องค์ประกอบทางเคมีของใบลางสาดป่าและใบประยงค์ใบใหญ่และฤทธิ์ทางชีวภาพ

นางสาวนันทิยา จ้อยชะรัด

สถาบันวิทยบริการ
จุฬาลงกรณ์มหาวิทยาลัย

วิทยานิพนธ์นี้เป็นส่วนหนึ่งของการศึกษาตามหลักสูตรปริญญาวิทยาศาสตรดุษฎีบัณฑิต
สาขาวิชาเภสัชเคมีและผลิตภัณฑ์ธรรมชาติ
คณะเภสัชศาสตร์ จุฬาลงกรณ์มหาวิทยาลัย
ปีการศึกษา 2550
ลิขสิทธิ์ของจุฬาลงกรณ์มหาวิทยาลัย

CHEMICAL CONSTITUENTS OF *AGLAIA FORBESII* AND *AGLAIA OLIGOPHYLLA* LEAVES AND THEIR BIOLOGICAL ACTIVITIES

Miss Nantiya Joycharat

สถาบันวิทยบริการ
จุฬาลงกรณ์มหาวิทยาลัย

A Dissertation Submitted in Partial Fulfillment of the Requirements
for the Degree of Doctor of Philosophy Program in Pharmaceutical Chemistry and Natural Products
Faculty of Pharmaceutical Sciences
Chulalongkorn University
Academic Year 2007

Copyright of Chulalongkorn University

Thesis Title	CHEMICAL CONSTITUENTS OF *AGLAIA FORBESII* AND *AGLAIA OLIGOPHYLLA* LEAVES AND THEIR BIOLOGICAL ACTIVITIES
By	Miss Nantiya Joycharat
Field of Study	Pharmaceutical Chemistry and Natural Products
Thesis Advisor	Associate Professor Ekarin Saifah, Ph.D.

Accepted by the Faculty of Pharmaceutical Sciences, Chulalongkorn University in Partial Fulfillment of the Requirements for the Doctoral Degree

.....Dean of the Faculty of Pharmaceutical Sciences

(Associate Professor Pornpen Pramyothin, Ph.D.)

THESIS COMMITTEE

.....Chairman

(Witchuda Thanakijcharoenpath, Ph.D.)

.....Thesis Advisor

(Associate Professor Ekarin Saifah, Ph.D.)

.....Member

(Associate Professor Rutt Suttisri, Ph.D.)

.....Member

(Associate Professor Nijsiri Ruangrungsi, Ph.D.)

.....Member

(Assistant Professor Srunya Vajrodaya, Ph.D.)

นันทิยา จ้อยชะรัด : องค์ประกอบทางเคมีของใบลางสาดป่าและใบประยงค์ใบใหญ่และฤทธิ์ทางชีวภาพ (CHEMICAL CONSTITUENTS OF *AGLAIA FORBESII* AND *AGLAIA OLIGOPHYLLA* LEAVES AND THEIR BIOLOGICAL ACTIVITIES) อ. ที่ปรึกษา : รศ. ดร. เอกรินทร์ สายฟ้า, 257 หน้า.

การศึกษาองค์ประกอบทางเคมีของใบลางสาดป่า (วงศ์ Meliaceae) สามารถแยกสารใหม่ในกลุ่ม cyclopenta[*bc*]-benzopyran flavaglines 3 ชนิด คือ desacetylpyramidaglains A, C และ D และสารใหม่ในกลุ่มของ cycloartane triterpenoid 1 ชนิด คือ (23*R*,24*S*)-23,24,25-trihydroxycycloartan-3-one รวมทั้งพบสารที่เคยมีรายงานมาแล้วอีก 8 ชนิด ได้แก่ สารกลุ่ม bisamide 1 ชนิด คือ pyramidatine, สารกลุ่ม sesquiterpenoid 1 ชนิด คือ spathulenol, สารกลุ่ม pregnane steroids 2 ชนิด คือ 2β,3β-dihydroxy-5α-pregn-17(20)-(*Z*)-en-16-one และ 2β,3β-dihydroxy-5α-pregn-17(20)-(*E*)-en-16-one, สารกลุ่ม stigmastane steroids 2 ชนิด คือ สารผสมของ β-sitosterol และ stigmasterol และ สารกลุ่ม triterpenoids ซึ่งพบได้ทั่วไป 2 ชนิด คือ lupeol และ lupenone ส่วนการศึกษาองค์ประกอบทางเคมีของใบประยงค์ใบใหญ่ สามารถแยกสารได้ 11 ชนิด โดยเป็นสารกลุ่ม cyclopenta[*b*]benzofuran flavagline 1 ชนิด คือ rocaglaol, สารกลุ่ม dammarane triterpenoids 8 ชนิด คือ dipterocarpol, สารผสมของ ocotillone และ cabraleone, ocotillol-II, 20*S*,24*S*-dihydroxydammar-25-en-3-one, 20*S*,25-epoxy-24*R*-hydroxy-3-dammaranone และ สารผสมของ 20*S*,25-epoxy-24*R*-hydroxydammar-3α-ol และ 20*S*,25-epoxy-24*R*-hydroxydammar-3β-ol และสารกลุ่ม bisamides 2 ชนิด คือ สารผสมของ odorine และ 2′-epi-odorine การพิสูจน์โครงสร้างทางเคมีของสารที่แยกได้นี้ อาศัยการวิเคราะห์สเปคตรัมของ UV, IR, MS และ NMR ร่วมกับการเปรียบเทียบข้อมูลของสารที่ทราบโครงสร้างแล้ว โดยสารแต่ละชนิดที่สกัดได้จากพืชทั้งสองชนิดได้ถูกนำไปทดสอบฤทธิ์ต้านเชื้อวัณโรค (*Mycobacterium tuberculosis* $H_{37}Ra$), ฤทธิ์ต้านไวรัสเริม HSV-1, และ ฤทธิ์ความเป็นพิษต่อเซลล์มะเร็งปอด (NCI-H187)

สารสกัดจากลางสาดป่าทั้งหมดแสดงฤทธิ์ต้านเชื้อวัณโรคยกเว้น desacetylpyramidaglains A และ C โดยพบว่า desacetylpyramidaglain D และ pyramidatine แสดงฤทธิ์ได้ดีที่สุด และยังพบว่าสารสกัดบางชนิดจากพืชนี้แสดงฤทธิ์ต้านไวรัสเริม HSV-1 โดยสารดังกล่าวประกอบด้วย 23,24,25-trihydroxycycloartan-3-one, desacetylpyramidaglain D, และ 2β,3β-dihydroxy-5α-pregn-17(20)-(*E*)-en-16-one ในขณะที่พบว่า lupeol นั้นแสดงความเป็นพิษปานกลางต่อเซลล์มะเร็งปอด (NCI-H187) นอกจากนี้ยังพบว่าสารสกัดจากประยงค์ใบใหญ่ 4 ชนิด ได้แก่ สารผสมของ 20*S*,25-epoxy-24*R*-hydroxydammar-3α-ol และ 20*S*,25-epoxy-24*R*-hydroxydammar-3β-ol และ สารผสมของ odorine และ 2′-epi-odorine แสดงฤทธิ์ต้านเชื้อวัณโรค

สาขาวิชา เภสัชเคมีและผลิตภัณฑ์ธรรมชาติ ลายมือชื่อนิสิต นางสาว นันทิยา จ้อยชะรัด

ปีการศึกษา 2550 ลายมือชื่ออาจารย์ที่ปรึกษา .....

4576958433 : MAJOR PHARMACEUTICAL CHEMISTRY AND NATURAL PRODUCTS

KEY WORD : *AGLAIA FORBESII* / *AGLAIA OLIGOPHYLL* / MELIACEAE / FLAVAGLINES / BISAMIDES / CYCLOPENTA[*bc*] BENZOPYRAN

NANTIYA JOYCHARAT : CHEMICAL CONSTITUENTS OF *AGLAIA FORBESII* AND *AGLAIA OLIGOPHYLLA* LEAVES AND THEIR BIOLOGICAL ACTIVITIES. THESIS ADVISOR : ASSOC. PROF. EKARIN SAIFAH, Ph.D., 257 pp.

Investigation of the chemical constituents of the leaves of *Aglaia forbesii* King. (Meliaceae) led to the isolation of three new cyclopenta[*bc*]benzopyran type flavaglines, desacetylpyramidaglains A, C and D, and a new cycloartane type triterpenoid, (23*R*,24*S*)-23,24,25-trihydroxycycloartan-3-one, together with the bisamide pyramidatine, the sesquiterpene spathulenol, two pregnane steroids, 2β,3β-dihydroxy-5α-pregn-17(20)-(*Z*)-en-16-one and 2β,3β-dihydroxy-5α-pregn-17(20)-(*E*)-en-16-one, two stigmastane steroids, a mixture of β-sitosterol and stigmasterol and two common triterpenoids, lupeol and lupenone. Similar study on the leaves of *A. oligophylla* Miq. yielded eleven of its constituents including the cyclopenta[*b*]benzofuran flavagline, rocaglaol, eight dammarane type triterpenoids, including dipterocarpol, a mixture of ocotillone and cabraleone, ocotillol-II, 20*S*,24*S*-dihydroxydammar-25-en-3-one, 20*S*,25-epoxy-24*R*-hydroxy-3-dammaranone, and a mixture of 20*S*,25-epoxy-24*R*-hydroxydammar-3α-ol and 20*S*,25-epoxy-24*R*-hydroxydammar-3β-ol, and a mixture of the bisamides odorine and 2′-epi-odorine. The structures of these isolates were determined by extensive spectroscopic studies, including comparison of their UV, IR, MS and NMR properties with previously reported data. Each isolated compounds from the two plants was evaluated for anti-tuberculosis activity against *Mycobacterium tuberculosis* $H_{37}Ra$, anti-herpes simplex activity, and cytotoxic activity against NCI-H187 small cell lung cancer cell line.

All of the compounds from *Aglaia forbesii* except desacetylpyramidaglains A and C exhibited anti-TB activity, of which desacetylpyramidaglain D and pyramidatine showed the highest activity. Furthermore, some of the compounds isolated from this plant, including 23,24,25-trihydroxycycloartan-3-one, desacetylpyramidaglain D and 2β,3β-dihydroxy-5α-pregn-17(20)-(*E*)-en-16-one, also exhibited anti-HSV-1 activity, while lupeol showed moderately cytotoxic activity against NCI-H187 cancer cell line. In addition, four compounds from *Aglaia oligophylla*, a mixture of 20*S*,25-epoxy-24*R*-hydroxydammar-3α-ol and 20*S*,25-epoxy-24*R*-hydroxydammar-3β-ol, and a mixture of the bisamides odorine and 2′-epi-odorine exhibited anti-TB activity .

Field of Study: Pharmaceutical Chemistry and Natural Products Student's Signature Nantiya Joycharat

Academic Year: 2007 Advisor's Signature Ekarin Saifah

ACKNOWLEDGEMENTS

The success of this research would not be realized without the support and assistance of some persons and various institutions to whom I would like to express my deepest gratitude:

Associate Professor Dr. Ekarin Saifah, my thesis advisor, for his excellent advice and untiring supervision during the entire duration of the work.

Prof. Dr. Harald Greger of the Comparative and Ecological Phytochemistry Section, Institute of Botany, University of Vienna, for providing research opportunities and invaluable suggestions during my research in Vienna, Austria.

Prof. Dr. Otmar Hofer of the Institute of Organic Chemistry, University of Vienna, for his kind assistance in NMR measurement and discussion on structure elucidation.

Associate Professor Dr. Rapepol Bavovada of the Department of Pharmaceutical Botany for his useful discussion on structure elucidation.

All the members of my thesis committee for their constructive suggestions and critical review of this thesis.

The Thailand Research Fund (TRF) for financial support (grant no. PHD/0063/2546) through the 2003 Royal Golden Jubilee Ph.D. program.

Nuclear magnetic resonance and infrared spectrometer operators of the Scientific and Technological Research Equipment Center, Chulalongkorn University for providing the spectral data and helpful assistance in spectroscopic experiments.

BIOTEC laboratories, NSTD, Thailand for the evaluation of antituberculosis, antimalarial, antiviral and anticancer activities of the plant extracts and pure compounds.

The students and all staff members of the Department of Pharmaceutical Botany, Faculty of Pharmaceutical Sciences, Chulalongkorn University for their friendship, kind support and encouragement throughout the period of my study.

Finally, the most special thanks are due to the late Mr. Patiparn Treechorvitaya and my family for their love, encouragement and moral support.

CONTENTS

Page

ABSTRACT (THAI) ……... iv

ABTRACT (ENGLISH) ……... v

ACKNOWLEDGEMENTS …… vi

CONTENTS ……... vii

LIST OF FIGURES …… xi

LIST OF TABLES …….. xvii

LIST OF SCHEMES ……... xix

LIST OF ABBREVIATIONS ..……... xx

CHAPTER

I INTRODUCTION…….. 1

II HISTORICAL……. 7

1. Chemical constituents of *Aglaia* spp. ……... 7

2. Biological Activity of the genus *Aglaia*……..... 47

III EXPERIMENTAL…… 53

1. Source of Plant Material ……... 53

2. General Techniques …….. 53

2.1 Analytical Thin-Layer Chromatography (TLC)…… 53

2.2 Preparative Thin Layer Chromatography (PTLC)……..... 53

2.3 Column Chromatography……. 54

2.3.1 Liquid Column Chromatography ……... 54

2.3.2 Gel filtration Chromatography…… 54

2.4 Spectroscopy…….. 54

2.4.1 Ultraviolet (UV) Absorption Spectra……... 54

2.4.2 Infrared (IR) Absorption Spectra……. 55

2.4.3 Mass Spectra (MS)……... 55

2.4.4 Nuclear Magnetic Resonance (NMR) spectra……. 55

2.5 Physical properties…….. 55

2.3.1 Melting Points……. 55

2.3.2 Optical Rotations……. 55

Page

2.6 Solvents……. 56
3. Extraction and Isolation…… 56
3.1 Extraction and Isolation of Compounds from the Leaves of *Aglaia forbesii*…… 56
3.1.1 Extraction ……. 56
3.1.2 Isolation of Compounds from the Hexane Extract of *A. forbesii* Leaves….. 56
3.1.2.1 Isolation of Compounds HAF1 and HAF3…… 56
3.1.2.2 Isolation of Compound HAF2……... 56
3.1.2.3 Isolation of Compound HAF4……... 57
3.1.3 Isolation of Compounds from the CH_2Cl_2 Extract of *A. forbesii* Leaves….. 57
3.1.3.1 Isolation of Compound CAF1…….. 57
3.1.3.2 Isolation of Compounds CAF2 and CAF3……... 57
3.1.3.3 Isolation of Compound CAF4…….. 58
3.1.3.4 Isolation of Compound CAF5 ……. 58
3.1.3.5 Isolation of Compound CAF6…….. 58
3.1.3.6 Isolation of Compounds CAF6 and CAF7…….. 58
3.2 Extraction and Isolation of Compounds from the Leaves of *A. oligophylla*…… 59
3.2.1 Extraction…… 59
3.2.2 Isolation of Compounds from the Hexane Extract of *A. oligophylla* leaves 59
3.2.2.1 Isolation of Compounds HAO1 and HAO2 ……. 59
3.2.2.2 Isolation of Compound HAO3…….. 60
3.2.2.3 Isolation of Compound HAO4……. 60
3.2.2.4 Isolation of Compound HAO5 ……. 60
3.2.2.5 Isolation of Compound HAO6…….. 61
3.2.2.6 Isolation of Compound HAO7……. 61
3.2.3 Isolation of Compounds from the EtOAc Extract of *A. oligophylla* leaves… 61
3.2.3.1 Isolation of Compound EAO1……... 61
4. Physical and Spectral Data of Isolated Compounds……. 75
4.1 Compound HAF1…… 75
4.2 Compound HAF2……..... 75
4.3 Compound HAF3…… 75
4.4 Compound HAF4…… 75

Page

4.5 Compound CAF1……. 76
4.6 Compound CAF2……. 76
4.7 Compound CAF3……. 76
4.8 Compound CAF4……. 77
4.9 Compound CAF5……. 77
4.10 Compound CAF6……... 78
4.11 Compound CAF7…….. 78
4.12 Compound HAO1…….. 79
4.13 Compound HAO2…….. 79
4.14 Compound HAO3…….. 79
4.15 Compound HAO4 ……. 80
4.16 Compound HAO5…….. 80
4.17 Compound HAO6…….. 80
4.18 Compound HAO7…….. 81
4.19 Compound EAO1……... 81
5. Evaluation of Biological Activities……... 82
5.1 Determination of Antimycobacterial Activity…… 82
5.2 Determination of Antimalarial Activity ……. 82
5.3 Determination of Cytotoxic Activity …….. 83
5.3.1 Human Small Cell Lung Carcinoma (NCI-H187)…….. 83
5.3.2 Vero cell ……. 84
5.4 Determination of Anti-Herpes Simplex Activity ……... 84
IV RESULTS AND DISCUSSION……... 85
1. Structure Determination of Compounds Isolated from *Aglaia forbesii*……. 85
1.1 Identification of Compound HAF1…….. 85
1.2 Identification of Compound HAF2…….. 88
1.3 Identification of Compound HAF3…….. 90
1.4 Identification of Compound HAF4…….. 92
1.5 Identification of Compound CAF1…….. 95
1.6 Identification of Compound CAF2…….. 99
1.7 Identification of Compound CAF3…….. 102

Page

1.8 Identification of Compound CAF4…….. 104
1.9 Identification of Compound CAF5…….. 106
1.10 Identification of Compound CAF6…… 110
1.11 Identification of Compound CAF7…… 114
2. Structure Determination of Compounds Isolated from *Aglaia oligophylla*…….. 117
2.1 Identification of Compound HAO1……. 117
2.2 Identification of Compound HAO2……. 120
2.3 Identification of Compound HAO3…….. 124
2.4 Identification of Compound HAO4…….. 127
2.5 Identification of Compound HAO5…….. 130
2.6 Identification of Compound HAO6…….. 133
2.7 Identification of Compound HAO7…….. 136
2.8 Identification of Compound EAO1…….. 139
3. Bioactivities of Compounds Isolated from *Aglaia forbesii* and *Aglaia oligophylla*……. 142
3.1 Bioactive Compounds from *Aglaia forbesii*…… 142
3.1.1 Cytotoxic Activity……..... 142
3.1.2 Antituberculosis Activity…… 142
3.1.3 Anti HSV-1 Activity……... 143
3.2 Bioactive Compounds from *Aglaia oligophylla*…….. 145
3.2.1 Cytotoxic activity…… 145
3.2.2 Antituberculosis activity……. 145
3.2.3 Anti HSV-1 activity……..... 145
3.2.4 Antimalarial activity……... 145
V CONCLUSION……... 147
REFERENCES……. 149
APPENDIX…….. 158
VITA……. 235

LIST OF FIGURES

Figure		Page
1	*Aglaia forbesii* King.....	5
2	*Aglaia oligophylla* Miq…….	6
3	Chemical constituents of plants in the genus *Aglaia*……	29
4	Chemical structures of compounds isolated from *Aglaia forbesii* leaves…….	70
5	Chemical structures of compounds isolated from *Aglaia oligophylla* leaves……...	72
6	ESI-TOF Mass Spectrum of compound HAF1……	159
7	IR Spectrum of compound HAF1 (KBr disc)…….	159
8	^{1}H NMR (400 MHz) Spectrum of compound HAF1 ($CDCl_3$)…….....	160
9	^{13}C APT (100 MHz) Spectrum of compound HAF1 ($CDCl_3$)……..	160
10	IR Spectrum of compound HAF2 (KBr disc)……..	161
11	^{1}H NMR (300 MHz) Spectrum of compound HAF2 ($CDCl_3$)…….	161
12	^{13}C NMR (75 MHz) and DEPT Spectra of compound HAF2 ($CDCl_3$)……	162
13	EI Mass Spectrum of compound HAF3 …….	162
14	IR Spectrum of compound HAF3 (KBr disc)……...	163
15	^{13}H NMR (400 MHz) Spectrum of compound HAF3 ($CDCl_3$)……	163
16	^{13}C APT (100 MHz) Spectrum of compound HAF3 ($CDCl_3$)…….....	164
17	HMBC Spectrum of compound HAF3 ($CDCl_3$)……...	164
18	IR Spectrum of compound HAF4 (KBr disc)……...	165
19	^{1}H NMR (300 MHz) Spectrum of compound HAF4 ($CDCl_3$)……..	165
20	^{13}C NMR (75 MHz) Spectrum of compound HAF4 (in $CDCl_3$)……..	166
21	HRESI-TOF Mass spectrum of compound CAF1.....	166
22	IR Spectrum of compound CAF1 (KBr disc)……...	167
23	^{1}H NMR (500 MHz) Spectrum of compound CAF1 ($CDCl_3$)……..	167
24	^{13}C NMR (125 MHz) Spectrum of compound CAF1 ($CDCl_3$)…….	168
25	^{1}H–^{1}H COSY Spectrum of compound CAF1 ($CDCl_3$)…….	168
26	HSQC Spectrum of compound CAF1 ($CDCl_3$) [δ_H 0.5-2.0 ppm, δ_C 17-36 ppm].....	169
27	HSQC Spectrum of compound CAF1 ($CDCl_3$) [δ_H 0.0-4.2 ppm, δ_C 10-78 ppm].....	169
28	HMBC Spectrum of compound CAF1 ($CDCl_3$) [δ_H 0.5-2.0 ppm, δ_C 18-31 ppm]…..	170

Figure		Page
29	HMBC Spectrum of compound CAF1 ($CDCl_3$) [δ_H 0.5-1.3 ppm, δ_C 32-56 ppm]…..	170
30	HMBC Spectrum of compound CAF1 ($CDCl_3$) [δ_H 0.0-2.8 ppm, δ_C 70-220 ppm]…	171
31	HMBC Spectrum of compound CAF1 ($CDCl_3$) [δ_H 2.6-4.6 ppm, δ_C 20-75 ppm]….	171
32	HMBC Spectrum of compound CAF1 ($CDCl_3$) [δ_H 0.8-1.9 ppm, δ_C 69-76 ppm]…..	172
33	NOESY Spectrum of compound CAF1 ($CDCl_3$)……..	172
34	EI Mass spectrum of compound CAF2…….	173
35	UV Spectrum of compound CAF2……	173
36	IR Spectrum of compound CAF2 (KBr disc)……	174
37	^{1}H NMR (500 MHz) Spectrum of compound CAF2 ($CDCl_3$)…….....	174
38	^{1}H NMR (400 MHz) Spectrum of compound CAF2 ($CDCl_3$)…….....	175
39	^{13}C APT (100 MHz) Spectrum of compound CAF2 ($CDCl_3$)…….....	175
40	^{1}H–^{1}H COSY Spectrum of compound CAF2 ($CDCl_3$)……..	176
41	HMQC Spectrum of compound CAF2 ($CDCl_3$)……	176
42	HMBC Spectrum of compound CAF2 ($CDCl_3$) [δ_H 3.4-6.7 ppm, δ_C 10-70 ppm]…..	177
43	HMBC Spectrum of compound CAF2 ($CDCl_3$) [δ_H 3.4-6.7 ppm, δ_C 120-210 ppm]..	177
44	HMBC Spectrum of compound CAF2 ($CDCl_3$) [δ_H 0.7-2.3 ppm, δ_C 10-70 ppm]…..	178
45	HMBC Spectrum of compound CAF2 ($CDCl_3$) [δ_H 0.9-2.3 ppm, δ_C 120-210 ppm]..	178
46	ESI-TOF Mass spectrum of compound CAF3……..	179
47	UV Spectrum of compound CAF3……	179
48	IR Spectrum of compound CAF3 (KBr disc)……	180
49	^{1}H NMR (400 MHz) Spectrum of compound CAF3 ($CDCl_3$)……...	180
50	^{13}C APT (100 MHz) Spectrum of compound CAF3 ($CDCl_3$)……...	181
51	ESI-TOF Mass spectrum of compound CAF4……..	181
52	UV Spectrum of compound CAF4……	182
53	IR Spectrum of compound CAF4 (KBr disc)……	182
54	^{1}H NMR (400 MHz) Spectrum of compound CAF4 (DMSO-d_6)…….	183
55	^{13}C NMR (100 MHz) Spectrum of compound CAF4 (DMSO-d_6)……	183
56	^{13}C NMR (100 MHz) Spectrum of compound CAF4 (DMSO-d_6) (expanded)…….	184
57	HRESI-TOF Mass spectrum of compound CAF5…….	184
58	UV Spectrum of compound CAF5……	185

Figure		Page
59	IR Spectrum of compound CAF5 (KBr disc)……	185
60	^{1}H NMR (500 MHz) Spectrum of compound CAF5 ($CDCl_3$)…….....	186
61	^{13}C NMR (125 MHz) Spectrum of compound CAF5 ($CDCl_3$)…….	186
62	^{1}H–^{1}H COSY Spectrum of compound CAF5 ($CDCl_3$) [δ_H 1.0-4.0 ppm]…….	187
63	^{1}H–^{1}H COSY Spectrum of compound CAF5 ($CDCl_3$) [δ_H 0.0-7.0 ppm]…….	187
64	HMBC Spectrum of compound CAF5 ($CDCl_3$) [δ_H 2.6-4.2 ppm, δ_C 125-175 ppm]..	188
65	HMBC Spectrum of compound CAF5 ($CDCl_3$) [δ_H 1.0-5.0 ppm, δ_C 20-65 ppm]…..	188
66	HMBC Spectrum of compound CAF5 ($CDCl_3$) [δ_H 5.5-8.0 ppm, δ_C 20-65 ppm]…..	189
67	HMBC Spectrum of compound CAF5 ($CDCl_3$) [δ_H 3.8-5.4 ppm, δ_C 78-110 ppm]…	189
68	HMBC Spectrum of compound CAF5 ($CDCl_3$) [δ_H 3.9-5.4 ppm, δ_C 128-138 ppm]..	190
69	HMBC Spectrum of compound CAF5 ($CDCl_3$) [δ_H 3.8-4.5 ppm, δ_C 128-138 ppm]..	190
70	NOESY Spectrum of compound CAF5 ($CDCl_3$)…….	191
71	HRESI-TOF Mass spectrum of compound CAF6……...	191
72	UV Spectrum of compound CAF6……	192
73	IR Spectrum of compound CAF6 (KBr disc)……	192
74	^{1}H NMR (500 MHz) Spectrum of compound CAF6 ($CDCl_3$)……...	193
75	^{13}C NMR (125 MHz) Spectrum of compound CAF6 ($CDCl_3$)…….	193
76	^{1}H–^{1}H COSY Spectrum of compound CAF6 ($CDCl_3$) [δ_H 1.6-6.6 ppm]…….	194
77	^{1}H–^{1}H COSY Spectrum of compound CAF6 ($CDCl_3$) [δ_H 6.4-7.8 ppm]…….	194
78	HSQC Spectrum of compound CAF6 ($CDCl_3$) [δ_H 4.0-8.0 ppm, δ_C 80-135 ppm]….	195
79	HMBC Spectrum of compound CAF6 ($CDCl_3$) [δ_H 1.5-5.0 ppm, δ_C 20-70 ppm]…..	195
80	HMBC Spectrum of compound CAF6 ($CDCl_3$) [δ_H 3.2-5.0 ppm, δ_C 76-115 ppm]…	196
81	HMBC Spectrum of compound CAF6 ($CDCl_3$) [δ_H 3.0-8.0 ppm, δ_C 76-115 ppm]…	196
82	HMBC Spectrum of compound CAF6 ($CDCl_3$) [δ_H 4.0-8.0 ppm, δ_C 80-135 ppm]…	197
83	HMBC Spectrum of compound CAF6 ($CDCl_3$) [δ_H 3.2-5.0 ppm, δ_C 125-175 ppm]..	197
84	HMBC Spectrum of compound CAF6 ($CDCl_3$) [δ_H 6.0-7.8 ppm, δ_C 125-175 ppm]..	198
85	NOESY Spectrum of compound CAF6 ($CDCl_3$)……..	198
86	HRESI-TOF Mass spectrum of compound CAF7…….	199
87	UV Spectrum of compound CAF7……	199

Figure		Page
88	IR Spectrum of compound CAF7 (KBr disc)……	200
89	^{1}H NMR (500 MHz) Spectrum of compound CAF7 ($CDCl_3$)……....	200
90	^{13}C NMR (125 MHz) Spectrum of compound CAF7 ($CDCl_3$)……..	201
91	^{1}H–^{1}H COSY Spectrum of compound CAF7 ($CDCl_3$) [δ_H 6.7-7.9 ppm]…….	201
92	HSQC Spectrum of compound CAF7 ($CDCl_3$) [δ_H 1.0-5.0 ppm, δ_C 25-75 ppm]……	202
93	HSQC Spectrum of compound CAF7 ($CDCl_3$) [δ_H 6.8-7.9 ppm, δ_C 125-130 ppm]…	202
94	HMBC Spectrum of compound CAF7 ($CDCl_3$) [δ_H 0.9-4.0 ppm, δ_C 10-76 ppm]…..	203
95	HMBC Spectrum of compound CAF7 ($CDCl_3$) [δ_H 4.5-8.0 ppm, δ_C 25-75 ppm]…..	203
96	HMBC Spectrum of compound CAF7 ($CDCl_3$) [δ_H 2.0-4.2 ppm, δ_C 80-176 ppm]…	204
97	HMBC Spectrum of compound CAF7 ($CDCl_3$) [δ_H 4.6-8.0 ppm, δ_C 80-174 ppm]…	204
98	NOESY Spectrum of compound CAF7 ($CDCl_3$)……..	205
99	EI Mass spectrum of compound HAO1……	205
100	IR Spectrum of compound HAO1 (KBr disc)……..	206
101	^{1}H NMR (400 MHz) Spectrum of compound HAO1 ($CDCl_3$)…….	206
102	^{13}C APT (100 MHz) Spectrum of compound HAO1 ($CDCl_3$)…….....	207
103	HMBC Spectrum of compound HAO1 ($CDCl_3$)……..	207
104	EI Mass spectrum of compound HAO2……	208
105	IR Spectrum of compound HAO2 (KBr disc)……..	208
106	^{1}H NMR (500 MHz) Spectrum of compound HAO2 ($CDCl_3$)…….	209
107	^{13}C NMR (125 MHz) Spectrum of compound HAO2 ($CDCl_3$)…….	209
108	^{13}C APT (100 MHz) Spectrum of compound HAO2 ($CDCl_3$)…….....	210
109	HSQC Spectrum of compound HAO2 ($CDCl_3$) [δ_H 0.80-1.9 ppm, δ_C15-29 ppm]….	210
110	HSQC Spectrum of compound HAO2 ($CDCl_3$)[δ_H 0.80-3.5 ppm, δ_C 70-90 ppm]….	211
111	HMBC Spectrum of compound HAO2 ($CDCl_3$) [δ_H 0.8-2.5 ppm, δ_C 80-220 ppm]…	211
112	HMBC Spectrum of compound HAO2 ($CDCl_3$) [δ_H 3.3-3.7 ppm, δ_C 14-42 ppm]…..	212
113	EI Mass spectrum of compound HAO3……	212
114	IR Spectrum of compound HAO3 (KBr disc)……..	213
115	^{1}H NMR (400 MHz) Spectrum of compound HAO3 ($CDCl_3$)……..	213
116	^{13}C NMR (100 MHz) Spectrum of compound HAO3 ($CDCl_3$)…….	214

Figure		Page
117	HMBC Spectrum of compound HAO3 ($CDCl_3$)…….....	214
118	NOESY Spectrum of compound HAO3 ($CDCl_3$)…….	215
119	EI Mass spectrum of compound HAO4……	215
120	IR Spectrum of compound HAO4 (KBr disc)……...	216
121	^{1}H NMR (400 MHz) Spectrum of compound HAO4 (in $CDCl_3$)……..	216
122	^{13}C NMR (100 MHz) Spectrum of compound HAO4 (in $CDCl_3$)……	217
123	HSQC Spectrum of compound HAO4 ($CDCl_3$)……	217
124	HMBC Spectrum of compound HAO4 ($CDCl_3$) [δ_H 0.9-1.7 ppm, δ_C 68-77 ppm]….	218
125	HMBC Spectrum of compound HAO4 ($CDCl_3$) [δ_H 4.6-5.6 ppm, δ_C 60-95 ppm]**....**	218
126	HMBC Spectrum of compound HAO4 ($CDCl_3$) [δ_H 0.9-2.6 ppm, δ_C 110-220 ppm]..	219
127	ESI-TOF Mass spectrum of compound HAO5…….	219
128	UV Spectrum of compound HAO5……...	220
129	IR Spectrum of compound HAO5 (KBr disc)……...	220
130	^{1}H NMR (500 MHz) Spectrum of compound HAO5 ($CDCl_3$)……..	221
131	^{13}C NMR (125 MHz) Spectrum of compound HAO5 ($CDCl_3$)…….	221
132	HSQC Spectrum of compound HAO5 ($CDCl_3$)……	222
133	NOESY Spectrum of compound HAO5 ($CDCl_3$)…….	222
134	ESI-TOF Mass spectrum of compound HAO6……	223
135	UV Spectrum of compound HAO6……...	223
136	IR Spectrum of compound HAO6 (KBr disc)……..	224
137	^{1}H NMR (500 MHz) Spectrum of compound HAO6 ($CDCl_3$)……..	224
138	^{13}C NMR (125 MHz) Spectrum of compound HAO6 ($CDCl_3$)…….**....**	225
139	^{1}H–^{1}H COSY Spectrum of compound HAO6 ($CDCl_3$) [δ_H 2.0-7.0 ppm]……	225
140	HMBC Spectrum of compound HAO6 ($CDCl_3$) [δ_H 0.7-8.0 ppm, δ_C 15-180 ppm]…	226
141	HMBC Spectrum of compound HAO6 ($CDCl_3$) [δ_H 6.0-6.2 ppm, δ_C 20-48 ppm]….	226
142	EI Mass spectrum of compound HAO7……	227
143	IR Spectrum of compound HAO7 (KBr disc)……..	227
144	^{1}H NMR (400 MHz) Spectrum of compound HAO7 ($CDCl_3$)……..	228
145	^{13}C APT (100 MHz) Spectrum of compound HAO7 ($CDCl_3$)…….....	228
146	^{13}C APT (100 MHz) Spectrum of compound HAO7 ($CDCl_3$) (expanded)……...	229
147	HMBC Spectrum of compound HAO7 ($CDCl_3$)…….....	229

Figure		Page
148	EI Mass spectrum of compound EAO1……	230
149	IR Spectrum of compound EAO1 (KBr disc)……....	230
150	^{1}H NMR (500 MHz) Spectrum of compound EAO1 ($CDCl_3$)……..	231
151	^{13}C NMR (125 MHz) Spectrum of compound EAO1 ($CDCl_3$)…….	231
152	^{13}C NMR (125 MHz) Spectrum of compound EAO1 ($CDCl_3$) (expanded)…….	232
153	HSQC Spectrum of compound EAO1 ($CDCl_3$) [δ_H 0.7-2.0 ppm, δ_C 15-29 ppm]…..	232
154	HSQC Spectrum of compound EAO1 ($CDCl_3$) [δ_H 3.1-3.4 ppm, δ_C 71-80 ppm]…..	233
155	HMBC Spectrum of compound EAO1 ($CDCl_3$) [δ_H 0.7-1.2 ppm, δ_C 33-58 ppm]….	233
156	HMBC Spectrum of compound EAO1 ($CDCl_3$) [δ_H 0.7-1.3 ppm, δ_C 72-88 ppm]….	234
157	HMBC Spectrum of compound EAO1 ($CDCl_3$) [δ_H 3.1-3.6 ppm, δ_C 26-80 ppm]**…..**	234

สถาบันวิทยบริการ
จุฬาลงกรณ์มหาวิทยาลัย

LIST OF TABLES

Table		Page
1	Chemical constituents of plants in the genus *Aglaia*……..	8
2	Biological activities of *Aglaia* species……	48
3	Comparison of the ^{13}C-NMR spectral data of lupenone and compound HAF1 ($CDCl_3$, 100 MHz)……	87
4	Comparison of the ^{13}C-NMR spectral data of lupeol and compound HAF2 ($CDCl_3$, 75 MHz)……	89
5	Comparison of the NMR spectral data of spathulenol and compound HAF3 ($CDCl_3$, 400 MHz)……	91
6	Comparison of the ^{13}C NMR spectral data of β-sitosterol and stigmasterol and compound HAF4 (a mixture of HAF4A and HAF4B) ($CDCl_3$, 75 MHz)……..	93
7	NMR spectral data of CAF1 and partial comparison of the ^{13}C resonances with those of 21*S*,24*R*-dihydroxycycloart-25-en-3-one ($CDCl_3$, 500 MHz)……	97
8	Comparison of the NMR spectral data of 2β,3β-Dihydroxy-5α-pregn-17(20)-(*E*)-en-16-one and compound CAF2 ($CDCl_3$, 500 MHz)……..	100
9	Comparison of the NMR spectral data of 2β,3β-Dihydroxy-5α-pregn-17(20)-(*Z*)-en-16-one and compound CAF3 ($CDCl_3$, 500 MHz)……..	103
10	Comparison of the NMR spectral data of pyramidatine and compound CAF4 (DMSO-d_6, 400 MHz)……	105
11	NMR spectral data of CAF5 ($CDCl_3$, 500 MHz)…….	108
12	NMR spectral data of CAF6 ($CDCl_3$, 500 MHz)……	112
13	NMR spectral data of CAF7 ($CDCl_3$, 500 MHz)……	115
14	Comparison of the NMR spectral data of dipterocapol and compound HAO1 ($CDCl_3$, 400 MHz)……	118
15	Comparison of the ^{13}C NMR spectral data of ocotillone and cabraleone and compound HAO2 ($CDCl_3$, 100 MHz)	122
16	Comparison of the NMR spectral data of ocotillol-II and compound HAO3 ($CDCl_3$, 400 MHz)……	125
17	Comparison of the NMR spectral data of 20(*S*),24(*S*)-dihydroxydammar-25-en-3-one and compound HAO4 ($CDCl_3$, 400 MHz)…….	128

Table		Page
18	Comparison of the NMR spectral data of rocaglaol and compound HAO5 ($CDCl_3$, 500 MHz)……..	131
19	Comparison of the NMR spectral data of odorine and compound HAO6 ($CDCl_3$, 500 MHz)…….	134
20	NMR spectral data of HAO7 and partial comparison of ^{13}C resonances with cabraleone ($CDCl_3$, 400 MHz)…….	137
21	NMR spectral data of EAO1 ($CDCl_3$, 500 MHz)…….	140
22	Bioactivities of isolated compounds from *Aglaia forbesii*……...	144
23	Bioactivities of isolated compounds from *Aglaia oligophylla*…….	146

สถาบันวิทยบริการ
จุฬาลงกรณ์มหาวิทยาลัย

LIST OF SCHEMES

Scheme		Page
1	Separation of the hexane extract of the leaves of *Aglaia forbesii*…….....	62
2	Separation of the CH_2Cl_2 extract of the leaves of *Aglaia forbesii*……..	63
3	Separation of the hexane extract of the leaves of *Aglaia oligophylla* …….	66
4	Separation of the EtOAc extract of the leaves of *Aglaia oligophylla* …….	69

สถาบันวิทยบริการ
จุฬาลงกรณ์มหาวิทยาลัย

LIST OF ABBREVIATIONS

$[\alpha]^{25}_{D}$	=	Specific rotation at 25 ^{o}C and sodium D line (589 nm)
δ	=	Chemical shift
APT	=	Attachted Proton Test Spectrum
ax	=	Axial
br	=	Broad (for NMR spectra)
^{13}C NMR	=	Carbon-13 Nuclear Magnetic Resonance
c	=	Concentration
^{o}C	=	Degree Celsius
calcd	=	Calculated
$CDCl_3$	=	Deuterated chloroform
CFU	=	Colony forming unit
CH_2Cl_2	=	Dichloromethane
$CHCl_3$	=	Chloroform
cm	=	Centimetre
cm^{-1}	=	Reciprocal centimeter (unit of wave number)
1-D	=	One dimensional
2-D	=	One dimensional
d	=	Doublet (for NMR spectra)
dd	=	Doublet of doublets (for NMR spectra)
DEPT	=	Distortionless Enhancement by Polarization Transfer
DMSO-d_6	=	Deuterated dimethyl sulfoxide
EIMS	=	Electron Impact Mass Spectrometry
eq	=	Equatorial
ESI-TOFMS	=	Electrospray Ionized Time of Flight Mass Spectrometry
EtOAc	=	Ethyl acetate
Fr.	=	Fraction
g	=	Gram
^{1}H-^{1}H COSY	=	Homonuclear (Proton-Proton) Correlation Spectroscopy
^{1}H-NMR	=	Proton Nuclear Magnetic Resonance
HMBC	=	^{1}H-detected Heteronuclear Multiple Bond Coherence

สถาบันวิทยบริการ
จุฬาลงกรณ์มหาวิทยาลัย

HMQC	=	^{1}H-detected Heteronuclear Multiple Quantum Coherence
HRESIMS	=	High Resolution Electrospray Ionization Mass Spectrometry
HSQC	=	Heteronuclear Single Quantum Correlation
HSV-1	=	Herpes Simplex Virus type 1
Hz	=	Hertz
IC_{50}	=	Median inhibitory concentration
IR	=	Infrared Spectrum
J	=	Coupling constant
KBr	=	Potassium bromide
kg	=	Kilogram
L	=	Litre
λ_{max}	=	Wave length at maximal absorption
ε	=	Molar absorptivity
m	=	Multiplet
m/z	=	Mass to charge ratio
MS	=	Mass Spectrometry
mult.	=	Multiplicity
M^{+}	=	Molecular ion
MeOH	=	Methanol
MHz	=	Megahertz
MIC	=	Minimum inhibitory concentration
min	=	Minute
mm	=	Millimetre
mM	=	Millimolar
Mp	=	Melting point
nm	=	Nanometre
NMR	=	Nuclear Magnetic Resonance
NOESY	=	Nuclear Overhauser Enhancement Spectroscopy
ps d	=	Pseudo doublet
ps t	=	Pseudo triplet
PLC	=	Preparative Thin Layer Chromatography
q	=	Quartet (for NMR spectra)

สถาบันวิทยบริการ
จุฬาลงกรณ์มหาวิทยาลัย

ν_{max}	=	Wave number at maximal absorption
s	=	Singlet (for NMR spectra)
t	=	Triplet (for NMR spectra)
TLC	=	Thin Layer Chromatography
UV	=	Ultraviolet
UV-VIS	=	Ultraviolet and Visible Spectrophotometry
µl	=	Microlitre

สถาบันวิทยบริการ
จุฬาลงกรณ์มหาวิทยาลัย

CHAPTER I

INTRODUCTION

Aglaia, the largest genus in the family Meliaceae, is separated from most other genera in the Meliaceae by its characteristic indumentum of stellate hairs or peltate scales. The hairs and scales collectively known as trichomes which are described as scales if they lie flat on the surface of the plant and as hairs if the arms project at various angles outwards from the plant surface. All species of *Aglaia* are woody, ranging from treelets a few metres high to large trees up to 40 m high. Latex is often present, sometimes flowing rapidly when the trunk is cut. Twigs are stout or slender, apical bud always with dense stellate hairs or peltate scales. Leaves are usually imparipinnate, but occasionally simple or trifoliolate. Leaflets are (1-)3-25, lanceolate, oblanceolate, ovate, obovate, elliptical or oblong, the margin is entire or slightly wavy, one or both surfaces may be rugulose or pitted, in some species almost without indumentum but usually the lower surface has few, numerous or dense hairs or scales like those on the twigs. Inflorescences are usually axillary, occasionally ramiflorous, often several on an apical shoot. Flowers are small (1-10 mm long) and subglobose, ellipsoid or obovoid. They are unisexual, the structure of female flowers is similar to the male but usually slightly larger. Corolla aestivation is imbricate or quincuncial, petals are 3-5, free or united at the base, usually yellow, sometimes pink or white, subrotund, elliptical or obovate, occasionally with stellate hairs or peltate scales on the outside. Stamens are united to form a tube 0.5-8 mm long; anthers are (3-)5-10(-21), usually in a single whorl; anthers in the female flowers are similar but sterile. Ovary is superior, depressed globose or ovoid with dense stellate hairs or peltate scales; style is absent; stigma is ovoid, entire at the apex or with 2,3 or rarely 4 small lobes; ovary and stigma in the male are either poorly developed or similar to the female but sterile. Fruit is subglobose, obovoid or ellipsoids, dehiscence (section *Amoora*) or indehiscence (section *Aglaia*), covered with stellate hairs or peltate scales (Pannell, 1992).

According to Pannell (1992) and Smitinand (2001), the genus *Aglaia* consists of over 100 species distributed in the tropical rain forests of Southeast Asia. In Thailand, twenty-eight species can be found as follows; *A. argentea* (Sang khriat klong), *A. aspera*, *A. chittagonga* (Pra song), *A. crassinervia*, *A. cuculata* (Samae daeng), *A. edulis* (Khang khao), *A. elaeagnoidea* (Kraduk - khiat), *A. elliptica*, *A. erythrosperma*, *A. eximia*, *A. exstipulata* (Sang khriat rai hu), *A. forbesii*, *A. grandis*, *A. korthalsii* (Lang sat kao), *A. lawii* (Sang katong), *A. leptantha*, *A. leucophylla*, *A. odorata* (Prayong),

A. odoratissima (Prayong pa), *A. oligophylla* (Pra youg bai yai), *A. pachyphylla*, *A. perviridis*, *A. silvestris* (Chan-chamot), *A. simplicifolia* (Khaduk ling), *A. spectabilis*, *A. tenuicaulis* (Sang khriat bai yai), *A. teymanniana* and *A. tomentosa* (Sang khriat langsat).

Several species of the genus *Aglaia* are traditionally used in folk medicine. In Indo-china, the roots and leaves of *A. odorata* are recommended as pectoral, heart stimulant, febrifuge, tonic, and as a remedy for convulsions; in Malay Peninsula, an infusion of the flowers is administered as a cooling drink for eruptive fevers; in Indonesia, a decoction of the leaves is ingested as a remedy for excessive menses during the menopause (Perry, 1980). In Nepal, the use of *A. roxburghiana* (syn. *A. elaeagnoidea*) to treat a wide range of physical ailments such as asthma, bronchitis, rheumatism, and inflammatory skin diseases has been reported (Kumar and Muller, 1999). Furthermore, the leaves and flowers of *A. duperreana* and *A. odorata* are used in the traditional medicine of several Southeast Asian countries for treatment of asthma and inflammatory skin diseases (Baumann *et al*., 2002). In China, a decoction of the bark of *A. tsangii* is rubbed on the affected areas **(rubbed** into the hair and scalp) to kill lice. In Indo-China, a decoction of *A. baillonii* is considered to be antifebrile. A decoction of the roots of *A. pleuropteris* is a remedy for jungle fever (malaria). In Thailand, the scented wood of *A. silvestris* (syn. *A. pyramidata*) is used medicinally as antifebrile and antitussive (Perry, 1980). In the Philippines, a decoction of the roots of *A. iloilo* is drunk as an emetic to relieve colic; the bark of *A. elliptica* is boiled and used to treat tumors, while the leaves are applied to wounds (Cui *et al*., 1997; Perry, 1980).

Previous phytochemical investigations of plants in the genus *Aglaia* have revealed the presence of a variety of compounds with interesting biological activities, including the flavonol-cinnamate derivatives, named flavaglines (cyclopenta[*b*]benzofurans, cyclopenta[*bc*]benzopyrans, and benzo[*b*]oxepines) (Dumontet *et al*., 1996; Bacher *et al*., 1999; Proksch *et al*., 2001), the cinnamic acid-derived bisamides (Brader *et al*., 1998; Saifah *et al*., 1988), triterpenoids (dammarane, cycloartane, tirucallane, glabretal, and baccharane types) (Weber *et al*, 2000; Hwang *et al*., 2004), steroids (pregnane, cholestane, stigmastane, and ergostane types) (Mohamad *et al*., 1999; Rivero-Cruz *et al*., 2004; Su *et al*., 2006), limonoids (Fuzzati *et al*., 1996, sesquiterpenes (Roux *et al*., 1998, lignans (Greger *et al*., 2000), and flavonoids (Greger *et al*., 2001). Among these previously known isolates, flavaglines have attracted considerable interest due to their unusual carbon skeleton, and these compounds are confined to the members of the genus *Aglaia*. Inaddition, some of flavaglines were shown to possess high insecticidal activity, antifungal activity as well as significant cytotoxicity in many different cancer cell lines (Cui *et al*., 1997; Proksch *et al*., 2001), while bisamides have been

reported as cytotoxic (Duh *et al*., 1993) and antiviral (Joshi *et al*., 1987).

Aglaia forbesii King (Lang Sat Pa) is a large tree of up to 35 metre in height. The leaves (**Figure 1**) are imparipinnate, up to 100 cm long and 60 cm wide, elliptical in outline. The 9-15 leaflets are alternate or subopposite. They all are 8.5-30 cm long and 2-10 cm wide, elliptical or oblong, brown or greenish-brown on lower surface when dry. The inflorescence is up to 35 cm long and 25 cm wide. The peduncle is up to 6 cm in length. The flowers are up to 2 mm long, ovoid, and fragrant . Each flower has 5-6 petals which are obovate, white, yellow or orange-yellow. The fruit is up to 4 cm long and 3.8 cm wide, ellipsoid or subglobose. The grey or greenish-grey pericarp is up to 4 mm thick with white latex, soft, fibrous and flexible. The seed is 1.5-3 cm long, 2-2.2 cm wide, and about 1.5 cm thick, with yellow or pink aril up to 3 mm thick.

The isolation of flavaglines including the cyclopenta[*b*]benzofuran type rocaglaol and ethylrocaglaol, the cyclopenta[*bc*]benzopyran type aglaforbesins A-B, and the benzo[*b*]oxepine type forbaglins A-B from the CH_2Cl_2 extract of the bark of *Aglaia forbesii*. has been earlier described (Dumontet *et al*., 1996). However, the chemical constituents and biological activity of the leaves of *Aglaia forbesii* have never been recorded. Preliminary evaluation of the biological activity of *A. forbesii* leaves revealed that the dichloromethane extract exhibited antimycobacterial activity against *Mycobacterium tuberculosis* with MIC values of 25 μg/ml. The extract was also moderately active (35-50%) against herpes simplex virus type 1 (HSV-1) at the non-cytotoxic concentration of 38.1 μg/ml .

Aglaia oligophylla Miq. (Prayong bai yai) is a tree up to 20 (-25) m, with small buttresses. The leaves (**Figure 2**) are imparipinnate, up to 40 cm long and 30 cm wide, obovate in outline. The 3-11 leaflets are opposite or subopposite. They are 4.5-22 cm long, 2-9 cm wide, obovate or elliptical, both surfaces are rather shiny when dry. The inflorescence is up to 10-20 cm long and 9-15 cm wide. The peduncle is up to 4 cm in length. The depressed-globose flower is up to 2 mm long, each of which has 5-6 yellow and obovate petals. The fruit is 1-3 cm in diameter, subglobose. Its pericarp is brown or yellow, either thin, hard and brittle or thick. The seeds are white or brown with sweet edible aril.

Previous phytochemical studies on this plant have revealed the presence of flavaglines including the cyclopenta[*b*]benzofuran type aglaroxins A-B, aglaroxin F, pannellin 1-O-acetate, C-1-oxo, C-2-piriferineaglaroxin A and cyclorocaglamide, and the cyclopenta[*bc*]benzopyran type homothapsakin A and C-8-demethoxy-C7, C8-methylenedioxyaglaforbesin in the CH_2Cl_2 extract of the twigs of *Aglaia oligophylla* Miq. (Dreyer *et al*., 2001; Bringmann *et al*., 2003). Preliminary

evaluation for bioactivity activity revealed that the hexane and EtOAc extracts of its leaves exhibited strong cytotoxic activity against NCI-H187 cancer cell line at the IC_{50} values of 3.86 and 4.22 µg/ml, respectively, as well as antimalarial activity against *Plasmodium falciparum* (KI stain) at the IC_{50} values of 2.5 and 5.1 µg/ml, respectively. In addition, the EtOAc extract also showed antimycobacterial activity against *Mycobacterium tuberculosis* with the MIC value of 100 µg/ml.

Therefore, these plants were selected for further investigation of their chemical constituents and biological activity. The purposes of this research are as follows:

1. Isolation and purification of compounds from the leaves of *Aglaia forbesii* and *A. oligophylla*.
2. Determination of chemical structures of the isolated compounds.
3. Evaluation of biological activities of the isolated compounds.

สถาบันวิทยบริการ
จุฬาลงกรณ์มหาวิทยาลัย

Figure 1 *Aglaia forbesii* King.

Figure 2 *Aglaia oligophylla* Miq.

CHAPTER II

HISTORICAL

1. Chemical constituents of *Aglaia* spp.

According to previous phytochemical studies, a number of compounds have been isolated from the genus *Aglaia*. They can be classified as flavaglines (cyclopenta[*b*]benzofurans, cyclopenta[*bc*]benzopyrans, and benzo[*b*]oxepines), bisamides (pyrrolidine and putrescine types), triterpenoids (dammarane, cycloartane, tirucallane, glabretal, and baccharane types), steroids (pregnane, cholestane, stigmastane, and ergostane types), limonoids, sesquiterpenes, lignans, and flavonoids. The distribution of these compounds in *Aglaia* spp. is summarized in **Table 1** and their chemical structures are shown in **Figure 3**.

สถาบันวิทยบริการ
จุฬาลงกรณ์มหาวิทยาลัย

Table 1. Chemical constituents of plants in the genus *Aglaia*

Chemical type / Chemical compounds	Sources / Plant part	References
Flavaglines Cyclopenta[*b*]benzofuran-type C-1-O-Acetyl-N-butanoyl-didesmethylrocaglamide **(1)**	*A. elliptica* (fruits)	Nugroho *et al*., 1997b
C-1-O-Acetyldemethylrocaglamide **(2)**	*A. duperreana* (roots, flowers)	Chaidir *et al*., 1999; Hiort *et al*., 1999
C-1-O-Acetyldidemethylrocaglamide **(3)**	*A. duperreana* (flowers)	Chaidir *et al*., 1999
C-1-O-Acetyl-3′-hydroxydemethylrocaglamide **(4)**	*A. duperreana* (roots, flowers)	Chaidir *et al*., 1999; Hiort *et al*., 1999
C-1-O-Acetyl-3′-hydroxymethylrocaglate **(5)**	*A. duperreana* (roots, flowers)	Chaidir *et al*., 1999; Hiort *et al*., 1999
C-1-O-Acetyl-3′-hydroxyrocaglamide **(6)**	*A. duperreana* (roots , twigs, flowers) *A. odorata* (twigs)	Nugroho *et al*., 1997a; Chaidir *et al*., 1999; Hiort *et al*., 1999; Nugroho *et al*., 1999
C-1-O-Acetylmethylrocaglate **(7)**	*A. duperreana* (roots , flowers) *A. rubiginosa* (twigs)	Chaidir *et al*., 1999; Hiort *et al*., 1999; Rivero-Cruz *et al*., 2004
C-1-O-Acetylrocaglamide **(8)**	*A. duperreana* (roots)	Hiort *et al*., 1999
C-1-O-Acetylrocaglaol **(9)**	*A. rubiginosa* (twigs)	River-Cruz *et al*., 2004
N-Butanoyl-didesmethylrocaglamide **(10)**	*A. duperreana* (flowers) *A. elliptica* (fruits) *A. odorata* (flowers)	Nugroho *et al*., 1997a; Nugroho *et al*.,1997b; Baumann *et al*., 2002

Table 1. Chemical constituents of plants in the genus *Aglaia* (continued)

Chemical type / Chemical compounds	Sources / Plant part	References
Desmethylrocaglamide **(11)**	*A. duperreana* (flowers, roots, twigs) *A. odorata* (leaves, flowers , root bark)	Nugroho *et al*., 1997a; Chaidir *et al*., 1999; Hiort *et al*., 1999; Ishibashi *et al*., 1993; Engelmeier *et al*., 2000; Baumann *et al*., 2002
Didesmethylrocaglamide **(12)**	*A. argentea* (leaves) *A. duperreana* (flowers, roots) *A. elliptica* (fruits) *A. odorata* (flowers)	Dumontet *et al*., 1996; Nugroho *et al*., 1997a; Hiort *et al*., 1999; Nugroho *et al*., 1997b Baumann *et al*., 2002
C-8b-O-Ethyl-3′-hydroxymethylrocaglamide **(13)**	*A. duperreana* (flowers)	Chaidir *et al*., 1999
C-8b-O-Ethyl-3′-hydroxyrocaglamide **(14)**	*A. duperreana* (flowers)	Chaidir *et al*., 1999
Ethylrocaglaol **(15)**	*A. forbesii* (bark)	Dumontet *et al*., 1996
C-1-O-Formyloxy-3′-hydroxymethylrocaglate **(16)**	*A. dasyclada* (leaves) *A. spectabilis* (bark)	Chaidir *et al*., 2001; Schneider *et al*., 2000
C-1-O-Formyloxymethylrocaglate **(17)**	*A. dasyclada* (leaves) *A. spectabilis* (bark)	Chaidir *et al*., 2001; Schneider *et al*., 2000
C-3′-Hydroxydemethylrocaglamide **(18)**	*A. duperreana* (roots) *A. odorata* (twigs)	Hiort *et al*., 1999; Nugroho *et al*., 1999

Table 1. Chemical constituents of plants in the genus *Aglaia* (continued)

Chemical type / Chemical compounds	Sources / Plant part	References
C-3′-Hydroxydemethylrocaglate **(19)**	*A. duperreana* (roots) *A. odorata* (flowers) *A. spectabilis* (bark)	Hiort *et al*., 1999; Nugroho *et al*.,1999; Schneider *et al*., 2000
C-3′-Hydroxydidesmethylrocaglamide **(20)**	*A. odorata* (twigs)	Nugroho *et al*., 1999
C-3′-Hydroxyrocaglamide **(21)**	*A. duperreana* (roots, twigs , flowers) *A. odorata* (twigs)	Nugroho *et al*., 1997a; Chaidir *et al*., 1999; Hiort *et al*., 1999; Nugroho *et al*., 1999
C-3′-Methoxyrocaglamide **(22)**	*A. duperreana* (twigs) *A. odorata* (twigs)	Nugroho *et al*., 1997a; Nugroho *et al*., 1999
C-8b-O-Methyl-methylrocaglate **(23)**	*A. duperreana* (roots)	Hiort *et al*., 1999
C-3′-Methylrocaglaol **(24)**	*A. odorata* (twigs & leaves)	Nugroho *et al*.,1999
C-8b-O-Methylrocaglaol **(25)**	*A. duperreana* (roots)	Hiort *et al*., 1999
Methylrocaglate (aglafolin) **(26)**	*A. dasyclada* (leaves) *A. duperreana* (flowers, roots) *A. elaeagnoidea* (bark) *A. elliptica* (stem & fruits) *A. elliptifolia* (stem)	Chaidir *et al*., 2001; Chairdir *et al*., 1999; Hiort *et al*., 1999; Fuzzati *et al*., 1996; Cui *et al*., 1997; Lee *et al*., 1998; Wu *et al*., 1997;

Table 1. Chemical constituents of plants in the genus *Aglaia* (continued)

Chemical type / Chemical compounds	Sources / Plant part	References
Methylrocaglate (aglafolin) **(26)**	*A. odorata* (leaves) *A. ponapensis* (leaves & twigs)	Ishibashi *et al*., 1993; Salim *et al*., 2007
C-1-Oxime-C-3′-methoxymethylrocaglate **(27)**	*A. odorata* (twigs)	Nugroho *et al*.,1999
Rocaglamide **(28)**	*A. duperreana* (roots, twigs) *A. elliptifolia* (stems) *A. odorata* (leaves , twigs, flowers, root bark)	Nugroho *et al*., 1997a; Hiort *et al*., 1999; Wu *et al*., 1997; Ishibashi *et al*., 1993; Janprasert *et al*., 1993; Engelmeier *et al*., 2000; Baumann *et al*., 2002
Rocaglaol (Ferrugin) **(29)**	*A. crassinervia* (leaves) *A. dasyclada* (leaves) *A. ferruginea* (syn. *A. tomentosa*) (bark) *A. forbesii* (bark) *A. odorata* (leaves, root bark) *A. spectabilis* (bark)	Su *et al*., 2006; Chaidir *et al*., 2001; Dean *et al*., 1993; Mulhollane and Naidoo, 1998; Mohamad *et al*., 1999; Dumontet *et al*., 1996; Ishibashi *et al*., 1993; Ohse *et al*., 1996; Engelmeier *et al*., 2000
Rocagloic acid **(30)**	*A. dasyclada* (leaves) *A. rubiginosa* (twigs)	Chaidir *et al*., 2001; Rivero-Cruz *et al*., 2004

Table 1. Chemical constituents of plants in the genus *Aglaia* (continued)

Chemical type / Chemical compounds	Sources / Plant part	References
Episilvestrol **(31)**	*A. silvestris* (twigs)	Hwang *et al*., 2004
Silvestrol **(32)**	*A. silvestris* (twigs)	Hwang *et al*., 2004
C-3′-Rhamnosyl-rocaglamide **(33)**	*A. harmsiana* (leaves)	Nugroho *et al*., 1997b
N-tetrahydrofuran-didesmethylrocaglamide **(34,35)**	*A. elliptica* (fruits)	Nugroho *et al*., 1997b
C-3′-Hydroxymarikarin **(36)**	*A. gracilis* (roots & stem bark)	Greger *et al*., 2001
C-3′-Hydroxypyrimidone **(37)**	*A. duperreana* (flowers) *A. testicularis* (leaves)	Chaidir *et al*., 1999; Wang *et al*., 2004
Marikarin **(38)**	*A. gracilis* (roots & stem bark)	Greger *et al*., 2001
Pyrimidone **(39)**	*A. duperreana* (roots , twigs, flowers) *A. odorata* (leaves) *A. testicularis* (leaves)	Nugroho *et al*., 1997a; Chaidir *et al*., 1999; Hiort *et al*., 1999; Ohse *et al*., 1996; Wang *et al*., 2004
Aglaiastatin (Aglaroxin D) **(40)**	*A. duperreana* (roots, twigs) *A. odorata* (leaves)	Nugroho *et al*., 1997a; Hiort *et al*., 1999; Ohse *et al*., 1996
C-1-O-Acetyl-4′-demethoxy-3′-4′-methylenedioxymethylrocaglate **(41)**	*A. dasyclada* (leaves) *A. spectabilis* (bark)	Lin *et al*., 2001; Schneider *et al*., 2000

Table 1. Chemical constituents of plants in the genus *Aglaia* (continued)

Chemical type / Chemical compounds	Sources / Plant part	References
C-4′-Demethoxy-3′,4′-methylenedioxyrocaglaol **(42)**	*A. dasyclada* (leaves) *A. elliptica* (stem & fruits) *A. spectabilis* (bark)	Chaidir *et al*., 2001; Cui *et al*., 1997; Lee *et al*., 1998; Schneider *et al*., 2000
C-4′-Demethoxy-3′,4′-methylenedioxymethylrocaglate **(43)**	*A. dasyclada* (leaves) *A. elliptica* (stem & fruits) *A. spectabilis* (bark)	Chaidir *et al*., 2001; Cui *et al*., 1997; Lee *et al*., 1998; Schneider *et al*., 2000
C-1-O-Formyl-4′-demethoxy-3′,4′-methylenedioxymethylrocaglate **(44)**	*A. elliptica* (stem & fruits) *A. dasyclada* (leaves)	Chaidir *et al*., 2001; Cui *et al*., 1997; Lee *et al*., 1998
C-1-Oxo-4′-demethoxy-3′,4′-methylenedioxyrocaglaol **(45)**	*A. dasyclada* (leaves) *A. elliptica* (stem & fruits) *A. spectabilis* (bark)	Chaidir *et al*., 2001; Cui *et al*., 1997; Lee *et al*., 1998; Schneider *et al*., 2000
Aglaroxin A **(46)**	*A. edulis* (root bark , roots) *A. oligophylla* (twigs)	Engelmeier *et al*., 2000; Bacher *et al*., 1999; Dreyer *et al*., 2001
Aglaroxin B **(47)**	*A. oligophylla* (twigs) & *A. roxburghiana* (syn. *A. elaeagnoidea*) (stem bark)	Dreyer *et al*., 2001
Aglaroxin F **(48)**	*A. oligophylla* (twigs)	Bringmann *et al*., 2003

Table 1. Chemical constituents of plants in the genus *Aglaia* (continued)

Chemical type / Chemical compounds	Sources / Plant part	References
C-3′-Methoxypannellin **(49)**	*A. elaeagnoidea* (bark)	Brader *et al*., 1998
Pannellin **(50)**	*A. edulis* (root bark , roots) *A. elaeagnoidea* (bark)	Bacher *et al*., 1999; Engelmeier *et al*., 2000; Brader *et al*., 1998
Pannellin-1-O-acetate **(51)**	*A. elaeagnoidea* (bark) *A. oligophylla* (twigs)	Brader *et al*., 1998; Dreyer *et al*., 2001
Cyclorocaglamide **(52)**	*A. oligophylla* (twigs)	Bringmann *et al*., 2003
C-1-Oxo,C-2-piriferineaglaroxin A **(53)**	*A. oligophylla* (twigs)	Dreyer *et al*., 2001
Cyclopenta[*bc*]benzopyran-type Aglaxiflorin D **(54)**	*A. testicularis* (syn. *A. edulis*) (leaves)	Wang *et al*., 2004
C-19,C-3′-Dihydroxyaglain C **(55)**	*A. odorata* (twigs & leaves)	Nugroho *et al*., 1999
C-3 ′-Hydroxyaglain C **(56,57)**	*A. odorata* (twigs & leaves)	Nugroho *et al*., 1999
C-19-Hydroxy,C-3′-methoxyaglain C **(58)**	*A. odorata* (twigs & leaves)	Nugroho *et al*., 1999
C-10-O-Acetylaglain B **(59)**	*A. ponapensis* (leaves & twigs)	Salim *et al*., 2007
Aglain A **(60)**	*A. argentea* (leaves) & *A. forbesii* (bark)	Dumontet *et al*., 1996
Aglain B **(61)**	*A. argentea* (leaves)	Dumontet *et al*., 1996
Aglain C **(62)**	*A. argentea* (leaves)	Dumontet *et al*., 1996

Table 1. Chemical constituents of plants in the genus *Aglaia* (continued)

Chemical type / Chemical compounds	Sources / Plant part	References
Desacetylaglain A **(63)**	*A. gracilis* (roots)	Greger *et al*., 2001
4-Epi-aglain A **(64)**	*A. ponapensis* (leaves & twigs)	Salim *et al*., 2007
Aglain-O-glycoside **(65)**	*A. dasyclada* (leaves)	Chaidir *et al*., 2001
Grandiamide **(66)**	*A. grandis* (leaves)	Inada *et al*., 1997a
Ponapensin **(67)**	*A. ponapensis* (leaves & twigs)	Salim *et al*., 2007
Pyramidaglain A **(68)**	*A. andamanica* (leaves)	Puripattanavong *et al*., 2000
Pyramidaglain B **(69)**	*A. andamanica* (leaves)	Puripattanavong *et al*., 2000
Homothapsakin A **(70)**	*A. edulis* (roots) *A. oligophylla* (twigs)	Bacher *et al*., 1999; Dreyer *et al*., 2001
Isothapsakin B **(71)**	*A. edulis* (roots)	Bacher *et al*., 1999
Thapsakin A acetate **(72)**	*A. edulis* (roots, root bark)	Bacher *et al*., 1999; Engelmeier *et al*., 2000
Thapsakin B **(73)**	*A. edulis* (roots)	Bacher *et al*., 1999
Thapsakon A **(74)**	*A. edulis* (roots)	Bacher *et al*., 1999
Thapsakon B **(75)**	*A. edulis* (roots)	Bacher *et al*., 1999
Aglaforbesin-O-glycoside **(76)**	*A. dasyclada* (leaves)	Chaidir *et al*., 2001
Aglaforbesins A **(77)**	*A. argentea* (leaves) & *A. forbesii* (bark)	Dumontet *et al*., 1996

Table 1. Chemical constituents of plants in the genus *Aglaia* (continued)

Chemical type / Chemical compounds	Sources / Plant part	References
Aglaforbesins B **(78)**	*A. argentea* (leaves) & *A. forbesii* (bark)	Dumontet *et al*., 1996
C-8-Demethoxy-C7,C8-methylenedioxy-aglaforbesin **(79)**	*A. oligophylla* (twigs)	Bringmann *et al*., 2003
Benzo[*b*]oxepine-type Homothapoxepine A **(80)**	*A. edulis* (roots, bark)	Bacher *et al*., 1999; Engelmeier *et al*., 2000
Thapoxepine A **(81)**	*A. edulis* (roots, bark)	Bacher *et al*., 1999; Engelmeier *et al*., 2000
Thapoxepine B **(82)**	*A. edulis* (roots, bark)	Bacher *et al*., 1999; Engelmeier *et al*., 2000
Edulisones A **(83)**	*A. edulis* (bark)	Kim *et al*., 2005
Edulisones B **(84)**	*A. edulis* (bark)	Kim *et al*., 2005
Forbaglins A **(85)**	*A. forbesii* (bark)	Dumontet *et al*., 1996
Forbaglins B **(86)**	*A. forbesii* (bark)	Dumontet *et al*., 1996
Forbaglin-O-glycoside **(87)**	*A. dasyclada* (leaves)	Chaidir *et al*., 2001
Bisamides Pyrrolidine-type Dehydroodorine **(88)**	*A. formosana* (leaves) *A. tomentosa* (leaves)	Duh *et al*., 1993; Brader *et al*., 1998

Table 1. Chemical constituents of plants in the genus *Aglaia* (continued)

Chemical type / Chemical compounds	Sources / Plant part	References
2′-Epiodorine (2′-Epiroxburghilin) **(89)**	*A. roxburghiana* (leaves)	Purushothaman and Sarada, 1979
Odorine (Roxburghilin) **(90)**	*A. argentea* (bark) *A. elaeagnoidea* (leaves) *A. gracilis* (leaves) *A. harmsiana* (leaves) *A. odorata* (leaves) *A. roxburghiana* (leaves)	Dumontet *et al*., 1996; Brader *et al*., 1998; Greger *et al*., 2001; Inada *et al*., 1995; Shiengthong and Ungphakorn, 1979; Inada *et al*., 2001; Purushothaman and Sarada, 1979
Odorinol **(91)**	*A. elaeagnoidea* (leaves) *A. odorata* (leaves) *A. testicularis* (syn. *A. edulis*) (leaves)	Brader *et al*., 1998; Shiengthong and Ungphakorn, 1979; Inada *et al*., 2001; Hayashi *et al*., 1982; Wang *et al*., 2004
Piriferine **(92)**	*A. elaeagnoidea* (leaves) *A. gracilis* (leaves) *A. testicularis* (syn. *A. edulis*) (leaves)	Brader *et al*., 1998; Greger *et al*., 2001; Wang *et al*., 2004
Piriferinol **(93)**	*A. elaeagnoidea* (leaves)	Brader *et al*., 1998
Agleptin **(94)**	*A. edulis* (leaves)	Brader *et al*., 1998
Isoagleptin **(95)**	*A. leptantha* (stem bark & leaves)	Greger *et al*., 2000

Table 1. Chemical constituents of plants in the genus *Aglaia* (continued)

Chemical type / Chemical compounds	Sources / Plant part	References
Leptanthin **(96)**	*A. leptantha* (stem bark & leaves)	Greger *et al*., 2000
Putrescine-type Agladuline **(97)**	*A. edulis* (leaves) *A. leptantha* (stem bark & leaves)	Saifah *et al*., 1999; Greger *et al*., 2000
Aglairubine **(98)**	*A. australiensis* (leaves), *A. meridionalis* (leaves) & *A. spectabilis* (leaves)	Seger *et al*., 2002
Dasyclamide **(99)**	*A. dasyclada* (leaves)	Lin *et al*., 2001
Edulimide **(100)**	*A. edulis* (leaves)	Brader *et al*., 1998
Grandiamides B **(101)**	*A. leptantha* (stem bark & leaves)	Greger *et al*., 2000
Grandiamides C **(102)**	*A. leptantha* (stem bark & leaves)	Greger *et al*., 2000
Pyramidatine **(103)**	*A. grandis* (leaves) & *A. silvestris* (*A. pyramidata*) *A. gracilis* (leaves)	Brader *et al*., 1998; Greger *et al*., 2001
Secopiriferine **(104)**	*A. gracilis* (leaves)	Greger *et al*., 2001
Secoodorine **(105)**	*A. gracilis* (leaves)	Greger *et al*., 2001
Aglaidithioduline **(106)**	*A. edulis* (leaves)	Saifah *et al*., 1999
Aglaithioduline **(107)**	*A. leptantha* (stem bark & leaves)	Greger *et al*., 2000

Table 1. Chemical constituents of plants in the genus *Aglaia* (continued)

Chemical type / Chemical compounds	Sources / Plant part	References
Aglaithioduline **(107)**	*A. edulis* (leaves)	Saifah *et al*., 1999
Triterpenoids Dammarane-type Aglinins A **(108)**	*A. lawii* (leaves)	Mohamad *et al*., 1999
Aglinins B **(109)**	*A. lawii* (leaves)	Mohamad *et al*., 1999
Dammarenolic acid **(110)**	*A. rubiginosa* (twigs)	Rivero-Cruz *et al*., 2004
Eichlerianic acid **(111)**	*A. elliptica* (stems) *A. foveolata* (bark) *A. lawii* (bark)	Cui *et al*., 1997; Roux *et al*., 1998; Mohamad *et al*., 1999
Shoreic acid **(112)**	*A. elliptica* (stems) *A. foveolata* (bark) *A. gracilis* (leaves) *A. rubiginosa* (twigs)	Cui *et al*., 1997; Roux *et al*., 1998; Greger *et al*., 2001; Rivero-Cruz *et al*., 2004
Foveolin A **(113)**	*A. foveolata* (bark) *A. lawii* (leaves)	Roux *et al*., 1998; Mohamad *et al*., 1999
Foveolin B **(114)**	*A. foveolata* (bark)	Roux *et al*., 1998

Table 1. Chemical constituents of plants in the genus *Aglaia* (continued)

Chemical type / Chemical compounds	Sources / Plant part	References
(20*S*,23*E*)-20,25-Dihydroxy-3,4-secodammara-4(28),23-dienoic acid **(115)**	*A. rubiginosa* (twigs)	Rivero-Cruz *et al*., 2004
(20*S*,23*E*)-20,25-Dihydroxy-3,4-secodammara-4(28),23-dienoic acid methyl ester **(116)**	*A. rubiginosa* (twigs)	Rivero-Cruz *et al*., 2004
Aglinins C **(117)**	*A. lawii* (leaves)	Mohamad *et al*., 1999
Aglinins D **(118)**	*A. lawii* (leaves)	Mohamad *et al*., 1999
Cabraleadiol **(119)**	*A. crassinervia* (bark)	Su *et al*., 2006
Cabraleadiol-3-acetate **(120)**	*A. tomentosa* (bark)	Mohamad *et al*., 1999
3-Epiocotillol **(121)**	*A. crassinervia* (bark) *A. foveolata* (bark)	Su *et al*., 2006; Roux *et al*., 1998
Ocotillol II **(122)**	*A. elliptica* (stems)	Cui *et al*., 1997
Ocotillone **(123)**	*A. rubiginosa* (twigs) *A.silvestris* (fruits & twigs)	Rivero-Cruz *et al*., 2004 Hwang *et al*., 2004
20*S*,24*S*-Epoxy-25-hydroxydammaran-3-one (Cabraleone) **(124)**	*A. elaeagnoidea* (bark) *A. lawii* (leaves) & *A. tomentosa* (bark) *A. rubiginosa* (twigs)	Fuzzati *et al*., 1996; Mohamad *et al*., 1999; Rivero-Cruz *et al*., 2004

Table 1. Chemical constituents of plants in the genus *Aglaia* (continued)

Chemical type / Chemical compounds	Sources / Plant part	References
20*S*,24*S*-Epoxy-25-hydroxymethyldammaran-3-one **(125)**	*A. elaeagnoidea* (bark)	Fuzzati *et al*., 1996
Cabralealactone **(126)**	*A. lawii* (leaves) & *A. tomentosa* (bark)	Mohamad *et al*., 1999
Cabralealactone-3-acetate **(127)**	*A. tomentosa* (bark)	Mohamad *et al*., 1999
Cabraleahydroxylactone **(128)**	*A. crassinervia* (bark)	Su *et al*., 2006
3-Epicabraleahydroxylactone **(129)**	*A. crassinervia* (bark)	Su *et al*., 2006
Cycloartane-type Argenteanol **(130)**	*A. argentea* (leaves)	Omobuwajo *et al*., 1996
Argenteanone B **(131)**	*A. argentea* (leaves)	Omobuwajo *et al*., 1996
Argenteanone C **(132)**	*A. argentea* (leaves)	Mohamad *et al*., 1997
Argenteanol B **(133)**	*A. argentea* (leaves)	Mohamad *et al*., 1997
Argenteanol C **(134)**	*A. argentea* (leaves)	Mohamad *et al*., 1997
Argenteanol D **(135)**	*A. argentea* (leaves)	Mohamad *et al*., 1997
Argenteanol E **(136)**	*A. argentea* (leaves)	Mohamad *et al*., 1997
24-Hydroperoxycycloart-25-en-3β-ol **(137)**	*A. grandis* (leaves)	Inada *et al*., 1997a
28,29-Bis-norcycloarten-3β,6α-diol **(138)**	*A. elaeagnoidea* (leaves)	Brader *et al*., 1998

Table 1. Chemical constituents of plants in the genus *Aglaia* (continued)

Chemical type / Chemical compounds	Sources / Plant part	References
28,29-Bis-norcycloarten-3β,4α,6α-triol **(139)**	*A. elaeagnoidea* (leaves)	Brader *et al*., 1998
3β-Hydroxy-28,29-bis-norcycloarten-6-one **(140)**	*A. elaeagnoidea* (leaves)	Brader *et al*., 1998
Cycloartane-3β,29-diol-24-one **(141)**	*A. grandis* (leaves)	Inada *et al*., 1997a
(24*R*)-Cycloartane-24,25-diol-3-one **(142)**	*A. harmsiana* (leaves)	Inada *et al*., 1995
(24*R*)-Cycloartane-3β,24,25-triol **(143)**	*A. harmsiana* (leaves)	Inada *et al*., 1997b
(24*R*)-Cycloartane-3α,24,25-triol **(144)**	*A. harmsiana* (leaves)	Inada *et al*., 1997b
(24*R*)-Cycloartane-3β,24,25,28-tetrol **(145)**	*A. harmsiana* (leaves)	Inada *et al*., 1997b
Cycloartenol **(146)**	*A. harmsiana* (leaves)	Inada *et al*., 1997b
Cycloart-23*E*-ene-3β,25-diol **(147)**	*A. andamanica* (leaves)	Puripattanavong *et al*., 2000
25-Hydroperoxycycloart-23-en-3β-ol **(148)**	*A. grandis* (leaves)	Inada *et al*., 1997a
24S,25-Epoxycycloartanol **(149)**	*A. lawii* (bark)	Mohamad *et al*., 1999
3β-Hydroxy-24-methylene-28,29-bis-norcycloarten-6-one **(150)**	*A. elaeagnoidea* (leaves)	Brader *et al*., 1998
24-Methylene-28,29-bis-norcycloarten-3β,4α,6α-triol **(151)**	*A. elaeagnoidea* (leaves)	Brader *et al*., 1998

Table 1. Chemical constituents of plants in the genus *Aglaia* (continued)

Chemical type / Chemical compounds	Sources / Plant part	References
Roxburghiadiol A **(152)**	*A. elaeagnoidea* (syn. *A. roxburghiana*) (leaves, fruits & stem)	Brader *et al*., 1998; Janaki *et al*., 1999
Roxburghiadiol B **(153)**	*A. elaeagnoidea* (leaves) *A. roxburghiana* var. *beddomei* (syn. *A. elaeagnoidea*) (fruits & stem)	Brader *et al*., 1998; Janaki *et al*., 1999
Argenteanone A **(154)**	*A. argentea* (leaves)	Omobuwajo *et al*., 1996
Argenteanone D **(155)**	*A. argentea* (leaves)	Mohamad *et al*., 1997
Argenteanone E **(156)**	*A. argentea* (leaves)	Mohamad *et al*., 1997
Tirucallane-type Leucophyllone **(157)**	*A. leucophylla* (stem bark)	Benosman *et al*., 1995
24-Epi-piscidinol A **(158)**	*A. andamanica* (leaves)	Puripattanavong *et al*., 2000
Piscidinol A **(159)**	*A. leucophylla* (stem bark)	Benosman *et al*., 1995
Glabretal-type Aglaiaglabretol A **(160)**	*A. crassinervia* (bark)	Su *et al*., 2006
Aglaiaglabretol B **(161)**	*A. crassinervia* (bark)	Su *et al*., 2006

Table 1. Chemical constituents of plants in the genus *Aglaia* (continued)

Chemical type / Chemical compounds	Sources / Plant part	References
Aglaiaglabretol C **(162)**	*A. crassinervia* (bark)	Su *et al*., 2006
7-Deacetylglabretal-3-acetate **(163)**	*A. ferruginaea* (syn. *A. tomentosa*) (wood)	Mulhollane and Monkne, 1993
7-Deacetylglabretal-3-tiglate **(164)**	*A. ferruginaea* (syn. *A. tomentosa*) (wood)	Mulhollane and Monkne, 1993
Baccharane-type 17,24-Epoxy-25-hydroxybaccharan-3-one **(165)**	*A. silvestris* (fruits & twigs)	Hwang *et al*., 2004
3-Monomethyl ester leucophyllic acid **(166)**	*A. silvestris* (fruits & twigs)	Hwang *et al*., 2004
Steroids Pregnane-type Aglatonins A **(167)**	*A. tomentosa* (bark)	Mohamad *et al*., 1999
2β,3β-Dihydroxy-5α-prenane-16-one **(168)**	*A. grandis* (leaves)	Inada *et al*., 1997a
Aglatonins B **(169)**	*A. tomentosa* (bark)	Mohamad *et al*., 1999
2β,3β-Dihydroxy-5α-pren-17(20)-(*Z*)-en-16-one **(170)**	*A. grandis* (leaves)	Inada *et al*., 1997a
2β,3β-Dihydroxy-5α-pren-17(20)-(*E*)-en-16-one **(171)**	*A. crassinervia* (bark) *A. grandis* (leaves)	Su *et al*., 2006; Inada *et al*., 1997a
(*E*)-Volkendousin **(172)**	*A. crassinervia* (bark)	Su *et al*., 2006

Table 1. Chemical constituents of plants in the genus *Aglaia* (continued)

Chemical type / Chemical compounds	Sources / Plant part	References
(*Z*)-Volkendousin **(173)**	*A. crassinervia* (bark)	Su *et al*., 2006
Cholestane-type (3*S*,4*R*,24*R*)-Cholest-7,24-diene-3,4,22-triol **(174)**	*A. rubiginosa* (leaves)	Rivero-Cruz *et al*., 2004
Ergostane-type (3β,4β,22*R*)-Ergosta-5,24(24')-dien-3,4,22-triol **(175)**	*A. rubiginosa* (leaves)	Rivero-Cruz *et al*., 2004
Stigmastane-type β-Sitosterol **(176)**	*A. andamanica* (leaves) *A. rubiginosa* (leaves)	Puripattanavong *et al*., 2000; Rivero-Cruz *et al*., 2004
Stigmasterol **(177)**	*A. crassinervia* (bark)	Su *et al*., 2006
Sesquiterpenoids 9,10-Dihydroxy-4,7-megastigmadien-3-one **(178)**	*A. gracilis* (leaves)	Greger *et al*., 2001
4β,10α-Dihydroxyaromadendrane **(179)**	*A. grandis* (leaves)	Inada *et al*., 2000
(-)-Ledol **(180)**	*A. foveolata* (leaves)	Roux *et al*., 1998
Spathulenol **(181)**	*A. foveolata* (leaves) *A. lawii* (bark)	Roux *et al*., 1998
(+)-T-Cadinol **(182)**	*A. foveolata* (leaves)	Roux *et al*., 1998

Table 1. Chemical constituents of plants in the genus *Aglaia* (continued)

Chemical type / Chemical compounds	Sources / Plant part	References
1β,4β-Dihydroxy-6α,15-epoxyeudesmane **(183)**	*A. silvestris* (fruits & twigs)	Hwang *et al*., 2004
1β,6β-Dihydroxy-4 (15)-eudesmene **(184)**	*A. silvestris* (fruits & twigs)	Hwang *et al*., 2004
Lignans Aglacins E **(185)**	*A. cordata* (stem bark)	Wang *et al*., 2002
Aglacins F **(186)**	*A. cordata* (stem bark)	Wang *et al*., 2002
Aglacins G **(187)**	*A. cordata* (stem bark)	Wang *et al*., 2002
Aglacins H **(188)**	*A. cordata* (stem bark)	Wang *et al*., 2002
trans-2,3-Bis (3,4,5-trimethoxybenzyl)-1,4-butanediol diacetate **(189)**	*A. elaeagnoidea* (bark)	Fuzzati *et al*., 1996
trans-3,4-Bis (3,4,5-trimethoxybenzyl)-tetrahydrofuran **(190)**	*A. elaeagnoidea* (bark)	Fuzzati *et al*., 1996
Secoisolariciresinol dimethyl ether **(191)**	*A. testicularis* (syn. *A. edulis*) (leaves)	Wang *et al*., 2004
Epigrandisin **(192)**	*A. leptantha* (stem bark & leaves)	Greger *et al*., 2000
Grandisin **(193)**	*A. leptantha* (stem bark & leaves)	Greger *et al*., 2000

Table 1. Chemical constituents of plants in the genus *Aglaia* (continued)

Chemical type / Chemical compounds	Sources / Plant part	References
Lariciresinol-3-acetate **(194)**	*A. elaeagnoidea* (leaves)	Brader *et al*., 1998
Methylarctigenin **(195)**	*A. tomentosa* (leaves)	Brader *et al*., 1998
Syringaresinol **(196)**	*A. odorata* (leaves)	Nugroho *et al*., 1999
Yangambin **(197)**	*A. andamanica* (leaves) *A. grandis* (leaves) *A. leptantha* (stem bark & leaves)	Puripattanavong *et al*., 2000; Brader *et al*., 1998; Greger *et al*., 2000
Flavonoids 3,3′-Dihydroxy-5,7,4′-trimethoxyflavone **(198)**	*A. odorata* (twigs & leaves)	Nugroho *et al*., 1999
3-Hydroxy-5,7,4′-trimethoxyflavone **(199)**	*A. gracilis* (leaves)	Greger *et al*., 2001
3′-Hydroxy-5,7,4′-trimethoxyflavone **(200)**	*A. odorata* (twigs & leaves)	Nugroho *et al*., 1999
3,5,7,3′,4′- pentamethoxyflavone **(201)**	*A. odorata* (twigs & leaves)	Nugroho *et al*., 1999
5-Hydroxy-3,7,4′-trimethoxyflavone **(202)**	*A.andamanica* (leaves) *A. rubiginosa* (twigs)	Puripattanavong *et al*., 2000; Rivero-Cruz *et al*., 2004
Pachypodol **(203)**	*A.andamanica* (leaves) *A. rubiginosa* (twigs)	Puripattanavong *et al*., 2000; Rivero-Cruz *et al*., 2004

Table 1. Chemical constituents of plants in the genus *Aglaia* (continued)

Chemical type / Chemical compounds	Sources / Plant part	References
Rutusin **(204)**	*A. andamanica* (leaves) *A. rubiginosa* (twigs)	Puripattanavong *et al*., 2000; Rivero-Cruz *et al*., 2004
Eryodicitiol **(205)**	*A. andamanica* (leaves) *A. rubiginosa* (twigs)	Puripattanavong *et al*., 2000; Rivero-Cruz *et al*., 2004
Naringenin **(206)**	*A. rubiginosa* (twigs)	Rivero-Cruz *et al*., 2004
Limonoids 6,11-Diacetoxygedunin **(207)**	*A. elaeagnoidea* (bark)	Fuzzati *et al*., 1996
24-Epi-melianodiol **(208)**	*A. andamanica* (leaves)	Puripattanavong *et al*., 2000
Melianodiol **(209)**	*A. andamanica* (leaves)	Puripattanavong *et al*., 2000
Aromatic butyrolactones Aglalactone **(210)**	*A. elaeagnoidea* (leaves)	Engelmeier *et al*., 2000
5,6-Desmetylenedioxy-5-methoxy-aglalactone **(211)**	*A. ponapensin* (twigs)	Salim *et al*., 2007

สถาบันวิทยบริการ
จุฬาลงกรณ์มหาวิทยาลัย

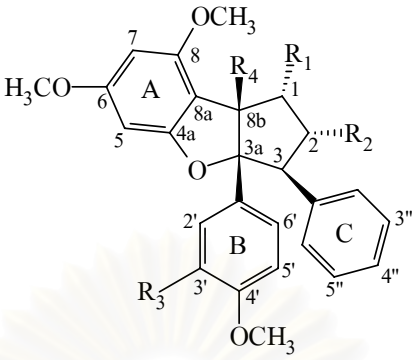

	R_1	R_2	R_3	R_4		R_1	R_2	R_3	R_4
1.	OAc	$CONH(CH_2)_4OH$	H	OH	**16.**	OCHO	$COOCH_3$	OH	OH
2.	OAc	$CONHCH_3$	H	OH	**17.**	OCHO	$CON(CH_3)_2$	H	OH
3.	OAc	$CONH_2$	H	OH	**18.**	OH	$CONHCH_3$	OH	OH
4.	OAc	$CONHCH_3$	OH	OH	**19.**	OH	$COOCH_3$	OH	OH
5.	OAc	$COOCH_3$	OH	OH	**20.**	OH	$CONH_2$	OH	OH
6.	OAc	$CON(CH_3)_2$	OH	OH	**21.**	OH	$CON(CH_3)_2$	OH	OH
7.	OAc	$COOCH_3$	H	OH	**22.**	OH	$CON(CH_3)_2$	OCH_3	OH
8.	OAc	$CON(CH_3)_2$	H	OH	**23.**	OH	$COOCH_3$	H	OCH_3
9.	OAc	H	H	OH	**24.**	OH	H	OCH_3	OH
10.	OH	$CONH(CH_2)_4OH$	H	OH	**25.**	OH	H	H	OCH_3
11.	H	$CONHCH_3$	H	OH	**26.**	OH	$COOCH_3$	H	OH
12.	OH	$CONH_2$	H	OH	**27.**	=NOH	$COOCH_3$	OCH_3	OH
13.	OH	$CONHCH_3$	OH	OEt	**28.**	H	$CON(CH_3)_2$	H	OH
14.	OH	$CON(CH_3)_2$	OH	OEt	**29.**	H	H	H	OH
15.	OH	H	H	OEt	**30.**	H	COOH	H	OH

Figure 3. Chemical constituents of plants in the genus *Aglaia*

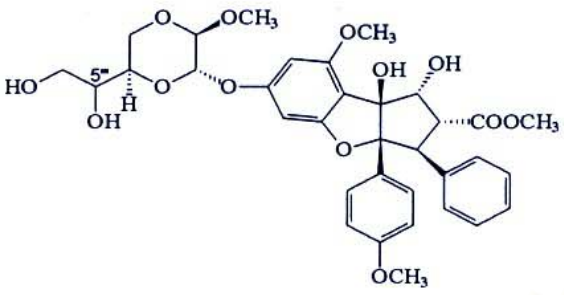

31. $5'''S$

32. $5'''R$

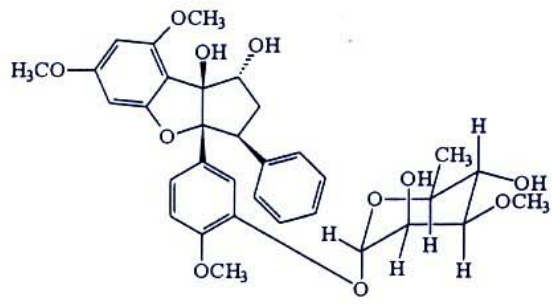

33.

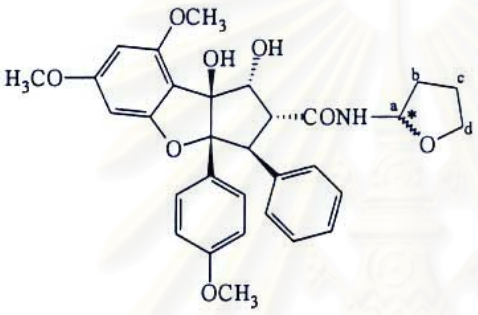

34,35

(*stereocentre)

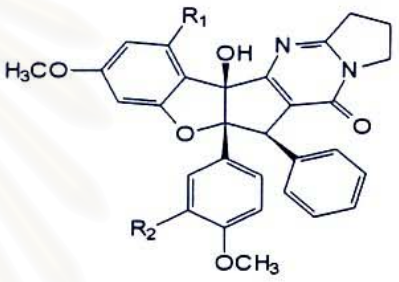

	R_1	R_2
36.	OH	OH
37.	OCH_3	OH
38.	OH	H
39.	OCH_3	H

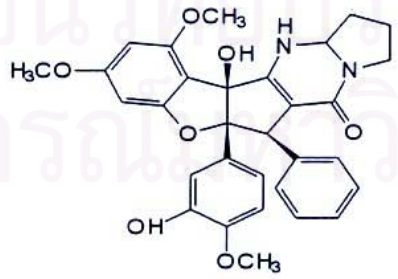

40

Figure 3. Chemical constituents of plants in the genus *Aglaia* (continued)

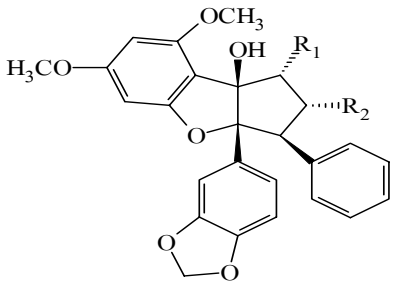

	R_1	R_2
41.	OAc	$COOCH_3$
42.	OH	$COOCH_3$
43.	OH	H
44.	OCHO	$COOCH_3$
45.	=O	H

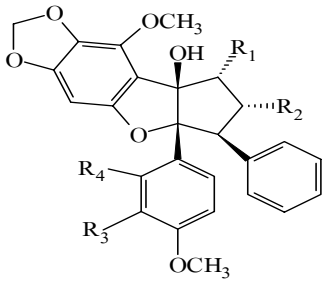

	R_1	R_2	R_3	R_4
46.	OH	$CON(CH_3)_2$	H	H
47.	OH	$CON(CH_3)_2$	OCH_3	H
48.	OH	$CON(CH_3)_2$	OCH_3	OH
49.	OAc	$COOCH_3$	H	H
50.	OH	$COOCH_3$	H	H
51.	OH	$CON(CH_3)_2$	OCH_3	H

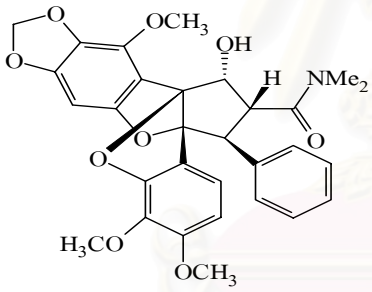

52

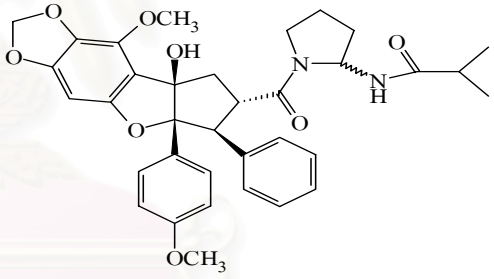

53

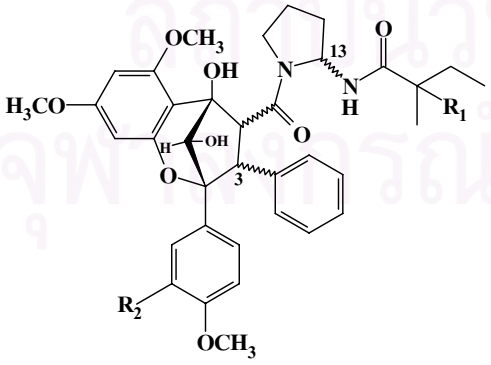

	R_1	R_2	
54.	OH	H	[H-3α, H-4β, 13*S*]
55.	OH	OH	[H-3α, H-4β, 13*S*]
56.	H	OH	[H-3α, H-4β, 13*S*]
57.	H	OH	[H-3β, H-4α, 13*S*]
58.	OH	OCH_3	[H-3α, H-4β, 13*S*]

Figure 3. Chemical constituents of plants in the genus *Aglaia* (continued)

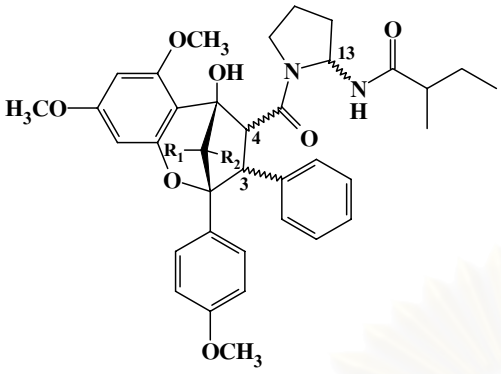

	R_1	R_2	
59.	H	OAc	[H-3β, H-4α, 13*S*]
60.	OAc	H	[H-3β, H-4α, 13*S*]
61.	H	OH	[H-3β, H-4α, 13*S*]
62.	H	OH	[H-3α, H-4β, 13*S*]
63.	OH	H	[H-3β, H-4α, 13*S*]
64.	OAc	H	[H-3β, H-4β, 13*S*]

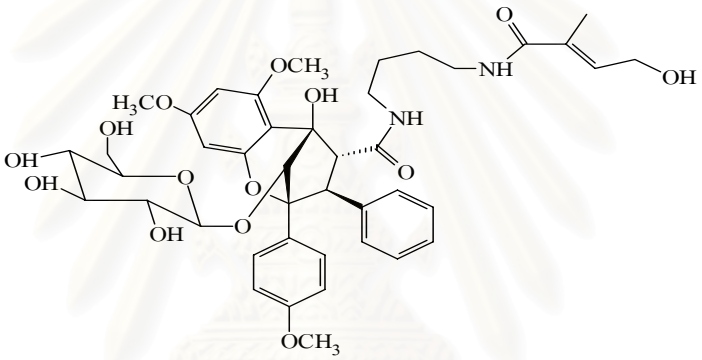

65

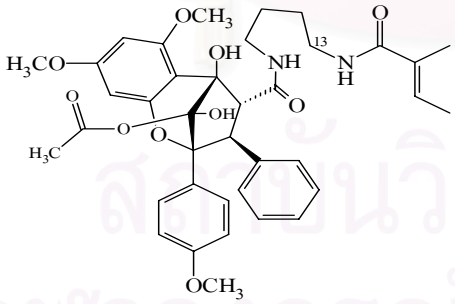

66

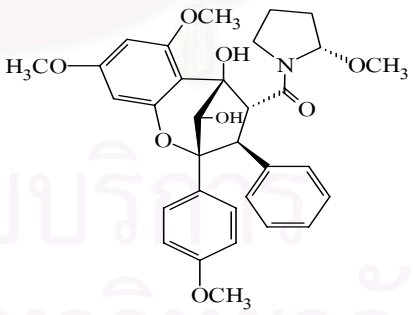

67

Figure 3. Chemical constituents of plants in the genus *Aglaia* (continued)

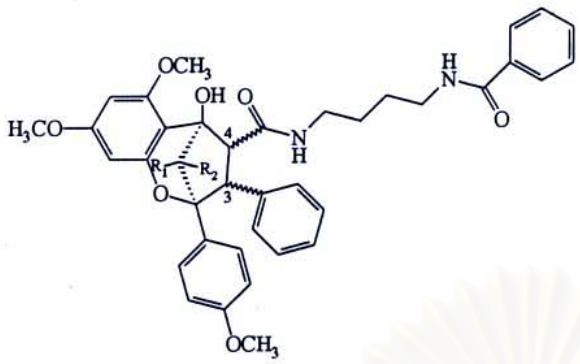

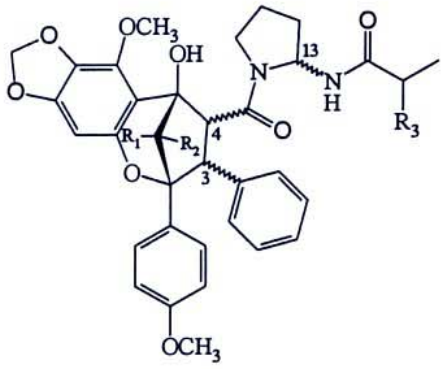

	R_1	R_2
68.	H	OAc (H-3β, H-4α)
69.	OAc	H (H-3α, H-4α)

	R_1	R_2	R_3
70.	H	OH	C_2H_5 [H-3α, H-4β, 13*S*]
71.	OH	H	CH_3 [H-3β, H-4α, 13*S*]
72.	H	OAc	CH_3 [H-3α, H-4β, 13*S*]
73.	H	OH	CH_3 [H-3β, H-4α, 13*RS*]
74.	=O		CH_3 [H-3α, H-4β, 13*S*]
75.	=O		CH_3 [H-3β, H-4α, 13*S*]

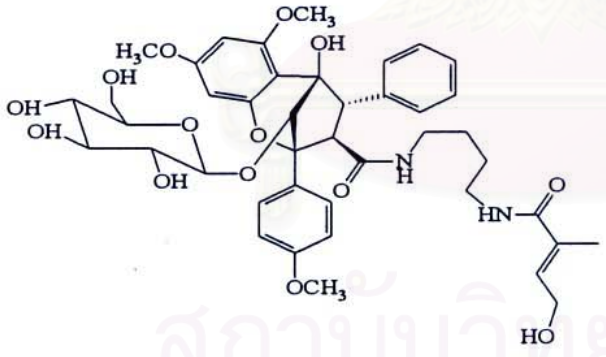

76

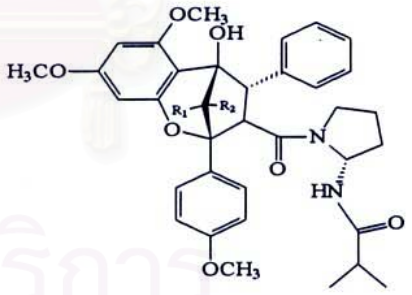

	R_1	R_2
77.	OH	H
78.	H	OH

Figure 3. Chemical constituents of plants in the genus *Aglaia* (continued)

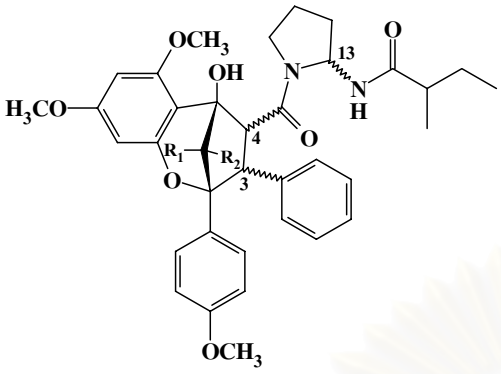

	R_1	R_2	
59.	H	OAc	[H-3β, H-4α, 13*S*]
60.	OAc	H	[H-3β, H-4α, 13*S*]
61.	H	OH	[H-3β, H-4α, 13*S*]
62.	H	OH	[H-3α, H-4β, 13*S*]
63.	OH	H	[H-3β, H-4α, 13*S*]
64.	OAc	H	[H-3β, H-4β, 13*S*]

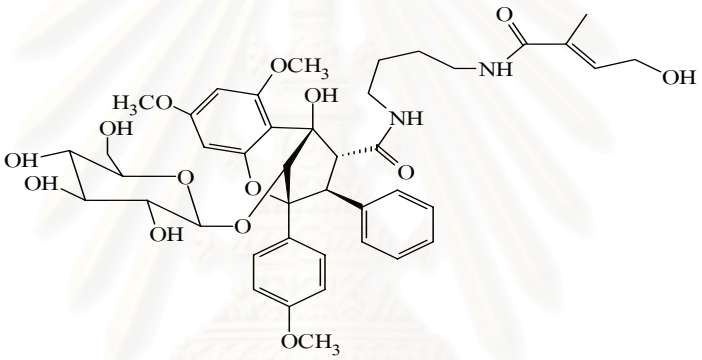

65

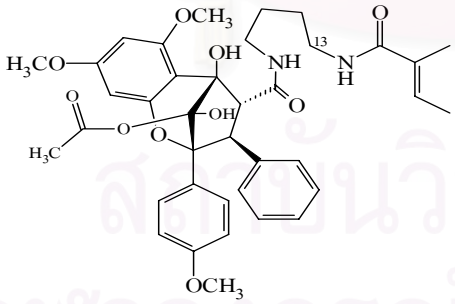

66

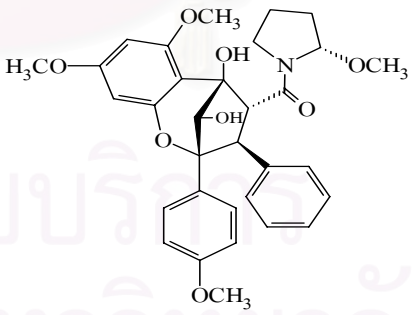

67

Figure 3. Chemical constituents of plants in the genus *Aglaia* (continued)

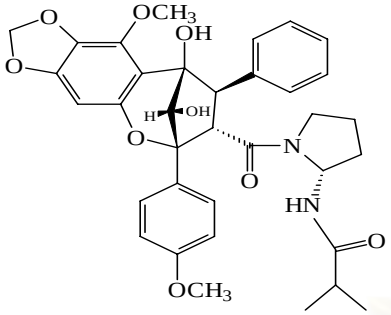

79

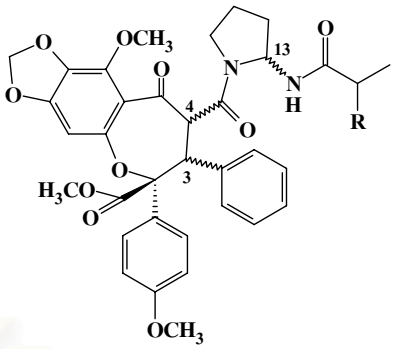

80. R = C_2H_5 [H-3α, H-4β, 13*S*]

81. R = CH_3 [H-3α, H-4β, 13*RS*]

82. R = CH_3 [H-3β, H-4α, 13*RS*]

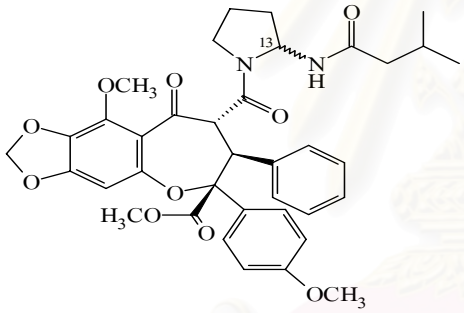

83. 13*R*

84. 13*S*

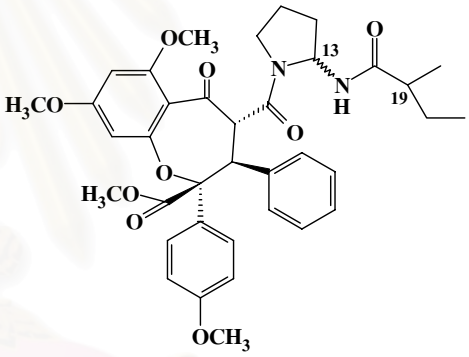

85. 13*R*, 19S

86. 13*S*

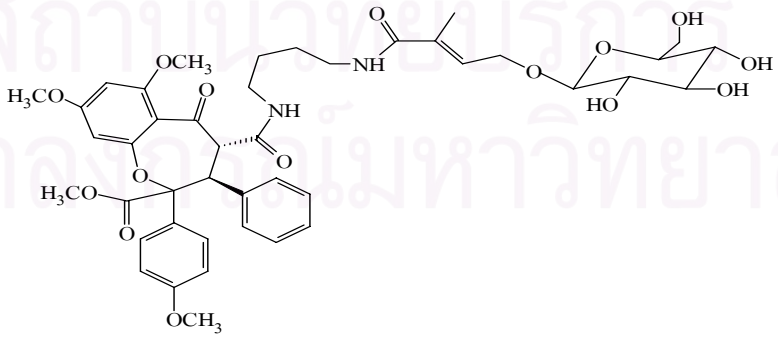

87

Figure 3. Chemical constituents of plants in the genus *Aglaia* (continued)

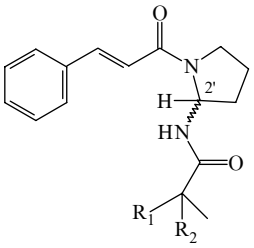

	R_1	R_2	
88.	$=C_2H_4$ (Z)		
89.	CH_2CH_3	H	(H-2′α)
90.	CH_2CH_3	H	(H-2′β)
91.	CH_2CH_3	OH	(H-2′β)
92.	CH_3	H	
93.	CH_3	OH	

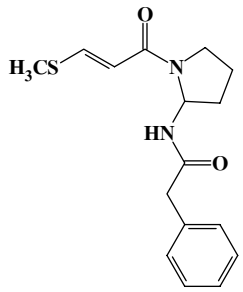

94

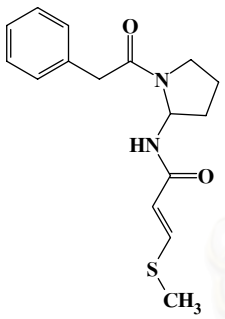

95

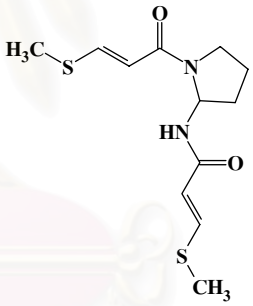

96

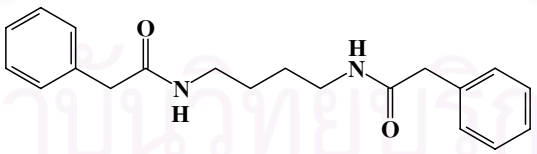

97

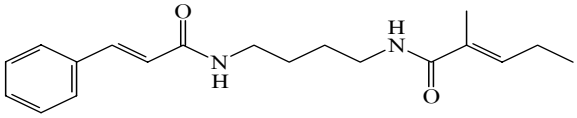

98

Figure 3. Chemical constituents of plants in the genus *Aglaia* (continued)

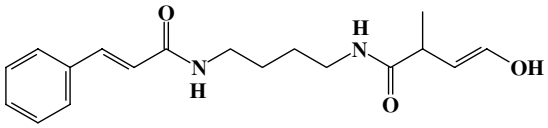

99

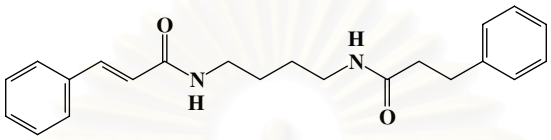

100

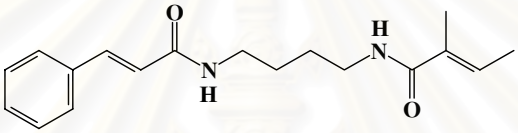

101

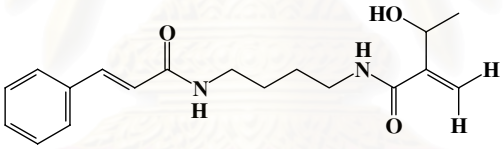

102

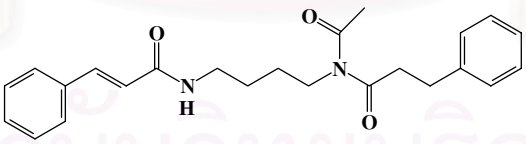

103

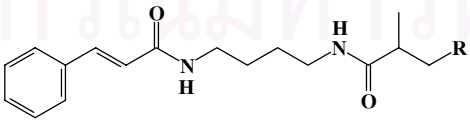

104. R = H

105. R = CH_3

Figure 3. Chemical constituents of plants in the genus *Aglaia* (continued)

สถาบันวิทยบริการ
จุฬาลงกรณ์มหาวิทยาลัย

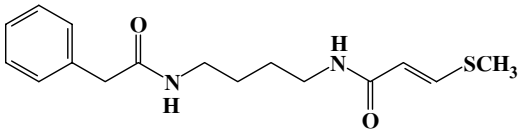

106

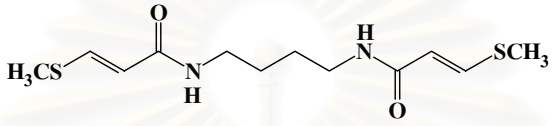

107

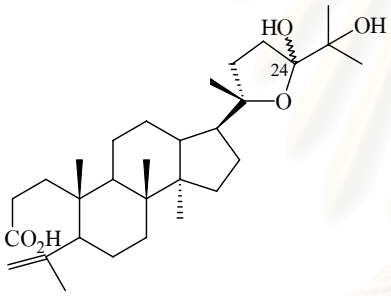

108. 24*RS*

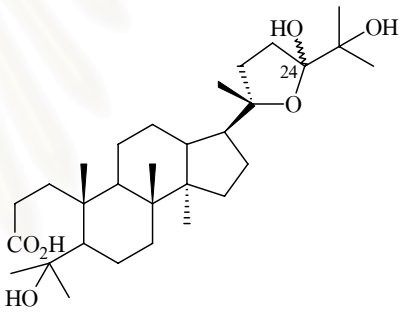

109. 24*RS*

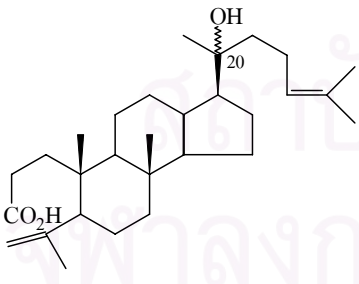

110

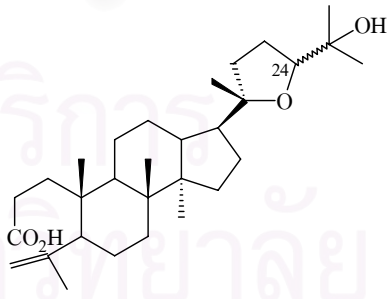

111. 24*R*

112. 24*S*

Figure 3. Chemical constituents of plants in the genus *Aglaia* (continued)

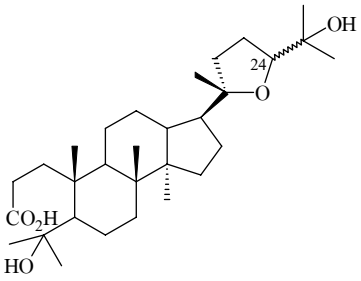

113. 24*S*

114. 24*R*

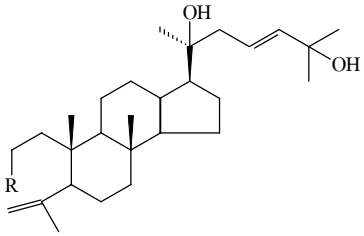

115. R = CO_2H

116. R = CO_2CH_3

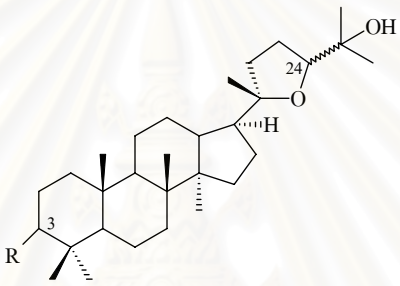

	R		R
117.	3α-OH (24*RS*)	**121.**	3α-OH (24*R*)
118.	=O (24*RS*)	**122.**	3β-OH (24*R*)
119.	3α-OH (24*S*)	**123.**	=O (24*R*)
120.	3α-OAc (24*S*)	**124.**	=O (24*S*)

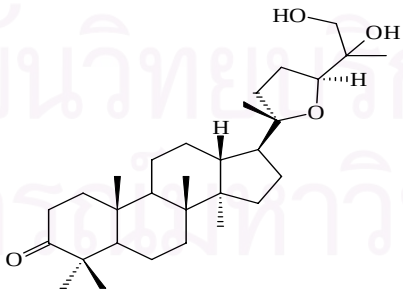

125

Figure 3. Chemical constituents of plants in the genus *Aglaia* (continued)

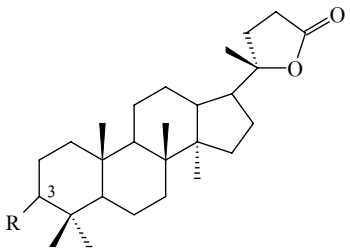

126. R = =O

127. R = α-OAc

128. R = α-OH

129. R = β-OH

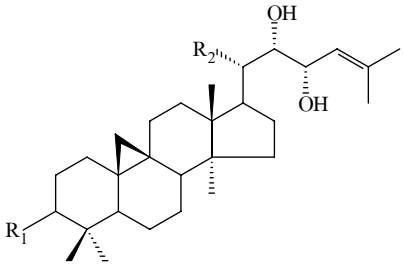

	R_1	R_2
130.	β-OH	CH_2OH
131.	=O	CH_2OH
132.	=O	CH_3
133.	β-OH	CH_3

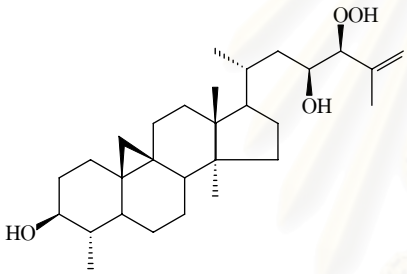

134

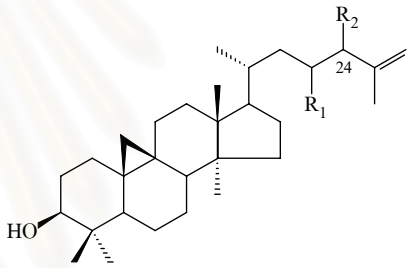

	R_1	R_2
135.	α-OH	α-OOH
136.	H	OOH (24*RS*)

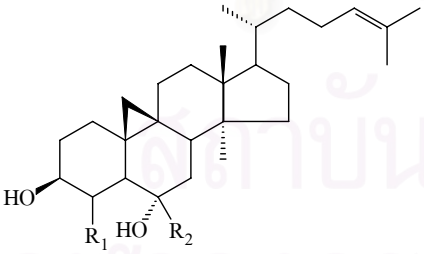

	R_1	R_2
137.	H	H
138.	α-OH	H
139.	H	β-OH

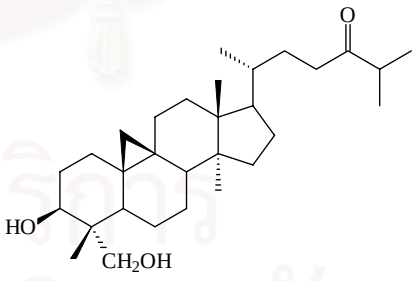

140

Figure 3. Chemical constituents of plants in the genus *Aglaia* (continued)

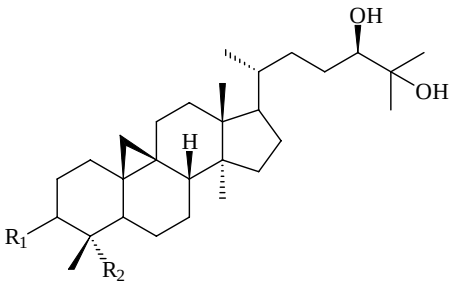

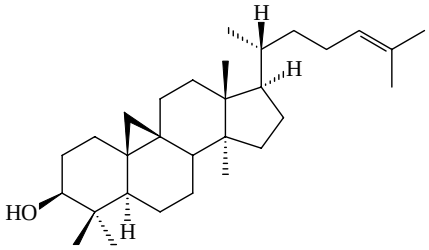

	R_1	R_2
141.	=O	CH_3
142.	β-OH	CH_3
143.	β-OH	CH_2OH
144.	α-OH	CH_3

145

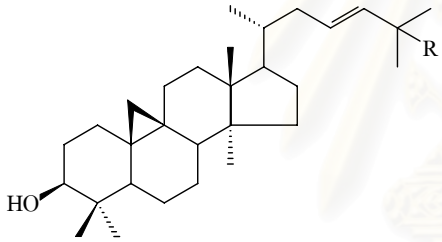

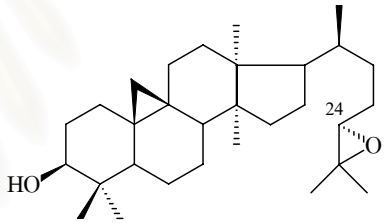

146. R = OH

147. R = OOH

148

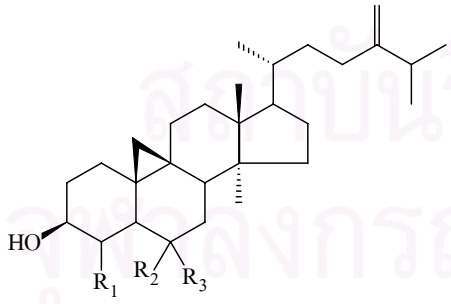

	R_1	R_2	R_3
149.	H	α-OH	β-OH
150.	α-OH	α-OH	H
151.	H	β-OH	H
152.	H	α-OH	H

Figure 3. Chemical constituents of plants in the genus *Aglaia* (continued)

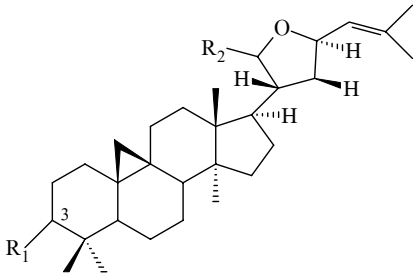

	R_1	R_2
153.	β-OH	β-OH
154.	=O	=O

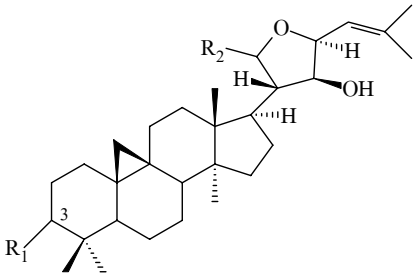

	R_1	R_2
155.	=O	β
156.	=O	OCH_2CH_3

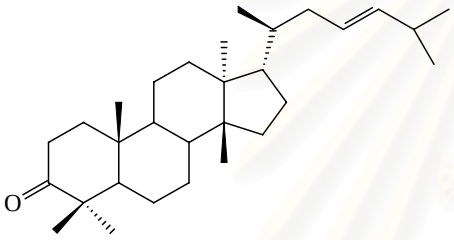

157

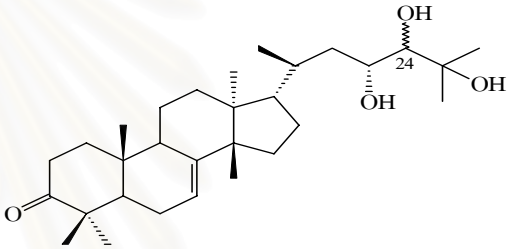

158. 24*R*

159. 24*S*

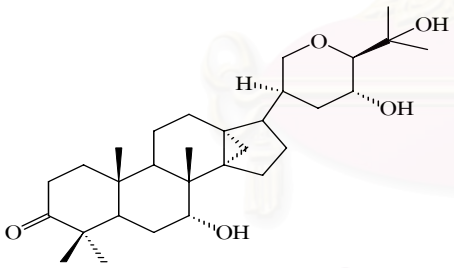

160

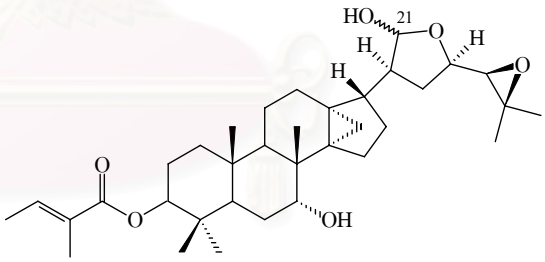

161. 21*RS*

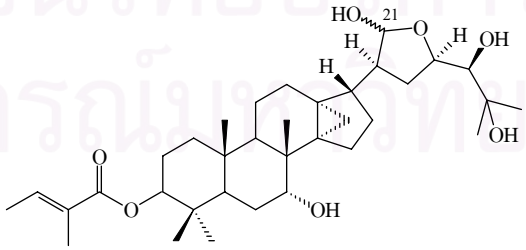

162. 21*RS*

Figure 3. Chemical constituents of plants in the genus *Aglaia* (continued)

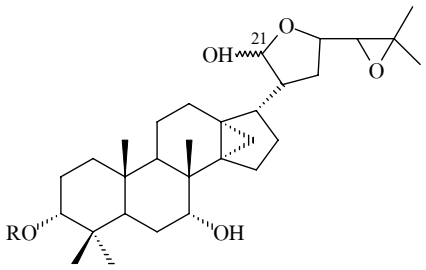

163. R = Ac (21*RS*)

164. R = Tig (21*RS*)

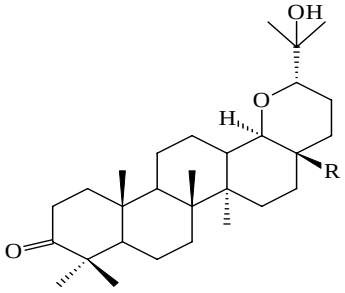

165. R = CH_3

166. R= COOH

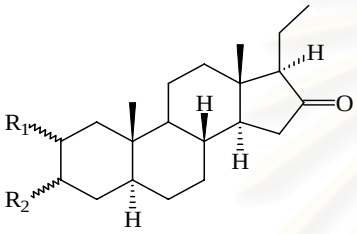

	R_1	R_2
167.	α-OH	α-OCH_3
168.	β-OH	β-OH

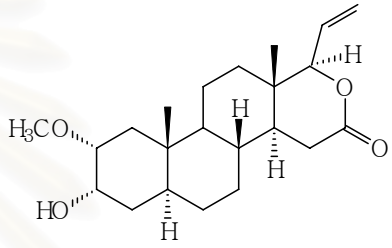

169

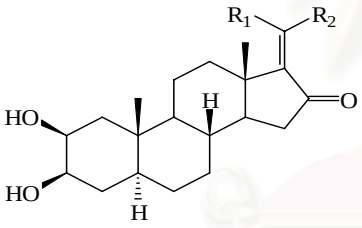

	R_1	R_2
170.	CH_3	H
171.	H	CH_3

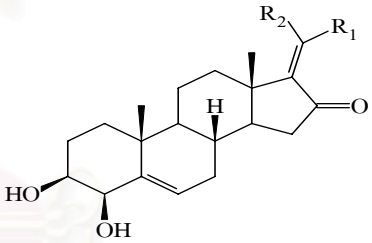

	R_1	R_2
172.	H	CH_3
173.	CH_3	H

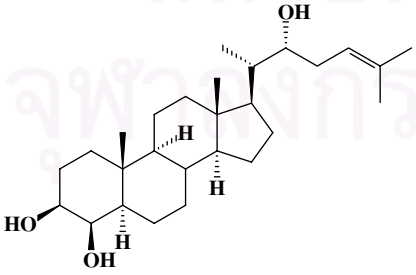

174

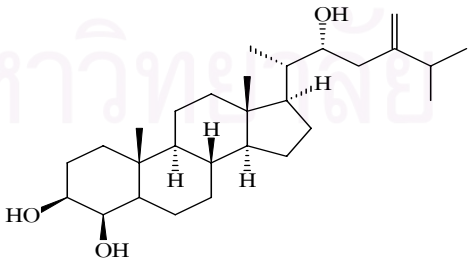

175

Figure 3. Chemical constituents of plants in the genus *Aglaia* (continued)

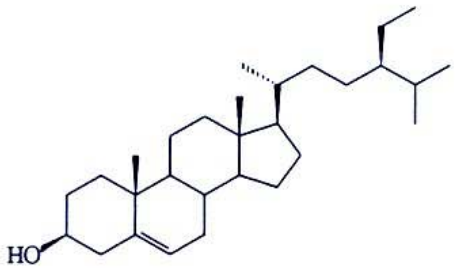

176

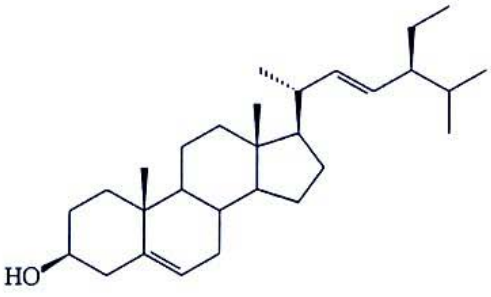

177

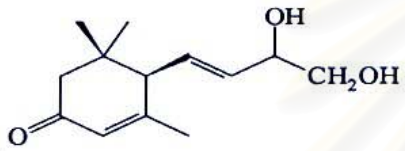

178

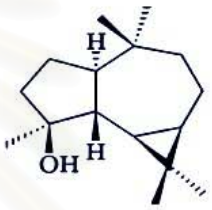

179

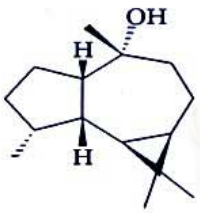

180

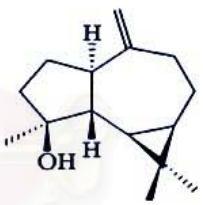

181

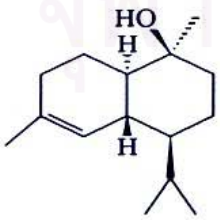

182

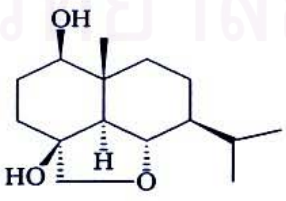

183

Figure 3. Chemical constituents of plants in the genus *Aglaia* (continued)

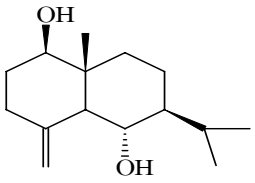

184

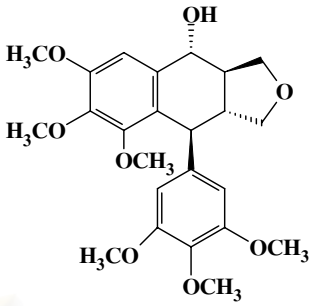

185

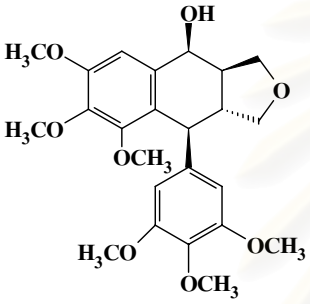

186

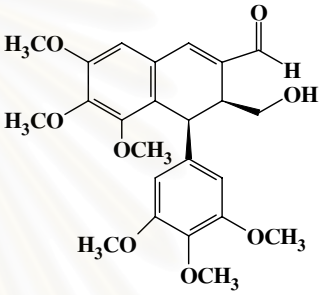

187

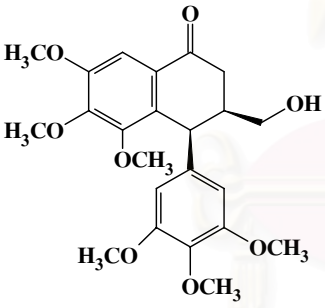

188

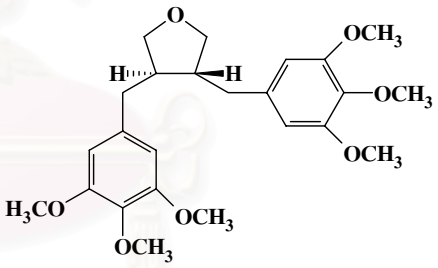

189

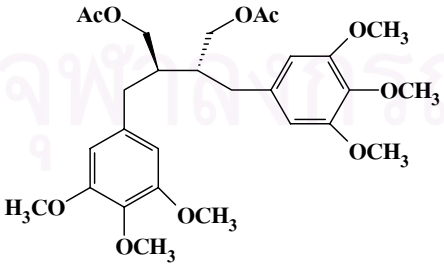

190

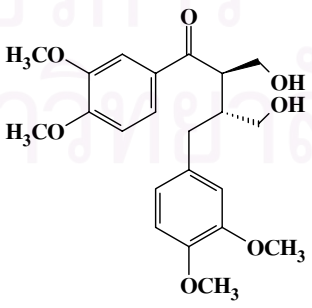

191

Figure 3. Chemical constituents of plants in the genus *Aglaia* (continued)

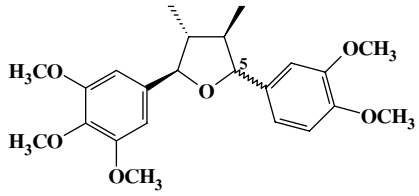

192. 5α-H

193. 5β-H

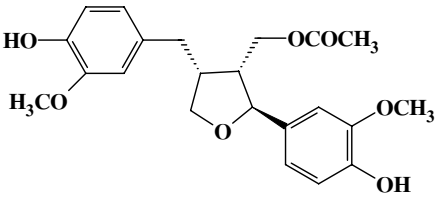

194

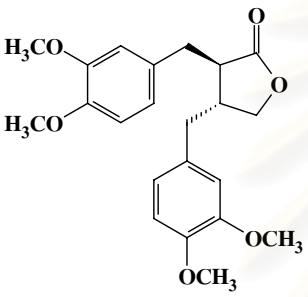

195

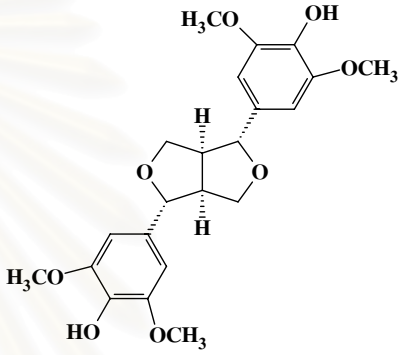

196

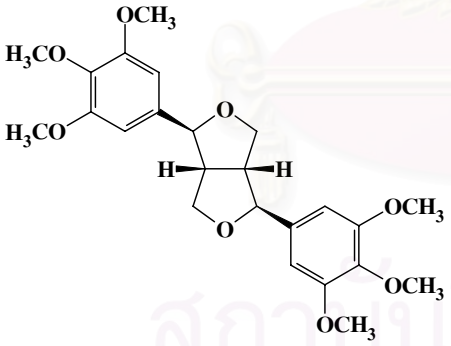

197

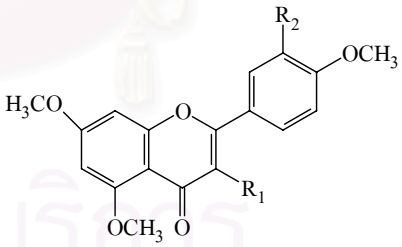

	R_1	R_2
198.	OH	OH
199.	OH	H
200.	H	OH
201.	OCH_3	OCH_3

Figure 3. Chemical constituents of plants in the genus *Aglaia* (continued)

สถาบันวิทยบริการ
จุฬาลงกรณ์มหาวิทยาลัย

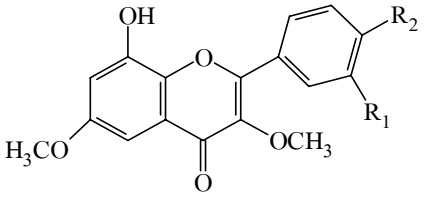

	R_1	R_2
202.	H	OCH_3
203.	OCH_3	OH
204.	OCH_3	OCH_3

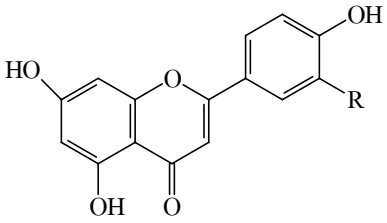

205. R= OH

206. R= H

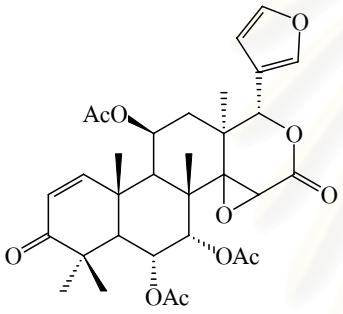

207

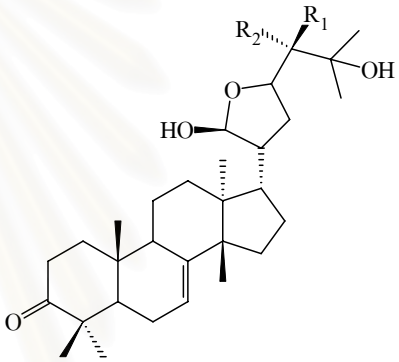

	R_1	R_2
208.	H	OH
209.	OH	H

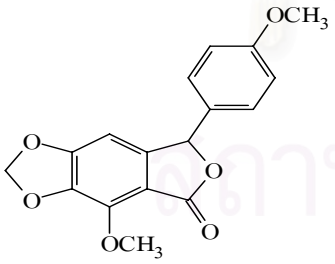

210

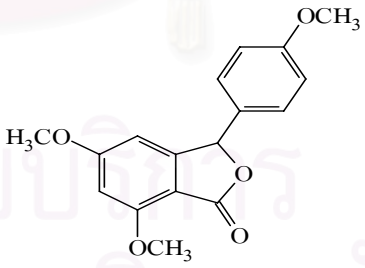

211

Figure 3. Chemical constituents of plants in the genus *Aglaia* (continued)

2. Biological Activities of plants in the genus *Aglaia*

From various phytochemical reports on plants of the genus *Aglaia*, with only a few exceptions all naturally occurring flavaglines of the cyclopenta[*b*]benzofuran type exhibited strong insecticidal activity, the most active of which are comparable in their activity to the well-known natural insecticide azadirachtin from *Azadirachta indica*. The insecticidal activity of the cyclopenta[*b*]benzofuran flavaglines seems to be largely linked to the integrity of the furan ring system, since two biogenetically closely related compounds of the benzo[*b*c]pyrans and benzo[*b*]oxepines which the oxygen heterocycle of the dihydrobenzofuran nucleus in the cyclopenta[*b*]benzofuran flavaglines is replaced by a bridged pyran and an oxepine ring, respectively, were shown to be inactive. However, the substitution pattern, especially the nature of substitutes at C-1, C-2, C-3′ and C-8b was also shown to be important for the insecticidal activity. Acylation of the OH group at C-1 (e.g. with formic or acetic acid) always caused a reduction of insecticidal activity. The nature of the amide substituents present at C-2, on the other hand, had little or no influence on the insecticidal activity. Additional oxygen substituents in ring A or B (compared to the substitution pattern of the parent compound rocaglamide) were also shown to have only marginal influences on the insecticidal activity of the respective products. However, a dramatic effect was observed for analogues with replacement of the OH-group at C-8b by a CH_3O or C_2H_5O- substituent, resulting in a total loss of insecticidal activity (Proksch *et al*., 2001). In addition to insecticidal activity, cytotoxic and antifungal activity of the cyclopenta[*b*]benzofuran flavaglines were also recorded. Furthermore, several studies have shown that the other classes of compounds isolated from the genus *Aglaia*, especially the bisamides, were also exhibited interesting biological activities. Summary of the biological activities of isolated compounds from *Aglaia* plants is shown in **Table 2.**

สถาบันวิทยบริการ
จุฬาลงกรณ์มหาวิทยาลัย

Table 2. Biological Activities of *Aglaia* species

Plant	Compound	Biological Activity	References
A. argentea	didesmethylrocaglamide **(12)**, argenteanol **(130)**, argenteanol B **(133)**, argenteanol C **(153)**, argenteanol D **(134)**, argenteanol E **(135)**, argenteanone A **(154)**, argenteanone B **(131)**, argenteanone C **(132)**, argenteanone D **(155)**, argenteanone E **(156)**	Cytotoxicity	Dumontet *et al*., 1996; Omobuwajo *et al*., 1996; Mohamad *et al*., 1997
	odorine **(90)**	Cancer chemopreventive activity	Inada *et al*., 2001
A. crassinervia	aglaiaglabretol B **(161)**, aglaiaglabretol B **(162),** rocaglaol **(29)**	Cytotoxicity	Su *et al*., 2006
A. duperreana	C-1-O-acetyldemethylrocaglamide **(2)**, C-1-O-acetyldidemethylrocaglamide **(3)**, C-1-O-acetyl-3′-hydroxydemethylrocaglamide **(4)**, C-1-O-acetyl-3′-hydroxymethylrocaglate **(5)**, C-1-O-acetyl-3′-hydroxyrocaglamide **(6)**, C-1-O-acetylmethylrocaglate **(18)**, C-1-O-acetylrocaglamide **(8)**, desmethylrocaglamide **(11)**, didesmethylrocaglamide **(12)**, C-8b-O-ethyl-3′-hydroxymethylrocaglamide **(13)**	Insecticidal activity	Nugroho *et al*., 1997; Chaidir *et al*., 1999; Hiort *et al*., 1999

Table 2. Biological Activities of *Aglaia* species

Plant	Compound	Biological Activity	References
A. duperreana	C-8b-O-ethyl-3′-hydroxyrocaglamide **(14)** C-3′-hydroxydemethylrocaglamide **(18)**, C-3′-hydroxydemethylrocaglate **(19)**, C-3′-hydroxyrocaglamide **(21)**, C-3′-methoxyrocaglamide **(22)**, C-8b-O-methyl-methylrocaglate **(20)**, C-8b-methylrocaglate **(25)**, methylrocaglate **(26)**, rocaglamide **(28)**	Insecticidal activity	Nugroho *et al*., 1997; Chaidir *et al*., 1999; Hiort *et al*., 1999
	N, N-didesmethyl-N-4-hydroxybutylrocaglamide **(10)**, didesmethylrocaglamide **(12)**	Inhibitor of NF-ΚB activation	Baumann *et al*., 2002
A. edulis	aglaroxin A **(46)**, pannellin **(50)**	Antifungal activity	Engelmeier *et al*., 2000
		Insecticidal activity	Bacher *et al*., 1999
	aglaidithioduline **(106)**, aglaithioduline **(107)**	Antiviral activity	Saifah *et al*., 1999
A. elaeagnoidea	aglaroxin B **(47)**, C-3′-methoxypannellin **(49)**, pannellin **(50)**, pannellin-1-O-acetate **(51)**	Insecticidal activity	Brader *et al*., 1998 ; Dreyer *et al*., 2001
	methylrocaglate **(26)**	Antifungal activity	Fuzzati *et al*., 1996
	Roxburghiadiol A **(151)**, Roxburghiadiol B **(152)**	Antiinflammatory activity	Janaki *et al*., 1999

Table 2. Biological Activities of *Aglaia* species

Plant	Compound	Biological Activity	References
A. elliptica	C-4′-demethoxy-3′,4′-methylenedioxyrocaglaol **(42)**, C-4′-demethoxy-3′,4′-methylenedioxymethylrocaglate **(43)**, C-1-O-formyl-4′-demethoxy-3′,4′-methylenedioxymethylrocaglate **(44)**, methylrocaglate **(26)**, C-1-oxo-4′-demethoxy-3′,4′-methylenedioxyrocaglaol **(45)**	Cytotoxic activity	Cui *et al*., 1997; Lee *et al*., 1998
	N-tetrahydrofuran- didesmethylrocaglamide **(34,35)**	Insecticidal activity	Nugroho *et al*., 1997b
A. elliptifolia	methylrocaglate **(26)**, rocaglamide **(28)**	Cytotoxic activity	Wu *et al*., 1997
		Antiplatelet aggregation	Wu *et al*., 1997
A. gracilis	C-3′-hydroxymarikarin **(36)**, marikarin **(38)**	Insecticidal activity	Greger *et al*., 2001
A. harmsiana	C-3′-rhamnosyl-rocaglamide **(33)**	Insecticidal activity	Nugroho *et al*., 1997b
A. leptantha	isoagleptin **(95)**	Antifungal activity	Greger *et al*., 2000
A. odorata	C-1-O-acetyl-3′-hydroxyrocaglamide **(6)**, C-3′-hydroxydemethylrocaglamide **(18)**, C-3′-hydroxydemethylrocaglate **(19)**, C-3′-hydroxydidesmethylrocaglamide **(20)**	Insecticidal activity	Nugroho *et al*., 1999

ศูนย์วิทยทรัพยากร
จุฬาลงกรณ์มหาวิทยาลัย

Table 2. Biological Activities of *Aglaia* species

Plant	Compound	Biological Activity	References
A. odorata	C-3′-hydroxyrocaglamide **(21)**, C-3′-methylrocaglaol **(24)**, C-3′-methylrocaglate **(22)**, C-1-oxime-C-3′-methoxymethylrocaglate **(27)**	Insecticidal activity	Nugroho *et al*., 1999
	desmethyrocaglamide **(11)**, methylrocaglate **(26)**, rocaglamide **(28)**, rocaglaol **(29)**	Insecticidal activity/Antifungal activity	Ishibashi *et al*., 1993; Janprasert *et al*., 1993; Engelmeier *et al*., 2000
	N,N-didesmethyl-N-4-hydroxybutylrocaglamide **(10)**, didesmethylrocaglamide **(12)**	Inhibitor of NF-ΚB- activation	Baumann *et al*., 2002
	aglaiastatin **(38)**, pyrimidone **(34)**, rocaglaol **(29)**	Protein synthesis inhibitor	Ohse *et al*., 1996
	odorine **(90)**, odorinol **(91)**	Cancer chemopreventive activity	Inada *et al*., 2001
	odorinol **(91)**	Anti-leukemic activity	Hayashi *et al*., 1982
A. ponapensis	methylrocaglate **(26)**, ponapensin **(75)**	Inhibitor of NF-ΚB- activation	Salim *et al*., 2007
A. rubiginosa	C-1-O-acetylmethylrocaglate **(7),** C-1-O-acetylrocaglaol **(9)**, rocagloic acid **(30)**	Cytotoxic activity	Rivero-Cruz *et al*., 2004
A. silvestris	episilvestrol **(31)**, silvestrol **(32)**	Cytotoxic activity	Hwang *et al*., 2004
A. spectabilis	C-1-O-acetyl-4′-demethoxy-3′-4′-methylenedioxymethylrocaglate **(41)**	Insecticidal activity	Schneider *et al*., 2000

Table 2. Biological Activities of *Aglaia* species

Plant	Compound	Biological Activity	References
A. spectabilis	C-4′-demethoxy-3′,4′-methylenedioxyrocaglaol **(42)**, C-4′-demethoxy-3′,4′-methylenedioxymethylrocaglate **(43)**, C-1-O-formyloxy-3′-hydroxymethylrocaglate **(16)**, C-1-O-formyloxymethylrocaglate **(18)**, C-3′-hydroxydemethylrocaglate **(19)**, C-1-oxo-4′-demethoxy-3′,4′-methylenedioxyrocaglaol **(45)**, rocaglaol **(29)**	Insecticidal activity	Schneider *et al*., 2000
A. tomentosa	rocaglaol **(29)**	Cytotoxic activity	Mohamad *et al*., 1999

สถาบันวิทยบริการ
จุฬาลงกรณ์มหาวิทยาลัย

CHAPTER III

EXPERIMENTAL

1. Sources of Plant Materials

The leaves of *Aglaia forbesii* King. and *Aglaia oligophylla* Miq. were collected from Khao Luang National Park, Nakhon Sri Thammarat Thailand in March, 2004 and compared with authentic specimens of the Herbarium of the Institute of Botany, University of Vienna, Austria (identified by Dr. Caroline Pannell, University of Oxford, England). Voucher specimens of both plants have been deposited at the herbarium of the Department of Pharmaceutical Botany, Faculty of Pharmaceutical Sciences, Chulalongkorn University, Bangkok, Thailand.

2. General Techniques

2.1 Analytical Thin-Layer Chromatography (TLC)

Technique	:	One dimension, ascending
Adsorbent	:	Silica gel 60 F_{254} (E. Merck) pre-coated plate
Layer thickness	:	0.2 mm
Distance	:	5.0 cm
Temperature	:	Laboratory temperature (30-35 ºC)
Detection	:	1) Ultraviolet light (254 and 365 nm) 2) Spraying with anisaldehyde-sulfuric acid solution or 10% sulfuric acid and heating at 100-110 ºC for 5 min.

2.2 Preparative Thin Layer Chromatography (PLC)

Technique	:	One dimension, ascending
Adsorbent	:	Silica gel 60 F_{254} (E. Merck) pre-coated plate
Layer thickness	:	1 mm
Distance	:	15 cm
Temperature	:	Laboratory temperature (30-35 ºC)
Detection	:	UV light (254 and 365 nm)

2.3 Column Chromatography

2.3.1 Liquid Column Chromatography

Column	:	Flat bottom glass column (various diameter)
Adsorbent	:	Silica gel (Merck 60, No. 7734) particle size 0.063-0.200 mm or Silica gel (Merck 60, No. 9385) particle size 0.040-0.063 mm
Solvent	:	Various solvent systems depending on materials
Packing method	:	Dry and wet packing
Sample loading	:	1) Dry packing: The sample was dissolved in a small amount of suitable organic solvent, mixed with small quantity of adsorbent, triturated, dried and then placed gently on top of the column. 2) Wet packing: The sample was dissolved in a small amount of eluent and then applied gently on top of the column.
Detection	:	Fractions were examined by TLC technique in the same manner as described in section 2.1. Fractions with similar chromatographic pattern were combined.

2.3.2 Gel Filtration Chromatography

Column size	:	Glass column, 2.2 cm in diameter
Gel Filter	:	Sephadex LH-20 (Pharmacia Biotech AB)
Solvent	:	CH_2Cl_2-MeOH (1:1)
Packing method	:	Gel filter was suspended in the eluent and left standing to swell for 24 hours prior to use, then poured into the column and allowed to set tightly.
Sample loading	:	The sample was dissolved in a small amount of the eluent and then applied gently on top of the column.
Detection	:	Fractions were examined by TLC technique in the same manner as described in section 2.3.1

2.4 Spectroscopy

2.4.1 Ultraviolet (UV) Absorption Spectra

UV absorption spectra were obtained on a Shimadzu UV-160A spectrophotometer (Pharmaceutical Research Instrument Center, Faculty of Pharmaceutical Sciences, Chulalongkorn University)

2.4.2 Infrared (IR) Absorption Spectra

IR absorption spectra (KBr disc and film) were recorded on a Perkin Elmer FT-IR 1760X spectrometer (Scientific and Technological Research Equipment Center, Chulalongkorn University).

2.4.3 Mass Spectra (MS)

Electrospray Ionization Time of Flight (ESI-TOF) mass spectra were obtained on a Micromass LCT mass spectrometer (National Center for Genetic Engineering and Biotechnology, BIOTEC, Thailand). Electron impact and high-resolution electron impact mass spectra (EIMS and HREIMS) were obtained with a Finnigan MAT 900S apparatus (University of Vienna, Wein, Austria).

2.4.4 Nuclear Magnetic Resonance (NMR) spectra

^{1}H (300 MHz) and ^{13}C (75 MHz) NMR spectra were obtained on a Bruker DPX-300 FT-NMR spectrometer (Pharmaceutical Research Instrument Center, Faculty of Pharmaceutical Sciences, Chulalongkorn University).

^{1}H (400 MHz) and ^{13}C (100 MHz) NMR spectra were obtained on a Bruker DRX-400 spectrometer (University of Vienna, Wein, Austria).

^{1}H (500 MHz) and ^{13}C (125 MHz) NMR spectra were obtained on a JEOL JMN-A 500 spectrometer (Scientific and Technological Research Equipment Center, Chulalongkorn University).

The solvents for NMR spectra were deuterated chloroform ($CDCl_3$) and deuterated dimethylsulfoxide (DMSO-d_6). The chemical shifts were reported in ppm scale using the chemical shift of the solvent as the reference signal.

2.5 Physical Properties

2.5.1 Melting Points

Melting points were obtained on a Fisher-John melting point apparatus (Department of Pharmaceutical Botany, Faculty of Pharmaceutical Sciences, Chulalongkorn University).

2.5.2 Optical Rotations

Optical rotations were measured on a Perkin-Elmer 241 Polarimeter (University of Vienna, Wein, Austria).

2.6 Solvents

Organic solvents used in the extraction were commercial grade. For column chromatography, solvents were redistilled prior to use.

3. Extraction and Isolation

3.1 Extraction and Isolation of Compounds from the Leaves of *Aglaia forbesii*

3.1.1 Extraction

The dried, powdered leaves (3.5 kg.) of *A. forbesii* were exhaustively extracted with MeOH (3 x 6 L) and filtered. After removing the solvent in *vacuo*, the residue was mixed with Kieselguhr, packed in a column and eluted with n-hexane, CH_2Cl_2, EtOAc and MeOH, successively. Each filtrate was pooled and evaporated to dryness under reduced pressure at temperature not exceeding 40 ºC to yield the hexane extract (190 g, 5.42% based on dried weight of leaves), CH_2Cl_2 extract (20 g, 0.57% yield), EtOAc extract (15 g, 0.42% yield) and MeOH extract (17 g, 0.48% yield).

3.1.2 Isolation of Compounds from the Hexane Extract of *A. forbesii* Leaves

The hexane extract (15.0 g) was subjected to column chromatography using silica gel (No. 7734, 400 g) as adsorbent and eluted with 8% EtOAc in hexane to give 100 fractions of approximately 40 ml each and then washed down with MeOH. The fractions were then combined on the basis of their TLC profiles, to give seven fractions: fraction A1 (1.69 g), A2 (1.19 g), A3 (1.33 g), A4 (0.62 g), A5 (2.09 g), A6 (1.86 g) and A7 (5.56 g).

3.1.2.1 Isolation of Compound HAF1

Fraction A2 (1.19 g), which displayed one main orange-brown spot on TLC plate (solvent system: 8% acetone in hexane), was further purified by gel filtration chromatography using a Sephadex LH20 column (100 g, 2.2 x 85 cm) with CH_2Cl_2-MeOH (1:1) as the eluent to yield 10 mg of compound HAF1 as colorless needles.

3.1.2.2 Isolation of Compounds HAF2 and HAF3

Fraction A3 (1.33 g), when developed with 8% acetone in hexane, displayed one major orange-brown spot and another dark violet spot on TLC plate upon detection with 10% sulfuric acid in EtOH. Crystallization of fraction A3 with MeOH yielded 5.6 mg of compound HAF2 as colorless needles while the filtrate, after drying (approximately 1.27 g), was further separated on Sephadex LH20 column (100 g, 2.2 x 85 cm) with CH_2Cl_2-MeOH (1:1) as the

eluent to yield another 9.4 mg of compound HAF2 and 5 mg of compound HAF3 as pale yellow oil.

3.1.2.3 Isolation of Compound HAF4

When developed with 8% acetone in hexane, fraction A4 (0.62 g) displayed one main violet-red spot on TLC plate under detection with 10% sulfuric acid in EtOH. Crystallization of fraction A4 with MeOH yielded 31 mg of compound HAF4 as colorless needles.

3.1.3 Isolation of Compounds from the CH_2Cl_2 Extract of *A. forbesii* Leaves

The CH_2Cl_2 extract (20.0 g) was fractionated by column chromatography using silica gel (No. 7734, 600 g) as adsorbent and eluted with CH_2Cl_2-EtOAc (1:1) to give 88 fractions of approximately 40 ml each and then washed down with MeOH. The fractions with similar chromatographic pattern were then combined to give six fractions: fraction B1 (4.70 g), B2 (2.0 g), B3 (2.0 g), B4 (4.36 g), B5 (1.88 g) and B6 (2.93 g).

3.1.3.1 Isolation of Compound CAF1

Fraction B2 (2 g) was further chromatographed on a silica gel 60 (No. 9385, 60 g) column, eluting with 2% MeOH in CH_2Cl_2, to give sixty fractions of approximately 20 ml each and then washed down with MeOH. The fractions were then combined according to their TLC profile to give five fractions: fraction B21 (64 mg), B22 (58 mg), B23 (457 mg), B24 (226 mg) and B25 (629 mg).

Fraction B23 (457 mg) was purified on Sephadex LH20 column (100 g, 2.2 x 85 cm), eluting with CH_2Cl_2-MeOH (1:1). Twenty-seven fractions, approximately 20 ml each, were collected and then combined according to their TLC behavior into three fractions: fraction B231 (132 mg), B232 (68 mg) and B233 (48 mg). Fraction B232 (68 mg) was further purified on silica gel 60 (No. 9385, 30g) column with 4% MeOH in CH_2Cl_2 as the eluent to give thirty fractions of approximately 10 ml each, then wash down with MeOH. The combined fractions 13-14 from this column yielded 5 mg of the compound CAF1 as white amorphous solid.

3.1.3.2 Isolation of Compounds CAF2 and CAF3

Fraction B233 (48 mg) displayed two spots close together under UV light and appeared as yellow spots on TLC plate (solvent system: hexane-acetone = 72:28) upon detection with 10% sulfuric acid. This fraction was further purified by preparative TLC developed with hexane-acetone (72:28) to give compounds CAF2 (3 mg) and CAF3 (3 mg).

3.1.3.3 Isolation of Compound CAF4

Fraction B3 (2 g) was further chromatographed on a silica gel 60 (No. 9385, 60 g) column, eluting with 40% acetone in hexane to give forty-seven fractions of

approximately 20 ml each and then washed down with MeOH. The fractions with similar TLC profiles were then combined to give four fractions: fraction B31 (694 mg), B32 (112 mg), B33 (468 mg) and B34 (525 mg).

Fraction B32 (112 mg), which displayed one Dragendorff - positive spot on TLC plate, precipitated after partial evaporation of the solvent. The precipretate (52 mg) was further purified by recrystallization in MeOH to yield 12 mg of compound CAF4 as colorless needles.

3.1.3.4 Isolation of Compound CAF5

Fraction B33 (468 mg), was applied to a silica gel 60 (No. 9385, 60 g) column eluted with 6% MeOH in CH_2Cl_2 to yield twenty-two fractions of approximately 10 ml each, then washed down with MeOH. The fractions were then combined on the basis of their TLC profiles to give three fractions: fraction B331 (130.0 mg), B332 (36.8 mg) and B333 (142.5 mg).

Fraction B331 (130 mg), which displayed a Dragendorff - positive spot on TLC plate (R_f 0.5, Hexane-CH_2Cl_2-EtOAc-MeOH = 10:54:26:10), was further purified by PLC developed with hexane-acetone-methanol (60:34:6) to afford 10 mg of CAF5 as white amorphous powder.

3.1.3.5 Isolation of Compound CAF6

Fraction B333 (142.5 mg) appeared a Dragendorff - positive spot on TLC plate (R_f 0.38, Hexane-CH_2Cl_2-EtOAc-MeOH = 10:54:26:10). This fraction was further purified on Sephadex LH20 column (100 g, 2.2 x 85 cm), eluting with CH_2Cl_2-MeOH (1:1), followed by PLC developed with hexane-acetone-methanol (60:34:6) to give 4.8 mg of CAF6 as white amorphous powder.

3.1.3.6 Isolation of Compounds CAF6 and CAF7

Fractions B34 (525 mg) was fractionated on a silica gel 60 (No. 9385, 60 g) column (solvent system: CH_2Cl_2-EtOAc-MeOH = 80:15:5) to yield fifteen fractions of approximately 20 ml each and then washed down with MeOH. The fractions were then combined according to their TLC profiles to give four fractions: fraction B341 (72 mg), B342 (275 mg), B343 (163 mg) and B344 (49 mg).

Fraction B343 (163 mg), which displayed two Dragendorff - positive spots on TLC plate (R_f 0.42 and 0.38, Hexane-CH_2Cl_2-EtOAc-MeOH = 10:54:26:10), was further separated by silica gel chromatography, eluting with CH_2Cl_2-EtOAc-MeOH (80:15:5) to afford fifteen fractions of approximately 15 ml each, then washed down with MeOH. The fractions were combined according to their TLC behavior to afford four main fractions: fraction B343A (5 mg), B343B (20

mg), B343C (17 mg) and B343D (55 mg). Fraction B343C (17 mg) displaying a Dragendorff - positive spot on TLC plate (R_f 0.38, Hexane-CH_2Cl_2-EtOAc-MeOH = 10:54:26:10) was further purified by PLC (solvent system: CH_2Cl_2-EtOAc-MeOH = 80:15:5) to yield another 5.2 mg of compound CAF6 while fraction B343B (20 mg), which displayed a Dragendorff - positive spot on TLC plate (R_f 0.42, Hexane-CH_2Cl_2-EtOAc-MeOH = 10:54:26:10), was further purified in the same manner to yield 6 mg of compound CAF7 as white amorphous powder.

3.2 Extraction and Isolation of Compounds from the Leaves of *A. oligophylla*

3.2.1 Extraction

The dried leaves (1.7 kg) of *A. oligophylla* were ground, macerated with MeOH (3 x 6 L) and filtered. After removing the solvent in *vacuo*, the residue was mixed with Kieselguhr, packed into a column and eluted with n-hexane, EtOAc and MeOH, successively. Each filtrate was pooled and evaporated to dryness under reduced pressure at temperature not exceeding 40 ºC to yield the hexane extract (76.86 g, 4.52% based on dried weight of leaves), EtOAc extract (53.14 g, 3.12% yield) and MeOH extract (46.41 g, 2.73% yield).

3.2.2 Isolation of Compounds from the Hexane Extract of *A. oligophylla* leaves

The hexane extract (16.0 g) was separated by column chromatography using silica gel 60 (No. 7734, 500 g) as adsorbent and eluted with 8% acetone in hexane. A total of one-hundred and seventy fractions (30 ml each) were collected and combined according to their TLC behavior into eight fractions: fraction C1 (2.36 g), C2 (1.88 g), C3 (1.62 g), C4 (3.59 g), C5 (3.14 g), C6 (385 mg), C7 (149 mg) and C8 (2.26 g).

3.2.2.1 Isolation of Compounds HAO1 and HAO2

Fraction C2 (1.88 g) was subjected to repeated gel filtration chromatography, using two successive Sephadex LH 20 columns (100 g, 2.2 x 85 cm) eluted with CH_2Cl_2-MeOH (1:1). The fractions, approximately 10 ml each, were combined according to their TLC profiles to give three main fractions: fraction C21 (22.3 mg), C22 (43.4 mg), and C23 (79.8 mg). Fraction C22 (43.4 mg) was recrystallized in MeOH to yield 17.8 mg of HAO1 as colorless needles. Furthermore, fraction C23 (79.8 mg) was applied to silica gel 60 (No. 9385, 60 g) column, eluting with 6% EtOAc in hexane to give forty-five fractions of approximately 20 ml each, then washed down with MeOH. The fractions were combined according to their TLC patterns into five fractions: C231 (93.6 mg), C232 (52.4 mg), C233 (126 mg), C234 (76.9 mg) and C235 (223.6 mg).

Fraction C232 (52.4 mg) gave another 12.6 mg of compound HAO1 by recrystallization in MeOH, while fraction C234 (76.9 mg), which displayed one main yellow spot on

TLC plate (Hexane-EtOAc = 4:1), was further purified by recrystallization in MeOH to yield 24.7 mg of compound HAO2 as colorless needles.

3.2.2.2 Isolation of Compound HAO3

Fraction C3 (1.62 g) was fractionated on silica gel 60 (No. 9385, 60 g) column eluted with hexane-acetone (76:24) to give forty-five fractions of approximately 20 ml each, then washed down with MeOH. The fractions with similar chromatographic pattern were combined to afford four fractions: C31 (55.6 mg), C32 (565 mg), C33 (38 mg) and C34 (529 mg).

Fraction C32 (565 mg) dissolved in acetone, precipitated after partial evaporation of the solvent. The precipitate was chromatographed on a silica gel column using 16% acetone in hexane as the eluent. A total of forty fractions (fraction size: 20 ml) were collected and combined to give five main fractions: fraction C321 (187.3 mg), C322 (12.2 mg), C323 (26.2 mg), C324 (38.4 mg) and C325 (264.7 mg).

Fraction C322, after recrystallized in MeOH, gave 12.2 mg of a mixture of β-sitosterol and stigmasterol. Fraction C324 (38.4 mg) was further purified by Sephadex LH20 column (100g, 2.2 x 85 cm) eluted with CH_2Cl_2:MeOH (1:1) to yield 13 mg of compound HAO3 as colorless needles.

3.2.2.3 Isolation of Compound HAO4

Fraction C33 (38 mg) was recrystallized in MeOH to give 5.8 mg of compound HAO4 as colorless needles.

3.2.2.4 Isolation of Compound HAO5

Chromatographic separation of fraction C6 (385.2 mg) using silica gel 60 (No. 9385, 60 g) column eluted with hexane-acetone (72:26) yield forty-two fractions (fraction size: 20 ml). The fractions were then combined according to their TLC profile into four fractions: fraction C61 (43.3 mg), C62 (64.0 mg), C63 (116.0 mg) and C64 (98.5 mg). Fraction C61 (43.3 mg) showed a major dark green spot on TLC plate after being detected with anisaldehyde-sulfuric acid solution. This fraction was further purified by Sephadex LH20 column (100 g, 2.2 x 85 cm) eluted with CH_2Cl_2-MeOH (1:1) to afford 8 mg of compound HAO5 as white amorphous solid.

3.2.2.5 Isolation of Compound HAO6

When developed with CH_2Cl_2-EtOAc-Hexane (40:40:20), fraction C63 (116 mg) displayed two spots of similar R_f values under UV light and appeared as yellow spots on TLC plate upon detection with anisaldehyde-sulfuric acid solution. This fraction was subjected to silica gel chromatography, eluting with CH_2Cl_2-EtOAc-Hexane (60:20:20). The eluates (40 fractions)

were collected 15 ml per fraction and then combined on the basis of their TLC behavior to give three main fractions: fraction C631 (8.3 mg), C632 (77.6 mg) and C633 (24.6 mg). Fraction C632 (77.6 mg) was chromatographed on a silica gel 60 (No. 9385, 50 g) column eluted with CH_2Cl_2-EtOAc-Hexane (40:40:20) to yield 5 mg of HAO6A (R_f 0.36, CH_2Cl_2-EtOAc-Hexane = 40:40:20) and 6.2 mg of HAO6B (R_f 0.30, CH_2Cl_2-EtOAc-Hexane = 40:40:20).

3.2.2.6 Isolation of Compound HAO7

Fraction C7 (149 mg) gave a precipitate after partial evaporation of the solvent. This precipitate was further subjected to column chromatography using a column of Sephadex LH 20 (100 g, 2.2 x 85 cm) eluted with CH_2Cl_2-MeOH (1:1), followed by recrystallization in MeOH to give 13.3 mg of compound HAO7 as colorless needles.

3.2.3 Isolation of Compound from the EtOAc Extract of *A. oligophylla* leaves

The EtOAc extract (20 g) was fractionated by column chromatography using silica gel (No. 7734, 600 g) as adsorbent and eluted with 4% EtOAc in CH_2Cl_2 to give two hundred fractions of approximately 40 ml each and then washed down with MeOH. These fractions were then combined according to their TLC patterns to afford six fractions: fraction D1 (3.70 g), D2 (4.12 g), D3 (2.0 g), D4 (2.36 g), D5 (2.07 g) and D6 (3.97 g).

3.2.3.1 Isolation of Compound EAO1

Fraction D3 (2.0 g) gave a precipitate after partial evaporation of the solvent. This fraction was further subjected to column chromatography using silica gel 60 (No. 9385, 150 g) eluted with CH_2Cl_2-EtOAc- MeOH (60:35:5), followed by Sephadex LH 20 (100 g, 2.2 x 85 cm) eluted with CH_2Cl_2:MeOH (1:1) to yield, after recrystallization in acetone, 6.8 mg of compound EAO1 as colorless needles.

สถาบันวิทยบริการ
จุฬาลงกรณ์มหาวิทยาลัย

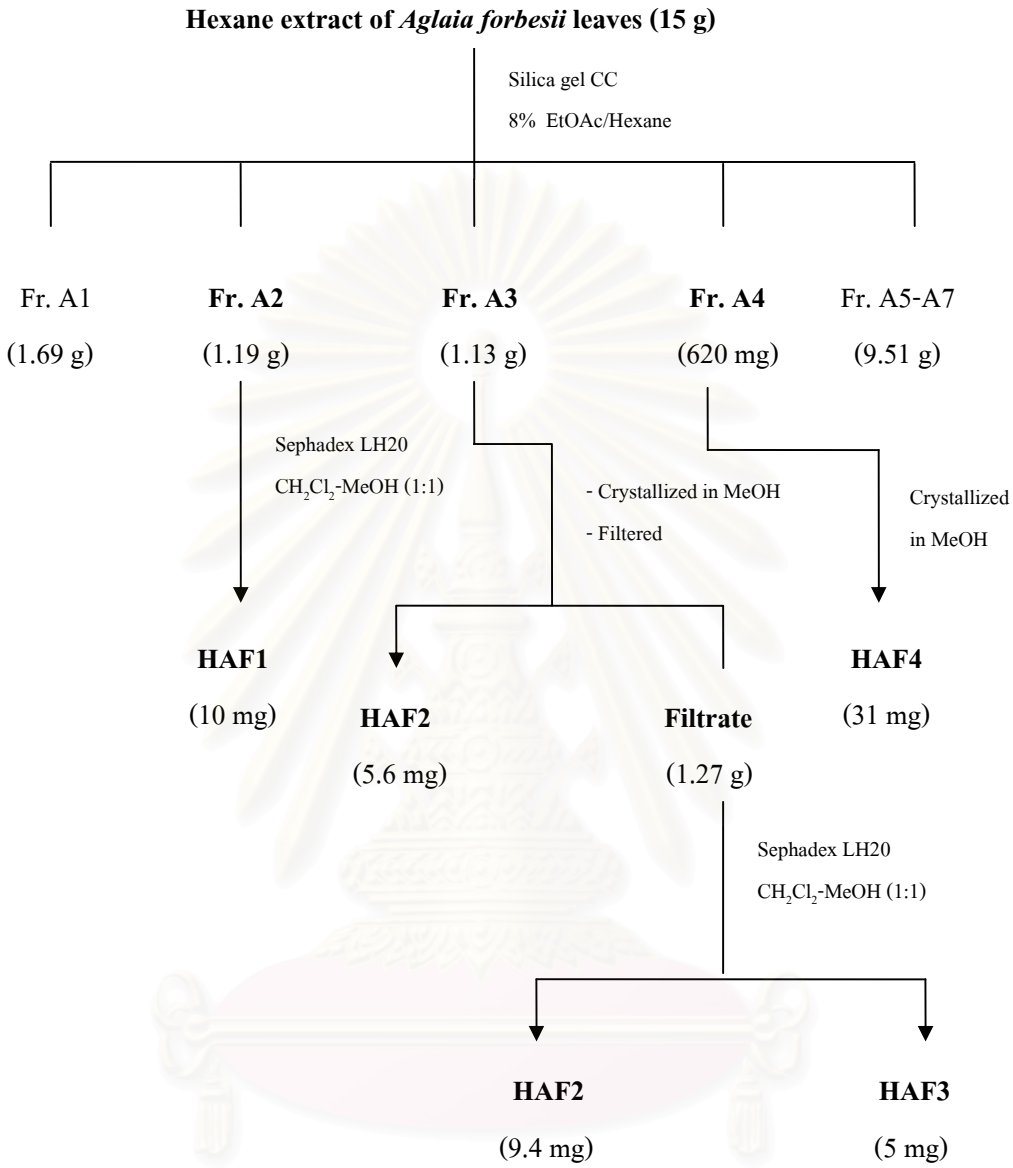

สถาบันวิทยบริการ
จุฬาลงกรณ์มหาวิทยาลัย

Scheme 1 Separation of the hexane extract of the leaves of *Aglaia forbesii*

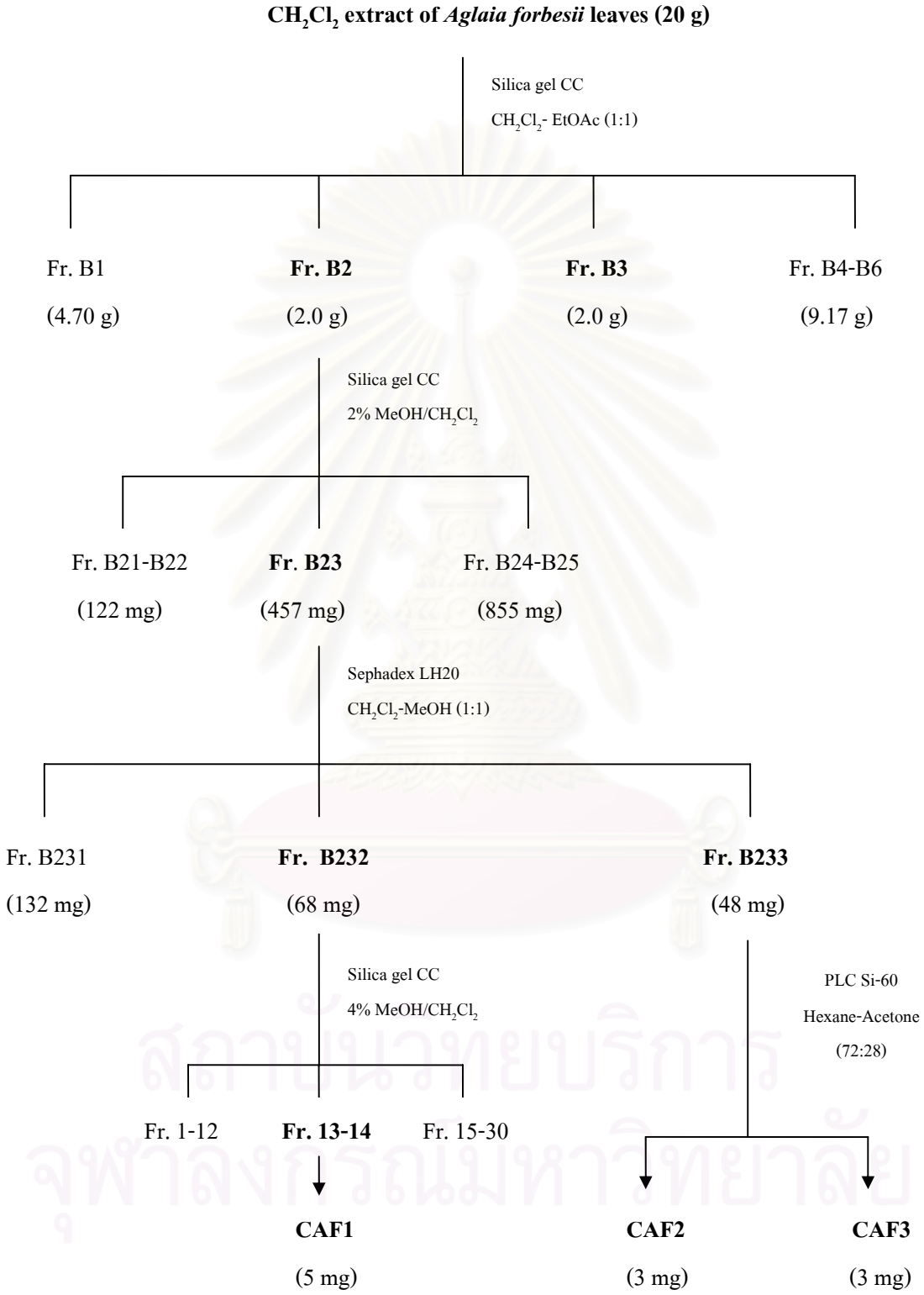

Scheme 2 Separation of the CH_2Cl_2 extract of the leaves of *Aglaia forbesii*

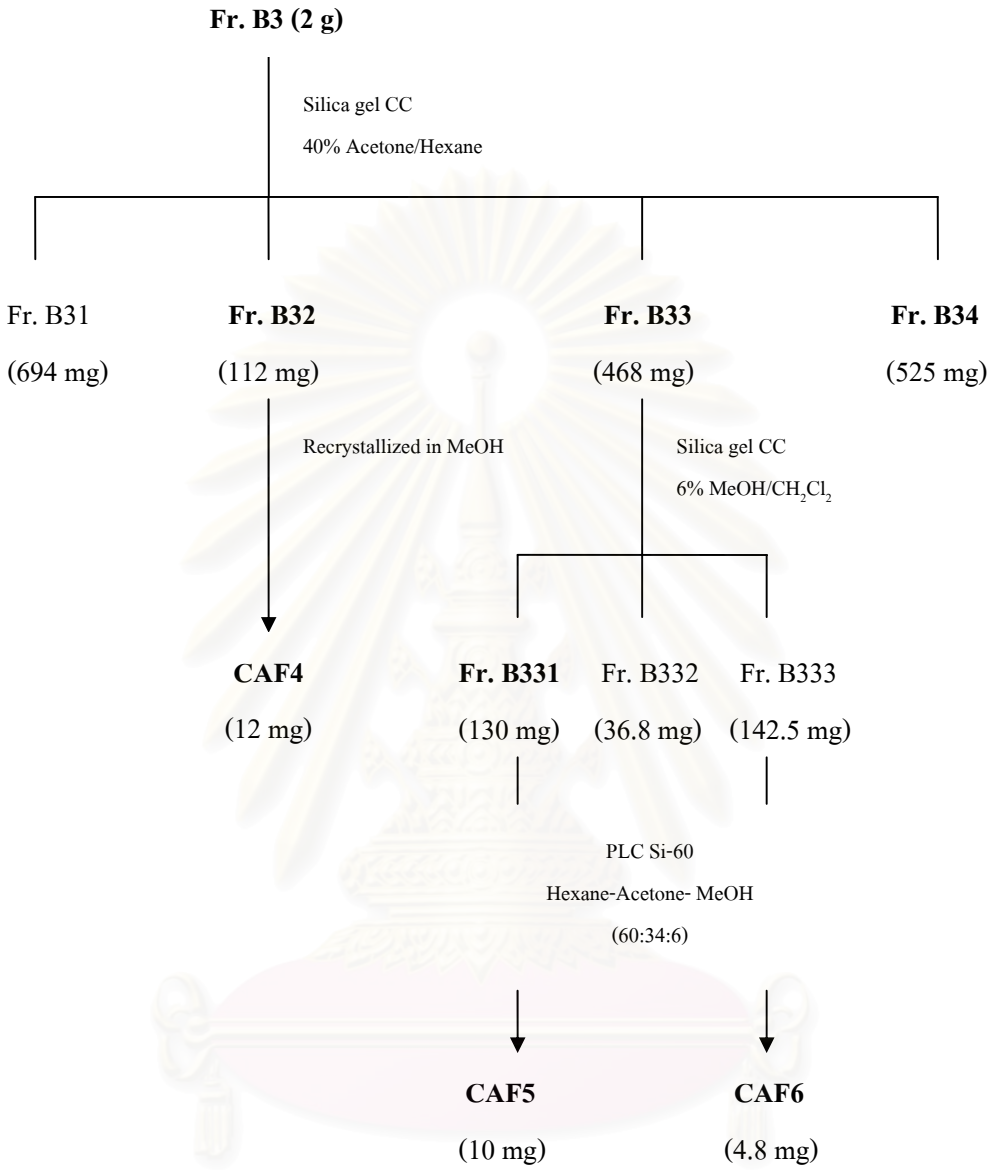

Scheme 2 Separation of the CH_2Cl_2 extract of the leaves of *Aglaia forbesii* (continued)

สถาบันวิทยบริการ
จุฬาลงกรณ์มหาวิทยาลัย

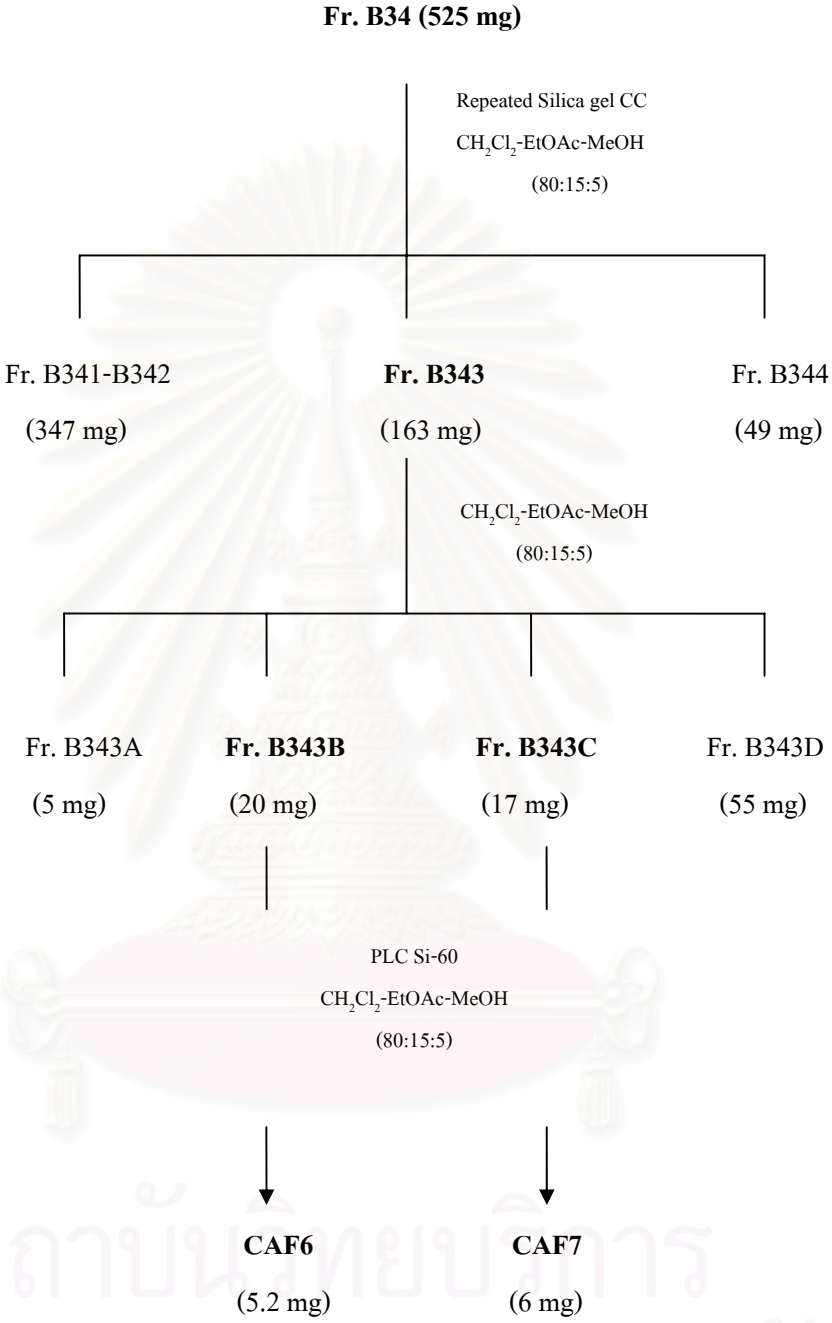

Scheme 2 Separation of the CH_2Cl_2 extract of the leaves of *Aglaia forbesii* (continued)

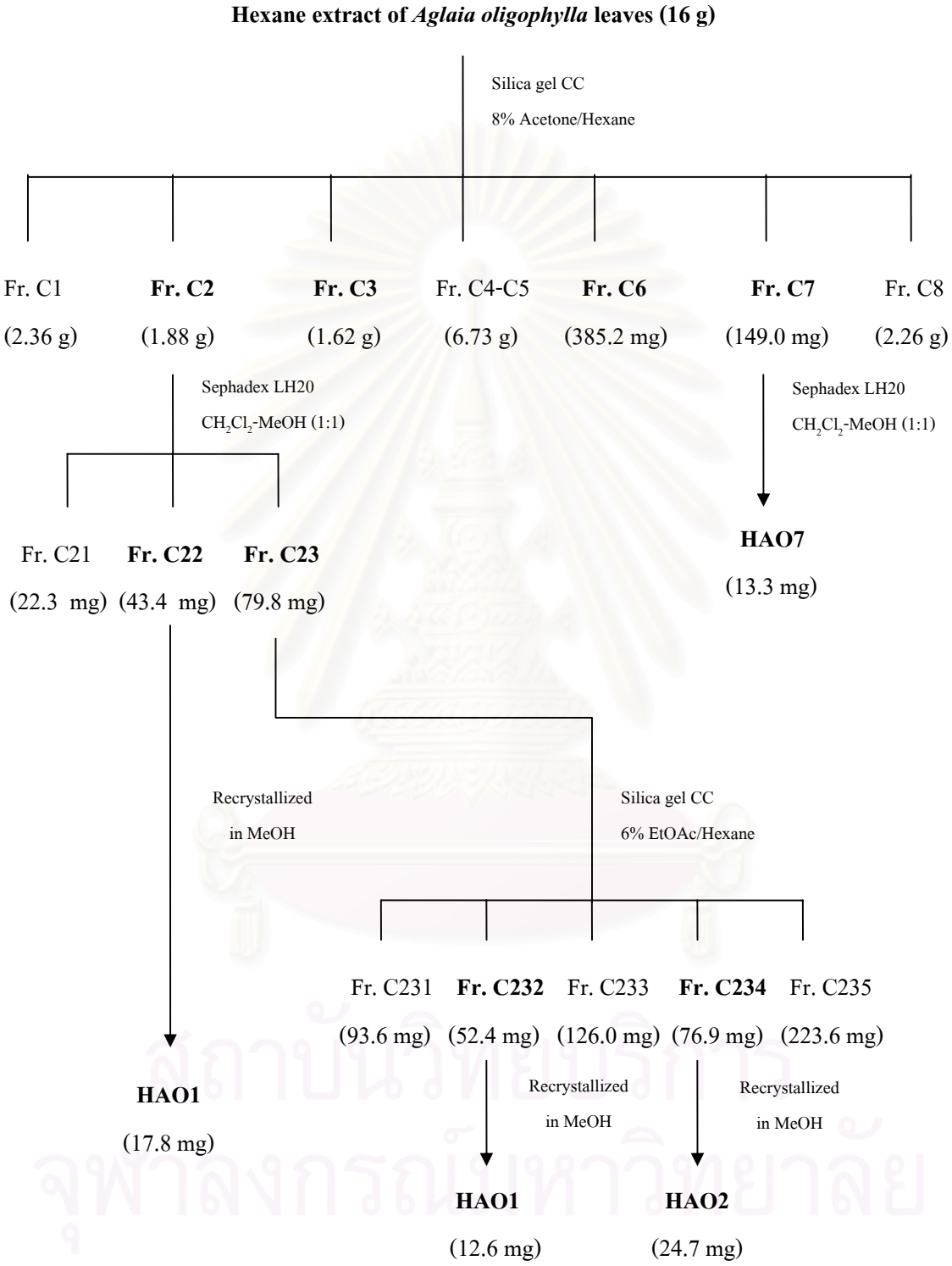

Scheme 3 Separation of the Hexane extract of the leaves of *Aglaia oligophylla*

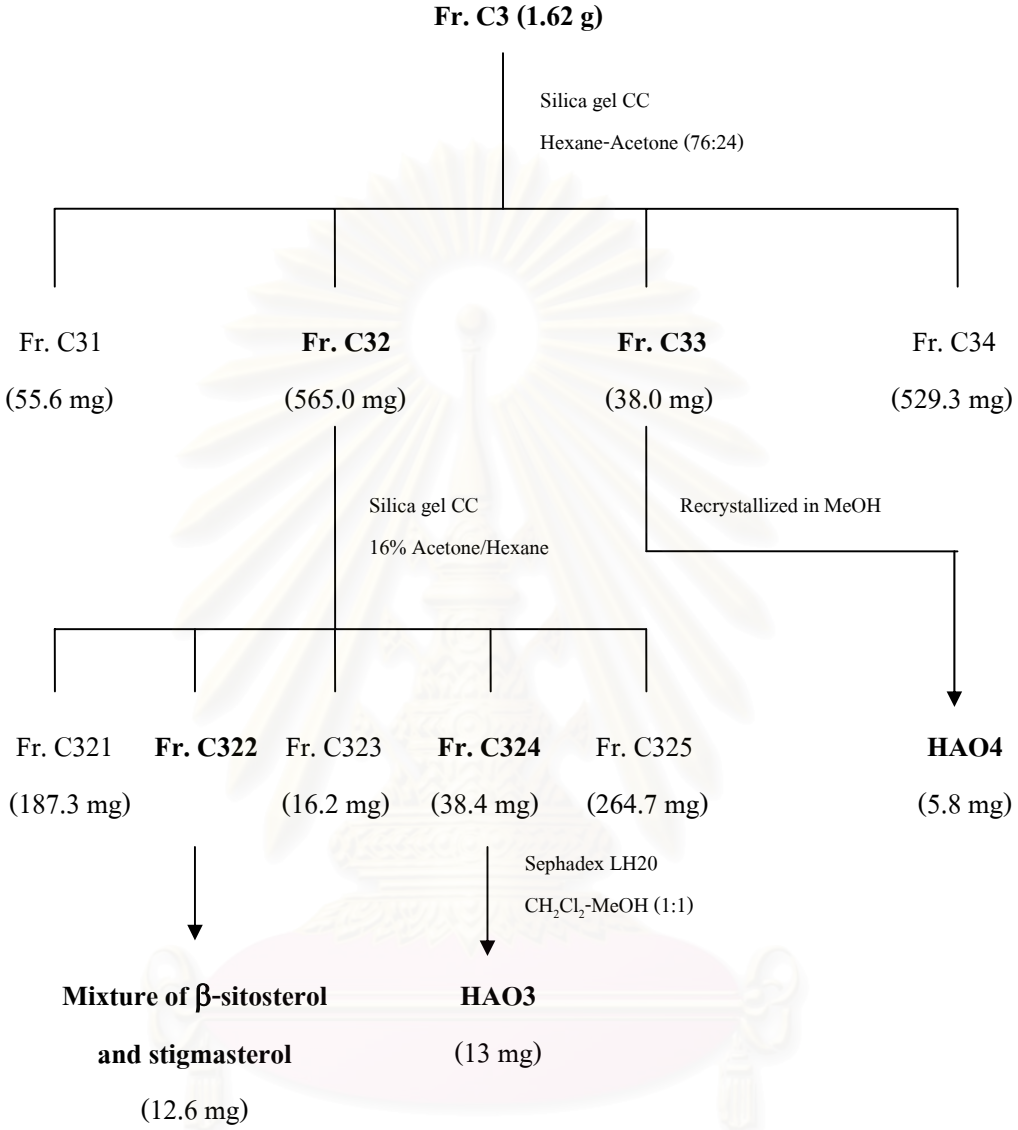

Scheme 3 Separation of the Hexane extract of the leaves of *Aglaia oligophylla* (continued)

สถาบันวิทยบริการ
จุฬาลงกรณ์มหาวิทยาลัย

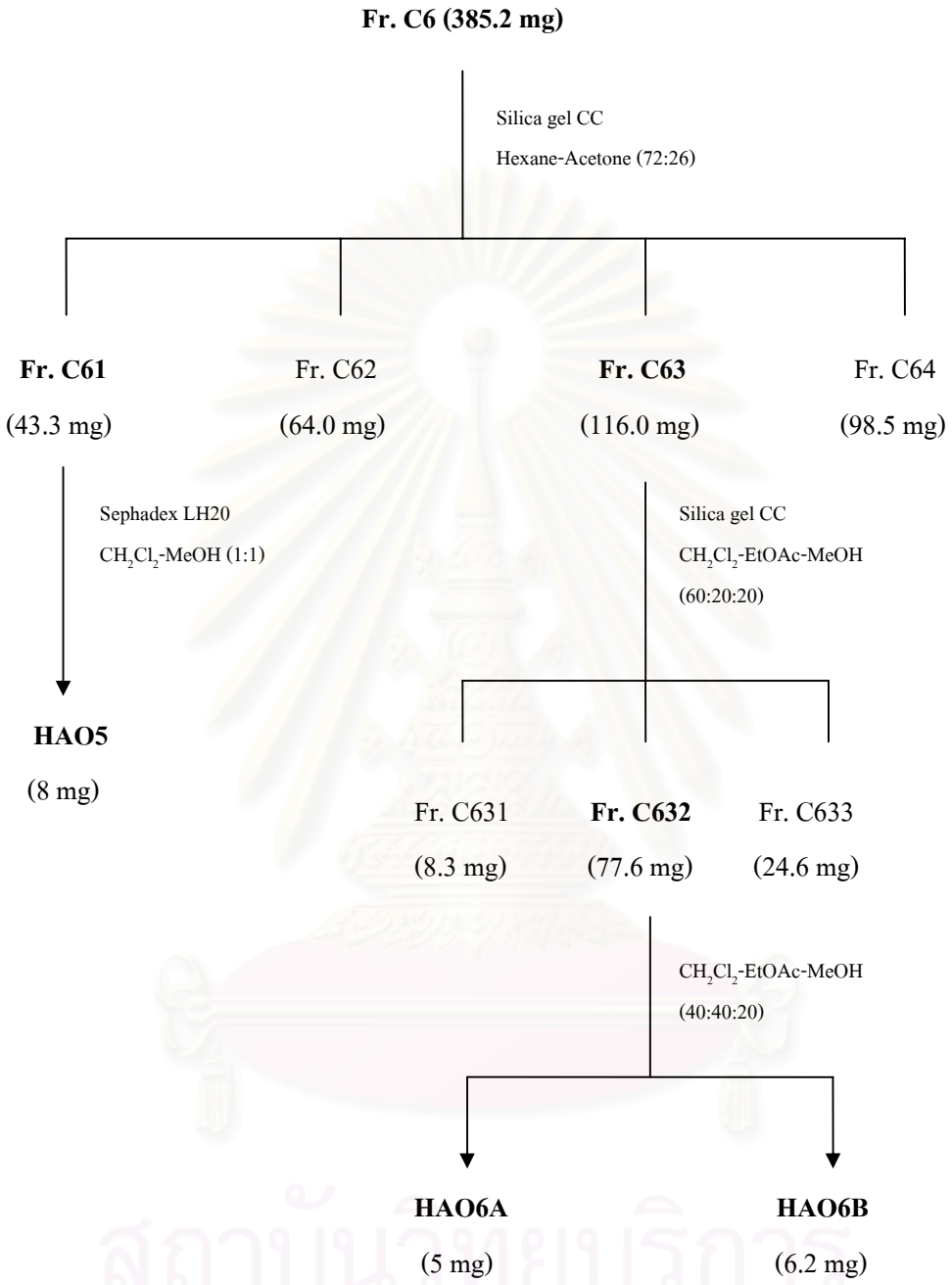

Scheme 3 Separation of the Hexane extract of the leaves of *Aglaia oligophylla* (continued)

สถาบันวิทยบริการ
จุฬาลงกรณ์มหาวิทยาลัย

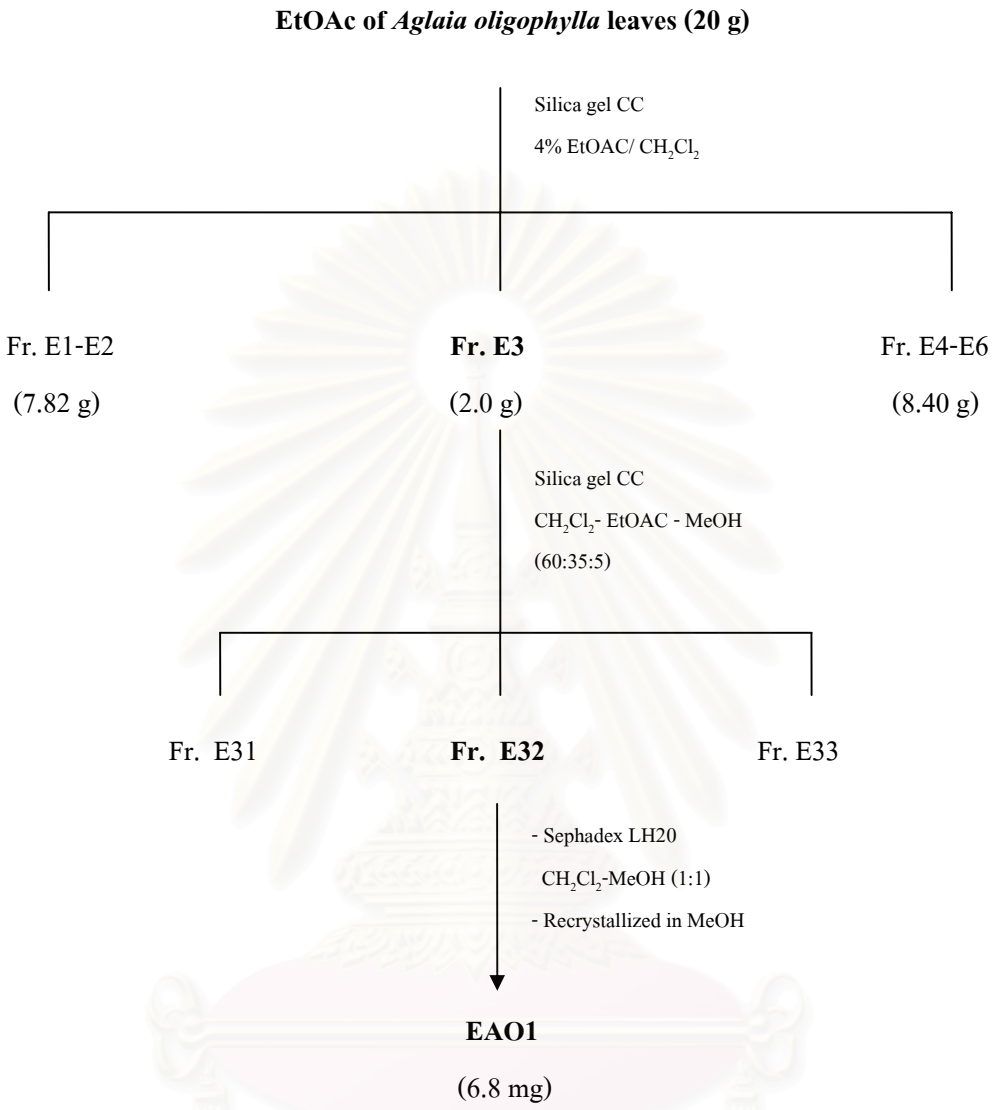

Scheme 4 Separation of the EtOAc extract of the leaves of *Aglaia oligophylla*

สถาบันวิทยบริการ
จุฬาลงกรณ์มหาวิทยาลัย

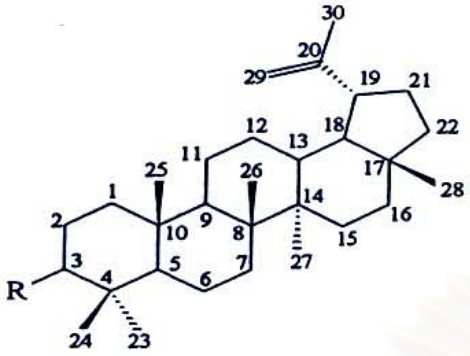

HAF1 R = =O

HAF2 R = β-OH

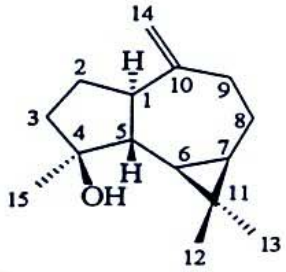

HAF3

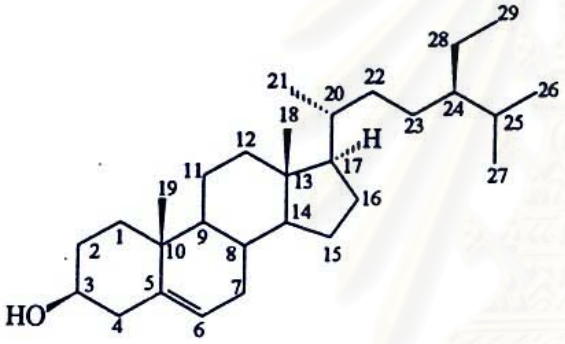

HAF4A

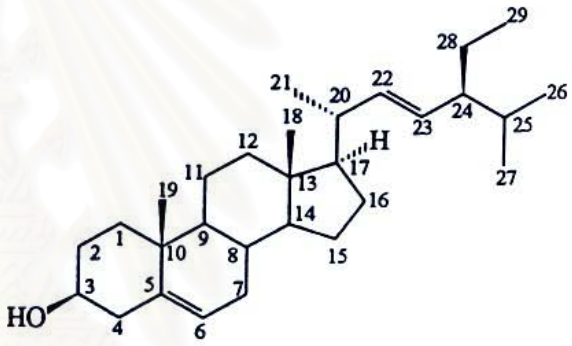

HAF4B

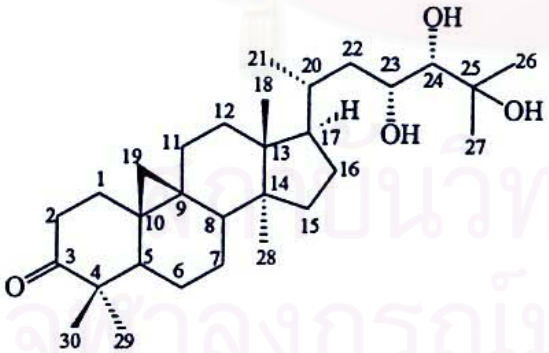

CAF1

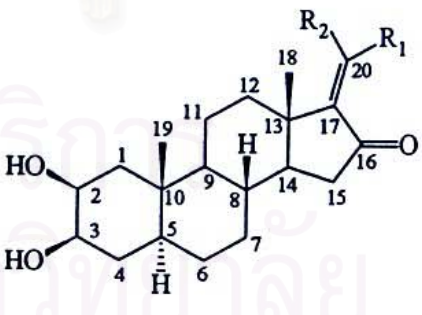

	R_1	R_2
CAF2	H	CH_3
CAF3	CH_3	H

Figure 4. Chemical structures of compounds isolated from *Aglaia forbesii* leaves

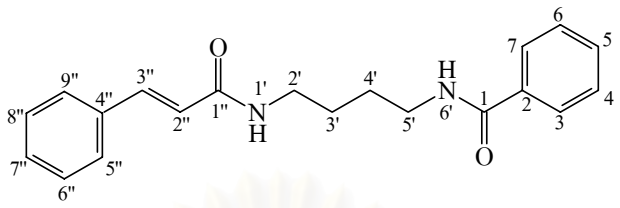

CAF4

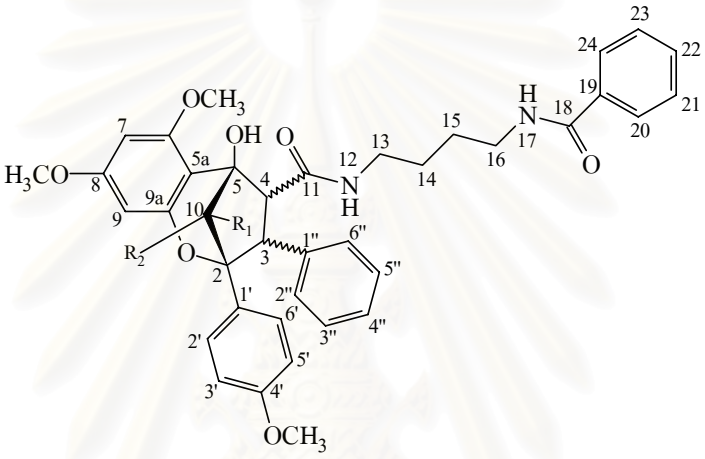

	R_1	R_2
CAF5	OH	H (3Hα,4Hβ)
CAF6	H	OH (3Hα,4Hβ)
CAF7	OH	H (3Hβ,4Hα)

สถาบันวิทยบริการ
จุฬาลงกรณ์มหาวิทยาลัย

Figure 4. Chemical structures of compounds isolated from *Aglaia forbesii* leaves (continued)

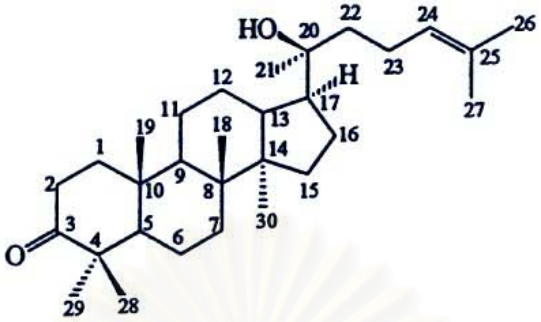

HAO1

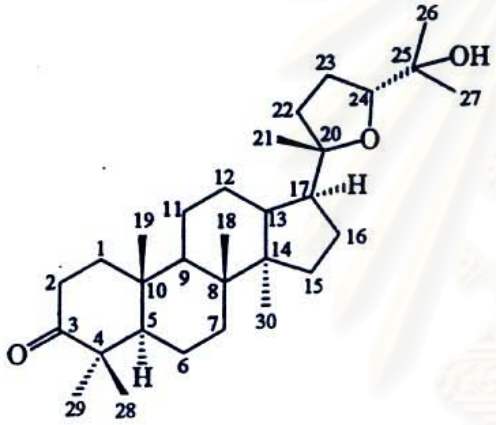

HAO2A

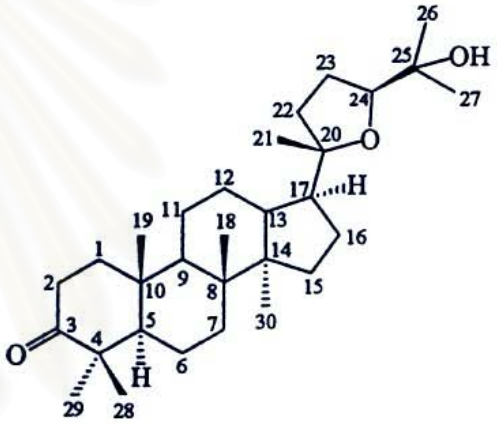

HAO2B

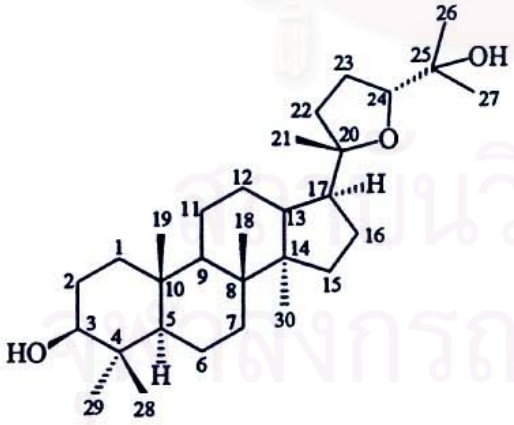

HAO3

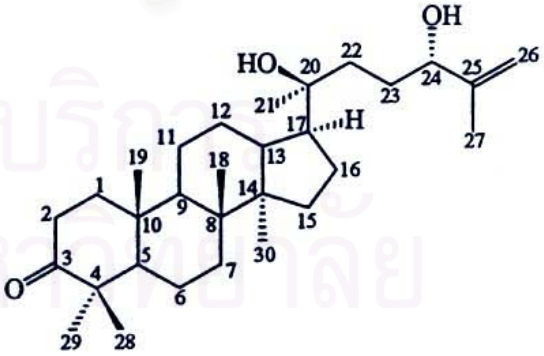

HAO4

Figure 5. Chemical structures of compounds isolated from *Aglaia oligophylla* leaves

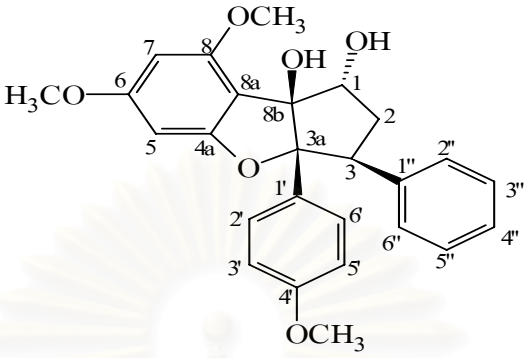

HAO5

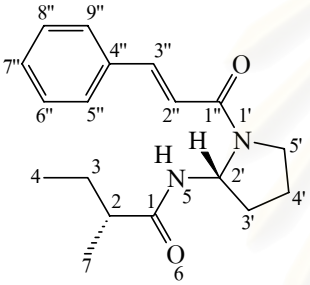

HAO6A

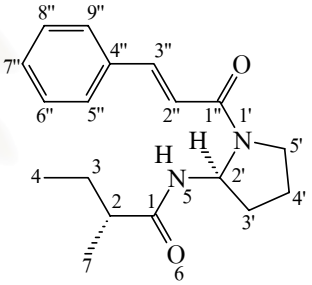

HAO6B

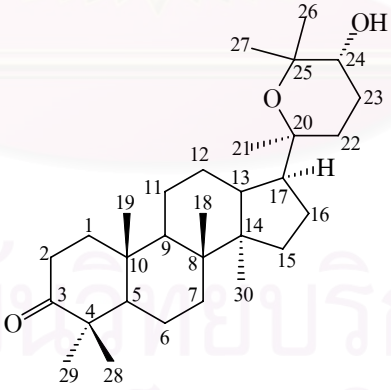

HAO7

Figure 5. Chemical structures of compounds isolated from *Aglaia oligophylla* leaves (continued)

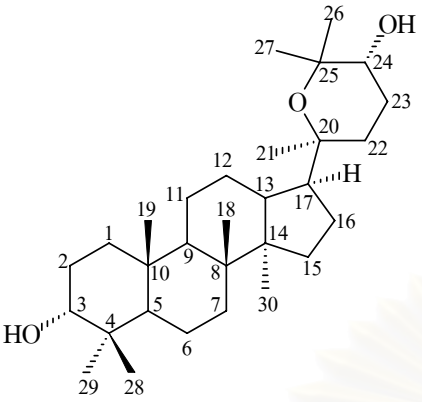

EAO7A

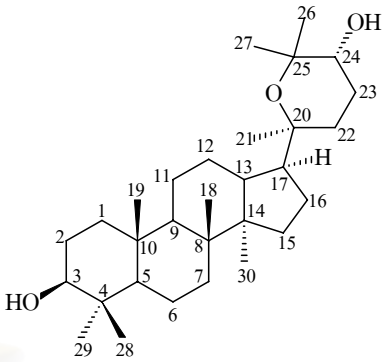

EAO7B

สถาบันวิทยบริการ
จุฬาลงกรณ์มหาวิทยาลัย

Figure 5. Chemical structures of compounds isolated from *Aglaia oligophylla* leaves (continued)

4. Physical and Spectral Data of Isolated Compounds

4.1 Compound HAF1

Compound HAF1 was obtained as colorless needles (10 mg, 0.0029 % yield).

ESITOFMS : *m/z* 424; $[M+H]^+$; **Figure 6**

Mp : 165-167 ^{o}C

$[\alpha]^{25}_{D}$: +60.6 ^{o} (*c* 0.5, $CHCl_3$)

IR : ν_{max} cm^{-1}, KBr disc; **Figure 7**

2941, 2870, 2857, 1705, 1644, 1455, 1381

^{1}H NMR : δ ppm, 400 MHz, in $CDCl_3$; **Figure 8, Table 3**

^{13}C NMR : δ ppm, 100 MHz, in $CDCl_3$; **Figure 9, Table 3**

4.2 Compound HAF2

Compound HAF2 was obtained as colorless needles (15 mg, 0.0016 % yield).

Mp : 213-215 ^{o}C

IR : ν_{max} cm^{-1}, KBr disc; **Figure 10**

3436, 2934, 2863, 1644, 1454, 1378, 1040, 881, 758, 476

^{1}H NMR : δ ppm, 300 MHz, in $CDCl_3$; **Figure 11, Table 4**

^{13}C NMR : δ ppm, 75 MHz, in $CDCl_3$; **Figure 12, Table 4**

4.3 Compound HAF3

Compound HAF3 was obtained as pale yellow oil (5 mg, 0.00014 % yield).

EIMS : *m/z* (% relative intensity); **Figure 13**

220 $[M]^+$ (40.4), 205 (100), 202 (30), 187 (37), 162 (49.5), 147 (45.2)

Mp : 147-149 ^{o}C

IR : ν_{max} cm^{-1}, KBr disc; **Figure 14**

3383, 2930, 2871, 1704, 1654, 1458, 1376, 917

^{1}H NMR : δ ppm, 400 MHz, in $CDCl_3$; **Figure 15, Table 5**

^{13}C NMR : δ ppm, 100 MHz, in $CDCl_3$; **Figure 16, Table 5**

4.4 Compound HAF4

Compound HAF4 was obtained as colorless needles (31 mg, 0.00089 % yield).

IR : ν_{max} cm^{-1}, KBr disc; **Figure 18**

3437, 2940, 2868, 1639, 1465, 1102, 1050, 477

^{1}H NMR : δ ppm, 300 MHz, in $CDCl_3$; **Figure 19**

^{13}C NMR : δ ppm, 75 MHz, in $CDCl_3$; **Figure 20, Table 6**

4.5 Compound CAF1

Compound CAF1 was obtained as white amorphous solid (5 mg, 0.000086 % yield).

EIMS : *m/z* (% relative intensity); **Figure 21**

474 $[M]^+$(12), 384 (7), 340 (11), 313 (8), 147 (13), 121(14), 91 (23), 59 (100)

HRESITOFMS : *m/z* = 497.3539 $[M+Na]^+$, $[M]^+$ = 474; **Figure 21**

Mp : 77-79 ^{o}C

$[\alpha]^{25}_{D}$: +17 ^{o} (*c* 0.3, $CHCl_3$)

IR : ν_{max} cm^{-1}, KBr disc; **Figure 22**

3419, 2928, 2870, 1706, 1462, 1456, 1378

^{1}H NMR : δ ppm, 400 MHz, in $CDCl_3$; **Figure 23, Table 7**

^{13}C NMR : δ ppm, 100 MHz, in $CDCl_3$; **Figure 24, Table 7**

4.6 Compound CAF2

Compound CAF2 was obtained as white amorphous solid (3 mg, 0.000086 % yield).

EIMS : *m/z* (% relative intensity); **Figure 34**

332 $[M]^+$ (100), 317 (77.9), 299 (29.6), 121 (87.1)

Mp : 208-211 ^{o}C

$[\alpha]^{25}_{D}$:-108.9 ^{o} (*c* 0.1, $CHCl_3$)

UV : λ_{max} nm (log ε), in MeOH; **Figure 35**

241 (3.35), 215 (3.14), 206 (3.23)

IR : ν_{max} cm^{-1}, KBr disc; **Figure 36**

3396, 2928, 1712, 1646, 1598, 1577, 1453, 1417, 1378, 1047

^{1}H NMR : δ ppm, 400 MHz, in $CDCl_3$; **Figure 38, Table 8**

^{13}C NMR : δ ppm, 100 MHz, in $CDCl_3$; **Figure 39, Table 8**

4.7 Compound CAF3

Compound CAF3 was obtained as white amorphous solid (3 mg, 0.000086 % yield).

ESITOFMS : *m/z* 332; $[M+H]^+$; **Figure 46**

Mp : 110-113 ^{o}C

$[\alpha]^{25}_{D}$: -85.0 ^{o} (*c* 0.12, $CHCl_3$)

UV : λ_{max} nm (log ε), in MeOH; **Figure 47**

206.2 (3.50)

IR : ν_{max} cm^{-1}, KBr disc; **Figure 48**

3390, 2926, 2853, 1716, 1737, 1645, 1598, 1558, 1453, 1415, 1379, 1047

^{1}H NMR : δ ppm, 400 MHz, in $CDCl_3$; **Figure 49, Table 9**

^{13}C NMR : δ ppm, 100 MHz, in $CDCl_3$; **Figure 50, Table 9**

4.8 Compound CAF4

Compound CAF4 was obtained as colorless needles (12 mg, 0.00034 % yield).

ESITOFMS : *m/z* 322; $[M+H]^{+}$; **Figure 51**

Mp : 173-174 ^{o}C

UV : λ_{max} nm (log ε), in MeOH; **Figure 52**

206.2 (4.54), 243.2 (4.54), 272 (4.46)

IR : ν_{max} cm^{-1}, KBr disc; **Figure 53**

3427, 3316, 1634, 1620, 1533, 1327, 1219, 986, 975, 715, 689

^{1}H NMR : δ ppm, 400 MHz, in DMSO-d_6; **Figure 54**, **Table 10**

^{13}C NMR : δ ppm, 100 MHz, in DMSO-d_6; **Figures 55-56, Table 10**

4.9 Compound CAF5

Compound CAF5 was obtained as white amorphous powder (10 mg, 0.0029 % yield).

EIMS : *m/z* (% relative intensity)

502 (3), 416 (11), 330 (26), 322 (44), 313 (60), 281 (15), 181 (21), 135 (44), 105 (74), 55 (100)

HRESITOFMS : *m/z* = 675.2690 $[M+Na]^{+}$, $[M]^{+}$ = 652; **Figure 57**

Mp : 129-131 ^{o}C

$[\alpha]^{25}_{D}$: +75 ^{o} (*c* 0.5, $CHCl_3$)

UV : λ_{max} nm, in MeOH; **Figure 58**

208.6 (4.3)

IR : ν_{max} cm^{-1}, KBr disc; **Figure 59**

3479, 3299, 2927, 2855, 1633, 1620, 1588, 1519, 1455, 1305, 1254, 1214, 1200, 1149, 1087, 832, 756, 669

^{1}H NMR : δ ppm, 500 MHz, in $CDCl_3$; **Figure 60, Table 11**

^{13}C NMR : δ ppm, 125 MHz, in $CDCl_3$; **Figure 61, Table 11**

4.10 Compound CAF6

Compound CAF6 was obtained as white amorphous powder (10 mg, 0.0029 % yield).

EIMS : *m/z* (% relative intensity)

416 (7), 330 (15), 322 (42), 313 (100), 181 (35), 135 (35), 131 (54), 105 (93), 55 (40)

HRESITOFMS : *m/z*= 675.2678 $[M+Na]^+$, $[M]^+$ = 652; **Figure 71**

Mp : 120-122 ^{o}C

$[\alpha]^{25}_{D}$: +20 ^{o} (*c* 0.5, $CHCl_3$)

UV : λ_{max} nm, in MeOH; **Figure 72**

207.6 (4.19)

IR : ν_{max} cm^{-1}, KBr disc; **Figure 73**

3478, 3287, 2931, 1633, 1620, 1589, 1539, 1515, 1455, 1303, 1252, 1215, 1201, 1182, 1151, 1101, 1085, 1051, 830, 817, 753, 700, 667

^{1}H NMR : δ ppm, 500 MHz, in $CDCl_3$; **Figure 74, Table 12**

^{13}C NMR : δ ppm, 125 MHz, in $CDCl_3$; **Figure 75, Table 12**

4.11 Compound CAF7

Compound CAF7 was obtained as white amorphous powder (6 mg, 0.00017 % yield).

EIMS : *m/z* (% relative intensity)

416 (22), 254 (11), 218 (18), 162 (52), 134 (25), 105 (100), 77 (95), 55 (44)

HRESITOFMS : *m/z* = 675.2684 $[M+Na]^+$, $[M]^+$ = 652; **Figure 86**

Mp : 144-146 ^{o}C

$[\alpha]^{25}_{D}$: -36 ^{o} (*c* 0.5, $CHCl_3$)

UV : λ_{max} nm, in MeOH; **Figure 87**

210 (4.33)

IR : ν_{max} cm^{-1}, KBr disc; **Figure 88**

3480, 3315, 2937, 1640, 1619, 1589, 1538, 1517, 1455, 1304, 1252, 1215, 1201, 1146,

1098, 832, 753, 700, 666

^{1}H NMR : δ ppm, 500 MHz, in $CDCl_3$; **Figure 89**, **Table 13**

^{13}C NMR : δ ppm, 125 MHz, in $CDCl_3$; **Figure 90, Table 13**

4.12 Compound HAO1

Compound HAO1 was obtained as colorless needles (30.4 mg, 0.018 % yield).

EIMS : *m/z* (% relative intensity); **Figure 99**

442$[M]^+$ (2.3), 424 (100), 355 (25.4), 313(14), 205 (48.7), 109 (84.2)

Mp : 134-136 ^{o}C

$[\alpha]^{25}_{D}$: +66 ^{o} (*c* 1.2 , $CHCl_3$)

IR : ν_{max} cm^{-1}, KBr disc; **Figure 100**

3480, 2950, 2869, 1704, 1455, 1376, 755

^{1}H NMR : δ ppm, 400 MHz, in $CDCl_3$; **Figure 101, Table 14**

^{13}C NMR : δ ppm, 100 MHz, in $CDCl_3$; **Figure 102, Table 14**

4.13 Compound HAO2

Compound HAO2 was obtained as colorless needles (24.7 mg, 0.015 % yield).

EIMS : *m/z* (% relative intensity); **Figure 104**

458 $[M]^+$ (0.4), 443 (3.3), 440 (3.8), 399 (26.9), 143 (100)

IR : ν_{max} cm^{-1}, KBr disc; **Figure 105**

3474, 1705, 2963, 2870,1459, 1382, 1376

^{1}H NMR : δ ppm, 500 MHz, in $CDCl_3$; **Figure 106, Table 15**

^{13}C NMR : δ ppm, 125 MHz, in $CDCl_3$; **Figure 107, Table 15**

4.14 Compound HAO3

Compound HAO3 was obtained as colorless needles (13 mg, 0.00076 % yield).

EIMS : *m/z* (% relative intensity); **Figure 113**

445 $[M\text{-}Me]^+$ (2.5), 427 (2.6), 401 (10.3), 383 (7.7), 143 (100)

Mp : 198-200 ^{o}C

$[\alpha]^{25}_{D}$: + 39 ^{o} (*c* 0.35, $CHCl_3$)

IR : ν_{max} cm^{-1}, KBr disc; **Figure 114**

3399, 2965, 2947, 1465, 1453, 1386, 1376, 1165, 1079, 1045, 984

^{1}H NMR : δ ppm, 400 MHz, in $CDCl_3$; **Figure 115, Table 16**

^{13}C NMR : δ ppm, 100 MHz, in $CDCl_3$; **Figure 116, Table 16**

4.15 Compound HAO4

Compound HAO4 was obtained as colorless needles (5.8 mg, 0.00034 % yield).

EIMS : *m/z* (% relative intensity); **Figure 119**

440 $[M-H_2O]^+$ (3.5), 313 (2.3), 143 (12.6), 125 (100), 107 (10.7), 81 14.3)

IR : ν_{max} cm^{-1}, KBr disc; **Figure 120**

3388, 2924, 2953, 2853, 1705, 1455, 1376, 757

^{1}H NMR : δ ppm, 400 MHz, in $CDCl_3$; **Figure 121, Table 17**

^{13}C NMR : δ ppm, 100 MHz, in $CDCl_3$; **Figure 122, Table 17**

4.16 Compound HAO5

Compound HAO5 was obtained as white amorphous solid (8 mg, 0.0047 % yield).

ESITOFMS : *m/z* = 455 $[M+Na]^+$; **Figure 127**

Mp : 75-77 ^{o}C

$[\alpha]^{25}_{D}$: - 125 ^{o} (*c* 0.48, $CHCl_3$)

UV : λ_{max} nm, in MeOH; **Figure 128**

207.4 (4.8)

IR : ν_{max} cm^{-1}, KBr disc; **Figure 129**

3500, 2927, 2853, 1610, 1514, 1498, 1454, 1441, 1250, 1217, 1201, 1183, 1147, 1128, 1116, 1062, 1034, 996, 819, 756, 699

^{1}H NMR : δ ppm, 500 MHz, in $CDCl_3$; **Figure 130, Table 18**

^{13}C NMR : δ ppm, 125 MHz, in $CDCl_3$; **Figure 131, Table 18**

4.17 Compound HAO6

Compound HAO6 was obtained as colorless needles (11.2 mg, 0.00071 % yield).

ESITOFMS : *m/z* = 323 $[M+Na]^+$; **Figure 134**

UV : λ_{max} nm, in MeOH; **Figure 135**

283.2 (3.92), 241.2 (4.06), 206.8 (3.54)

IR : ν_{max} cm^{-1}, KBr disc; **Figure136**

3291, 2961, 2924, 2853, 1648, 1727, 1734, 1599, 1535, 1453, 1416, 1260, 1094, 1026

^{1}H NMR : δ ppm, 500 MHz, in $CDCl_3$; **Figure 137, Table 19**

^{13}C NMR : δ ppm, 125 MHz, in $CDCl_3$; **Figure 138, Table 19**

4.18 Compound HAO7

Compound HAO7 was obtained as colorless needles (13.3 mg, 0.00078 % yield).

EIMS : *m/z* (% relative intensity); **Figure 142**

458 $[M]^+$ (3.1), 443 (4.1), 440 (6.8), 425 (2.3), 399 (17.9), 359 (6.2), 315 (3.2), 245 (9.2), 205 (18.1), 143 (100)

IR : ν_{max} cm^{-1}, KBr disc; **Figure 143**

3407, 2964, 2870, 1699, 1461, 1383, 1074, 755

Mp : 233-236 ^{o}C

^{1}H NMR : δ ppm, 400 MHz, in $CDCl_3$; **Figure 144, Table 20**

^{13}C NMR : δ ppm, 100 MHz, in $CDCl_3$; **Figures 145-146, Table 20**

4.19 Compound EAO1

Compound EAO1 was obtained as colorless needles (6.8 mg, 0.0004 % yield).

EIMS : *m/z* (% relative intensity); **Figure 148**

460 $[M]^+$ (0.3), 458 (0.8), 440 (1.5), 425 (2.3), 315 (3.2), 143 (100), 125 (13.4)

IR : ν_{max} cm^{-1}, KBr disc; **Figure 149**

3399, 2942, 2871, 1465, 1452, 1385, 1376, 1076, 1031, 932

^{1}H NMR : δ ppm, 500 MHz, in $CDCl_3$; **Figure 150, Table 21**

^{13}C NMR : δ ppm, 125 MHz, in $CDCl_3$; **Figures 151-152, Table 21**

สถาบันวิทยบริการ
จุฬาลงกรณ์มหาวิทยาลัย

5. Evaluation of Biological Activities

5.1 Determination of Antimycobacterial Activity

Antimycobacterial activity was assessed against *Mycobacterium tuberculosis* $H_{37}Ra$ using the Microplate Alamar Blue Assay (MABA) (Collins and Franzblau, 1997). The mycobacteria were grown in 100 ml of 7H9GC broth containing 0.005 % Tween 80. Culture was incubated in 500 ml plastic flask on a rotary shaker at 200 rpm and 37 °C until they reached an optical density of 0.4-0.5 at 550 nm. Bacteria were washed and suspended in 20 ml of phosphate-buffered saline and passed through a filter. The filtrates were aliquoted and stored at -80°C. The susceptibility testing was performed in 96-well microplates. Samples were initially diluted with either dimethyl sulfoxide or distilled deionized water, then diluted by Middlebrook 7H9 media containing 0.2 % v/v glycerol and 1.0 g/L 7H9GC broth, and subsequent two-fold dilutions were performed in 0.1 ml of 7H9CG broth in microplates. Frozen inocula were diluted 100 times in 7H9GC broth and adding of 0.1 ml to the well resulted in final bacterial titers of about 5 x 10^4 CFU/ml. The wells containing sample only were used to determine whether the test samples themselves can reduce the dye. Additional control wells were consisted of bacteria only (B) and medium only (M). Plates were incubated at 37 °C. Starting at day 6 of the incubation, 20 µl of Alamar Blue solution and 12.5 µl of 20 % Tween 80 were added to one B well and one M well, and the plates were reincubated at 37 °C. The B wells were observed for a color change from blue to pink, at which time reagents were added to all remaining wells. Plates were then incubated at 37 °C, and results were recorded at 24 h after the addition of reagents. Visual MIC values were defined as the lowest concentration of sample that prevented a color change. Rifampicin, isoniazid and kanamycin sulfate, which are standard drugs in the treatment of tuberculosis, were used as the reference compounds.

5.2 Determination of Antimalarial Activity

The parasite *Plasmodium falciparum* (K1, multi-drug resistant strain) was cultivated *in vitro* using the method of Trager and Jensen (Trager and Jensen, 1976) in RPMI 1640 medium containing 20 mM HEPES (N-2-hydroxyethylpiperazine-N′-2-ethanesulfonic acid), 32 mM $NaHCO_3$ and 10 % heat-inactivated human serum with 3 % erythrocytes and incubated at 37 ºC in an incubator with 3 % CO_2. The cultures were diluted with fresh medium and erythrocytes every day according to cell growth. Quantitative assessment of antimalarial activity *in vitro* was determined by microculture radioisotope

techniques based upon the method of Desjardins *et al.* (1979). Briefly, a mixture of 200 µl of 1.5 % erythrocytes with 1 % parasitemia at the early ring stage was pre-exposed to 25 µl of the medium containing a test sample dissolved in 1% DMSO (0.1 % final concentration) for 24 h, employing the incubation condition described above. Subsequently, 25 µl of [^{3}H]-hypoxanthine (Amersham, USA) in culture medium (0.5 µCi) were added to each well and the plates were incubated for an additional 24 h. Levels of incorporated labeled hypoxanthine indicating parasite growth were determined using the TopCount microplate scintillation counter (Packard, USA). The IC_{50} value represents the concentration which indicates 50 % reduction of parasite growth. The standard sample for positive control was dihydroartemisinine (DHA).

5.3 Determination of Cytotoxic Activity

5.3.1 Human Small Cell Lung Carcinoma (NCI-H187)

Cytotoxicity to NCI-H187 cells (human small cell lung carcinoma, ATCCCRL-5804) was determined by MTT assay (Plumb, Milroy and Kaye, 1989). Briefly, cells were diluted to 10^5 cells/ml. Test compounds were diluted in distilled water and added to microplates in a total volume of 200 µl. Plates were incubated at 37 °C, 5% CO_2 for 5 days. Then, 50 µl of 2 mg/ml MTT solution (3-[4,5-dimethylthiazol-2-yl]-2,5-diphenyltetrazolium bromine; thiazolyl blue) was added to each well of the plate. The plates were wrapped with aluminium foil and incubated for 4 h. After the incubation period, the microplates were spun at 200 rpm for 5 min. MTT was then removed from the wells and the formazan crystals were dissolved in 200 µl of DMSO and 25 µl of Sorensen's glycine buffer. Absorbance was read in microplate reader at the wavelength of 510 nm. The reference substance was ellipticine and doxorubicin. The activity was expressed as 50 % inhibitory concentration (IC_{50}). The criteria of cytotoxic potency of the compound testing in this system are as follows:

IC_{50} (µg/ml)	**Activity**
> 20	Inactive
> 10 – 20	Weakly active
5 – 10	Moderately active
< 5	Strongly active

5.3.2 Vero cell

Compounds were tested for their toxicity against Vero cells (African green monkey kidney fibroblast), using colorimetric microplate assay (Skehan *et al.*, 1990). Briefly, cells at a logarithmic growth phase were harvested and diluted to 10^5 cells/ml with fresh medium and gently mixed. Extracts or test compounds were diluted in distilled water and put into microplates in a total volume of 200 µl. Plates were incubated at 37 ºC, 5 % CO_2 for 72 h. After the incubation period, cells were fixed by 50 % trichloroacetic acid. The plates were incubated at 4 ºC for 30 min, washed with tap water and air-dried at room temperature. The plates were then stained with 0.05 % sulforhodamine B (SRB), dissolved in 1 % acetic acid for 30 min. After the staining period, SRB was removed with 1 % acetic acid. Plates were air-dried before the bound dye was solubilized with 10 mM Tris-base for 5 min on shaker. Absorbance was read in microplate reader at the wavelength of 510 nm. If % cell viability $\geq$ 50%, IC_{50} was reported as > 50 µg/ml and if % cell viability < 50%, IC_{50} was reported from two-fold serial dilution. Ellipticine and DMSO were used as positive and negative control, respectively.

5.4 Determination of Anti-Herpes Simplex Activity

Anti-herpes simplex virus type 1 (HSV-1) activity of pure compounds was tested against HSV-1 strain ATCC VR 260, using colorimetric microplate assay (Skehan et al., 1990). The growth of host cells (Vero cell line ATCC CCL-81) infected with the virus and treated with the extract was compared with control cells, which were infected with virus only. Acyclovir and DMSO were used as positive and negative control, respectively. The extracts were tested at non-cytotoxic concentrations (inhibition of cell growth < 50 %). The potency of activity criteria are as follows:

% Inhibition	**Potency of Activity**
25-35 %	weak active
35-50 %	moderate active
> 50 %	active

Extracts that inhibited virus more than 50 % were further tested to determine the IC_{50} values.

CHAPTER IV

RESULTS AND DISCUSSION

Chromatographic separation of the n-hexane fraction of the methanolic leaf extract of *Aglaia forbesii* King. yielded 5 compounds (HAF1, HAF2, HAF3 and HAF4; a mixture of HAF4A and HAF4B, whereas the CH_2Cl_2 fraction afforded 7 compounds (CAF1, CAF5, CAF6, CAF7, CAF2, CAF3 and CAF4).

The methalolic leaf extract of *Aglaia oligophylla* Miq. was mixed with Kieselguhr, packed in a column and eluted with n-hexane, EtOAc and MeOH, successively. Nine compounds (HAO1, HAO2; a mixture of HAO2A and HAO2B, HAO3, HAO4, HAO5, HAO6; a mixture of HAO6A and HAO6B, and HAO7) were isolated from the n-hexane fractions while the EtOAc fraction was chromatographed to yield compound EAO1 (a mixture of EAO1A and EAO1B).

The structure determination of these isolated compounds was based on spectroscopic methods (UV, IR, MS, 1D and 2D NMR), and comparison with those reported in the literature.

1. Structure Determination of Compounds Isolated from *Aglaia forbesii*

1.1 Identification of Compound HAF1

Compound HAF1 was isolated as colorless needle crystals. The molecular formula $C_{30}H_{49}O$ for this compound was deduced from its mass spectrum ($[M]^+$ at *m/z* 424) (**Figure 6**) in combination with the ^1H and ^{13}C APT spectrum (**Figures 8** and **9**) and its IR spectrum (**Figure 7**) which indicated the presence of carbonyl function (1705 cm^{-1}) and a terminal methylene group (1644 cm^{-1}).

Preliminary comparison of the ^1H and ^{13}C NMR spectral data (**Figures 8** and **9**) of this compound with those of HAF2 revealed that their NMR spectra were closely similar, including the presence of seven tertiary methyl groups and one isopropenyl group. However, instead of secondary alcohol as in HAF2, a keto carbonyl could be detected at δ_C 218 in this compound. Two singlet signals at δ_H 4.66/4.54 (each *br s*, H_2-29) in the ^1H NMR spectra indicated that an exomethylene group was still present in this molecule. All these data suggested that the compound has a lupane skeleton system identical to that of HAF1.

The assignment of ketone carbonyl at the C-3 position was deduced from the signal at δ_C 218

in the ^{13}C spectrum together with the deshielded methylene protons in the region δ_H 2.34-2.54 in the ^{1}H NMR spectrum, typical for H_2-2 vicinal to ketone group in a keto-triterpenoid (Tanaka, Tabuse and Matsunaga, 1988).

According to the above spectral evidence and by comparison of its ^{13}C NMR spectral data (**Table 3**) with the reported data (Carpenter, Sotheeswaran, and Sultanbawa, 1980), compound HAF1 was identifield as lupenone.

Lupenone, one of the most common triterpene, has previously been reported to exhibit strong viral plaque inhibitory effect against HSV-1 and HSV-2 (Madureira *et al*., 2003).

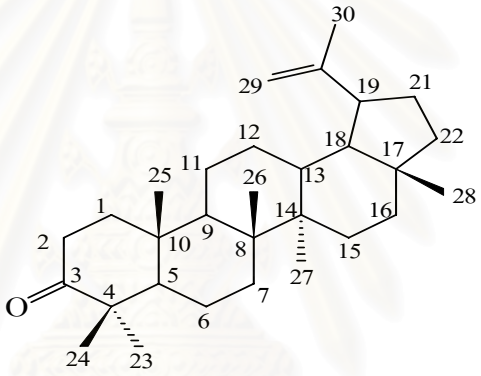

lupenone

สถาบันวิทยบริการ
จุฬาลงกรณ์มหาวิทยาลัย

Table 3. Comparison of the ^{13}C-NMR spectral data of lupenone and compound HAF1 ($CDCl_3$, 100 MHz)

Position	HAF1	Lupenone*	Position	HAF1	Lupenone*
	^{13}C (mult.)	^{13}C		^{13}C (mult.)	^{13}C
1	39.6 (*t*)	39.6	16	35.5 (*t*)	35.6
2	34.1 (*t*)	34.1	17	42.9 (*s*)	42.9
3	218.0 (*s*)	217.9	18	48.2 (*d*)	48.3
4	47.3 (*s*)	47.3	19	47.9 (*d*)	47.9
5	54.3 (*d*)	55.0	20	150.7 (*s*)	150.7
6	19.6 (*t*)	19.6	21	29.8 (*t*)	29.9
7	33.7 (*t*)	33.6	22	39.9 (*t*)	40.0
8	40.7 (*s*)	40.9	23	26.6 (*q*)	26.6
9	49.7 (*d*)	49.8	24	20.9 (*q*)	21.0
10	36.8 (*s*)	36.9	25	15.8 (*q*)	15.8
11	21.4 (*t*)	21.5	26	15.9 (*q*)	15.9
12	25.2 (*t*)	25.2	27	14.4 (*q*)	14.4
13	38.1 (*d*)	38.2	28	17.9 (*q*)	18.0
14	42.8 (*s*)	42.9	29	109.3 (*t*)	109.2
15	27.4 (*t*)	27.4	30	19.3 (*q*)	19.3

***** Carpenter, Sotheeswaran and Sultanbawa, 1980 (in $CDCl_3$, 100 Mz)

สถาบันวิทยบริการ
จุฬาลงกรณ์มหาวิทยาลัย

1.2 Identification of Compound HAF2

Compound HAF2 was obtained as colorless needle crystals. The compound gave violet color to Liebermann-Burchard test, indicating the presence of triterpenoid. The IR (**Figure 10**) spectrum showed the presence of hydroxyl group in this molecule (3436 cm^{-1})**.**

The ^{1}H NMR (**Figure 11**) spectrum exhibited signals corresponded to the lupane-type triterpenoid (Tanaka, Tabuse and Matsunaga, 1988) which including six tertiary methyl groups (δ_H 0.98, 0.77, 0.84, 1.04, 0.96 and 0.80; Me-23-Me-28, respectively), one vinylic methyl (δ_H 1.68, Me-30), one terminal methylene (δ_H 4.66/4.54, each *br s*, H_2-29), a C-3α carbinolic methine proton (δ_H 3.17, *dd*, *J* = 10.8, 5.4 Hz, H-3) and the remaining signals due to methylene and methine protons in the high field region (δ_H 0.90-1.70).

The ^{13}C NMR spectrum (**Figure 12**) together with the DEPT experiment resolved the 30 carbon signals as seven methyl, eleven methylene, six methine and six quaternary carbons, thus also supporting the triterpenoid structure. The presence of isopropenyl group was deduced from the signals of two olefinic carbons and the vinylic methyl carbon resonated at δ_C 150.9 (C-20), 109.3 (C-29) and 19.3 (C-30), respectively, in the ^{13}C spectrum and the corresponding signals in ^{1}H NMR spectrum including the resonances at δ_H 4.66/4.54 (each *br s*, H_2-29), and 1.69 (*s*, Me-30).

The assignment of the relative configuration at C-3 was based on the large coupling constant (δ_H 3.17, *dd*, *J* = 10.8, 5.4 Hz, H-3) of the axial carbinolic methine proton, indicating the β-equatorial orientation of 3-OH group.

HAF2 was finally identified to be lupeol, a pentacyclic triterpene of the lupane-type, by TLC comparison with authentic sample and comparison of the ^{1}H and ^{13}C NMR spectral data (**Table 4**) with those already reported (Reynolds, McLean and Poplawski, 1986).

Lupeol have recently been investigated for its various pharmacological and medicinal properties including anti-inflammatory activity (Geetha and Varalakshmi, 2001), cytotoxicity against human hepatocellular carcinoma (Hep-G2), human epidermoid carcinoma (A-431) and human leukemia HL-60 cells (Aratanechemuge *et al*., 2004; Moriarity *et al*., 1998), anti-angiogenic activity on *in vitro* tube formation of human umbilical vein endothelial cells (HUVEC) (You *et al*., 2003), and antimicrobial activity (Ajaiyeoba *et al*., 2003).

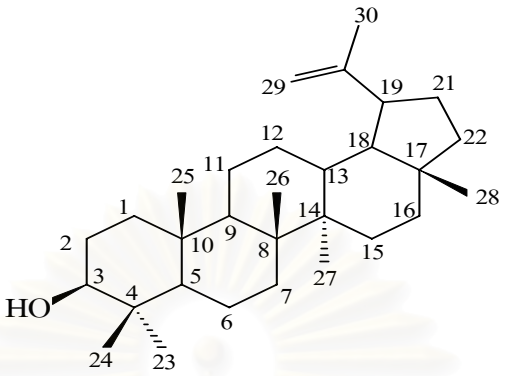

lupeol

Table 3. Comparison of the NMR spectral data of lupeol and compound HAF2 ($CDCl_3$, 75 MHz)

Position	Compound HAF2	Lupeol*	Position	Compound HAF2	Lupeol*
	^{13}C (mult.)	^{13}C		^{13}C (mult.)	^{13}C
1	38.7 (*t*)	38.6	16	35.5 (*t*)	35.5
2	27.4 (*t*)	27.3	17	42.9 (*s*)	42.9
3	79.9 (*d*)	78.9	18	48.3 (*d*)	48.2
4	38.8 (*s*)	38.8	19	47.9 (*d*)	47.9
5	55.3 (*d*)	55.2	20	150.9 (*s*)	150.8
6	18.3 (*t*)	18.2	21	29.8 (*t*)	29.8
7	34.2 (*t*)	34.2	22	40.0 (*t*)	39.9
8	40.8 (*s*)	40.7	23	27.9 (*q*)	27.9
9	40.4 (*d*)	50.3	24	15.3 (*q*)	15.3
10	37.1 (*s*)	37.1	25	16.1 (*q*)	16.1
11	20.9 (*t*)	20.9	26	15.9 (*q*)	15.9
12	25.1 (*t*)	25.0	27	14.4 (*q*)	14.4
13	38.0 (*d*)	38.0	28	17.9 (*q*)	18.0
14	42.8 (*s*)	42.7	29	109.3 (*t*)	109.2
15	27.4 (*t*)	27.4	30	19.3 (*q*)	19.3

***** Reynolds, McLean and Poplawski, 1986 (in $CDCl_3$, 100 Mz)

1.3 Identification of Compound HAF3

Compound HAF3 was obtained as pale yellow oil. The EI mass spectrum (**Figure 13**) displayed $[M]^+$ ion peak at *m/z* 220 corresponding to the molecular formula $C_{15}H_{24}O$. The EIMS also gave mass fragment peak at m/z 202 $([M-H_2O])^+$, suggesting the presence of hydroxyl group in this molecule. This was also confirmed by IR absorption band (**Figure 14**) at 3383 cm^{-1}.

The APT experiment (**Figure 16**) revealed 15 carbons including three tertiary methyl groups, five methylenes, four methines and three quaternary carbons, one of which was the oxygenated methine carbon (δ_C 80.9, C-4). Two quaternary carbons which resonated at δ_C153.4 (C-10) and 106.2 (C-14) were those of an exomethylene function.

The ^{1}H NMR spectra (**Figure 15**) also exhibited the signals of three tertiary methyl groups (δ_H 1.04, 1.05 and 1.28, 3H each, *s*), an exomethylene function (δ_H 4.69/4.67, each *br s*, H_2-14) and two most upfield signals of typical methine protons (δ_H 0.5, *dd*, *J* = 9.5, 11.3 Hz, H-6 and δ_H 0.5, *ddd*, *J* = 9.5, 11.3, 6.2 Hz, H-7) of the aromadendrane framework (Vizzotto *et al*., 2003) .

This compound was further proved to be an aromadendrane sesquiterpenoid by the analysis of 2D NMR (^{1}H-^{1}H COSY, HMQC and HMBC) spectra. The assignment of the hydroxyl group at C-4 was achieved by the downfield shift of this position and was further confirmed by the prominent cross peaks from Me-15 (δ_H 1.28, *s*) to C-3 (δ_C 41.7), C-4 (δ_C 80.9) and C-5 (δ_C 54.3) in the HMBC spectrum (**Figure 17**). Furthermore, HMBC correlations (**Figure 17**) from H_2-14 (δ_H 4.67/4.69, each *br s*) to C-1 (δ_C 53.4) and C-9 (δ_C 38.8), clearly indicated that an exomethylene function was placed in the position 10.

Based on analysis of the above spectral data (**Table 5**) and confirmed by comparison of previously published data (Brochini and Roque, 2000), HAF3 was identified as spathulenol.

The aromadendrane sesquiterpene spathulenol has already been isolated from *A. foveolata* and *A. lawii* (Roux *et al*., 1998). In addition, it was also reported to be the constituent of *Callicarpa japonica* (Verbenaceae), *Esenbeckia conspecta* (Rutaceae), *Nepeta macrosiphon* Boiss. (Lamiaceae) and the softcoral *Sinularia kavarattiensis* (Fraga, 2003).

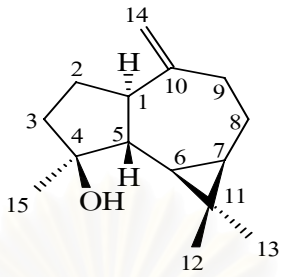

spathulenol

Table 5. Comparison of the NMR spectral data of spathulenol and compound HAF3 ($CDCl_3$, 400 MHz)

Position	HAF3		Spathulenol*	
	^{1}H (mult., *J* in Hz)	^{13}C (mult.)	^{1}H	^{13}C
1	2.20 (*m*)	53.4 (*d*)		53.4
2	1.92/1.64 (each *m*)	26.7 (*t*)		26.7
3	1.91/1.58 (each *m*)	41.7 (*t*)		41.7
4		80.9 (*s*)		81.0
5	1.30 (*m*)	54.3 (*d*)		54.3
6	0.50 (*dd*, 9.5, 11.3)	29.9 (*d*)	0.4-0.6	29.9
7	0.70 (*ddd*, 9.5, 11.3, 6.2)	27.5 (*d*)	0.4-0.6	27.5
8	1.98/1.01 (each *m*)	24.8 (*t*)		24.8
9	2.42/2.04 (each *m*)	38.8 (*t*)	2.42 (*m*)	38.8
10		153.4 (*s*)		153.4
11		20.2 (*s*)		20.2
12	1.04 (*s*)	28.6 (*q*)	1.04 (*s*)	28.6
13	1.05 (*s*)	16.3 (*q*)	1.05 (*s*)	16.3
14	4.67/4.69 (each *br s*)	106.2 (*t*)	4.66/4.69 (each *br s*)	106.2
15	1.28 (*s*)	26.1 (*q*)	1.29 (*s*)	26.1

***** Brochini and Roque, 2000 (in $CDCl_3$, 400 Mz)

1.4 Identification of Compound HAF4

Compound HAF4 was obtained as colorless needle crystals. TLC comparison of this compound with an authentic sample (Solvent system: Hexane-Acetone = 84:16), suggested HAF4 could be a mixture of β-sitosterol (HAF4A) and stigmasterol (HAF4B). This was further confirmed by the following evidences.

The ^{1}H NMR spectrum (**Figure 19**) exhibited the olefinic proton signal at δ_H 5.33, typical for position 6 of both β-sitosterol and stigmasterol, while two double doublet signals at δ_H 5.01 and 5.12 were assigned to H-22 and H-23 of stigmasterol, respectively. A desheilded signal at δ_H 3.54 in the ^{1}H NMR spectrum corresponded to the carbinolic methine proton of position 3. This was also confirmed by IR absorption (**Figure 18**) band at 3357 cm^{-1} (hydroxyl group).

The ^{13}C NMR spectrum (**Figure 20**) showed four olefinic carbons, two of which resonated at δ_C 138.3 and 129.3 were due to the signals for C-22 and C-23 of stigmasterol, respectively. The ratio of the mixture was deduced from the intregration value between H-6 and H-22 or H-23 to be 1:1.

Further comparison of the ^{13}C NMR spectral data of HAF4 with the data reported in the literature (Jahodar, Grygarova and Budesinsky, 1988; Rubinstein *et al.*, 1976), confirmed that this compound was a mixture of β-sitosterol and stigmasterol.

β-sitosterol, the most common plant sterol, has previously demonstrated to have interesting therapeutic properties such as antihyperglycemic (Invorra *et al.*, 1988), anti-inflammatory, and antipyretic activities (Gupta *et al.*, 1980).

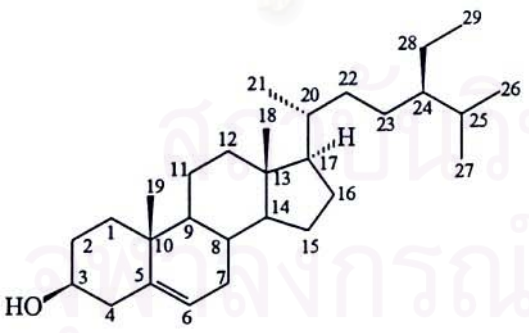

β-sitosterol

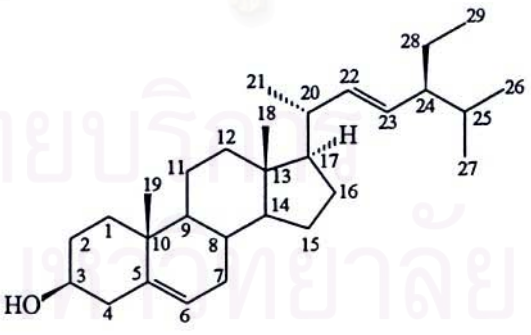

stigmasterol

Table 6. Comparison of the ^{13}C NMR spectral data of β-sitosterol and stigmasterol and compound HAF4 (a mixture of HAF4A and HAF4B) ($CDCl_3$, 75 MHz)

position	HAF4A (mult.)	β-Sitosterol*	HAF4B (mult.)	Stigmasterol*
1	37.2 (*t*)	37.2	37.2 (*t*)	37.2
2	31.7 (*t*)	31.7	31.7 (*t*)	31.7
3	71.7 (*d*)	71.7	71.7 (*d*)	71.8
4	42.3 (*t*)	42.3	42.2 (*t*)	42.4
5	140.8 (*s*)	140.8	140.8 (*s*)	140.8
6	121.7 (*d*)	121.7	121.7 (*d*)	121.7
7	31.9 (*t*)	31.9	31.9 (*t*)	32.0
8	31.9 (*d*)	31.9	31.9 (*d*)	32.0
9	50.1 (*d*)	50.1	50.1 (*d*)	50.2
10	36.5 (*s*)	36.5	36.5 (*s*)	36.6
11	21.1 (*t*)	21.1	21.1 (*t*)	21.1
12	39.8 (*t*)	39.8	39.7 (*t*)	39.7
13	42.3 (*s*)	42.3	42.3 (*s*)	42.4
14	56.8 (*d*)	56.8	56.9 (*d*)	56.9
15	24.3 (*t*)	24.3	24.4 (*t*)	24.4
16	28.2 (*t*)	28.2	28.9 (*t*)	29.0
17	56.0 (*d*)	56.0	56.1 (*d*)	56.1
18	12.0 (*q*)	11.9	12.2 (*q*)	12.1
19	19.4 (*q*)	19.4	19.4 (*q*)	19.4
20	36.1 (*d*)	36.1	40.5 (*d*)	40.5
21	18.8 (*q*)	18.8	21.2 (*q*)	21.1
22	33.9 (*t*)	33.9	138.3 (*d*)	138.0
23	26.1 (*t*)	26.1	129.3 (*d*)	129.3
24	45.8 (*d*)	45.8	51.2 (*d*)	51.3
25	29.1 (*d*)	29.1	32.0 (*d*)	32.0

Table 6. Comparison of the ^{13}C NMR spectral data of β-sitosterol and stigmasterol and compound HAF4 (a mixture of HAF4A and HAF4B) ($CDCl_3$, 75 MHz) (continued)

position	HAF4A (mult.)	β-Sitosterol*	HAF4B (mult.)	Stigmasterol*
26	19.8 (*q*)	19.8	21.3 (*q*)	21.3
27	19.0 (*q*)	19.0	18.9 (*q*)	19.0
28	23.1 (*t*)	23.1	25.4 (*t*)	25.4
29	12.0 (*q*)	11.9	12.2 (*q*)	12.3

* Rubinstein *et al*., 1976 (in $CDCl_3$, 100 Mz)

สถาบันวิทยบริการ
จุฬาลงกรณ์มหาวิทยาลัย

1.5 Structure Elucidation of Compound CAF1

Compound CAF1 was obtained as white amorphous solid. Its IR spectrum (**Figure 22**) indicated the presence of hydroxy group (3419 cm^{-1}) and ketone carbonyl (1706 cm^{-1}). EI mass apectrum (**Figure 21**) of this compound showed a molecular mass of *m/z* = 474 corresponding to the molecular formula $C_{30}H_{50}O_4$.

The ^{1}H and ^{13}C NMR spectra (**Figures 23** and **24**) were typical for triterpenes of the cycloartane series. The high field pair of doublets at δ_H 0.76 (H-19a) and 0.55 (H-19b) with a geminal coupling constant of 4.3 Hz was characteristic for this class of triterpenes (Inada *et al*., 1995). The typical 3-keto carbonyl resonated in the ^{13}C NMR at δ_C 216.6 and the pair H-2ax and H-2eq at δ_H 2.71 and 2.30 in the ^{1}H NMR. Two deshielded signals at δ_H 4.13 and 3.18 indicated two secondary alcohol functions. This was supported by the corresponding doublets in the ^{13}C NMR at δ_C 75.0 and 69.7. Additionally, a singlet at δ_C 74.3 indicated a tertiary alcohol. The molecular formula $C_{30}H_{50}O_4$ (*m/z* 474) is in agreement with one keto and three alcohol functions. The ^{13}C resonances (see **Table 7**) of the basic tetracyclic system of cycloartanes were almost identical with literature data, e.g. 21*S*,24*R*-dihydroxycycloart-25-en-3-one isolated from *A. rubiginosa* (Weber *et al*., 2000). The structure and shift assignments of the remaining 23,24,25-triol side chain atoms were straightforward using 2D methods (^{1}H-^{1}H COSY, HSQC, HMBC, NOESY) (**Figures 25-33**). Inspection of the ^{1}H-^{1}H COSY spectrum showed that a methyl-group doublet (δ_H 0.94) associated with C-21 formed part of a CH_3-CH-CH_2 fragment which allowed identification of positions C-21, C-20 and C-22, respectively. Furthermore, H_2-22 coupled to the oxygenated methine proton (δ_H 4.13, *dd*, *J* = 9.4, 4.8 Hz, H-23) , which show additional coupling to neigbouring oxygenated methine proton (δ_H 3.18, *br s*, *J* < 0.5 Hz, H-24) in the COSY spectrum. Analysis of the HMQC spectrum indicated that these two deshielded methines should be placed at C-23 and C-24, respectively. This was also supported by the HMBC spectrum, which showed correlations between H_2-22/C-23, C24, H-23/C-22, C-24, and Me-21/C-17, C-20, C-22. Finally, two geminal methyl groups could be placed on an oxygenated quaternary carbon (C-25) *via* their HMBC correlations to this carbon and to another carbon of position 24. This complete the side chain of compound CAF1.

Contrary to cycloartanes, this triol side chain is rather common in the related tirucallanes. An X-ray analysis of piscidinol A and 24-epi-piscidinol A proved 23*R*,24*S* configuration for the former and 23*R*,24*R* for the latter (McChesney *et al*., 1997). 24-Epi-piscidinol A was found also in *A.*

andamanica (Puripattanavong *et al*., 2000), however, the ^{13}C chemical shifts of the side chain did not agree with our data. The most striking difference in the ^{1}H NMR was the coupling constant $^{3}J_{(H\text{-}23,H\text{-}24)}$ which was 8.1 Hz, compared to almost zero in CAF1. The resonance for H-24 of CAF1 appeared as a slightly broad singlet (δ_H 3.18, $J < 0.5$ Hz) and as a consequence H-23 was a double doublet (δ_H 4.13, $J =$ 9.4, 4.8 Hz). A broad singlet for H-24 was also observed for piscidinol A and B (McChesney *et al*., 1997; Govindachari *et al*., 1995) and the ^{13}C resonances of the side chain agreed also quite well. This implied that the configurations of the side chain in CAF1 are 23*R*,24*S* or 24*S*,24*R*. These two possibilities would show the same NMR pattern and, additionally, one should have in mind that the configurations at carbon atoms 13, 14, 17, and 20 are reversed in the tirucallanes and the same may be true for positions 23 and 24. The known absolute configuration 20*R*, common for all cycloartanes, could be used for the correlation of the side chain configurations. Characteristic NOEs prove that 23*R*,24*S* is indeed correct. It is interesting that the absolute configurations of the two alcohol functions were identical in tirucallanes and cycloartanes, whereas all other comparable configurations were opposite in the two series.

The complete structure corresponds to the usual representation in literature. The partial structure shows a different conformation (rotation about the C20-C22 bond) and is based on the X-ray structure of piscidinol A. Note that a change in conformation by rotation about a single bond inverts the up and down positions within the chain attached to this bond, the absolute configurations remain of course unchanged. Only this more natural presentation is compatible with the NOEs and all observed couplings. Large coupling constants were observed for transoid arrangements like $^{3}J_{(H\text{-}22a,H\text{-}20)} = 9.6$ Hz and $^{3}J_{(H\text{-}22b,H\text{-}23)} = 9.4$ Hz and small values for cisoid relationships like $^{3}J_{(H\text{-}22a,H\text{-}23)} = 4.8$ Hz, $^{3}J_{(H\text{-}22a,H\text{-}20)} \sim 4.0$ Hz, and $^{3}J_{(H\text{-}23,H\text{-}24)} < 0.5$ Hz (transoid means one H up and the other one down, cisoid means both protons on the same side, either both up or both down). The resonances of Me-26 and Me-27 can also be discriminated by means of different NOE effects. Both terminal methyl groups show NOE contacts to both protons H-23 and H-24, however, in the case of H-23 the NOE to H_3-26 is clearly stronger, in the case of H-24 the NOE to H_3-27. This results in ageometry with all three OH groups pointing upwards in the correct stereochemical view of CAF1, an arrangement which is stabilized by hydrogen bonding. Optimized hydrogen bonds are also the reason that the vicinal torsional angle between H-23 and H-24 is widened up to 80 or 90° (therefore $^{3}J_{(H\text{-}23,H\text{-}24)} < 0.5$ Hz). This results in a smaller torsional angle of about 30 or 40° between 23-OH and 24-OH, allowing a better formation of a hydrogen bond. Due to the many substituents

and extensive hydrogen bridging of the three OH functions the chain is relatively rigid and a detailed conformational analysis was possible. The derived structure of CAF1 was (23*R*,24*S*)-23,24,25-trihydroxycycloartan-3-one. This compound have not been described yet in the literature.

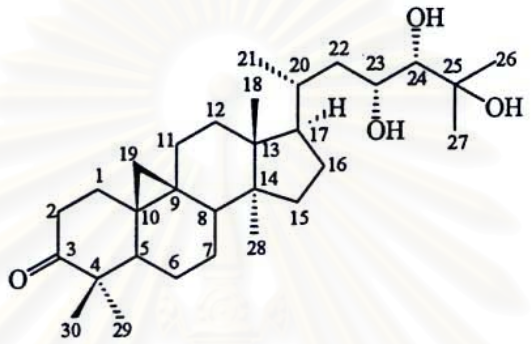

(23*R*,24*S*)-23,24,25-trihydroxycycloartan-3-one

Table 7. NMR spectral data of CAF1 and partial comparison of the ^{13}C resonances with those of 21*S*,24*R*-dihydroxycycloart-25-en-3-one ($CDCl_3$, 500 MHz)

position	CAF1			21*S*,24*R*-Dihydroxycycloart-25-en-3-one*
	^{1}H (mult., *J* in Hz) *	^{13}C (mult.)	HMBC	^{13}C
1	1.80/1.48 (each *m*)	33.4 (*t*)	C-3, C-10, C-19	33.4
2	2.71/2.30 (each *m*)	37.5 (*t*)	C-3	37.4
3		216.6 (*s*)		216.5
4		50.2 (*s*)		50.2
5	1.63 (*m*)	48.4 (*d*)	C-3, C-10, C-19, C-28	48.4
6	1.50/1.02 (each *m*)	21.5 (*t*)		21.4
7	1.98/1.10 (each *m*)	25.8 (*t*)	C-9, C-18	25.8
8		47.8 (*d*)		47.8
9		21.0 (*s*)		21.0
10		26.0 (*s*)		26.0

Table 7. NMR spectral data of CAF1 and partial comparison of the ^{13}C resonances with those of 21*S*,24*R*-dihydroxycycloart-25-en-3-one ($CDCl_3$, 500 MHz) (continued)

position	CAF1			21*S*,24*R*-Dihydroxycycloart-25-en-3-one*
	^{1}H (mult., *J* in Hz)	^{13}C (mult.)	HMBC	^{13}C
11	1.30 (*m*)	26.7 (*t*)	C-9, C-12	26.6
12	1.60 (*m*)	32.9 (*t*)	C-11, C-18	32.1
13	1.50 (*m*)	54.4 (*s*)	C-14	45.1
14		48.8 (*s*)		48.8
15	1.24 (*m*)	35.5 (*t*)	C-30	35.4
16	1.90/1.26 (each *m*)	28.4 (*t*)	C-17	27.5
17	1.56 (*m*)	53.1 (*d*)	C-16	46.4
18	0.98 (*s*)	18.2 (*q*)	C-8, C-13, C-14, C-15	18.3
19	0.76/0.55 (each *d*, 4.3)	29.5 (*t*)	C-1, C-5, C-9, C-10, C-11	29.5
20	1.44 (*m*)	33.6 (*d*)		-
21	0.91 (*d*, 6.0)	18.8 (*q*)	C-17, C-20, C-22	-
22	1.12 (*dd*, 9.6, 4.8) 1.83 (*dd*, 9.4, 4.0)	40.7 (*t*)	C-23, C-24	-
23	4.13 (*dd*, 9.4, 4.8)	69.7 (*d*)	C-20, C-22, C-24, C-25	-
24	3.18 (*br s*)	75.0 (*d*)	C-22, C-23, C-26, C-27	-
25		74.3 (*s*)		-
26	1.29 (*s*)	26.2 (*q*)	C-23, C-24, C-25, C-27	-
27	1.31 (*s*)	27.5 (*q*)	C-23, C-24, C-25, C-26	-
28	1.07 (*s*)	22.2 (*q*)	C-3, C-4, C-5, C-29	22.2
29	1.02 (*s*)	20.8 (*q*)	C-3, C-4, C-5, C-28	20.7
30	0.91 (*s*)	19.3 (*q*)	C-8, C-12, C-14, C-17	19.4

***** Weber *et al.*, 2000 (in $CDCl_3$, 100 MHz)

1.6 Identification of Compound CAF2

Compound CAF2 was obtained as white amorphous solid. EI mass spectroscopy **(Figure 34)** showed molecular ion peak at *m/z* 332, suggesting the molecular formula of $C_{21}H_{32}O_3$. IR spectrum (**Figure 36**) exhibited both hydroxyl and α,β-unsaturated ketone absorption maxima at 3396 cm^{-1} and 1712 cm^{-1}, respectively.

The ^1H NMR spectrum (**Figures 37** and **38**) showed the presence of two tertiary methyls (δ_H 1.01, *s*, Me-18 and 1.05, *s*, Me-19) and one deshielded vinylic methyl (δ_H 1.84, *d*, *J* = 7.5 Hz, Me-21). In addition, there was one olefinic proton quartet (δ_H 6.48, *q*, *J* = 7.5 Hz), suggesting that this olefinic proton was coupled with the vinylic methyl.

The ^{13}C APT spectrum (**Figure 39**) of this compound showed three methyl groups (δ_C 17.6, 14.4 and 13.1), two olefinic carbons (δ_C147.9 and 129.9), two oxygenated methine carbons (δ_C 72.3 and 70.0) and one ketonic carbony (δ_C 206.5).

All these NMR spectral data, together with the detailed analysis of 2D-NMR (^1H-^1H COSY, HMQC and HMBC) (**Figures 40-45**) allowed the assignment for this compound to be a pregnane steroid. The signals at δ_H 3.66 (*ddd*, *J* = 11.3, 4.0, 2.8 Hz, H-3) and 4.03 (*dt*, *J* = 4.0, 2.8 Hz, H-2), were assigned to a pair of adjacent axial and equatorial carbinolic methine protons, and each of which was further coupled with a methylene group.

The ketone group was located at C-16 as assigned by the HMBC correlations (**Figure 43**) from the C-16 carbonyl carbon to both H_2-15 (δ_H 2.19/1.98, *m*) and H-20 (6.48, *q*, *J*=7.5 Hz). Furthermore, placement of double bond at C-17 was established by the prominent cross peaks from Me-21 (1.84, *d*, *J* = 7.5 Hz) to C-13 (δ_C 17.6) and C-16 (δ_C 206.5), in the HMBC spectrum (**Figures 44** and **45**).

Finally, from a detailed comparison of the NMR spectral data (**Table 8**) of CAF2 with those already reported (Inada *et al*., 1997a), the structure of this compound was established as 2β,3β-dihydroxy-5α-pregn-17(20)-(*E*)-en-16-one.

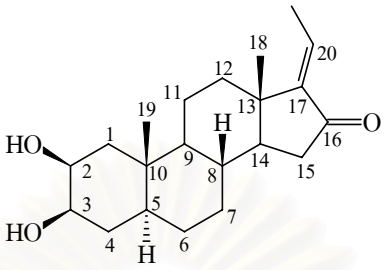

2β,3β-dihydroxy-5α-pregn-17(20)-(*E*)-en-16-one

Table 8. Comparison of the NMR spectral data of 2β,3β-dihydroxy-5α-pregn-17(20)-(*E*)-en-16-one and compound CAF2 ($CDCl_3$, 500 MHz)

Position	**CAF2**		**2β,3β-Dihydroxy-5α-pregn-17(20)-(*E*)-en-16-one***	
	^{1}H (mult., *J* in Hz)	**^{13}C (mult.)**	**^{1}H**	**^{13}C**
1	2.10/1.14 (each *m*)	42.7 (*t*)		42.8
2	4.03 (*dt*, 4.0, 2.8)	70.0 (*d*)	4.04 (*dt*, 4.0, 2.8)	70.1
3	3.66 (*ddd*, 11.3, 4.0, 2.8)	72.3 (*d*)	3.66 (*ddd*, 11.3, 4.0, 2.8)	72.3
4	1.69/1.38 (each *m*)	32.4 (*t*)		32.4
5	1.17 (*tt*, 11.4, 2.6)	45.2 (*d*)	1.17 (*tt*, 11.7, 2.8)	45.3
6	1.35 (*m*)	28.0 (*t*)		28.1
7	1.62 (*m*)	31.8 (*t*)		31.9
8	1.50 (*m*)	33.5 (*d*)		33.6
9	0.80 (*m*)	54.9 (*d*)		55.0
10		35.4 (*s*)		35.5
11	1.71 (*m*)	21.0 (*t*)		21.1
12	2.30 (*m*)	36.3 (*t*)		36.4
13		43.4 (*s*)		43.5
14	1.42 (*m*)	49.9 (*d*)		50.0

Table 8. Comparison of the NMR spectral data of 2β,3β-dihydroxy-5α-pregn-17(20)-(*E*)-en-16-one and compound CAF2 ($CDCl_3$, 500 MHz) (continued)

Position	**CAF2**		**2β,3β-Dihydroxy-5α-pregn-17(20)-(*E*)-en-16-one***	
	^{1}H (mult., *J* in Hz)	**^{13}C (mult.)**	**^{1}H**	**^{13}C**
15	2.19/1.98 (each *m*)	37.9 (*t*)	1.98 (*dd*, 16.9, 14.1, H-15a) 2.19 (*dd*, 16.9, 6.9, H-15b)	37.9
16		206.5 (*s*)		206.4
17		147.9 (*s*)		148.0
18	1.01 (*s*)	17.6 (*q*)	1.01 (*s*)	17.7
19	1.05 (*s*)	14.4 (*q*)	1.06 (*s*)	14.5
20	6.48 (*q*, 7.5)	129.0 (*d*)	6.49 (*q*, 7.7)	129.0
21	1.84 (*d*, 7.5)	13.1 (*q*)	1.84 (*d*, 7.7)	13.1

* Inada *et al.*, 1997a (in $CDCl_3$, 400 MHz)

สถาบันวิทยบริการ
จุฬาลงกรณ์มหาวิทยาลัย

1.7 Identification of Compound CAF3

Compound CAF3 was obtained as white amorphous solid. Its molecular formula was determined by ESI-TOF MS (**Figure 46**) as $C_{21}H_{32}O_3$, from its $[M+H]^+$ ion peak at *m/z* 333 and the IR absorption bands (**Figure 48**) at 3390 and 1716 cm^{-1} were suggestive of the presence of hydroxyl and carbonyl groups in this structure.

The ^1H and ^{13}C NMR spectra (**Figures 49** and **50**) were closely identical to those of CAF2 with the presence of two tertiary methyl groups, one vinylic methyl, two oxygenated methines and one ketone function. In the ^1H NMR spectrum, however, the chemical shift of the olefinic proton (δ_H 5.67, *q*, 7.3 Hz) of this compound significantly differed from that of CAF2.

The data above suggested that the two compounds are the *Z*/*E* isomers of the side chain moiety. The *Z* configuration of this compound was established based on the appearance of the olefinic proton signal at higher field (δ_H 5.67, *q*, 7.3, H-20) compared with CAF2 due to the orientation away from the ketonic carbonyl (δ_C 194.5).

Finally, from a detailed comparison of the NMR spectral data (**Table 9**) of CAF3 with previously reported data (Inada *et al*., 1997a), confirmed the structure of this compound as 2β,3β-dihydroxy-5α-pregn-17(20)-(*Z*)-en-16-one.

The occurrence of similar pregnane steroids to the ones isolated in this study is quite rare in the plant kingdom, and such compounds have only been isolated from three species in the Meliaceae family [*Melia volkensii* (Roger, Zeng and McLaughlin, 1998), *Aglaia grandis* (Inada *et al*, 1997) and *Aglaia ponapensis* (Angela *et al*., 2007)]

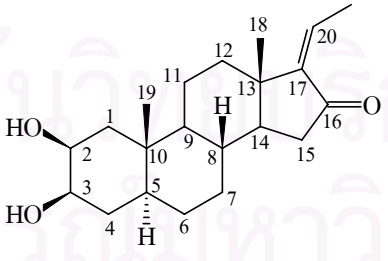

2β,3β-dihydroxy-5α-pregn-17(20)-(*Z*)-en-16-one

Table 9. Comparison of the NMR spectral data of 2β,3β-dihydroxy-5α-pregn-17(20)-(*Z*)-en-16-one and compound CAF3 ($CDCl_3$, 500 MHz)

Position	**CAF3**		**2β,3β-Dihydroxy-5α-pregn-17(20)-(*Z*)-en-16-one***	
	^{1}H (mult., *J* in Hz)	**^{13}C (mult.)**	**^{1}H**	**^{13}C**
1		42.1 (*t*)		42.9
2	4.02 (*dt*, 3.8, 2.6)	70.0 (*d*)	4.04 (*dt*, 4.0, 2.8)	70.1
3	3.62 (*ddd*, 11.8, 3.8, 2.5)	72.3 (*d*)	3.65 (*ddd*, 11.5, 4.0, 2.7)	72.3
4		32.4 (*t*)		32.5
5	1.17 (*tt*, 11.5 , 2.6)	45.3 (*d*)	1.17 (*tt*, 11.9 , 2.9)	45.4
6		28.0 (*t*)		28.1
7		31.8 (*t*)		31.9
8		33.8 (*d*)		34.0
9		55.2 (*d*)		55.2
10		35.4 (*s*)		35.6
11		20.7 (*t*)		21.0
12		35.7 (*t*)		35.8
13		42.8 (*s*)		43.4
14		49.4 (*d*)		49.5
15	2.00/2.16 (each *m*)	39.4 (*t*)	2.00 (*dd*, 17.3, 13.9, H-15a) 2.18 (*dd*, 17.3, 7.1, H-15b)	39.5
16		194.5 (*s*)		208.7
17		147.5 (*s*)		148.4
18	0.88 (*s*)	19.6 (*q*)	0.91 (*s*)	19.7
19	1.03 (*s*)	14.4 (*q*)	1.05 (*s*)	14.5
20	5.67 (*q*, 7.3)	129.9 (*d*)	5.69 (*q*, 7.3)	130.0
21	2.05 (*d*, 7.3)	13.2 (*q*)	2.07 (*d*, 7.3)	14.1

* Inada *et al*, 1997a (in $CDCl_3$, 400 MHz)

1.8 Identification of Compound CAF4

Compound CAF4 was obtained as colorless needle crystals. Its molecular formula was determined by ESI-TOFMS (**Figure 51**) as $C_{20}H_{22}N_2O_2$, from its $[M+H]^+$ ion peak at *m/z* 323. The prominent and broad maxima at 272 nm in the UV spectrum (**Figure 52**) as well as the typical IR absorption bands (**Figure 53**) at 3316-3427 cm^{-1} (NH) , 1620-1634 cm^{-1} (>N-C=O) and 1533 cm^{-1} (C=C), showed that this compound belongs to the group of bisamides characteristic for *Aglaia* species (Greger *et al*., 2001). In addition, the proton signals at δ_H 8.13 and 8.48 in the ^{1}H NMR spectrum (**Figure 54**) as well as the signals resonated at δ_C 164.9 and 166.2 in ^{13}C NMR spectrum (**Figures 55** and **56**) further confirmed the presence of two amide functions.

Previous phytochemical investigation of a number of *Aglaia* species (Brader *et al*., 1998; Greger *et al*., 2000; Seger *et al*., 2002) revealed that the cinnamic acid derived bisamides consist of two acid moieties linked with the diamine part (Brader *et al*., 1998). The occurrence of a pair of doublets at δ_H 7.42 (H-3$''$) and 6.63 (H-2$''$) and ten aromatic protons in the region δ_H 7.35-7.84 together with two carbonyl carbons at δ_C 164.9 and 166.2 suggested the two acid moieties in this molecule would be a cinnamic and a benzoic acid. The large coupling constant of 15.8 Hz between the pair of doublets at δ_H 7.42 and 6.63 suggested the *trans* double bond.

The analysis of the ^{1}H and ^{13}C APT spectral data indicated the signals of diamine part as including four methylene protons in the region δ_H 1.43-1.64 and four other deshielded methylene protons as two double doublets at δ_H 3.21 (*dd*, *J* =12.5, 6.6 Hz, H_2-2$'$) and 3.28 (*dd*, *J* =12.5, 6.6 Hz, H_2-5$'$)

Further comparison of the ^{1}H and ^{13}C spectral data (**Table 10**) to previous work (Saifah *et al*., 1993), identified compound CAF4 as pyramidatine.

A putrescine-type amide, pyramidatine, was previously isolated from a number of *Aglaia* species (see **Table 1**). Evaluation of the cytotoxic potential of this compound against eleven human cancer cell lines has been performed by Saifah *et al* (1993).

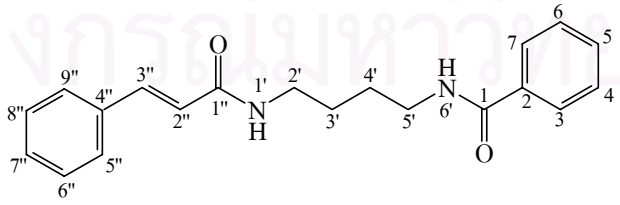

pyramidatine

Table 10. Comparison of the NMR spectral data of pyramidatine and compound CAF4 (DMSO-d_6, 400 MHz)

Position	CAF4		Pyramidatine*	
	^{1}H (mult., *J* in Hz)	**^{13}C (mult.)**	**^{1}H**	**^{13}C**
1		166.2 (*s*)		166.2
2		135.1 (*s*)		134.7
3,7	7.84 (*dd*, 8.3, 1.6)	127.3 (*d*)	7.84 (*dd*, 8.3, 1.6)	127.2
4,6	7.44 (*dd*, 8.3, 8.3)	128.4 (*d*)	7.44 (*dd*, 8.3, 8.3)	128.3
5	7.35-7.60 (*m*)	131.1 (*d*)	7.48 (*m*)	131.0
1′-NH	8.13 (*br t*)		8.13 (*dd*, 6.6, 6.6)	
2′	3.23 (*dd*, 12.5, 6.6)	38.5 (*t*)	3.21 (*dd*, 12.5, 6.6)	38.5
3′	1.43-1.64 (*m*)	26.8 (*t*)	1.43-1.58 (*m*)	26.8
4′	1.50-1.60 (*m*)	26.8 (*t*)	1.50-1.64 (*m*)	26.8
5′	3.25 (*dd*, 12.5, 6.6)	38.5 (*t*)	3.28 (*dd*, 12.5, 6.6)	38.5
6′-NH	8.48 (*br t*)		8.48 (*dd*, 6.6, 6.6)	
1″		164.9 (*s*)		164.9
2″	6.63 (*d*, 15.8)	122.3 (*d*)	6.63 (*d*, 15.8)	122.3
3″	7.42 (*d*, 15.8)	138.5 (*d*)	7.42 (*d*, 15.8)	138.5
4″		134.9 (*s*)		134.9
5″,9″	7.35-7.60	127.6 (*d*)	7.54 (*dd*, 8.0, 1.6)	127.5
6″,8″	7.35-7.60	129.1 (*d*)	7.39 (*dd*, 8.0, 8.0)	128.9
7″	7.35-7.60	129.5 (*d*)	7.35 (*m*)	129.4

* Saifah *et al*., 1993 (in DMSO-d_6, 300 MHz)

สถาบันวิทยบริการ
จุฬาลงกรณ์มหาวิทยาลัย

1.9 Structure Elucidation of Compound CAF5

Compound CAF5 was obtained as white amorphous powder. The HRESI-TOFMS (**Figure 57**) showed $[M+Na]^+$ peaks at *m/z* = 675.2678 matching a molecular formula of $C_{38}H_{40}N_2O_8$ and the IR (**Figure 59**) absorptions indicated the presence of hydroxyl at 3479 cm^{-1} and amide functions at 1620 and 1633 cm^{-1}.

The ^{13}C NMR spectrum (**Figure 61**) showed 38 carbons including signals for three methine carbons (δ_C 61.6, 61.7 and 78.7 ppm), four methylene carbons (δ_C 26.0, 26.5, 39.0 and 39.4 ppm), ten methine carbons of two mono-substituted aromatic rings, four methine carbons of a para-substituted aromatic ring, two mthine carbons of a fourfold substituted aromatic ring and the remaining resonances of twelve quaternary carbons, two of which resonated at δ_C 167.6 and 173.3 ppm were amide carbons.

The ^1H-NMR (**Figure 60**) spectrum indicated the presence of characteristic benzene ring signals, including ten aromatic proton signals of two mono-substituted rings at δ_H 6.98-7.15 (5H) and 7.45-7.78 (5H), four aromatic proton signals at δ_H 6.89 (2H, *ps d*) and 7.74 (2H, *ps d*) for a para-substituted ring and meta-coupled proton signals at δ_H 5.77 (*d*, *J* = 2.3) and 6.04 (*d*, *J* = 2.3) and resonances for three methoxy groups at δ_H 3.08 (*s*, 6-OMe), 3.71 (*s*, 8-OMe) and 3.77 (*s*, 4′-OMe). Furthermore, three methine proton signals at δ_H 3.91 (*d*, *J* = 8.6 Hz, H-3), 4.12 (*d*, *J* = 8.6 Hz, H-4) and 4.90 (*d*, *J* = 4.8 Hz, H-10) were typical of a cyclopenta[*bc*]benzopyran skeleton (Proksch *et al*., 2001).

The remaining amide proton signals at δ_H 6.79 (*br t*, *J* = 5.5, NH-12) and 6.31 (*br t*, *J* = 5.5, NH-17) and four methylene proton signals at δ_H 2.90/2.98 (each *m*, H_2-13), 1.14 (2H, *m*, H_2-14), 1.20 (2H, *m*, H_2-15) and 3.23 (2H, *m*, H_2-16) showed correlations in the COSY spectrum (**Figures 62** and **63**), suggesting the presence of 1,4-butanebisamide chain. In the HMBC spectrum (**Figure 64**), a cross peak was observed between signals at δ_H 7.78 (2H, *ps d*, H-20, 24) and δ_C 167.6 (C-18), indicated that one of the mono-substituted benzeng rings is connected to this 1,4-butanebisamide chain. Further HMBC (**Figures 65-69**) correlations from H-3 (δ_H 3.91, *d*, 8.6 Hz) to C-2 (δ_C 86.8), C-4 (δ_C 61.6), C-11 (δ_C 173.3), C-1″ (δ_C 136.7) and from H-4 (δ_H 4.12, *d*, 8.6 Hz) to C-3 (δ_C 61.7), C-5 (δ_C 83.2), C-5a (δ_C 106.0), C-11 (δ_C 173.3), C-1″(δ_C 136.7), established the connectivity of the benzoyl-1,4-butanebisamide moiety and the second monosubstituted benzeng ring to C-4 (δ_C 61.6) and C-3 (δ_C 61.7), respectively.

All these data corresponded to cyclopenta[*bc*]benzopyran flavagline with a benzoyl-1,4-butaneamine moiety linked to the flavagline skeleton by an amide function. The benzoyl-1,4-

butanebisamide structure was known from the pyramidaglains A and B and the bisamide pyramidatine.

The ^{1}H and ^{13}C NMR (**Table 11**) data of CAF5 were partially almost identical with those of pyramidaglain A (Puripattanavong *et al*., 2000). The only difference was the lack of the acetylation of the 10-OH function in CAF5. The relative configurations in the hydroxylated methano bridge and the two substituents at positions 3 and 4 could be derived from the characteristic NOESY (**Figure 70**) correlations from H-3 to H-4, NH-12, H-2′/6′ and H-2′′/6′′, from H-4 to H-3, 10-OH, NH-12 and H-2′′/6′′, from H-10 to H-2′/6′ and from 10-OH to H-4. The most important NOESY correlations was between 10-OH and H-4 because it proved directly the relative configurations at C-3, C-4 and C-10. Since the resonances for 10-OH and H-10 were accidentally very close at room temperature (δ_H 4.88 and 4.90), the NOESY spectrum (**Figure 70**) was recorded also at lower temperatures. At 278 K the broad doublet of 10-OH shifted to 5.25 ppm and the cross peak between 10-OH and H-4 allowed a clear decision. The structure of CAF5 corresponded to the acetylated derivative of pyramidaglain A (Puripattanavong *et al*., 2000) and was therefore designated as desacetylpyramidaglain A.

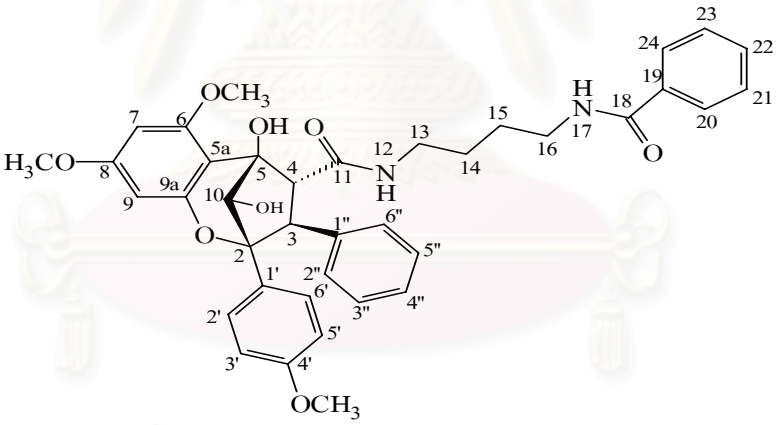

desacetylpyramidaglain A

สถาบันวิทยบริการ
จุฬาลงกรณ์มหาวิทยาลัย

Table 11. NMR spectral data of CAF5 ($CDCl_3$, 500 MHz)

position	CAF5			
	^{1}H (mult., *J* in Hz)	**^{13}C (mult.)**	**HMBC**	**NOESY**
2		86.8 (*s*)		
3	3.91 (*d*, 8.6)	61.7 (*d*)	C-2, C-4, C-11, C-1″	H-4, NH-12, H-2′/6′, H-2″/6″
4	4.12 (*d*, 8.6)	61.6 (*d*)	C-3, C-5, C-5a, C-11, C-1″	H-3, 10-OH, H-2″/6″
5		83.2 (*s*)		
5a		106.0 (*s*)		
6		158.8 (*s*)		
7	5.77 (*d*, 2.3)	92.8 (*d*)	C-5a, C-8	
8		161.0 (*s*)		
9	6.04 (*d*, 2.3)	93.7 (*d*)	C-5a, C-7, C-8	
9a		152.8 (*s*)		
10	4.90 (*d*, 4.8)	78.7 (*d*)	C-2, C-3, C-4, C-5a	H-4, H-2″/6″
11		173.3 (*s*)		
NH-12	6.79 (*br t*, 5.5)		C-11	
13	2.98, 2.90 (each *m*)	39.0 (*t*)	C-15, C-16	
14	1.14 (*m*)	26.0 (*t*)	C-13, C-15, C-16	
15	1.20 (*m*)	26.5 (*t*)	C-16	
16	3.23 (*m*)	39.4 (*t*)	C-13, C-14	
NH-17	6.31 (*br t*, 5.5)		C-18	
18		167.6 (*s*)		
19		134.5 (*s*)		
20,24	7.78 (*ps d*)	126.9 (*d*)	C-18, C-20/24, C-22	NH-17
21,23	7.45 (*ps t*)	128.6 (*d*)	C-19, C-20/24, C-22	
22	7.51 (*ps t*)	131.4 (*d*)	C-20/24, C-21/23	

Table 11. NMR spectral data of CAF5 ($CDCl_3$, 500 MHz) (continued)

position	CAF5			
	^{1}H (mult., *J* in Hz)	**^{13}C (mult.)**	**HMBC**	**NOESY**
1′		130.3 (*s*)		
2′ ,6′	7.74 (*ps d*)	127.7 (*d*)	C-2, C-1′, C-4′	
3′,5′	6.89 (*ps d*)	113.7 (*d*)	C-1′, C-2′, C-4′, C-6′	4′-OMe
4′		159.6 (*s*)		
1′′		136.7 (*s*)		
2′′,6′′	6.98 (*m*)	128.5 (*d*)	C-3, C-1′′,C-4′′	NH-12
3′′,5′′	7.15 (*m*)	127.7 (*d*)	C-1′′, C-2′′/6′′	
4′′	7.15 (*m*)	127.1 (*d*)	C-1′′, C-2′′/6′′	
5-OH	5.42 (*s*)		C-5, C-5a, C-10	
10-OH	4.88 (*br d*, 4.8)		C-2	H-4
6-OMe	3.08 (*s*)	55.7 (*q*)	C-6	
8-OMe	3.71 (*s*)	55.4 (*q*)	C-8	
4′-OMe	3.77 (*s*)	55.3 (*q*)	C-4′	H-3′/5′

สถาบันวิทยบริการ
จุฬาลงกรณ์มหาวิทยาลัย

1.10 Structure Elucidation of Compound CAF6

Compound CAF6 was obtained as white amorphous powder. The HRESI-TOF **(Figure 71)** mass spectrum exhibited $[M+Na]^+$ ion peak at *m/z* 675.2678, suggesting the molecular formula $C_{38}H_{40}N_2O_8$. The UV spectrum showed absorption maxima at 208 (**Figure 72**). The IR spectrum (**Figure 73**) exhibited absorption bands for hydroxy and two amide functionalities at 3479, 1620 and 1633 cm^1, respectively.

The ^{1}H-NMR (**Figure 74**) spectrum indicated the presence of characteristic benzene ring signals, including ten aromatic proton signals of two mono-substituted rings at 6.98-7.10 (5H) and 7.42-7.77 (5H), four aromatic proton signals at δ_H 6.86 (2H, *ps d*) and 7.64 (2H, *ps d*) for a para- substituted ring and meta-coupled proton signals at δ_H 6.10 (*d*, *J* = 2.3) and 6.12 (*d*, *J* = 2.3), resonances for three methoxy groups at δ_H 3.86 (*s*, 6-OMe), 3.77 (*s*, 8-OMe) and 3.79 (*s*, 4′-OMe), three methine proton signals at δ_H 4.67 (*d*, *J* = 6.0 Hz, H-3), 3.44 (*d*, *J* = 6.0 Hz, H-4) and 4.28 (*d*, *J* = 9.5 Hz, H-10), two amide proton signals at δ_H 6.49 (*br t*, *J* = 5.5, NH-12) and 6.52 (*br t*, *J* = 5.5, NH-17) and four methylene proton signals at δ_H 3.31/3.48 (each *m*, H_2-13) and 1.60-3.50 (H_2-14- H_2-16).

The ^{13}C NMR spectrum (**Figure 75**) showed 38 carbons including signals for three methine carbons at δ_C 55.9 (C-3), 65.6 (C-4) and 82.6 (C-10), four methylene carbons at δ_C 39.3 (C-13), 26.3 (C-14), 26.9 (C-15) and 39.7 (C-16), two amide carbons at δ_C 173.8 (C-11) and 1167.7 (C-18), ten methine carbons of two mono-substituted aromatic rings, four methine carbons of a para-substituted aromatic ring, two mthine carbons of a fourfold substituted aromatic ring and the remaining resonances of ten quaternary carbons (see **Table 12**).

The ^{1}H and ^{13}C NMR (**Figures 74-75** and **Table 12**) data of compounds CAF5 and CAF6 were comparable, suggesting that compound CAF6 also possesses the same carbon skeleton of cyclopenta[*bc*]benzopyran bearing benzoyl-1,4-butanebisamide moiety in the side chain bisamide.

The analysis of 2D-NMR (^{1}H-^{1}H COSY, HMQC and HMBC) (**Figures 76-84**) was further confirmed this compound to be a stereoisomer of CAF5. In the HMBC spectrum, the same correlations were also observed for both compounds (see **Table 12**), indicating in CAF6 the same connectivity of the diamide moiety and unsubstituted phenyl ring, as determined for CAF5. This compound was characterised by H-3β, H-4α, and 10-OH pointing towards positions 3 and 4. In the NOESY (**Figure 85**) spectrum, crosspeaks from H-3 to H-4, 10-OH, H-2′/6′ and H-2′′/6′′; from H-4 to H-3, NH-12 and H-2′′/6′′; from

H-10 to 10-OH and 2′/6′; and from 10-OH to H-3 and 5-OH were typical of the cyclopenta[*b*]benzofuran system. The stereochemistry followed immediately from the most informative NOESY correlation between H-3 and 10-OH. The compound was designated as desacetylpyramidaglain D.

According to previous studies on other cyclopenta[*bc*]benzopyran-type flavaglines, the configuration at positions 3 and 4 could be also determined from the analysis of ^{3}J coupling constants of these positions. The $^{3}J_{(H\text{-}3,\ H\text{-}4)}$ of 5-6 Hz is compatible with the H-3β, H-4α configuration, while the vicinal coupling constant of 9-10 Hz is compatible with the H-3α, H-4β configuration (Proksch *et al*., 2001; Kim *et al*., 2006). In accordance with previous finding, the vicinal coupling constant values between H-3 and H-4 were 6.0 and 8.6 Hz, indicating H-3β, H-4α and H-3α, H-4β in compounds CAF6 and CAF5, respectively.

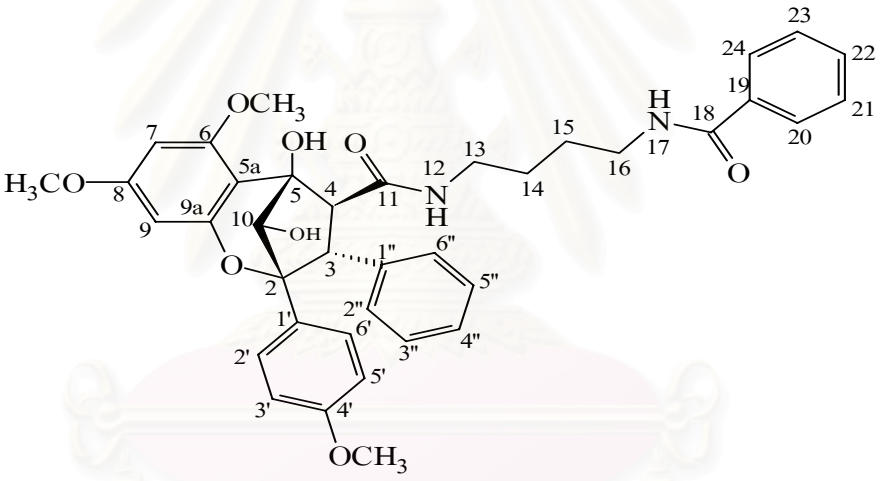

desacetylpyramidaglain D

สถาบันวิทยบริการ
จุฬาลงกรณ์มหาวิทยาลัย

Table 12. NMR spectral data of CAF6 ($CDCl_3$, 500 MHz)

position	CAF6			
	^{1}H (mult., *J* in Hz)	^{13}C (mult.)	HMBC	NOESY
2		89.9 (*s*)		
3	4.67 (*d*, 6.0)	55.9 (*d*)	C-2, C-4, C-11, C-1′′, C-2′′/6′′	H-4, 10-OH, H-2′/6′, H-2′′/6′′
4	3.44 (*d*, 6.0)	65.6 (*d*)	C-3, C-5, C-5a, C-11, C-1′′	H-3, NH-12, H-2′′/6′′
5		79.6 (*s*)		
5a		110.5 (*s*)		
6		156.3 (*s*)		
7	6.12 (*d*, 2.3)	92.5 (*d*)	C-5a, C-9	
8		160.9 (*s*)		
9	6.10 (*d*, 2.3)	93.9 (*d*)	C-5a, C-7	
9a		153.8 (*s*)		
10	4.28 (*d*, 9.5)	82.6 (*d*)	C-5a, C-2, C-3, C-4	10-OH, H-2′′/6′′
11		173.8 (*s*)		
NH-12	6.49* (*br t*, 5.5)		C-13	
13	3.31/3.48 (*each m*)	39.3 (*t*)		
14	1.60-1.70 (*m*)	26.3 (*t*)		
15	1.60-1.70 (*m*)	26.9 (*t*)		
16	3.44-3.50 (*m*)	39.7 (*t*)		
NH-17	6.52* (*br t*, 5.5)		C-16	
18		167.7 (s)		
19		134.4 (s)		
20,24	7.77 (*ps d*)	126.9 (*d*)	C-20/24, C-22	NH-17
21,23	7.42 (*ps t*)	128.6 (*d*)	C-19, C-21/23	
22	7.49 (*ps t*)	131.5 (*d*)	C-20/24	

Table 12. NMR spectral data of CAF6 ($CDCl_3$, 500 MHz) (continued)

position	CAF6			
	^{1}H (mult., *J* in Hz)	**^{13}C (mult.)**	**HMBC**	**NOESY**
1′		129.8 (*s*)		
2′,6′	7.64 (*ps d*)	128.6 (*d*)	C-2′/6′	
3′,5′	6.86 (*ps d*)	113.1 (*d*)	C-1′, C-2′/6′, C-4′	4′-OMe
4′		159.0 (*s*)		
1″		137.5 (*s*)		
2″,6″	6.89 (*m*)	129.2 (*d*)	C-1″, C-2″/6″, C-4″	NH-12
3″,5″	7.10 (*m*)	128.0 (*d*)	C-1″, C-2″/6″	4′-OMe
4″	7.10 (*m*)	127.0 (*d*)	C-1″, C-2″/6″	
5-OH	5.79 (*s*)			
10-OH	5.96 (*d*, 9.5)			H-3, 5-OH
6-OMe	3.86 (*s*)	56.2 (*q*)	C-6	
8-OMe	3.77 (*s*)	55.5 (*q*)	C-8	
4′-OMe	3.79 (*s*)	55.2 (*q*)	C-4′	H-3′/5′

*Assignments are interchangeable in the same column.

สถาบันวิทยบริการ
จุฬาลงกรณ์มหาวิทยาลัย

1.11 Structure Elucidation of Compound CAF7

Compound CAF7 was obtained as white amorphous powder. The molecular formula of $C_{38}H_{40}N_2O_8$ was established by $[M+Na]^+$ peaks at *m/z* = 675.2684 in the HRESI-TOFMS (**Figure 86**). The IR (**Figure 87**) absorption bands at 3479 cm^{-1}, 1620 and 1633 cm^{-1} indicated the presence of hydroxyl and two amide functions in this molecule, respectively.

Based on the comparison of the ^1H and ^{13}C NMR (**Figures 88-89** and **Table 13**) data of CAF7 with those of CAF5 together with the analysis of 2D-NMR (^1H-^1H COSY, HMQC and HMBC) (**Figures 90-97**) data indicated that CAF7 was also possessed the benzoyl-1,4-butaneamine moiety linked to the flavagline skeleton by an amide function. NOESY (**Figure 98**) correlations from H-3 to H-4, NH-12, H-2′/6′ and H-2′′/6′′; and from H-4 to H-3, H-10 and H-2′′/6′′, and the $^3J_{(H\text{-}3,\ H\text{-}4)}$ coupling constant (8.9 Hz) revealed that CAF7 was also have the same relative configuration at positions 3 and 4 as determined for compound CAF5. However, the lack of any NOE interactions between H-4 and H-10 in CAF7 suggested this compound is the C-10 epimer of CAF5. The most important cross peak for the position of the methano bridge 10-OH relative to the substituents at C-3 and C-4 was the strong cross peak between H-4 and H-10. The chemical shift of the OH group was at remarkable high field which was probably due to the ring current effect of the close aromatic ring 5a-9a. A model showed that the proton of the 10-OH group was situated above this ring. The compound was named desacetylpyramidaglain C.

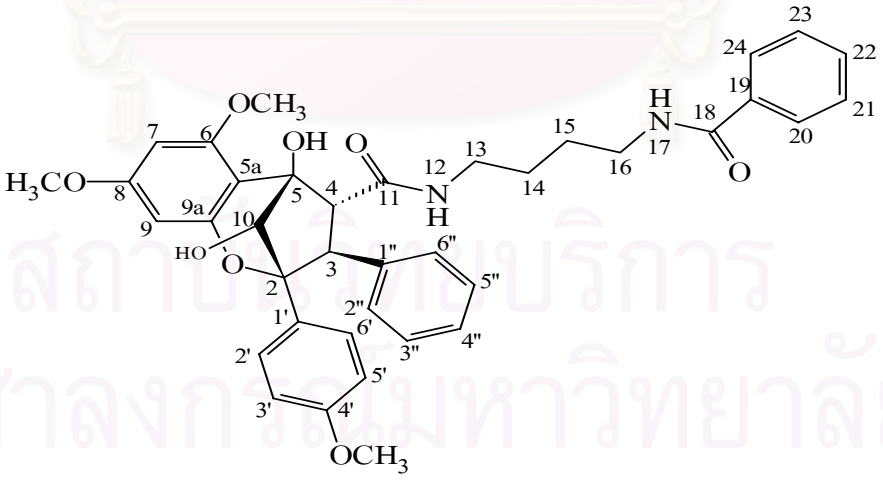

desacetylpyramidaglain C

Table 13. NMR spectral data of CAF7 ($CDCl_3$, 500 MHz)

position	CAF7			
	^{1}H (mult., *J* in Hz)	**^{13}C (mult.)**	**HMBC**	**NOESY**
2		85.6 (*s*)		
3	3.22 (*d*, 8.9)	59.0 (*d*)	C-2, C-4, C-10, C-11, C-1″	H-4, NH-12, H-2′/6′, H-2″/6″
4	4.00 (*d*, 8.9)	57.1 (*d*)	C-3, C-5,C-10, C5a, C-11, C-1″	H-3, 10-H, H-2″/6″
5		81.8 (*s*)		
5a		104.2 (*s*)		
6		160.3 (*s*)		
7	5.86 (*d*, 2.3)	93.0 (*d*)	C-5a, C-6, C-9	
8		160.8 (*s*)		
9	6.25 (*d*, 2.3)	93.9 (*d*)	C-5a, C-7, C-8	
9a		152.9 (*s*)		
10	4.90 (*d*, 4.4)	73.5 (*d*)	C-5, C-5a, C-1′	H-4, H-2″/6″
11		170.0 (*s*)		
NH-12	5.52 (*br t*, 5.5)		C-11,C-13	
13	2.62/2.92 (each *m*)	39.0 (*t*)	C-14	
14	0.98 (*m*)	26.2 (*t*)	C-13, C-15	
15	1.15 (*m*)	26.3 (*t*)	C-14, C-16	
16	3.28 (*m*)	39.4 (*t*)	C-13,C-14, C-15	
NH-17	6.46 (*br t*, 5.5)		C-16, C-18	
18		167.5 (s)		
19		134.5 (s)		
20,24	7.81 (*ps d*)	126.9 (*d*)	C-19, C-22	NH-17
21,23	7.46 (*ps t*)	128.6 (*d*)	C-19, C-20/24, C-22	
22	7.52 (*ps t*)	131.4 (*d*)	C-21/23	

Table 13. NMR spectral data of CAF7 ($CDCl_3$, 500 MHz) (continued)

position	CAF7			
	^{1}H (mult., *J* in Hz)	**^{13}C (mult.)**	**HMBC**	**NOESY**
1′		129.2 (*d*)		
2′ ,6′	7.61 (*ps d*)	128.0 (*d*)	C-2, C-3′/5′, C-4′	
3′,5′	6.89 (*ps d*)	113.6 (*d*)	2′ /6′, C-4′	4′-OMe
4′		159.3 (*s*)		
1′′		136.8 (*s*)		
2′′,6′′	6.92 (*m*)	128.6 (*d*)	C-3′′/5′′, C-4′′	NH-12
3′′,5′′	7.15 (*m*)	127.7 (*d*)	C-1′′, C-2′′/6′′	
4′′	7.15 (*m*)	127.0 (*d*)		
5-OH	5.43 (*s*)		C-10	
10-OH	2.32 (*br d*, 4.4)			H-4
6-OMe	3.11 (*s*)	55.5 (*q*)	C-6	
8-OMe	3.78 (*s*)*	55.4 (*q*)	C-8	
4′-OMe	3.77 (*s*)*	55.4 (*q*)	H-3′/5′, C-4′	H-3′/5′

*Assignments are interchangeable in the same column.

สถาบันวิทยบริการ
จุฬาลงกรณ์มหาวิทยาลัย

2. Structure Determination of Compounds Isolated from *Aglaia oligophylla*

2.1 Identification of Compound HAO1

Compound HAO1 was obtained as colorless needle crystals. EI mass spectrum (**Figure 99**) indicated the $[M]^+$ of this compound as *m/z* 442 which corresponded to the molecular formula $C_{30}H_{50}O_2$ and indicated an index of hydrogen deficiency of 6. The presence of ketonic carbonyl group and hydroxyl function were inferred from the IR absorbtion bands at 1704 and 3480 cm^{-1}, respectively (**Figure 100**).

The ^1H spectrum (**Figure 101**) exhibited eight tertiary singlet methyl groups at δ_H 0.94 (Me-18), 1.00 (Me-19), 1.15 (Me-21), 1.69 (Me-26), 1.62 (Me-27), 1.08 (Me-28), 1.03 (Me-29) and 0.88 (Me-30), an olefinic proton at δ_H 5.12 (*t*, *J* = 7.1 Hz, H-24), and the deshielded methylene protons at δ_H 2.42 (*ddd*, *J* = 13.6, 9.6, 7.6 Hz, H-2ax) and 2.51 (*ddd*, *J* = 13.6, 7.8, 4.5 Hz, H-2eq) typical for position 2 in 3-oxo triterpenoid.

The ^{13}C APT experiment (**Figure 102**) displayed 30 carbon signals, corresponding to eight tertiary C-Me groups, ten methylenes, four methines, five quaternary carbons, two sp^2 carbons at δ_C 124.6 (C-24) and 131.6 (C-25), and one carbonyl function at δ_C 218.8 (C-3).

These data suggested that this compound would be 3-oxodammarane-type triterpene. This hypothesis was supported by the following evidences. HMBC correlations (**Figure 103**) from both signals at Me-28 (δ_H 1.08) and Me-29 (δ_H 1.03) to δ_C 218.8 (C-3) indicated that ketonic carbonyl group was placed in position 3. Placement of hydroxyl group at C-20 (δ_C 75.3), judging from the downfield shift of this position, was further confirmed by the HMBC (**Figure 103**) correlation between the signal of Me-21 (δ_H 1.15, *s*) and this deshielded quaternary carbon of position 20. An olefinic proton resonated at δ_H 5.12 (*t*, *J* = 7.1 Hz) showed HMBC (**Figure 103**) cross peaks to sp^2 quaternary carbon at δ_C 131.6 (C-25) and both Me-26 (δ_C 25.7) and Me-27 (δ_C 17.7), clearly indicating the location of this olefinic proton as position 24.

HAO1 was identified as dipterocarpol based on the above spectral evidence and by comparison of the ^{13}C NMR (**Table 14**) with reported data (Tori *et al*., 1988).

Dipterocarpol was previously reported to be a constituent of various *Dipterocarpus* species (Cascon and Brown, 1972). Although there are also a number of dammarane triterpenes in the genus *Aglaia* (see **Table 1**), to our knowledge, this is the first report on the occurrence of dipterocarpol in the genus *Aglaia*.

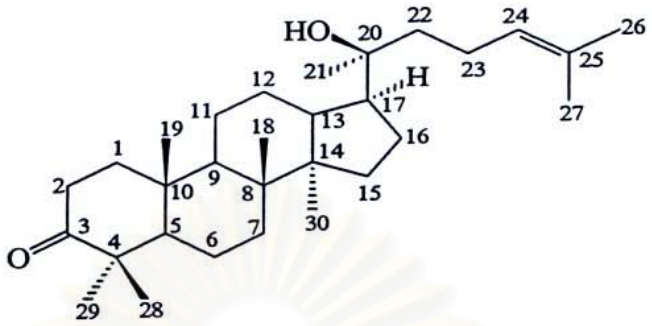

dipterocapol

Table 14. Comparison of the NMR spectral data of dipterocapol and compound HAO1 ($CDCl_3$, 400 MHz)

Position	Compound HAO1		Dipterocarpol*
	^{1}H (mult., *J* in Hz)	^{13}C (mult.)	^{13}C
1	1.92 (*m*)	39.8 (*t*)	39.8
2	2.42 (*ddd*, 13.6, 9.6, 7.6) 2.51 (*ddd*,13.6, 7.8, 4.5)	34.0 (*t*)	34.0
3		218.8 (*s*)	217.6
4		47.4 (*s*)	47.3
5	1.39 (*m*)	55.3 (*d*)	55.3
6	1.55/1.48 (each *m*)	19.6 (*t*)	19.6
7	1.60/1.30 (each *m*)	34.5 (*t*)	34.5
8		40.2 (*s*)	40.2
9	1.42 (*m*)	50.0 (*d*)	49.9
10		36.8 (*s*)	36.7
11	1.40 (*m*)	22.0 (*t*)	22.0
12	1.88 (*m*)	27.5 (*t*)	27.5
13	1.73 (*m*)	42.3 (*d*)	42.3
14		50.2 (*s*)	50.2
15	1.59/1.09 (each *m*)	31.5 (*t*)	31.1
16	1.76/1.51 (each *m*)	24.7 (*t*)	24.7

Table 14. Comparison of the NMR spectral data of dipterocapol and compound HAO1 ($CDCl_3$, 400 MHz) (continued)

Position	Compound HAO1		Dipterocarpol*
	^{1}H (mult., *J* in Hz)	**^{13}C (mult.)**	**^{13}C**
17	1.60 (*m*)	49.8 (*d*)	49.7
18	0.94 (*s*)	16.0 (*q*)	15.9
19	1.00 (*s*)	15.2 (*q*)	15.2
20		75.3 (*s*)	75.1
21	1.15 (*s*)	25.4 (*q*)	25.4
22	1.49 (*m*)	40.4 (*t*)	40.5
23	2.50 (*m*)	22.5 (*t*)	22.5
24	5.12 (*t*, 7.1)	124.6 (*d*)	124.7
25		131.6 (*s*)	131.3
26	1.69 (*s*)	25.7 (*q*)	25.7
27	1.62 (*s*)	17.7 (*q*)	17.6
28	1.08 (*s*)	26.7 (*q*)	26.6
29	1.03 (*s*)	21.0 (*q*)	21.0
30	0.88 (*s*)	16.3 (*q*)	16.2

* Tori *et al*., 1988 (in $CDCl_3$, 400 MHz)

สถาบันวิทยบริการ
จุฬาลงกรณ์มหาวิทยาลัย

2.2 Identification of Compound HAO2

Compound HAO2 was obtained as colorless needle crystals. The EI mass spectrum (**Figure 104**) displayed $[M]^+$ peak at *m/z* 458, corresponding to the molecular formula $C_{30}H_{50}O_3$. The IR spectrum (**Figure 105**) showed the strong carbonyl absorption at 1705 cm^{-1}, suggesting this structure belongs to the group of keto-triterpenoids.

Both ^1H and ^{13}C NMR spectra (**Figures 106** and **107**) showed double signals, indicating this compound as in a mixture state. Analysis of signal integration for the ^1H NMR spectrum of HAO2 indicated 4:1 ratio of the two components of this mixture.

Based on the ^{13}C APT and HSQC spectra (**Figures 108** and **109**), it was concluded that each triterpenoid possessed eight tertiary methyl groups, ten methylenes, five methines, six quaternary carbons and one carbonyl group. Two of six quaternary carbons (for the major component: δ_C 86.3, C-20 and 71.4, C-25; for the minor component: δ_C 86.5, C-20 and 70.2, C-25) and one of five methines (for the major component: δ_C 83.3, C-24; for the minor component: δ_C 86.4, C-24) were carrying oxygen function, judging from the downfield shift of these carbon signals.

The ^{13}C NMR spectrum (**Table 15**) of the major component, however, differed significantly from the minor one only in the chemical shifts of the side chain moiety, suggesting that they are C-24-epimers (epimers are indicated by the suffices **A** and **B**). The signals at δ_C 86.3 (C-20) and 83.3 (C-24) of the major component (HAO2A) and δ_C 86.5 (C-20) and 86.4 (C-24) of the minor component (HAO2B) were observed to be typical of C-20 and C-24 in the 20,24-epoxy-25-dammaranes reported earlier (Aalbersberge and singe, 1991). The mass spectrum also exhibited the fragment ion characteristic of 20,24-epoxy function at *m/z* 143 ($C_8H_{15}O_2$).

The ^1H NMR spectrum (**Figure 106**) from the major component (HAO2A) of this mixture exhibited the signals of eight tertiary methyl groups (δ_H 0.88, 0.93 , 0.99, 1.03, 1.07, 1.12, 1.13 and 1.21; Me-18, Me-30, Me-19, Me-29, Me-28, Me-27, Me-21 and Me-26, respectively) and of oxymethine proton at δ_H 3.73 (*t*, *J* = 7.3 Hz), typical for the H-24*R* in 20,24-epoxy chain at C-17 as described by Roux *et al* (1998). HSQC (**Figure 110**) correlation between the signal at δ_H 3.73 (*t*, *J* = 7.3 Hz, H-24) and the signal at δ_C 83.3 (C-24) was also supported the location of this oxymethine proton at position 24.

The HMBC (**Figures 111** and **112**) correlations from Me-21 (δ_H 1.13) to C-17 (δ_C 49.5) and C-20 (δ_C 86.3) and from H-24 (3.73, *t*, *J* = 7.3 Hz) to C-20 (δ_C 86.3), C-25 (δ_C71.4), C-26 (δ_C 24.2) and

C-27 (δ_C 27.4), further confirmed the presence of 20,24-epoxy function in the side chain. The assignment of ketonic carbonyl at C-3 was supported by the HMBC (**Figure 111**) correlations from H_2-2 (δ_H 2.44/2.48, *m*), H_3-28 (δ_H 1.03, *s*) and H_3-29 (δ_H 1.07, *s*) to this ketonic carbonyl (δ_C 218.5, C-3)

The ^{1}H NMR spectrum (**Figure 106**) from the minor component (HAO2B) also exhibited the signals of eight tertiary methyl groups (δ_H 0.88, 0.94, 1.01, 1.03, 1.07, 1.15, 1.11 and 1.19; Me-30, Me-18, Me-19, Me-29, Me-28, Me-26, Me-21 and Me-27, respectively), however, instead of signal typical for H-24*R* isomer (δ_H 3.73, *t*, *J* = 7.3 Hz) in HAO2A, showed an oxymethine proton at δ_H 3.64 (*dd*, *J* = 7.6 Hz, H-24), typical for the H-24*S* isomer in HAO2B (Roux *et al*., 1998).

The compound was finally identified by comparison of the ^{13}C NMR (**Table 15**) spectral data with the reported values (Aalbersberg and Singh, 1991) as a mixture of ocotillone (HAO2A) and cabraleone (HAO2B).

The co-occurrence of ocotillone and cabraleone in the same plant has previously been reported from several species of Meliaceae such as *Cabralea eichleriana* (Rao *et al*., 1975), *Dysoxylum richii* (Aalbersberg and Singh, 1991) and *Amoora yunnanensis* (Luo *et al*., 2000). Ocotillone was responsible for cytotoxic activity of an ethanolic extract of *Dysoxylum cauliflorum* Hiern against KB cells, previously reported by Benosman *et al* (1995).

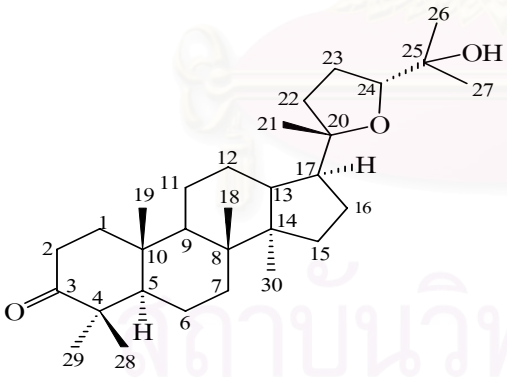

ocotillone

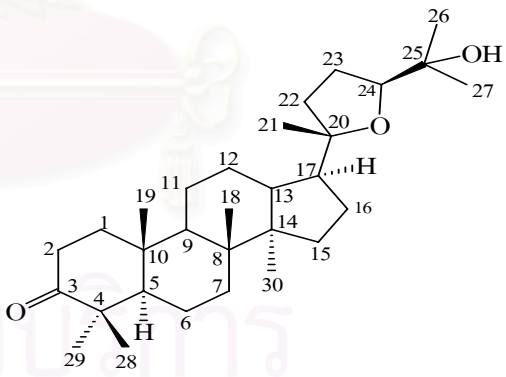

cabraleone

ศูนย์วิทยทรัพยากร
จุฬาลงกรณ์มหาวิทยาลัย

Table 15. Comparison of the ^{13}C NMR spectral data of ocotillone and cabraleone and compound HAO2 ($CDCl_3$, 100 MHz)

position	HAO2A (mult.)	Ocotillone (mult.)*	HAO2B (mult.)	Cabraleone (mult.)*
1	39.9 (*t*)	39.9 (*t*)	39.9 (*t*)	39.9 (*t*)
2	34.1(*t*)	34.1 (*t*)	34.0 (*t*)	34.1 (*t*)
3	218.1 (*s*)	218.1 (*s*)	218.1 (*s*)	218.0 (*s*)
4	47.4 (*s*)	47.4 (*s*)	47.4 (*s*)	47.4 (*s*)
5	55.3 (*d*)	55.4 (*d*)	55.3 (*d*)	55.4 (*d*)
6	19.6 (*t*)	19.7 (*t*)	19.6 (*t*)	19.7 (*t*)
7	34.6 (*t*)	34.8 (*t*)	34.6 (*t*)	34.6 (*t*)
8	40.3 (*s*)	40.3 (*s*)	40.3 (*s*)	40.3 (*s*)
9	50.1 (*d*)	49.8 (*d*)	50.1 (*d*)	49.6 (*d*)
10	36.8 (*s*)	36.9 (*s*)	36.8 (*s*)	36.9 (*s*)
11	22.0 (*t*)	22.3 (*t*)	22.3 (*t*)	22.1 (*t*)
12	25.6 (*t*)	25.8 (*t*)	25.8 (*t*)	25.8 (*t*)
13	43.1 (*d*)	42.9 (*d*)	43.0 (*d*)	43.4 (*d*)
14	50.0 (*s*)	50.0 (*s*)	50.0 (*s*)	50.0 (*s*)
15	31.4 (*t*)	31.4 (*t*)	31.4 (*t*)	31.5 (*t*)
16	27.4 (*t*)	27.0 (*t*)	27.1 (*t*)	27.8 (*t*)
17	49.5 (*d*)	50.2 (*d*)	49.8 (*d*)	49.8 (*d*)
18	16.0 (*q*)	16.1 (*q*)	16.1 (*q*)	16.1 (*q*)
19	15.1 (*q*)	15.2 (*q*)	15.1 (*q*)	15.2 (*q*)
20	86.3 (*s*)	86.5 (*s*)	86.5 (*s*)	86.5 (*s*)
22	35.7 (*t*)	34.6 (*t*)	34.8 (*t*)	34.9 (*t*)
23	26.1 (*t*)	26.4 (*t*)	26.3 (*t*)	27.1 (*t*)
24	83.3 (*d*)	83.4 (*d*)	86.4 (*d*)	86.4 (*d*)
25	71.4 (*s*)	71.4 (*s*)	70.2 (*s*)	70.3 (*s*)
26	24.3 (*q*)	24.3 (*q*)	27.2 (*q*)	26.4 (*q*)

Table 15. Comparison of the ^{13}C NMR spectral data of ocotillone and cabraleone and compound HAO2 ($CDCl_3$, 100 MHz) (continued)

position	HAO2A (mult.)	Ocotillone (mult.)	HAO2B (mult.)	Cabraleone (mult.)
27	27.4 (*q*)	27.1 (*q*)	27.1 (*q*)	27.2 (*q*)
28	26.7 (*q*)	26.8 (*q*)	27.8 (*q*)	27.8 (*q*)
29	21.0 (*q*)	21.0 (*q*)	21.0 (*q*)	21.0 (*q*)
30	16.3 (*q*)	16.3 (*q*)	16.3 (*q*)	16.3 (*q*)

*Aalbersberg and Singh, 1991 (in $CDCl_3$, 75 MHz)

สถาบันวิทยบริการ
จุฬาลงกรณ์มหาวิทยาลัย

2.3 Identification of Compound HAO3

Compound HAO3 was obtained as colorless needle crystals. The molecular formula, $C_{30}H_{52}O_3$, was determined for this compound, even though its EI mass spectrum (**Figure 113**) lack the $[M]^+$ peak and showed peak due to $[M\text{-}Me]^+$ at 445. The IR spectruym (**Figure 114**) showed the absorption of hydroxyl group at 3399 cm^{-1}.

Comparison of the ^{13}C (**Figure 116**) spectral data of HAO3 with those of HAO2 and the appearance of the characteristic base peak at *m/z* 143 in the mass spectrum suggested that the two compounds are based on the same carbon skeleton. However, the carbonyl was missing in this compound and an additional signal at δ_C 78.9 of oxymethine carbon was observed.

The ^1H NMR (**Figure 115**) spectrum showed the presence of eight tertiary methyl groups (δ_H 0.95, 0.83, 1.11, 1.12, 1.20, 0.97, 0.76 and 0.86). Two oxymethine protons could be located at positions 3 (δ_C 78.9, δ_H 3.19, *dd*, *J* = 11.4, 5.0 Hz) and 24 (δ_C 83.3, δ_H 3.72, *t*, *J* = 7.3 Hz), judging from the downfield shifts of the signals of these positions. In the HMBC (**Figure 117**) spectrum, prominent cross peaks from H_2-1 (1.68/0.94, *m*) and both Me-28 and Me-29 to δ_C 78.9 (C-3) and from H_2-22 (1.62/1.17, *m*), H_2-23 (1.86/1.78, *m*) and both Me-26 and Me-27 to δ_C 83.3 (C-24) further confirmed these assignments.

The assignment of the relative configuration of C-24 was based on a NOESY (**Figure 118**) correlation between Me-21 and H-24, suggesting that isopropanol group at C-24 is *trans* to the methyl group at C-20.

Further comparison of the ^1H and ^{13}C (**Table 16**) spectral data of this compound with those already reported (Tanaka, Masuda, and Matsunaga, 1993) confirmed the structure of HAO3 as ocotillol-II.

Ocotillol-II has previously been isolated from the stem of *Aglaia elliptica* and was shown to be devoid of cytotoxic activity against human cancer cell lines (Cui *et al*., 1997). It was also found as a constituent of *Fouquieria splendens* (Warnhoff and Halls, 1965), *Phyllanthus flexuosus* (Tanaka, Masuda, and Matsunaga, 1993) and *Camellia japonica* (Akihisa *et al*., 2004).

ศูนย์วิทยทรัพยากร
จุฬาลงกรณ์มหาวิทยาลัย

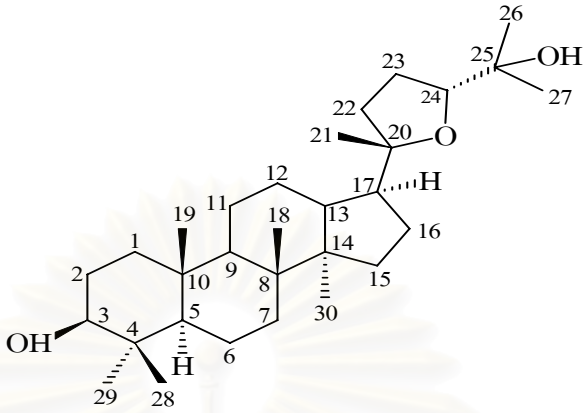

ocotillol-II

Table 16. Comparison of the NMR spectral data of ocotillol-II and compound HAO3 ($CDCl_3$, 400 MHz)

Position	Compound HAO3		Ocotillol II*	
	^{1}H (mult., *J* in Hz)	^{13}C (mult.)	^{1}H	^{13}C
1	1.68/0.94 (each *m*)	39.05 (*t*)		39.01
2	1.76/1.58 (each *m*)	27.42 (*t*)		27.43
3	3.19 (*dd*, 11.4, 5.0)	78.94 (*s*)	3.20 (*dd*, 11.5, 4.5)	78.95
4		38.96 (*s*)		38.96
5	0.72 (*m*)	55.86 (*d*)		55.85
6	1.54/1.42 (each *m*)	18.27 (*t*)		18.30
7	1.52/1.28 (each *m*)	35.28 (*d*)		35.29
8		40.36 (*s*)		40.38
9	1.31(*m*)	50.79 (*d*)		50.80
10		37.15 (*s*)		37.18
11	1.50 (*m*)	21.55 (*t*)		21.59
12	1.44 (*m*)	25.70 (*t*)		25.74
13	1.58 (*m*)	42.95 (*d*)		42.97
14		50.04 (*s*)		50.08
15	1.48/1.09 (each *m*)	31.44 (*t*)		31.48

Table 16. Comparison of the NMR spectral data of ocotillol-II and compound HAO3 ($CDCl_3$, 400 MHz) (continued)

Position	Compound HAO3		Ocotillol II*	
	^{1}H (mult., *J* in Hz)	^{13}C (mult.)	^{1}H	^{13}C
16	0.96 (*m*)	27.36 (*t*)		27.43
17	1.78 (*m*)	49.54 (*d*)		49.54
18	0.95 (*s*)	15.43 (*q*)	0.95 (*s*)	15.47
19	0.83 (*s*)	16.20 (*q*)	0.84 (*s*)	16.25
20		86.40 (*s*)		86.44
21	1.11(*s*)	23.52 (*q*)	1.12 (*s*)	23.55
22	1.62/1.17 (each *m*)	35.69 (*t*)		35.67
23	1.86/1.78 (each *m*)	26.12 (*t*)		26.13
24	3.72 (*t*, 7.3)	83.30 (*d*)	3.73 (*t*, 7.3)	83.31
25		71.42 (*s*)		71.43
26	1.11(*s*)	24.26 (*q*)	1.13 (*s*)	24.26
27	1.20 (*s*)	27.46 (*q*)	1.21 (*s*)	27.43
28	0.97 (*s*)	27.99 (*q*)	0.97 (*s*)	28.08
29	0.76 (*s*)	15.33 (*q*)	0.77 (*s*)	15.34
30	0.86 (*s*)	16.45 (*q*)	0.87 (*s*)	16.47

* Tanaka, Masuda and Matsunaga, 1993 (in $CDCl_3$, 300 MHz)

สถาบันวิทยบริการ
จุฬาลงกรณ์มหาวิทยาลัย

2.4 Identification of Compound HAO4

Compound HAO4 was obtained as colorless needle crystals. In the mass spectrum (**Figure 119**) the highest detectable peak is at *m/z* 440, evidently resulting from the loss of 18 units (H_2O) from *m/z* 458, the presumed molecular ion ($C_{30}H_{50}O_3$). The IR spectrum (**Figure 120**) displayed absorption bands for hydroxyl (3388 cm^{-1}) and carbonyl functionalities (1705 cm^{-1}).

The ^{1}H-NMR spectrum (**Figure 121**) showed signals for six tertiary methyl groups (δ_H 0.88, 0.93, 0.99, 1.03, 1.08, and 1.15) and one allyic methyl (δ_H 1.75). Evidence for the existence of an exomethylene function was provided by the presence of two broad singlets at δ_H 4.95/4.84 (H_2-26). In addition, signals representing the methylene protons at C-2 and an oxymethine proton at C-24 were located at δ_H 2.50/2.43 (each *m*, H_2-2) and 4.04 (*m*, H-24), respectively. HSQC spectrum (**Figure 123**) showed that the former methylene protons were correlated with a carbon peak at δ_C 34.1(C-2), while the latter exhibited cross peak with the carbon signal at δ_C 76.4 (C-24).

The ^{13}C-MNR (**Figure 122**) data of HAO4 also exhibited signals due to seven tertiary methyl groups (δ_C 16.0, 15.2, 25.5, 17.7, 26.6, 20.9 and 16.3) two olefinic carbons (δ_C 147.6 and 110.9), an oxygenated methine carbon (δ_C 76.4), an oxygenated quaternary carbon (δ_C 75.5), and one ketonic carbonyl (δ_C 218.1).

The ^{1}H and ^{13}C NMR (**Figures 121** and **122**) spectral data showed to be very similar to those of HAO1 and the observed differences in HAO4 of an isopropenyl moiety (δ_C 147.6, C-25; 110.9, C-26; and 17.7, C-27) in the side chain instead of a terminal isopropylidene moiety in HAO1.

All the signals of HAO4 and their connectivity were established by HMBC, HMQC and ^{1}H-^{1}H COSY experiments. The assignment of two hydroxyls at positions 20 (δ_C 75.1) and 24 (δ_C 76.4) was deduced from the downfield shift of these carbon atoms. The HMBC (**Figure 124**) correlations between Me-21 (δ_H 1.15) and C-20 and between Me-27 (δ_H 1.66) and C-24 further confirmed these assignment. Placement of an exomethylene function at C-25 was established by the correlations between δ_H 4.95/4.84 (H_2-26) and C-24 (δ_C 76.4) and between δ_H 1.75(Me-27) and δ_C 147.6 (C-25) and δ_C 110.9 (C-26) in the HMBC spectrum (**Figures 125** and **126**).

Based on these spectral data and comparison with earlier report (Mazinovskaya *et al*., 1992), compound HAO4 was identified as 20(*S*),24(*S*)-dihydroxydammar-25-en-3-one, previously isolated from *Aglaia rubiginosa* (Weber *et al*., 2000).

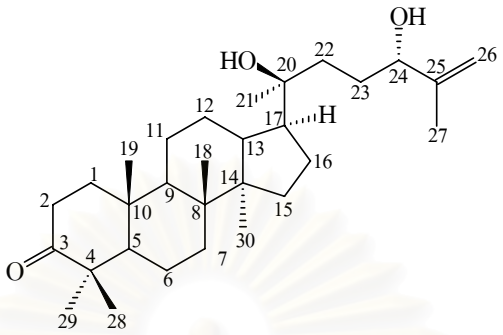

20(*S*),24(*S*)-dihydroxydammar-25-en-3-one

Table 17. Comparison of the NMR spectral data of 20(*S*),24(*S*)-dihydroxydammar-25-en-3-one and compound HAO4 ($CDCl_3$, 400 MHz)

Position	**Compound HAO4**		**20(*S*),24(*S*)-Dihydroxydammar-25-en-3-one***	
	^{1}H (mult., *J* in Hz)*	**^{13}C (mult.)**	**^{1}H**	**^{13}C**
1	1.84/1.38 (each *m*)	39.8 (*t*)		40.2
2	2.50 (*ddd*, 15.7, 9.6, 6.6) 2.43 (*ddd*, 15.7, 7.8, 4.3)	34.1 (*t*)		34.3
3		218.1 (*s*)		218.6
4		47.4 (*s*)		47.6
5	1.31 (*m*)	55.3 (*d*)		55.7
6	1.48/1.42 (each *m*)	19.6 (*t*)		19.9
7	1.38/1.26 (each *m*)	34.5 (*t*)		34.8
8		40.2 (*s*)		40.6
9	1.82 (*m*)	49.9 (*d*)		50.5
10		36.8 (*s*)		37.1
11	1.45/1.24 (each *m*)	21.9 (*t*)		22.3
12	1.78 (*m*)	27.4 (*t*)		27.7
13	1.59 (*m*)	42.4 (*d*)		42.8
14		50.2 (*s*)		50.4

Table 17. Comparison of the NMR spectral data of 20(*S*),24(*S*)-dihydroxydammar-25-en-3-one and compound HAO4 ($CDCl_3$, 400 MHz) (continued)

Position	Compound HAO4		20(*S*),24(*S*)-Dihydroxydammar-25-en-3-one*	
	^{1}H (mult., *J* in Hz)*	^{13}C (mult.)	^{1}H	^{13}C
15	1.42/1.30 (each *m*)	31.2 (*t*)		31.4
16	1.4 (*m*)	24.8 (*t*)		25.0
17	1.68 (*m*)	50.0 (*d*)		50.5
18	0.93 (*s*)	16.0 (*q*)	0.94 (*s*)	16.1
19	0.99 (*s*)	15.2 (*q*)	1.00 (*s*)	15.3
20		75.1 (*s*)		75.1
21	1.15 (*s*)	25.5 (*q*)	1.15 (*s*)	25.0
22	1.56 (*m*)	36.5 (*t*)		37.0
23	1.22 (*m*)	29.2 (*t*)		29.4
24	4.04 (*m*)	76.4 (*d*)	3.96 (t, 5.2)	76.4
25		147.6 (*s*)		147.8
26	4.95/4.84 (each *br s*)	110.9 (*t*)	4.96,4.84 (each *br s*)	110.9
27	1.75 (*s*)	17.7 (*q*)	1.74 (*s*)	17.6
28	1.08 (*s*)	26.6 (*q*)	1.08 (*s*)	26.9
29	1.03 (*s*)	20.9 (*q*)	1.04 (*s*)	21.1
30	0.88 (*s*)	16.3 (*q*)	0.89 (*s*)	16.5

* Mazinovskaya *et al*., 1992 ($CDCl_3$, 300 MHz)

สถาบันวิทยบริการ
จุฬาลงกรณ์มหาวิทยาลัย

2.5 Identification of Compound HAO5

Compound HAO5 was obtained as white amorphous solid. Its molecular formula, $C_{26}H_{26}O_6$ was determined from the $[M+H]^+$ peak at *m/z* 434 (**Figure 127**). The IR (**Figure 129**) absorptions suggested the presence of hydroxyl (3500 cm^{-1}) and aromatic (3061, 1610, 1454 cm^{-1}) in the molecule.

The ^1H NMR spectrum (**Figure 130**) of this compound exhibited signals for three aromatic rings, including two *meta*-coupled aromatic protons at δ_H 6.31 (*d*, *J* = 1.9 Hz, H-5) and 6.17 (*d*, *J* = 1.9 Hz, H-7), a characteristic AA′BB′ system (δ_H 7.02-7.20, *m*, 2H, H-2′/6′ and 6.68, *d*, *J* = 8.9 Hz, 2H, H-3′/5′) of a *p*-disubstitutted benzene ring and a monosubstituted benzene ring (δ_H 7.05-7.20, *m*, 3H, H-3″/5″ and H-4″, and 7.01, *dd*, *J* = 6.7, 1.3 Hz, 2H, H-2″/6″). The ^1H NMR spectrum further exhibited signals for methylene protons as a pair of geminally coupled multiplets at δ_H 2.75 (*ddd*, *J* =13.9, 13.9, 6.4 Hz, H-2α) and 2.20 (*ddd*, *J* = 13.7, 6.5, 1.2 Hz, H-2β), both of with showed vicinal couplings with the signals of methines at δ_H 4.81 (*d*, *J* = 5.5 Hz, H-1) and 4.01 (*dd*, *J* = 14.2, 6.5 Hz, H-3). Thus, the methylene signals at δ_H 2.20 and 2.75 should be connected between the methines.

Consistent with this ^1H NMR spectral data analysis, the ^{13}C NMR (**Figure 131**) and HSQC (**Figure 132**) spectra of HAO5 also displayed the signals for tetrasubstituted, a disubstituted and a monosubstituted benzene ring, one oxymethine carbon (δ_C79.1, C-1), and two carbons at δ_C 36.4 (C-2) and 53.2 (C-3) of methylene and methine, respectively, and two characteristic deshielded quaternary carbons at δ_C 103.5 and 94.8 of C-3a and C-8b of the cyclopenta[*b*]benzofuran skeleton (Rivero-Cruz *et al*., 2004).

The relative configuration of HAO5 was established primarily by analysis of the splitting patterns and the coupling constants (see **Table 18**) between H-1, H-2α, H-2β, and H-3 ($J_{1,2}$ *ca.* 5-7 Hz and $J_{2,3}$ *ca.* 13-14 Hz) indicated a 1α, 3β configuration, as well as a *cis*-B/C ring junction (Proksch *et al*., 2001). These relative configurations were confirmed by 2D NOESY (**Figure 133**) experiments, wherein correlations were observed between H-2′/6′ and both H-1α and H-2α but not between H-2′/6′ and H-3β.

On the basis of the above evidence and comparison with those already reported (Su *et al*., 2006), the structure of compound HAO5 was characterized as rocaglaol.

The cyclopenta[*b*]benzofuran flavagline, rocaglaol, which also exists in other species of *Aglaia* (see **Table 1**), show interesting pharmacological properties including cytotoxic (Su *et al*., 2006) and insecticidal activity (Schneider *et al*., 2000).

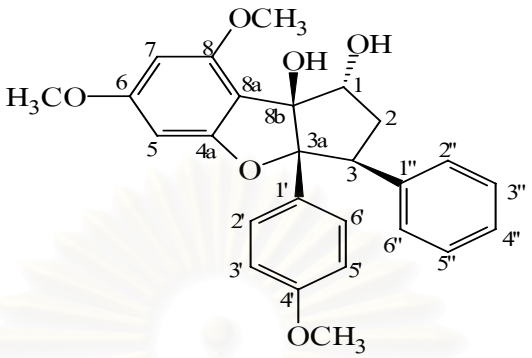

rocaglaol

Table 18. Comparison of the NMR spectral data of rocaglaol and compound HAO5 ($CDCl_3$, 500 MHz)

Position	Compound HAO5		Rocaglaol*	
	^{1}H (mult., *J* in Hz)	^{13}C (mult.)	^{1}H	^{13}C
1	4.81 (*d*, 5.5)	79.1 (*d*)	4.81 (*d*, 6.0)	79.1
2α	2.75 (*ddd*, 13.9, 13.9, 6.4)	36.4 (*t*)	2.75 (*ddd*, 13.8, 13.8, 6.4)	36.4
2β	2.20 (*ddd*, 13.7, 6.5, 1.2)		2.20 (*dd*, 13.6, 6.6)	
3	4.01 (*dd*, 14.2 , 6.5)	53.2 (*d*)	4.01 (*dd*, 14.1, 6.6)	53.2
3a		103.5 (*s*)		103.5
4a		161.0 (*s*)		161.0
5	6.31 (*d*, 1.9)	89.4 (*d*)	6.29 (*d*, 1.9)	89.4
6		163.9 (*s*)		163.9
7	6.17 (*d*, 1.9)	92.4 (*d*)	6.14 (*d*, 1.9)	92.5
8		157.0 (*s*)		157.0
8a		107.7 (*s*)		107.8
8b		94.8 (*s*)		94.8
1′		126.8 (*s*)		126.8
2′, 6′	7.02-7.20 (*m*)	128.1 (*d*)	7.05-7.13 (*m*)	128.1
3′, 5′	6.68 (*d*, 8.9)	112.7 (*d*)	6.68 (*d*, 8.9)	112.7
4′		158.6 (*d*)		158.6

Table 18. Comparison of the NMR spectral data of rocaglaol and compound HAO5 ($CDCl_3$, 500 MHz) (continued)

Position	Compound HAO5		Rocaglaol*	
	^{1}H (mult., *J* in Hz)	**^{13}C (mult.)**	**^{1}H**	**^{13}C**
1″		138.7 (*s*)		138.7
2″, 6″	7.01 (*dd*, 6.7, 1.3)	127.7 (*d*)	6.98-7.00 (*m*)	127.7
3″, 5″	7.05-7.20 (*m*)	128.9 (*d*)	7.05-7.13 (*m*)	128.9
4″	7.05-7.20 (*m*)	126.2 (*d*)	7.05-7.13 (*m*)	126.3
OMe-6	3.84 (*s*)	55.6 (*q*)	3.84 (*s*)	55.7
OMe-8	3.90 (*s*)	55.7 (*q*)	3.90 (*s*)	55.8
OMe-4′	3.71 (*s*)	55.1 (*q*)	3.71 (*s*)	55.1

* Su *et al*., 2006 (in $CDCl_3$, 300 MHz)

สถาบันวิทยบริการ
จุฬาลงกรณ์มหาวิทยาลัย

2.6 Identification of Compound HAO6

Compound HAO6 was obtained as colorless needle crystals. It has the molecular formula of $C_{18}H_{24}N_2O_2$ as determined by $[M+Na]^+$ peak at *m/z* = 323 in the ESI-TOF mass spectrum (**Figure 134**). The UV (**Figure 135**) spectrum was compatible with that expected for cinnamide derivative [λ_{max} (MeOH) 283 nm]. Absorption bands in the infrared (**Figure 136**) spectrum, characteristic of the amide group, was present at 3291, 1648 and 1535 cm^{-1}. These data suggested that this compound belong to the group of bisamides characteristic for *Aglaia* species. This was further confirmed by the following evidences.

The ^1H spectrum (**Figure 137**) displayed the characteristic lowfield signals at δ_H 6.8 (*d*, *J* = 15.5 Hz, H-2″), 7.6 (*d*, *J* = 15.5 Hz, H-3″) and 7.20-7.50 (5H, *m*, aromatic proton) of the cinnamyl moiety. The large coupling constant of 15.5 Hz indicated *trans*-double bond at position 2″. Furthermore, methylene proton at δ_H 1.40 (*m*, H-3), methine proton at δ_H 1.98 (*m*, H-2) and two methyl groups at δ_H 1.03 (*d*, *J* = 6.5 Hz, Me-2) and 0.85 (*t*, *J* = 6.5 Hz, Me-3) showed correlations in the COSY spectrum (**Figure 139**), indicating another acid part of this bisamide as isobutyric acid. The remaining methylenes in the region δ_H 2.02-3.68 and one amide proton at δ_H 5.91 (*d*, *J* = 9.0 Hz) suggested that the bifuntional amine part would be a cyclic 2-aminopyrrolidine.

The ^{13}C spectrum (**Figure 138** and **Table 19**) also exhibited signals which were consistent with the ^1H spectrum, including two amide carbonyl carbons, two olefinic carbons, two methyl groups, four methylenes, six aromatic carbons and two methine carbons. Among two methines one of which appeared at the low field (δ_C 62.50) was assigned for C-2′. This was further confirmed by the HMBC (**Figures 140** and **141**) correlation of δ_H 6.1 (H-2′) to δ_C 175.3 (C-1) of amide carbonyl carbon.

On standing in the $CDCl_3$, HAO6 underwent partial epimerization at C-2′. This was apparent in the ^{13}C NMR (**Table 19**) spectrum which exhibited two sets of some of the resonances. The ratio of epimer was about 1:1. The partial racemization at C-2′ may easily occur *via* a ring opening mechanism of the 2- amino-substituted pyrrolidine ring (acetal-like N-C-N arrangement) as described previously by Brader *et al*. (1998).

Based on these spectral data and comparison with earlier reported data (Shiengthong *et al*., 1979), HAO6 was identified as a mixture of odorine (HAO6A) and its 2′-epimer (HAO6B).

The pyrrolidine derivative, odorine, appears to be widely distributed within *Aglaia* and has

already been reported from *A. argentea* Blume and *A. forbesii* King (Dumontet *et al*., 1996) as well as from *A. elliptica* Blume (syn. *A. harmsiana* Perkins) (Inada *et al*., 1995). Furthermore, odorine and its 2′-epimer were found to inhibit the growth of the vinblastine-resistant KB cells by enhancing the anticancer activity of vinblastine (Saifah *et al*.,, 1993).

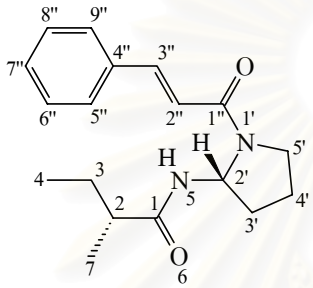

odorine

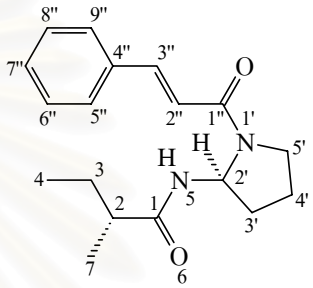

2′-*epi*-odorine

Table 19. Comparison of the NMR spectral data of odorine and compound HAO6 ($CDCl_3$, 500 MHz)

Position	**HAO6A**		**HAO6B (2′-epimer)**	**Odorine**	
	^{1}H (mult., *J* in Hz)	**^{13}C (mult.)**	**^{13}C (mult.)**	**^{1}H***	**^{13}C****
1		175.3 (*s*)	175.4 (*s*)		175.9
2	1.98 (*m*)	43.3 (*d*)	43.3 (*d*)		43.3
3	1.40 (*m*)	27.1 (*t*)	27.1 (*t*)	1.49 (*m*)	27.1
2′	6.13 (*t,* 7.5)	62.5 (*d*)	62.6 (*d*)	6.12 (*m*)	62.8
3′	2.22 (*m*)	34.7 (*t*)	34.5 (*t*)	2.00 (*m*)	34.6
4′	2.02 (*m*)	21.8 (*t*)	21.7 (*t*)	2.00 (*m*)	21.8
5′	3.44/3.68 (each *m*)	46.0 (*t*)	46.0 (*t*)	3.62 (*m*)	46.1
1′′		165.8 (*s*)	165.7 (*s*)		166.2
2′′	6.90 (*d*, 15.5)	142.9 (*d*)	143.0 (*d*)	6.94 (*d*, 16.0)	143.0
3′′	7.63 (*d*, 15.5)	117.9 (*d*)	117.9 (*d*)	7.64 (*d*, 16.0)	118.2

Table 19. Comparison of the NMR spectral data of odorine and compound HAO6 ($CDCl_3$, 500 MHz) (continued)

Position	HAO6A		HAO6B (2′-epimer)	Odorine	
	^{1}H (mult., *J* in Hz)	^{13}C (mult.)	^{13}C (mult.)	^{1}H*	^{13}C**
4′′		134.9 (*s*)	134.9 (*s*)		135.4
5′′,9′′	7.52 (*dd*, 8.0, 1.5)	128.8 (*d*)	128.8 (*d*)	7.40 (*m*)	128.8
6′′,8′′	7.25-7.32 (*m*)	129.2 (*d*)	129.2 (*d*)	7.40 (*m*)	129.8
7′′	7.25-7.32 (*m*)	129.8 (*d*)	129.8 (*d*)	7.40 (*m*)	128.2
Me-2	1.03 (*d*, 6.5)	17.3 (*q*)	17.4 (*q*)	1.12 (*d*, 7.0)	17.4
Me-3	0.85 (*t*, 6.5)	11.9 (*q*)	11.8 (*q*)	0.76 (*t*, 7.0)	11.8
NH-5	5.91 (*d*, 9.0)			6.60 (*d,* 8.0)	

***** Purushothaman and Sarada, 1979

****** Shiengthong *et al*., 1979

สถาบันวิทยบริการ
จุฬาลงกรณ์มหาวิทยาลัย

2.7 Identification of Compound HAO7

Compound HAO7 was obtained as colorless needle crystals. It has the molecular formula $C_{30}H_{50}O_3$ which was deduced from the peak $[M]^+$ at *m/z* 458 in the EIMS (**Figure 142**). IR (**Figure 143**) spectrum showed the presence of hydroxyl (3407 cm^{-1}) and carbonyl (1699 cm^{-1}) functionalities.

The ^{13}C APT spectrum (**Figures 145** and **146**) showed 30 carbons consisting of eight methyls, ten methylenes, five methines, six quaternary carbon atoms and one carbonyl carbon. The presence of carbons bearing an oxygen function can be observed in ^{13}C APT spectrum by the signals at δ_C 75.47 (C-20), 78.78 (C-24) and 73.14 (C-25). The ^1H-NMR spectrum (**Figure 144**) showed eight tertiary methyls at δ_H 0.98 (Me-18), 0.93 (Me-19), 1.15 (Me-21), 1.16 (Me-26), 1.21 (Me-27), 1.07 (Me-28), 1.03 (Me-29) and 0.87 (Me-30), the deshielded methine proton resonated at δ_H 3.38 (*dd*, *J* = 10.4, 1.5 Hz, H-24) and the α-methylene protons adjacent to 3-ketone group in ring A of the tetracyclic system appeared at δ_H 2.50 (H-2ax) and 2.44 (H-2eq). These data were typical of the dammarane group of triterpenes (Cascon and Brown, 1972; Asakawa, *et al*., 1977; Hasan *et al*., 1984).

The ^1H and ^{13}C NMR chemical shifts of ring A and B of cabraleone, previously isolated from *Aglaia elaeagnoidea* (Fuzzati *et al*., 1996), *A. tomentosa* (Mohamad *et al*., 1999) and *A. rubiginosa* (Rivero-Cruz *et al*., 2004), could be matched closely to HMQC data for HAO7, and the resulting signal assignments (**Table 20**) were consistent with the HMBC and ^1H-^1H COSY spectra. The similarity of the chemical shifts established that HAO7 has the same carbon skeleton and stereochemistry as cabraleon in the basis tetracyclic system. The assignment of the remaining 20,25-epoxy functionality came from the following evidence.

In the mass spectrum, HAO7 exhibited important fragments at *m/z* 143 ($C_8H_{15}O_2$) and 125 ($C_8H_{15}O_2$- H_2O), indicating the existence of one hydroxyl group in the cyclized side chain of epoxy triterpenoid. Cross peak correlations were depicted in HMBC spectrum (**Figure 147**) between Me-21 (δ_H 1.15) and C-20 and between both Me-26 (δ_H 1.16) and Me-27 (δ_H 1.21) and C-25 , indicated the location of two oxygenated quaternary carbons appearing at δ 75.47 and 73.14 as C-20 and C-25, respectively.

The observed HBMC (**Figure 147**) correlations from δ_H 1.15 (Me-21) to 49.94 (C-17), 75.47 (C-20) and 36.80 (C-22) and from δ_H 3.38 (H-24) to 25.64 (C-23) and 73.14 (C-25) clearly indicated the presence of an 20,25-epoxy functionality. Furthermore, inspection of the HMBC spectrum (**Figure 147**) showed that the signal of oxygenated methine proton at δ_H 3.38 (H-24) was coupled to δ

73.14 (C-25) of oxygenated quaternary carbon, suggesting the location of a hydroxyl group at C-24. The final consideration was to assign stereochemistry of hydroxyl group at C-24. The coupling constant for H-24 (δ_H 3.38) was 10.4 Hz indicated an axial-axial interaction with the axial partner of H_2-23. This would make H-24 axial (β) and the OH at this position therefore equatorial (α).

Based on these data, HAO7 was identified as 20*S*,25-epoxy-24*R*-hydroxy-3-dammaranone which had already been found from *Cistus libanotis* (Rutaceae) (De Pascual Teresa *et al*., 1982) and *Erythrophleum fordii* (Fabaceae) (Nan, Fang, and Shishan, 2004).

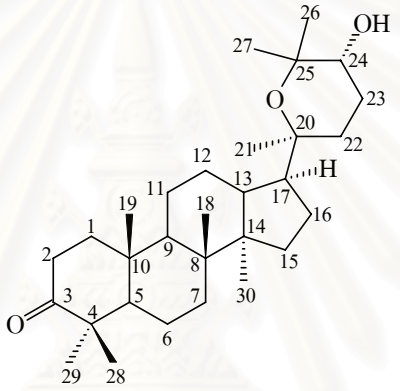

20*S*,25-epoxy-24*R*-hydroxy-3-dammaranone

Table 20. NMR spectral data of HAO7 and partial comparison of ^{13}C resonances with cabraleone ($CDCl_3$, 400 MHz)

position	HAO7			Cabraleone*
	^{1}H (mult., *J* in Hz)	**^{13}C (mult.)**	**HMBC**	**^{13}C (mult.)**
1	1.92/1.43 (each *m*)	39.84 (*t*)	C-2,C-3,C-5,C-10,C-19	39.96 (*t*)
2	2.50 (*ddd*, 15.7, 9.6, 7.5) 2.44 (*ddd*, 15.7, 7.8, 4.5)	34.07 (*t*)	C-1,C-3	34.12 (*t*)
3		218.08 (*s*)		217.96 (*s*)
4		47.40 (*s*)		47.42 (*s*)
5	1.37 (*m*)	55.30 (*d*)		55.41 (*d*)
6	1.56/1.47 (each *m*)	19.62 (*t*)		19.70 (*t*)

Table 20. NMR spectral data of HAO7 and partial comparison of ^{13}C resonances with cabraleone ($CDCl_3$, 400 MHz) (continued)

position	HAO7			Cabraleone*
	^{1}H (mult., *J* in Hz)	^{13}C (mult.)	HMBC	^{13}C (mult.)
7	1.57/1.32 (each *m*)	34.50 (*t*)		34.60 (*d*)
8		40.25 (*s*)		40.35 (*s*)
9	1.80 (*m*)	50.04 (*d*)		50.23 (*d*)
10		36.93 (*s*)		36.91 (*s*)
11	1.51/1.36 (each *m*)	21.99 (*t*)	C-9	22.10 (*t*)
12	1.83/1.3 (each *m*)	27.42 (*t*)		25.84 (*t*)
13	1.63 (*m*)	42.58 (*d*)		43.35 (*d*)
14		50.25 (*s*)		50.04 (*s*)
15	1.46/1.12 (each *m*)	31.11 (*t*)		31.46 (*t*)
16	1.79/1.4 (each *m*)	24.87 (*t*)		27.80 (*t*)
17	1.44 (*m*)	49.94 (*d*)	C-21	49.84 (*d*)
18	0.98 (*s*)	15.17 (*q*)	C-7, C-9	16.08 (*q*)
19	0.93 (*s*)	15.97 (*q*)	C-1,C-2,C-5,C-7,C-8,C-9,C-10	15.23 (*q*)
20		75.47 (*s*)		-
21	1.15 (*s*)	25.29 (*q*)	C-17,C-20,C-22	-
22	1.74/1.60 (each *m*)	36.80 (*t*)	C-23	-
23	1.63/1.42 (each *m*)	25.64 (*t*)		-
24	3.38 (*dd*, 10.4, 1.5)	78.78(*d*)	C-23, C-22, C-25	-
25		73.14 (*s*)		-
26	1.16 (*s*)	23.32 (*q*)	C-24,C-25,C-27	-
27	1.21 (*s*)	26.59 (*q*)	C-24,C-25,C-26	-
28	1.07 (*s*)	26.68 (*q*)	C-3,C-4,C-5,C-29	27.15 (*q*)
29	1.03 (*s*)	20.98 (*q*)	C-3,C-4,C-5,C-28	21.02 (*q*)
30	0.87 (*s*)	16.32 (*q*)	C-8,C-13,C-14,C-15	16.34 (*q*)

* Waterman and Ampofo, 1985 (in $CDCl_3$, 90.56 MHz)

2.8 Identification of Compound EAO1

Compound EAO1 was obtained as colorless needle crystals. The molecular formula $C_{30}H_{52}O_3$ for this compound was deduced from its mass spectrum ($[M]^+$ at *m/z* 460) (**Figure 148**) in combination with the IR (**Figure 149**) absorption band at 3399 cm^{-1}. The appearance of the fragment peak at *m/z* 143 strongly suggested that EAO1 would be the dammarane type triterpene with the cyclized side chain of the epoxy type (Cascon and Brown, 1972).

Both ^1H and ^{13}C NMR spectra (**Figures 150-152**) of EAO1 showed two sets of the resonances, suggesting that this compound, although homogeneous by TLC, was in fact a 1:1 mixture of epimers, EAO1A and EAO1B at C-3, judging from the presence of two oxymethine protons at δ_H 3.37 (*t*, *J* = 3 Hz) and 3.17 (*dd*, *J* = 11.5, 5 Hz) in the ^1H-NMR spectra and the signals resonated at δ_C 76.27 and 78.94 of oxymethine carbons in the ^{13}C NMR spectra.

The C-3 epimeric mixture, EAO1A and EAO1B, gave ^1H and ^{13}C NMR spectra which were similar to those of HAO7, but instead of a keto carbonyl, it showed an extra secondary alcohol suggesting its nature as the 3-hydroxy derivative of HAO7. This was confirmed by the following evidences.

The ^1H-NMR spectrum of each component of the mixture, EAO1A and EAO1B (**Figure 150**) showed almost identical signals, including eight tertiary methyls and an oxymethine protons resonated at δ_H 3.38 (*dd*, *J* = 10.5, 1.3 Hz, H-24), while a difference was found in the the splitting patterns and the coupling constants of oxymethine protons at C-3. In EAO1A an oxymethine proton formed triplet with small coupling constant of 3.0 Hz, while in EAO1B the corresponding proton formed double doublet with large coupling constant (11.5 Hz), indicating 3α-OH group in the former and 3β-OH group in the latter (Hasan et al., 1984; Waterman and Ampofo, 1985).

All signals of a C-3 epimeric mixture and their connectivity were established by HSQC, HMBC experiments (**Figures 153-157**). The observed HMBC (**Figures 155-157**) correlations from δ_H 1.03 (Me-21) to 49.54 (C-17), 75.57 (C-20) and 36.89 (C-22) and from δ_H 3.38 (*dd*, 10.5, 1.3, H-24) to 25.60 (C-23) and 73.15 (C-25) suggested an 20,25-epoxy functionality in this molecule. The relative stereochemistry at C-24 was determined from the large coupling constant (10.5 Hz) between H-23ax and H-24 which indicated the β orientation of H-24 (3.38, *dd*, *J* = 10.5, 1.3 Hz).

Based on the spectral data analysis (**Table 21**), the structure of EAO1 was identified as a mixture of 20*S*,25-epoxy-24*R*-hydroxydammarane 3α-ol (EAO1A) and its C3-epimer, 20*S*,25-epoxy-24*R*-

hydroxydammarane 3β-ol (EAO1B).

Previous study has revealed the co-occurrence of 20*S*,25-epoxy-24*R*-hydroxydammarane 3α-ol and its 3-oxodammarane derivative (20*S*,25-epoxy-24*R*-hydroxy-3-dammaranone) in *Cistus libanotis* (Rutaceae) (De Pascual Teresa *et al*., 1982). However, no information on the biological activities of these compounds is currently available.

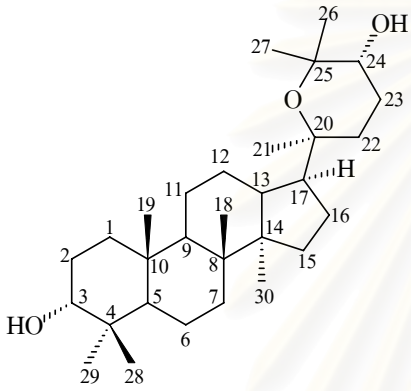

20*S*,25-epoxy-24*R*-hydroxydammarane 3α-ol

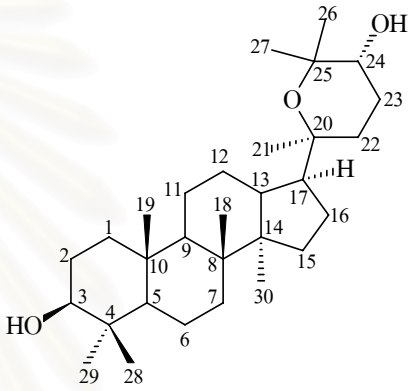

20*S*,25-epoxy-24*R*-hydroxydammarane 3β-ol

Table 21. NMR spectral data of EAO1 ($CDCl_3$, 500 MHz)

position	EAO1A		EAO1B	
	^{1}H (mult., *J* in Hz)	**^{13}C (mult.)**	**^{1}H (mult., *J* in Hz)**	**^{13}C (mult.)**
1		33.63 (*t*)		39.03 (*t*)
2		25.34 (*t*)		27.36 (*t*)
3	3.37 (*t*, 3.0)	76.28 (*d*)	3.17 (*dd*, 11.5, 5.0)	78.95 (*d*)
4		37.62 (*s*)		39.01 (*s*)
5		49.51 (*d*)		55.85 (*d*)
6		18.22 (*t*)		18.24 (*t*)
7		35.11 (*t*)		35.18 (*t*)
8		40.50 (*s*)		40.33 (*s*)
9		50.37 (*d*)		50.41 (*d*)

Table 21. NMR spectral data ($CDCl_3$, 500 MHz) of (continued)

position	EAO1A		EAO1B	
	^{1}H (mult., *J* in Hz)	^{13}C (mult.)	^{1}H (mult., *J* in Hz)	^{13}C (mult.)
10		37.24 (*s*)		37.12 (*s*)
11		21.36 (*t*)		21.50 (*t*)
12		27.42 (*t*)		27.42 (*t*)
13		42.54 (*d*)		42.50 (*d*)
14		50.30 (*s*)		50.30 (*s*)
15		31.12 (*t*)		31.14 (*t*)
16		24.89 (*t*)		24.87 (*t*)
17		49.88 (*d*)		49.88 (*d*)
18	0.93 (*s*)	15.47 (*q*)	0.93 (*s*)	15.45 (*q*)
19	0.83 (*s*)	16.01 (*q*)	0.83 (*s*)	16.19 (*q*)
20		75.58 (*s*)		75.77 (*s*)
21	1.13 (*s*)	25.16 (*q*)	1.13 (*s*)	23.28 (*q*)
22		36.90 (*t*)		36.96 (*t*)
23		25.60 (*t*)		25.61 (*t*)
24	3.38 (*dd*, 10.5, 1.3)	78.81 (*d*)	3.38 (*dd*, 10.5, 1.3)	78.81 (*d*)
25		73.15 (*s*)		73.00 (*s*)
26	1.15 (*s*)	23.28 (*q*)	1.15 (*s*)	25.16 (*q*)
27	1.21 (*s*)	26.59 (*q*)	1.21 (*s*)	26.59 (*q*)
28	0.91 (*s*)	28.21 (*q*)	0.95 (*s*)	27.97 (*q*)
29	0.83 (*s*)	22.10 (*q*)	0.83 (*s*)	15.34 (*q*)
30	0.86 (*s*)	16.53 (*q*)	0.87 (*s*)	16.43 (*q*)

3. Bioactivities of Compounds Isolated from *Aglaia forbesii* and *Aglaia oligophylla*

In the search for biologically active constituents of *Aglaia forbesii* and *A. oligophylla*, the hexane, dichloromethane, EtOAc and MeOH extracts of the leaves of *Aglaia forbesii*, as well as the hexane, EtOAc and MeOH extracts of the leaves *A. oligophylla*, were subjected to *in vitro* screenings for their cytotoxic activity against NCI-H187 (human small cell lung cancer), antimalarial activity against *Plasmodium falciparum*, antituberculosis activity against *Mycobacterium tuberculosis* $H_{37}Ra$ and anti-herpes simplex virus type 1 activity.

3.1 Bioactive Compounds from *Aglaia forbesii*

The hexane and dichloromethane extracts of the leaves of *Aglaia forbesii* were found to exhibit antiviral activity against herpes simplex virus type 1. The hexane extract was moderately active (>35-50 % viral inhibition) at the non-cytotoxic concentration of 27.8 μg/ml and the dichloromethane extract was active with IC_{50} value of 1.9 μg/ml at 38.1 μg/ml. In addition, the dichloromethane extract exhibited antituberculosis activity against *Mycobacterium tuberculosis* $H_{37}Ra$ with MIC value of 25 μg/ml.

Four compounds (lupeol, lupenone, spathulenol and a mixture of β-sitosterol and stigmasterol) were isolated from the hexane extracts of *Aglaia forbesii* leaves, whereas the dichloromethane extract afforded seven compounds, including three cyclopenta[*bc*]benzopyran flavaglines (desacetylpyramidaglains A, C and D), the cycloartane triterpenoid 23,24,25-trihydroxycycloartan-3-one, two pregnane steroids (2β,3β-dihydroxy-5α-pregn-17(20)-(*Z*)-en-16-one and 2β,3β-dihydroxy-5α-pregn-17(20)-(*E*)-en-16-one) and one bisamide (pyramidatine).

All of these isolated compounds, except spathulenol and β-sitosterol/stigmasterol mixture, were evaluated for their biological activities and the results are summarized in **Table 22**.

3.1.1 Cytotoxic Activity

Lupeol, previously reported as cytotoxic against human hepatocellular carcinoma (Hep-G2) and human epidermoid carcinoma (A-431) (Ajaiyeoba *et al*., 2003), was shown to be cytotoxic to small cell lung cancer cell line (NCI-H187) with IC_{50} of 6.84 μg/ml.

3.1.2 Antituberculosis Activity

As can be seen from Table 22, all compounds tested, except desacetylpyramidaglains A

and C, exhibited antituberculosis activity against *Mycobacterium tuberculosis* H_{37}Ra. Among these bioactive compounds, desacetylpyramidaglain D and pyramidatine showed strongest activity with MIC value of 25 μg/ml. Up to now, this is the first report on the antibacterial activity of the cyclopenta[*bc*]benzopyran flavaglines.

3.1.3 Anti HSV-1 Activity

The cycloartane triterpenoid, 23,24,25-trihydroxycycloartan-3-one, was shown to be moderately active against Herpes simplex virus type 1 at the non-cytotoxic concentration of 50 μg/ml. Other compounds subjected to this test were inactive, with the exception of 2β,3β-dihydroxy-5α-pregn-17(20)-(*E*)-en-16-one and desacetylpyramidaglain D, which were weakly active at the non-cytotoxic concentration of 50 μg/ml.

สถาบันวิทยบริการ
จุฬาลงกรณ์มหาวิทยาลัย

Table 22. Bioactivities of isolated compounds from *Aglaia forbesii*

Compound	Anti HSV-1 IC_{50} (µg/ml)	Anti TB MIC (µg/ml)	Cytotoxicity IC_{50} (µg/ml)	
			NCI-H187	Vero cell
Lupeol	inactive	100	6.84	43.0
Lupenone	inactive	50	inactive	> 50
pyramidatine	ND	25	ND	ND
2β,3β-dihydroxy-5α-pregn-17(20)-(*Z*)-en-16-one	inactive	200	inactive	> 50
2β,3β-dihydroxy-5α-pregn-17(20)-(*E*)-en-16-one	weakly active	100	inactive	> 50
(23*R*,24*S*)-23,24,25-trihydroxycycloartan-3-one	moderately active	50	inactive	> 50
Desacetylpyramidaglain A	inactive	inactive	inactive	> 50
Desacetylpyramidaglain C	inactive	inactive	inactive	> 50
Desacetylpyramidaglain D	weakly active	25	inactive	> 50
Rifampicin	-	0.047	-	-
Kanamycin sulfate	-	1.25	-	-
Isoniazid	-	0.05	-	-
Ellipticine	-	-	0.595	0.455
Doxorubicin	-	-	0.027	-
Acyclovir	2.09	-	-	-

ND = not determined

สถาบันวิทยบริการ
จุฬาลงกรณ์มหาวิทยาลัย

3.2 Bioactive Compounds from *Aglaia oligophylla*

Preliminary bioactivity evalution revealed that the hexane and EtOAc extracts of the leaves of *Aglaia oligophylla* exhibited strong cytotoxic activity against NCI-H187 cancer cell line at the IC_{50} values of 3.86 and 4.22 µg/ml, respectively, as well as antimalarial activity against *Plasmodium falciparum*, KI stain, at the IC_{50} values of 2.5 and 5.1 µg/ml, respectively. Furthermore, these two also displayed anti-HSV1 activity, of which the hexane extract was weakly active at 2 µg/ml and the EtOAc extract was moderately active at 23.5 ug/ml. The latter extract also showed antimycobacterial activity against *Mycobacterium tuberculosis* with the MIC value of 100 µg/ml.

Chemical investigation of the hexane extract of the leaves led to the isolation of six dammarane-type triterpenoids (dipterocarpol, a mixture of ocotillone and cabraleone, ocotillol-II, 20*S*,24*S*-dihydroxydammar-25-en-3-one, and 20*S*,25-epoxy-24*R*-hydroxy-3-dammaranone), a cyclopenta[*b*]benzofuran flavagline (rocaglaol) and a mixture of bisamide (odorine and 2′-epiodorine), while the EtOAc extract afforded a mixture of 20*S*,25-epoxy-24*R*-hydroxydammar-3α-ol and its C-3 epimer.

The results of the bioactivity evaluation of all of these isolated compounds except rocaglaol are presented in **Table 23**.

3.2.1 Cytotoxic activity

As shown in Table 23, none of these compounds were cytotoxic. The cytotoxic activity of the crude extract of *Aglaia oligophylla* might therefore be attributed to rocaglaol, previously reported as cytotoxic (Ishibashi *et al*., 1993; Dumontet *et al*., 1996; Mulholland and Nadoo, 1998).

3.2.2 Antituberculosis activity

The dammarane type triterpenoid (a mixture of 20*S*,25-epoxy-24*R* -hydroxydammmaran-3α-ol and its C-3 epimer) and a mixture of bisamide odorine and 2′-epiodorine, were able to inhibit the growth of *Mycobacterium tuberculosis* with MIC values of 50 and 200 µg/ml, respectively.

3.2.3 Anti HSV-1 activity

In this study, no anti HSV-1 activity was detected for any of these tested compounds.

3.2.4 Antimalarial acivity

All the compounds tested appeared to be devoid of antimalarial acivity against *Plasmodium falciparum*, KI stain**.** Since the cyclopenta[*b*]benzofuran flavagline, rocaglaol, was previously found to

exhibit significant insecticidal (Ishibashi *et al*., 1993) and cytotoxic (Rivero-Cruz *et al*., 2004) activity, it might be responsible for the antimalarial acivity of the crude extract.

Table 23. Bioactivities of isolated compounds from *Aglaia oligophylla*

Compound	Anti HSV-1 IC_{50} (µg/ml)	Anti TB MIC (µg/ml)	Antimalarial EC_{50} (µg/ml)	Cytotoxicity IC_{50} (µg/ml)	
				NCI-H187	Vero cell
Dipterocarpol	inactive	inactive	inactive	inactive	> 50
Ocotillone/cabraleone	inactive	inactive	inactive	inactive	> 50
Ocotillol II	inactive	inactive	inactive	inactive	> 50
20(*S*),24(*S*)-dihydroxydammar-25-en-3-one	inactive	inactive	inactive	inactive	> 50
Odorine and its 2′-epimer	inactive	200	ND	inactive	> 50
20*S*,25-epoxy-24*R*-hydroxy-3-dammmaranone	inactive	inactive	inactive	inactive	> 50
20*S*,25-epoxy-24*R*-hydroxydammmaran-3α –ol and its C-3 epimer	inactive	50	ND	inactive	> 50
Rifampicin	-	0.047	-	-	-
Kanamycin sulfate	-	1.25	-	-	-
Isoniazid	-	0.05	-	-	-
Ellipticine	-	-	-	0.595	0.455
Doxorubicin	-	-	-	0.027	-
Acyclovir	2.09	-	-	-	-
Dihydroartemisin	-	-	0.0043	-	-

ND = not determined

CHAPTER V

CONCLUSION

Chromatographic separation of the n-hexane fraction of the methanolic leaf extract of *Aglaia forbesii* led to the isolation of the sesquiterpene spathulenol, the ubiquitous triterpenoids lupeol and lupenone, and a mixture of β-sitosterol and stigmasterol. The CH_2Cl_2 fraction yielded three new cyclopenta[*bc*]benzopyran flavaglines, named desacetylpyramidaglains A, C, and D, and a new triterpene, 23,24,25-trihydroxycycloartan-3-one, together with two rare pregnane steroids, 2β,3β-dihydroxy-5α-pregn-17(*Z*)-en-16-one and 2β,3β-dihydroxy-5α-pregn-17(*E*)-en-16-one, and the bisamide pyramidatine.

Similar study on another meliaceous plant, *Aglaia oligophylla* Miq, afforded eleven of its constituents including eight dammarane-type triterpenoids (dipterocarpol, a mixture of ocotillone and cabraleone, ocotillol-II, 20*S*,24*S*-dihydroxydammar-25-en-3-one, 20*S*,25-epoxy-24*R*-hydroxy-3-dammaranone, and a mixture of 20*S*,25-epoxy-24*R*-hydroxydammar-3α-ol and its C-3 epimer (20*S*,25-epoxy-24*R*-hydroxydammar-3β-ol), a cyclopenta[*b*]benzofuran flavagline (rocaglaol) and a mixture of two pyrrolidine-type bisamides, odorine and 2′-epi-odorine.

All of the compounds from *Aglaia forbesii* , except desacetylpyramidaglains A and C, exhibited anti-TB activity, of which desacetylpyramidaglain D and pyramidatine showed the highest activity with MIC value of 25 μg/ml. 23,24,25-Trihydroxycycloartan -3-one, desacetylpyramidaglain D and 2β,3β-dihydroxy-5α-pregn-17(20)-(*E*)-en-16-one were shown to be moderately to weakly active against HSV-1 at the non-cytotoxic concentration of 50 μg/ml. Lupeol was moderately cytotoxic against NCI-H187 cancer cell line at the IC_{50} value of 6.84 μg/ml. However, all of the compounds isolated from *Aglaia oligophylla* were shown to be devoid of any bioactivity except 20*S*,25-epoxy-24*R*-hydroxydammar-3-ol and the mixture of odorine and 2′-epi-odorine which exhibited anti-TB activity with the MIC values of 50 and 200 μg/ml, respectively.

Based on present knowledge, the very characteristic bisamides and flavaglines occur only in *Aglaia* species. Hence, these natural products may be useful as chemotaxonomic markers for the genus *Aglaia*. In accordance with previous studies (Brader *et al*., 1998; Wang, *et al*., 2004), we obtained both

flavaglines and bisamide derivatives in addition to other compounds from the leaves of these two species of *Aglaia*. The results obtained in this study reinforce the view that a significant taxonomic contribution can also be expected from phytochemical characters.

สถาบันวิทยบริการ
จุฬาลงกรณ์มหาวิทยาลัย

REFERENCES

Aalbersberg, W., and Singn, Y. 1991. Dammarane triterpenoids from *Dysoxylum richii*. Phytochemistry 30: 921-926.

Ajaiyeoba, E. O., Onocha, P. A., Nwozo, S. O., and Sama, W. 2003. Antimicrobial and cytotoxicity evaluation of *Buchholzia coriacia* stem bark. Fitoterapia 74: 706-709.

Akihisa, T., Tokuda, H., Ukiya, M., Suzuki, T., Enjo, F., Koike, K., Nikaido, T., and Nishino, H. 2004. 3-Epicabraleahydroxylactone and other triterpenoids from Camellia oil and their inhibitory effect on Epstein-barr virus activation. Chem. Pharm. Bull. 52: 153-156.

Aratanechemuge, Y., Hibasami, H., Sanpin, K., Katsuzaki, H. Imai, K., and Komiya, T. 2004. Induction of apoptosis by lupeol isolated from mokumen (*Gossampinus malabarica* L. Merr) in human promyelotic leukemia HL-60 cells. Oncol. Rep. 11: 289-292.

Asakawa, J., Kasai, R., Yamasaki, K., and Tanaka, O. 1977. ^{13}C NMR study of ginseng sapogenins and their related dammarane type triterpenes. Tetrahedron 33: 1935-1939.

Bacher, M., Hofer, O., Brader, G., Vajrodaya, S., and Greger, H. 1999. Trapsakins: Possible biogenetic intermediates towards insecticidal cyclopenta[*b*] benzofurans from *Aglaia edulis*. Phytochemistry 52: 253-263.

Baumann, B., Bohnenstengel, F., Siegmund, D., Wajant, H., Weber, C., Herr, I., Debatin, K. M., Proksch, P., and Wirth, T. 2002. Rocaglamide derivatives are potent inhibitors of NF-ΚB activation in T-cells. J. Biol. Chem. 277: 44791-44800.

Benosman, A., Richomme, P., Sevenet, T., Perromat, G., Hadi, A. A. H., and Bruneton, J. 1995. Tirucallane triterpenes from the stem bark of *Aglaia leucophylla*. Phytochemistry 40: 1485-1487.

Brader, G., Vajrodaya, S., Greger, H., Bacher, M., Kalchhauser, H., and Hofer, O. 1998. Bisamides, lignans, triterpenes, and insecticidal cyclopenta[*b*]benzofurans from *Aglaia* species. J. Nat. Prod. 61: 1482-1490.

Bringmann, G., Muhlbacher, J., Messer, K., Dreyer, M., Ebel, R., Nugroho, B. W., Wray, V., and Proksch, P. 2003. Cyclorocaglamide, the first bridged, cyclopentatetrahydrobenzo-furan and a related " Open chain" rocaglamide derivative from *Aglaia oligophylla*. J. Nat. Prod. 66: 80-85.

Brochini, C. B. and Roque, N. F. 2000. Two new cneorubin related diterpenes from the leaves of *Guarea guidonia* (Meliaceae). J. Braz. Chem. Soc. 11: 361-364.

Campos, A. M., Oliveira, F. S., Machado, M. I. L., Braz-Filho, R., and Matos, F. J. A. 1991. Triterpenes from *Cedrela odorata*. Phytochemistry 30: 1225-1229.

Carpenter, R. C., Sotheeawaran, S., and Sultanbawa, M. U. S. 1980. ^{13}C NMR studies of some lupane and taraxerane triterpenes. Org. Mag. Res. 14: 462-465.

Cascon, S. C., and Brown, K. S. 1972. Biogenetically significant triterpenes in a species of Meliaceae : *Cabralea polytricha* A. Juss. Tetrahedron 28: 315-323.

Chaidir, Hiort, J., Nugroho, B. W., Bohnenstengel, F. I., Wray, V., Witte, L., Hung, P. D., Kiet, L.C., Sumaryono, W., and Proksch, P. 1999. New insecticidal rocaglamide derivatives from flowers of *Aglaia duperreana* . Phytochemistry 52: 837-842.

Chaidir, Lin, W.H., Ebel, R., Edrada, R., Wray, V., Nimtz, M., Sumaryono, W., and Proksch, P. 2001. Rocaglamides, glycosides and putrescine bisamides from *Aglaia dasyclada*. J. Nat. Prod. 64: 1216-1220.

Cui, B., Chai, H., Santisuk, T., Reutrakul, V., Farnsworth, N. R., Cordell, G. A., Pezzuto, J.M., and Kinghorn, A.D. 1997. Novel cytotoxic 1*H*-cyclopenta[*b*]benzofuran lignans from *Aglaia elliptica*. Tetrahedron 53: 17625-17632.

Collin, L. A., and Eranzblau, S. G. 1997. Microplate alamar blue assay versus BACTEC 460 system for high-throughput screening of compounds against *Mycobacterium tuberculosis* and *Mycobacterium avium*. Antimicrob. Agents Chemother. 41: 1004-1009.

Dean, F. M., Monkhe, T. V., Mulholland, D. A., and Taylor, A. H. 1993. An isoflavonoid from *Aglaia ferruginea*, an Australian member of the Meliaceae. Phytochemistry 34: 1537-1539.

De Pascual Teresa, J., Urones, J. G., Basabe, P., Sanchez, M., and Granell, F. 1982. Terpenoids and flavonoids from *Cistus libanotis* L. Ann. Quim. 78: 324-327.

Desjardins, R. E., Canfield, C. J., Haynes, J. D., and Chulay, J. D. 1979. Quantitative assessment of antimalarial activity *in vitro* by a semiautomated microdilution technique. Antimicrob. Agents Chemother. 16: 710-718.

Dreyer, M., Nugroho, B. W., Bohnenstengel, F. I., Ebel, R., Wray, V., Bringmann, G., Muhlbacher, J., Herold, M., Hung, P. D., Kiet, L. C., and Proksch, P. 2001. New insecticidal rocaglamide derivatives and related compounds from *Aglaia oligophylla*. J. Nat. Prod. 64: 415-420.

Duh, C. Y., Wang, S. K., R. S., Wu, Y. C., Wang, W. Y., Cheng, M. C., and Chang, T. T. 1993. Dehydroodorin, a cytotoxic diamide from the leaves of *Aglaia formosana*. Phytochemistry 34: 857-858.

Dumontet, V., Thoison, O., Omobuwajo, R., Martin, M. T., Perromat,G., Chiaroni, A., Riche, C., Pais, M., and Sevenet, T. 1996. New nitrogenous and aromatic derivatives from *Aglaia argentea* and *A. forbesii*. Tetrahedron 52: 6931-6942.

Engelmeier, D., Hadacek, F., Pacher, F., Vajrodaya, S., and Greger, H. 2000. Cyclopenta[*b*]-benzofurans from *Aglaia* species with pronounced antifungal activity against rice blast fungus (*Pyricularia grisea*). J. Agric. Food Chem. 48: 1400-1404.

Fraga B. M. 2003. Natural sesquiterpenoids. Nat. Prod. Rep. 20: 392-413.

Fuzzati, N., Dyatmiko, W., Rahman, A., Achmad, F., and Hostettmann, K. 1996. Triterpenoids, lignans and a benzofuran derivatives from the bark of *Aglaia elaeagnoidea*. Phytochemistry 42: 1395-1398.

Gauthier, C., Legault, J., Lebrun, M., Dufour, P., and Pichette, A. 2006. Glycosidation of lupine-type triterpenoids as potent in vitro cytotoxic agents. Bioorg. Med. Chem. 14: 6713-6725.

Geetha, T., and Varalakshmi, P. 2001. Anti-inflammatory activity of lupeol and lupeol linoleate in rats. J. Ethnopharmacol. 76: 77-80.

Greger, H., Pacher, T., Brem, B., Bacher, M., and Hofer, O. 2001. Insecticidal flavaglines and other compounds from Fijian *Aglaia* species. Phytochemistry 57: 57-64.

Greger, H., Pacher, T., Vajrodaya, S., Bacher, B., and Hofer, O. 2000. Infraspecific variation of sulfur-containing bisamides from *Aglaia leptantha*. J. Nat. Prod. 63: 616-620.

Govindachari, T. R., Kumari, G. N. K., and Suresh, G. 1995. Triterpenoids from *Walsura piscidia*. Phytochemistry 39: 167-170.

Gupta, M. B., Nath, R., Srivastava, N., Shanker, K., Kishor, K., and Bhargava, K. P. 1980. Anti-inflammatory and antipyretic activities of β-sitosterol. Planta Med. 39: 157-163.

Hasan, C. M., Islam, A., Ahmed, M., Ahmed, M-D., and Waterman, P. G. 1984. Capsugenin, a dammarane triterpene from *Corchorus capsularis*. Phytochemistry 23: 2583-2587.

Hayashi, N., Lee, K. H., Hall, I. H., Mcphail, A. T., and Huang H. C. 1982. Structure and stereochemistry of (-)-odorinol, an antileukemic diamide from *Aglaia odorata*. Phytochemistry 21: 2371-2373.

Hiort, J., Chaidir, Bohnenstengel, F. I., Nugroho, B. W., Schneider, C., Witte, L., Hung, P. D., Kiet, L. C., and Proksch. 1999. New Insecticidal rocaglamide derivatives from the roots of *Aglaia duperreana*. J. Nat. Prod. 62: 1632-1635.

Hwang, B. Y., Su, B. N., Chai, H. C., Leonardus, Q. M., Kardono, L. B. S., Afriastini, J. J., Riswan, S., Santarsiero, B. D., Mesecar, A. D., Wild, R., Fairchild, C. R., Vite,G. D., Rose, W. C., Farnsworth, N. R., Cordell, G. A., Pezzuto, J. M., Swanson, S. M., and Kinghorn, A. D. 2004. Silvestrol and episilvestrol , potential anticancer rocaglate derivatives from *Aglaia silvestris*. J. Org. Chem. 69: 3350-3358.

Inada, A., Murayta, H., Inatomi, Y., Nakanishi, T. 1995. Cycloartane triterpenoids from the leaves of *Aglaia harmsiana*. J. Nat. Prod. 58: 1143-1146.

Inada, A., Murayta, H., Inatomi, Y., Nakanishi, T., and Darnaedi, D. 1997a. Pregnanes and triterpenoid hydroperoxides from the leaves of *Aglaia grandis*. Phytochemistry 45: 1225-1228.

Inada, A., Nishino, H., Kuchide, M., Takayasu, J., Mukainaka, T., Nobukuni, Y., Okuda, M., and Tokuda, H. 2001. Cancer chemopreventive activity of odorine and odorinol from *Aglaia odorata*. Biol. Pharm. Bull. 24: 1282-1285.

Inada, A., Ohtsuki, S., Sorano, T., Murata, H., Inatomi, Y., Darnaedi, D., and Nakanishi, T. 1997b. Cycloartane triterpenenoids from *Aglaia harmsiana*. Phytochemistry 46: 379- 381.

Inada, A., Shono, K., Murata, H., Inatomi, Y., Darnaedi, D., and Nakanishi, T. 2000. Three putrescine bisamides from the leaves of *Aglaia grandis*. Phytochemistry 53: 1091- 1095.

Ishibashi, F., Satasook, C., Isman, M. B., and Towers, G. H. N. 1993. Insecticidal 1*H*-cyclopentatetrahydro[*b*]benzofurans from *Aglaia odorata*. Phytochemistry 32: 307-310.

Ivorra, M. D., D'Ocon, M. P., Paya, M., and Villar, A. 1988. Antihyperglycemic and insulin-releasing effects of β-sitosterol 3-β-D-glucoside and its aglycone, β-sitosterol. Arch Int Pharmacodyn. 296: 224-231.

Janaki, S., Vijayasekaran, V., Viswanathan, S., and Balakrishna, K. 1999. Anti- inflammatory activity of *Aglaia roxburghiana* var. *beddomei* extract and triterpenes roxburghiadiol A and B. J. Ethnopharmacol. 67: 54-51.

Janprasert, J., Satasook, C., Sukumalanand, P., Champagne, D. E., Isman, M. B., Wiriyachitra, P., and Towers, G. H. N. 1993. Rocaglamide, a natural benzofuran insecticide from *Aglaia odorata.* Phytochemistry 32: 67-69.

Joshi, M.N., Chowdhury, B.L., Vishnoi, S.P., Shoeb, A., and Kapil, R.S. 1987. Antiviral activity of (+) –odorinol. Planta Med. 53: 245-255.

Karam, M. A., and Shier, T. 1990. A simplified plaque reduction assay for antiviral agents from plants. J. Nat. Prod. 53: 340-344.

Kim, S., Su, B. N., Riswan, S., Kardono, L. B. S., Afriastini, J. J., Gallucci, J. C., Chai, H., Fransworth, N. R., Cordell, G. A., Swanson, S. M., and Kinghorn, A. D. 2005. Edulisidones A and B, two epimeric benzo[*b*]oxepine derivatives from the bark of *Aglaia edulis*. Tetrahedron Lett. 46: 9021-9024.

Kim, S., Salim, A. A., Swanson, S. M., and Kinghorn, A. D. 2006. Potential of cyclopenta[*b*]benzofurans from *Aglaia* species in cancer chemotherapy. Anticancer Agents Med. Chem. 6: 319- 345.

Kumar KC, S., and Müller, K. 1999. Medicinal plants from Nepal; II. Evaluation as inhibitors of lipid peroxidation in biological membranes. J. Etnopharmacol. 64: 135-139.

Lee, S. K., Cui, B., Mehta, R. R., Kinghorn, A. D., and Pezzuto, J. M. 1998. Cytostatic mechanism and antitumor potential of novel 1*H*-cyclopenta[*b*]benzofuran lignans isolated from *Aglaia elliptica*. Chem. Biol. Int. 115: 215-228.

Lin, C. W. H., Ebel, R., Edrada, R., Wray, V., and Nimtz, M. 2001. Rocaglamides, glucosides, and putrescine bisamides from *Aglaia dasyclada.* J. Nat. Prod. 64: 1216-1220.

Luo, X., Wu, S., Ma, Y., and Wu, D. 2000. Dammarane triterpenoids from *Amoora yunnanensis*. Heterocycles 53: 2795-2802.

Madureira, A. M., Ascenso, J. R., Valdeira, L., Duarte, A., Frade, J. P., Freitas, G., and Ferreira, M. J. U. 2003. Evaluation of the antiviral and antimicrobial activities of triterpenes isolated from *Euphorbia segetalis*. Nat. Prod. Res. 17: 375-380.

Malinovskaya, G. V., Novikov, V. L., Denisenko, V. A., and Uvarova, N. I. 1980. New triterpene from leaves of *Betula mandschurica*. Chem. Nat. Compd. (Engl. Transl.) 16: 257-261.

McChesney, J. D., Dou, J., Sindelar, R. D., Goins, D. K., Walker, L. A., and Rogers, R. D. 1997. Tirucallane-type triterpenoids: nmr and X-ray diffration analyses of 24-epi-piscidinol A and piscidinol A. J. Chem. Cryst. 27: 283-290.

Mohamad, K., Martin, M. T., Leroy, E., Tempete, C., Sevenet, T., Awang, K., and Pais, M. 1997. Argenteanones C-E and argenteanols B-E, cytotoxic cycloartanes from *Aglaia argentea*. J. Nat. Prod. 60: 81-85.

Mohamad, K., Sevenet, T., Dumontet, V., Pais, M., Tri, M. V., Hadi, H., Awang, K., and Martin, M. T. 1999. Dammarane triterpenes and pregnane steroids from *Aglaia lawii* and *A. tomentosa*. Phytochemistry 51: 1031-1037.

Moriarity, D. M., Huang, J., Yancey, C. A., Zhang, P., Setzer, W. N., Lawton, R. O., Bates, R. B., and Caldera, S. 1998. Lupeol is the cytotoxic principal in the leaf extract *of Dendropanax* cf. *querceti*. Planta Med. 64: 370-372.

Mulhollane, D. A., and Monkne, T. V. 1993. Two glabretal-type triterpenoids from the heartwood of *Aglaia ferruginaea*. Phytochemistry 34: 579-580.

Mulhollane, D. A., and Naidoo, N. 1998. A revision of the structure of ferrugin from *Aglaia ferruginea*. Phytochemistry 47: 1163.

Nan, L., Fang, Y., and Shishan, Y. 2004. Triterpenoids from *Erythrophleum fordii*. Acta Bot Sin. 40: 371-374.

Nugroho, B. W., Edrada, R. A., Wray, V., Witte, L., and Proksch, P. 1997a. Insecticidal rocaglamide derivatives from *Aglaia duppereana*. Phytochemistry 44: 1455-1461.

Nugroho, B. W., Gussregen, B., Wray, V., Witte, L., Bringmann, G., and Proksch, P. 1997b. Insecticidal rocaglamide derivatives from *Aglaia elliptica* and *A. harmsiana*. Phytochemistry 45: 1579-1585.

Nugroho, B. W., Edrada, R. A., Wray, V., Witte, L., Bringmann, G., Gehling, M., and Proksch, P. 1999. An insecticidal rocaglamide derivatives and related compounds from *Aglaia odorata* (Meliaceae). Phytochemistry 51: 367-376.

Omobuwajo, O. R., Martin, M. T., Perromat, G., Sevenet, T., Awang, K., and Pais, M. 1996. Cytotoxic cycloartanes from *Aglaia argentea*. Phytochemistry 41: 1325-1328.

Ohse, T., Ohba, S., Yamamoto, T., Koyano, T., and Umezawa, K. 1996. Cyclopentabenzofuran lignan protein synthesis inhibitors from *Aglaia odorata*. J. Nat. Prod. 59: 650-652.

Pannell, C.M. 1992. Taxonomic monograph of the genus *Aglaia* Lour. (Meliaceae), HMSO, London.

Perry, L.M. 1980. Medicinal Plants of East and Southeast Asia : Attributed Properties and Used. Cambridge: MIT Press.

Plumb, J. A., Milroy, R. and Kaye, S. B. 1989. Effects of the pH dependence of 3-(4,5-dimethylthiazol-2-yl)-2,5-diphenyl-tetrazolium bromide-formazan absorption on chemosensitivity determined by a novel tetrazolium-based assay. Cancer Res. 49: 4435-4440.

Proksch, P., Edrada, R. A., Ebel, R., Bohnenstengel, F. I., and Nugroho, B.W. 2001. Chemistry and biological activity of rocaglamide derivatives and related compounds in *Aglaia* species (Meliaceae). Curr. Org. Chem. 5: 923-938.

Puripattanavong, J., Weber, S., Brecht, V., and Frahm, A. W. 2000. Phytochemical investigation of *Aglaia andamanica*. Planta Med. 66: 740-745.

Purushothaman, K. K., and Sarada, A. 1979. The structure of roxburghilin, a bisamide of 2-aminopyrrolidine from the leaves of *Aglaia roxburghiana* (Meliaceae). J. Chem. Soc., Perkin Trans. 1. 5: 3171-3174.

Reynolds, W. F., McLene, S., Poplawski, J., Enriguez, R. G., Escobar, L. I., Leon, I. 1986. Total assignment of ^{13}C and ^{1}H spectra of three isomeric triterpenol derivatives by 2D NMR: An investigation of the potential utility of 1h chemical shifts in structural assignments of complex natural products. Tetrahedron 42: 3419-3428.

Rao, M. M., Meshulam, H., Zelnik, R., and Lavie, D. 1975. *Cabralea eichleriana* DC. (Meliaceae)-I. Structure and stereochemistry of wood extractives. Tetrahedron 31: 333-339.

Rivero-Cruz, J. F., Chai, H. B., Kardono, L. B. S., Setyowati, F. M., Afriatini, J. J., Riswan, S., Farnsworth, N. R., Cordell, G. A., Pezzuto, J. M., Swanson, S. M., and Kinghorn, A. D. 2004. Cytotoxic constituents of the twigs and leaves of *Aglaia rubiginosa*. J. Nat. Prod. 67: 343-347.

Roger, L. L., Zeng, L., and McLaughlin, J. L. 1998. New bioactive steroids from *Melia volkenzii*. J. Org. Chem. 63: 3781-3785.

Roux, D., Martin, M. T., Sevennet, T., Hadi, H. A., and Pais, M. 1998. Foveolin A and B, dammarane triterpenes from *Aglaia foveolata*. Phytochemistry 49: 1745-1748.

Rubinstein, I., Goad, L. J., Chague, A. D. H., Mulhein, L. J. 1976. The 220 MHz nmr spectra of phytosterols. Phytochemistry 15: 195-200.

Saifah, E., Jongbunprasert, V., and Kelley, C. J. 1988. Piriferine, a new pyrrolidine alkaloid from *Aglaia pirifera* leaves. J. Nat. Prod. 51: 80-82.

Saifah, E., Puripattanavong, J., Likhiwitayawuid, K., Cordell, G. A., Chai, H., and Pezzuto, J. M. 1993. Bisamides from *Aglaia* species: structure analysis and potential to reverse drug resistance with cultured cells. J. Nat. Prod. 56: 473-477.

Saifah, E., Suttisri, R., Shamsub, S., Pengsuparp, T., and Lipipun, V. 1999. Bisamides from *Aglaia edulis*. Phytochemistry 52: 1085-1088.

Salim, A. A., Pawlus, A. D., Chai, H. B., Franworth, N. R., Kinghorn, A. D., and Carcache-Blanco, E. J. 2007. Ponapensin, a cyclopenta[*bc*]benzopyran with potent NF-κB inhibitory activity from *Aglaia ponapensis*. Bioorg. Med. Chem. Lett. 17: 109-112.

Schneider, C., Bohnenstengel, F. I., Nugroho, B. W., Wray, V., Witte, V., Hung, P. D., Kiet, L. C., and Proksch, P. 2000. Insecticidal rocaglamide derivatives from *Aglaia spectabilis* (Meliaceae). Phytochemistry 54: 731-736.

Seger, C., Pacher, T., Greger, H., Saifah, E., and Hofer, O. 2002. Aglairubine: structure revision of a chemotaxonomiccally interesting bisamide in *Aglaia* (Meliaceae). Chem. Mont. 133: 97-100.

Shiengthong, D., Ungphakorn, A., Lewis, D. E., and Messy-Westropp, R. A. 1979. Constituents of Thai medicinal plants-IV; New nitrogenous compounds-odorine and odorinol. Tetrahedron Lett. 24: 2247-2250.

Skehan, R. S., Scudiero, D., Monks, A., Mcmahon, J., Vistica, D., Warren, J. T., Bokesch, H., Kenney, S., and Boyd, M. R. 1990. New colorimetric cytotoxic assay for anticancer drug screening. J. Natl. Cancer Int. 82: 1107-1112.

Smitinand, T. 2001. Thai plant names (botanical names-vernacular names) revised edition. Bangkok: The Forest Herbarium, Royal Forest Department. pp. 18-19.

Su, B. N., Chai, H., Mi, Q., Riswan, S., Kardono, L. B. S., Afriastini, J. J., Santarsiero, B. D., Mesecar, A. D., Fransworth, N. R., Cordell, G. A., Swanson, S. M., and Kinghorn, A. D. 2006. Activity-guided isolation of cytotoxic constituents from the bark of *Aglaia crassinervia* collected in Indonesia. Bioorg. Med. Chem. 14: 960-972.

Tanaka, R., Masuda, K., and Matsunaga, S. 1993. Lup-20(29)en-3β-15α-diol and ocotillol-II from the stem bark of *Phyllanthus flexuosus*. Phytochemistry 32: 472-474.

Tanaka, R., Tabuse, M., and Matsunaga, S. 1988. Triterpenes from the stem bark of *Phyllanthus flexuosus*. Phytochemistry 27: 3563-3567.

Tori, M., Matsuda, R., Sono, M., and Asakawa, Y. 1988. ^{13}C NMR assignment of dammarane triterpenes and dendropanoxide: Application of 2D long-rang e ^{13}C-^{1}H correlation spectra. Magn. Reson. Chem. 26: 581-590.

Trager, W. and Jensen, J. B. 1976. Human malaria parasites in continuous culture. Science 193: 673-675.

Wang, B. G., Ebel, R., Wang, C. Y., Wray, V., and Proksch, P. 2002. New methoxylated aryltetrahydronaphthalene lignans and a norlignan from *Aglaia cordata*. Tetrahedron Lett. 43: 5783-5787.

Wang, B. G., Peng, H., Huang, H. L., Li, X. M., Eck, G., Gong, X., and Proksch, P. 2004. Rocaglamide , aglain , and other related derivatives from *Aglaia testicularis* (Meliaceae). Biochem. System. Ecol. 32: 1223-1226.

Wanhoff, E. W., and Halls, C. M. M. 1965. Desert plant constituents: II. Ocotillol: an intermediate in the oxidation of hydroxyl isooctenyl side chains. Can. J. Chem. 43: 3311-3321.

Watermann, P. G., and Ampofo, S. 1985. Dammarane triterpenes from the stem bark of *Commiphora drazielii*. Phytochemistry 24: 2925-2928.

Weber, S., Puripattanavong, J., Brecht, V., and Frahm, A.W. 2000. Phytochemical investigation of *Aglaia rubiginosa.* J. Nat. Prod. 63: 636-642.

Wu, T. S., Liou, M. J., Kuoh, C. S., Teng, C. M., Nagao, T., and Lee, K. H. 1997. Cytotoxic and antiplatelet aggregation principles from *Aglaia elliptifolia*. J. Nat. Prod. 60: 606-608.

You, Y-J., Nam, N-H., Kim, Y., Bae, K-H., and Ahn, B-Z. 2003. Antiangiogenic activity of lupeol from *Bombax ceiba*. Phytother. Res. 17: 341-344.

สถาบันวิทยบริการ
จุฬาลงกรณ์มหาวิทยาลัย

APPENDICES

สถาบันวิทยบริการ
จุฬาลงกรณ์มหาวิทยาลัย

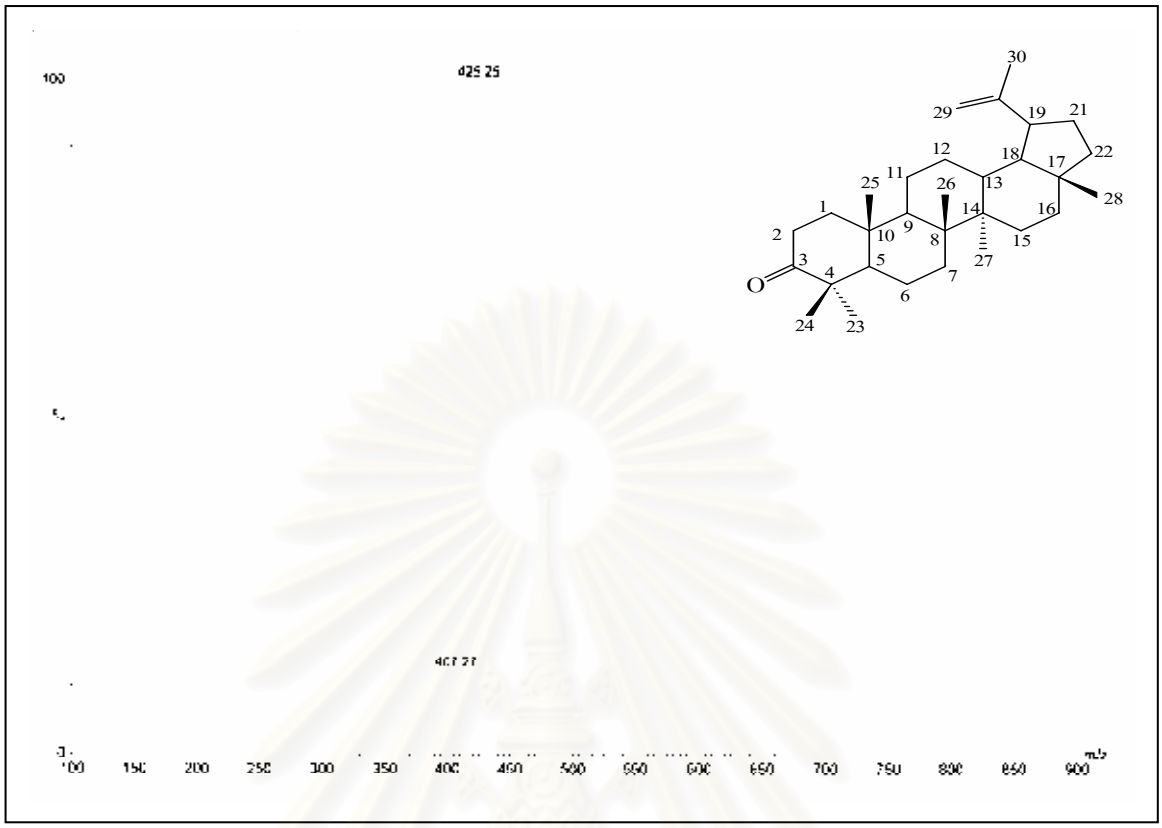

Figure 6. ESI-TOF Mass Spectrum of compound HAF1

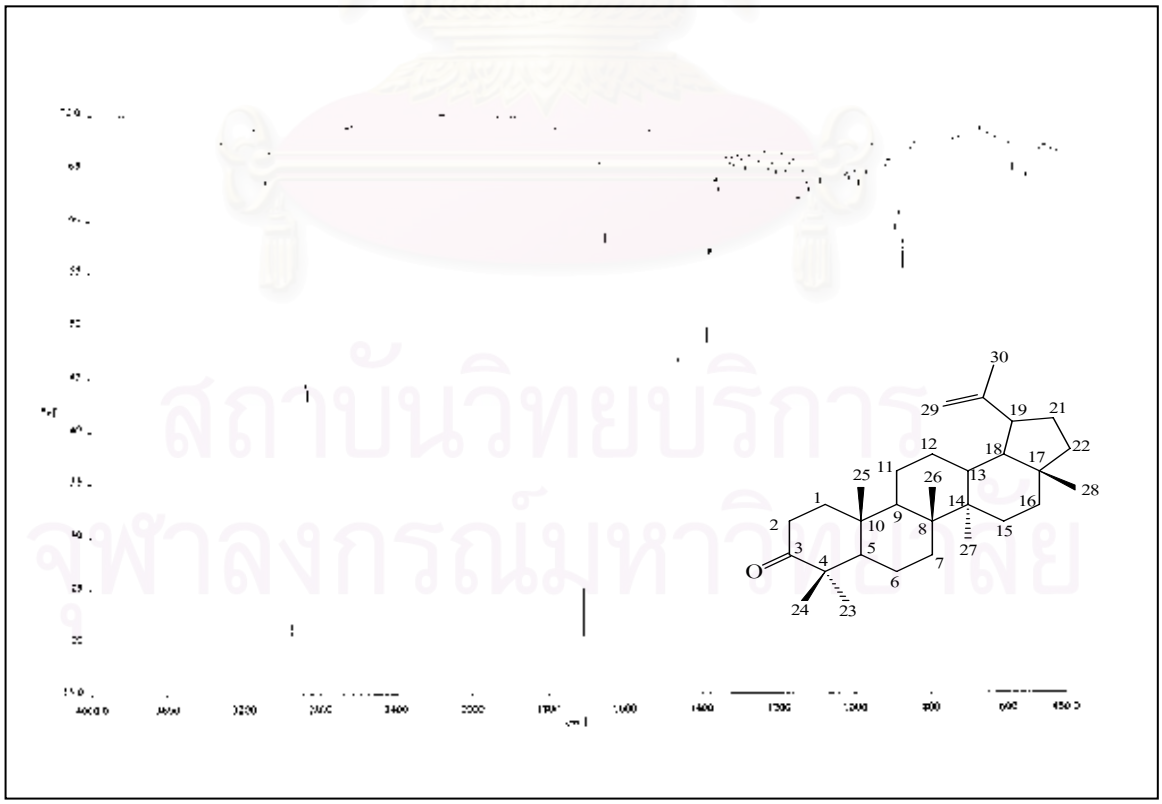

Figure 7. IR Spectrum of compound HAF1 (KBr disc)

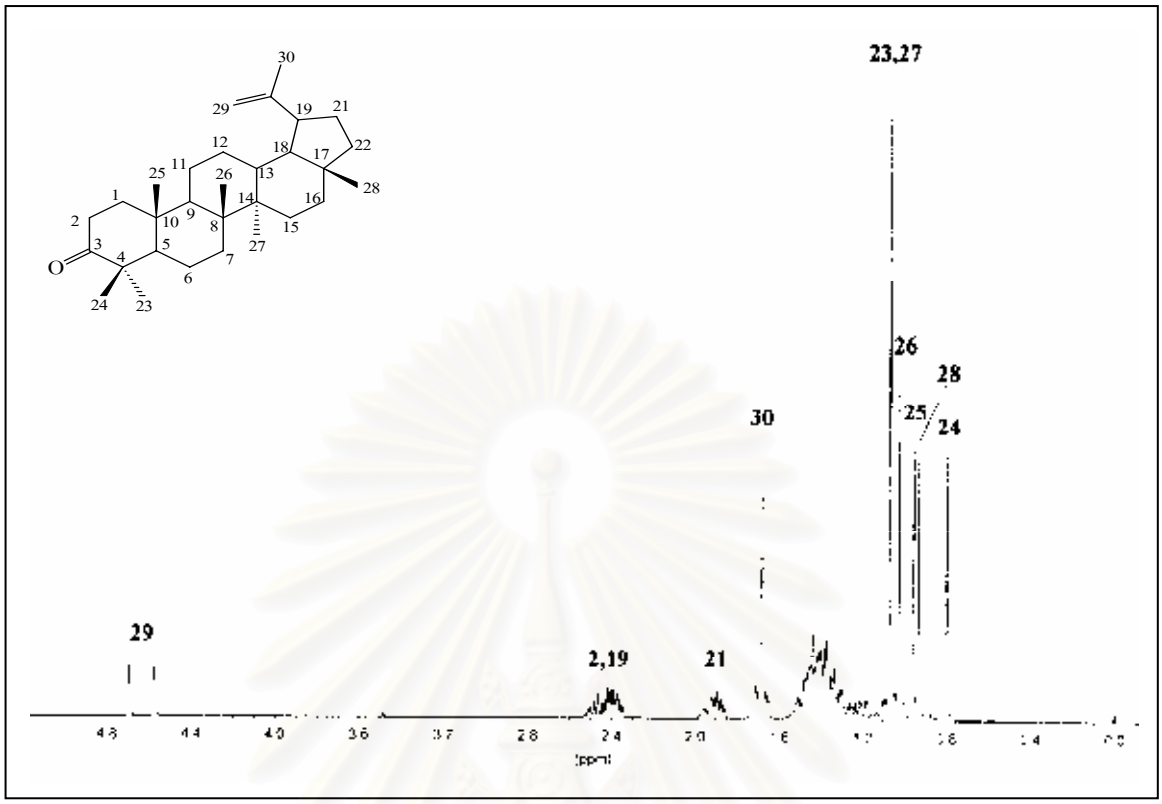

Figure 8. ^{1}H NMR (400 MHz) Spectrum of compound HAF1 ($CDCl_3$)

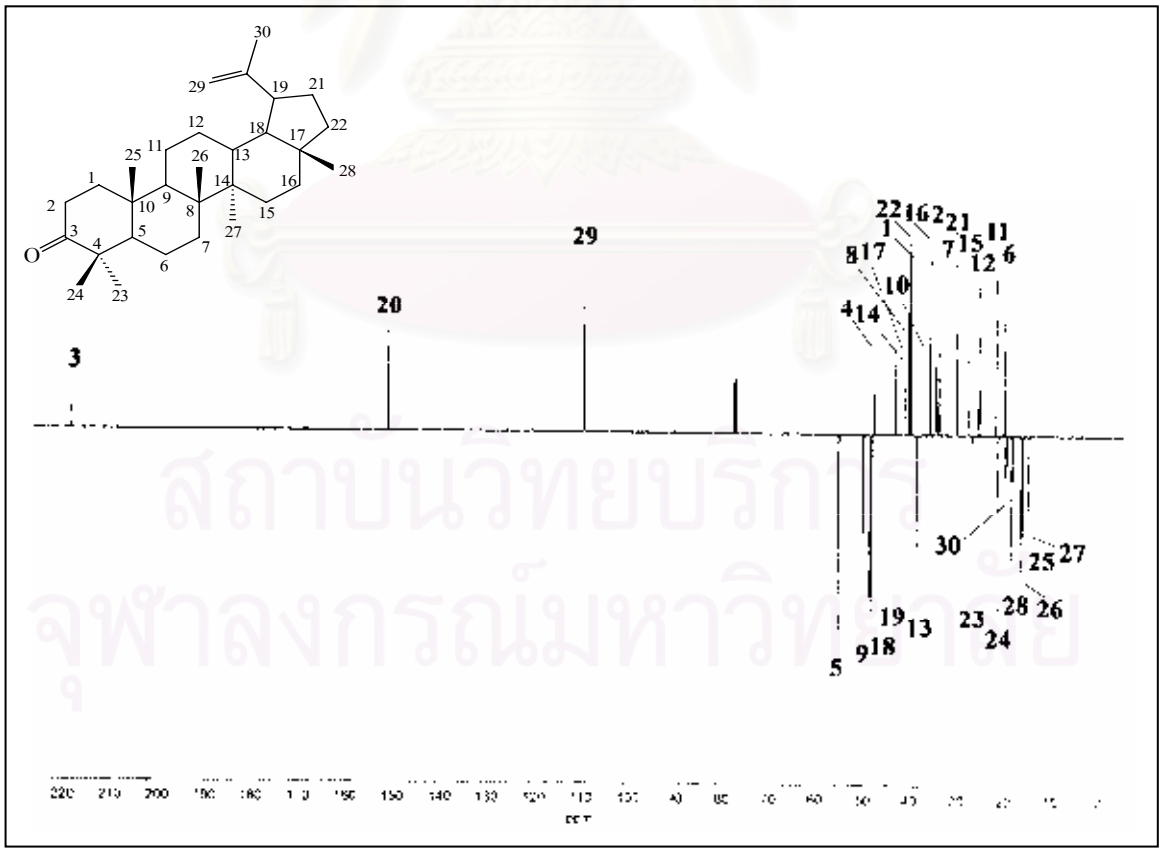

Figure 9. ^{13}C APT (100 MHz) Spectrum of compound HAF1 ($CDCl_3$)

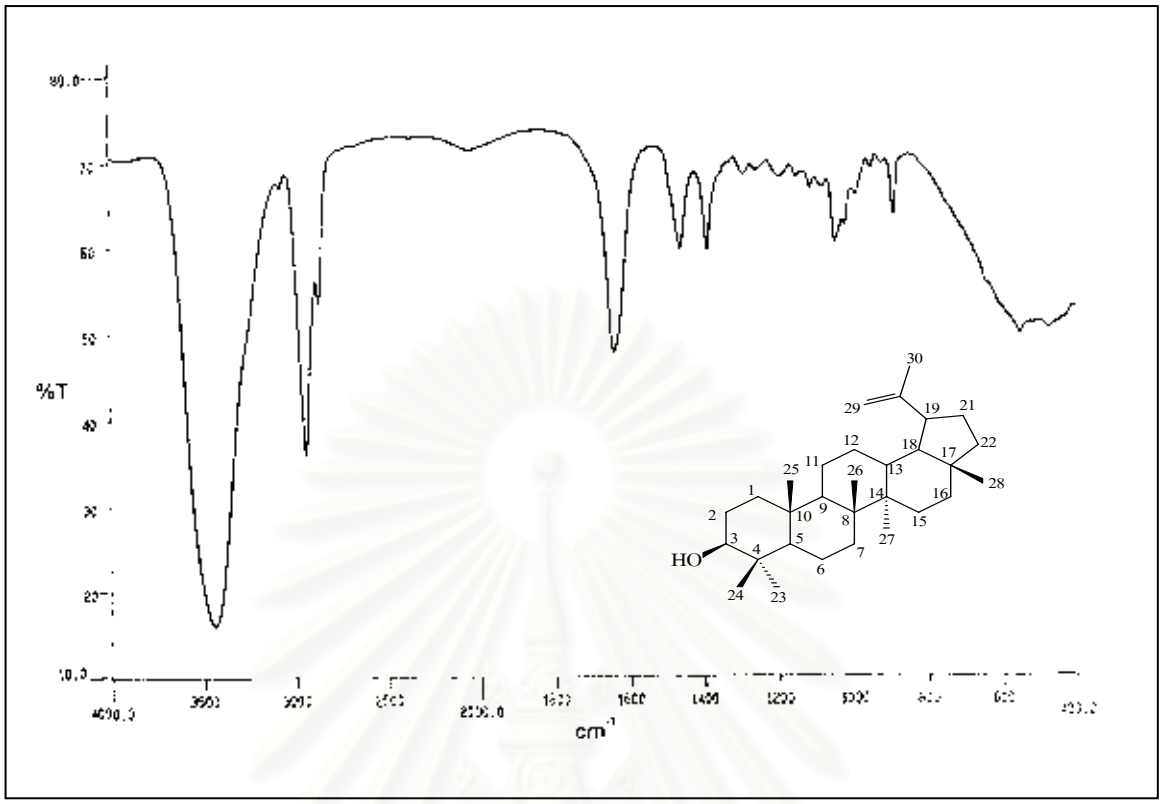

Figure 10. IR Spectrum of compound HAF2 (KBr disc)

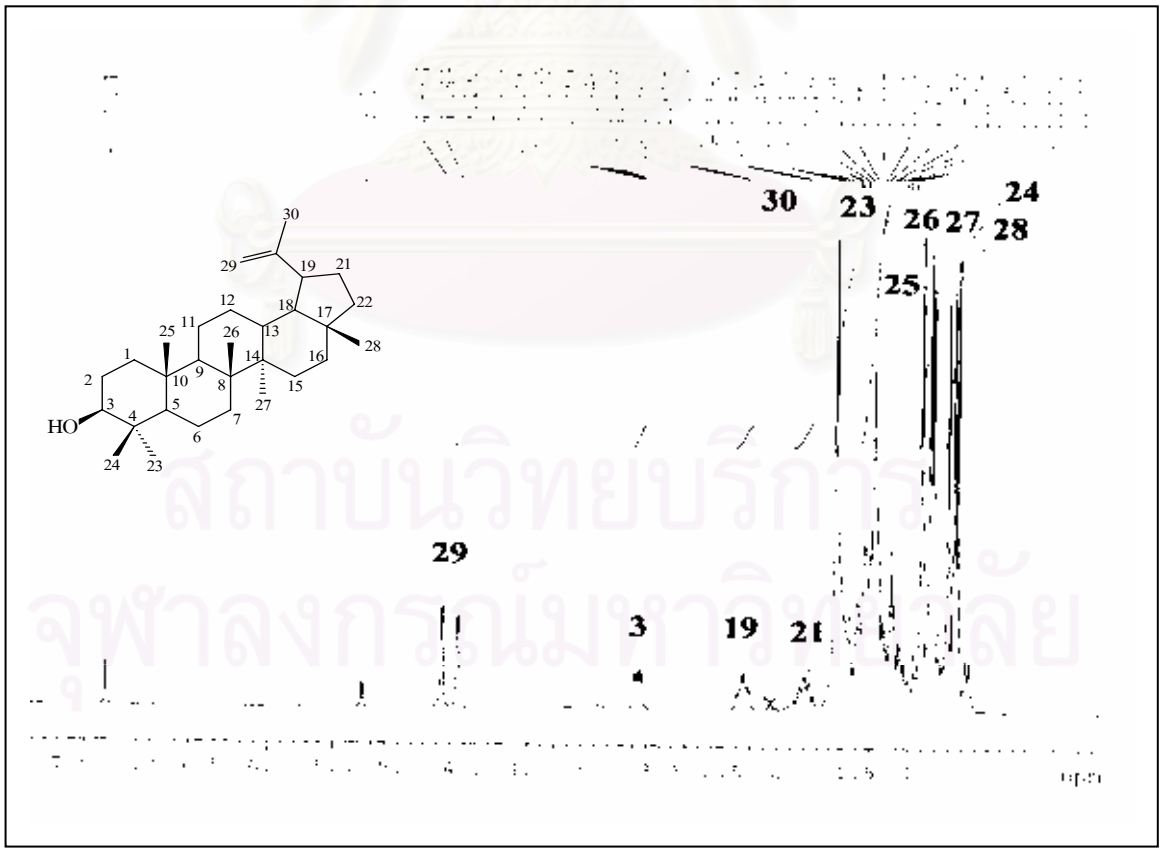

Figure 11. ^{1}H NMR (300 MHz) Spectrum of compound HAF2 ($CDCl_3$)

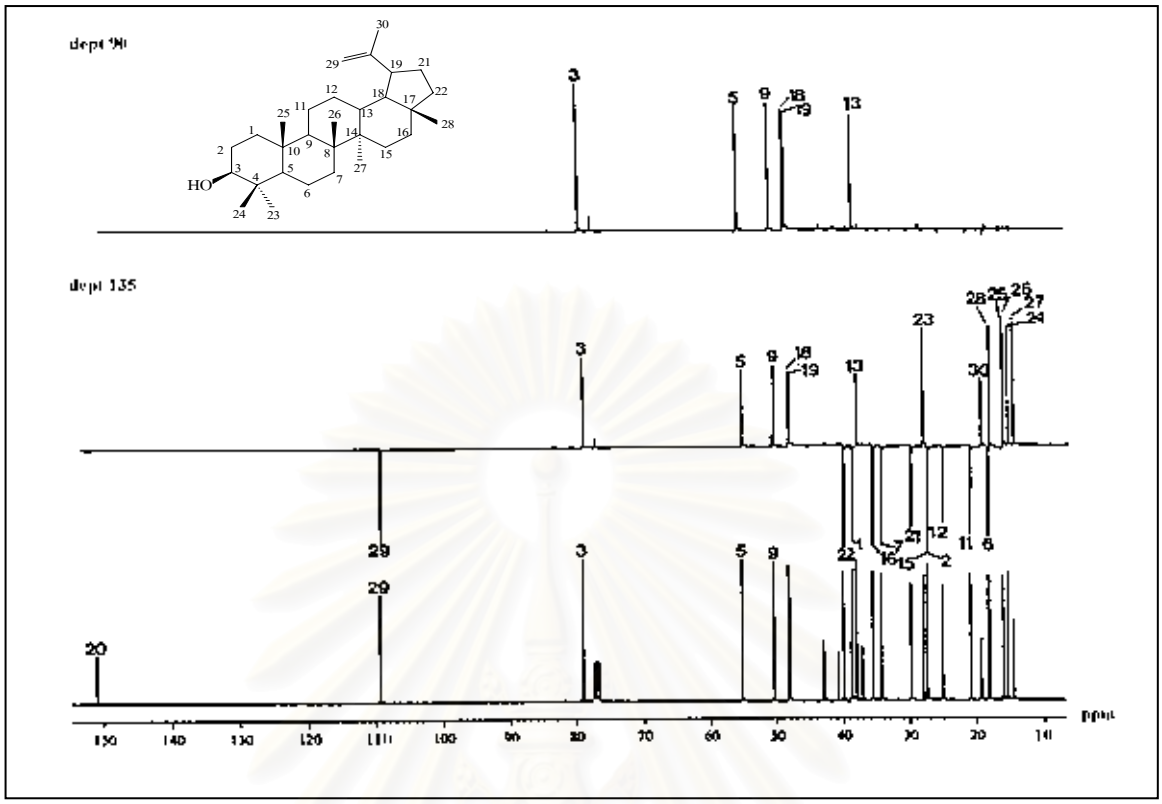

Figure 12. ^{13}C NMR (75 MHz) and DEPT Spectra of compound HAF2 ($CDCl_3$)

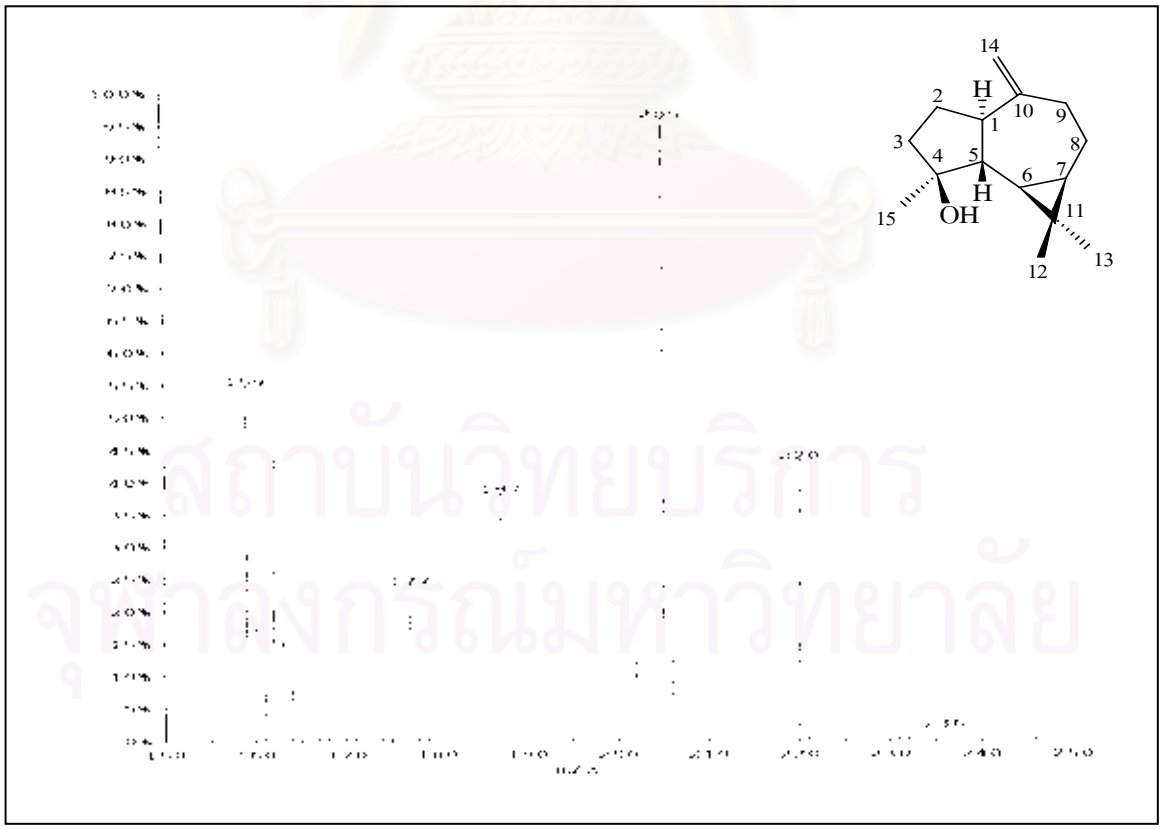

Figure 13. EI Spectrum of compound HAF3

สถาบันวิทยบริการ
จุฬาลงกรณ์มหาวิทยาลัย

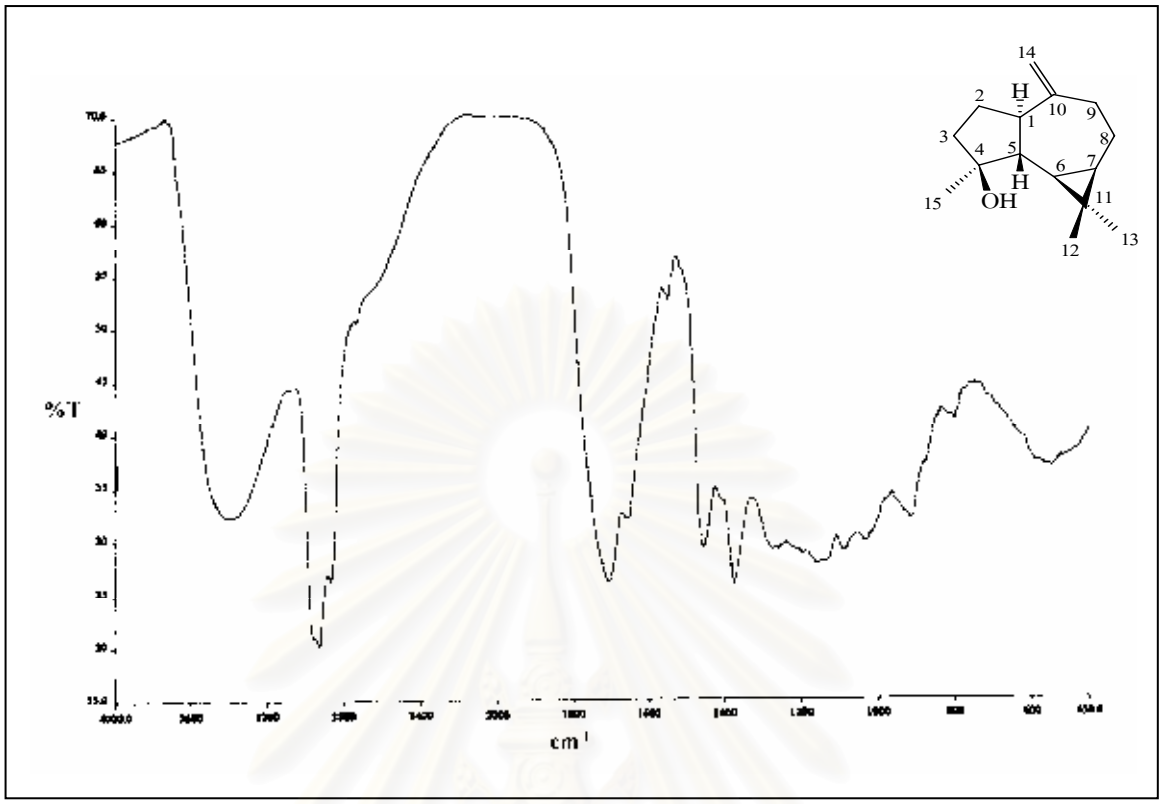

Figure 14. IR spectrum of compound HAF3 (KBr disc)

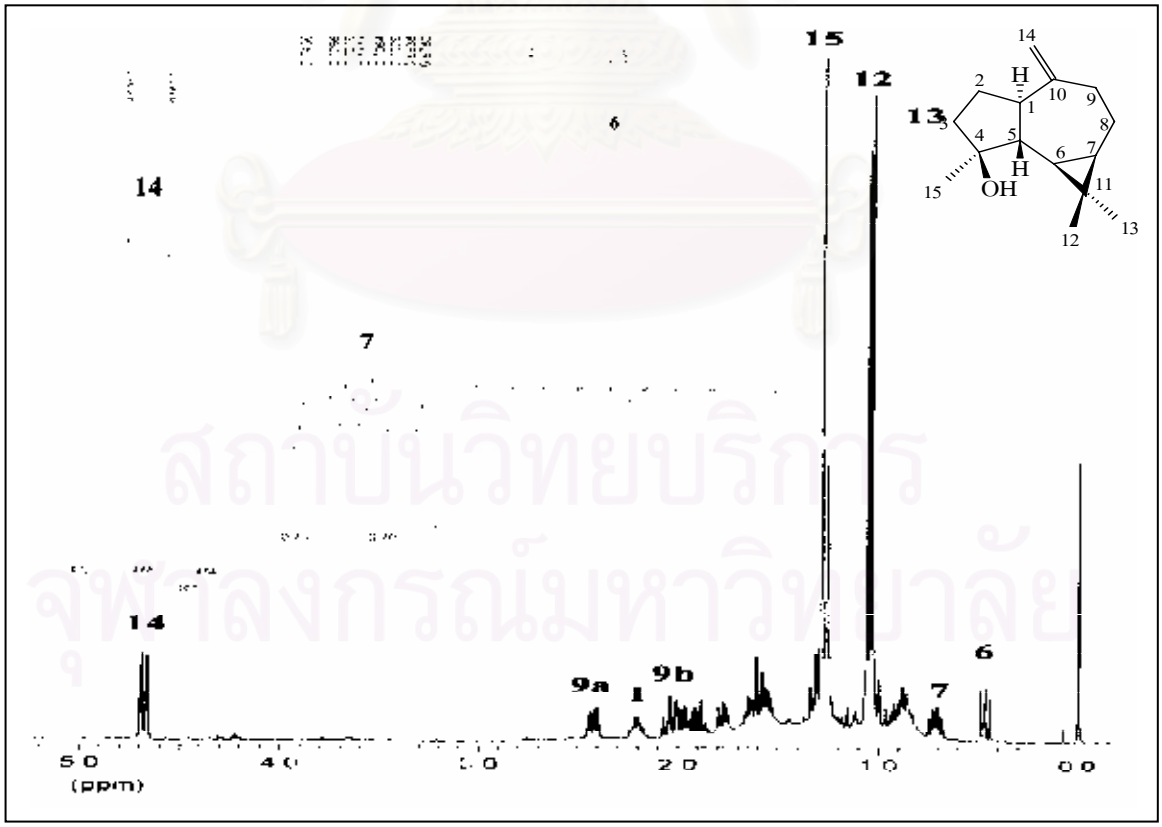

Figure. 15. ^{13}H NMR (400 MHz) Spectrum of compound HAF3 ($CDCl_3$)

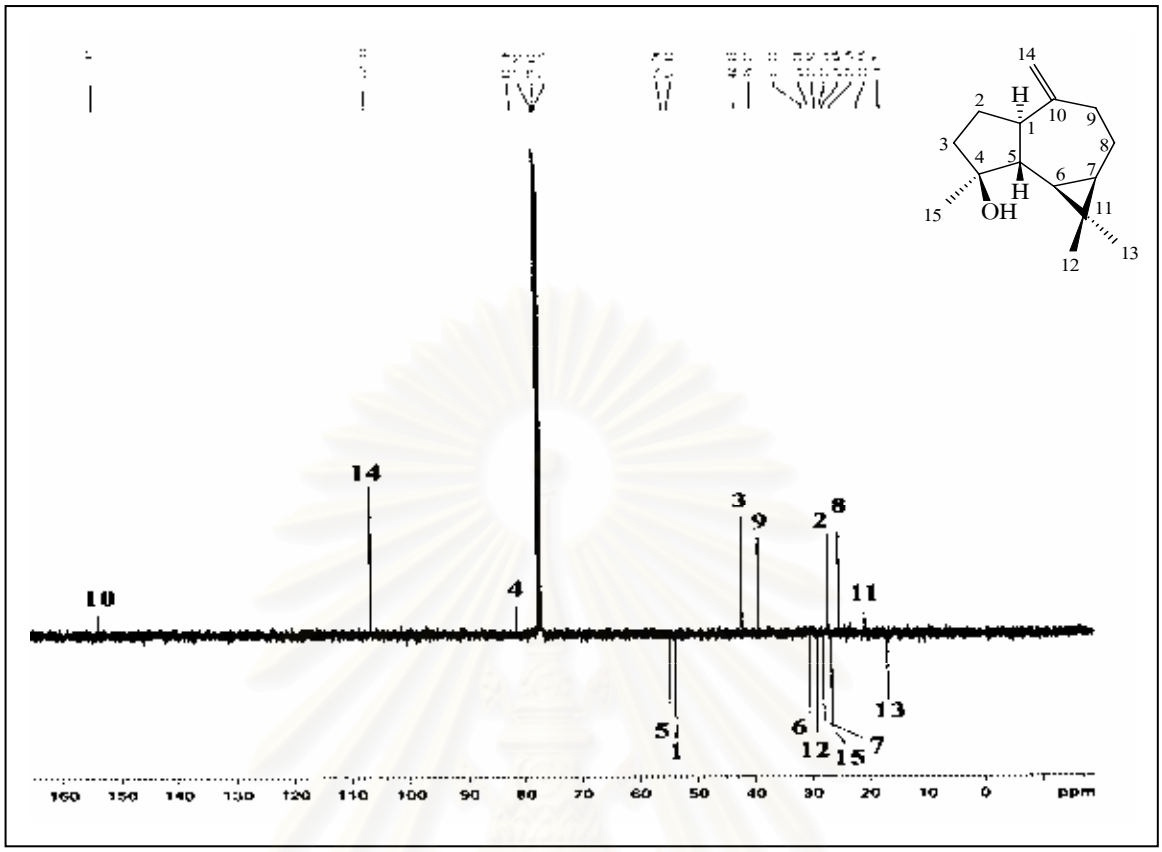

Figure 16. ^{13}C APT (100 MHz) Spectrum of compound HAF3 ($CDCl_3$)

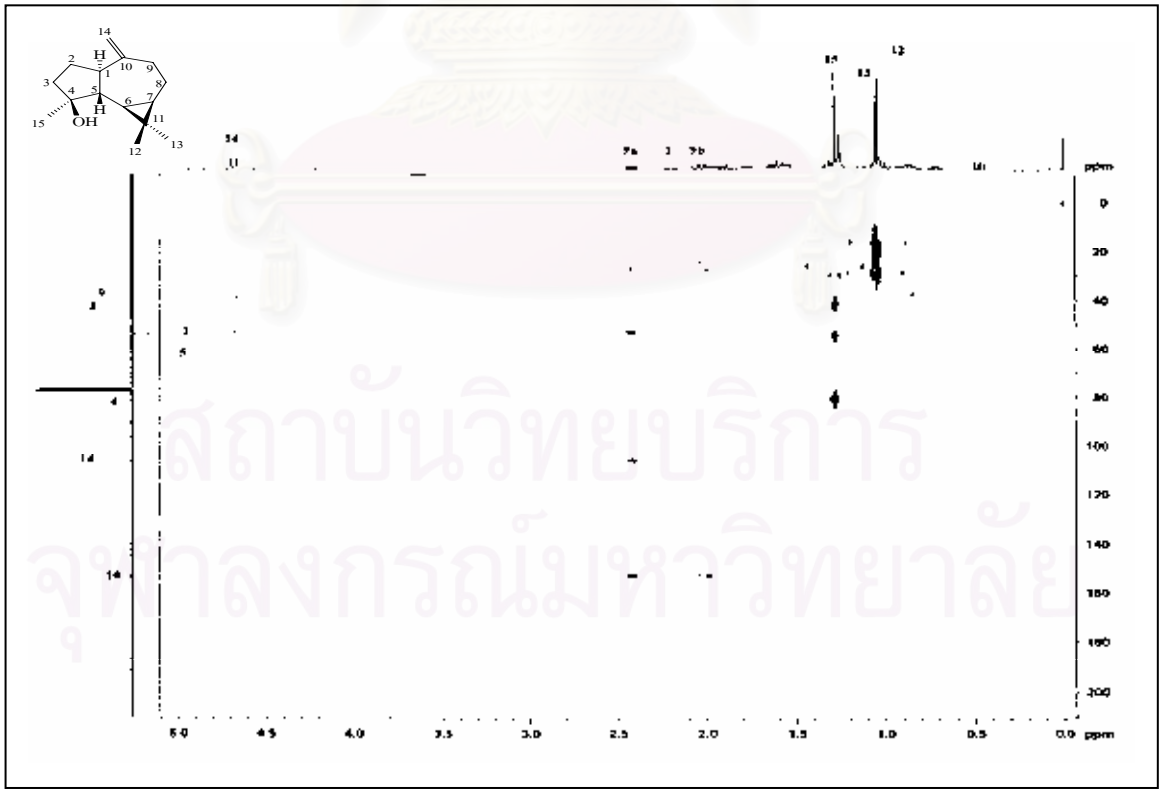

Figure 17. HMBC spectrum of compound HAF3 ($CDCl_3$)

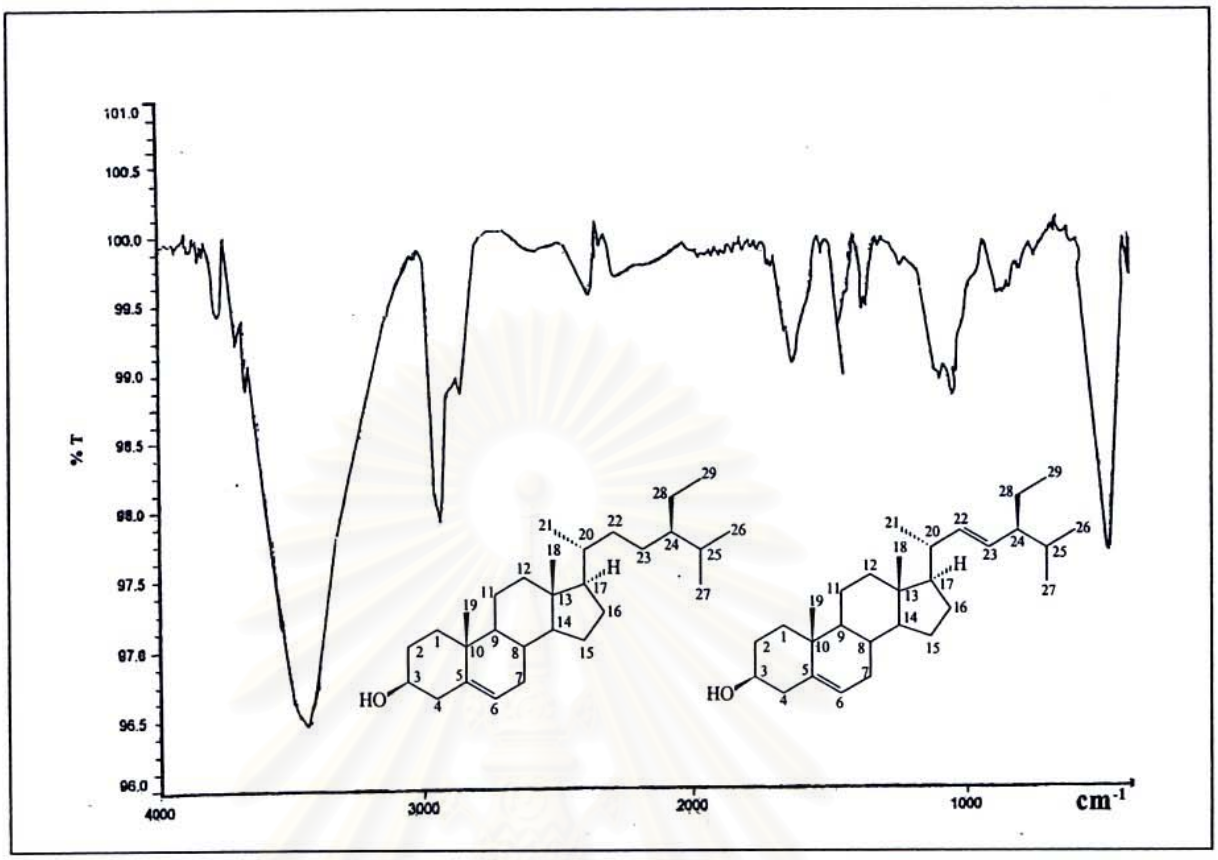

Figure 18. IR Spectrum of compound HAF4 (KBr disc)

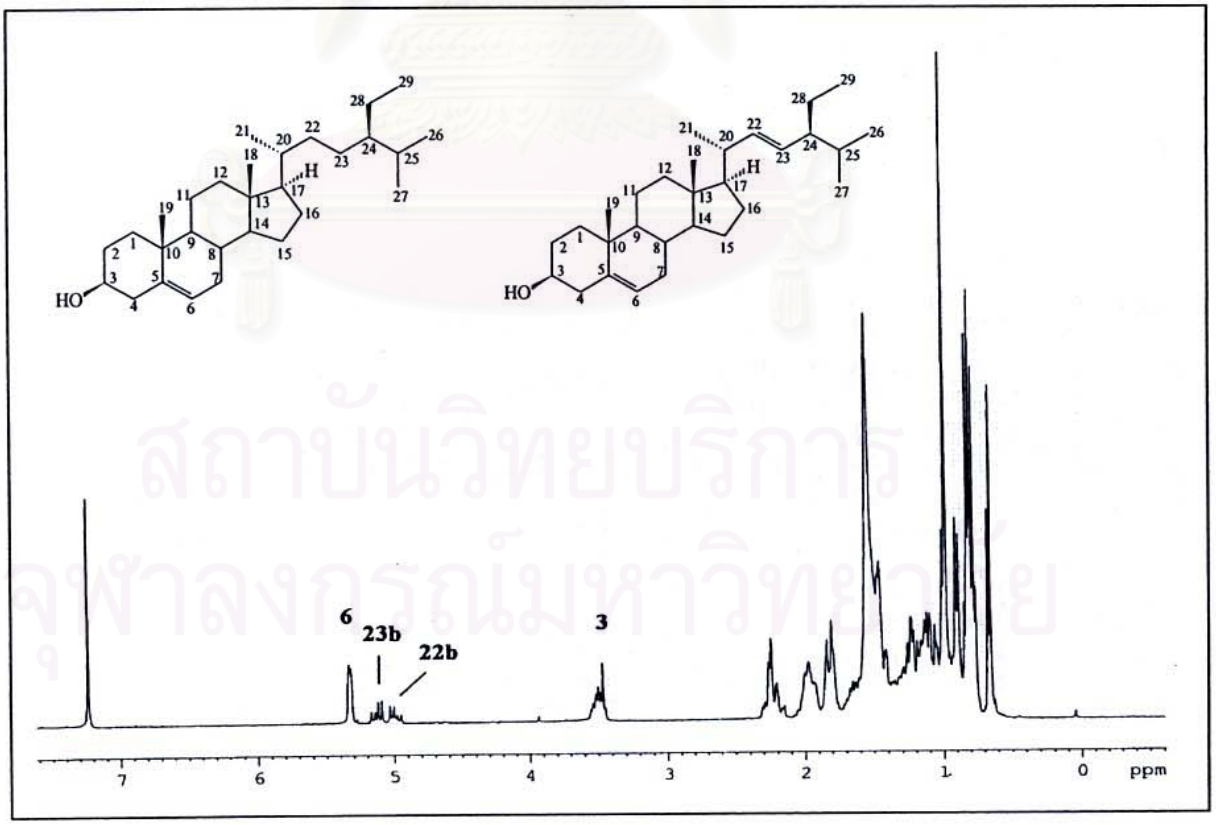

Figure 19. ^{1}H NMR (300 MHz) Spectrum of compound HAF4 ($CDCl_3$)

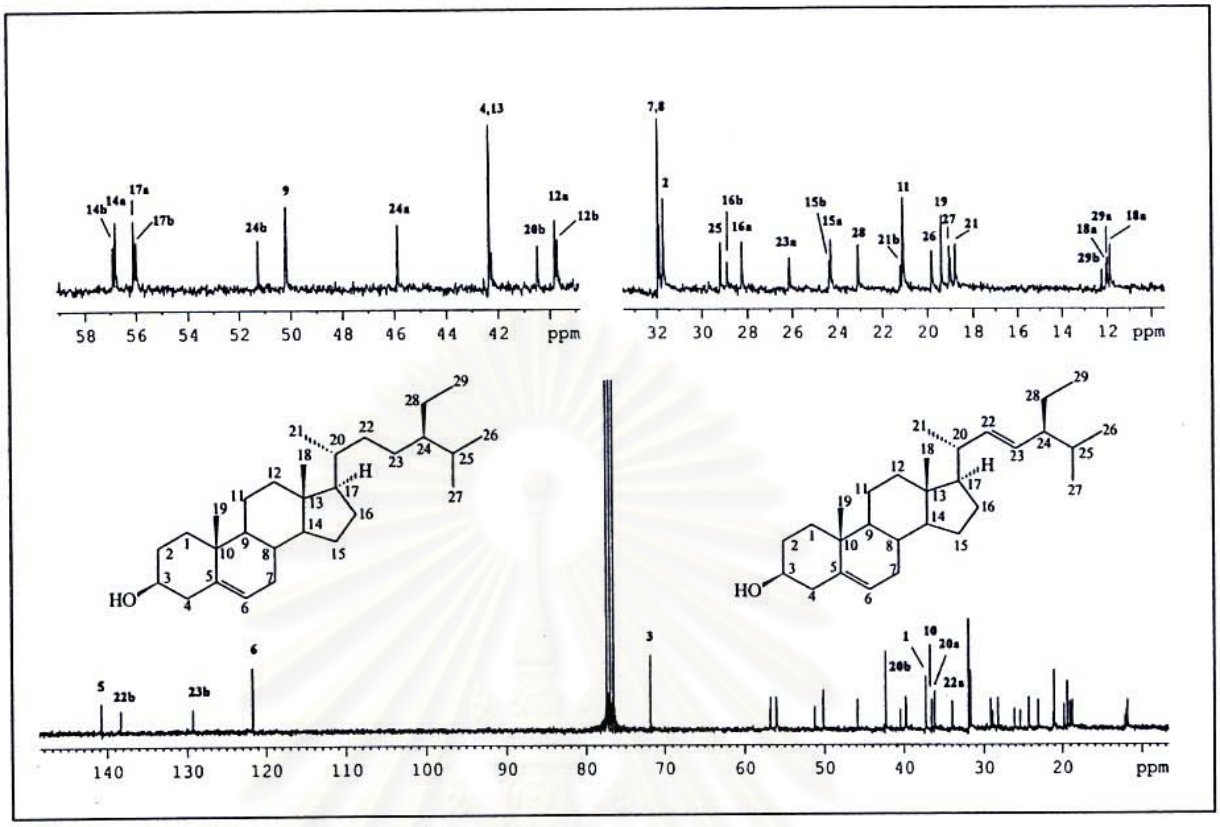

Figure 20. ^{13}C NMR (75 MHz) spectrum of compound HAF4 ($CDCl_3$)

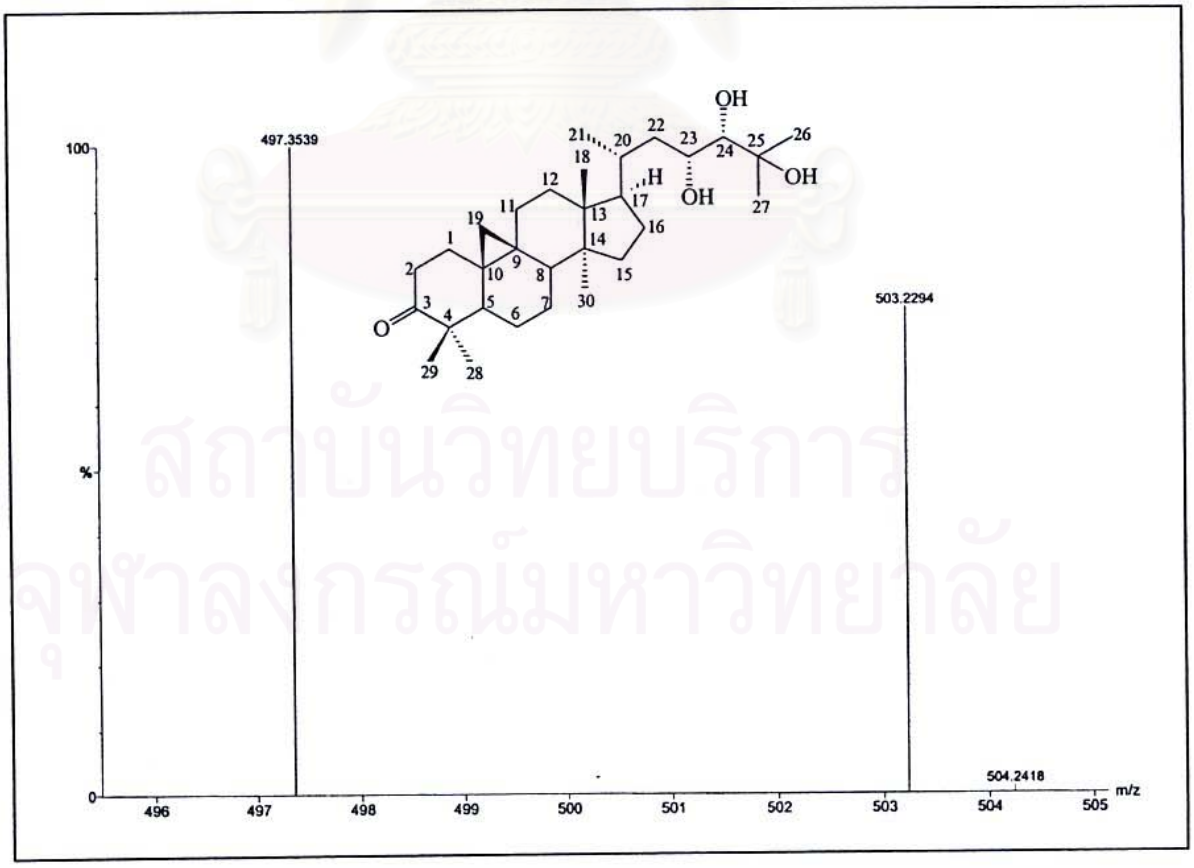

Figure 21. HRESI-TOF Mass spectrum of compound CAF1

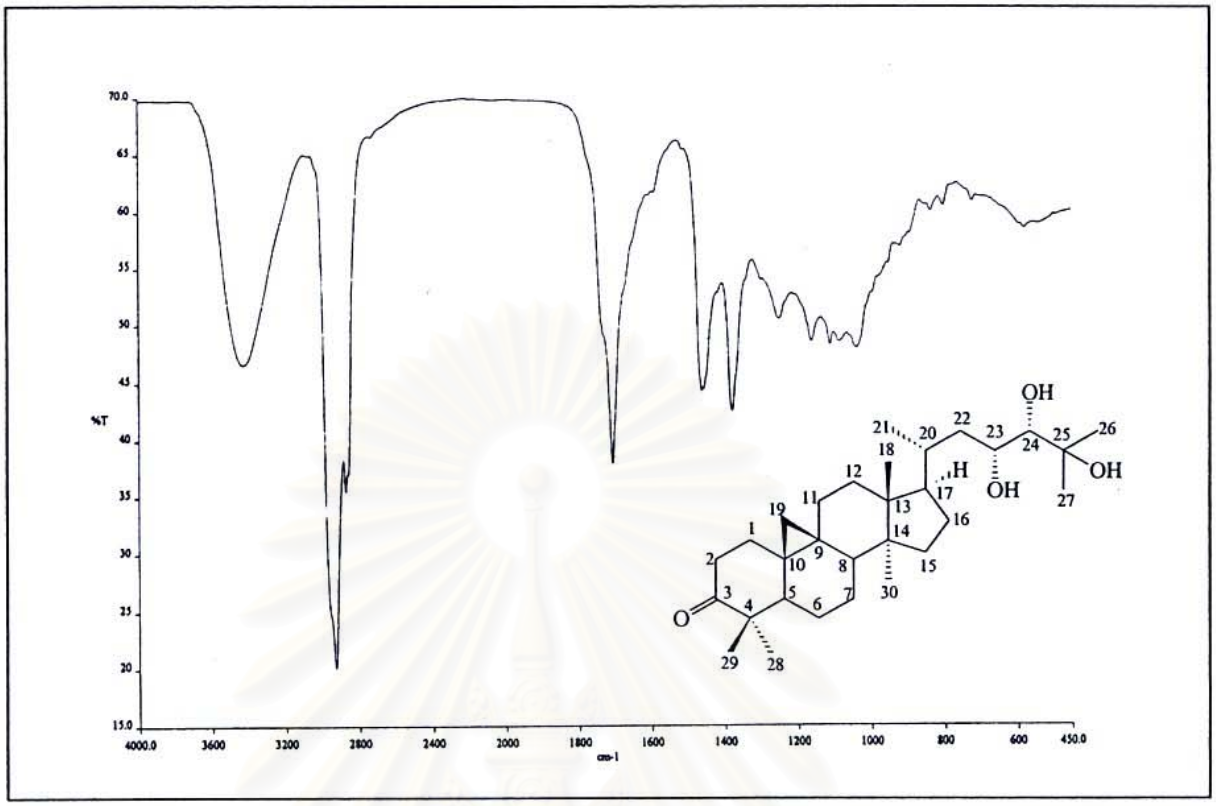

Figure 22. IR Spectrum of compound CAF1 (KBr disc)

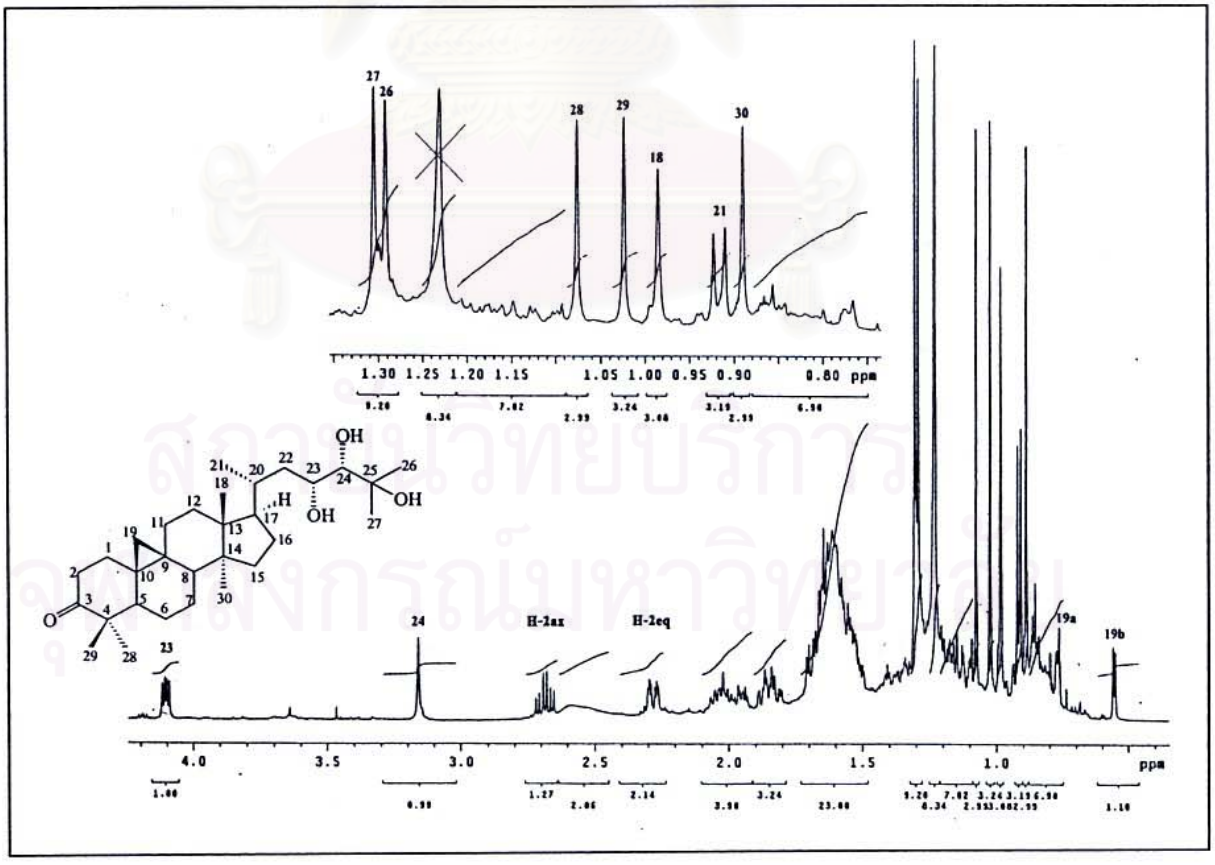

Figure 23. ^{1}H NMR (500 MHz) Spectrum of compound CAF1 ($CDCl_3$)

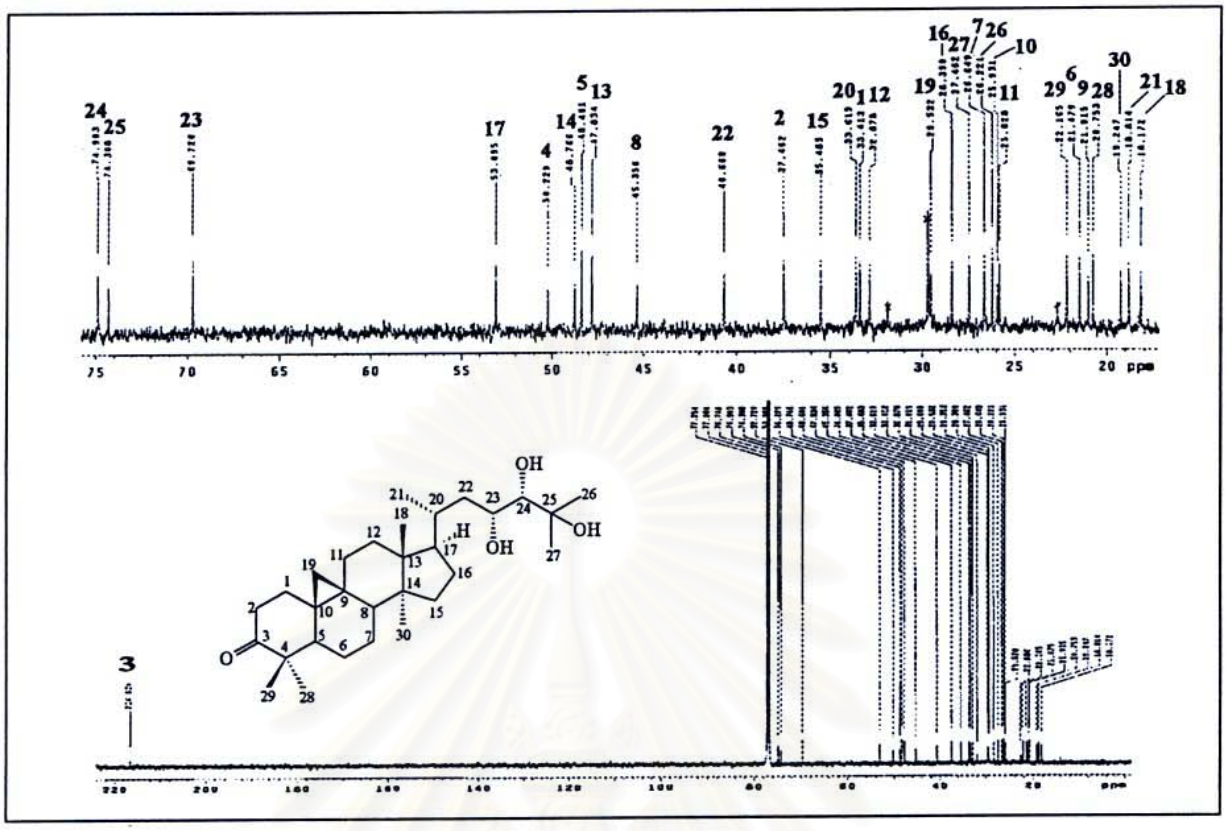

Figure 24. ^{13}C NMR (125 MHz) Spectrum of compound CAF1 ($CDCl_3$)

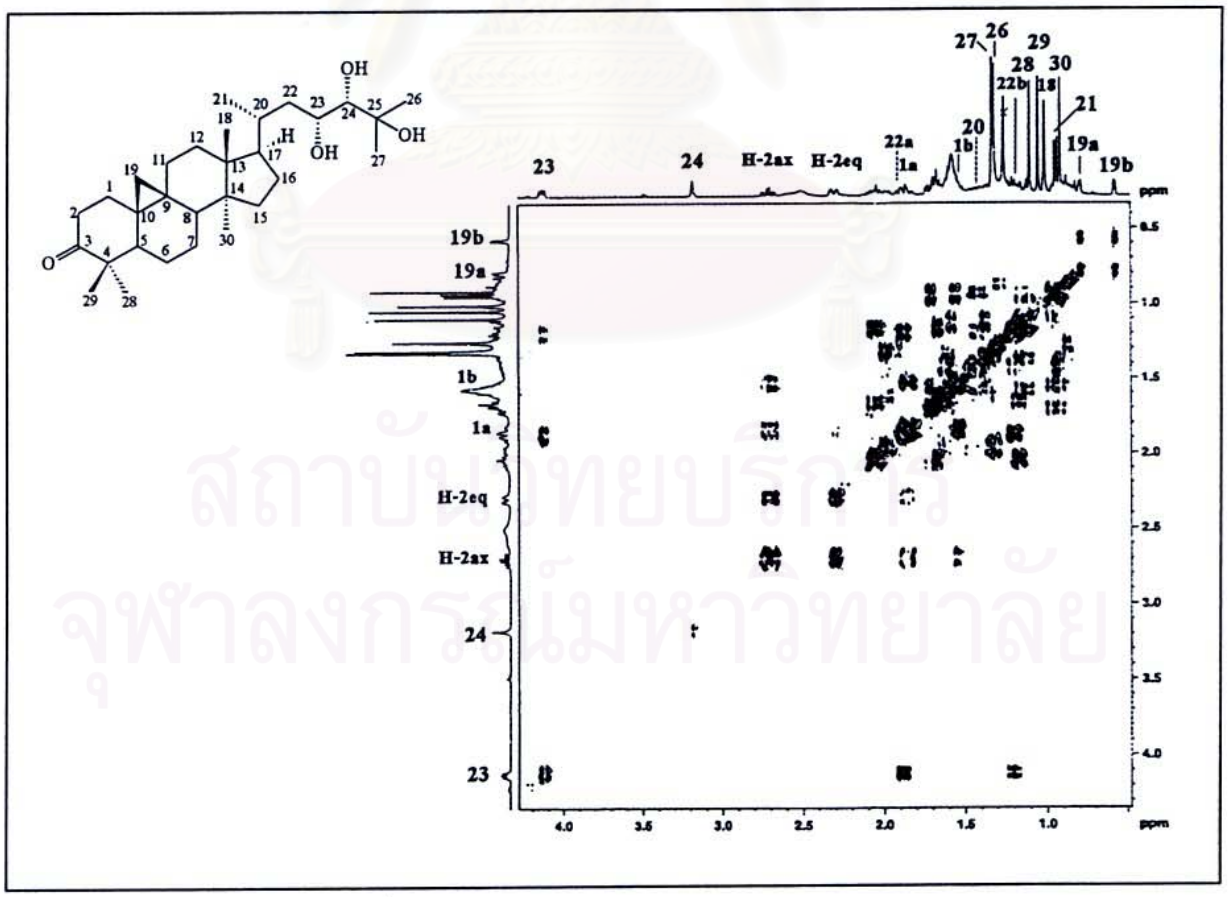

Figure 25. ^{1}H–^{1}H COSY Spectrum of compound CAF1 ($CDCl_3$)

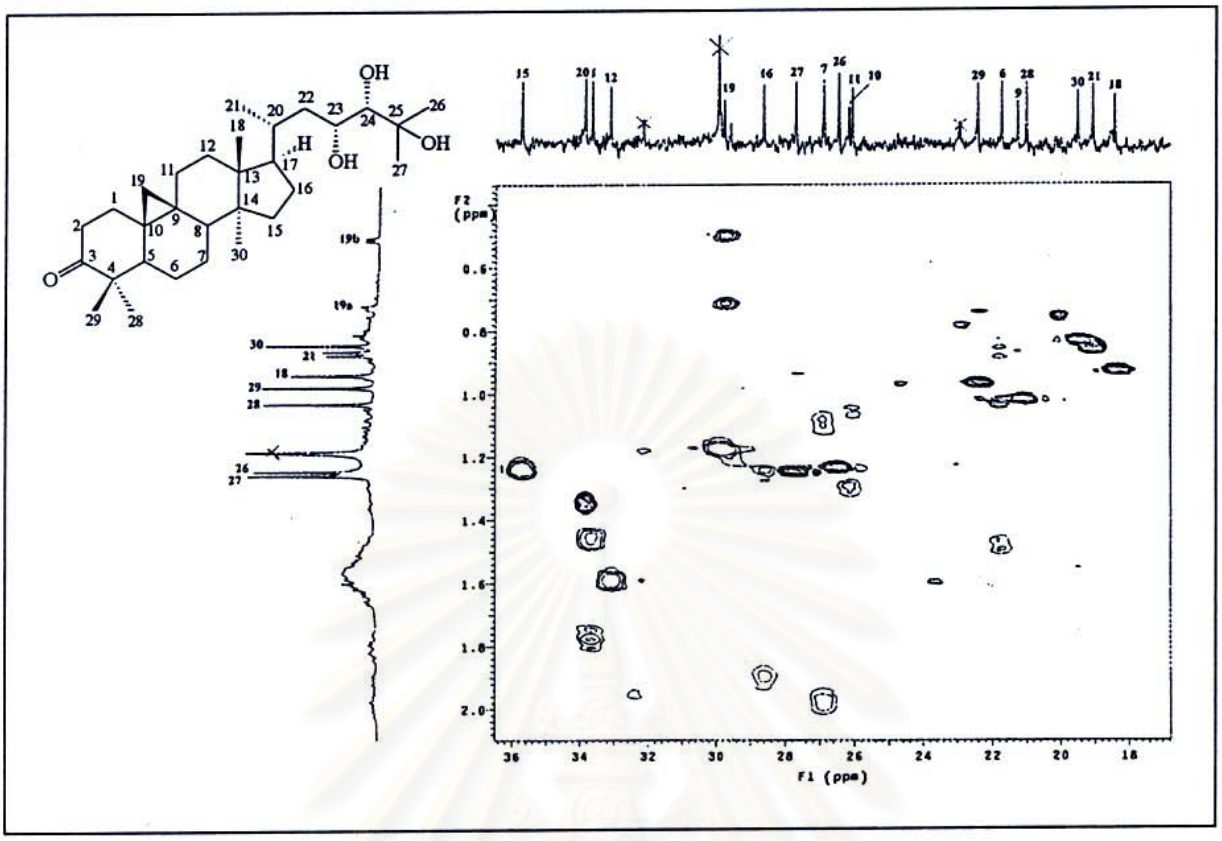

Figure 26. HSQC Spectrum of compound CAF1 ($CDCl_3$) [δ_H 0.5-2.0 ppm, δ_C 17-36 ppm]

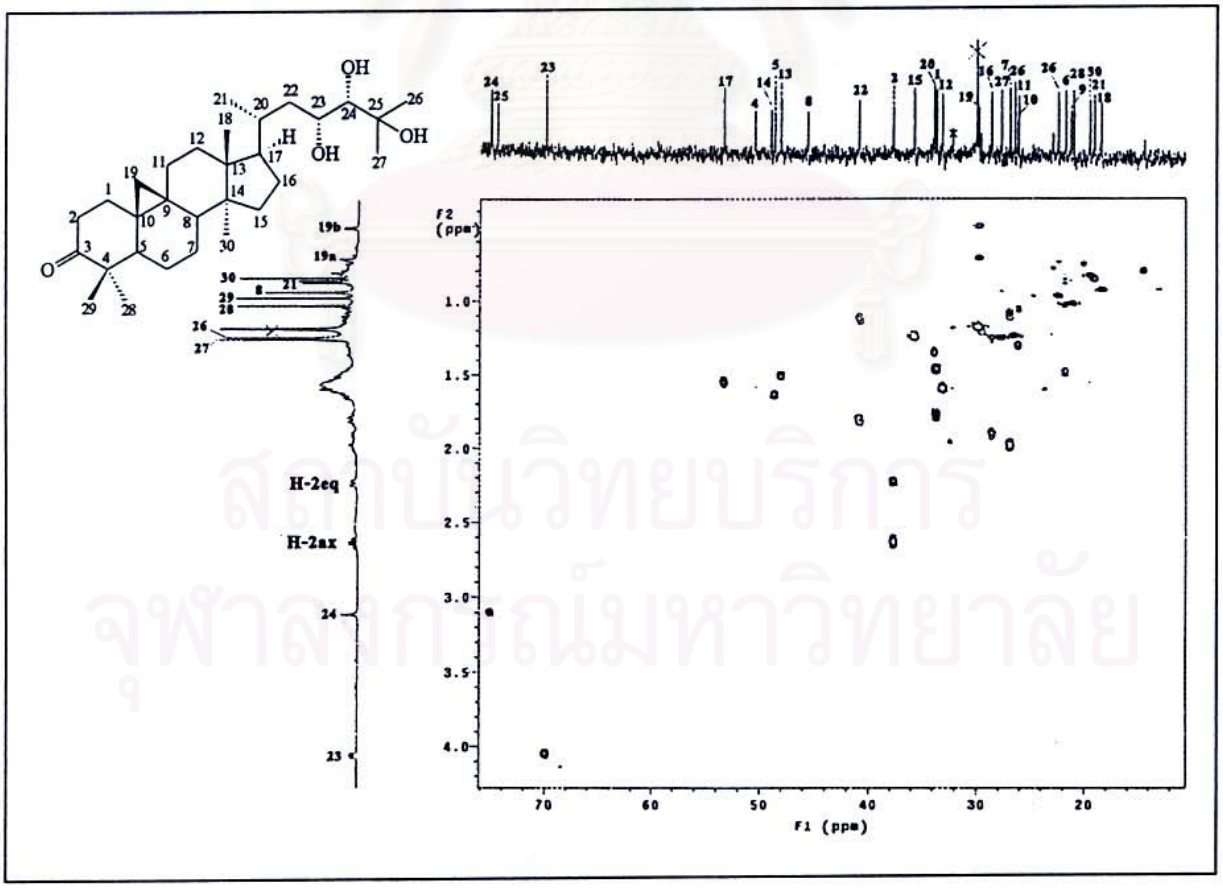

Figure 27. HSQC Spectrum of compound CAF1 ($CDCl_3$) [δ_H 0.0-4.2 ppm, δ_C 10-78 ppm]

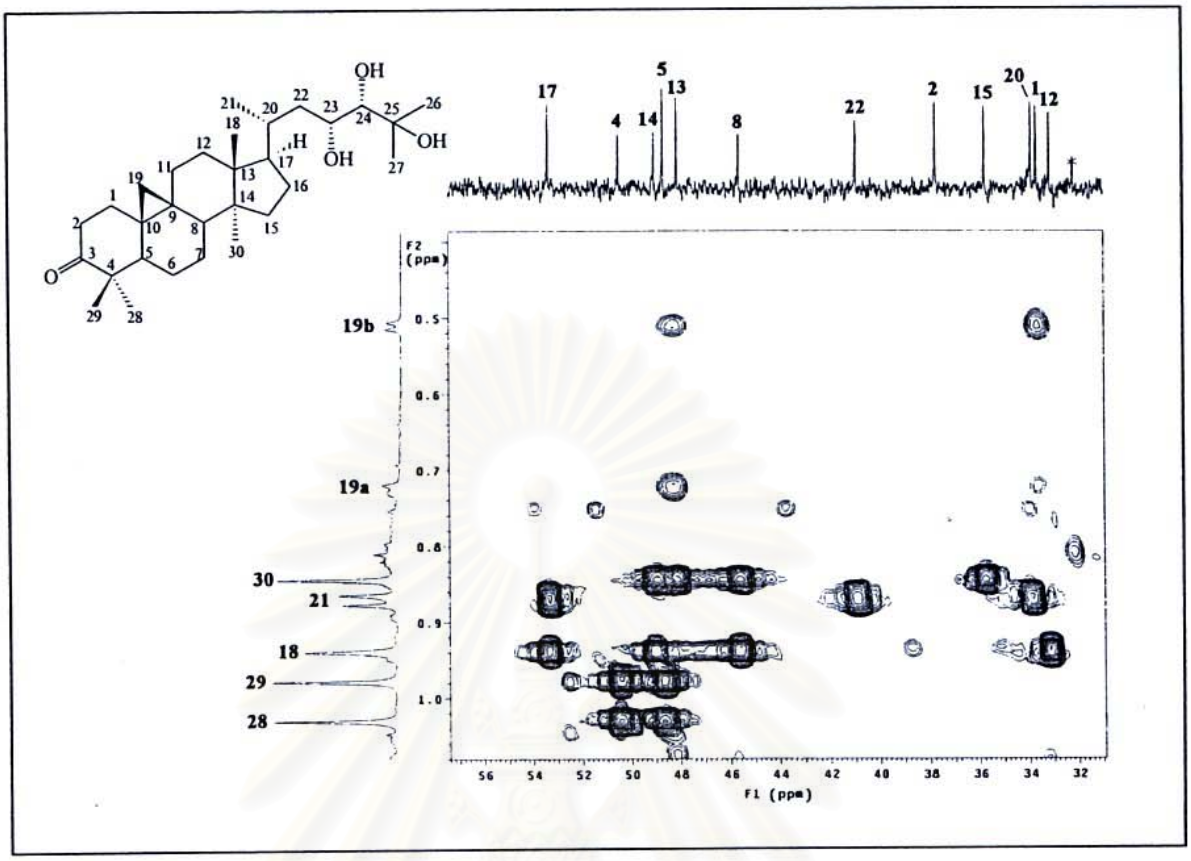

Figure 28. HMBC Spectrum of compound CAF1 ($CDCl_3$) [δ_H 0.5-2.0 ppm, δ_C 18-31 ppm]

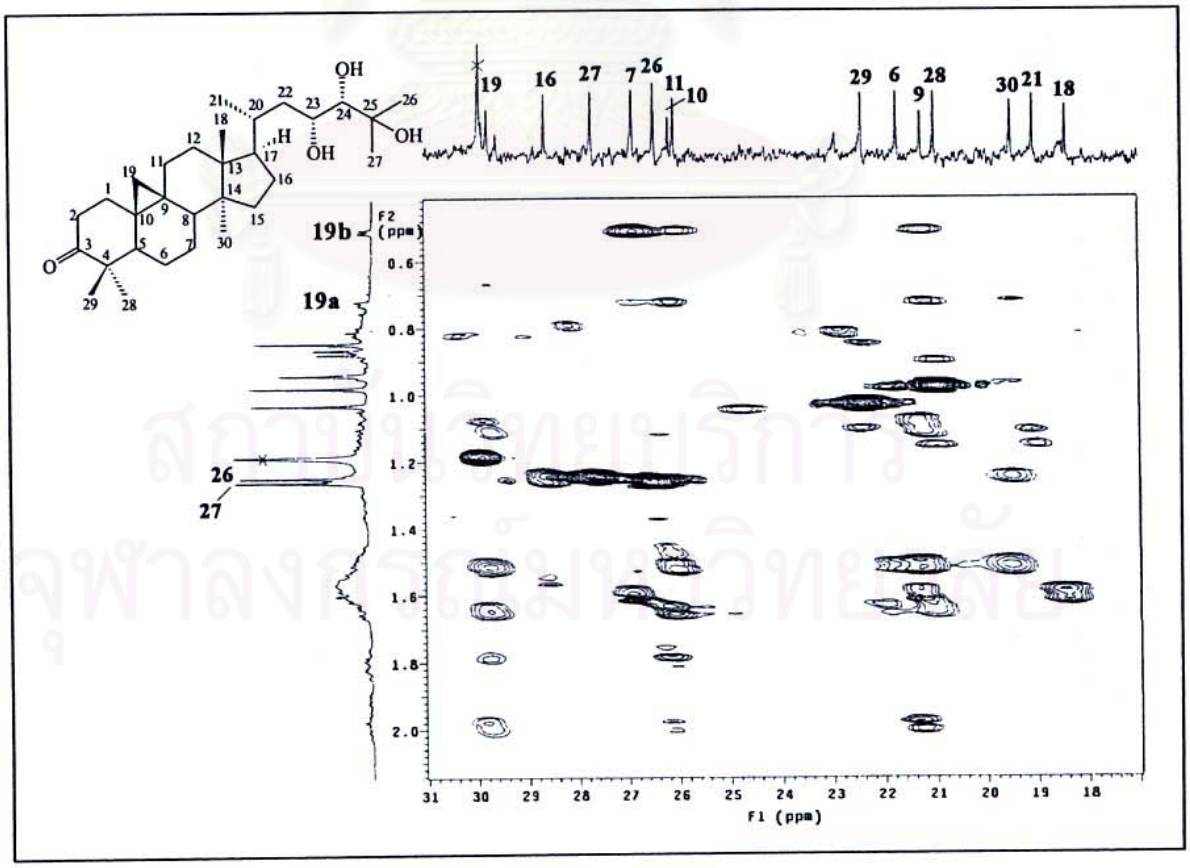

Figure 29. HMBC Spectrum of compound CAF1 ($CDCl_3$) [δ_H 0.5-1.3 ppm, δ_C 32-56 ppm]

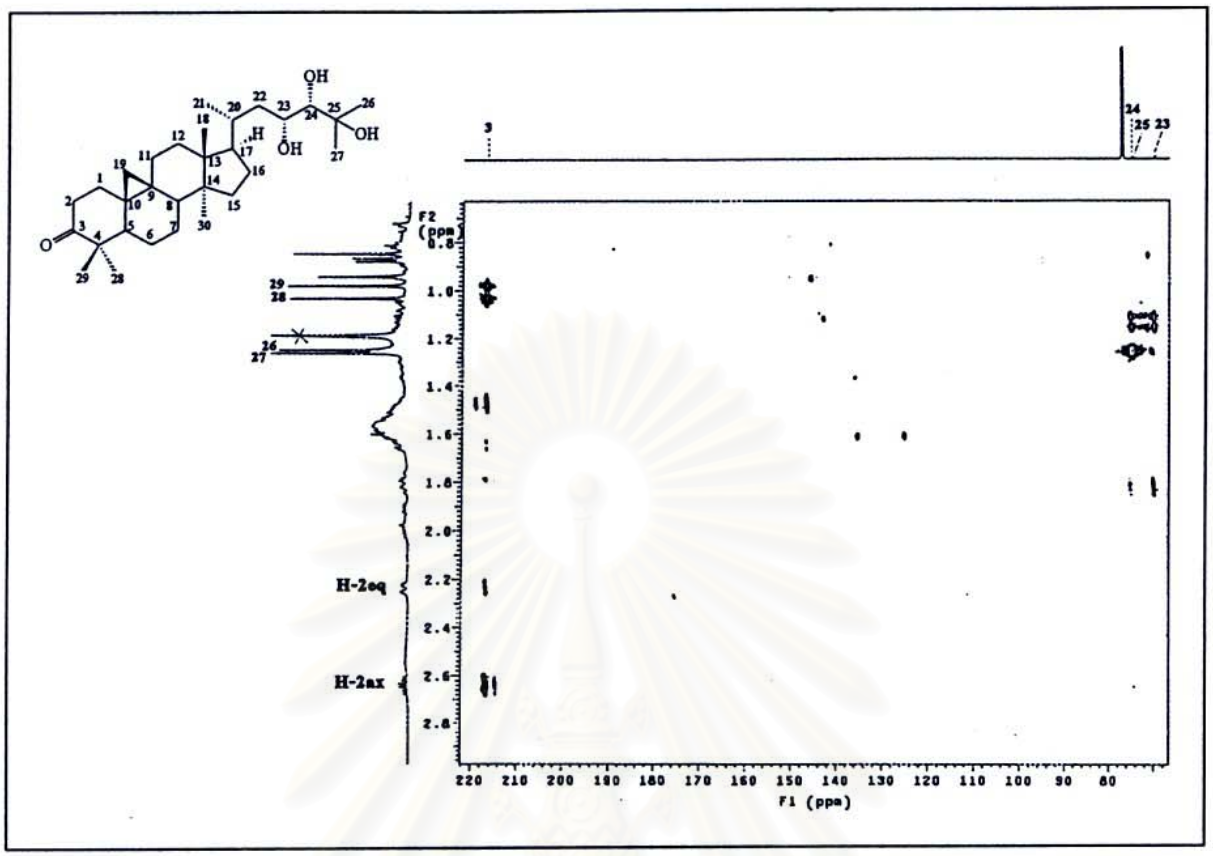

Figure 30. HMBC Spectrum of compound CAF1 ($CDCl_3$) [δ_H 0.0-2.8 ppm, δ_C 70-220 ppm]

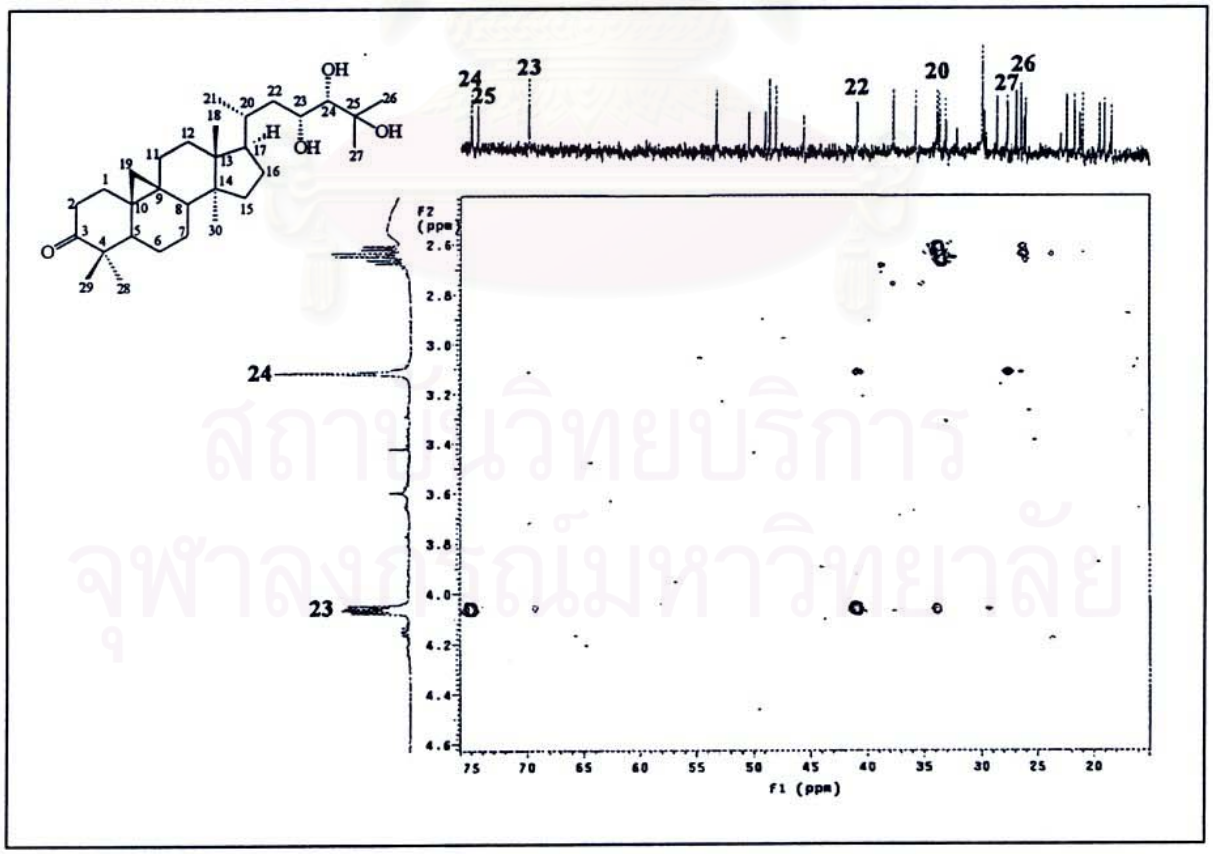

Figure 31. HMBC Spectrum of compound CAF1 ($CDCl_3$) [δ_H 2.6-4.6 ppm, δ_C 20-75 ppm]

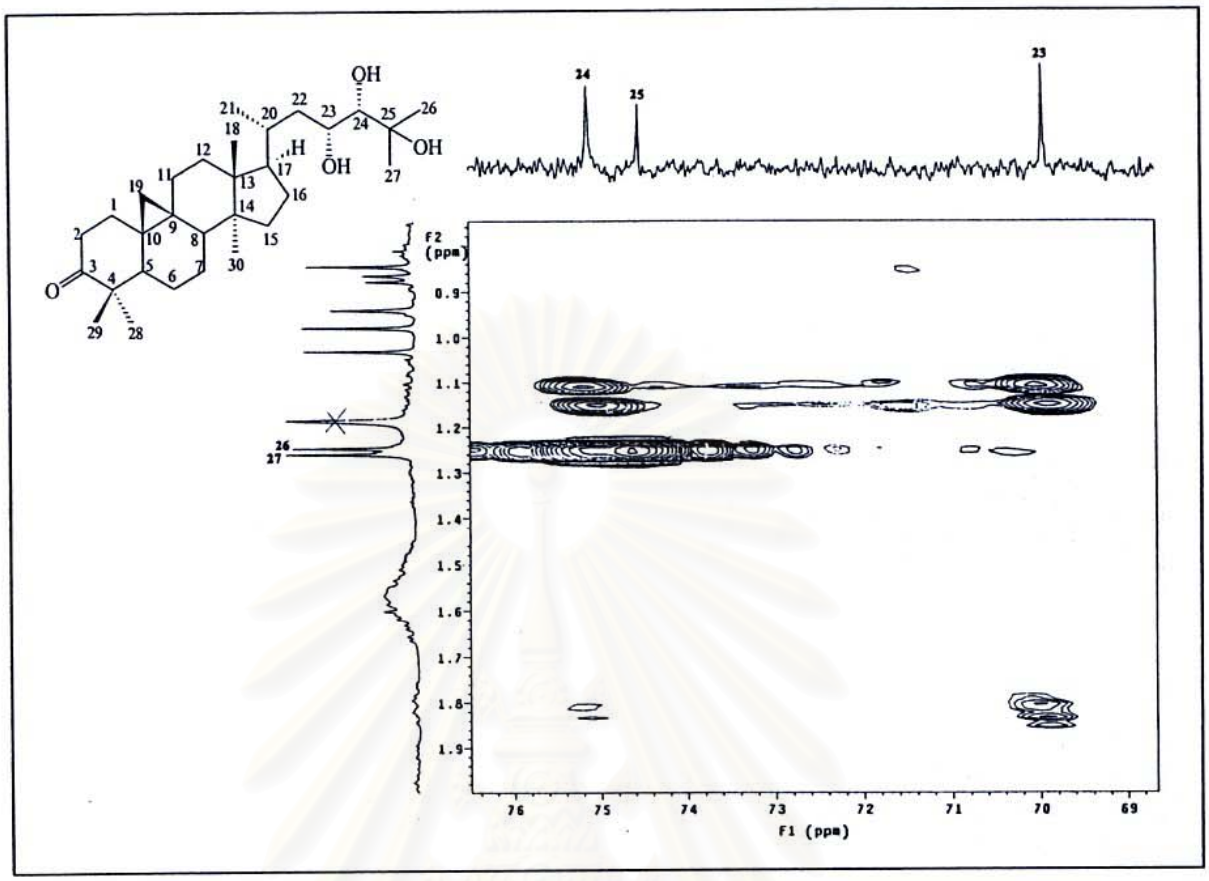

Figure 32. HMBC Spectrum of compound CAF1 ($CDCl_3$) [δ_H 0.8-1.9 ppm, δ_C 69-76 ppm]

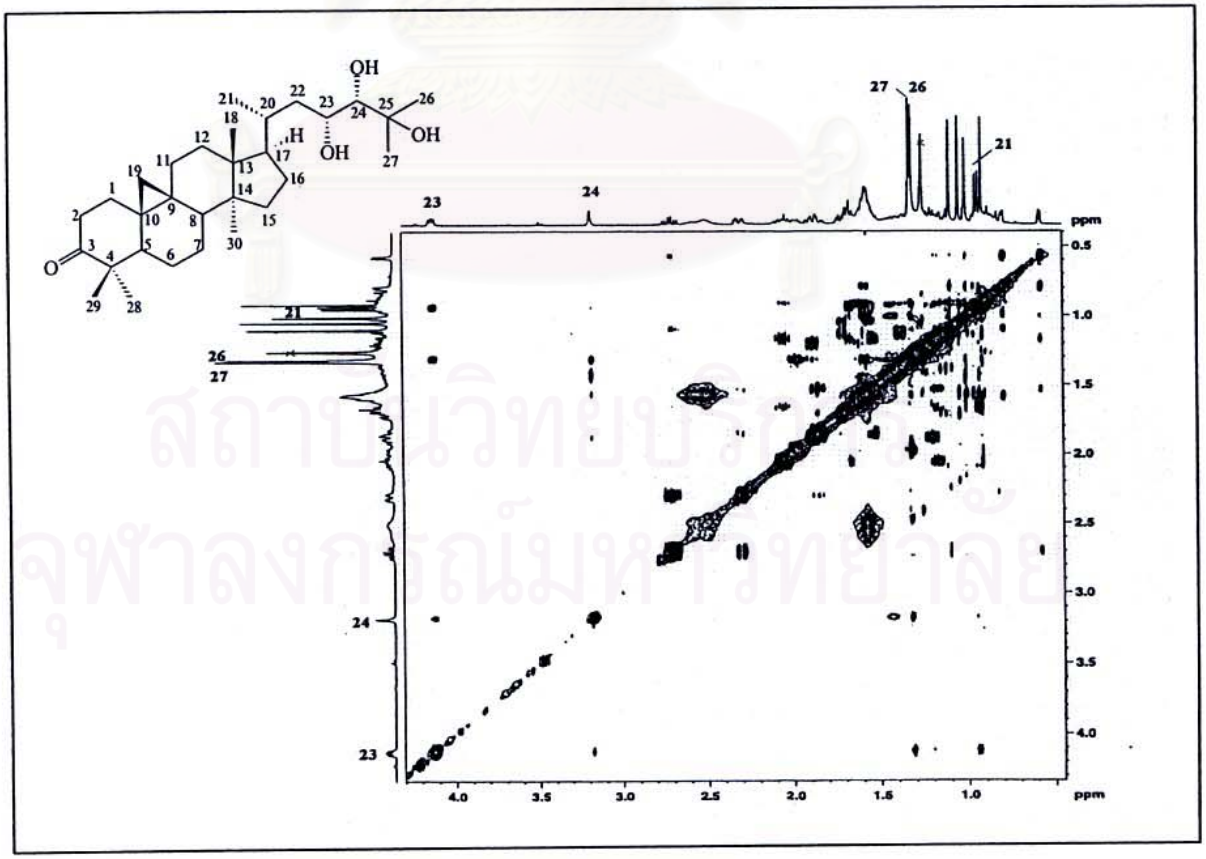

Figure 33. NOESY Spectrum of compound CAF1 ($CDCl_3$)

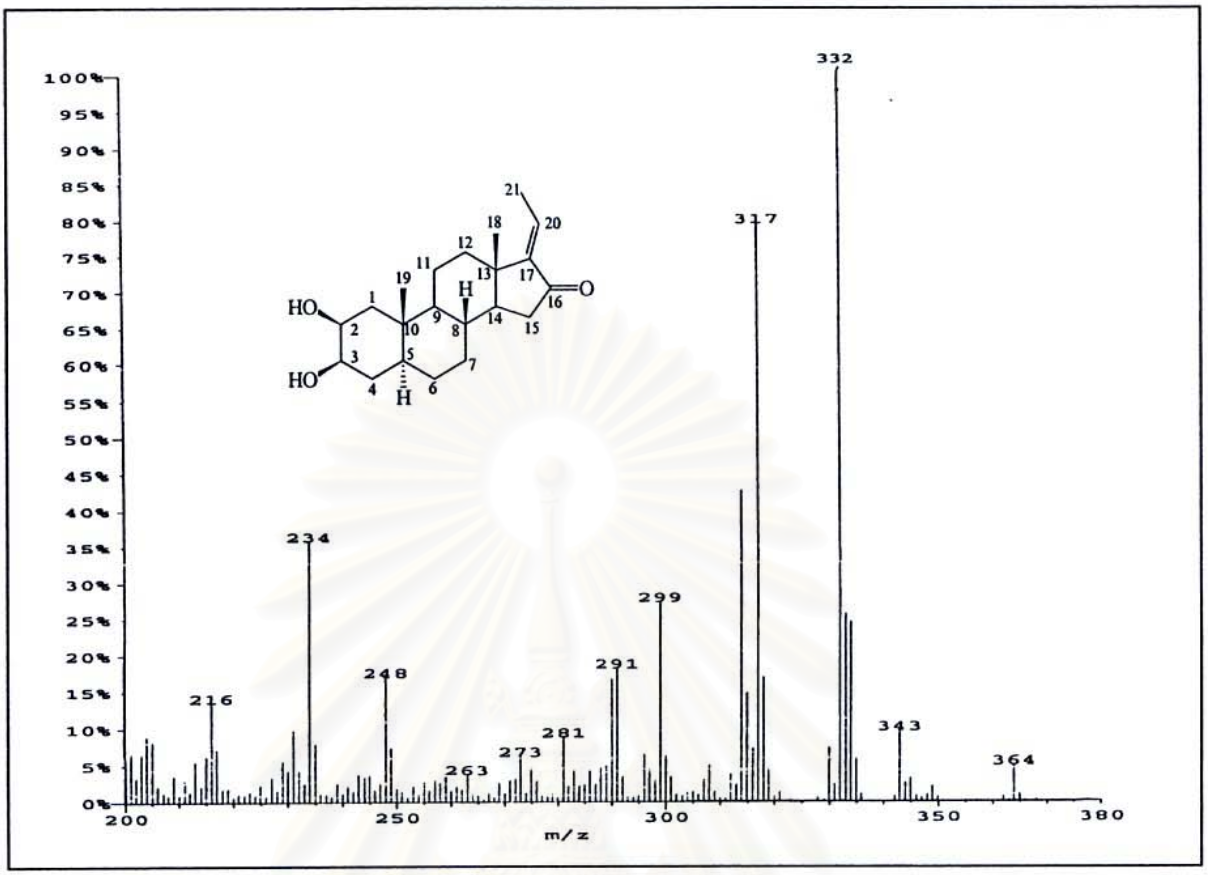

Figure 34. EI Mass spectrum of compound CAF2

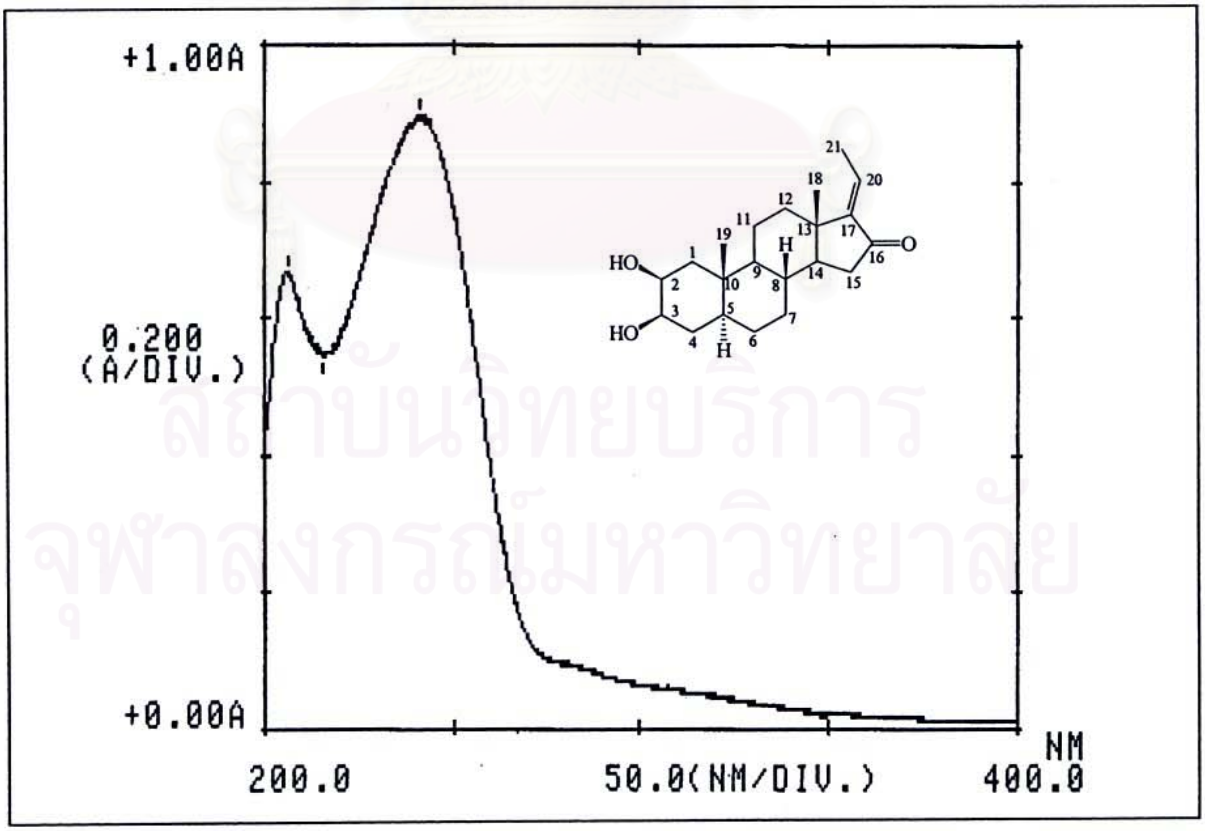

Figure 35. UV Spectrum of compound CAF2

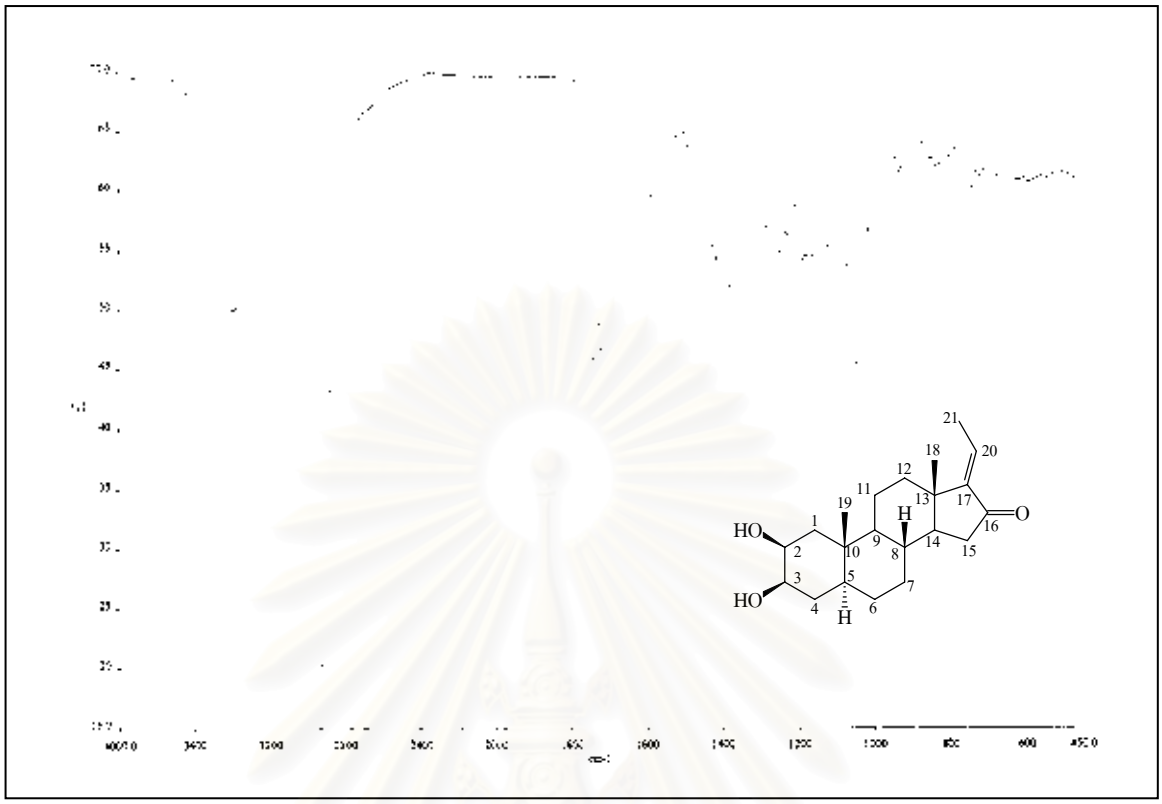

Figure 36. IR Spectrum of compound CAF2 (KBr disc)

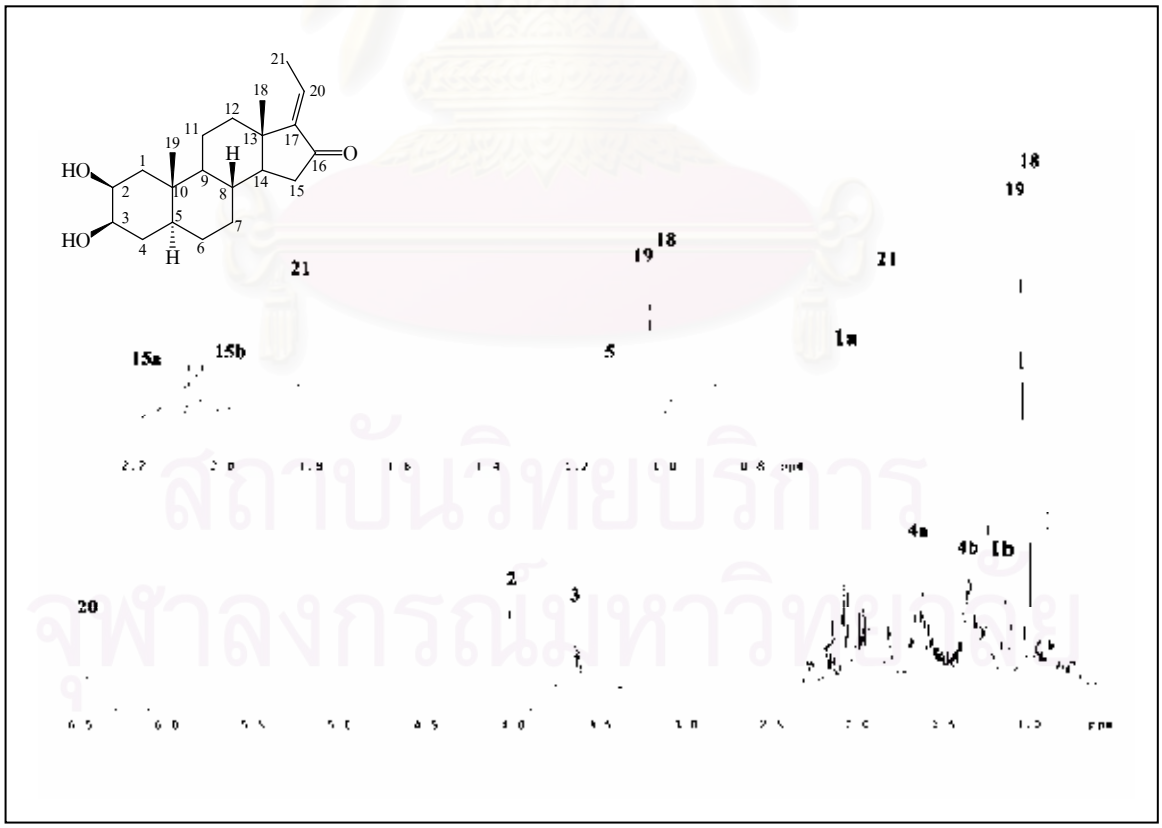

Figure 37. ^{1}H NMR (500 MHz) Spectrum of compound CAF2 ($CDCl_3$)

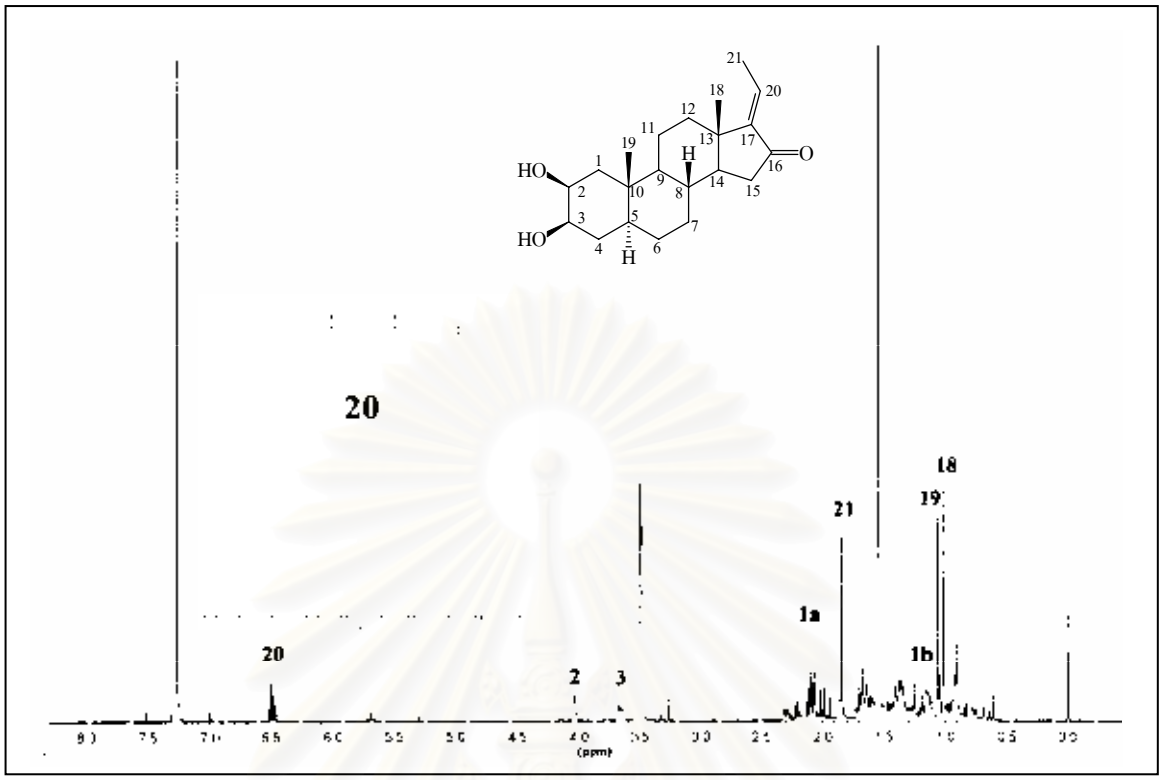

Figure 38. ^{1}H NMR (400 MHz) Spectrum of compound CAF2 ($CDCl_3$)

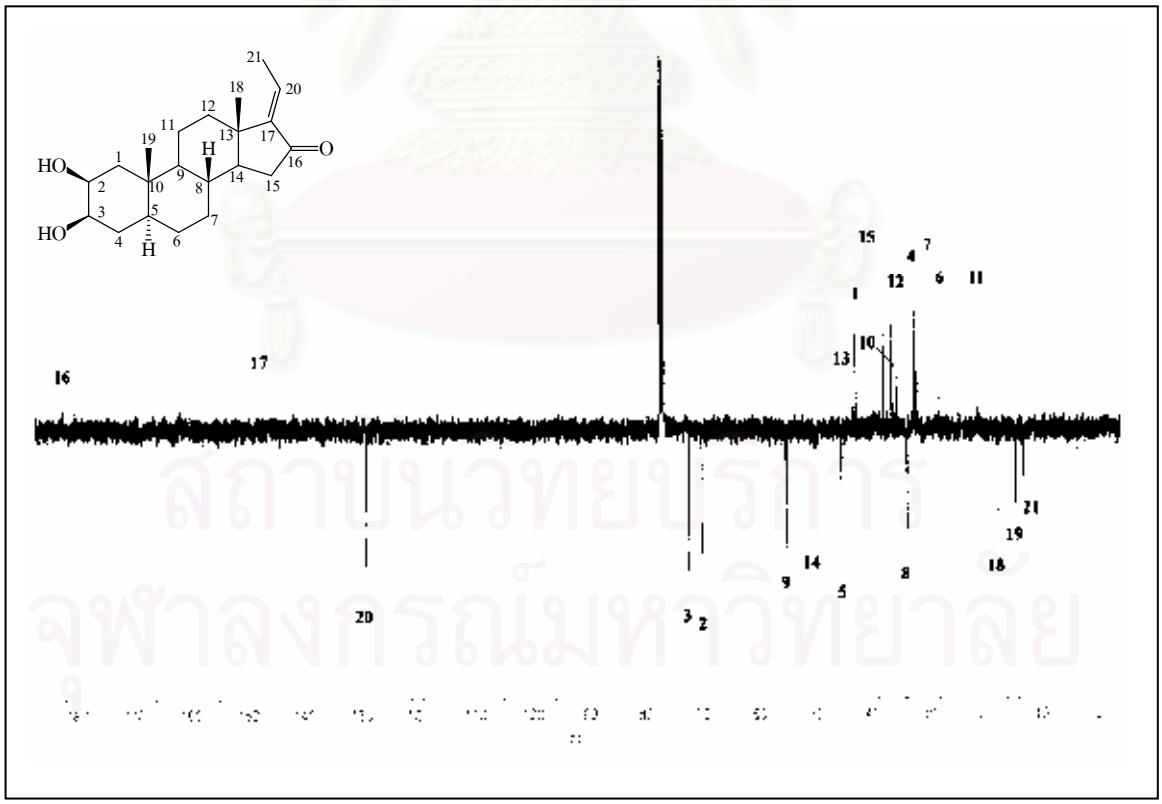

Figure 39. ^{13}C APT (100 MHz) Spectrum of compound CAF2 ($CDCl_3$)

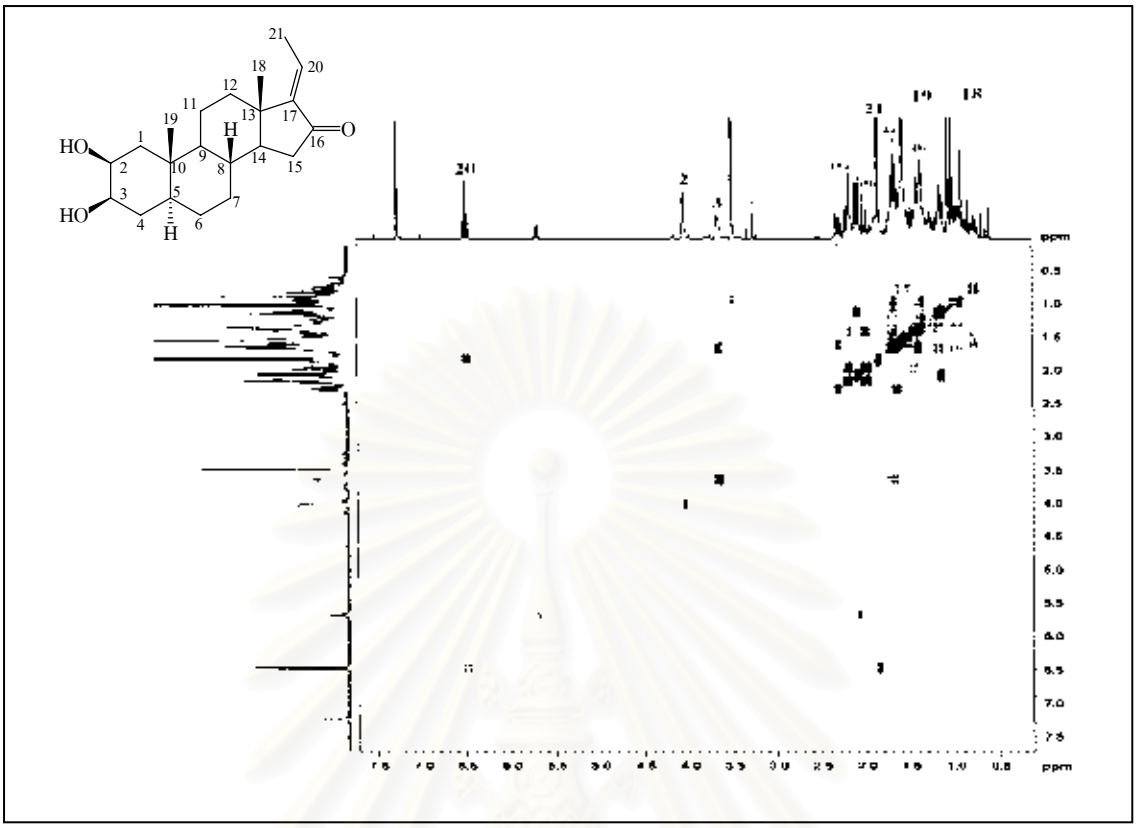

Figure 40. $^{1}H–^{1}H$ COSY Spectrum of compound CAF2 ($CDCl_3$)

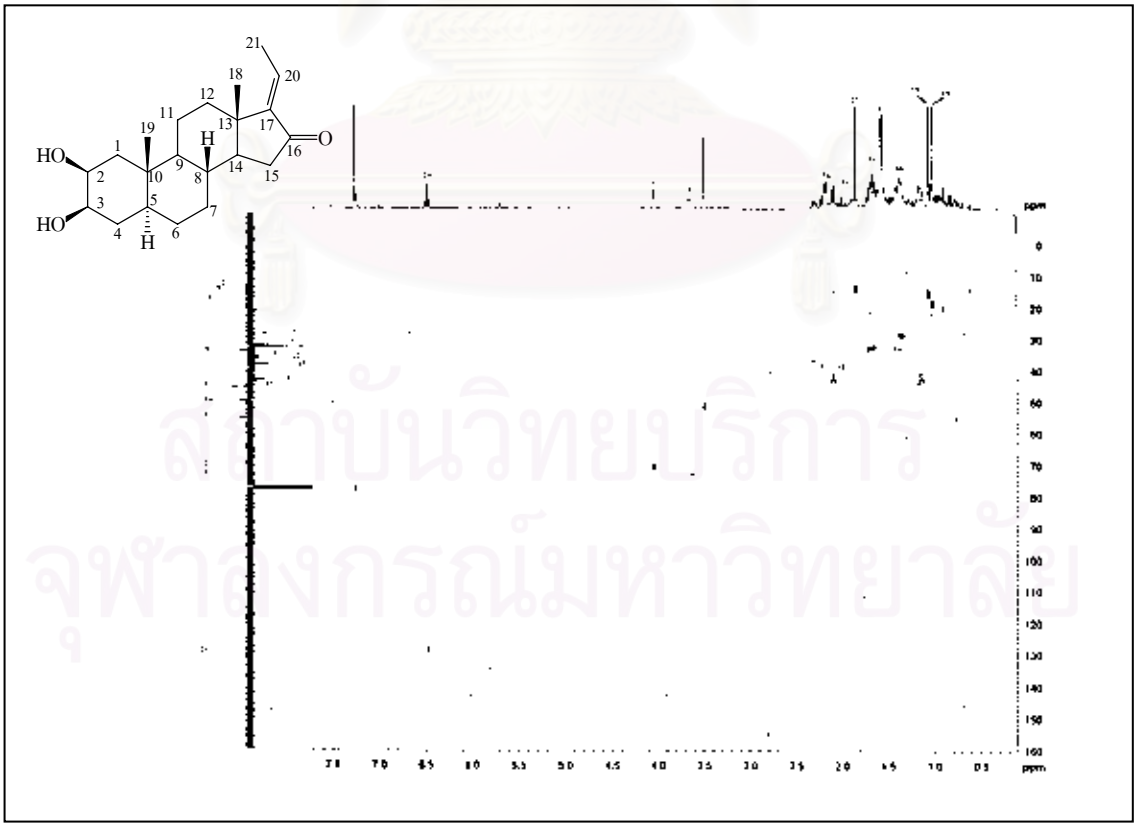

Figure 41. HMQC Spectrum of compound CAF2 ($CDCl_3$)

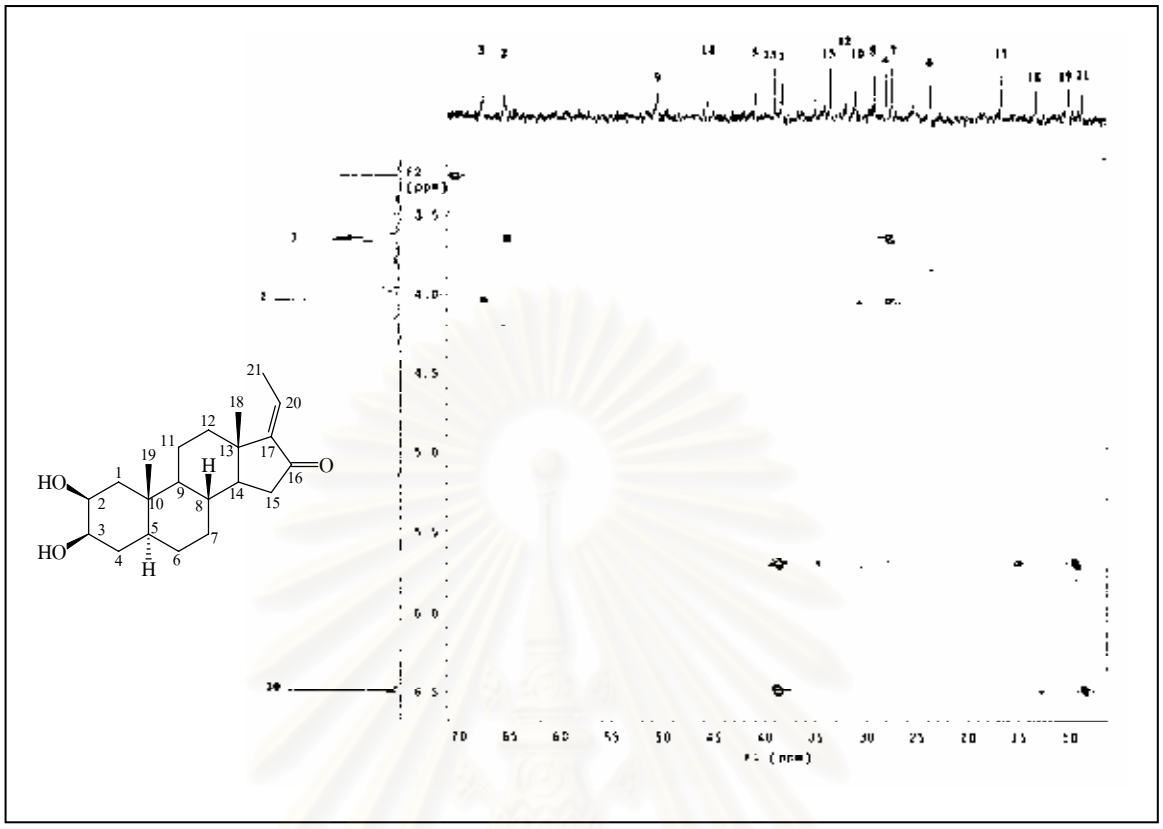

Figure 42. HMBC Spectrum of compound CAF2 ($CDCl_3$) [δ_H 3.4-6.7 ppm, δ_C 10-70 ppm]

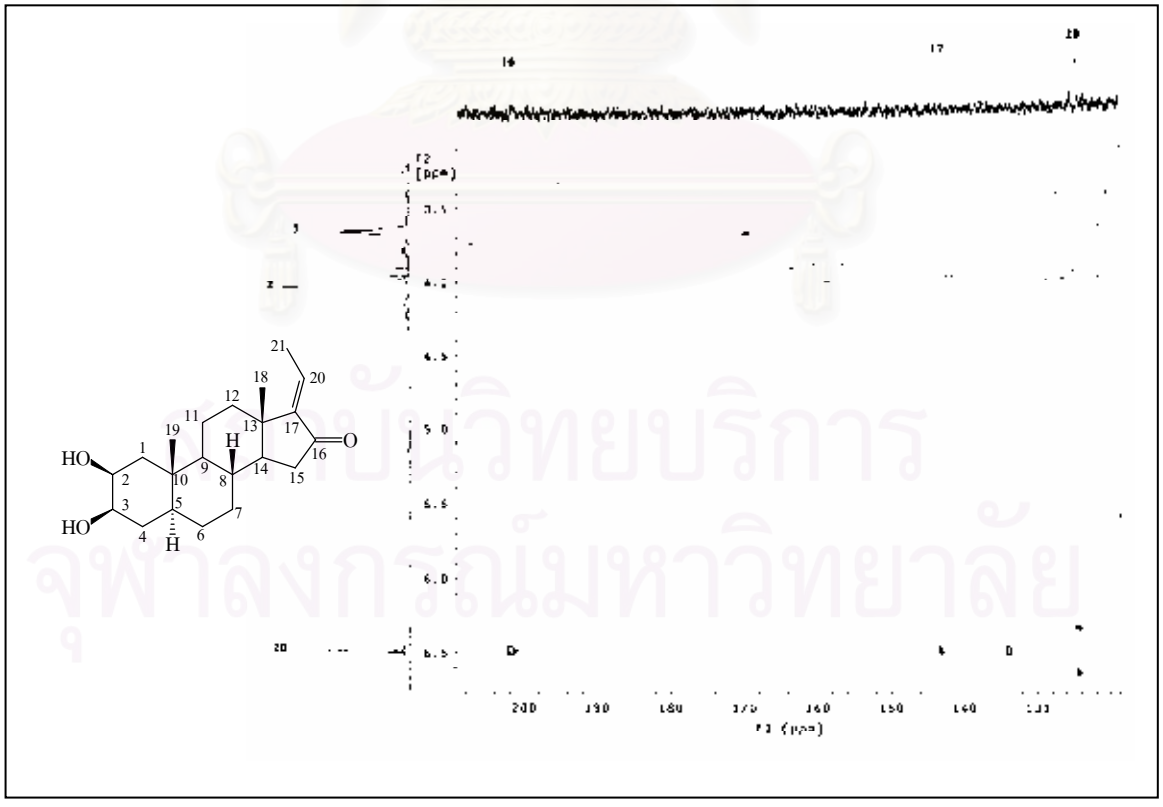

Figure 43. HMBC Spectrum of compound CAF2 ($CDCl_3$) [δ_H 3.4-6.7 ppm, δ_C 120-210 ppm]

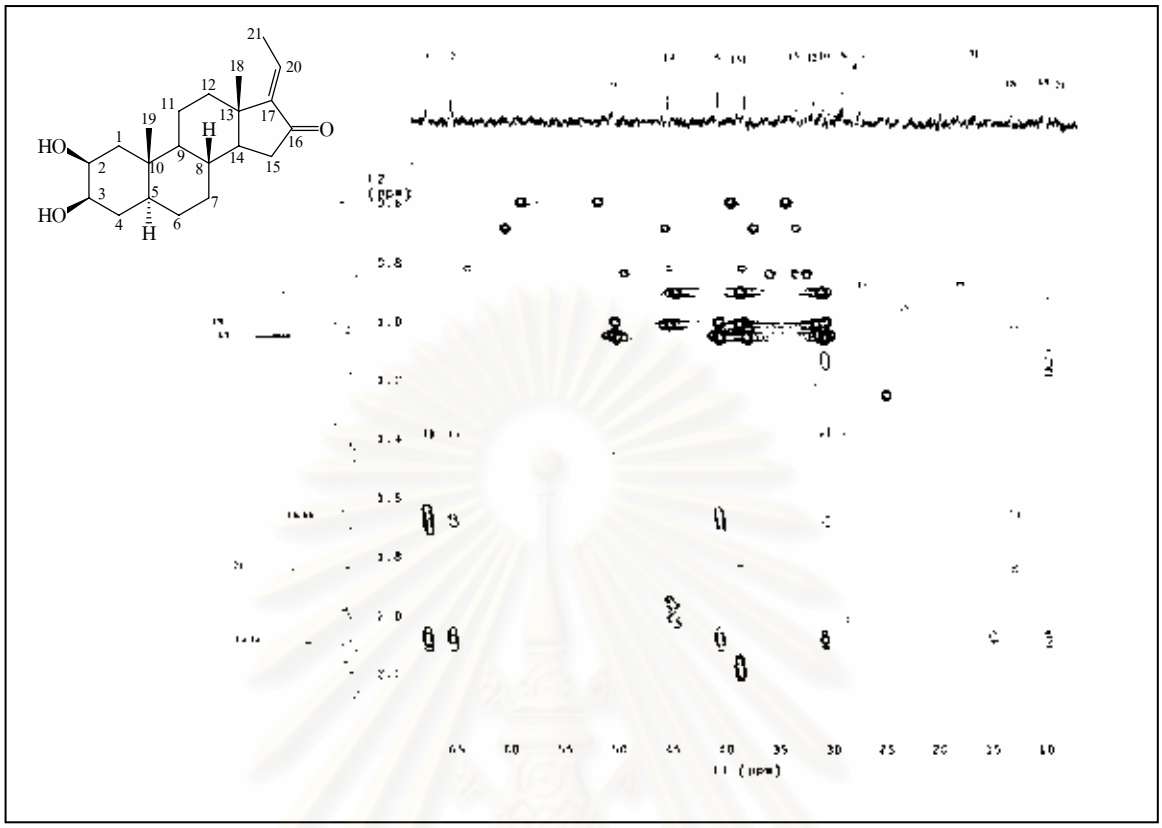

Figure 44. HMBC Spectrum of compound CAF2 ($CDCl_3$) [δ_H 0.7-2.3 ppm, δ_C 10-70 ppm]

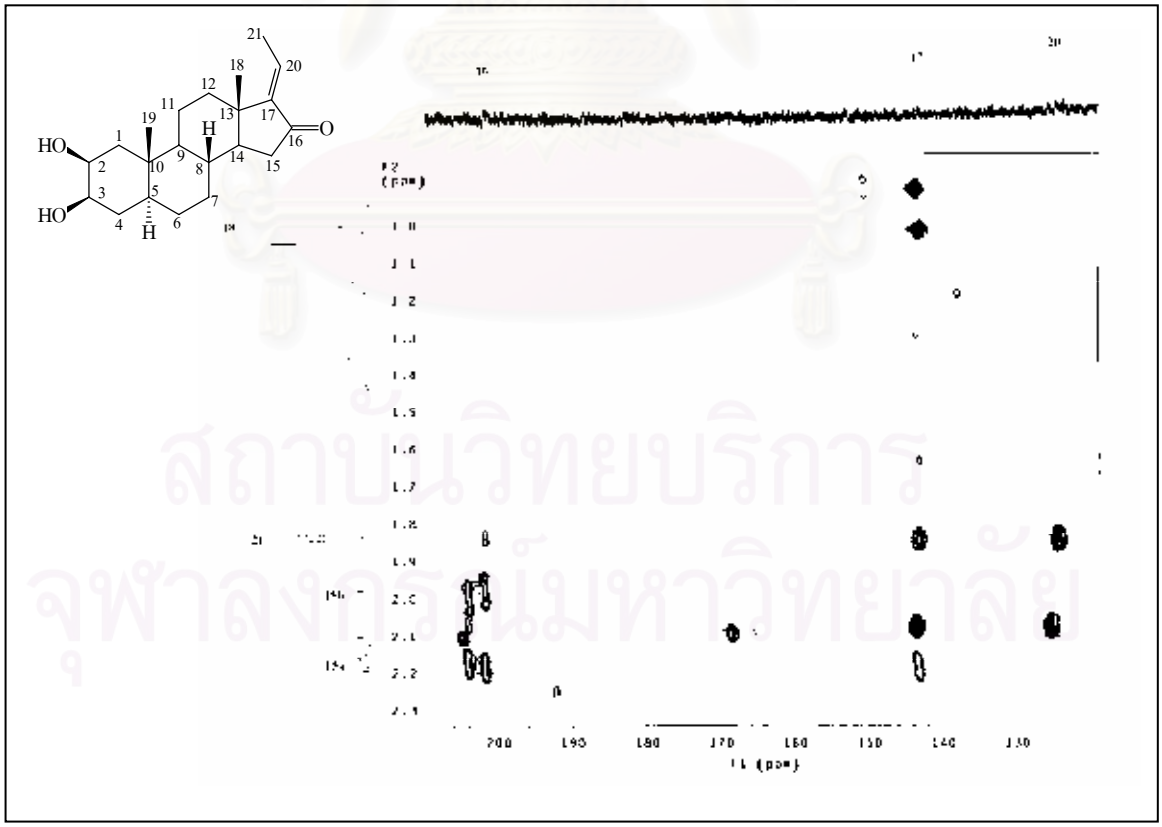

Figure 45. HMBC Spectrum of compound CAF2 ($CDCl_3$) [δ_H 0.9-2.3 ppm, δ_C 120-210 ppm]

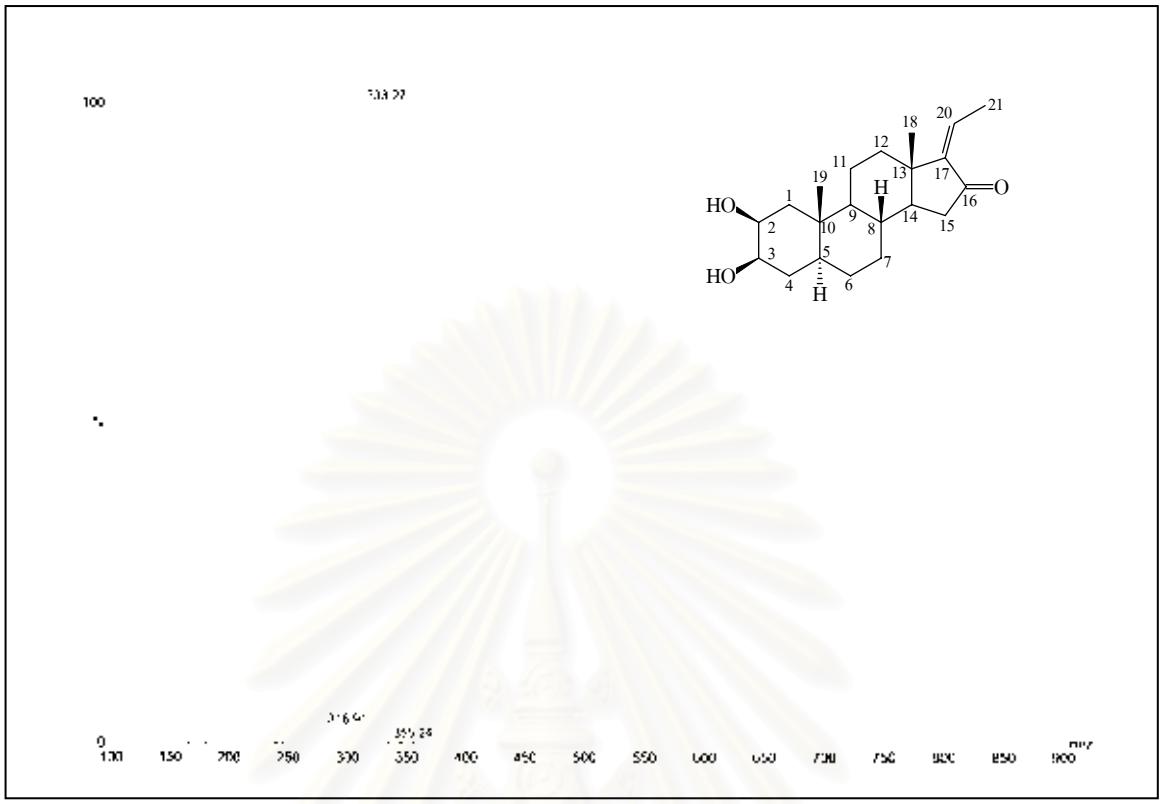

Figure 46. ESI-TOF Mass spectrum of compound CAF3

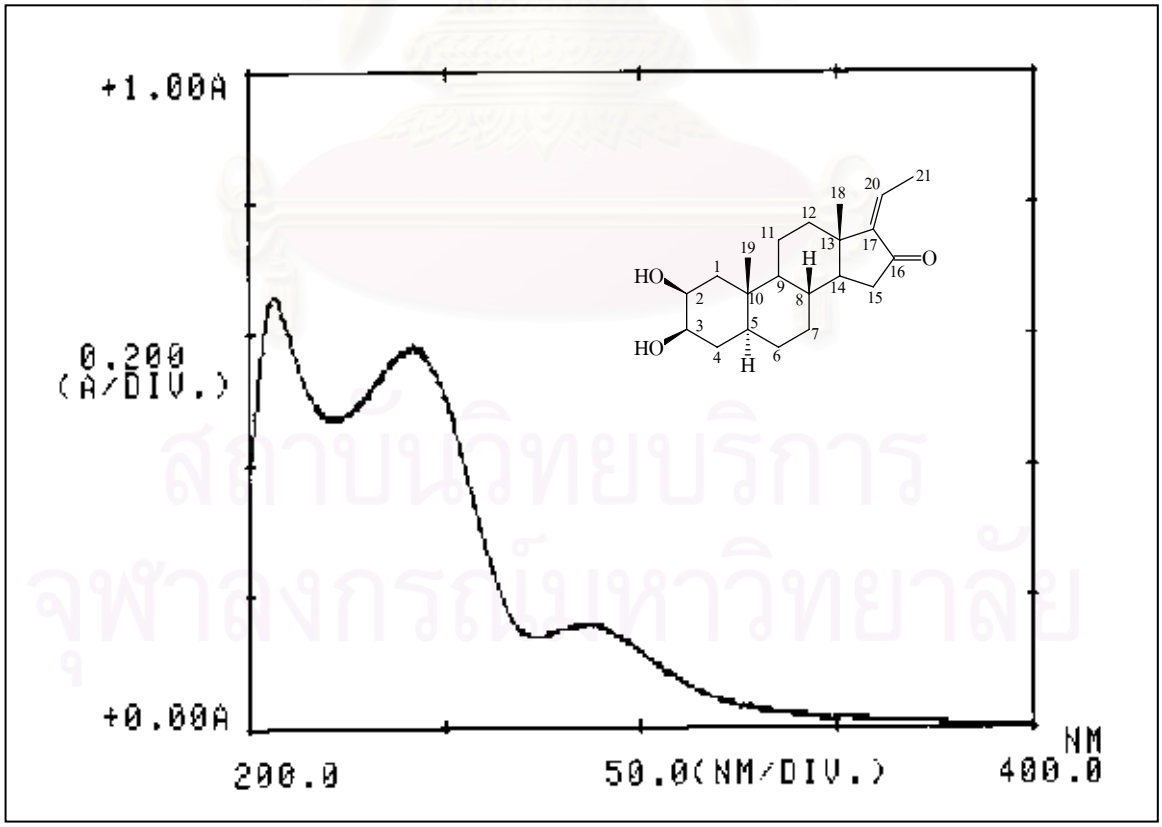

Figure 47. UV Spectrum of compound CAF3

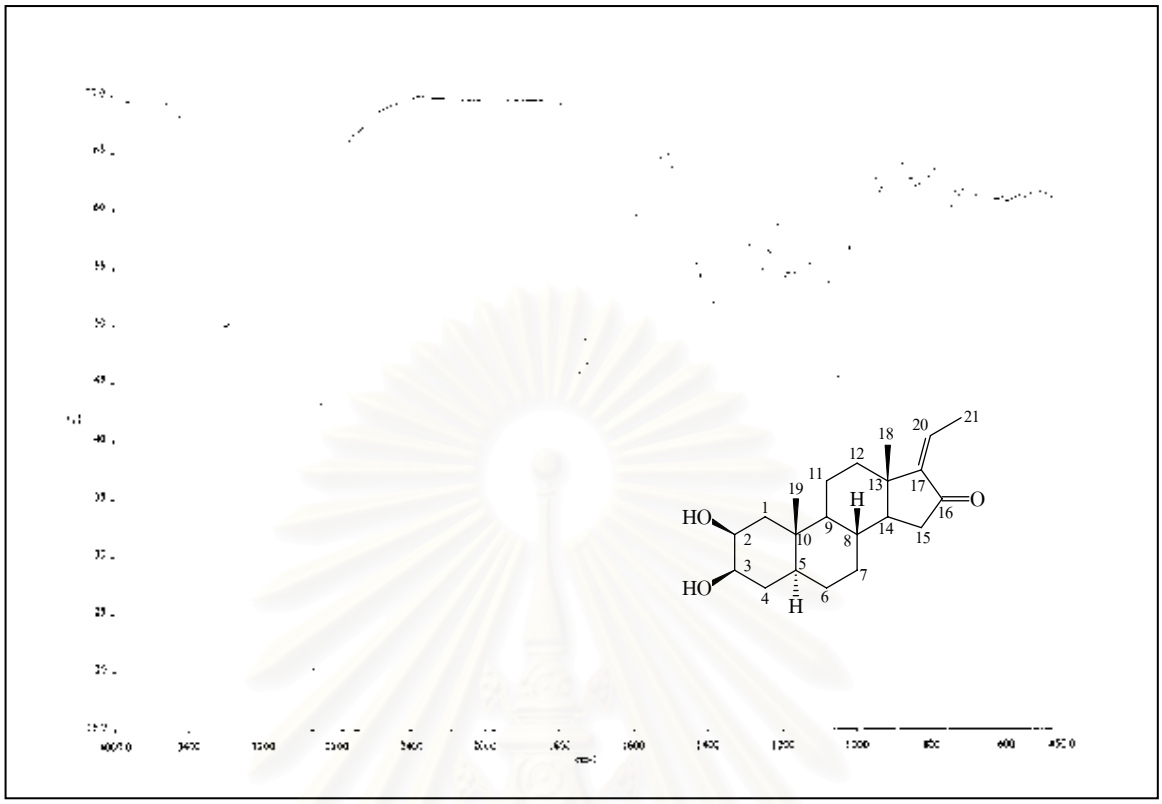

Figure 48. IR Spectrum of compound CAF3 (KBr disc)

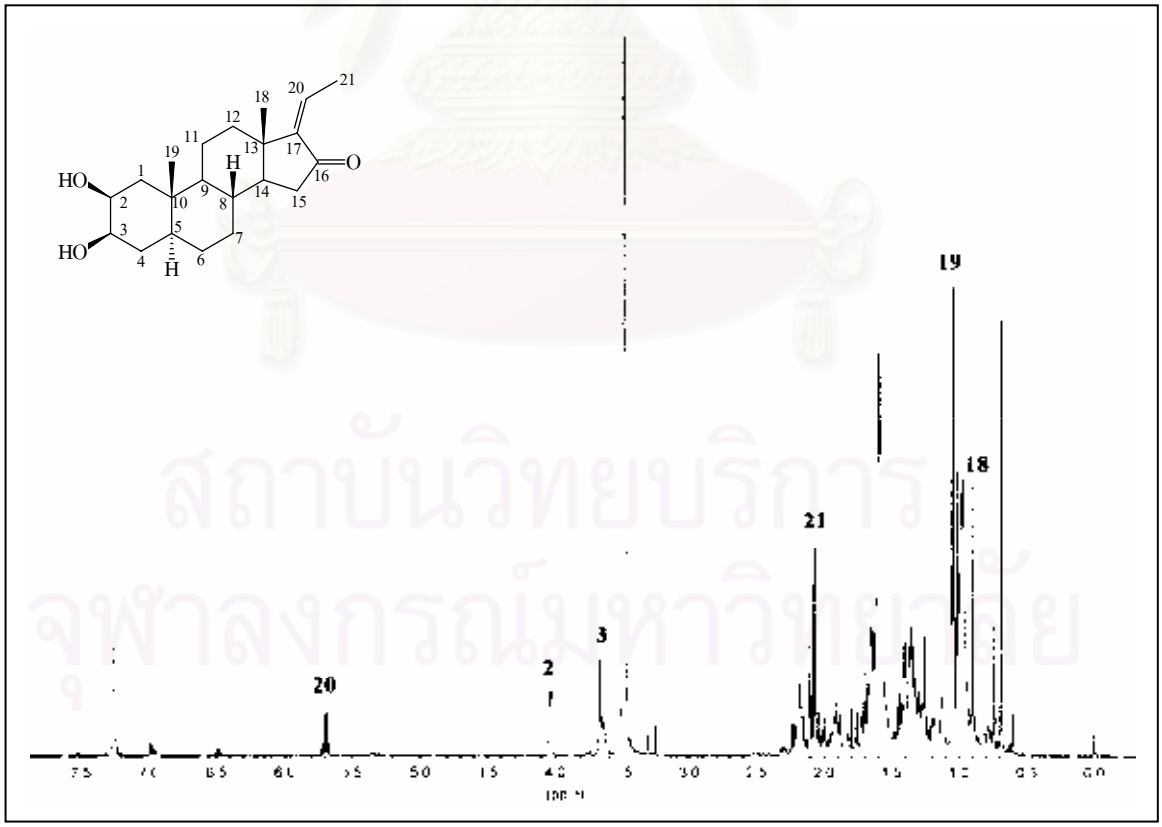

Figure 49. ^{1}H NMR (400 MHz) Spectrum of compound CAF3 ($CDCl_3$)

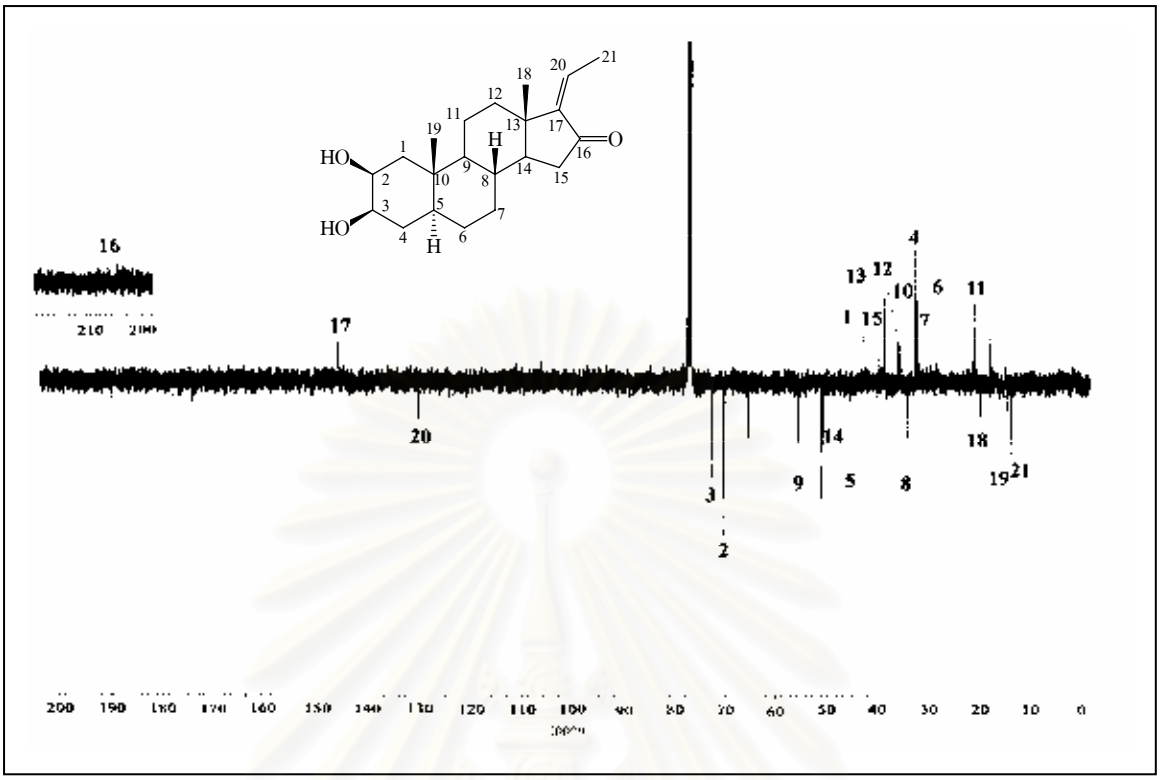

Figure 50. ^{13}C APT (100 MHz) Spectrum of compound CAF3 ($CDCl_3$)

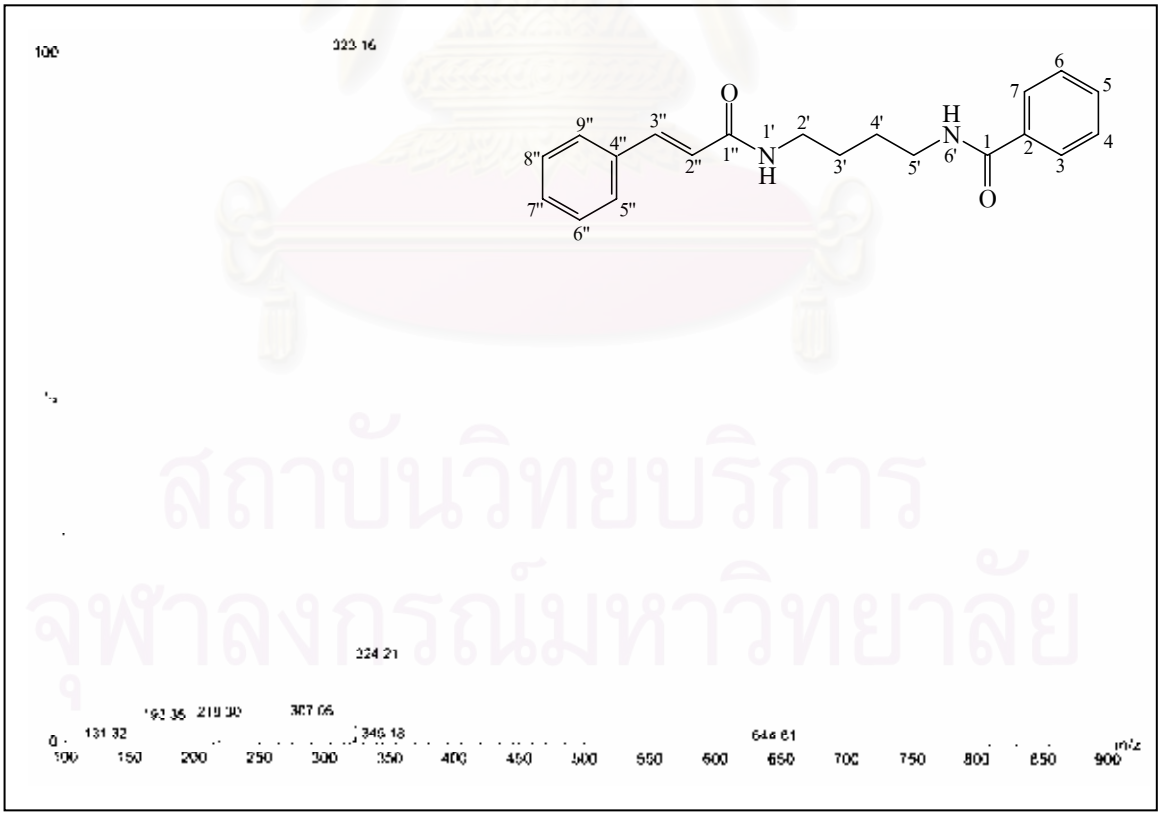

Figure 51. ESI-TOF Mass spectrum of compound CAF4

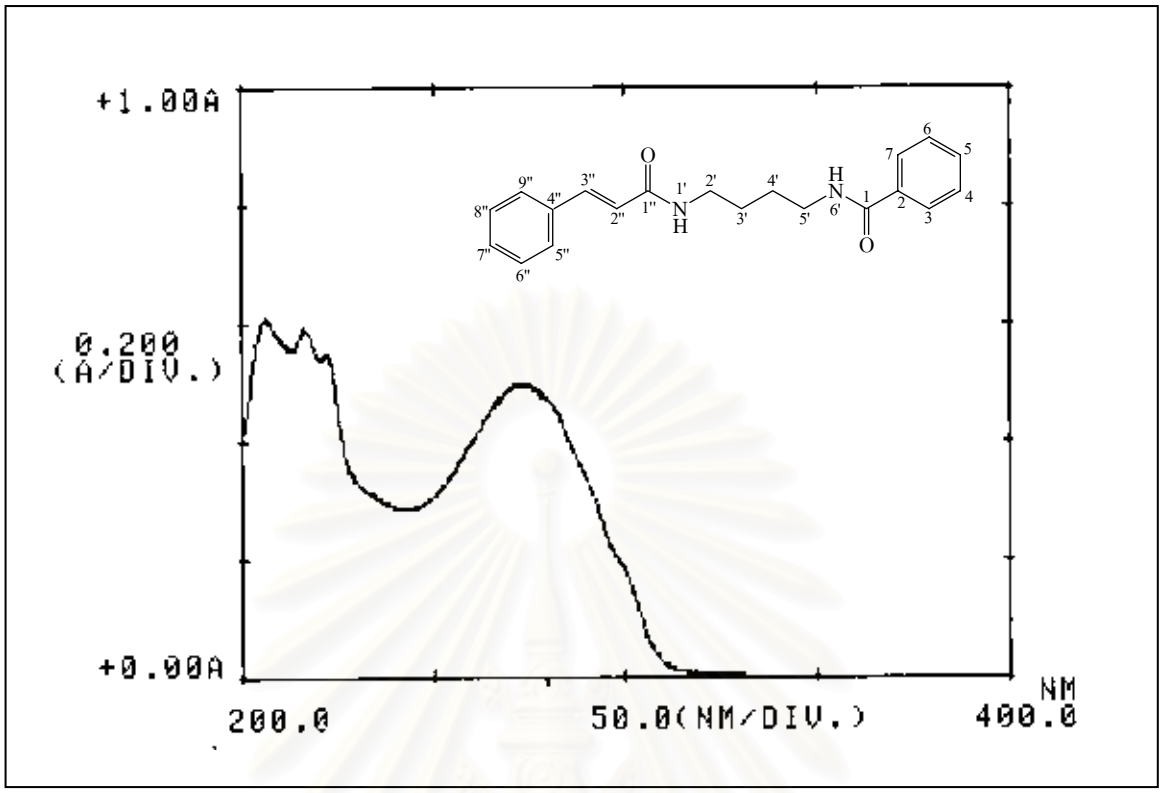

Figure 52. UV Spectrum of compound CAF4

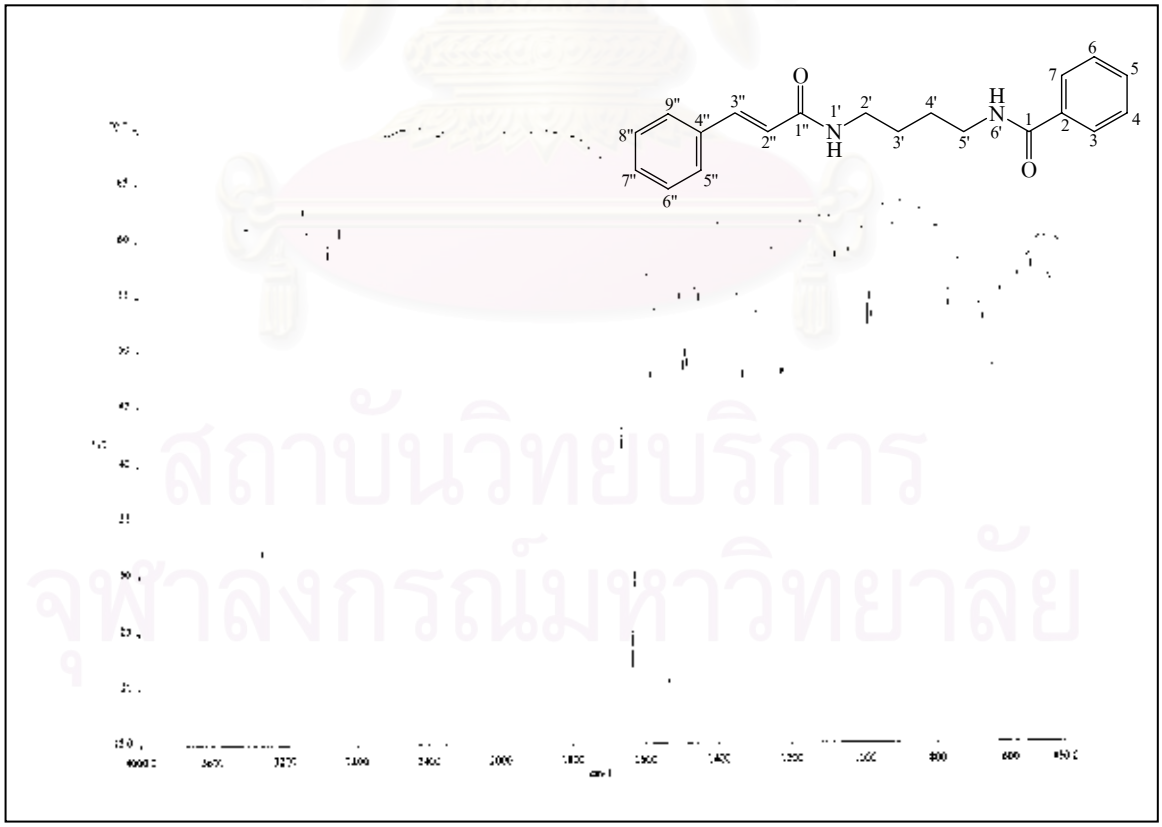

Figure 53. IR Spectrum of compound CAF4 (KBr disc)

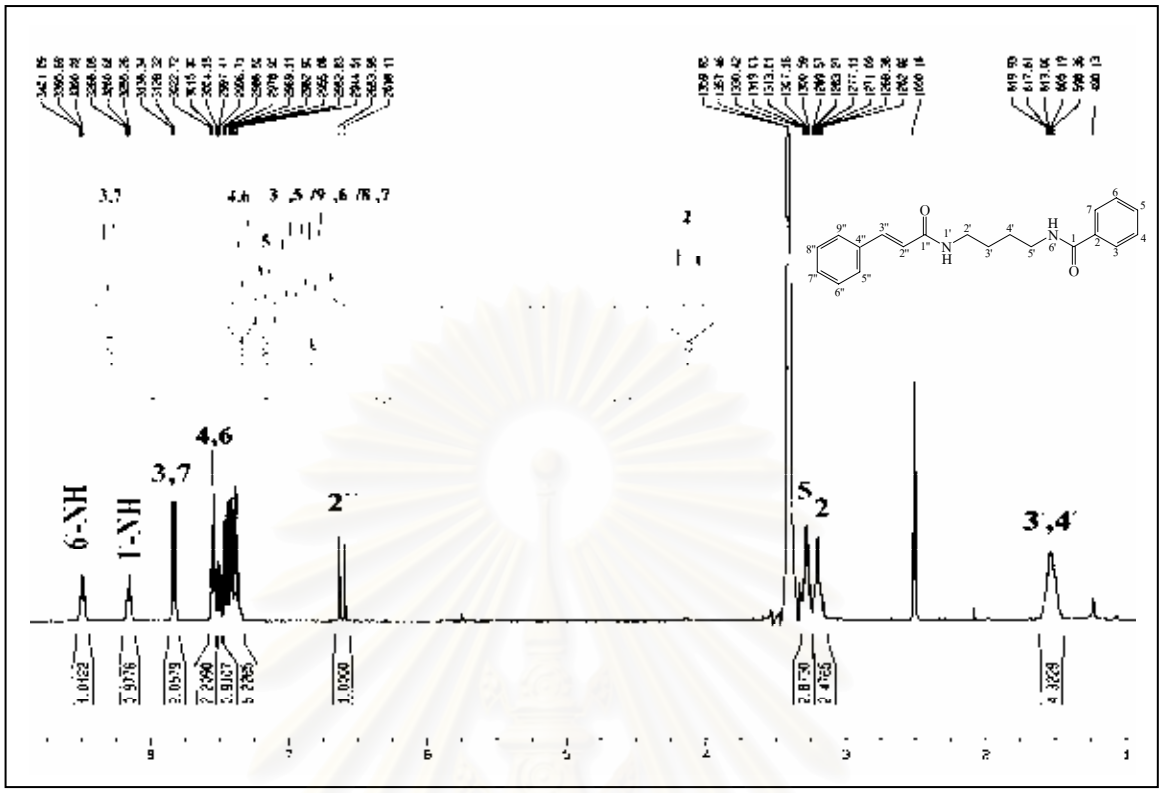

Figure 54. ^{1}H NMR (400 MHz) Spectrum of compound CAF4 (DMSO-d_6)

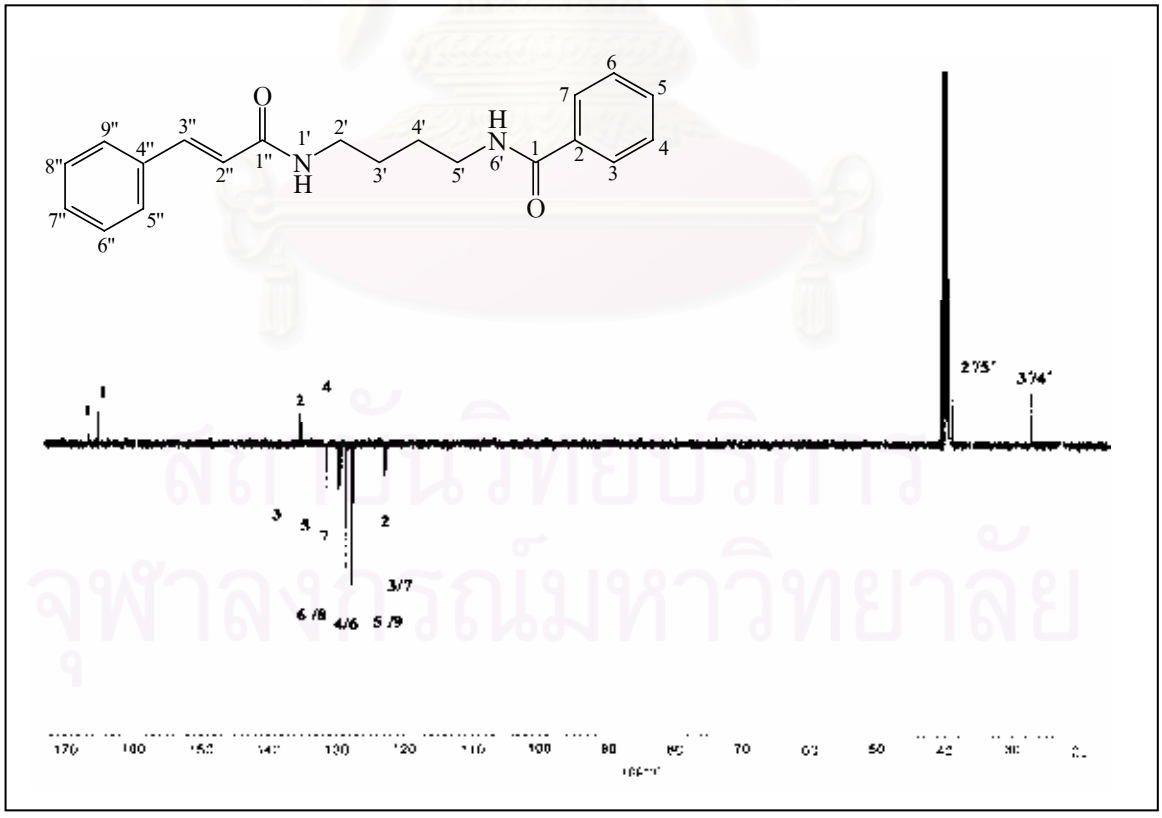

Figure 55. ^{13}C APT (100 MHz) Spectrum of compound CAF4 (DMSO-d_6)

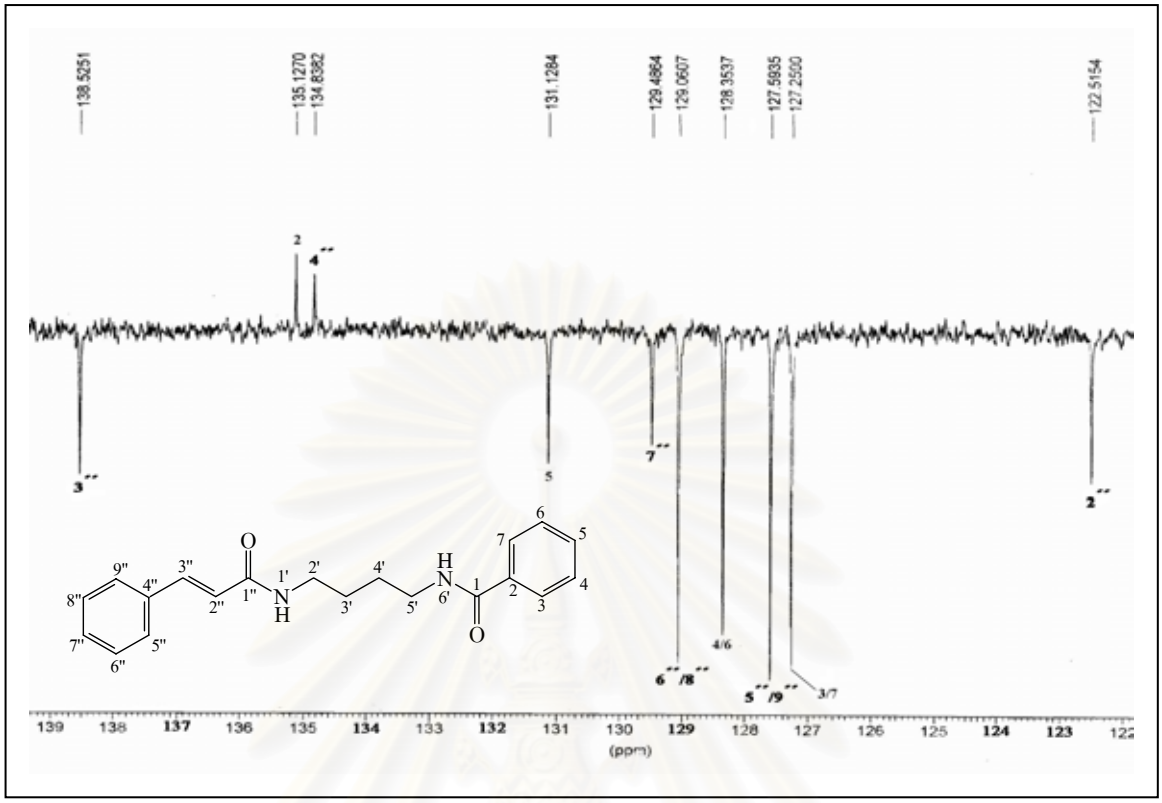

Figure 56. ^{13}C APT (100 MHz) Spectrum of compound CAF4 (DMSO-d_6) (expanded)

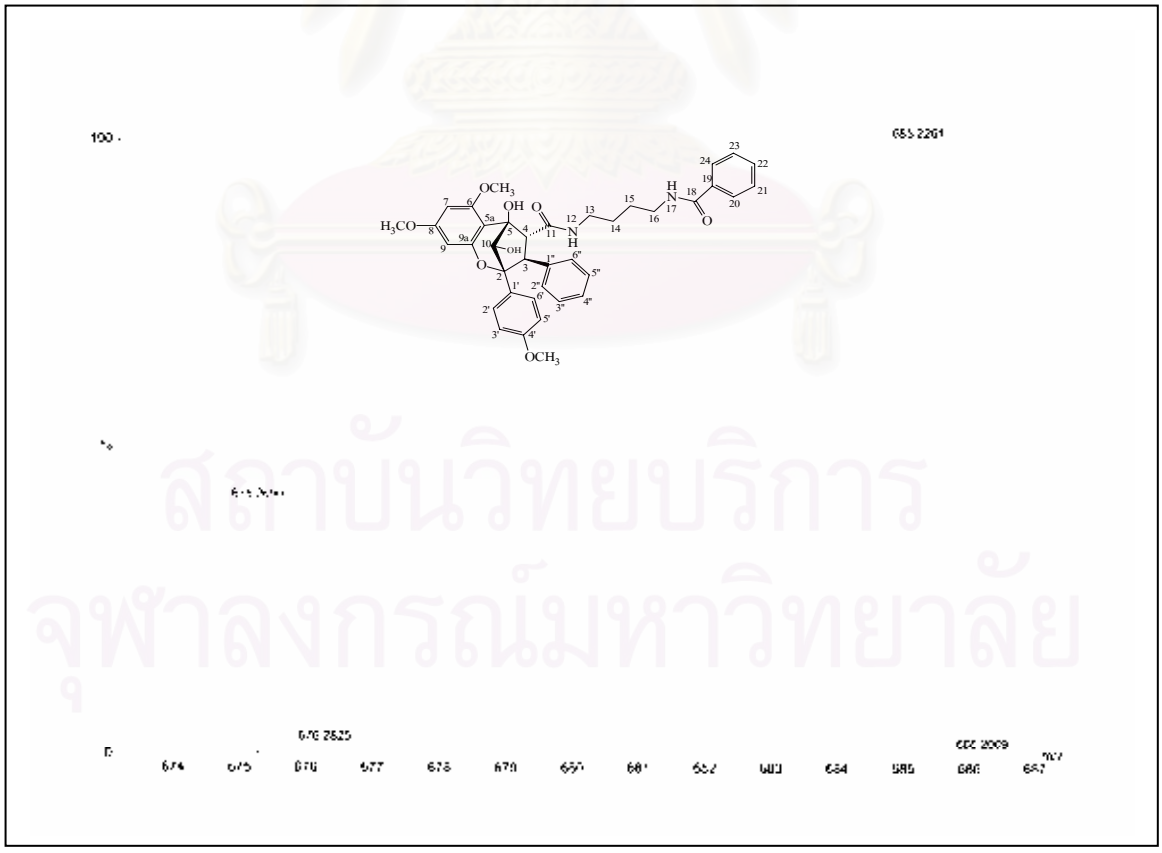

Figure 57. HRESI-TOF Mass spectrum of compound CAF5

สถาบันวิทยบริการ
จุฬาลงกรณ์มหาวิทยาลัย

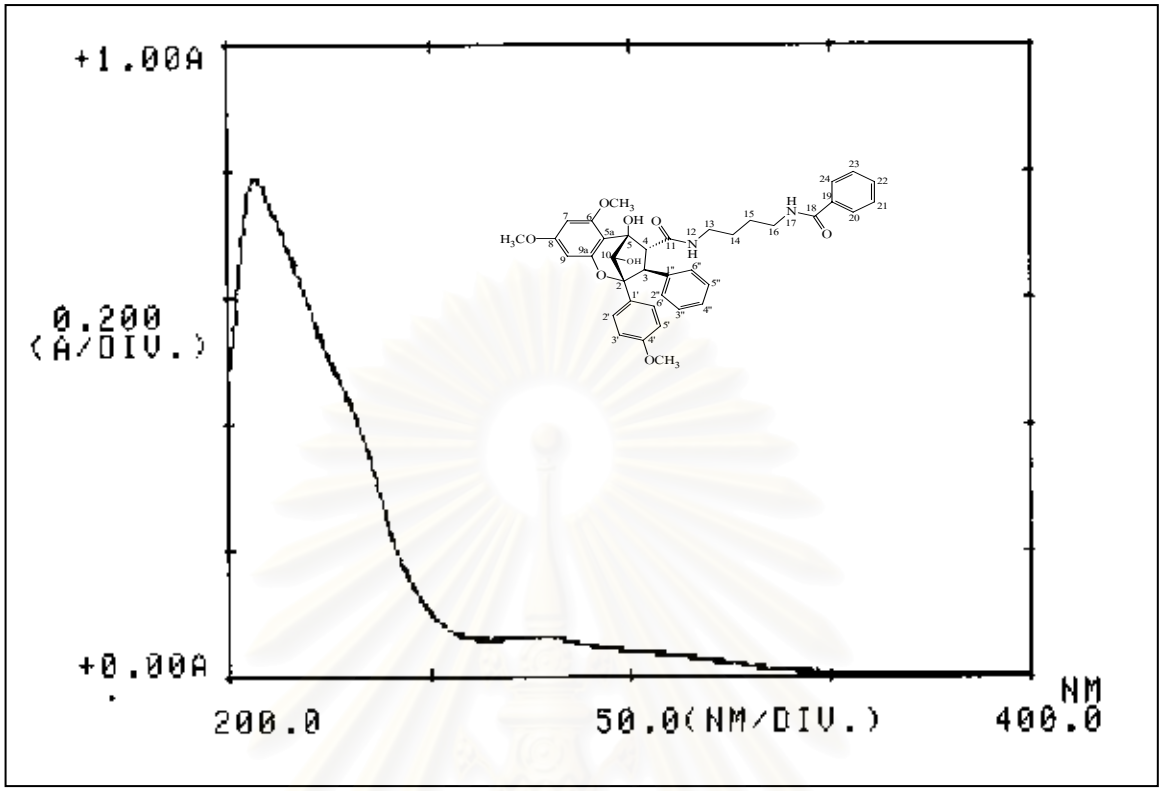

Figure 58. UV Spectrum of compound CAF5

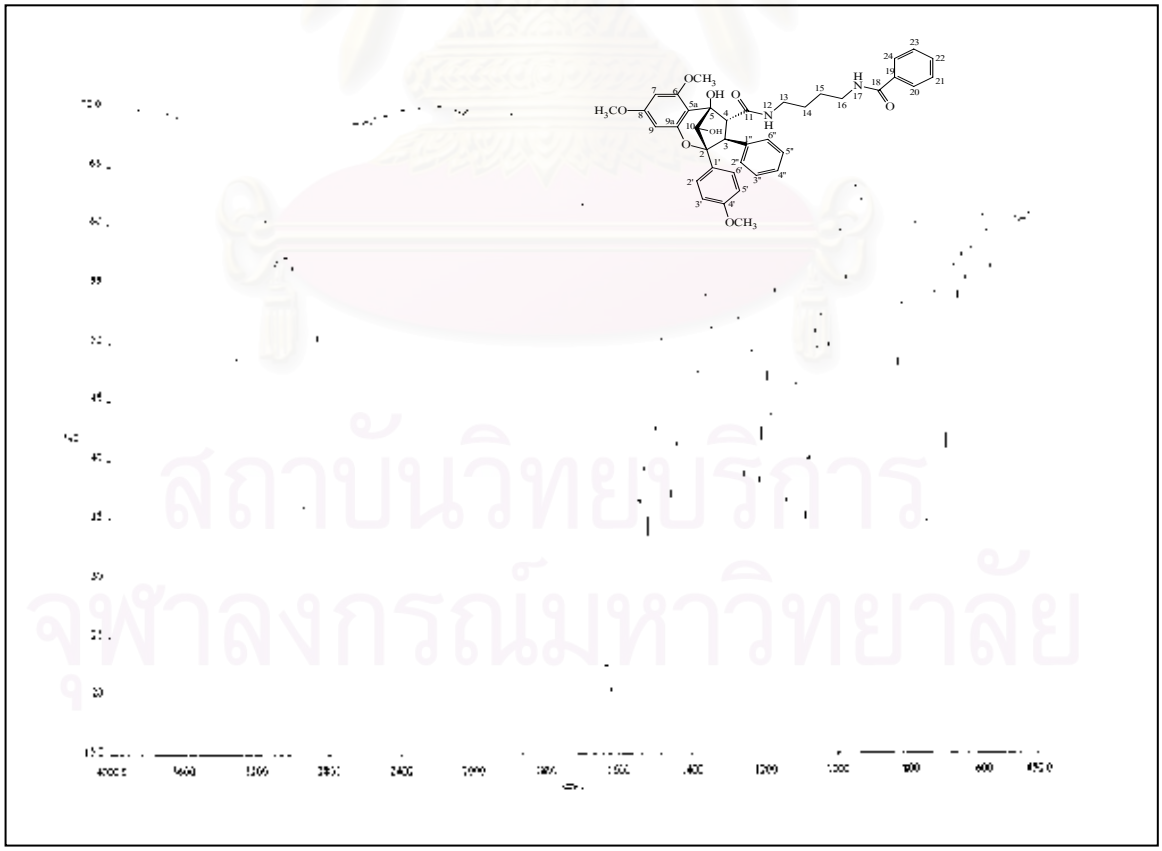

Figure 59. IR Spectrum of compound CAF5 (KBr disc)

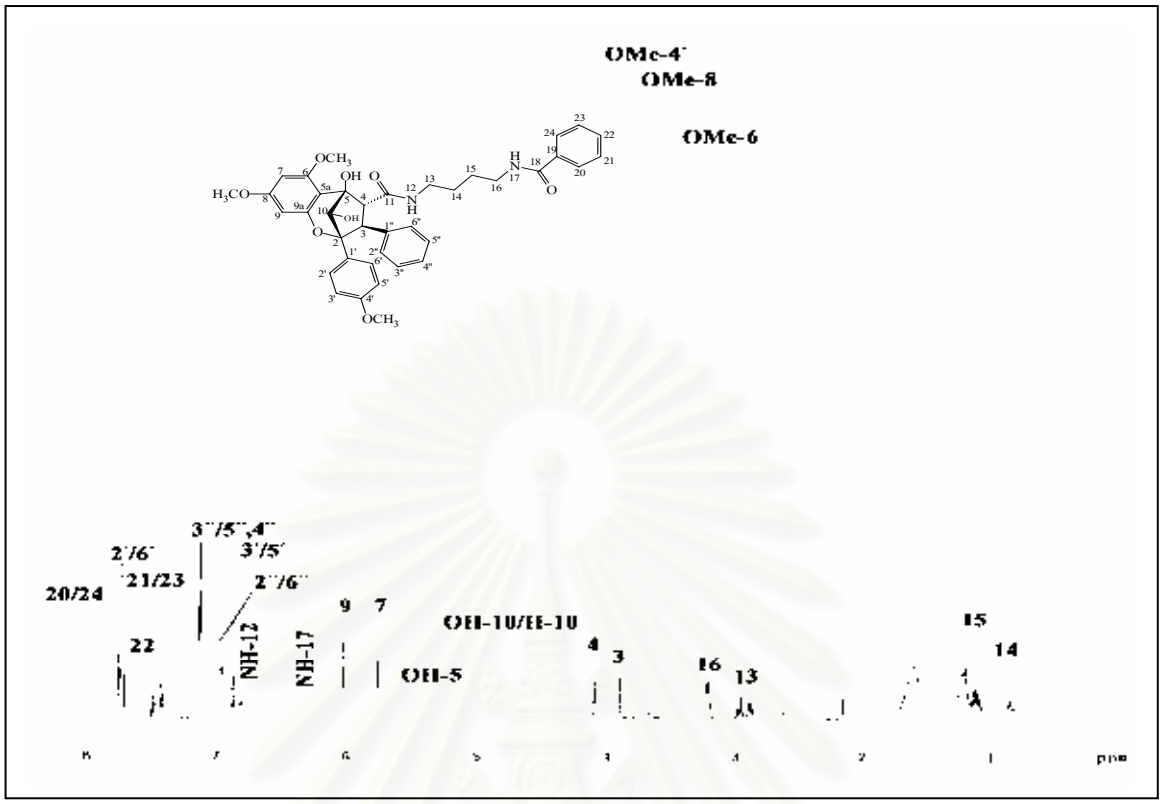

Figure 60. ^{1}H NMR (500 MHz) Spectrum of compound CAF5 ($CDCl_3$)

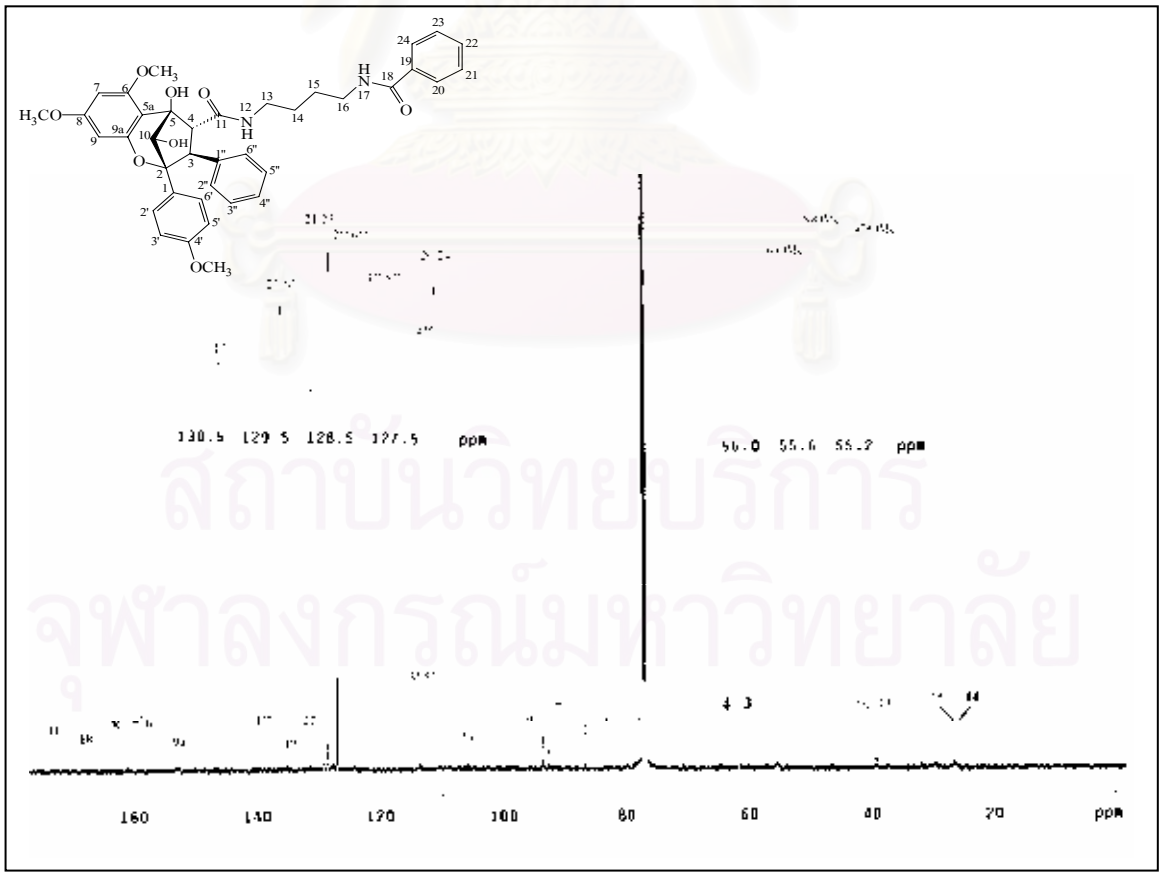

Figure 61. ^{13}C NMR (125 MHz) Spectrum of compound CAF5 ($CDCl_3$)

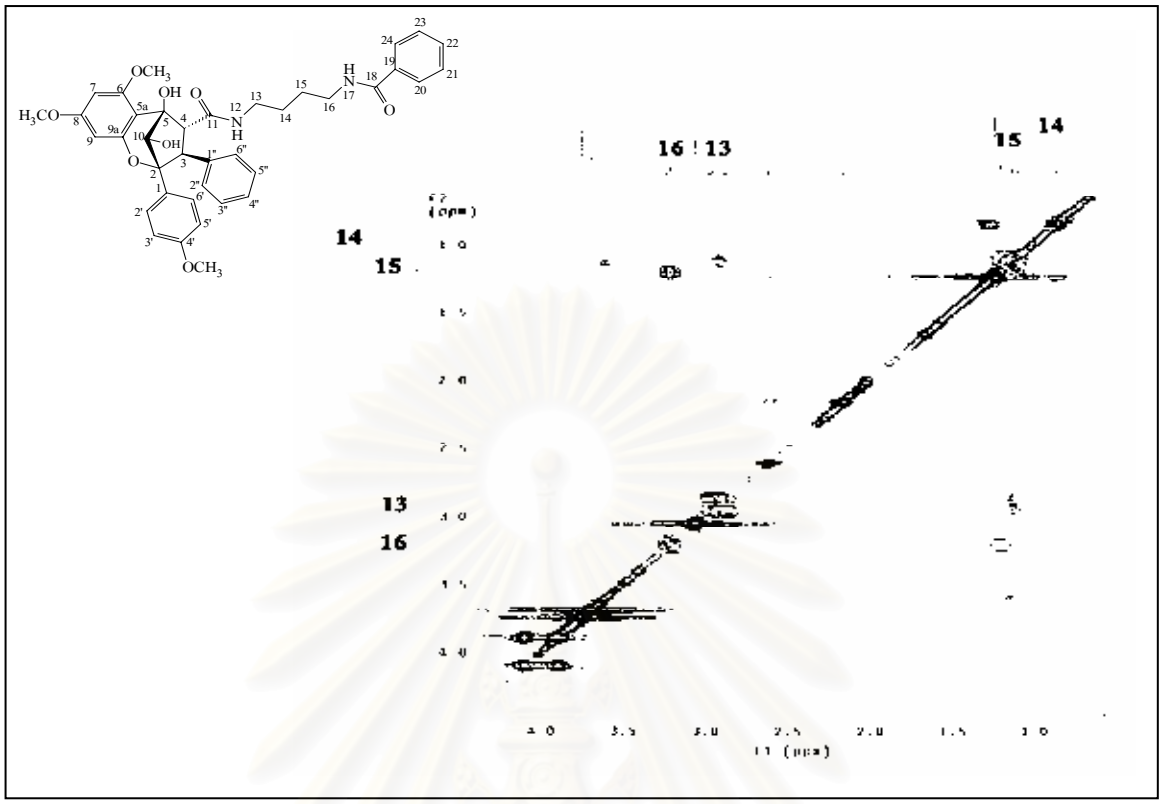

Figure 62. $^{1}H–^{1}H$ COSY Spectrum of compound CAF5 ($CDCl_3$) [δ_H 1.0-4.0 ppm]

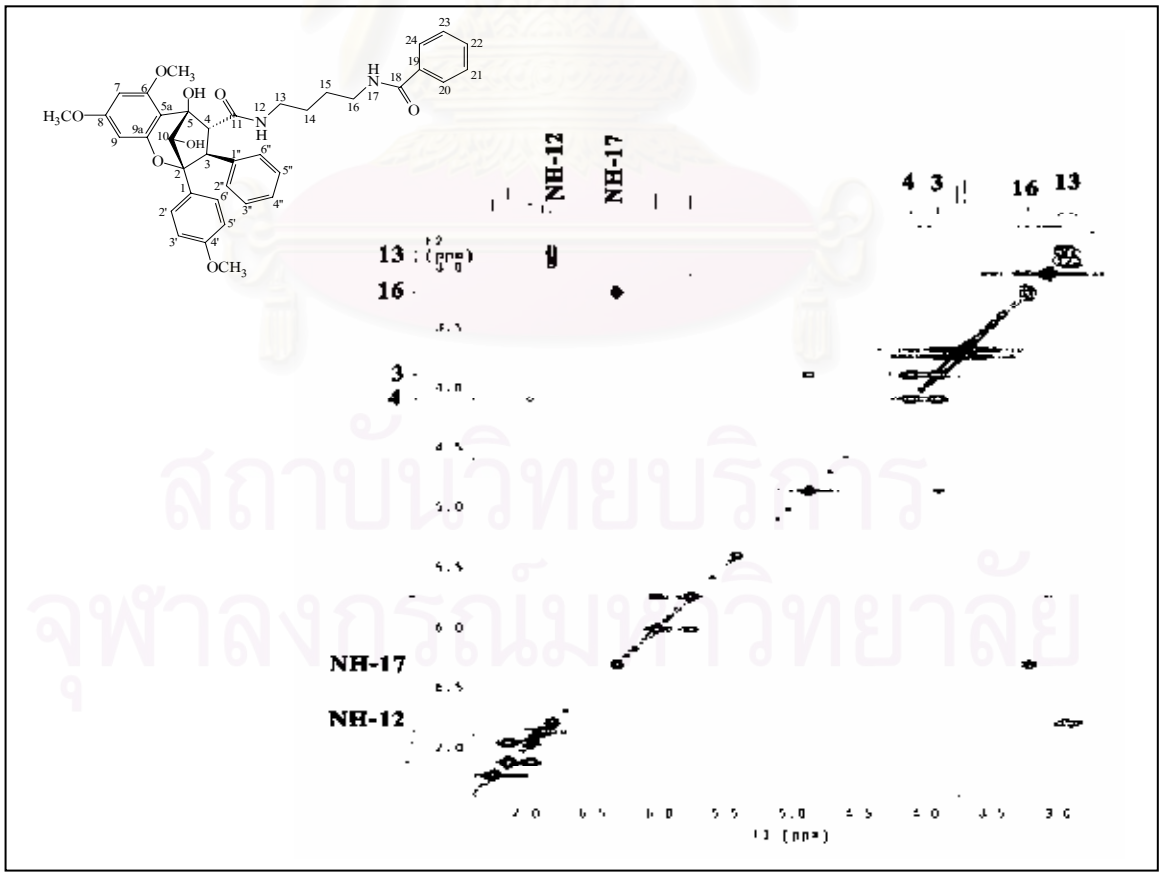

Figure 63. $^{1}H–^{1}H$ COSY Spectrum of compound CAF5 ($CDCl_3$) [δ_H 0.0-7.0 ppm]

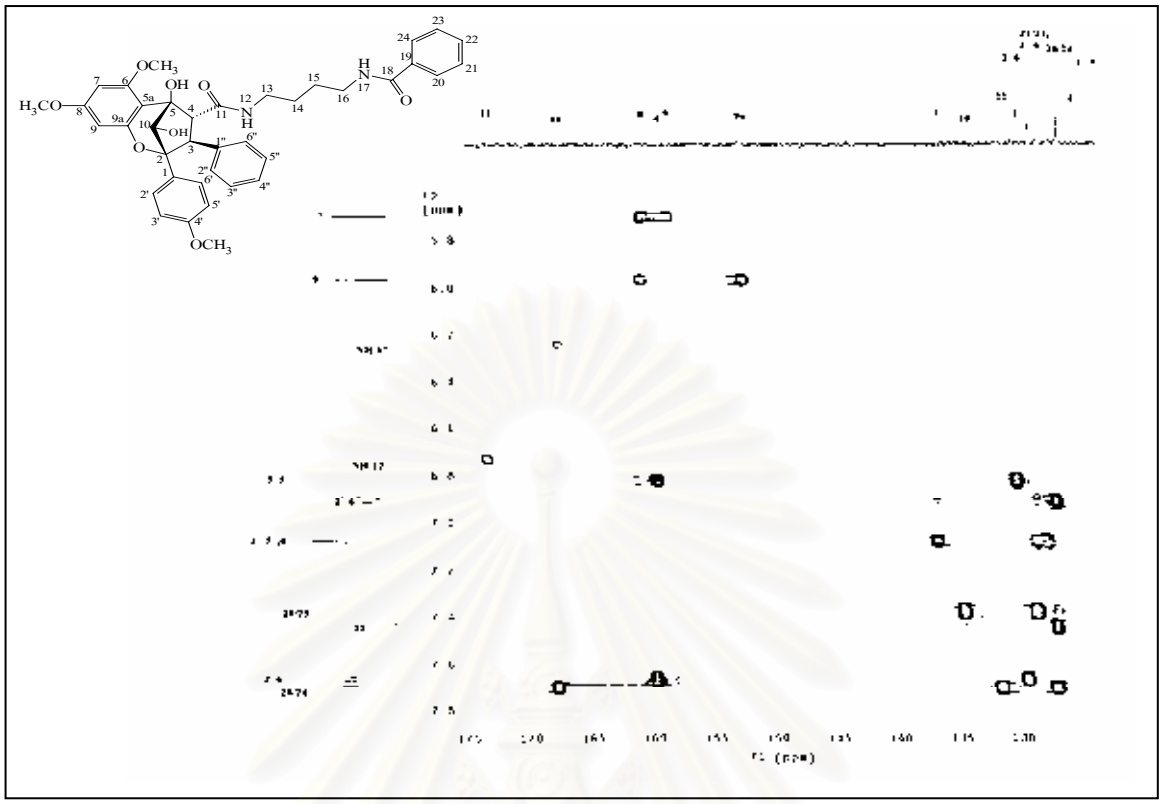

Figure 64. HMBC Spectrum of compound CAF5 ($CDCl_3$) [δ_H 2.6-4.2 ppm, δ_C 125-175 ppm]

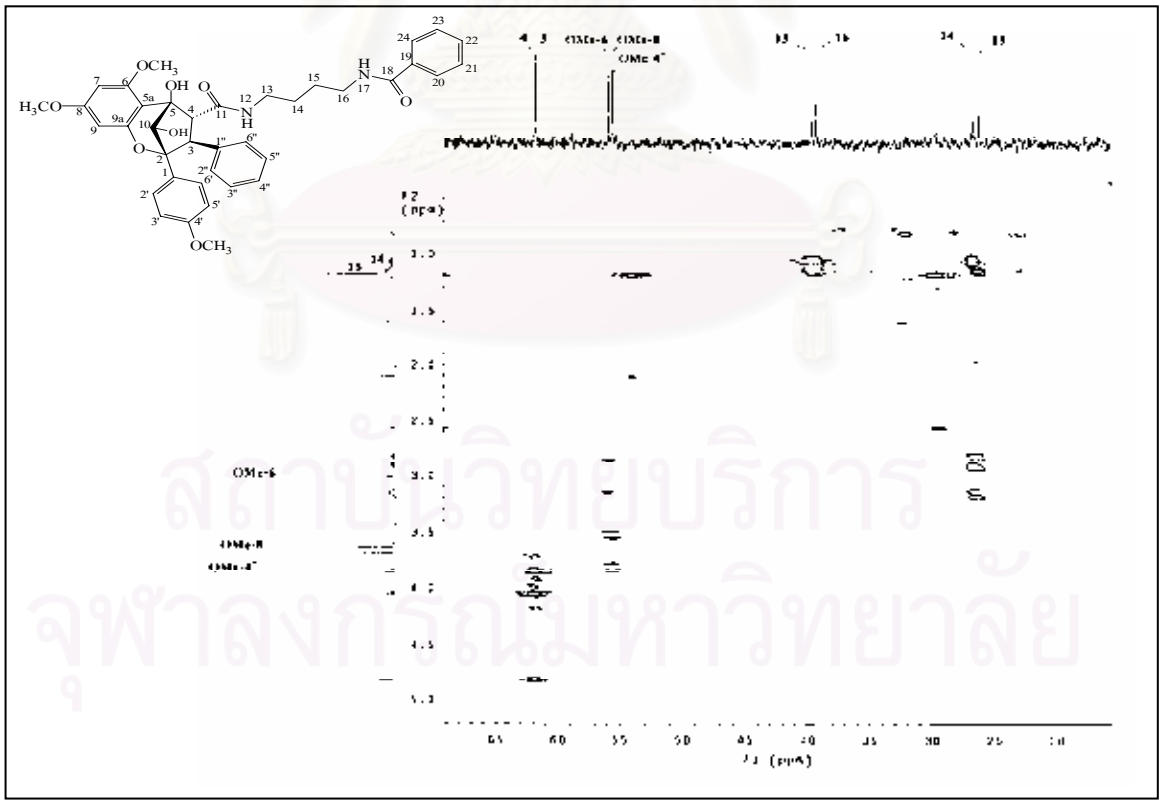

Figure 65. HMBC Spectrum of compound CAF5 ($CDCl_3$) [δ_H 1.0-5.0 ppm, δ_C 20-65 ppm]

สถาบันวิทยบริการ
จุฬาลงกรณ์มหาวิทยาลัย

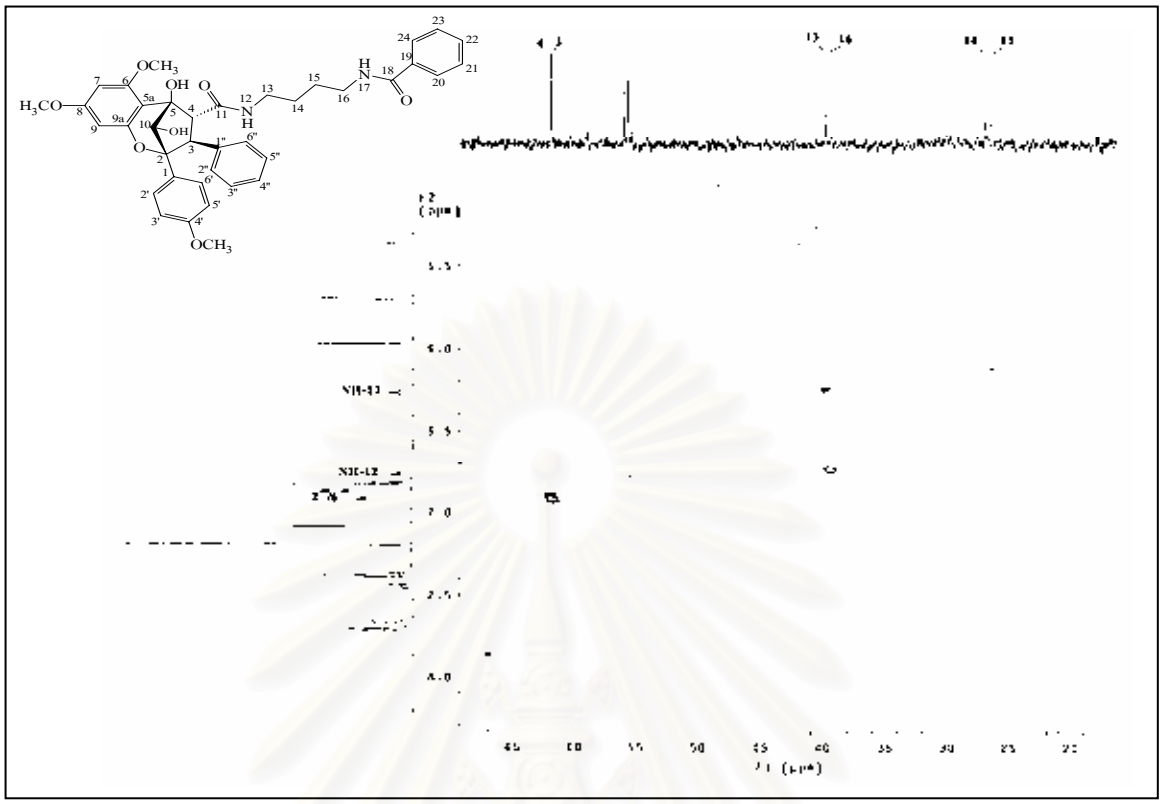

Figure 66. HMBC Spectrum of compound CAF5 ($CDCl_3$) [δ_H 5.5-8.0 ppm, δ_C 20-65 ppm]

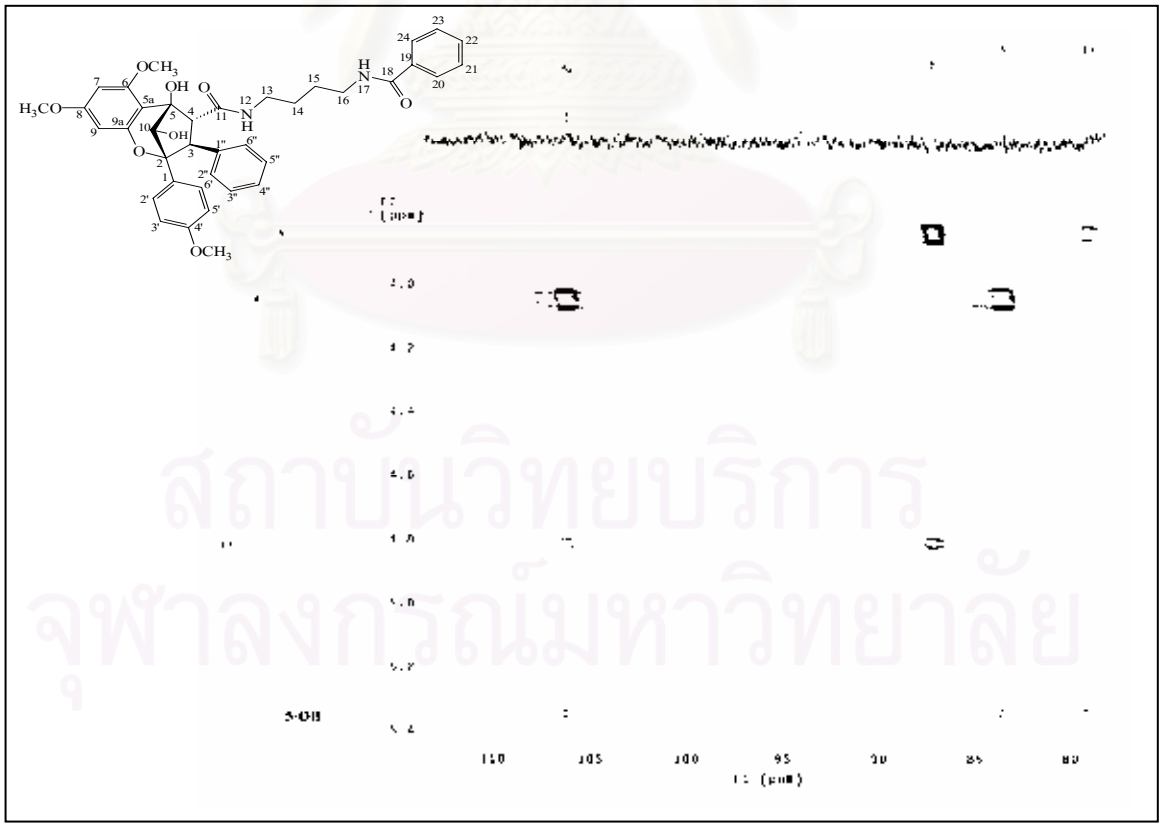

Figure 67. HMBC Spectrum of compound CAF5 ($CDCl_3$) [δ_H 3.8-5.4 ppm, δ_C 78-110 ppm]

สถาบันวิทยบริการ
จุฬาลงกรณ์มหาวิทยาลัย

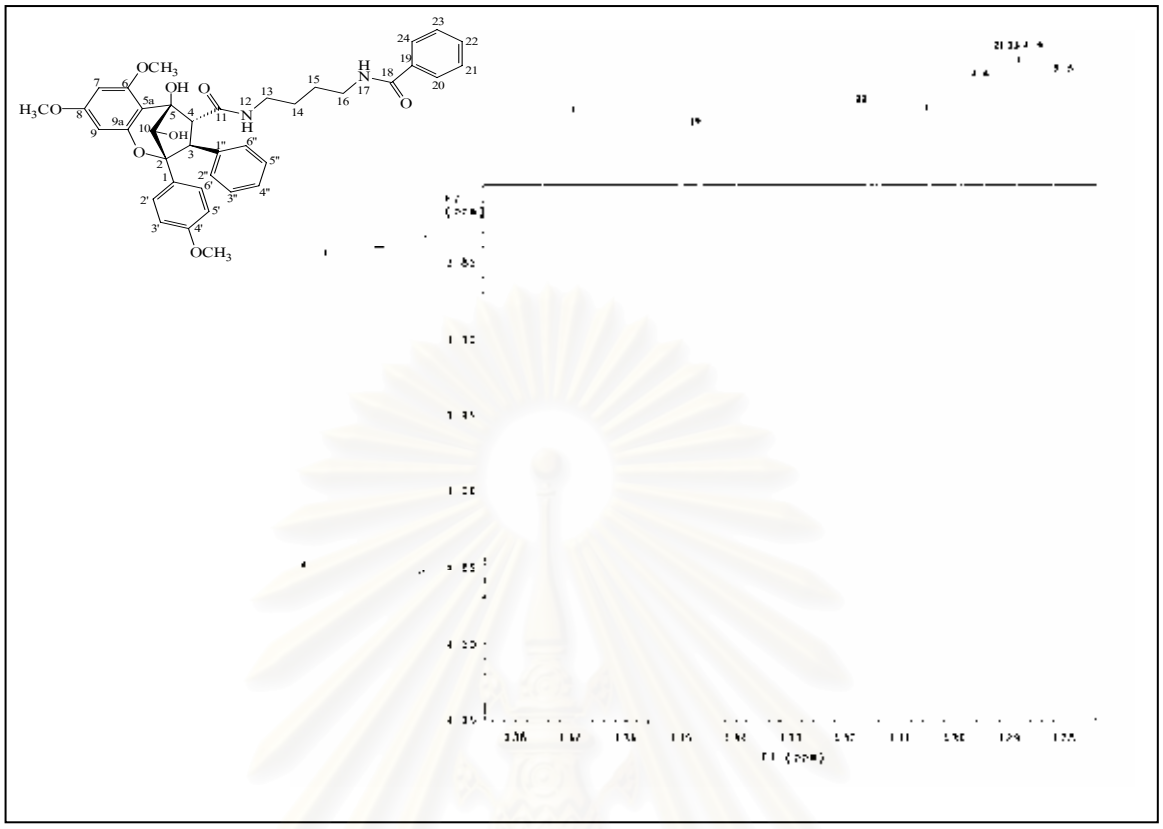

Figure 68. HMBC Spectrum of compound CAF5 ($CDCl_3$) [δ_H 3.9-5.4 ppm, δ_C 128-138 ppm]

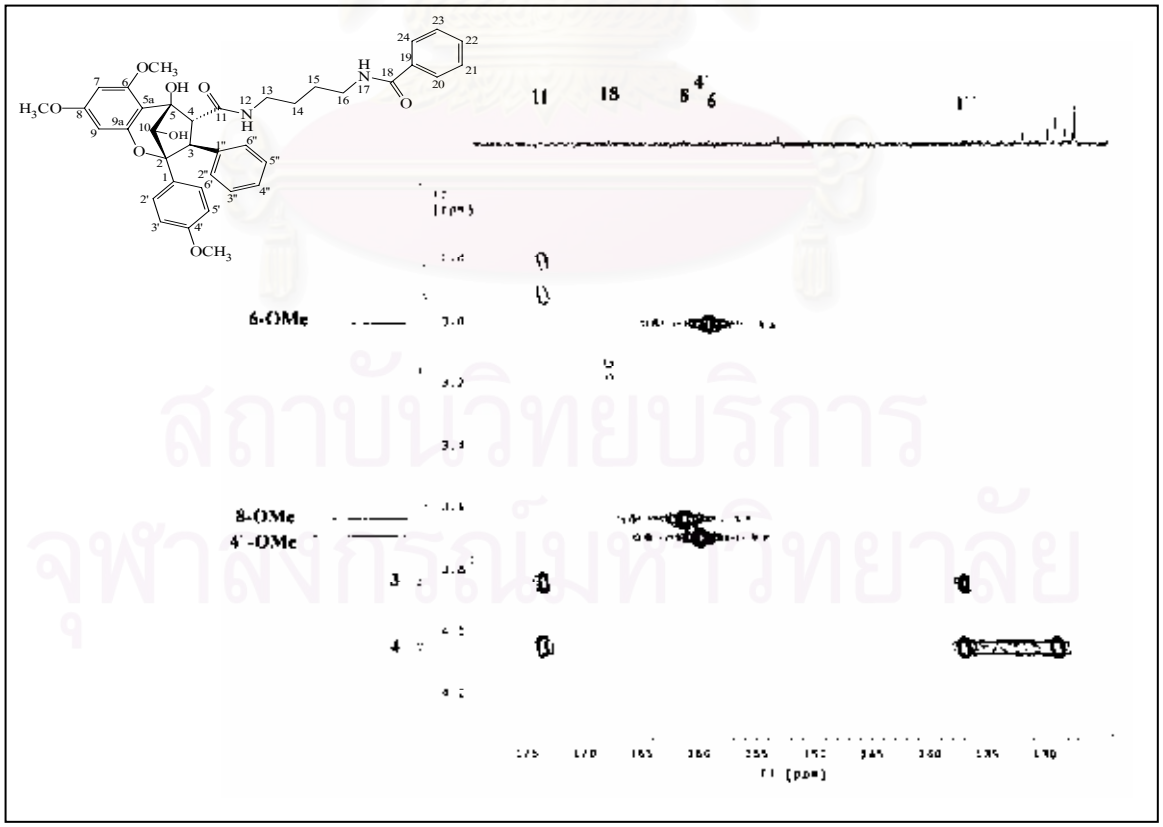

Figure 69. HMBC Spectrum of compound CAF5 ($CDCl_3$) [δ_H 3.8-4.5 ppm, δ_C 128-138 ppm]

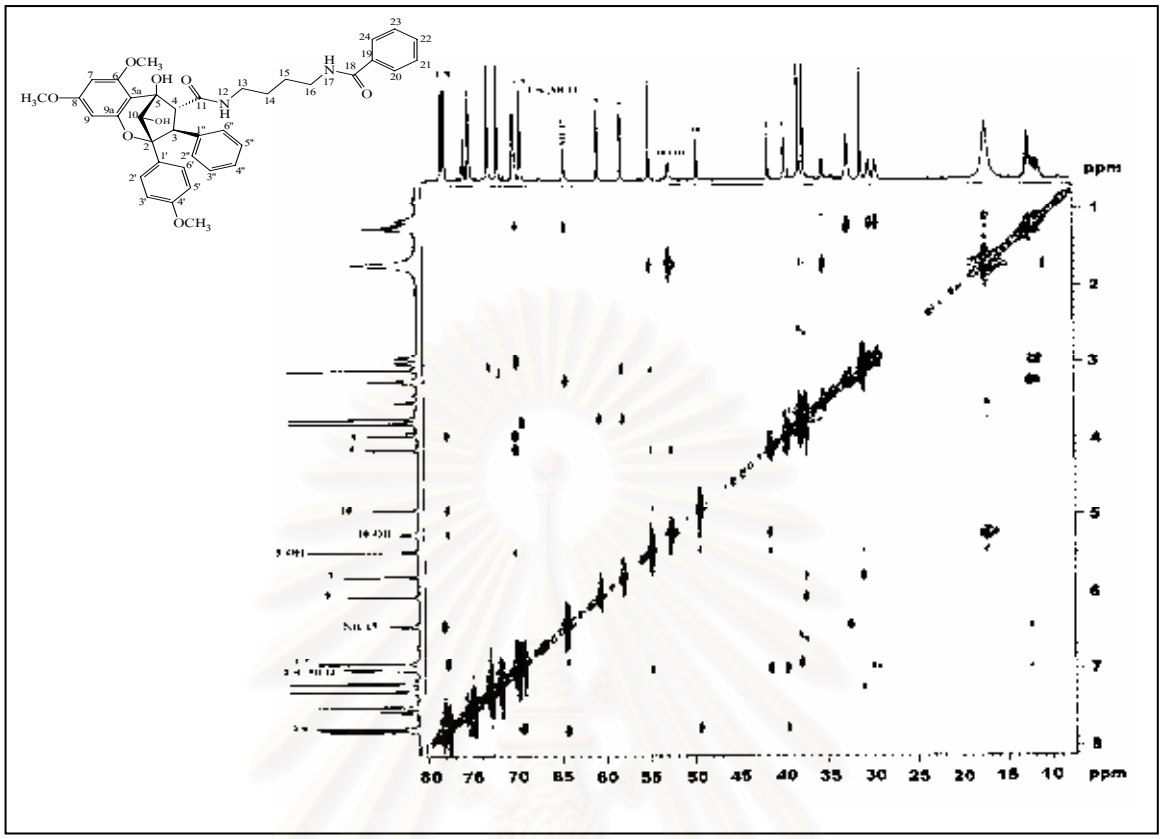

Figure 70. NOESY Spectrum of compound CAF5 ($CDCl_3$)

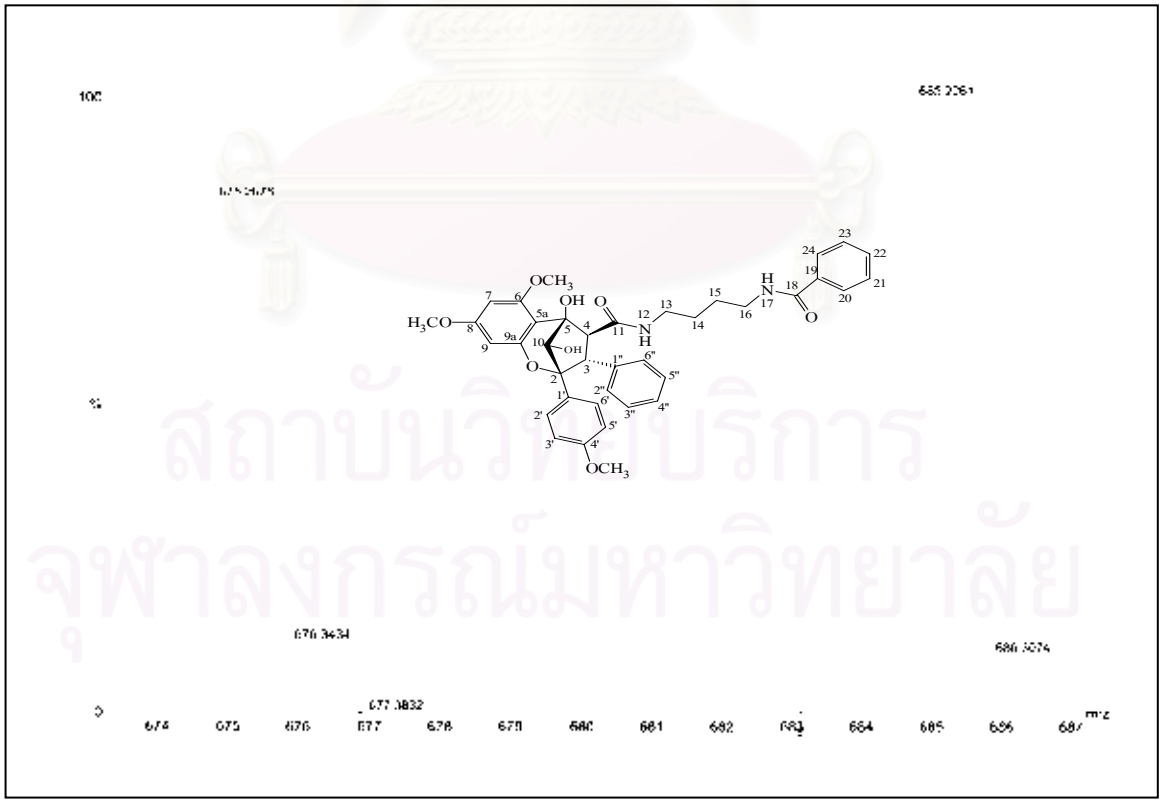

Figure 71. HRESI-TOF Mass spectrum of compound CAF6

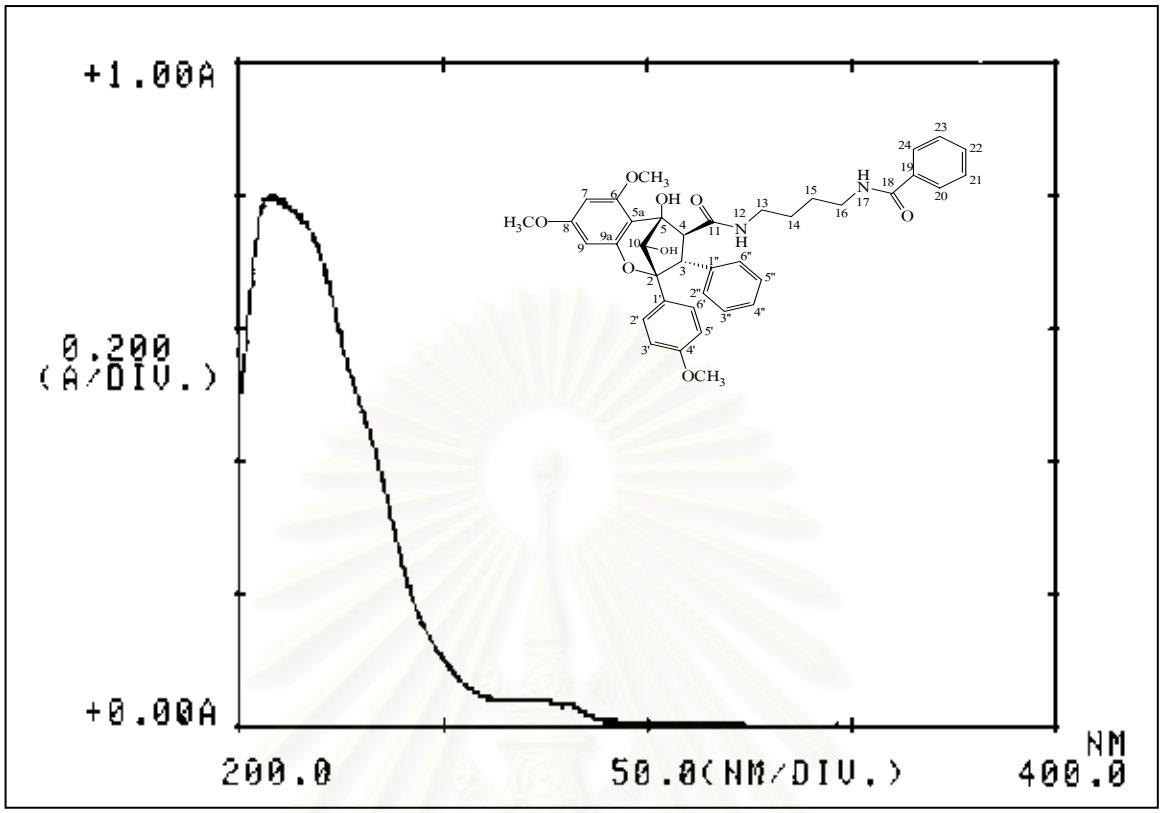

Figure 72. UV Spectrum of compound CAF6

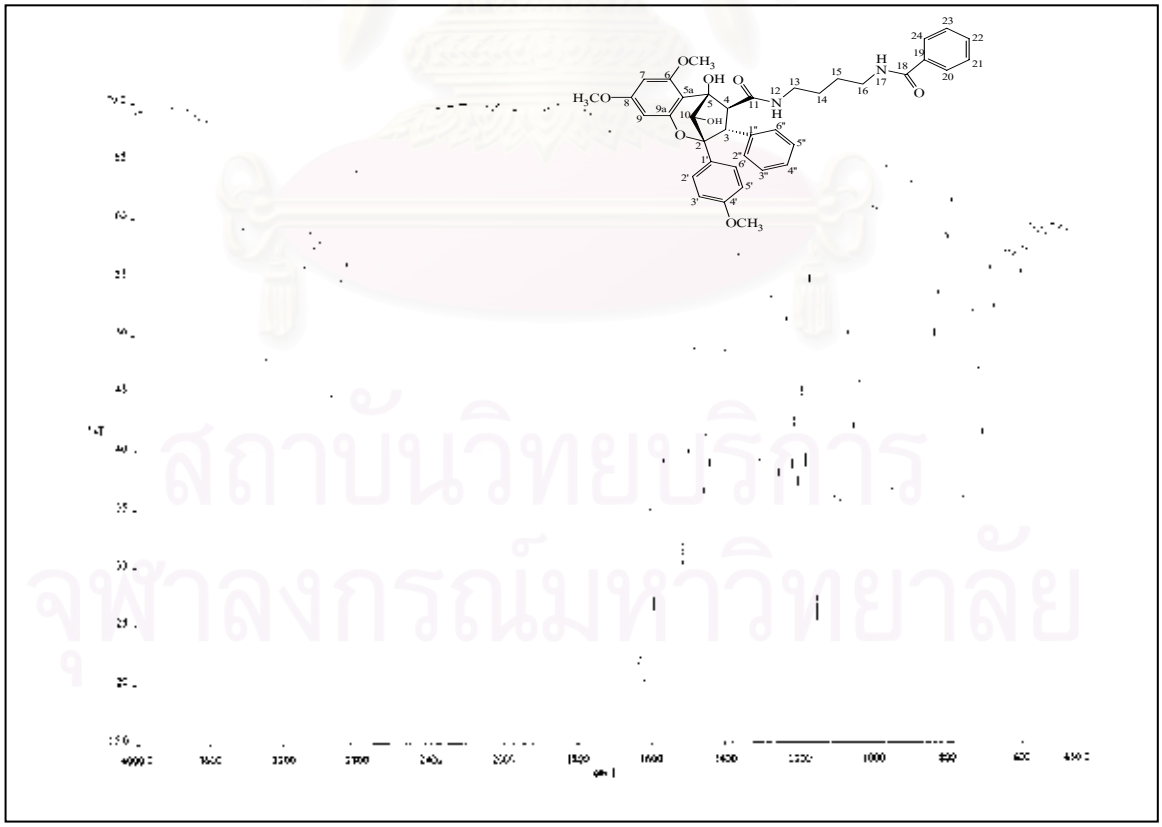

Figure 73. IR Spectrum of compound CAF6 (KBr disc)

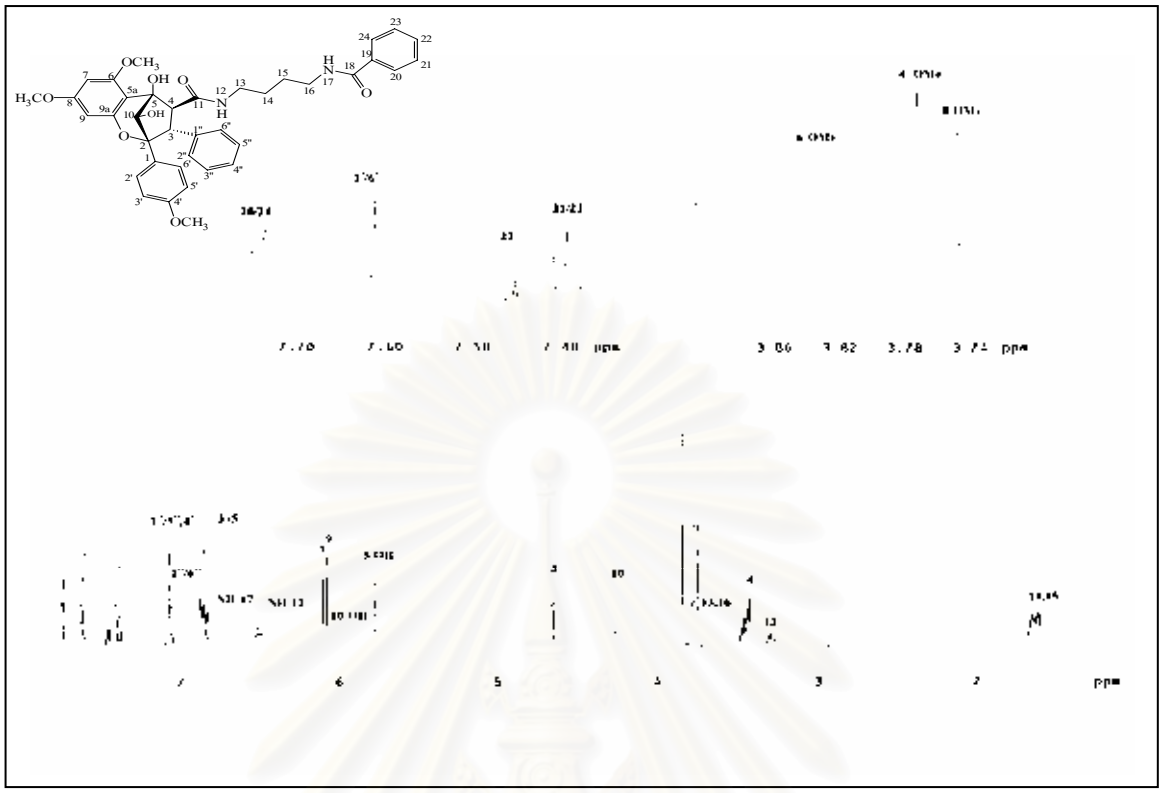

Figure 74. ^{1}H NMR (500 MHz) Spectrum of compound CAF6 ($CDCl_3$)

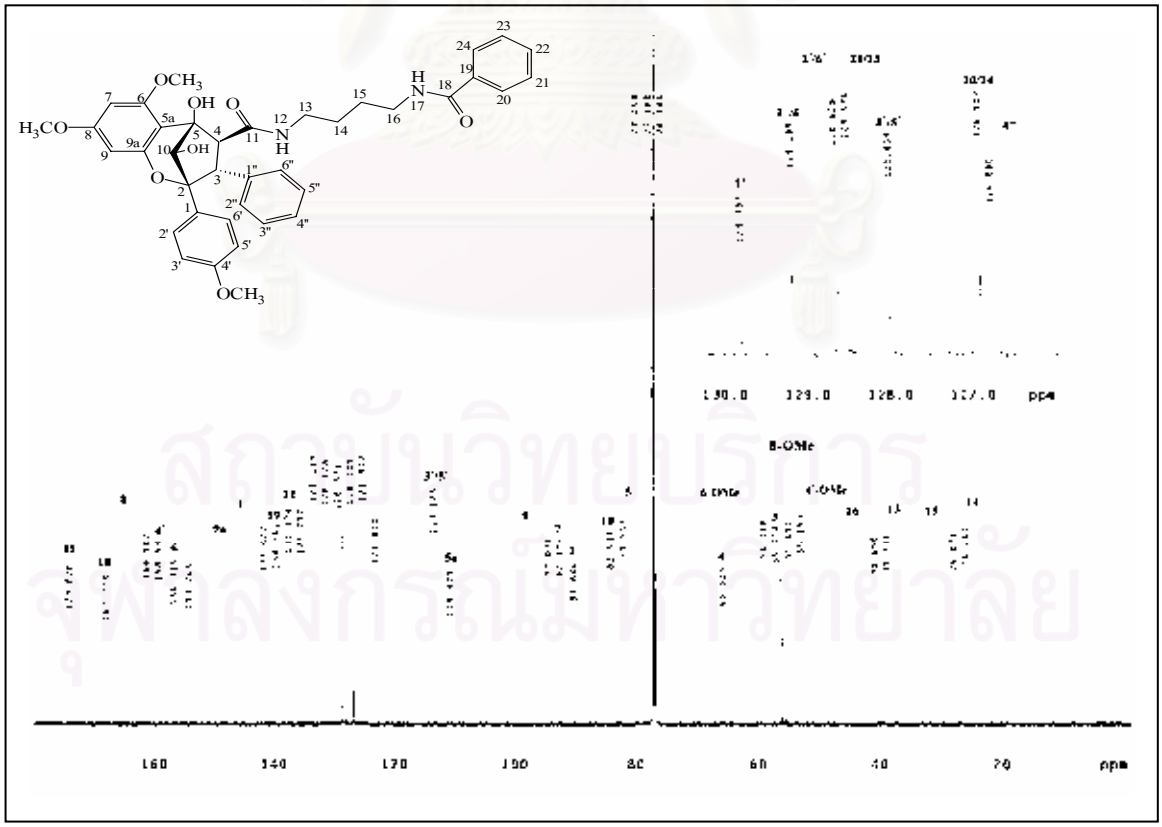

Figure 75. ^{13}C NMR (125 MHz) Spectrum of compound CAF6 ($CDCl_3$)

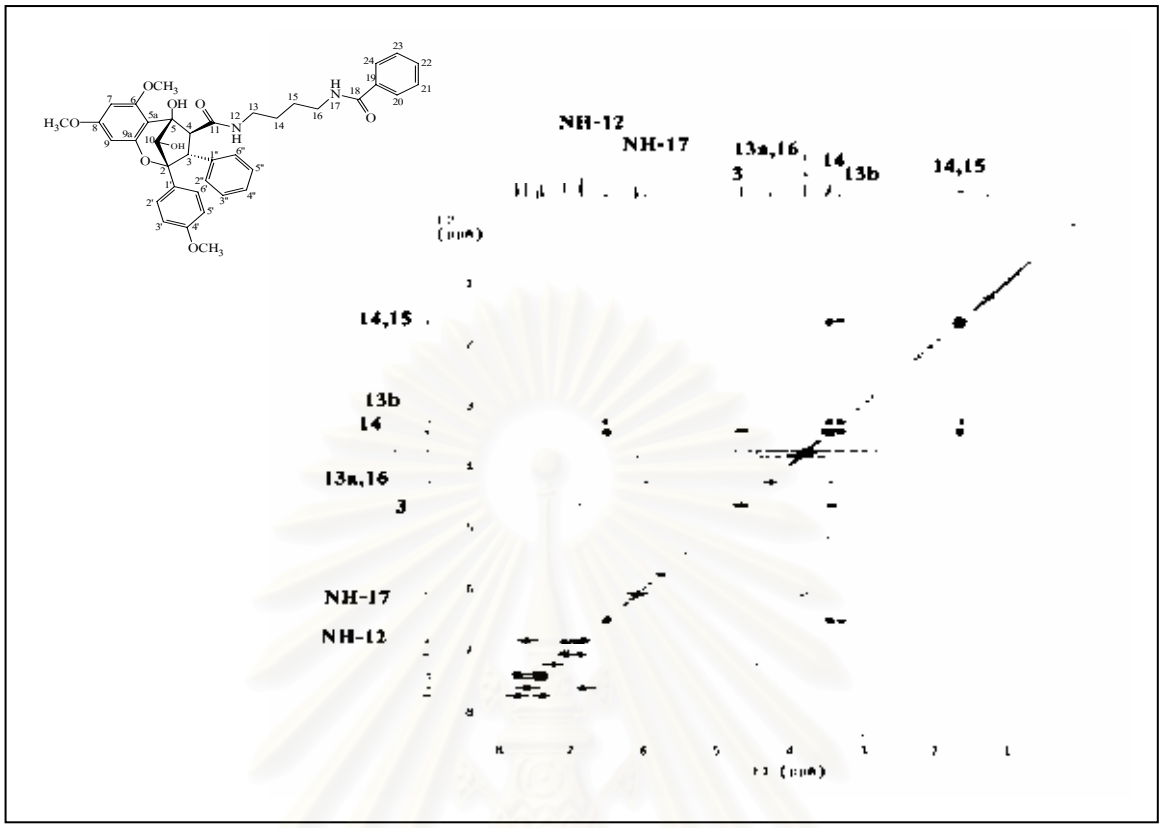

Figure 76. $^{1}H–^{1}H$ COSY Spectrum of compound CAF6 ($CDCl_3$) [δ_H 1.6-6.6 ppm]

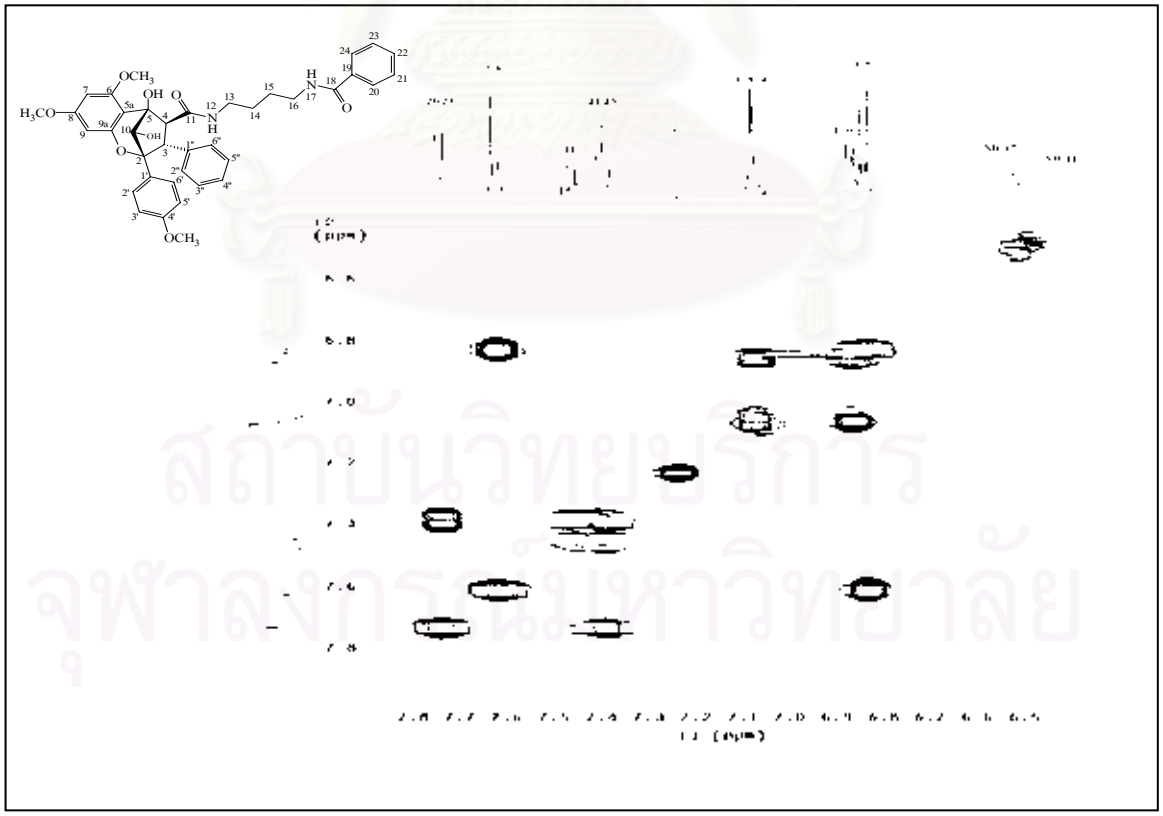

Figure 77. $^{1}H–^{1}H$ COSY Spectrum of compound CAF6 ($CDCl_3$) [δ_H 6.4-7.8 ppm]

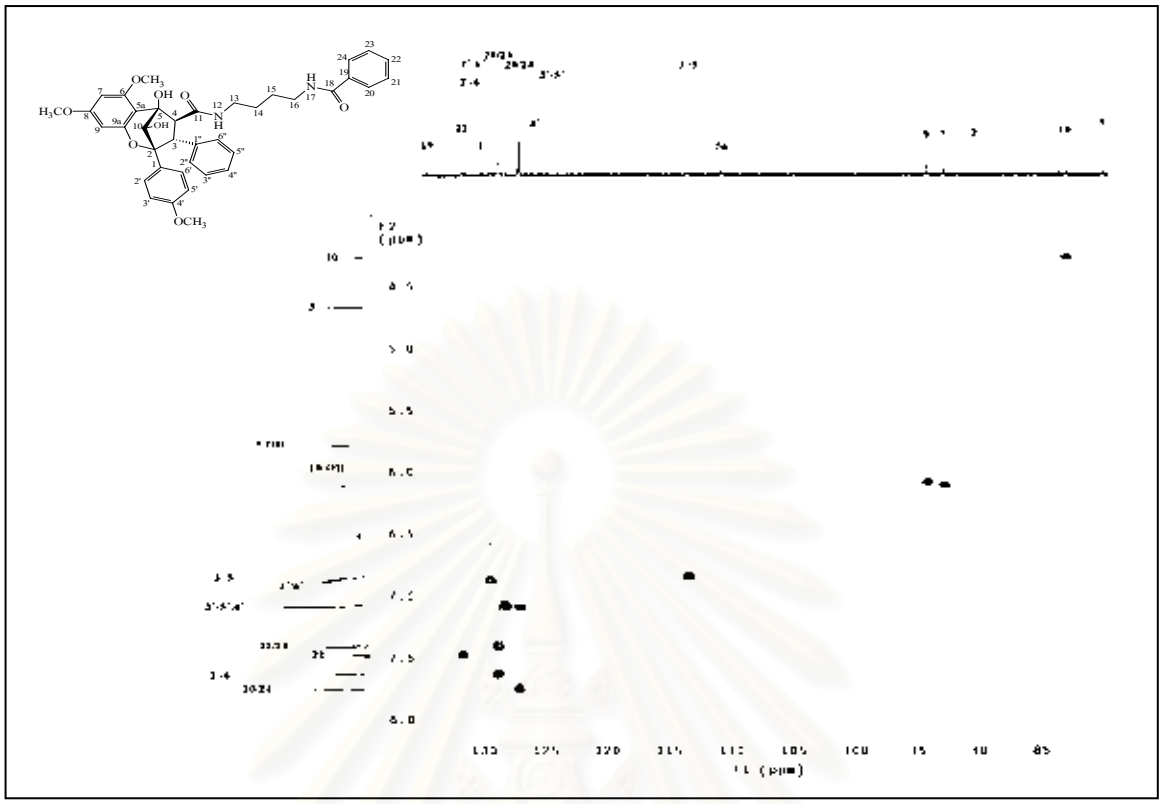

Figure 78. HSQC Spectrum of compound CAF6 ($CDCl_3$) [δ_H 4.0-8.0 ppm, δ_C 80-135 ppm]

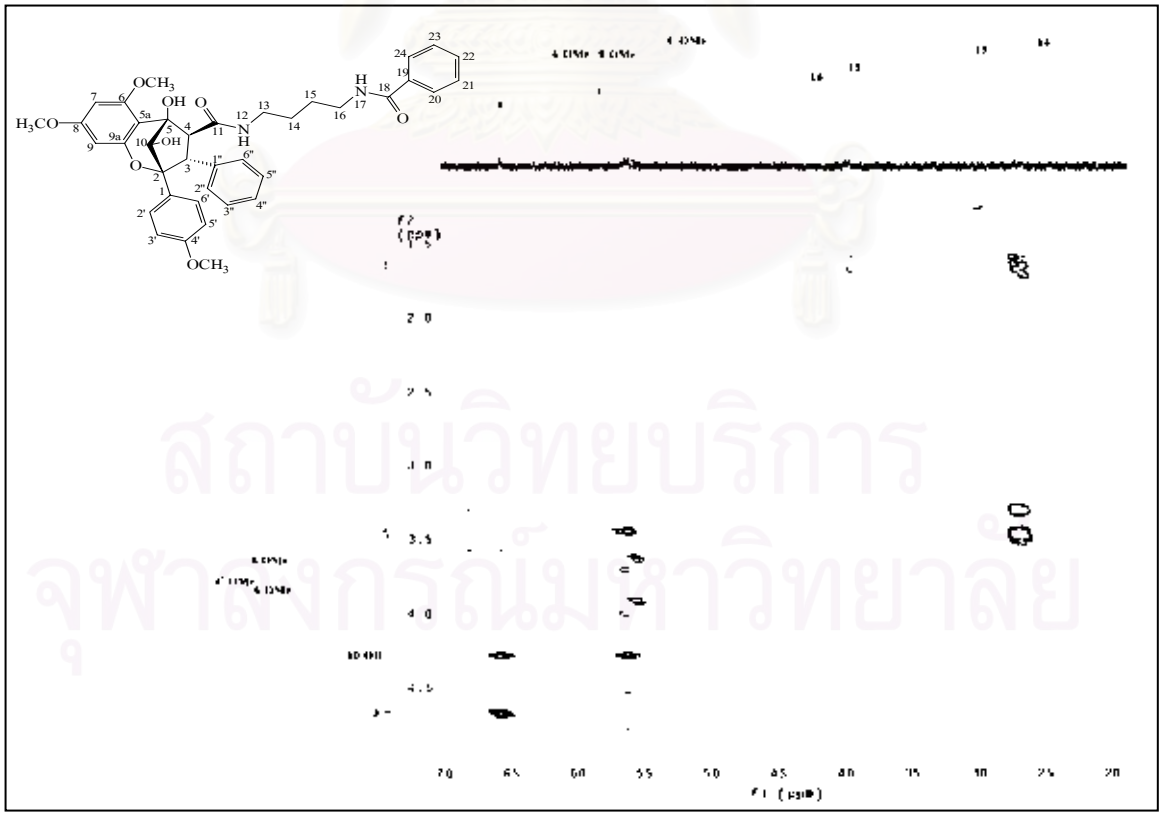

Figure 79. HMBC Spectrum of compound CAF6 ($CDCl_3$) [δ_H 1.5-5.0 ppm, δ_C 20-70 ppm]

สถาบันวิทยบริการ
จุฬาลงกรณ์มหาวิทยาลัย

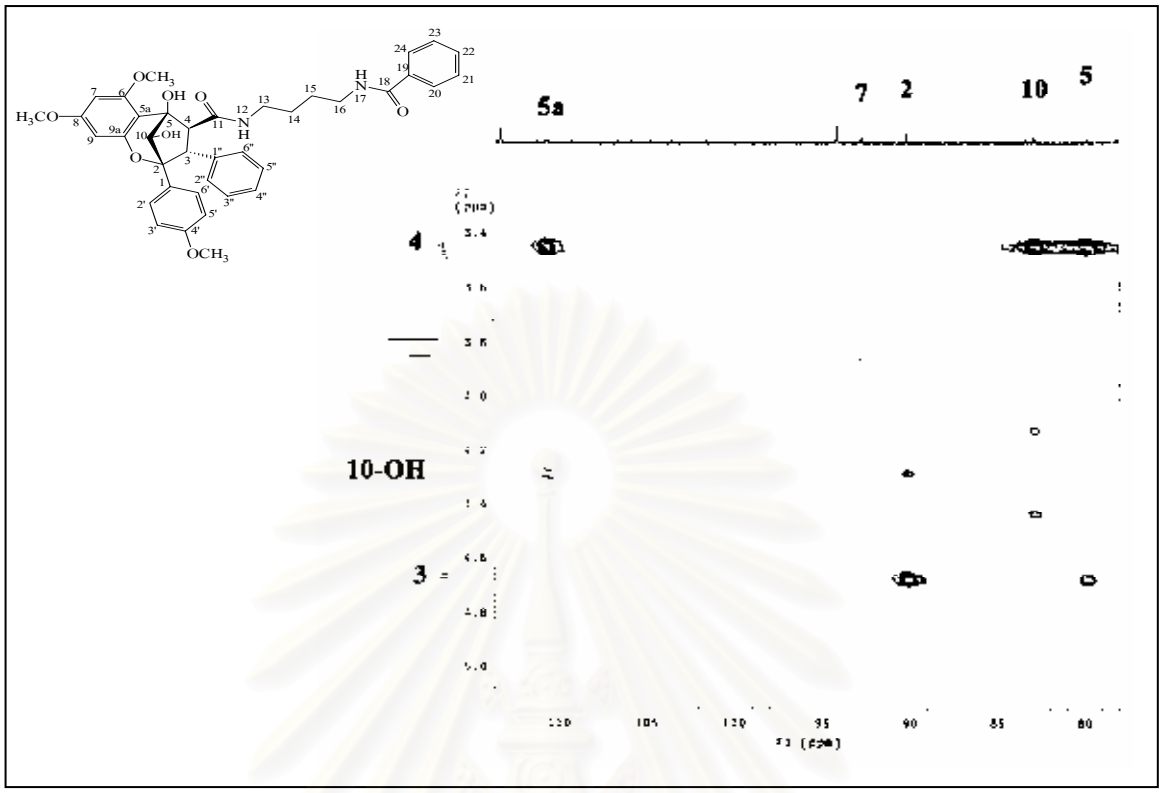

Figure 80. HMBC Spectrum of compound CAF6 ($CDCl_3$) [δ_H 3.2-5.0 ppm, δ_C 76-115 ppm]

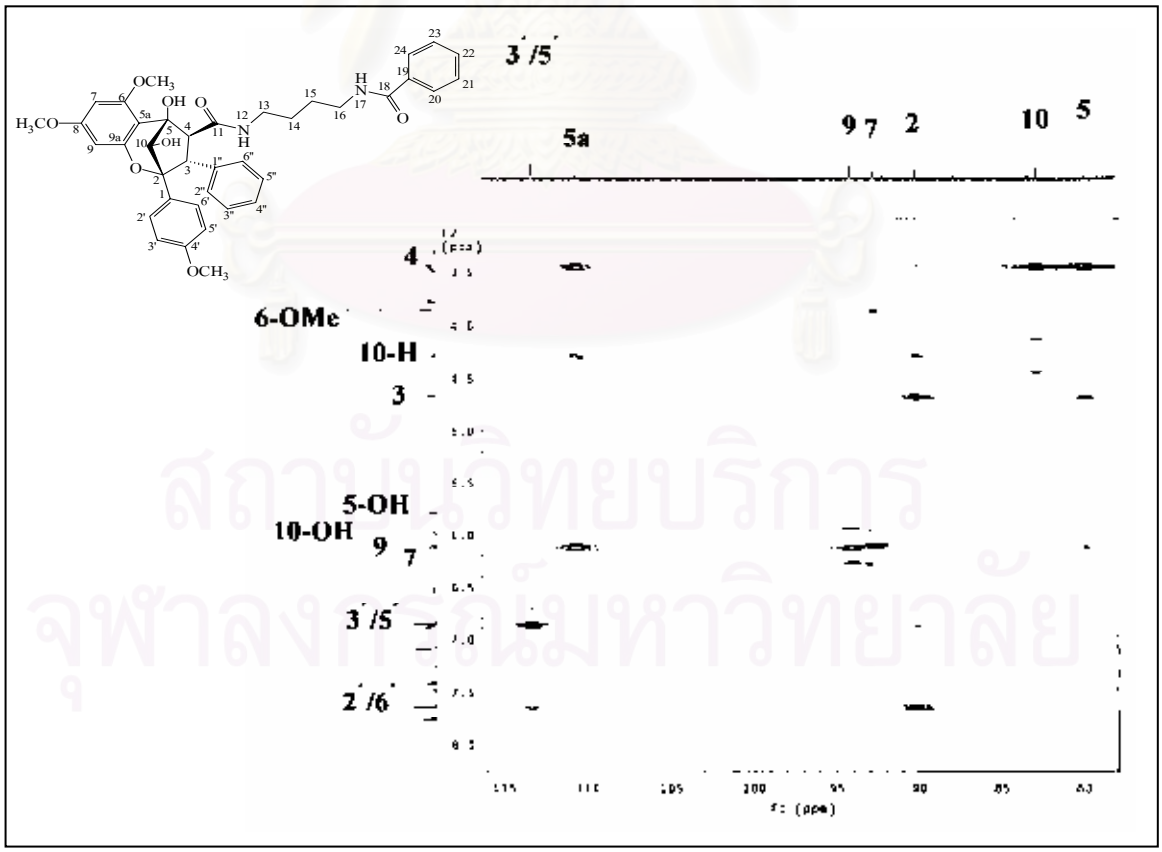

Figure 81. HMBC Spectrum of compound CAF6 ($CDCl_3$) [δ_H 3.0-8.0 ppm, δ_C 76-115 ppm]

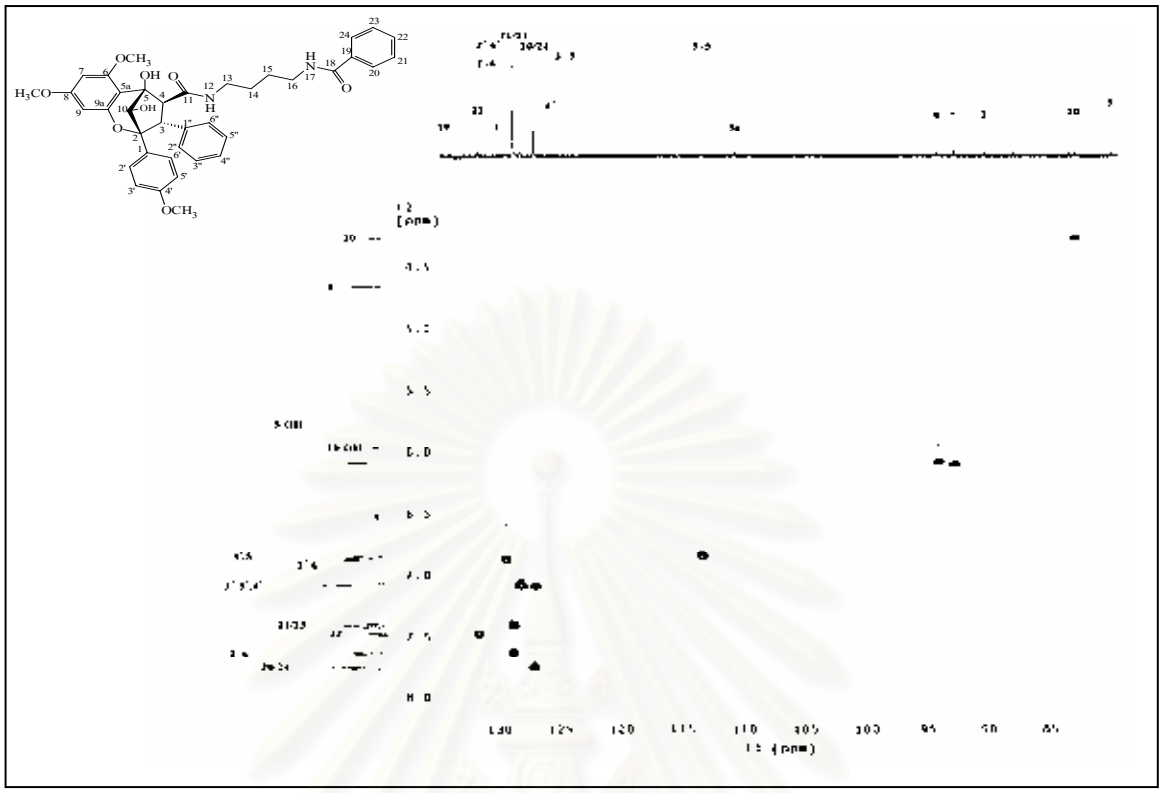

Figure 82. HMBC Spectrum of compound CAF6 ($CDCl_3$) [δ_H 4.0-8.0 ppm, δ_C 80-135 ppm]

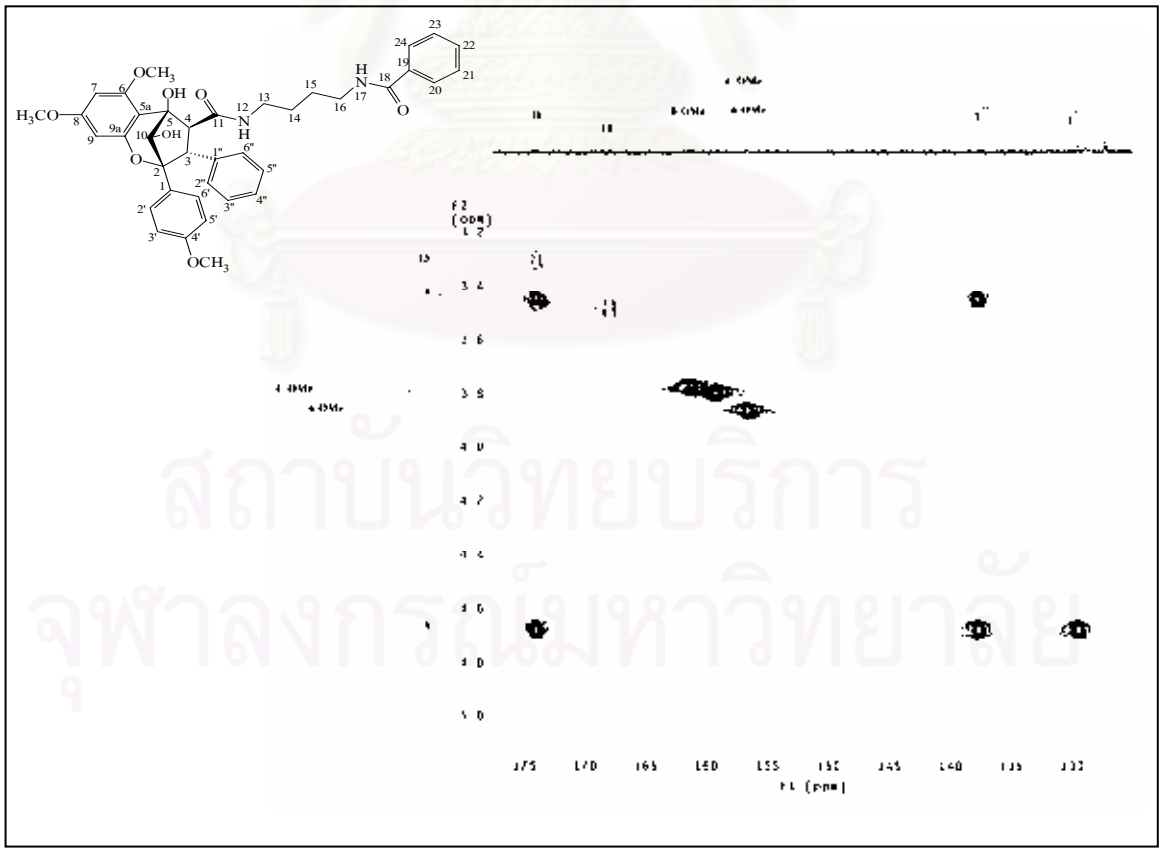

Figure 83. HMBC Spectrum of compound CAF6 ($CDCl_3$) [δ_H 3.2-5.0 ppm, δ_C 125-175 ppm]

สถาบันวิทยบริการ
จุฬาลงกรณ์มหาวิทยาลัย

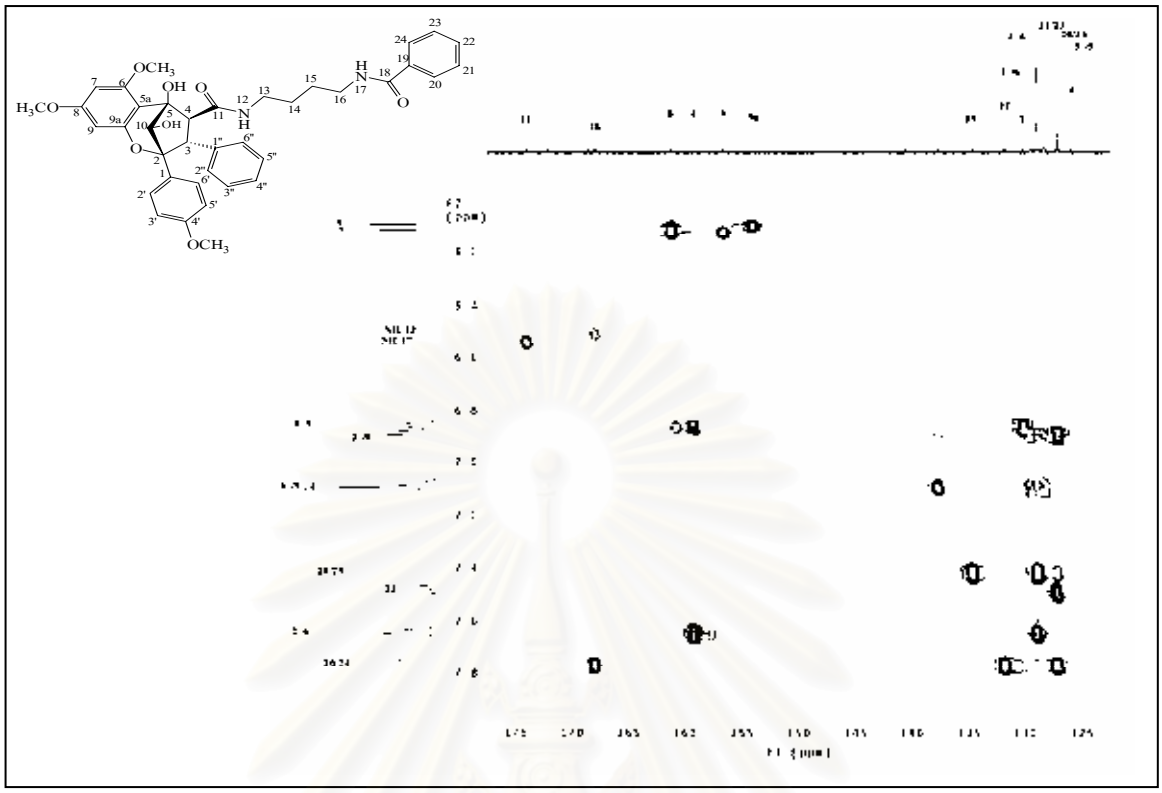

Figure 84. HMBC Spectrum of compound CAF6 ($CDCl_3$) [δ_H 6.0-7.8 ppm, δ_C 125-175 ppm]

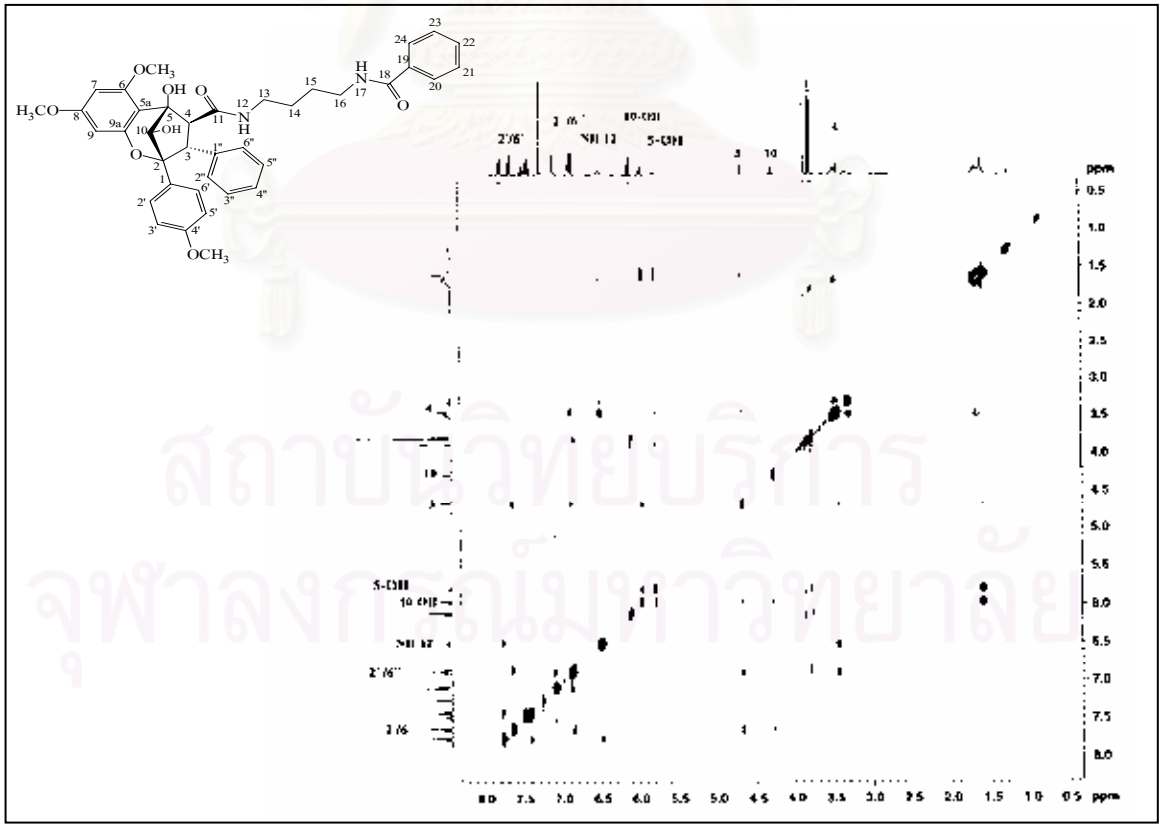

Figure 85. NOESY Spectrum of compound CAF6 ($CDCl_3$)

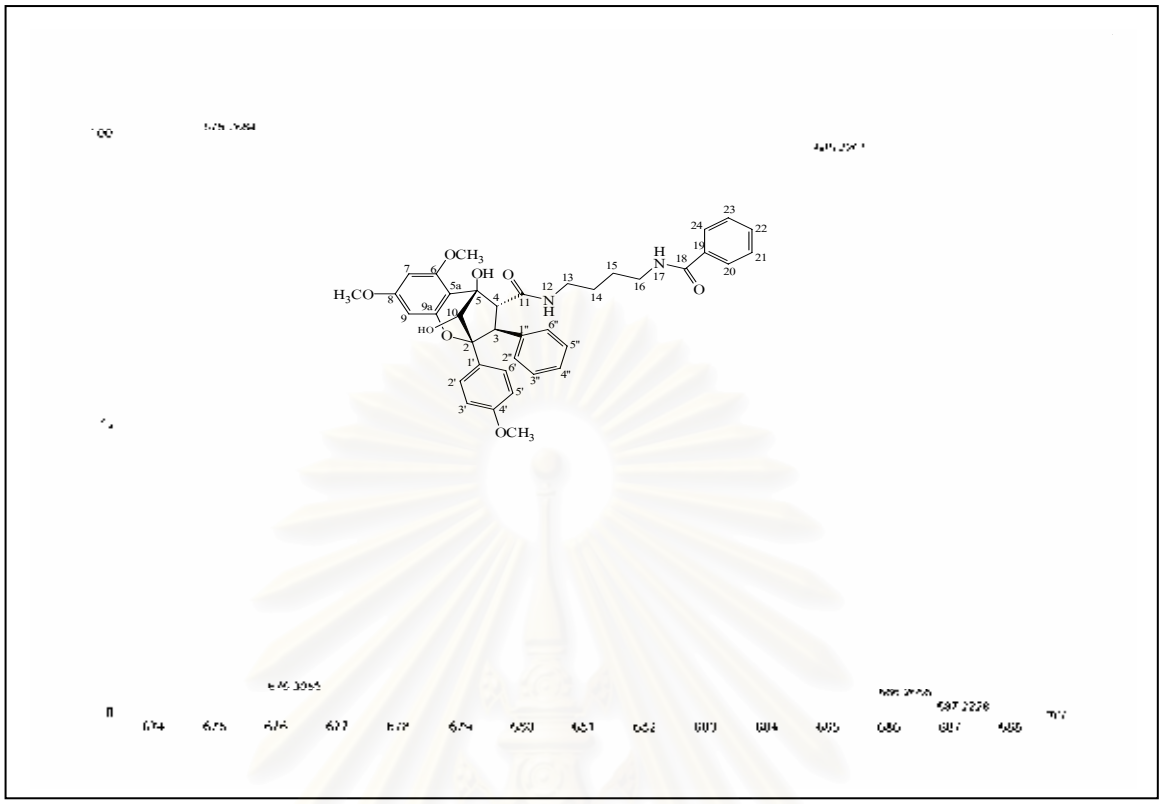

Figure 86. HRESI-TOF Mass spectrum of compound CAF7

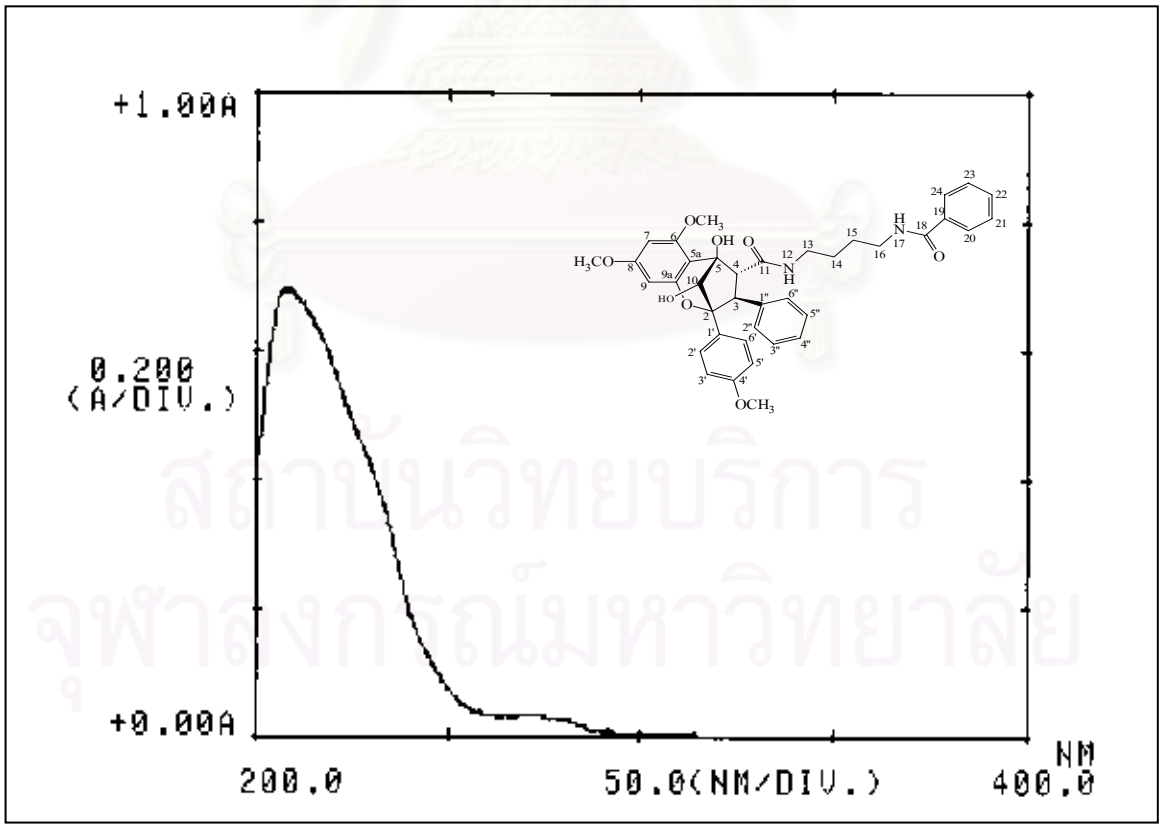

Figure 87. UV Spectrum of compound CAF7

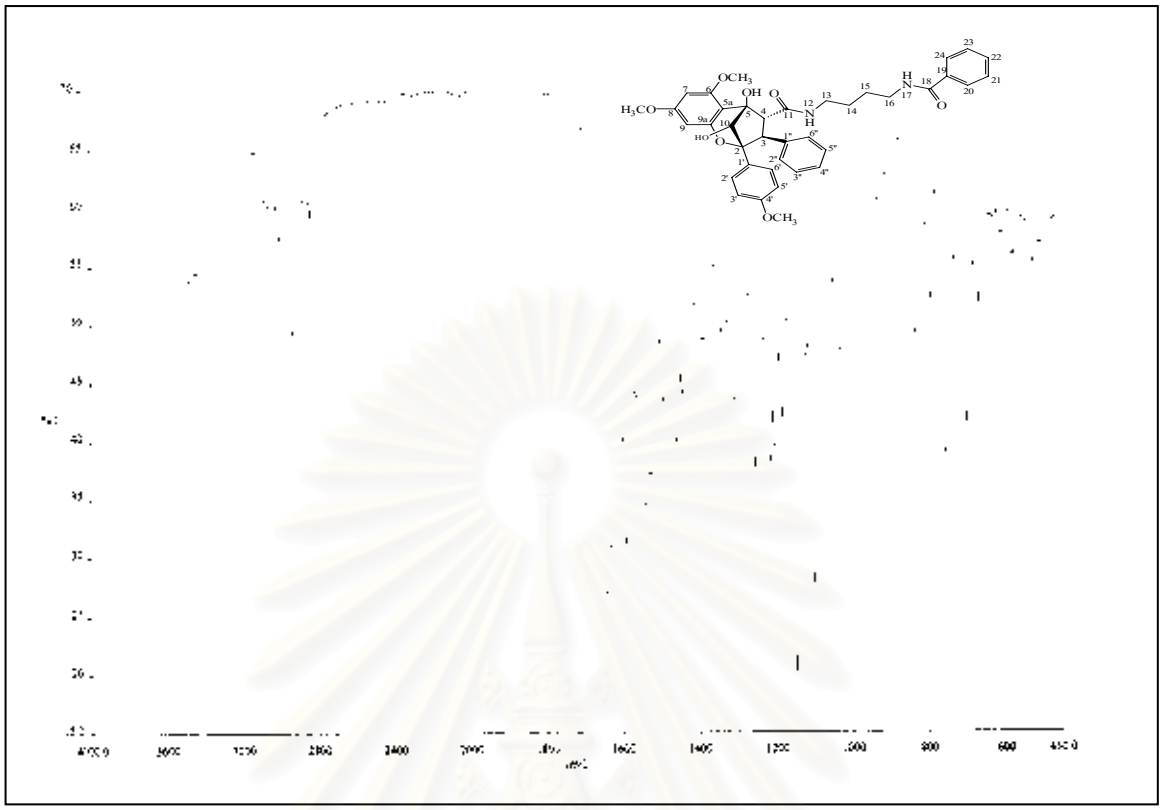

Figure 88. IR Spectrum of compound CAF7 (KBr disc)

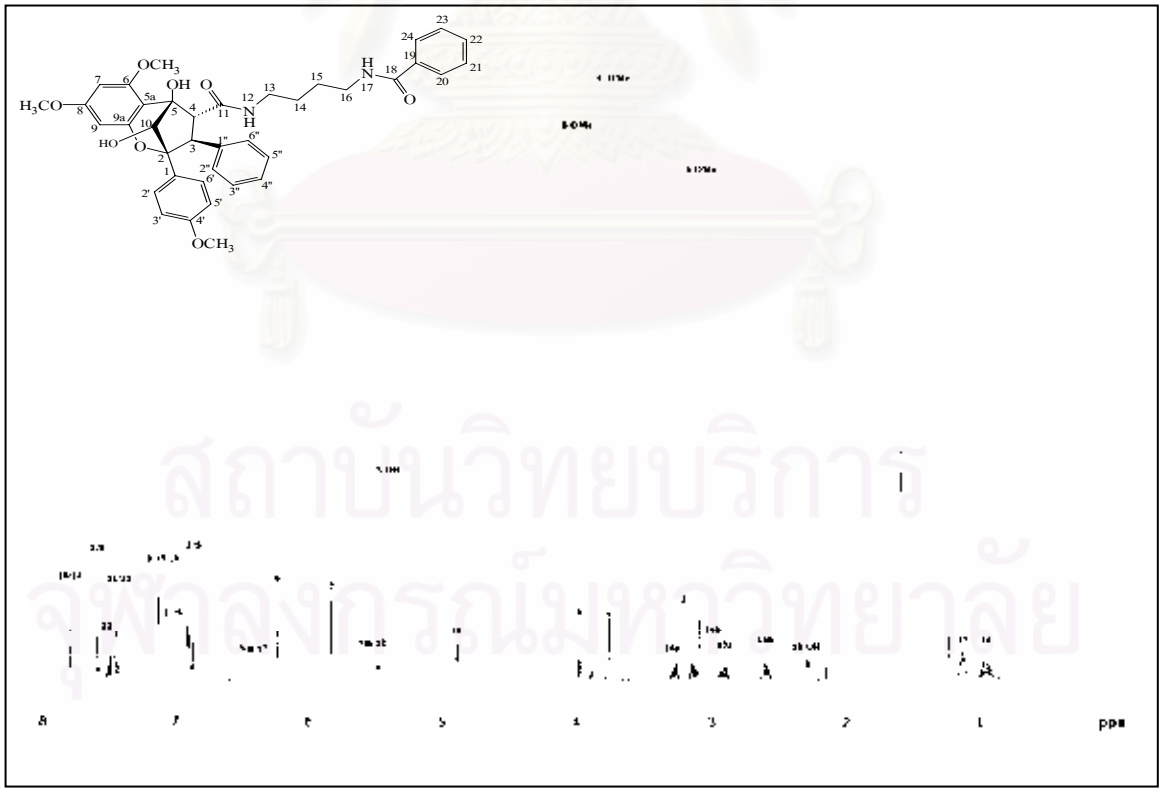

Figure 89. ^{1}H NMR (500 MHz) Spectrum of compound CAF7 ($CDCl_3$)

สถาบันวิทยบริการ
จุฬาลงกรณ์มหาวิทยาลัย

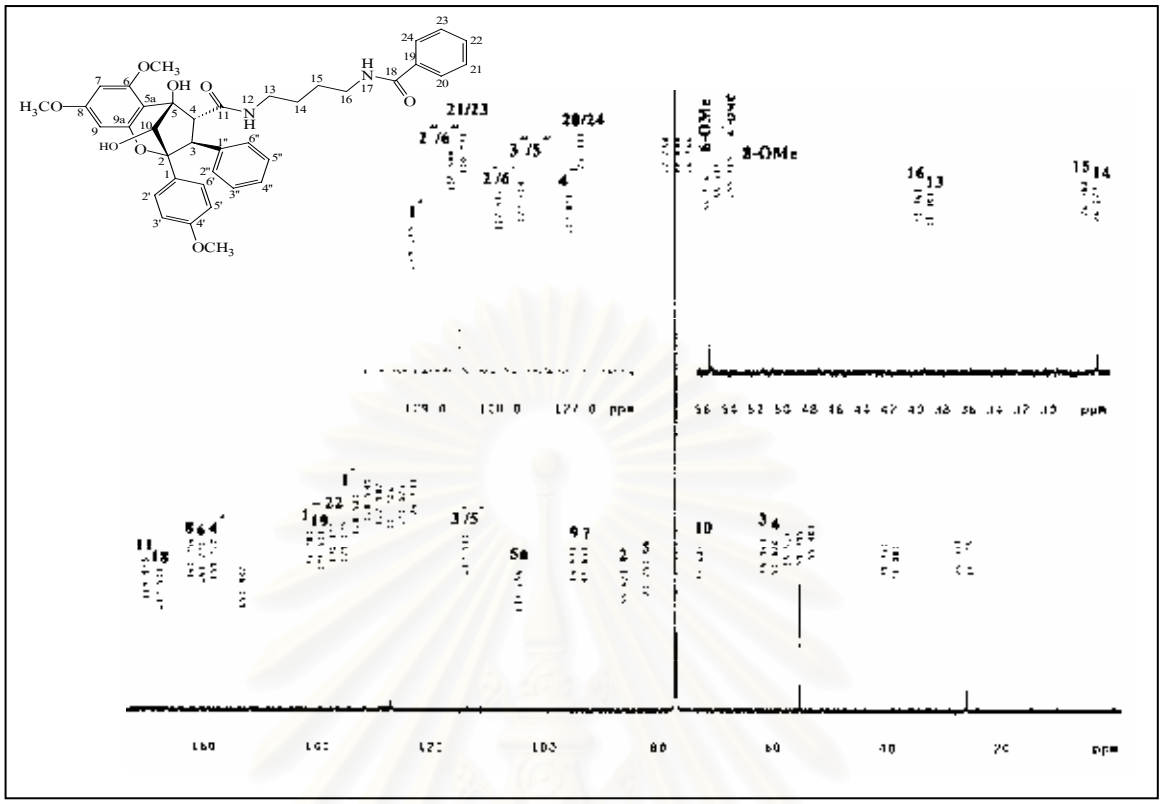

Figure 90. ^{13}C NMR (125 MHz) Spectrum of compound CAF7 ($CDCl_3$)

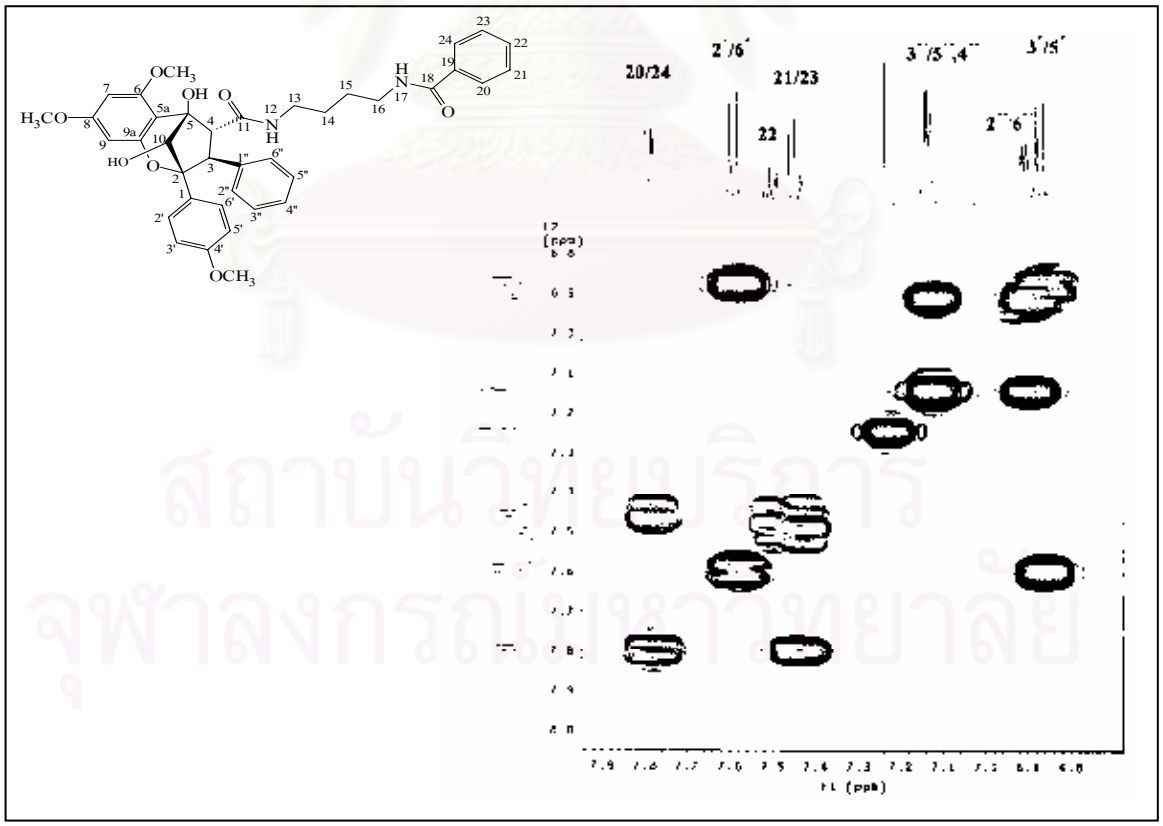

Figure 91. ^{1}H–^{1}H COSY Spectrum of compound CAF7 ($CDCl_3$) [δ_H 6.7-7.9 ppm]

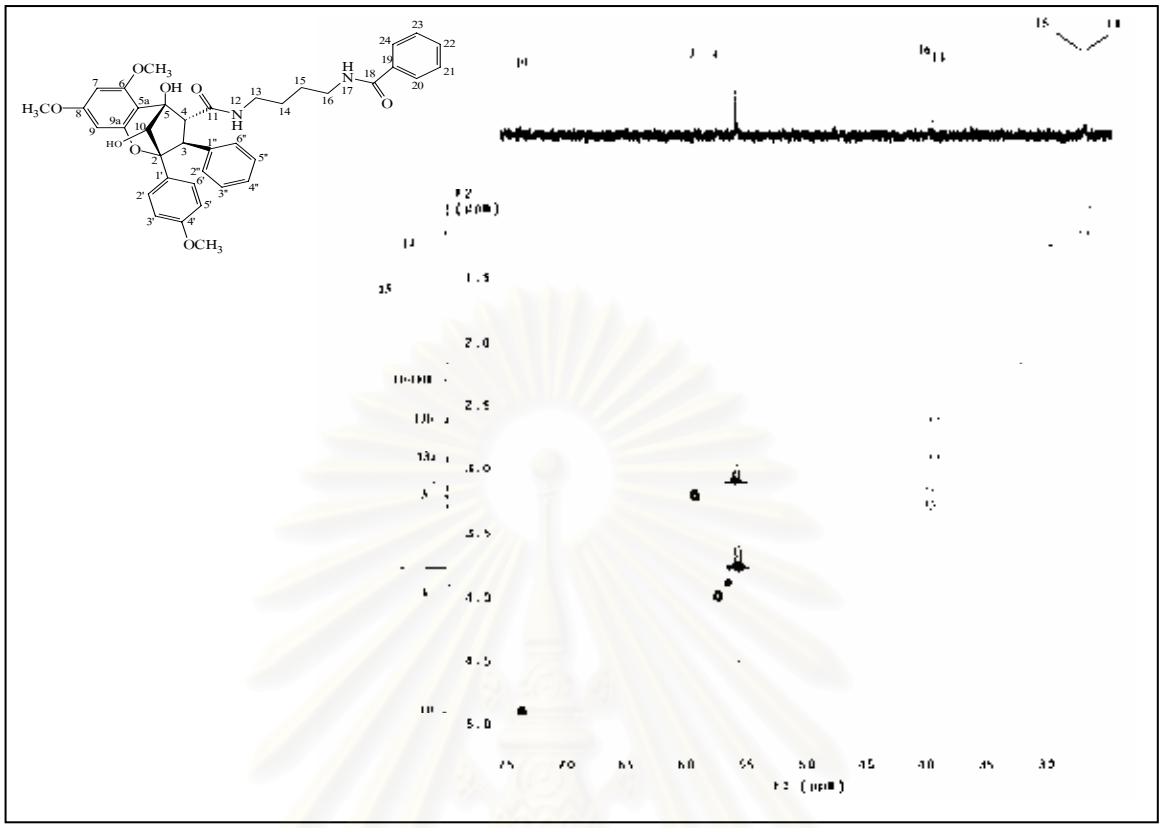

Figure 92. HSQC Spectrum of compound CAF7 ($CDCl_3$) [δ_H 1.0-5.0 ppm, δ_C 25-75 ppm]

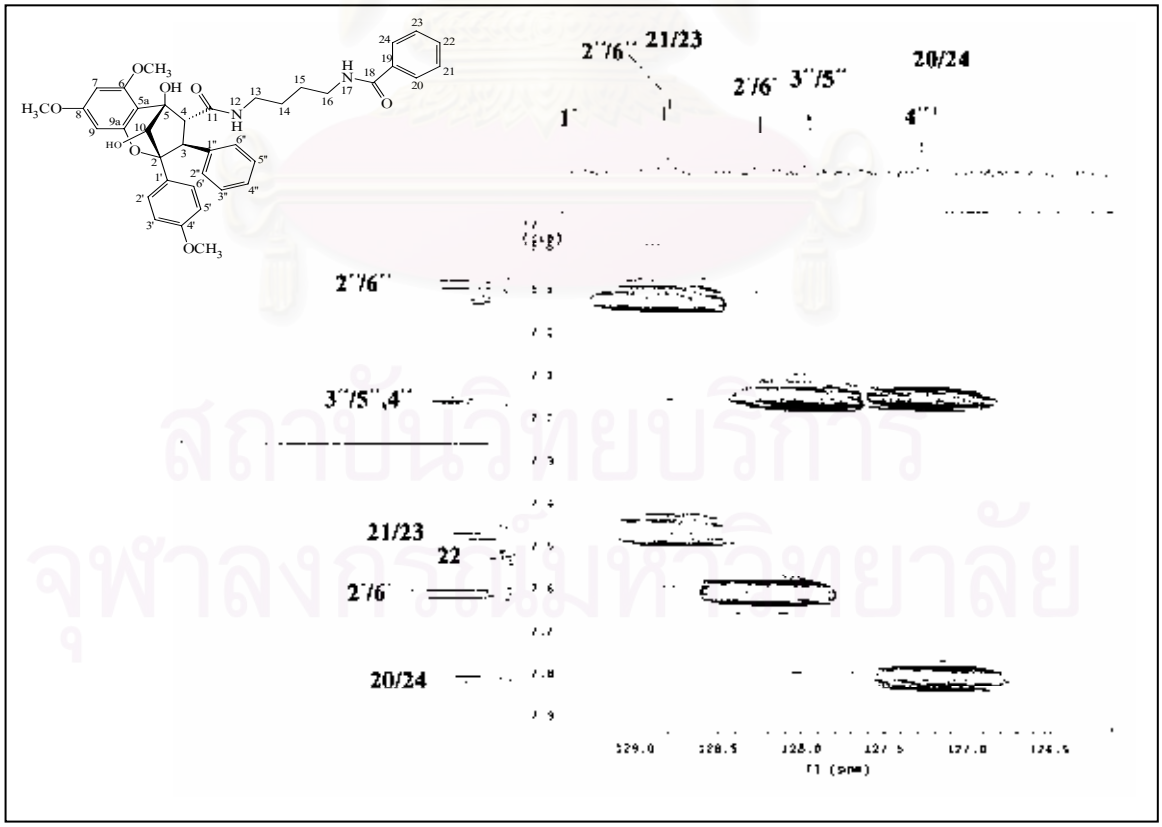

Figure 93. HSQC Spectrum of compound CAF7 ($CDCl_3$) [δ_H 6.8-7.9 ppm, δ_C 125-130 ppm]

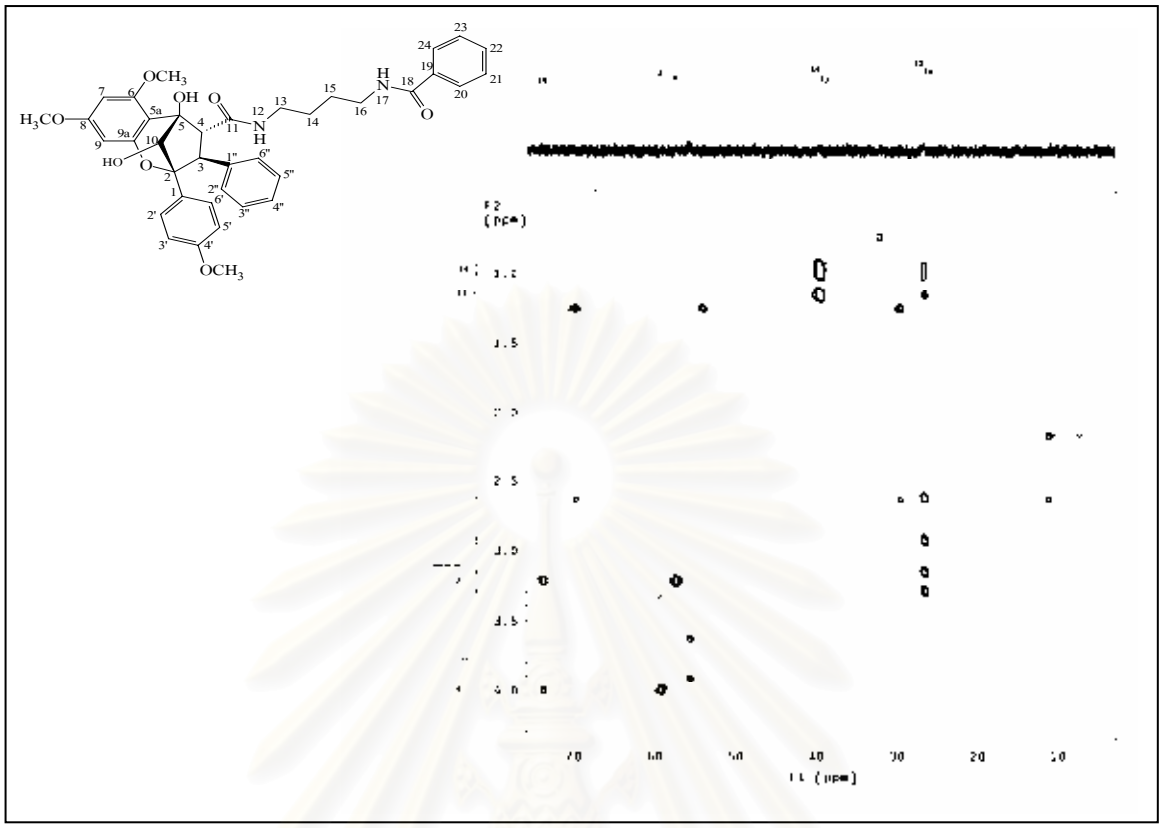

Figure 94. HMBC Spectrum of compound CAF7 ($CDCl_3$) [δ_H 0.9-4.0 ppm, δ_C 10-76 ppm]

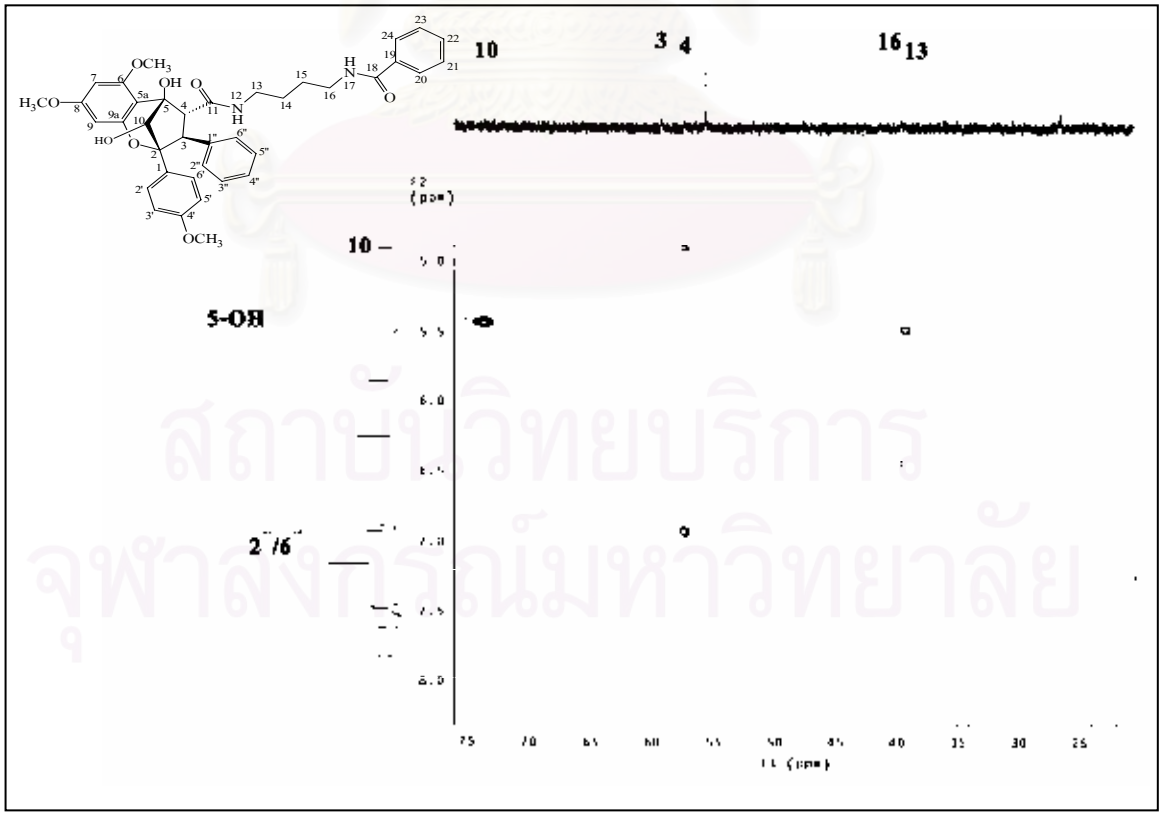

Figure 95. HMBC Spectrum of compound CAF7 ($CDCl_3$) [δ_H 4.5-8.0 ppm, δ_C 25-75 ppm]

สถาบันวิทยบริการ
จุฬาลงกรณ์มหาวิทยาลัย

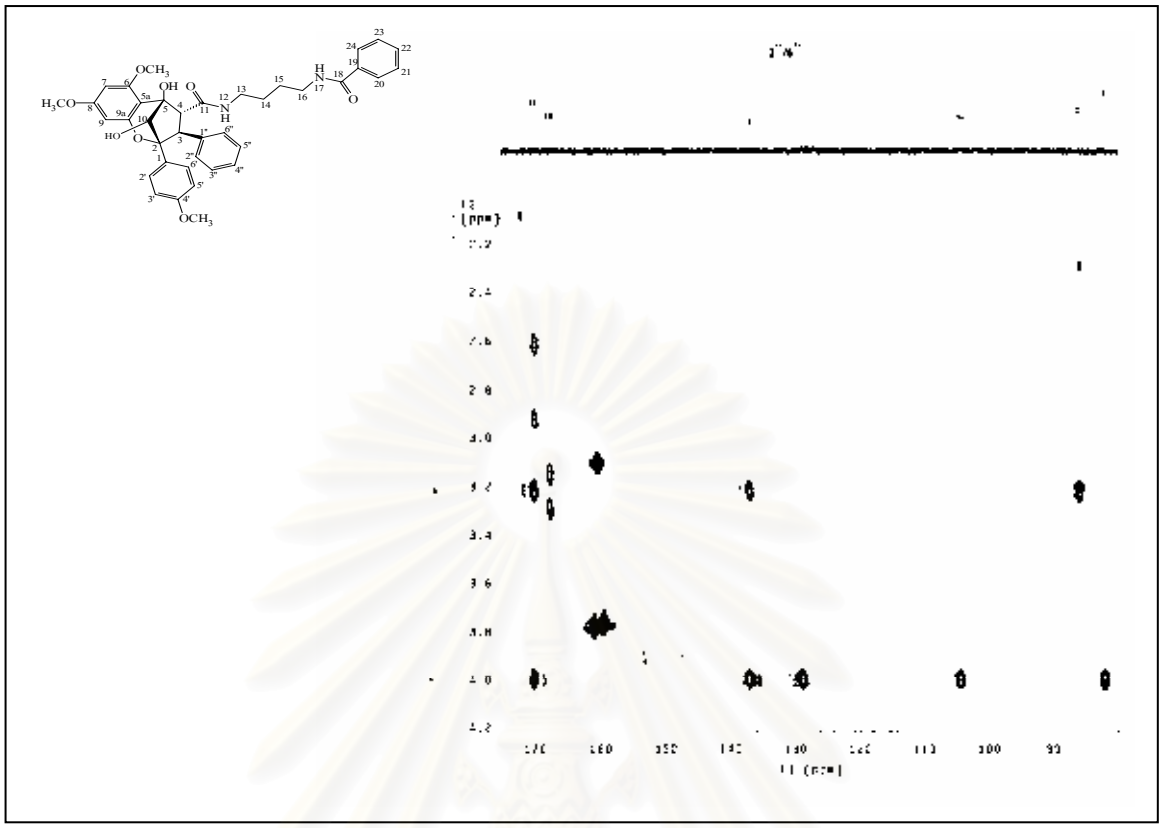

Figure 96. HMBC Spectrum of compound CAF7 ($CDCl_3$) [δ_H 2.0-4.2 ppm, δ_C 80-176 ppm]

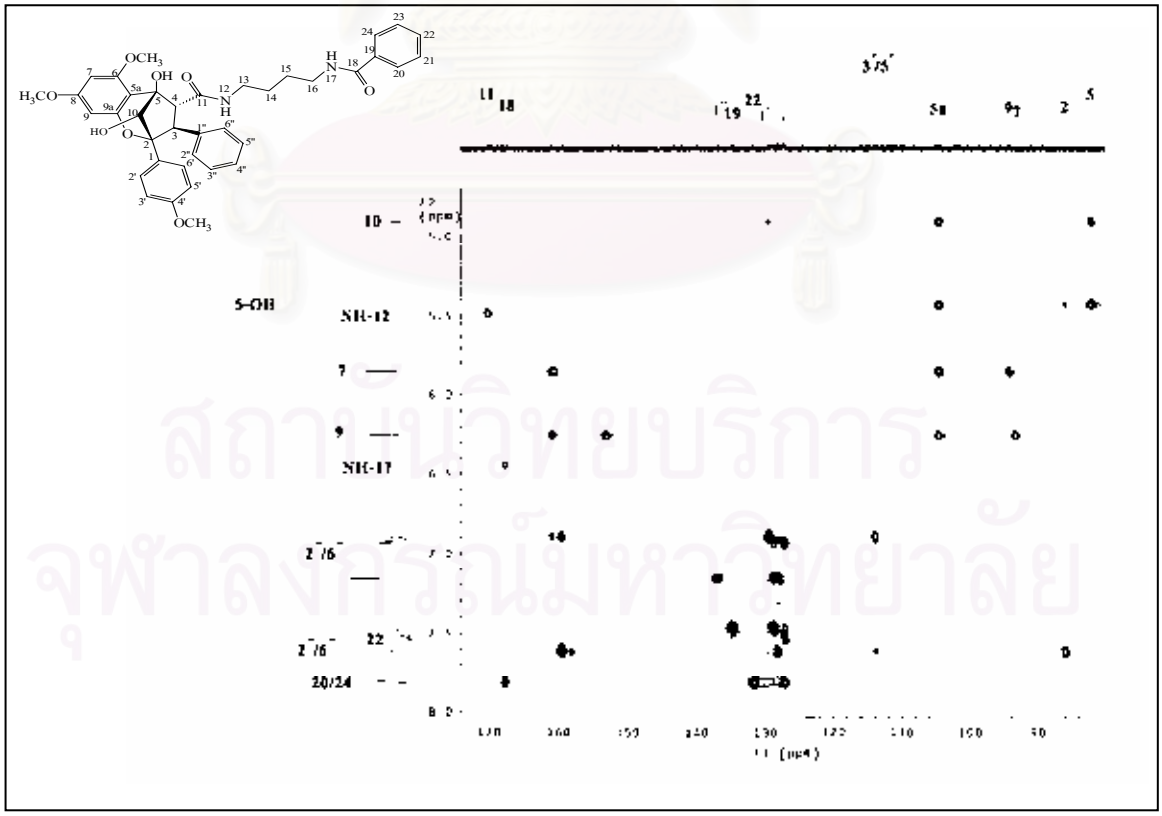

Figure 97. HMBC Spectrum of compound CAF7 ($CDCl_3$) [δ_H 4.6-8.0 ppm, δ_C 80-174 ppm]

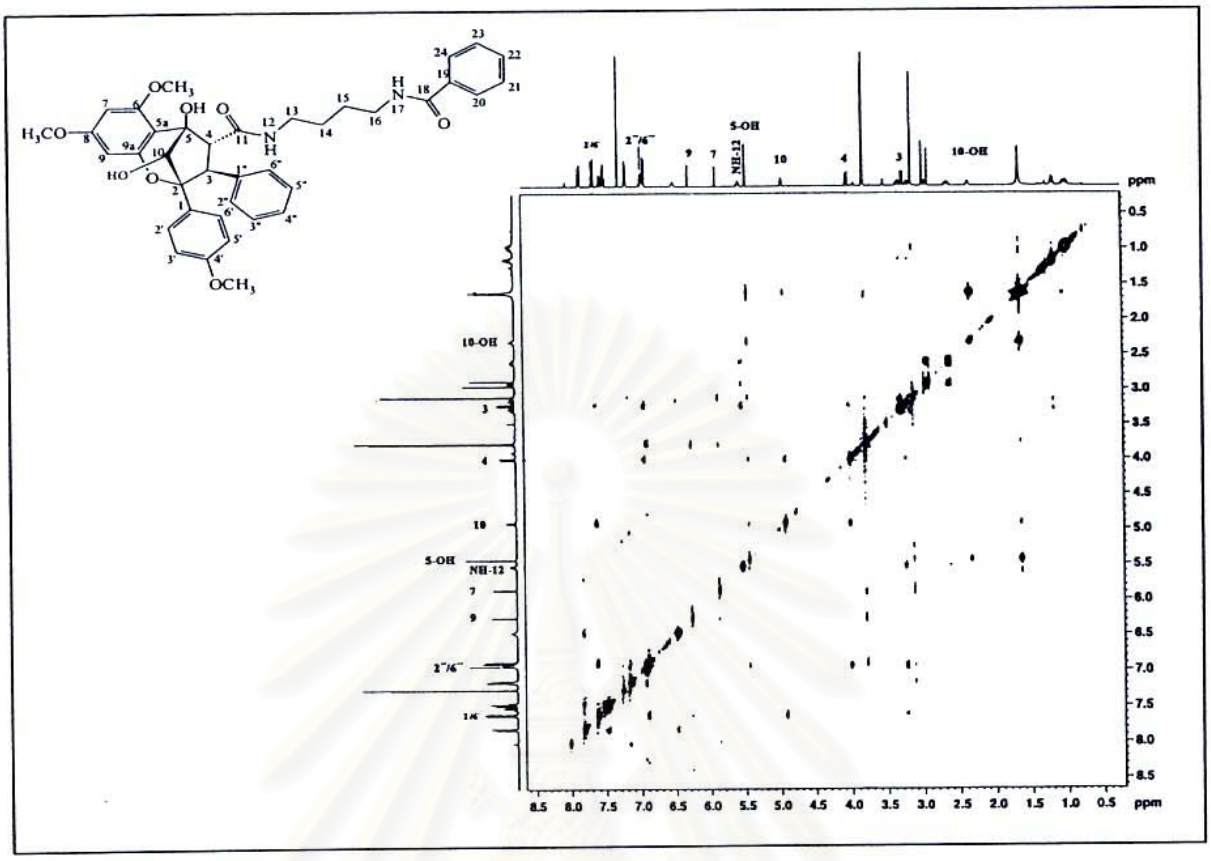

Figure 98. NOESY Spectrum of compound CAF7 ($CDCl_3$)

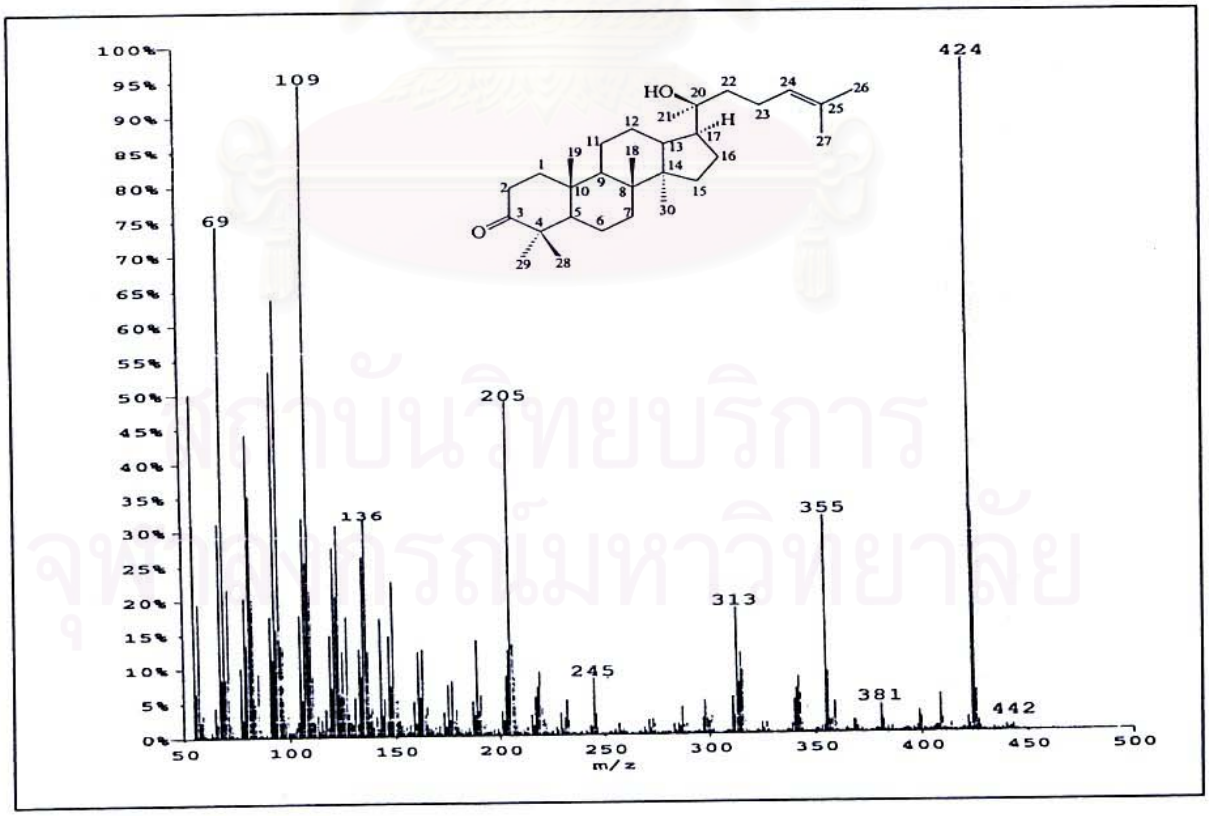

Figure 99. EI Mass spectrum of compound HAO1

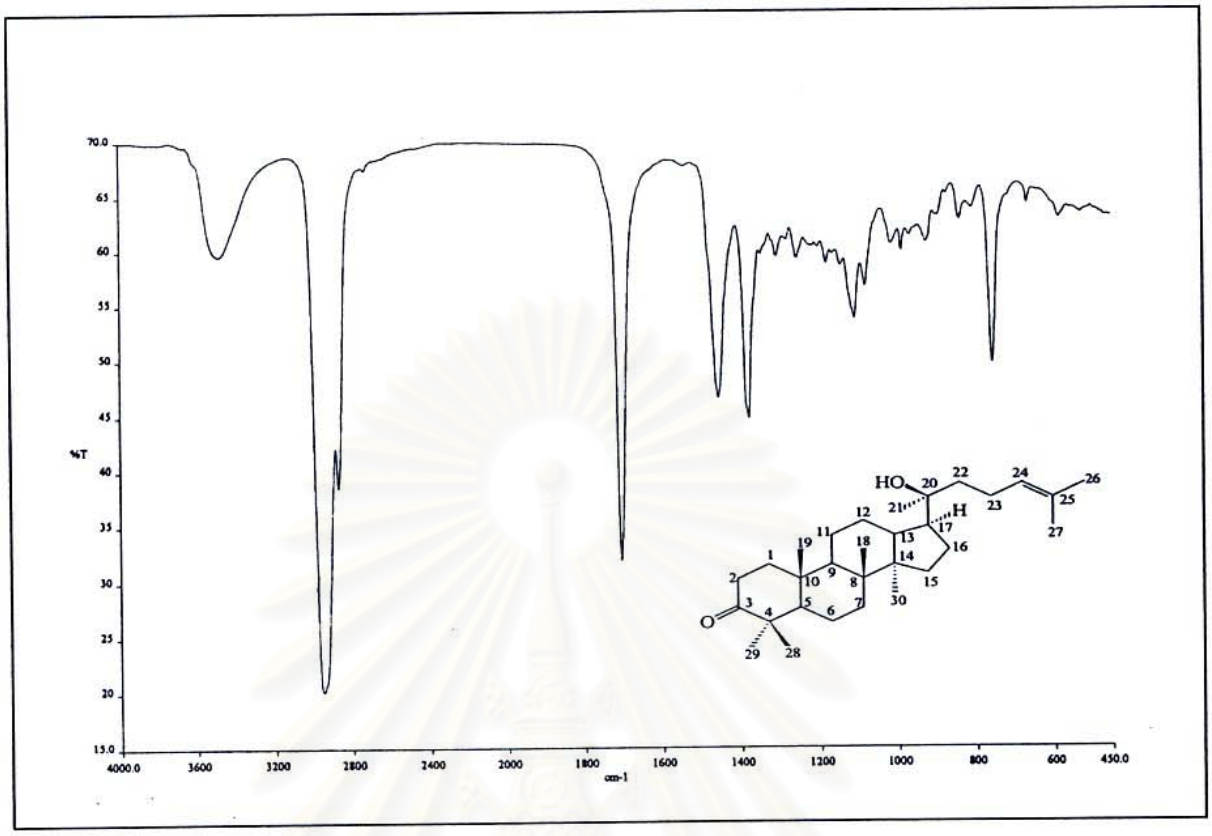

Figure 100. IR Spectrum of compound HAO1 (KBr disc)

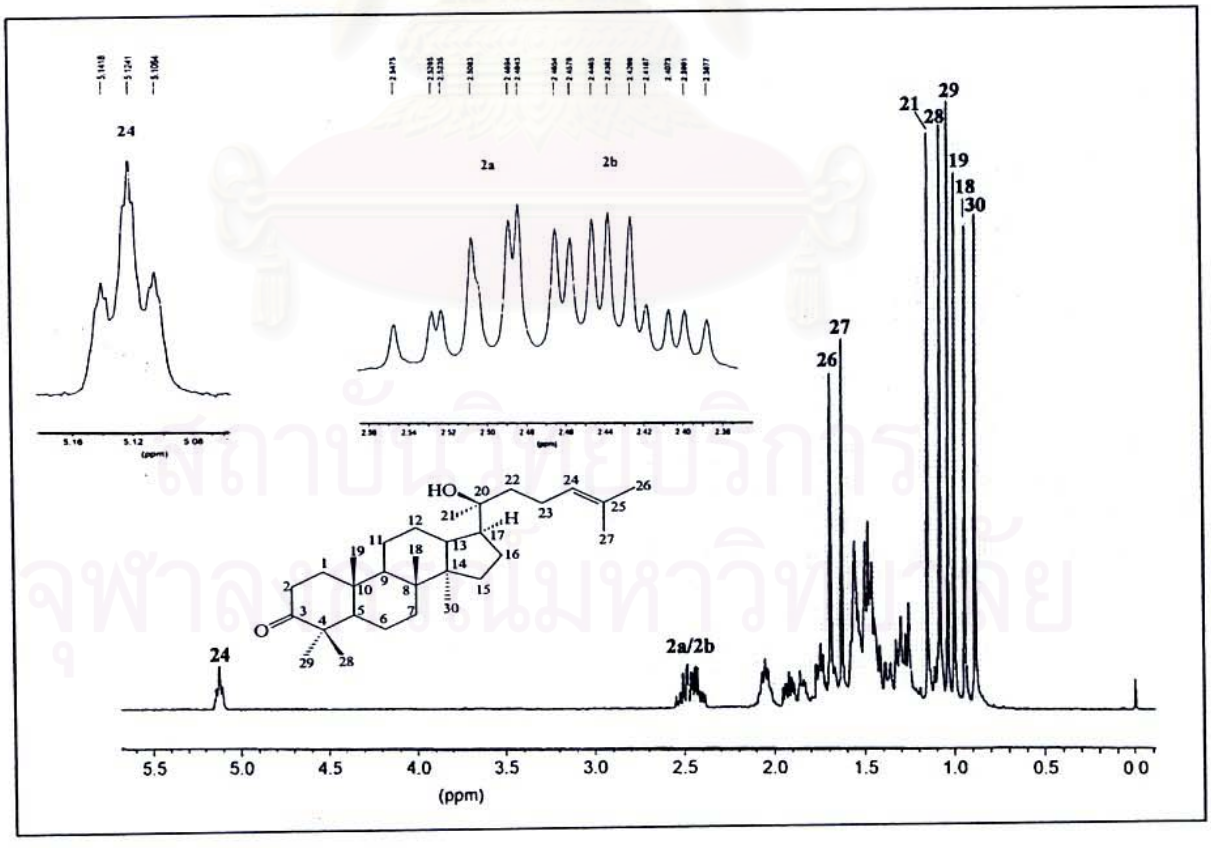

Figure 101. ^{1}H NMR (400 MHz) Spectrum of compound HAO1 ($CDCl_3$)

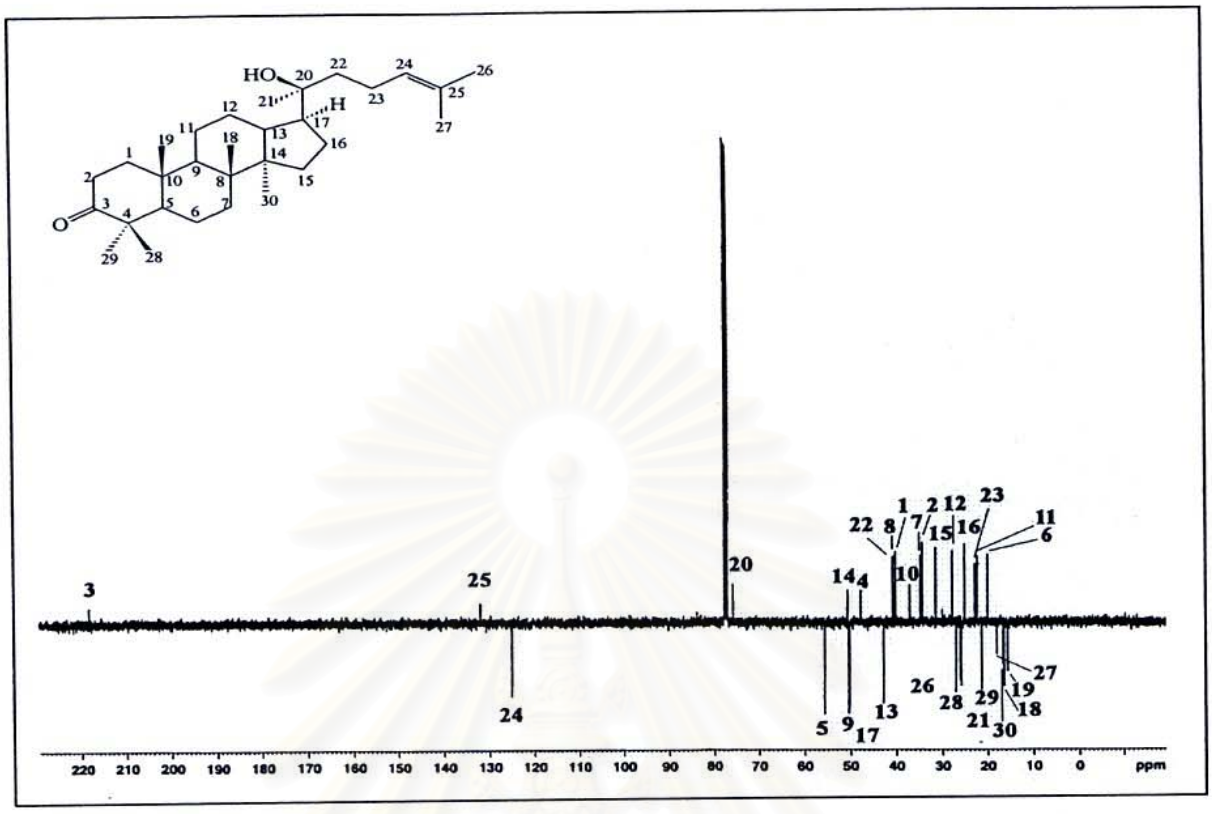

Figure 102. ^{13}C APT (100 MHz) Spectrum of compound HAO1 ($CDCl_3$)

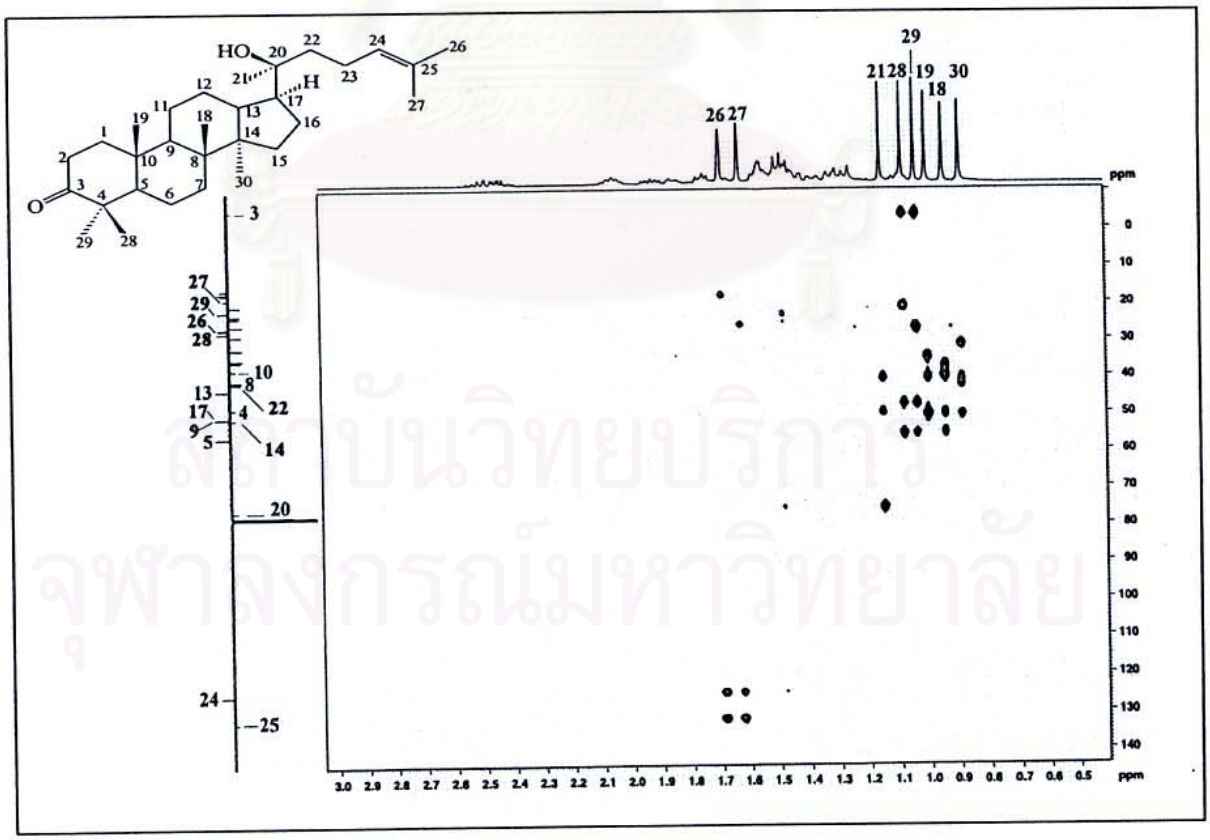

Figure 103. HMBC Spectrum of compound HAO1 ($CDCl_3$)

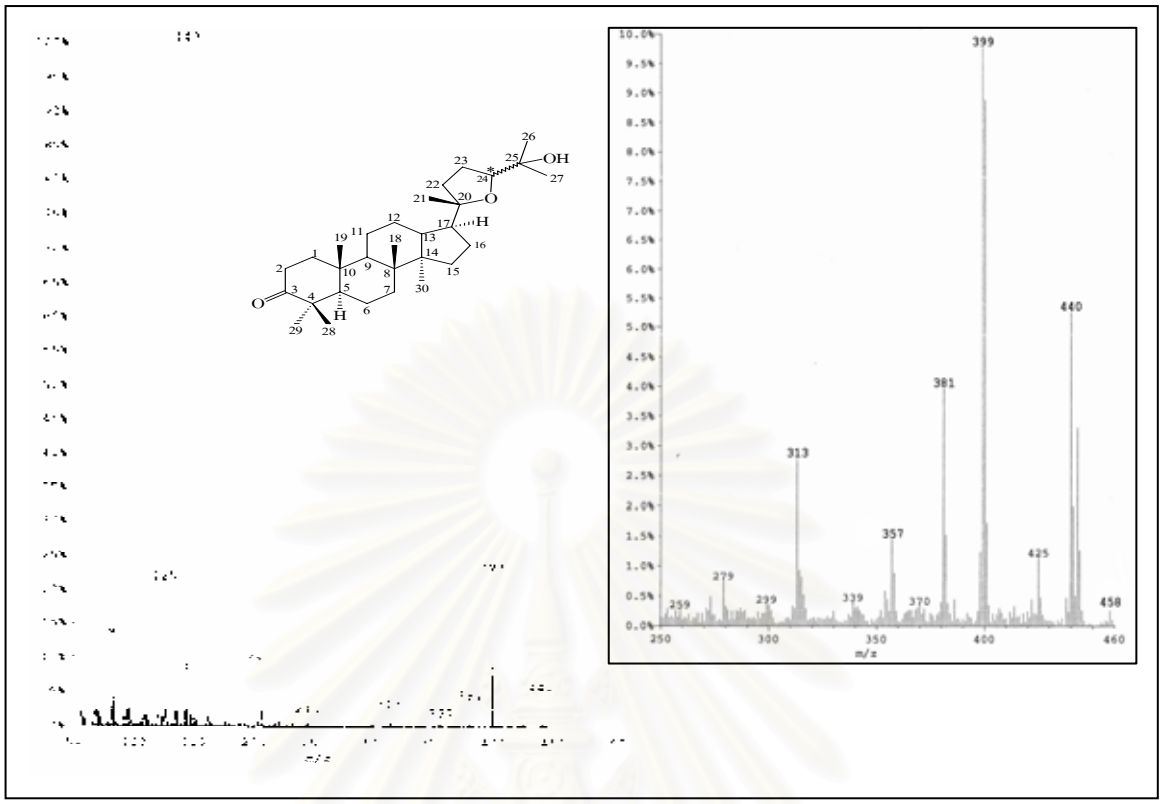

Figure 104. EI Mass spectrum of compound HAO2

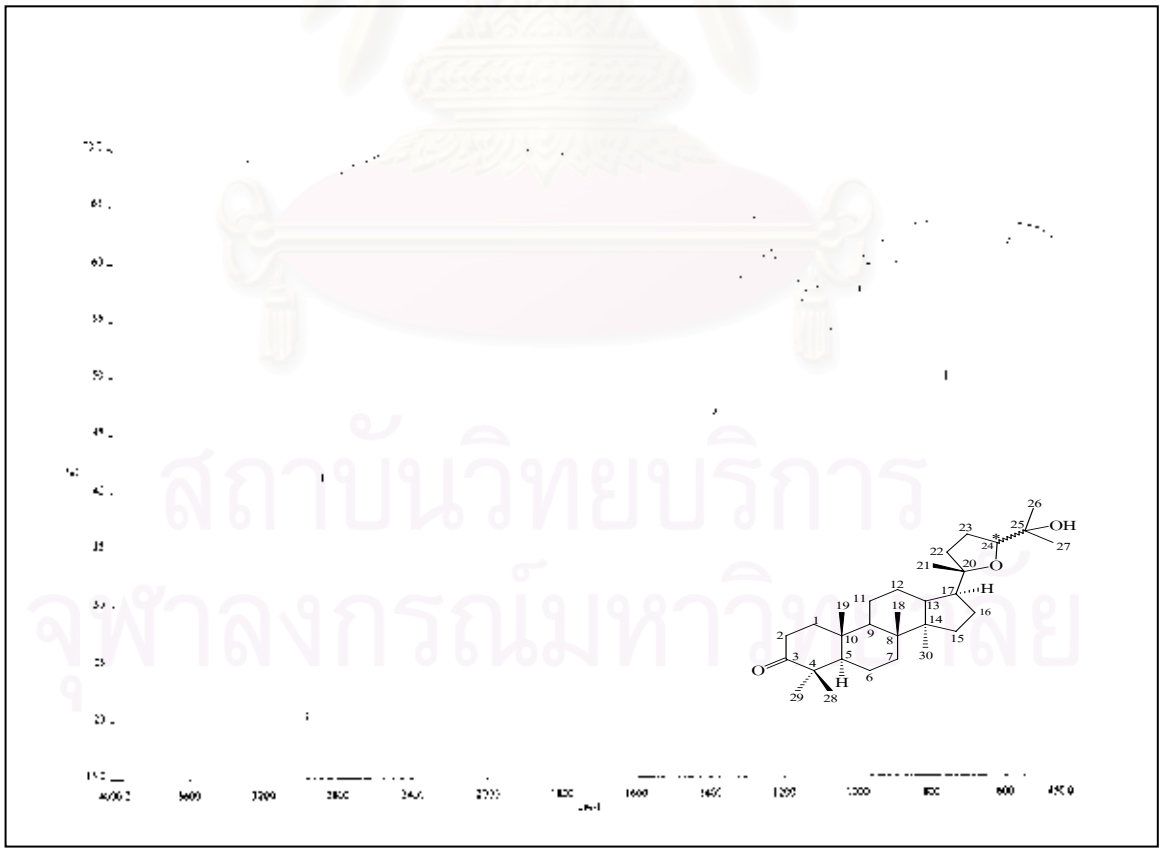

Figure 105. IR Spectrum of compound HAO2 (KBr disc)

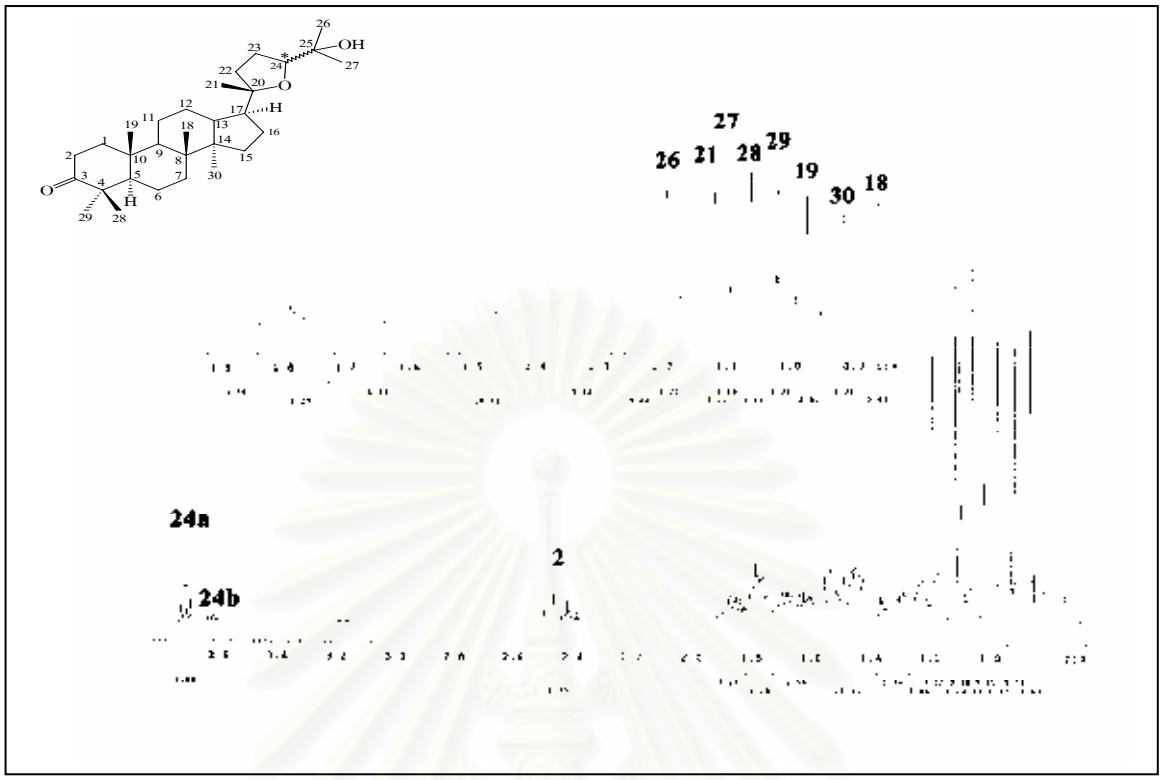

Figure 106. ^{1}H NMR (500 MHz) Spectrum of compound HAO2 ($CDCl_3$)

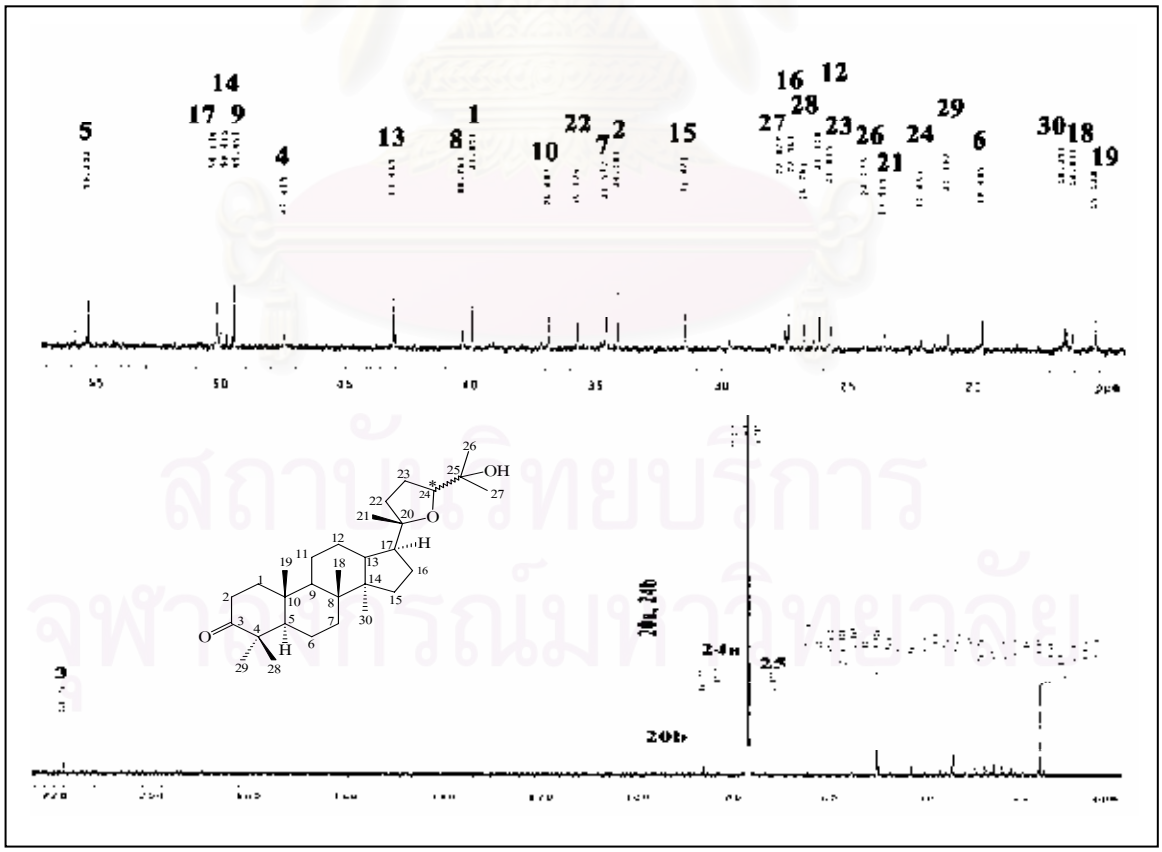

Figure 107. ^{13}C NMR (125 MHz) Spectrum of compound HAO2 ($CDCl_3$)

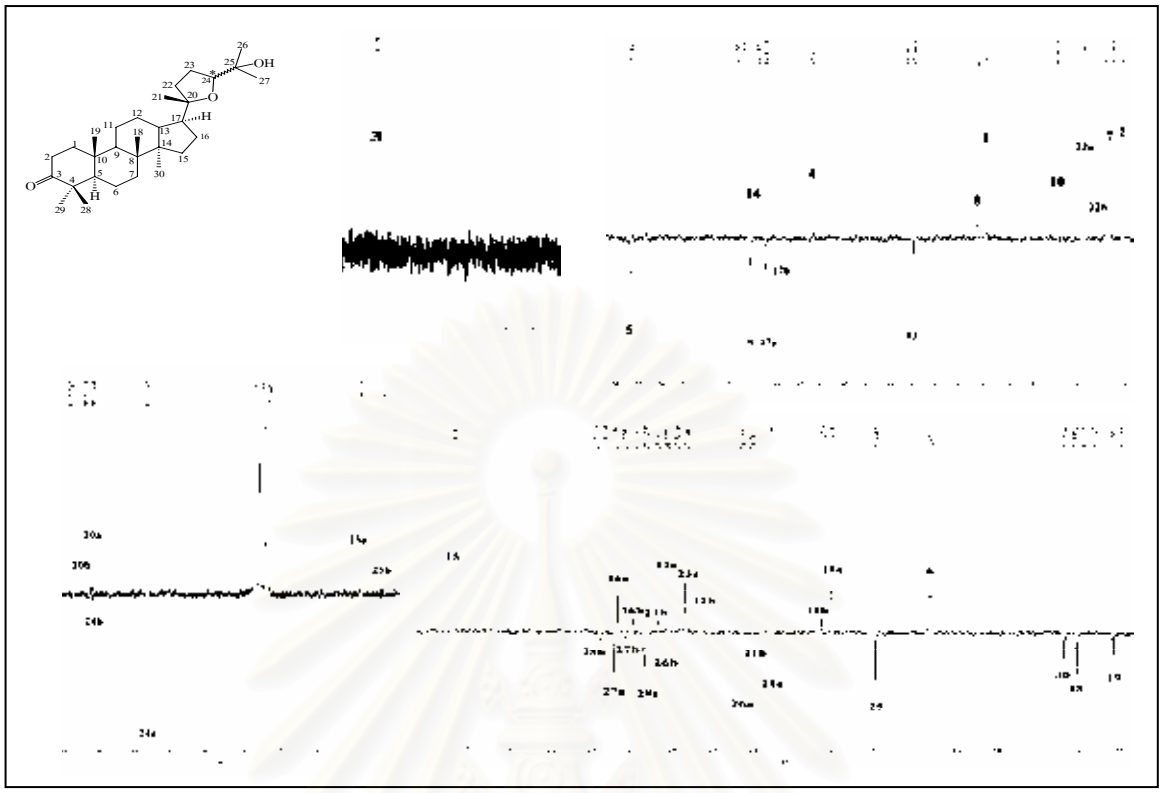

Figure 108. ^{13}C APT (100 MHz) Spectrum of compound HAO2 ($CDCl_3$)

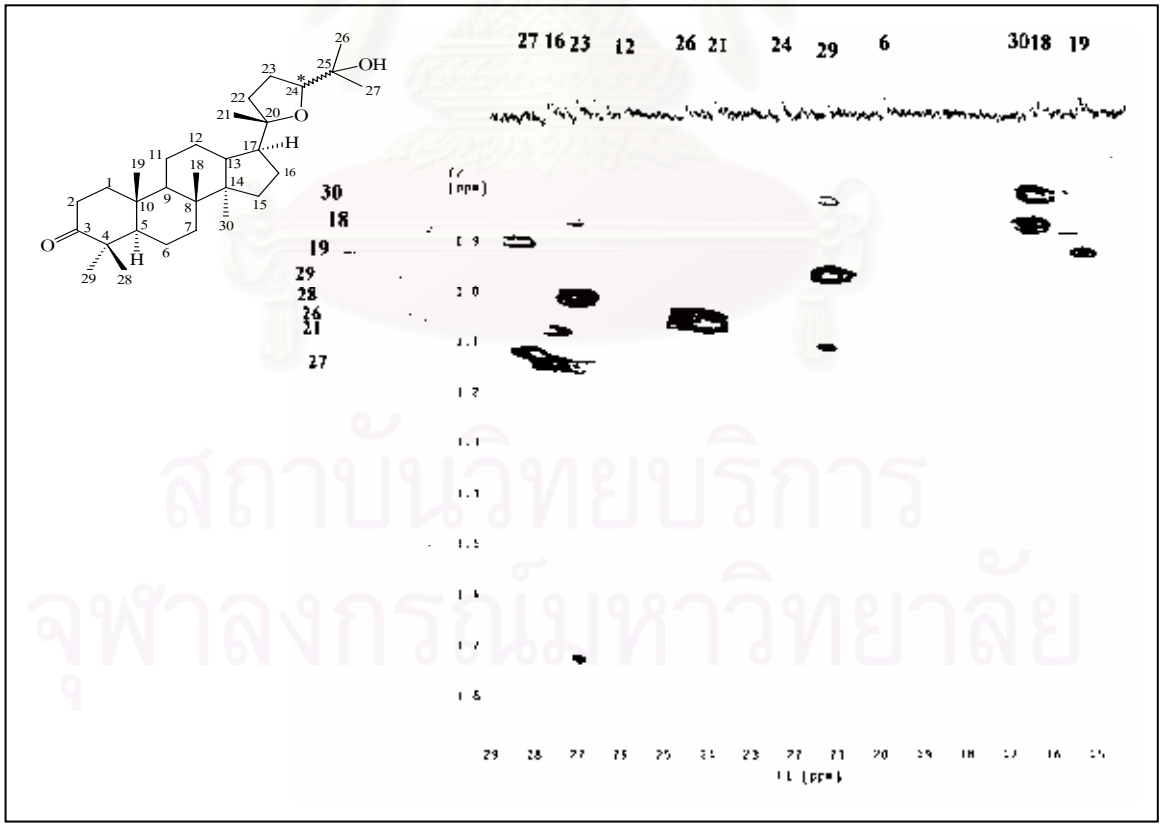

Figure 109. HSQC Spectrum of compound HAO2 ($CDCl_3$) [δ_H 0.80-1.9 ppm, δ_C15-29 ppm]

สถาบันวิทยบริการ
จุฬาลงกรณ์มหาวิทยาลัย

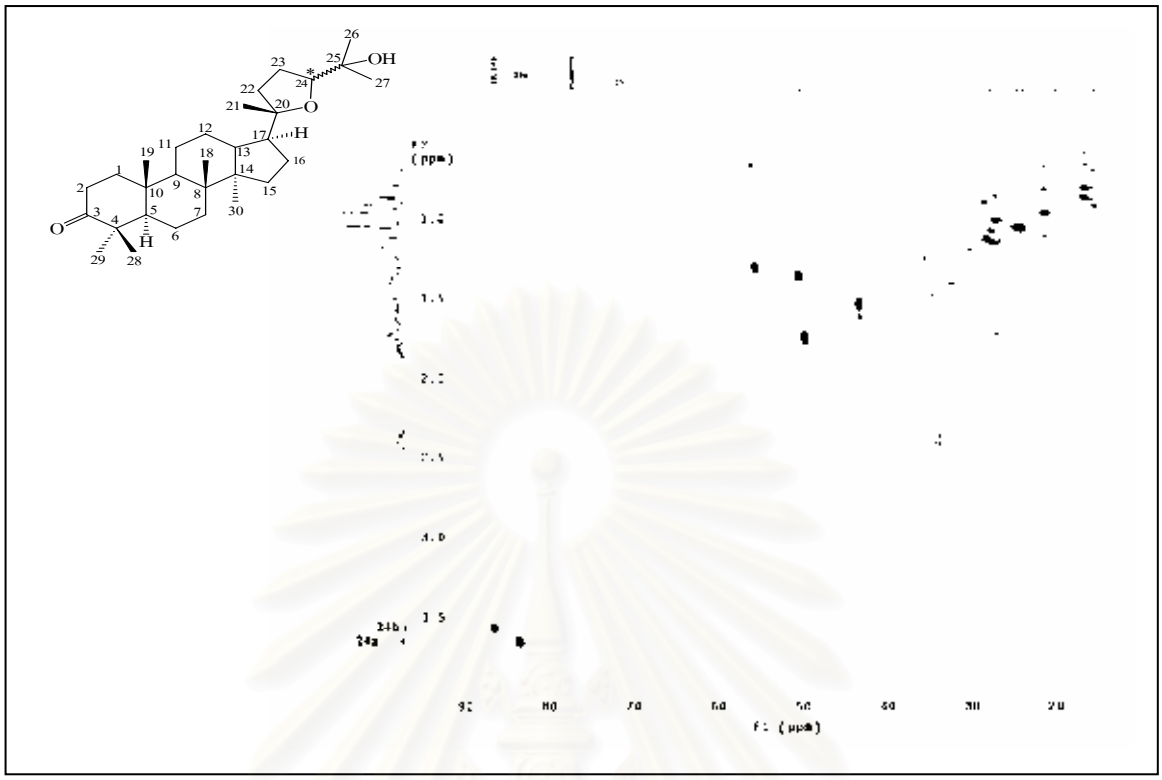

Figure 110. HSQC Spectrum of compound HAO2 ($CDCl_3$)[δ_H 0.80-3.5 ppm, δ_C 70-90 ppm]

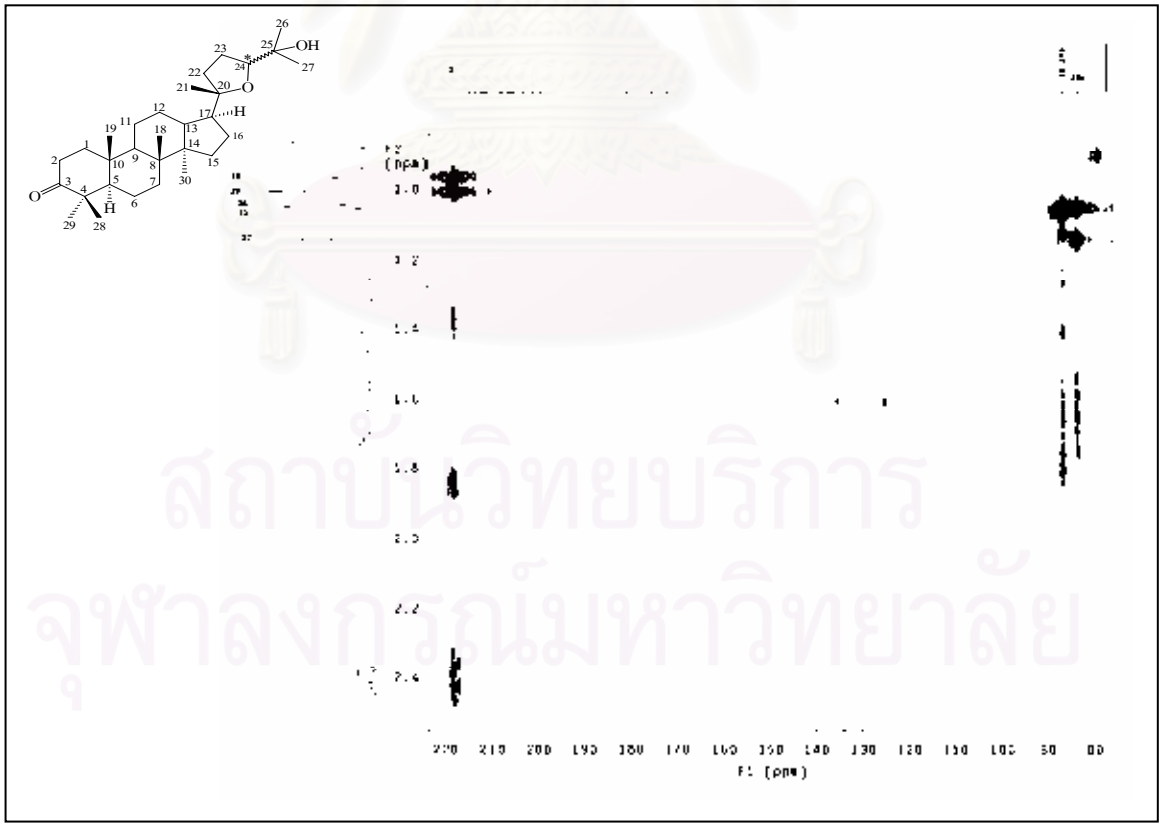

Figure 111. HMBC Spectrum of compound HAO2 ($CDCl_3$) [δ_H 0.86-2.5 ppm, δ_C 80-220 ppm]

สถาบันวิทยบริการ
จุฬาลงกรณ์มหาวิทยาลัย

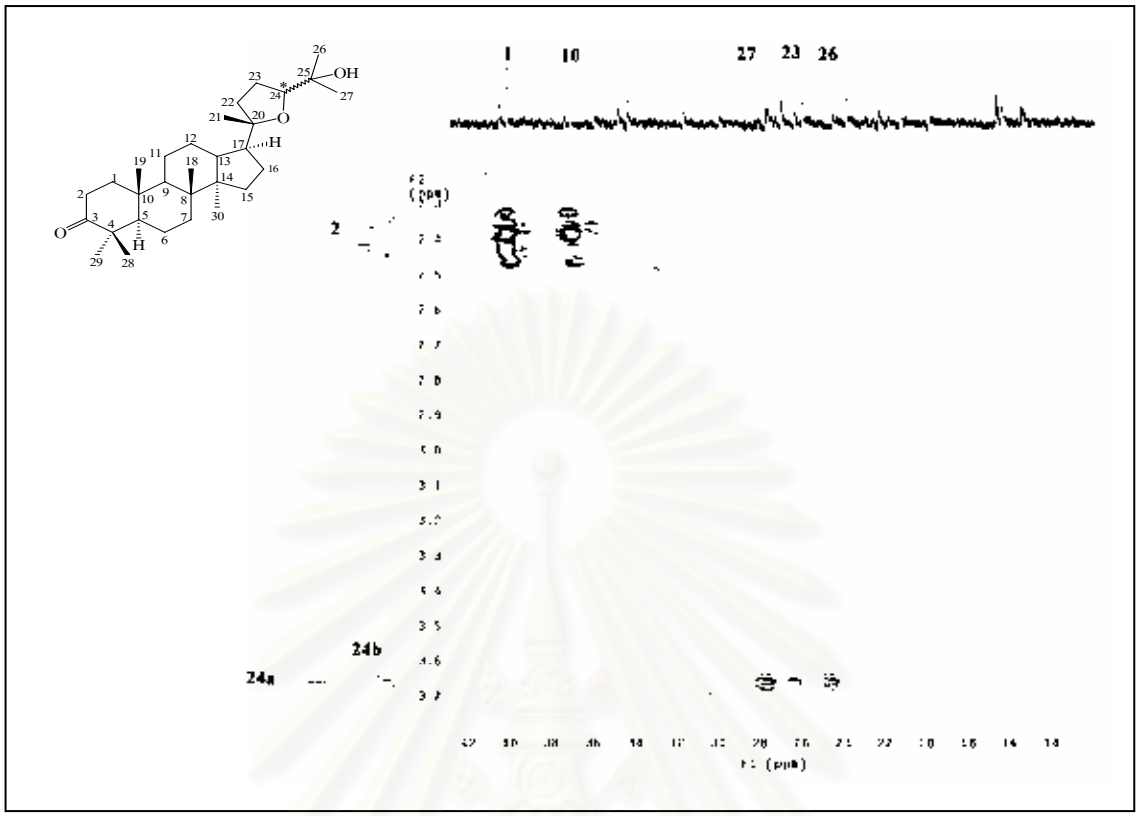

Figure 112. HMBC Spectrum of compound HAO2 ($CDCl_3$) [δ_H 3.3-3.7 ppm, δ_C 14-42 ppm]

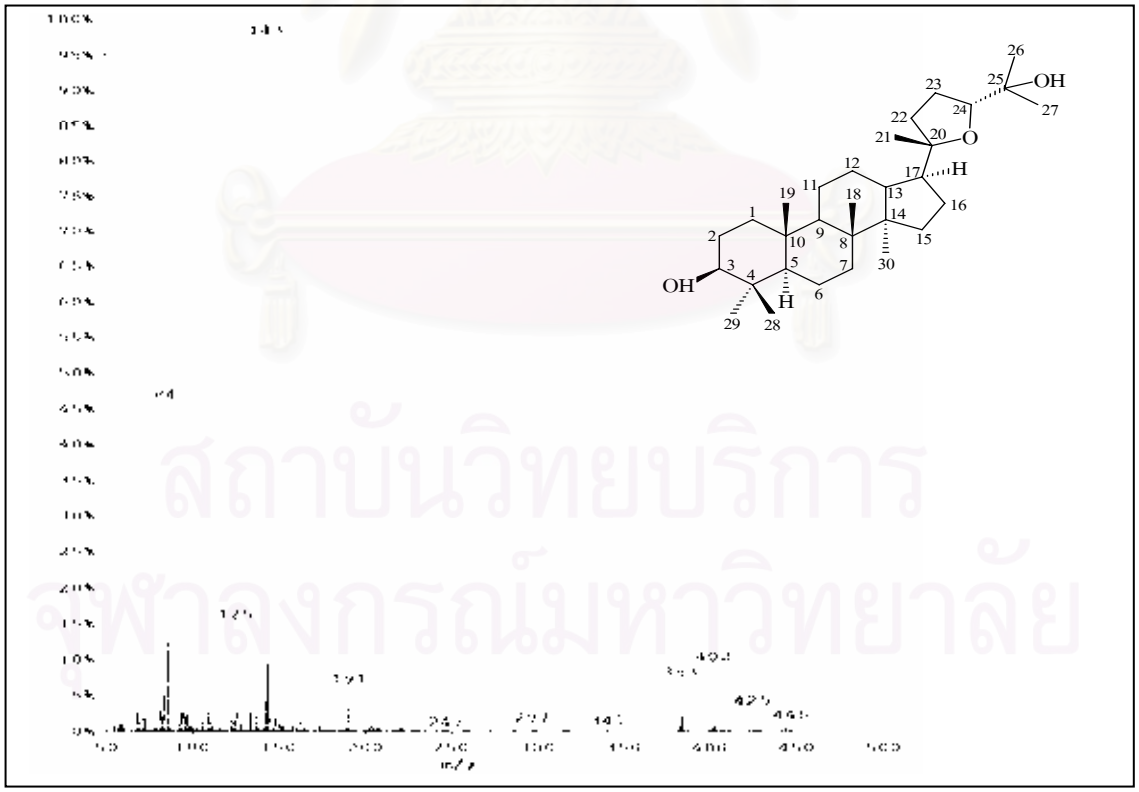

Figure 113. EI Mass spectrum of compound HAO3

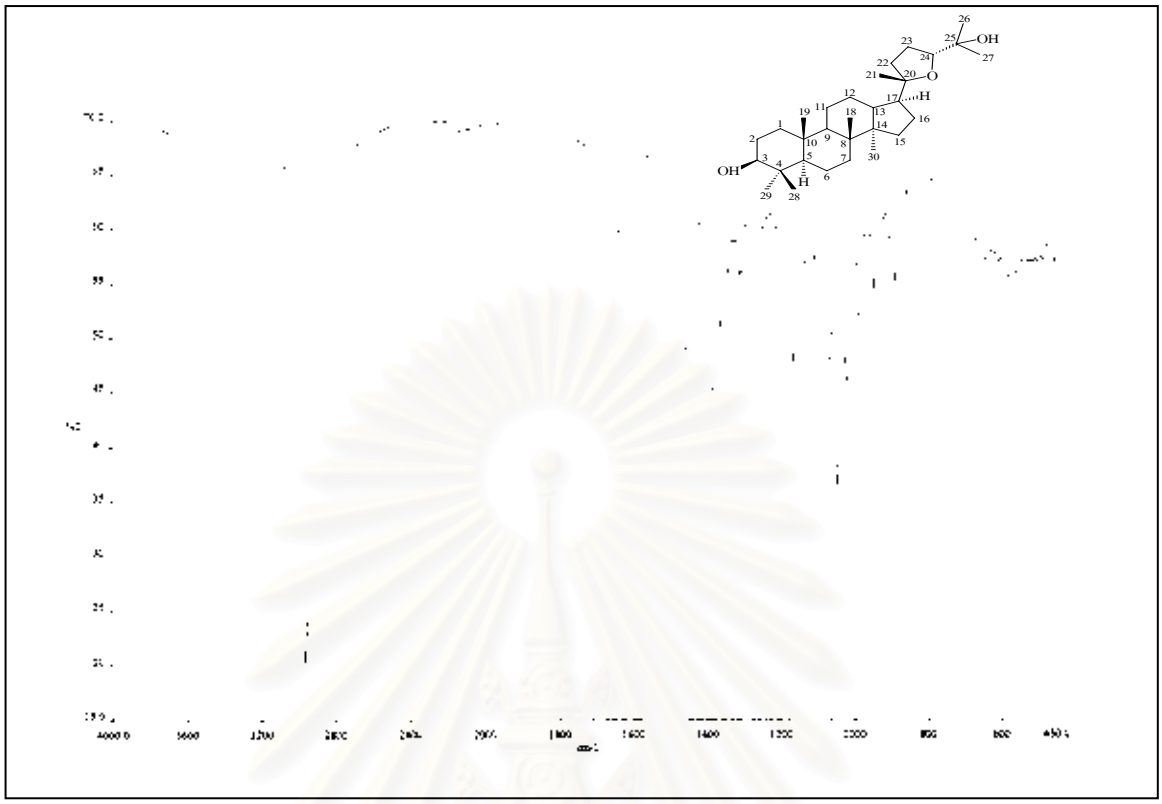

Figure 114. IR Spectrum of compound HAO3 (KBr disc)

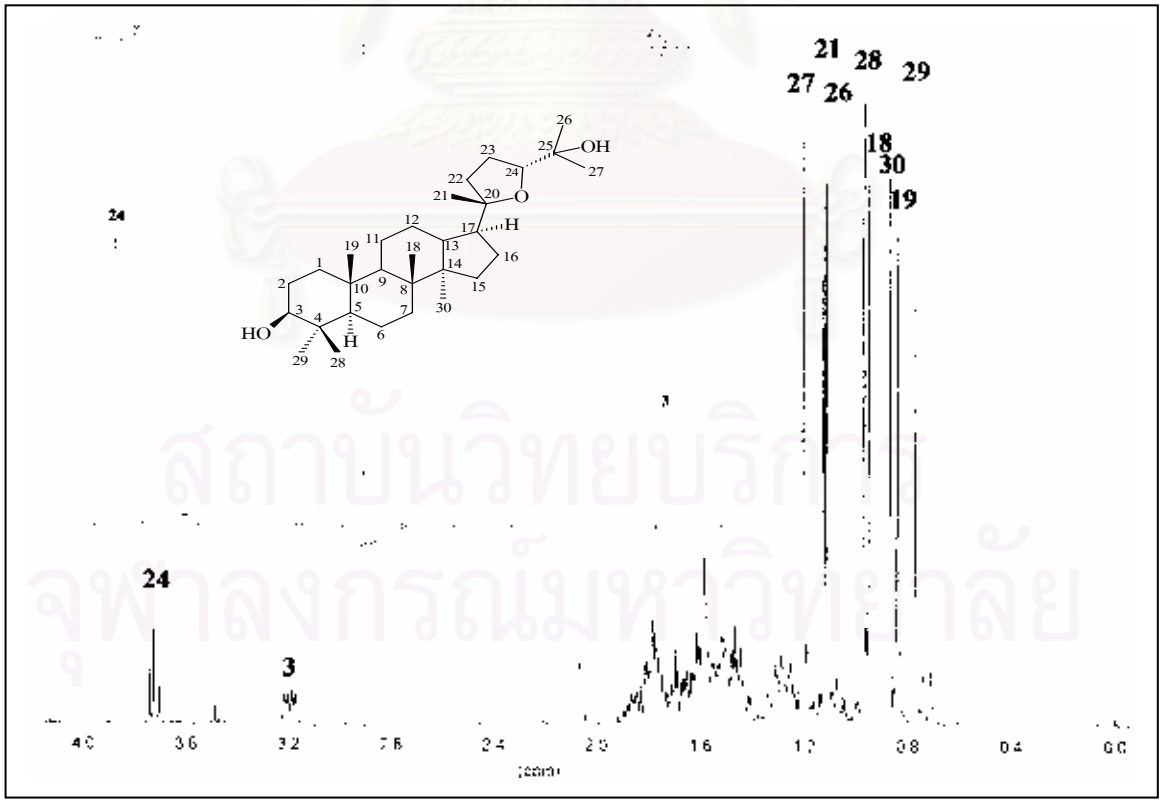

Figure 115. ^{1}H NMR (400 MHz) Spectrum of compound HAO3 ($CDCl_3$)

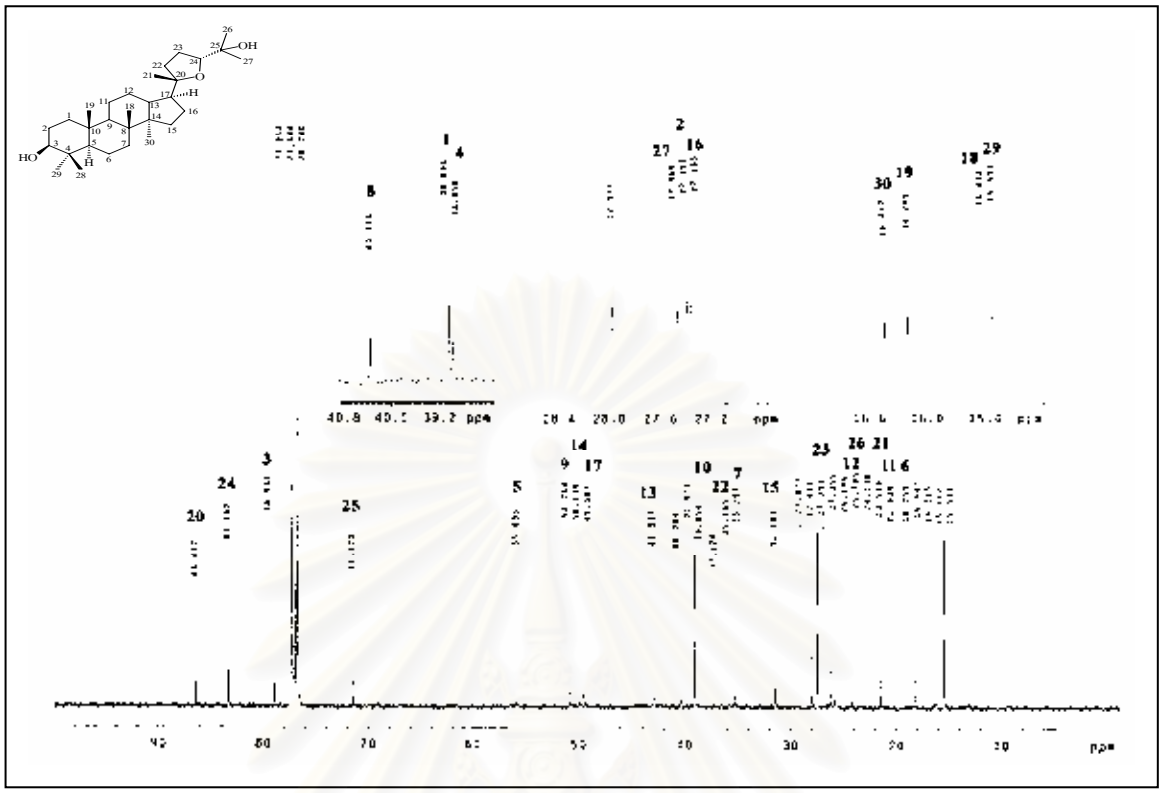

Figure 116. ^{13}C NMR (100 MHz) Spectrum of compound HAO3 ($CDCl_3$)

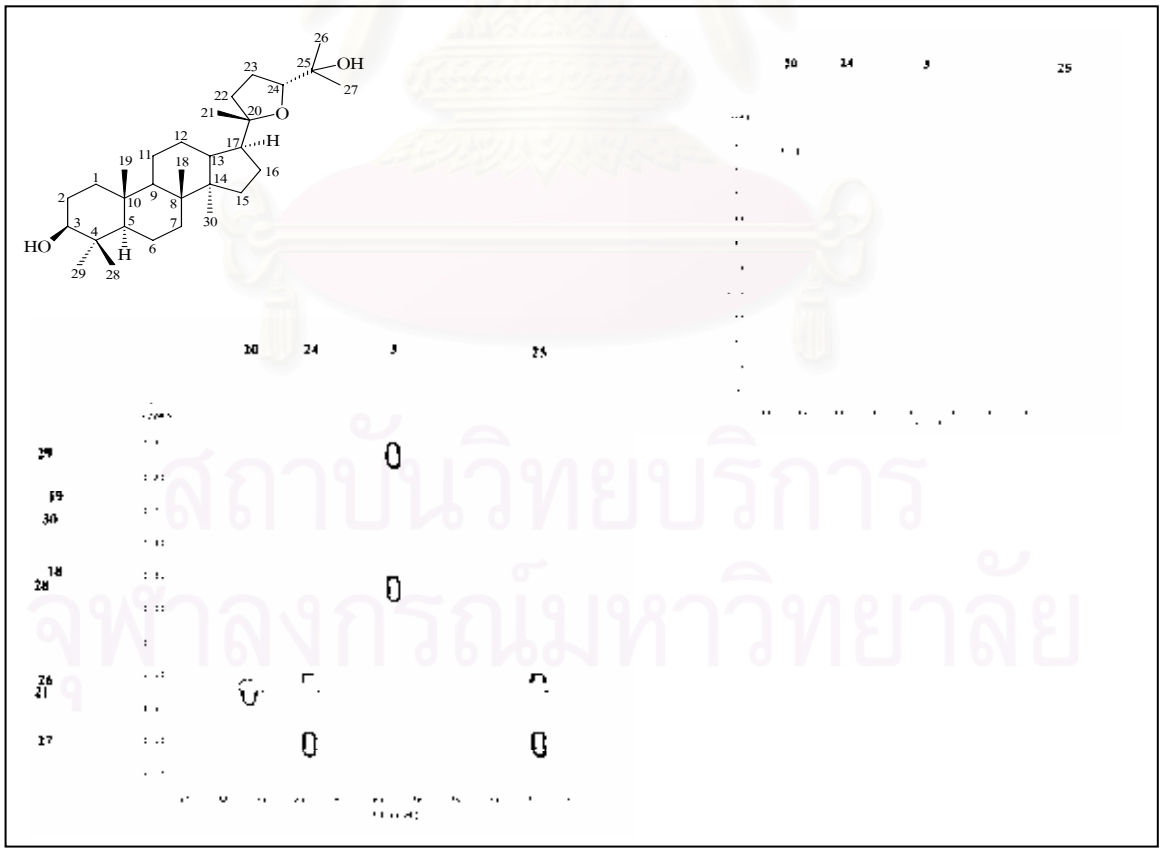

Figure 117. HMBC Spectrum of compound HAO3 ($CDCl_3$)

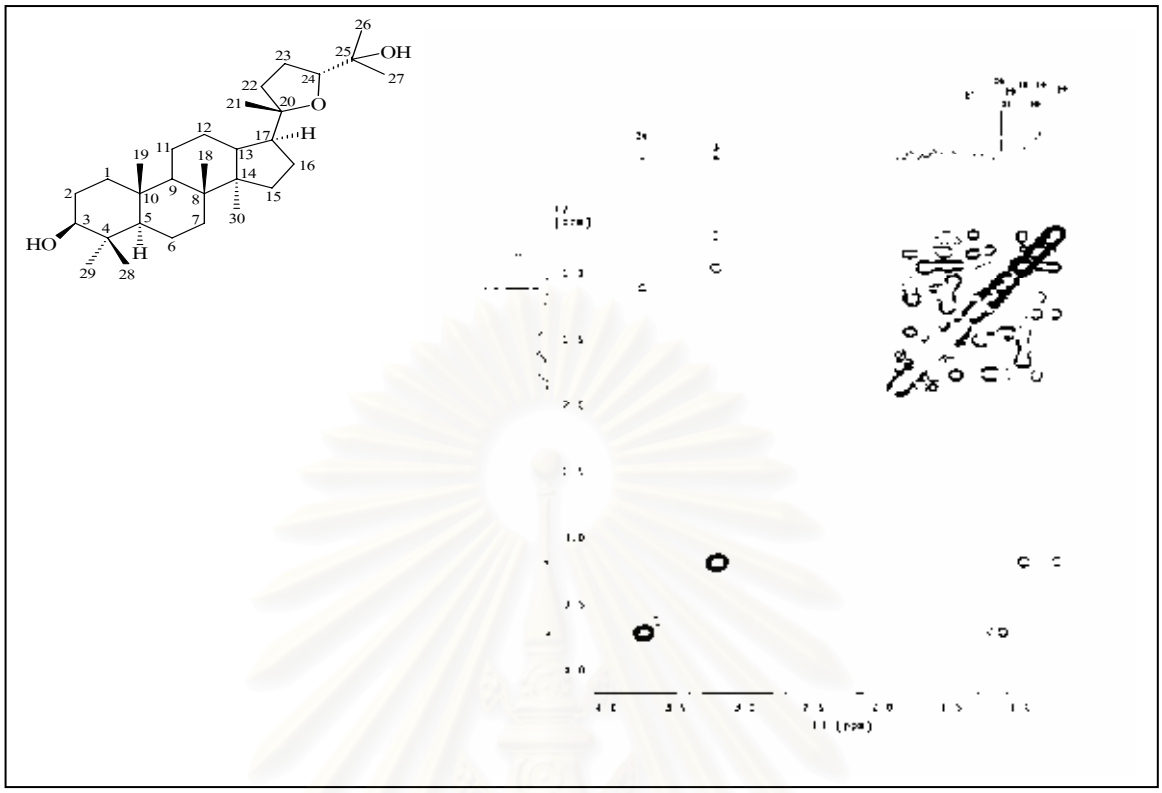

Figure 118. NOESY Spectrum of compound HAO3 ($CDCl_3$)

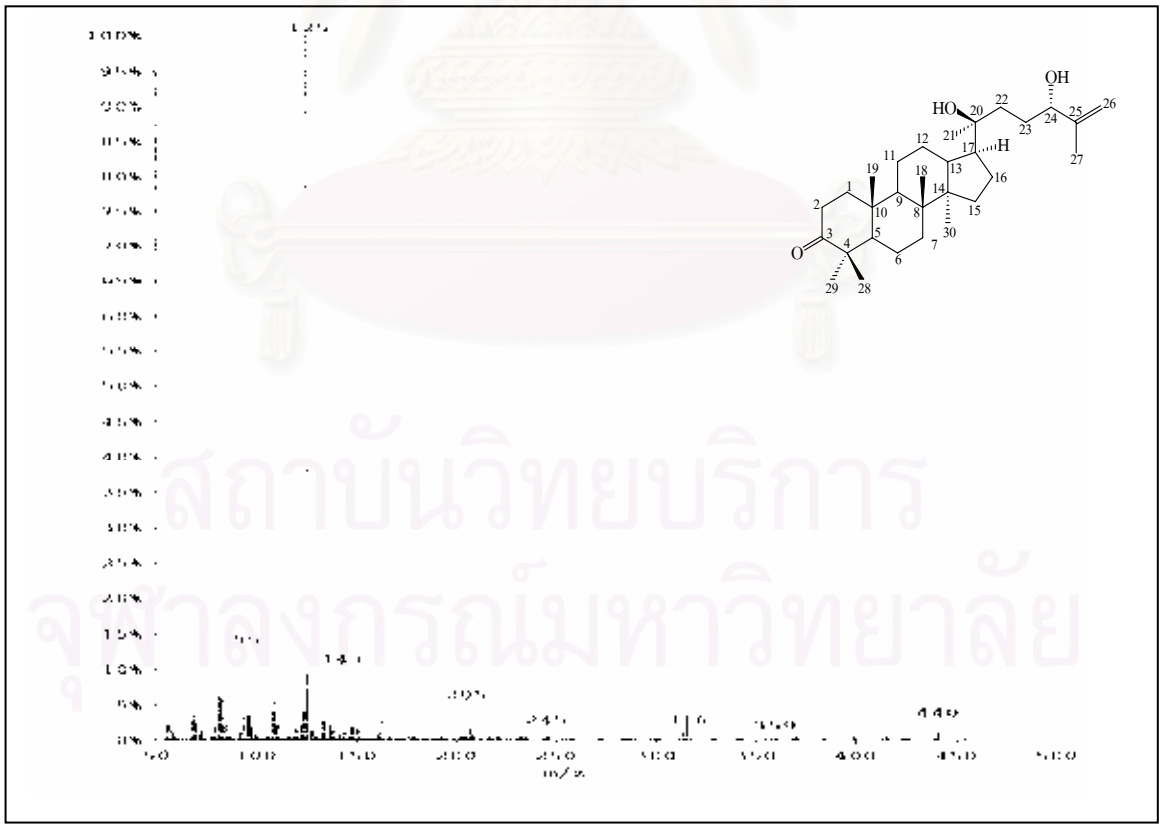

Figure 119. EI Mass spectrum of compound HAO4

สถาบันวิทยบริการ
จุฬาลงกรณ์มหาวิทยาลัย

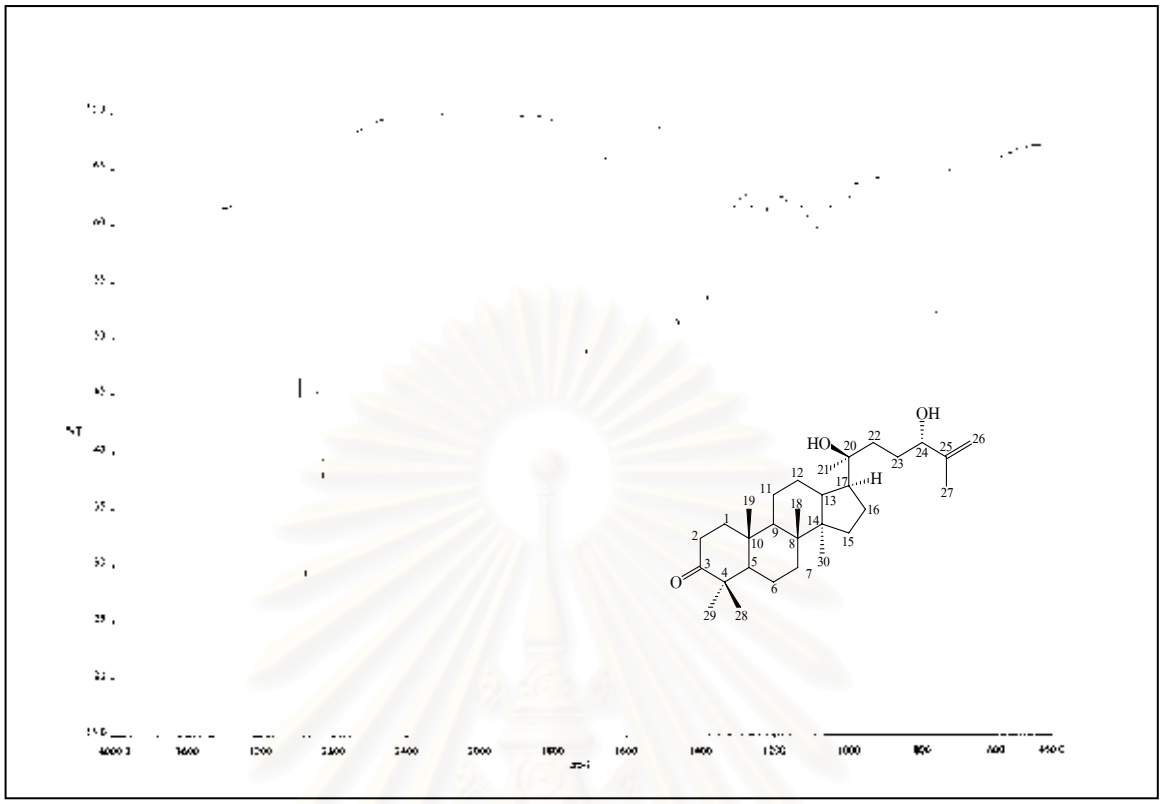

Figure 120. IR Spectrum of compound HAO4 (KBr disc)

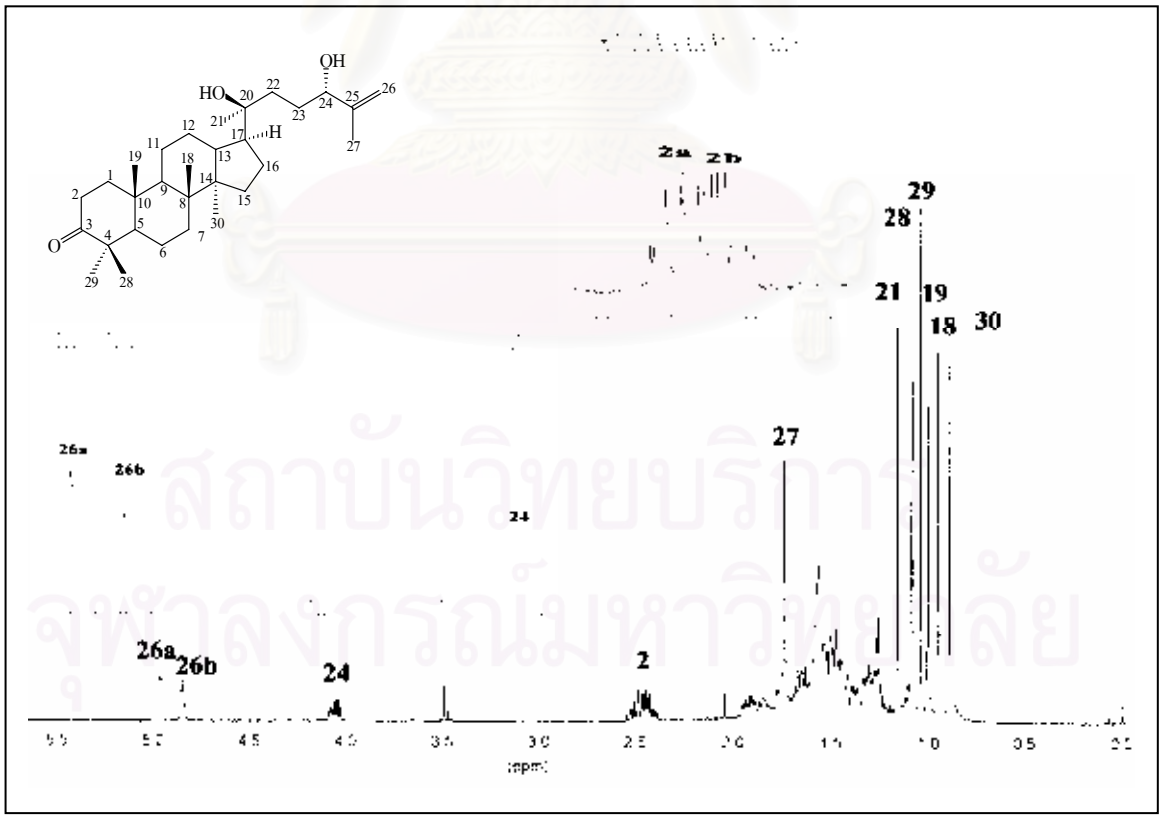

Figure 121. ^{1}H NMR (400 MHz) Spectrum of compound HAO4 ($CDCl_3$)

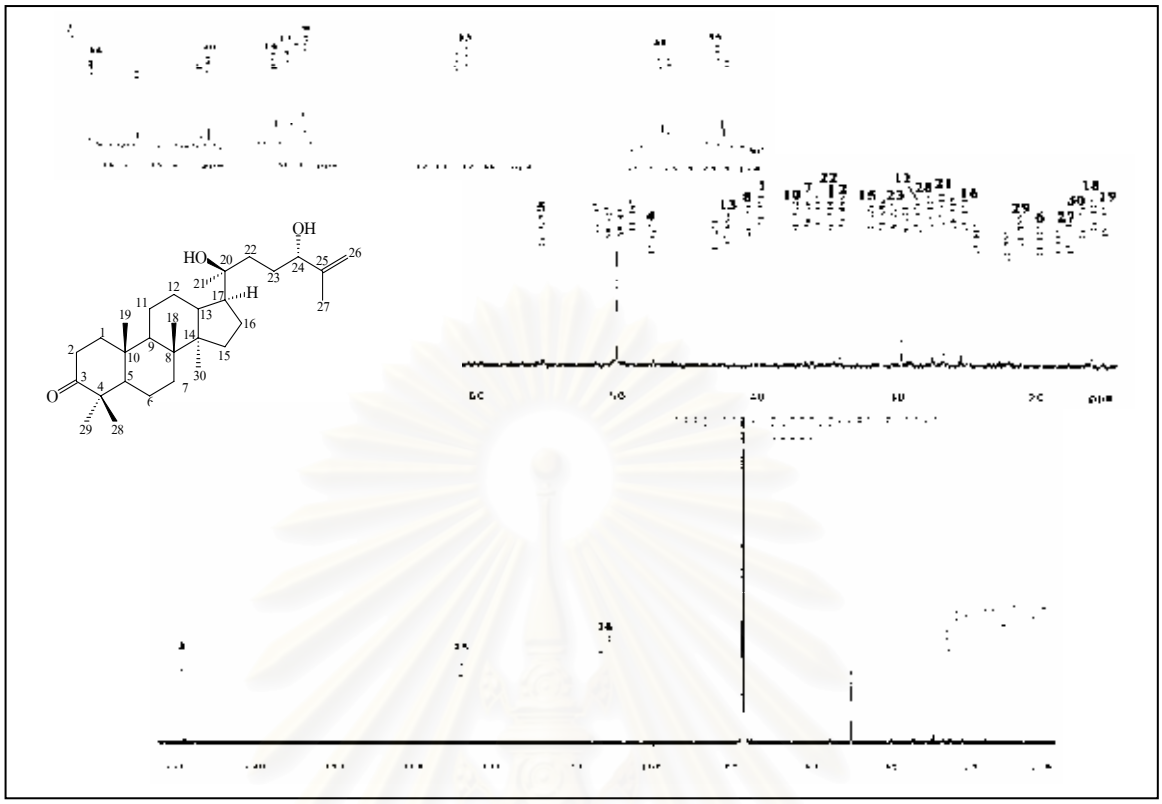

Figure 122. ^{13}C NMR (100 MHz) Spectrum of compound HAO4 ($CDCl_3$)

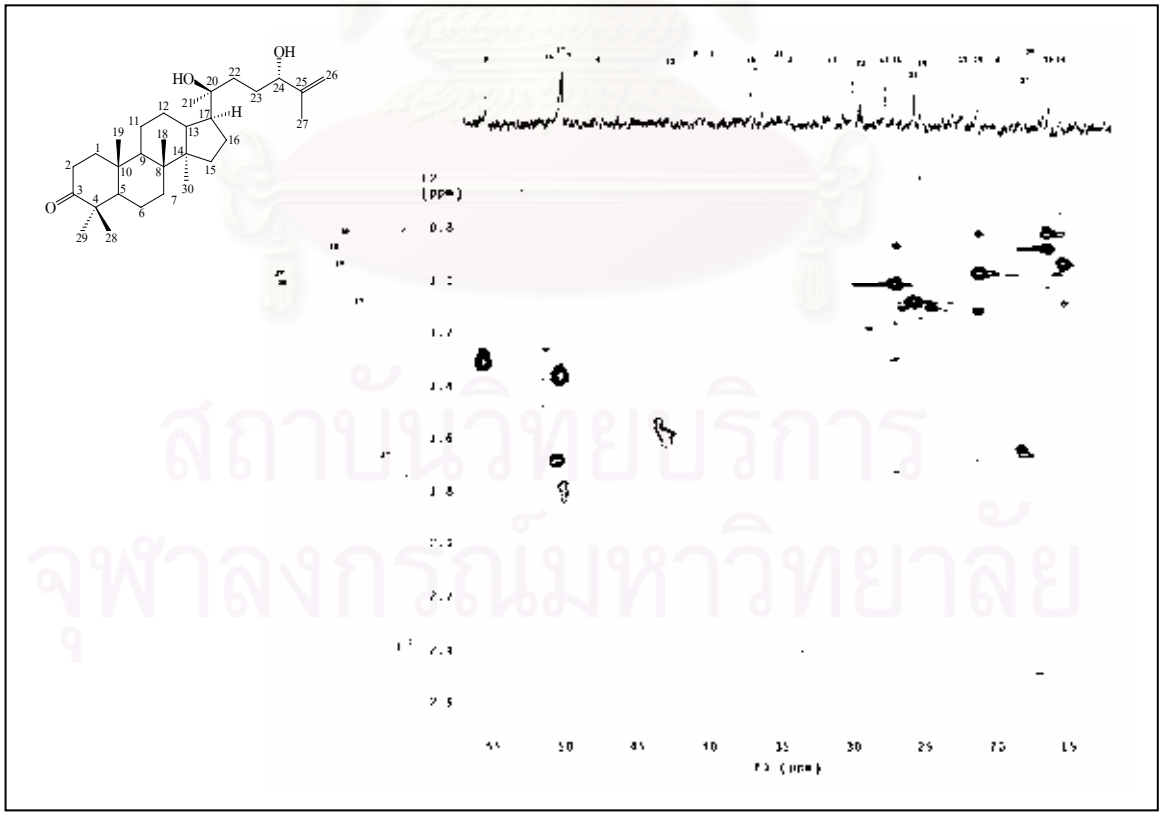

Figure 123. HSQC Spectrum of compound HAO4 ($CDCl_3$)

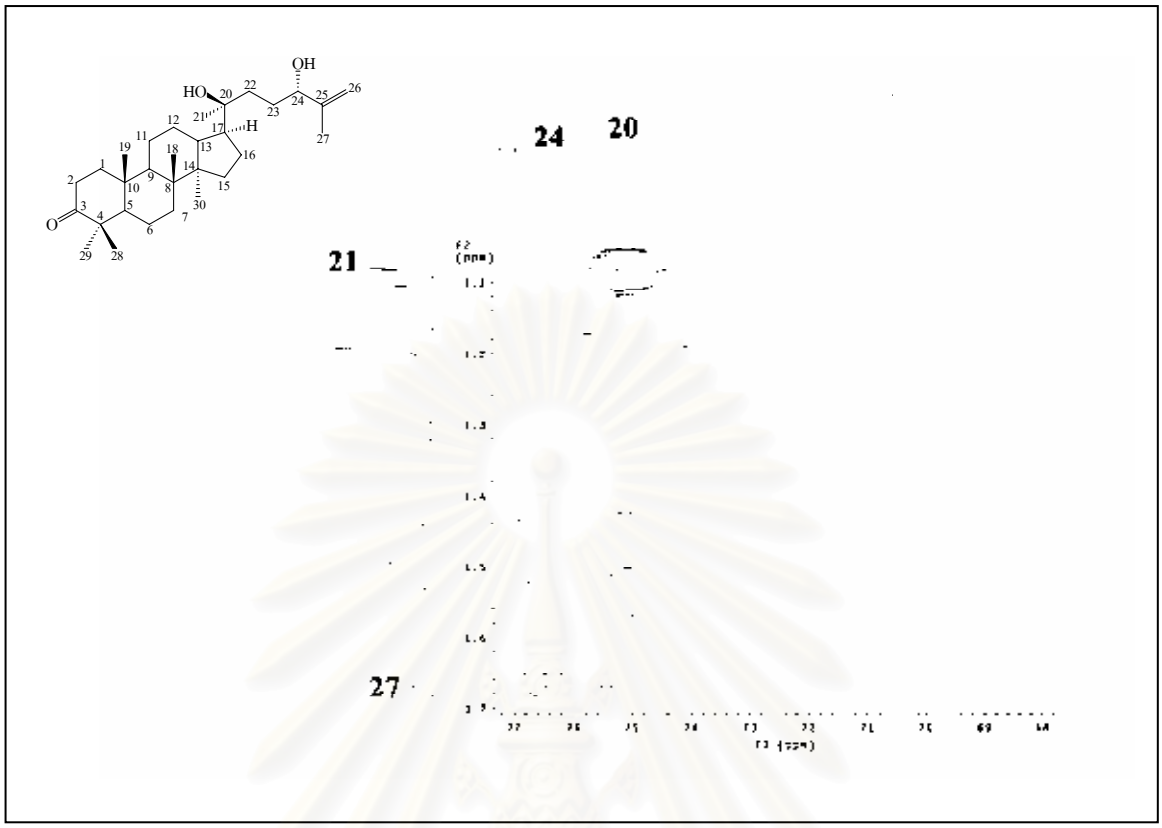

Figure 124. HMBC Spectrum of compound HAO4 ($CDCl_3$) [δ_H 0.9-1.7 ppm, δ_C 68-77 ppm]

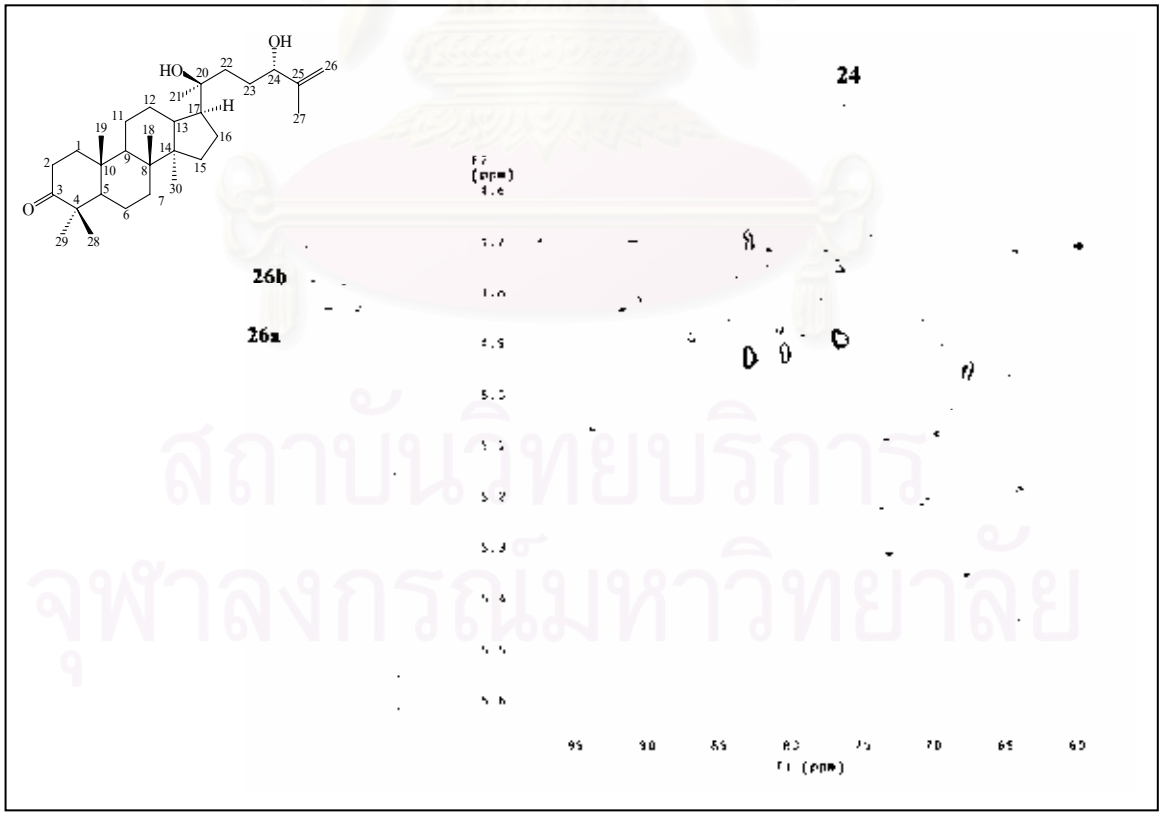

Figure 125. HMBC Spectrum of compound HAO4 ($CDCl_3$) [δ_H 4.6-5.6 ppm, δ_C 60-95 ppm]

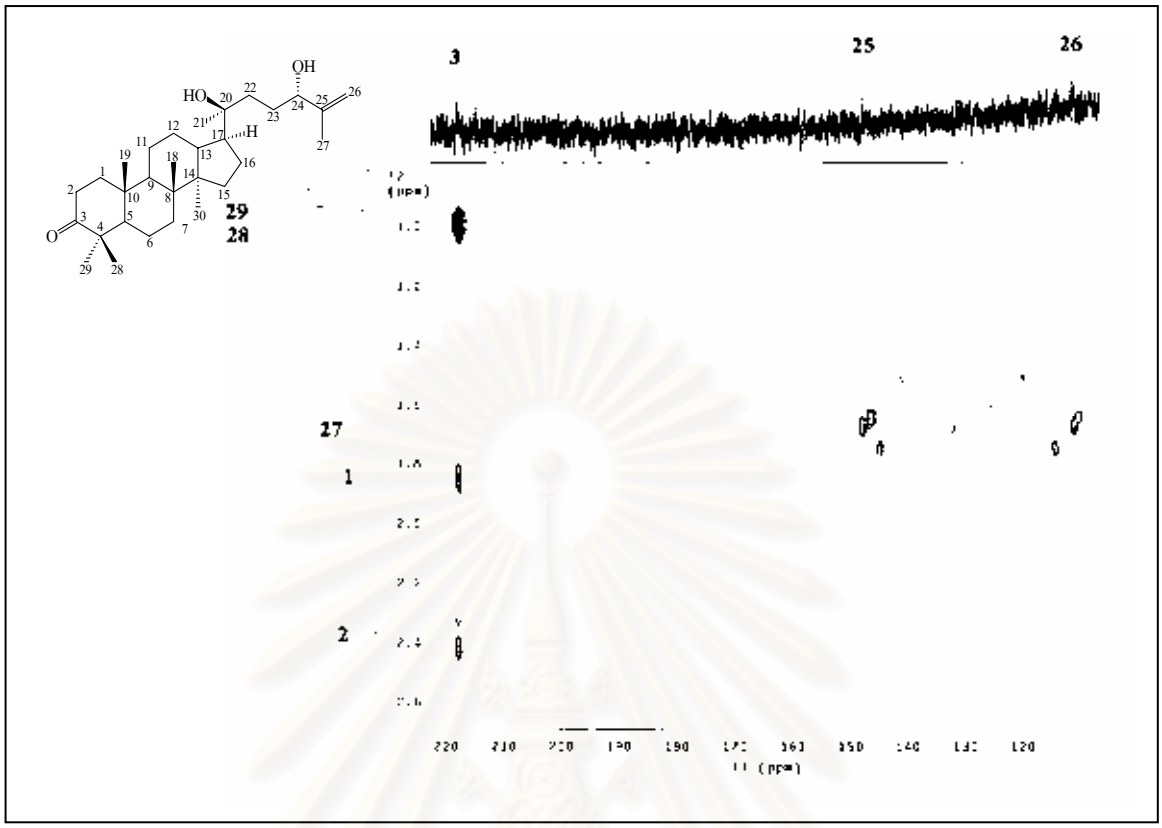

Figure 126. HMBC Spectrum of compound HAO4 ($CDCl_3$) [δ_H 0.9-2.6 ppm, δ_C 110-220 ppm]

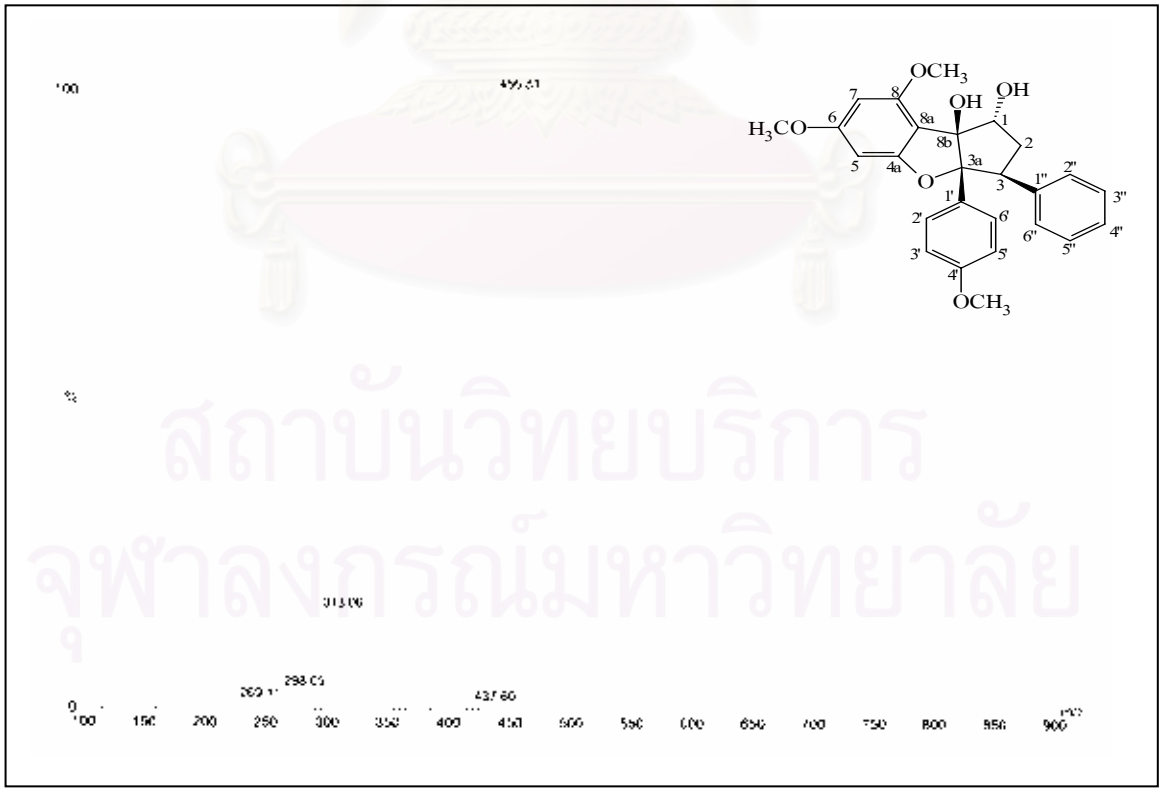

Figure 127. ESI-TOF Mass spectrum of compound HAO5

สถาบันวิทยบริการ
จุฬาลงกรณ์มหาวิทยาลัย

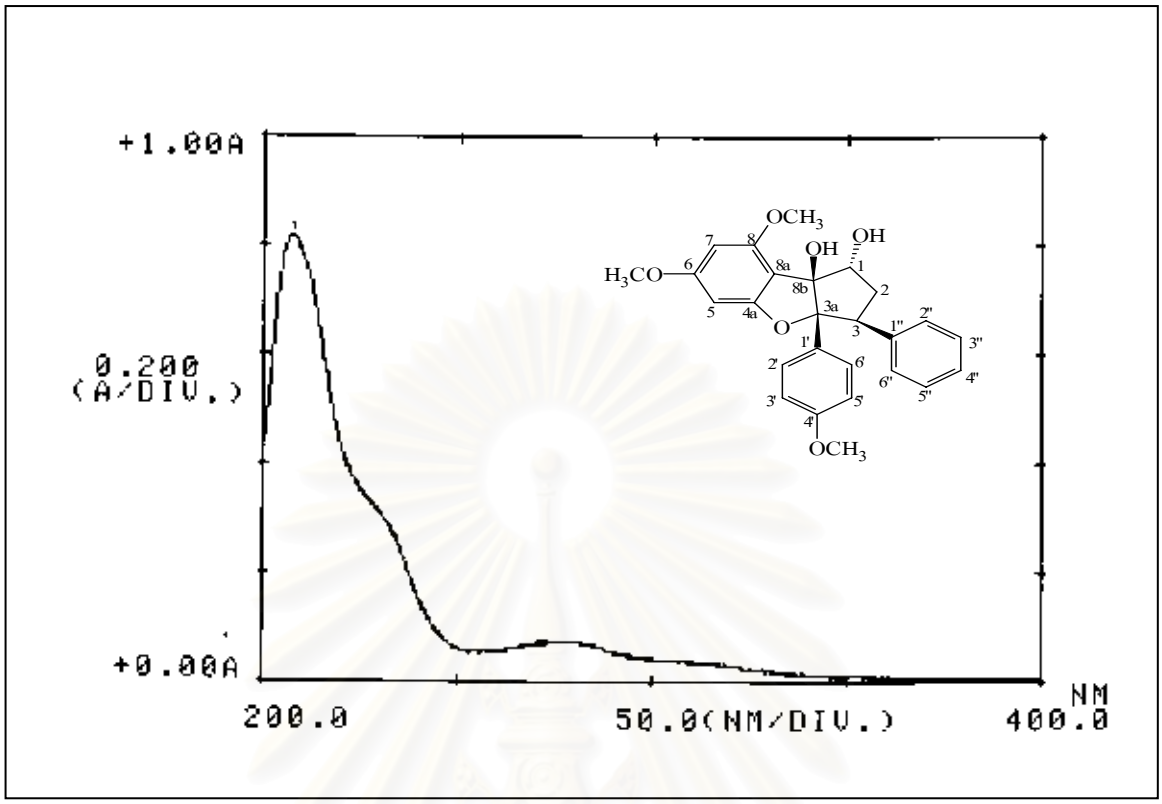

Figure 128. UV Spectrum of compound HAO5

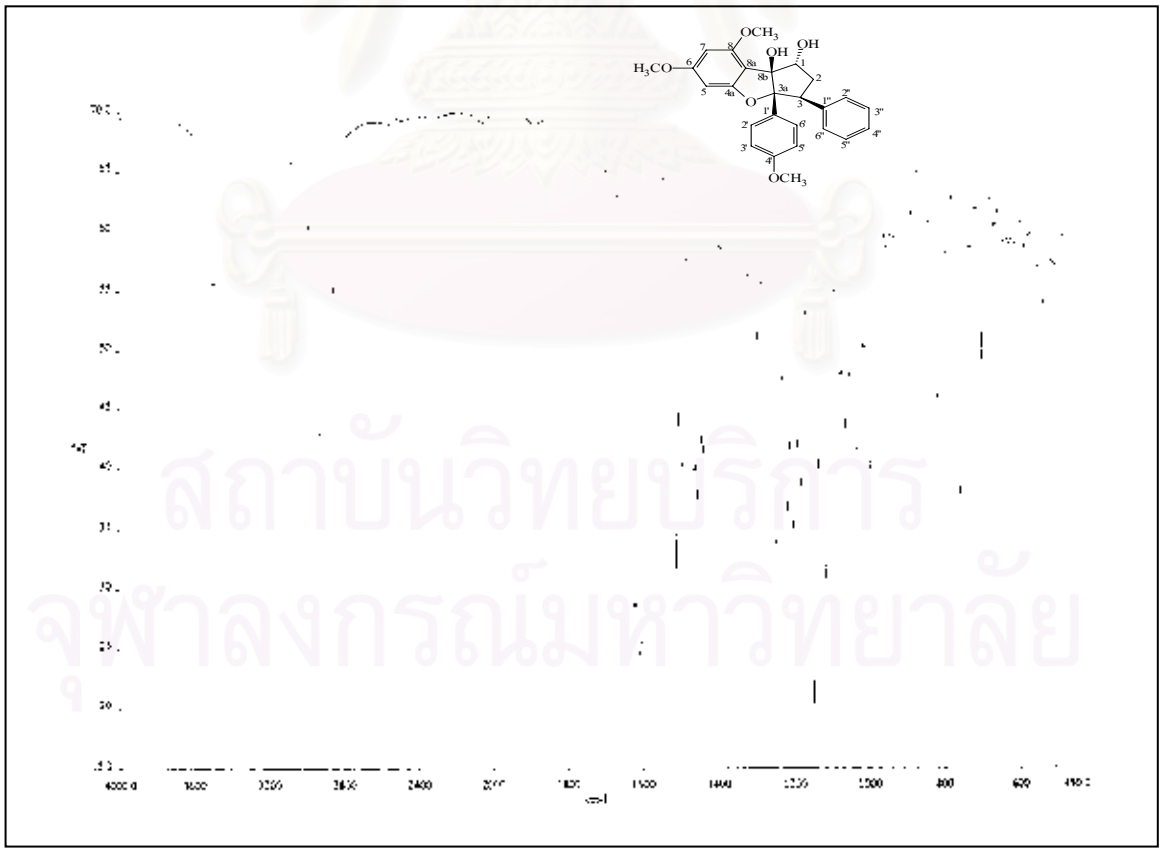

Figure 129. IR Spectrum of compound HAO5 (KBr disc)

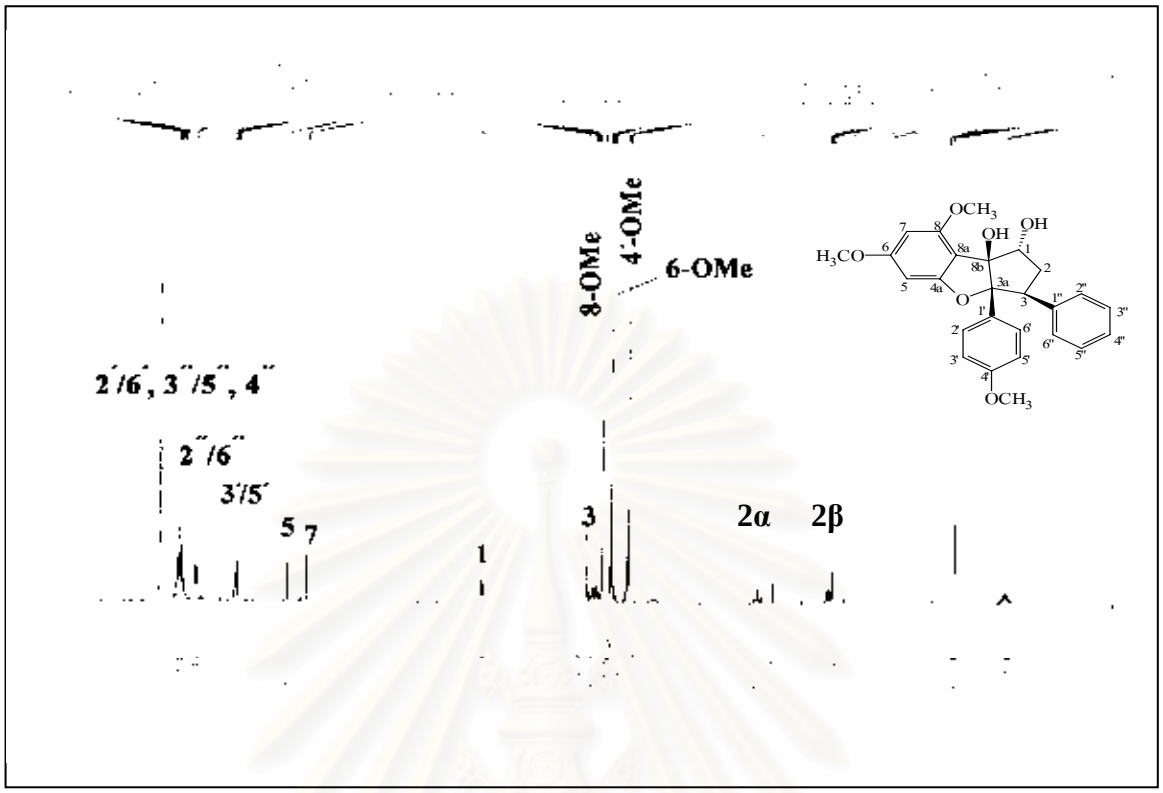

Figure 130. ^{1}H NMR (500 MHz) Spectrum of compound HAO5 ($CDCl_3$)

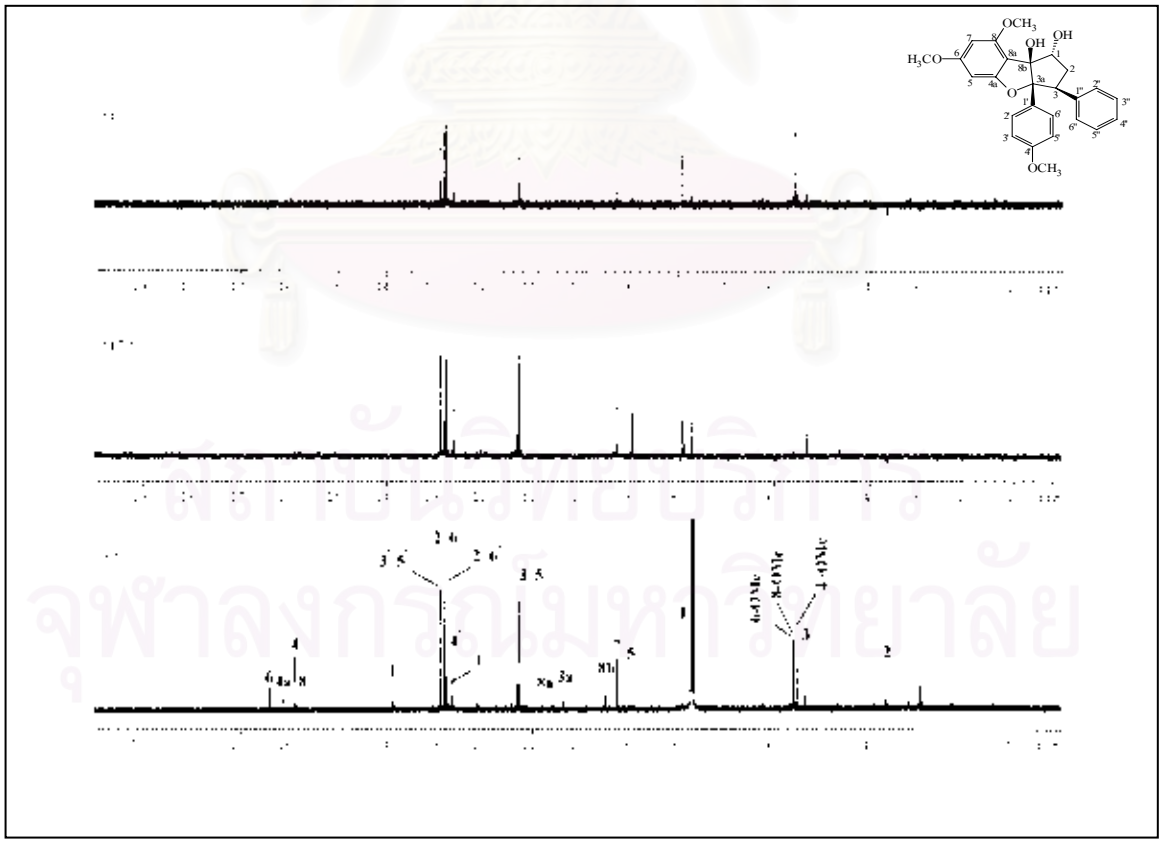

Figure 131. ^{13}C NMR (125 MHz) Spectrum of compound HAO5 ($CDCl_3$)

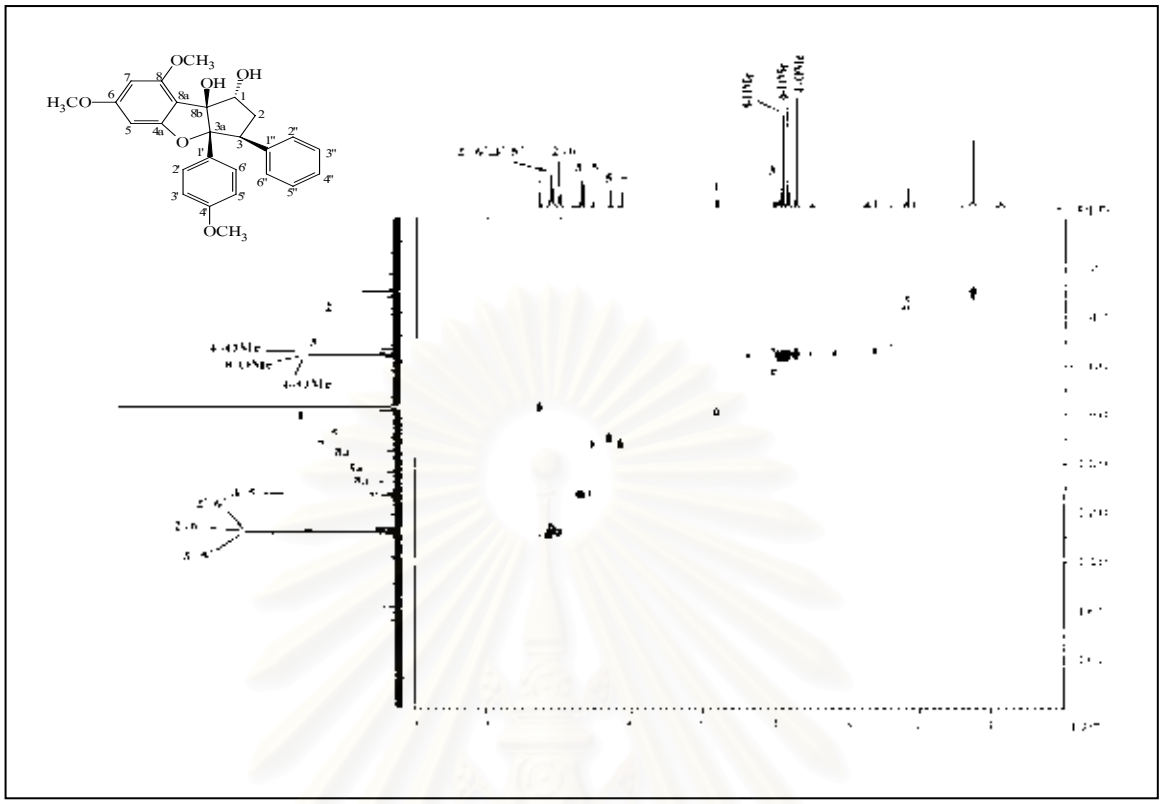

Figure 132. HSQC Spectrum of compound HAO5 ($CDCl_3$)

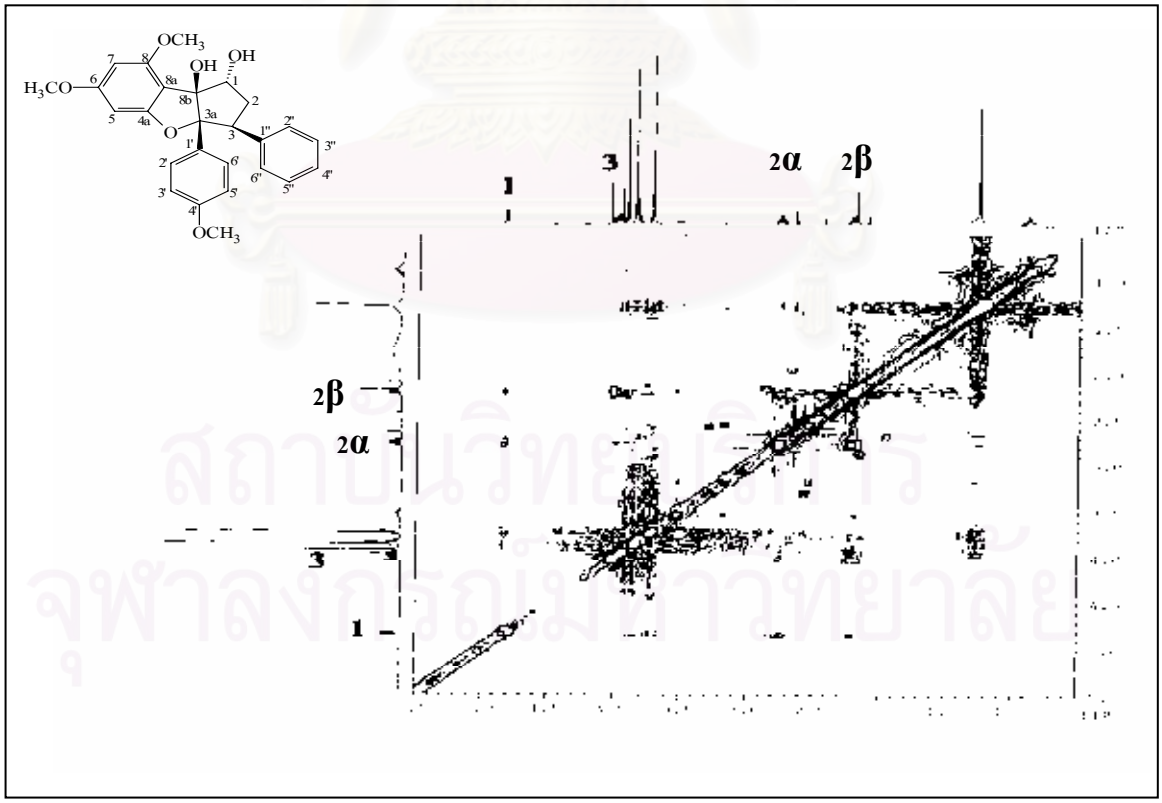

Figure 133. NOESY Spectrum of compound HAO5 ($CDCl_3$)

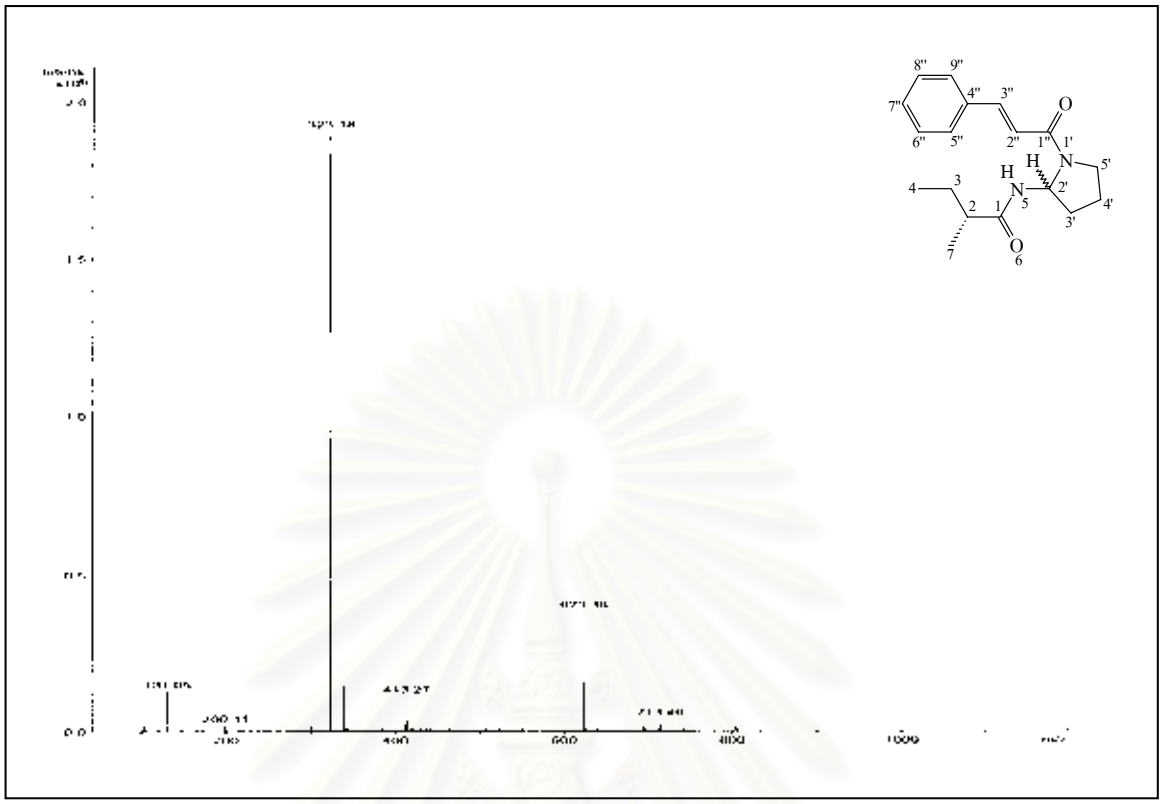

Figure 134. ESI-TOF Mass spectrum of compound HAO6

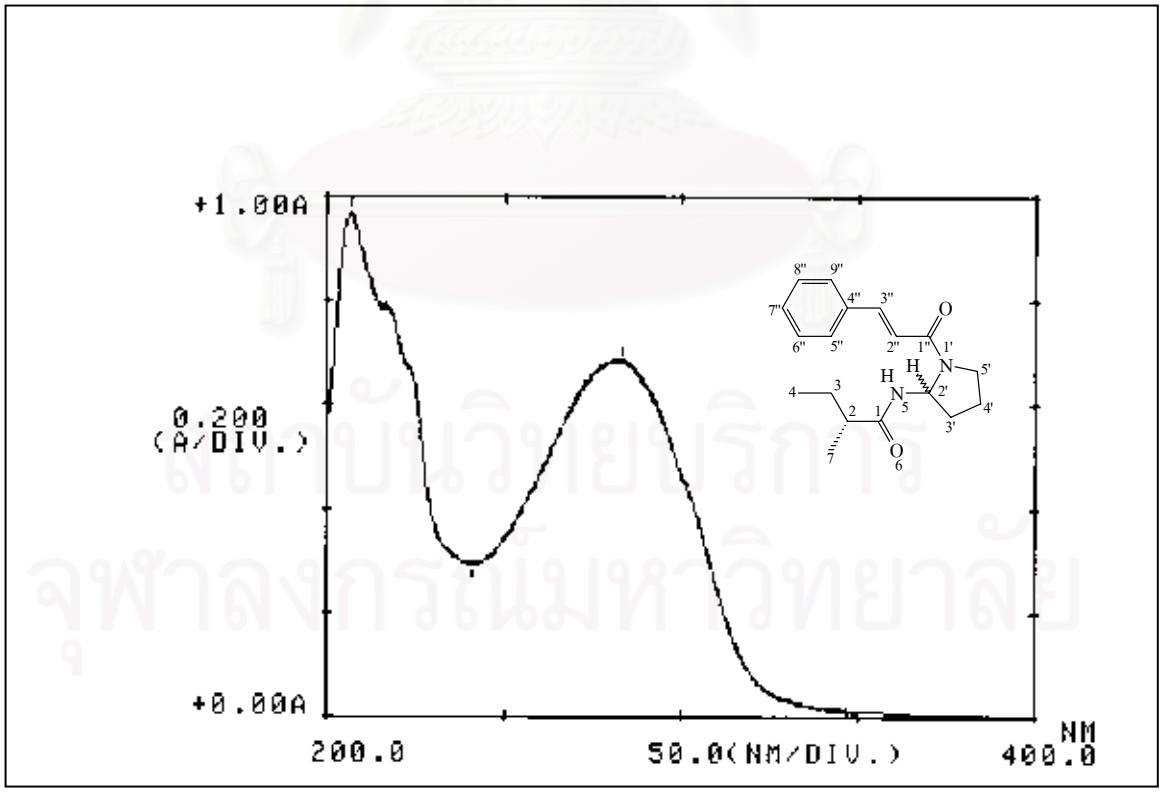

Figure 135. UV Spectrum of compound HAO6

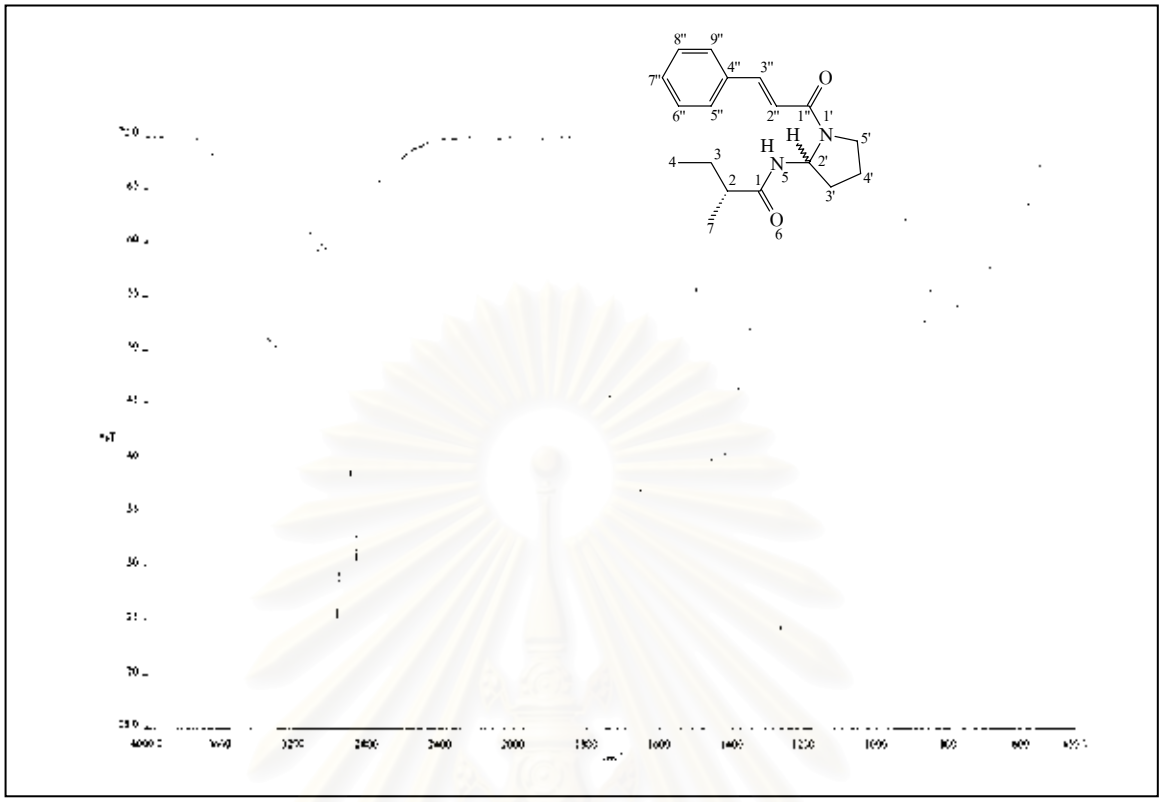

Figure 136. IR Spectrum of compound HAO6 (KBr disc)

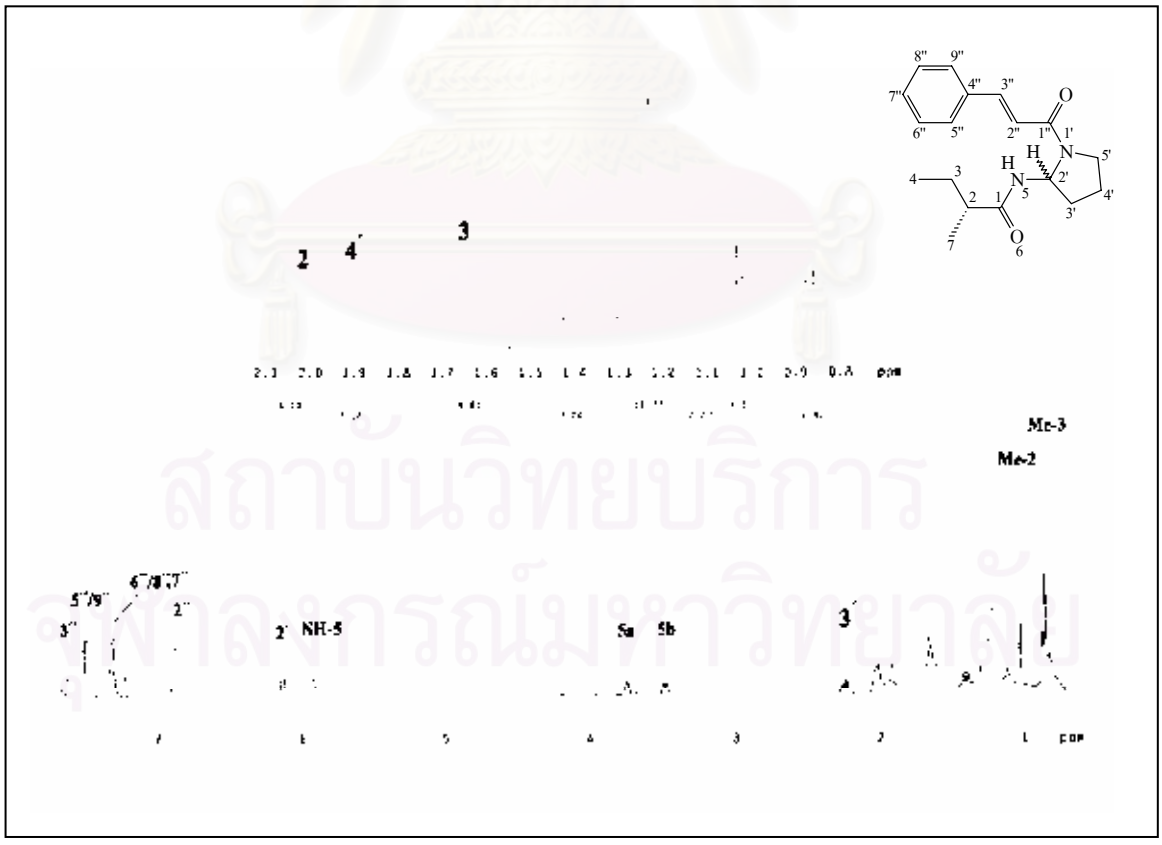

Figure 137. ^{1}H NMR (500 MHz) Spectrum of compound HAO6 $CDCl_3$)

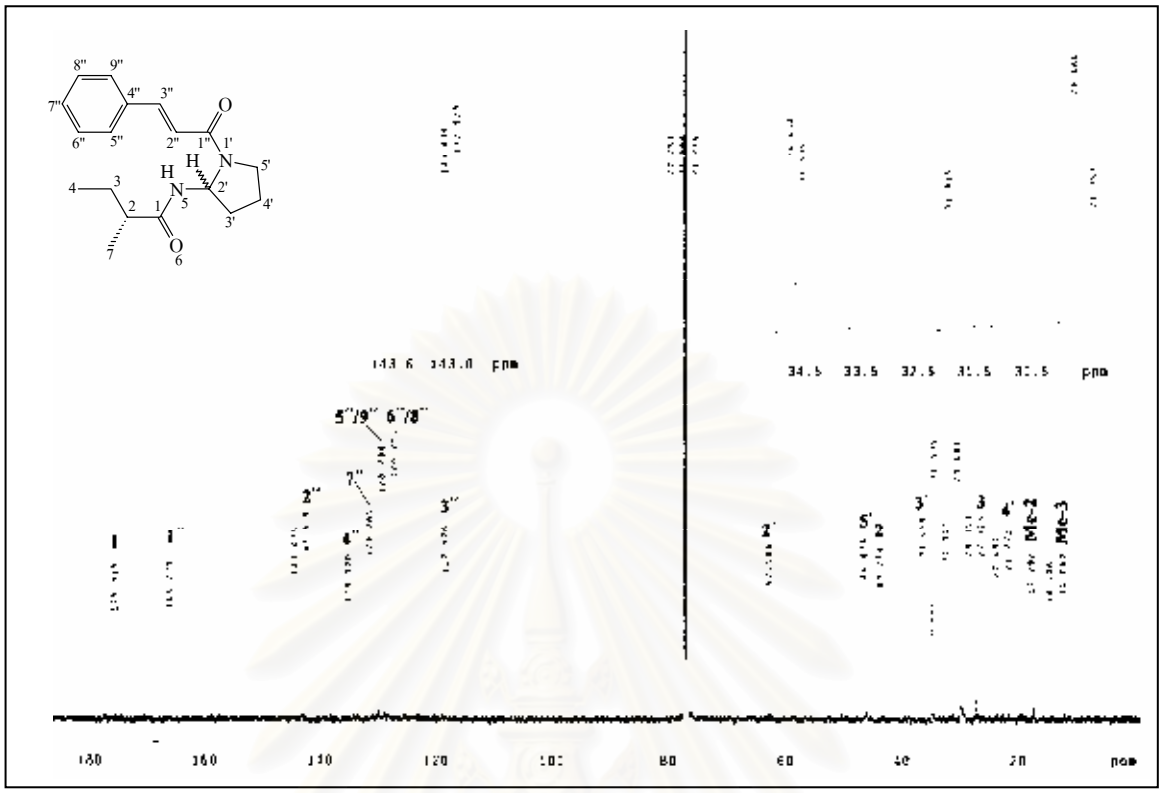

Figure 138. ^{13}C NMR (125 MHz) Spectrum of compound HAO6 ($CDCl_3$)

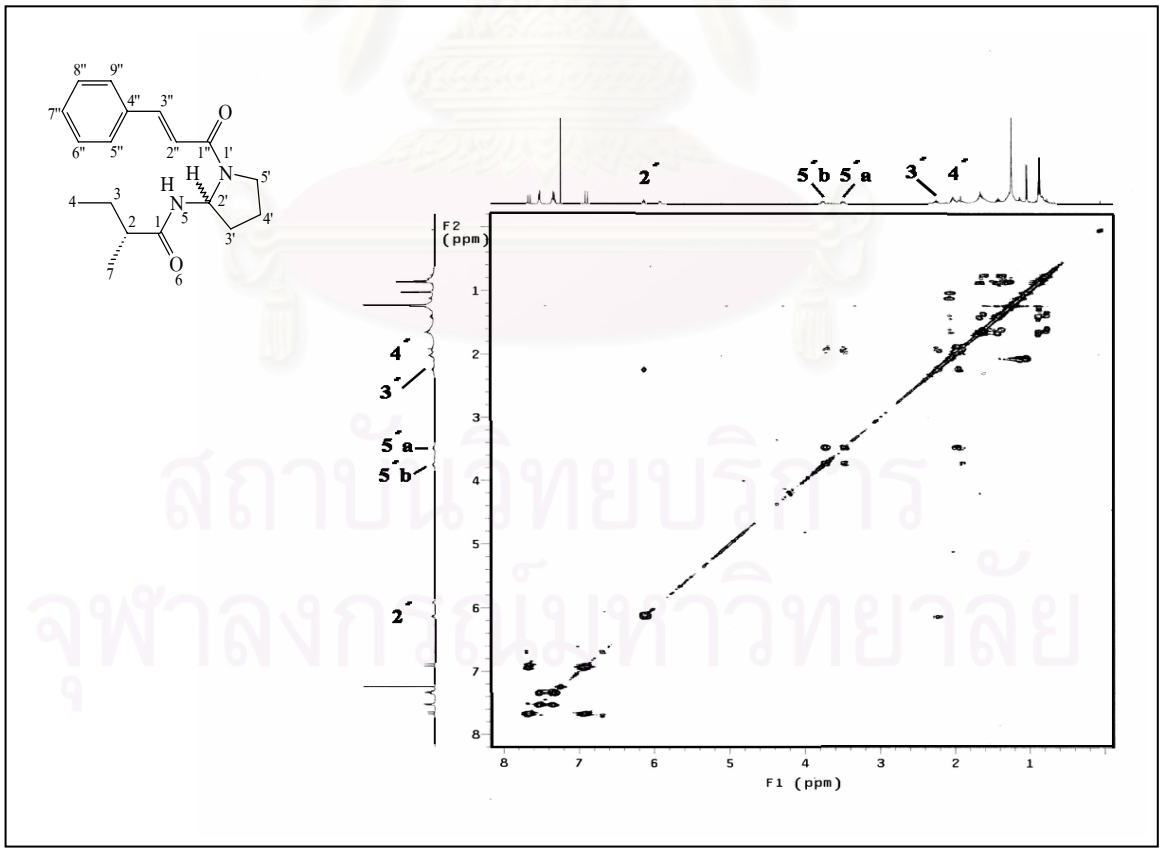

Figure 139. ^{1}H–^{1}H COSY Spectrum of compound HAO6 ($CDCl_3$) [δ_H 2.0-7.0 ppm]

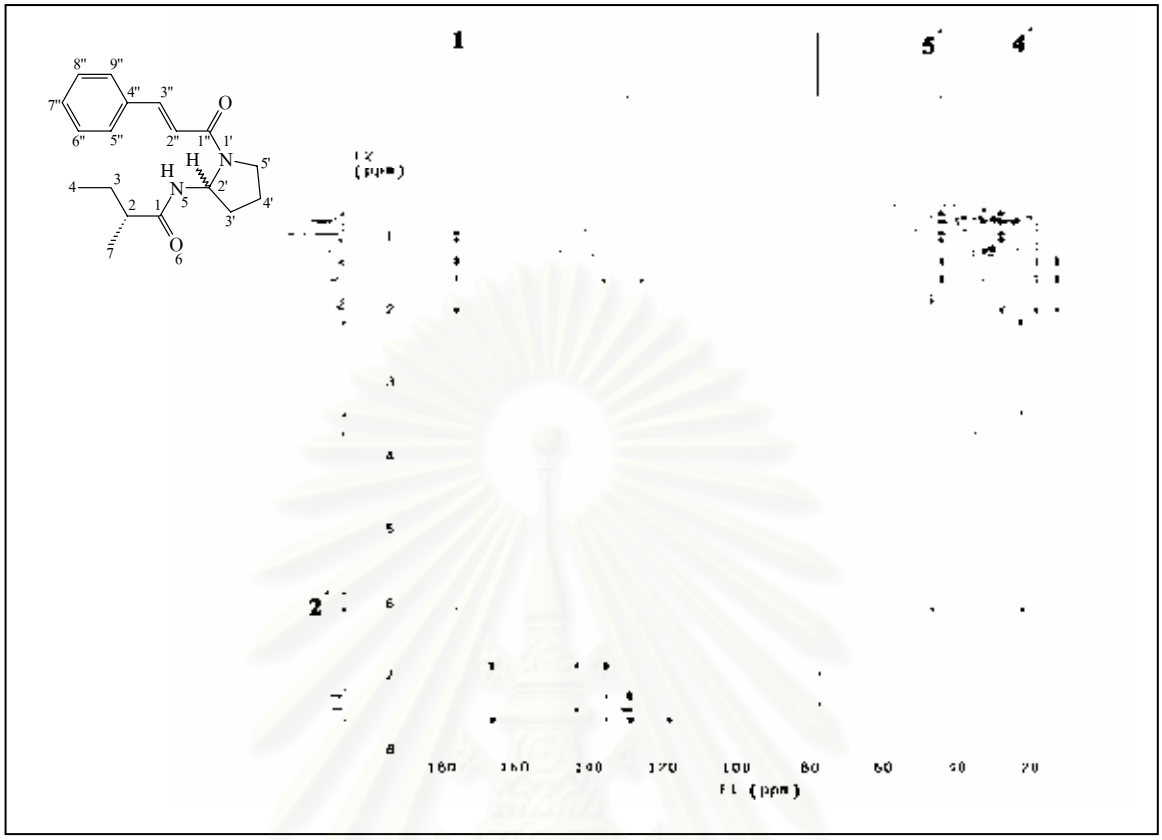

Figure 140. HMBC Spectrum of compound HAO6 ($CDCl_3$) [δ_H 0.7-8.0 ppm, δ_C 15-180 ppm]

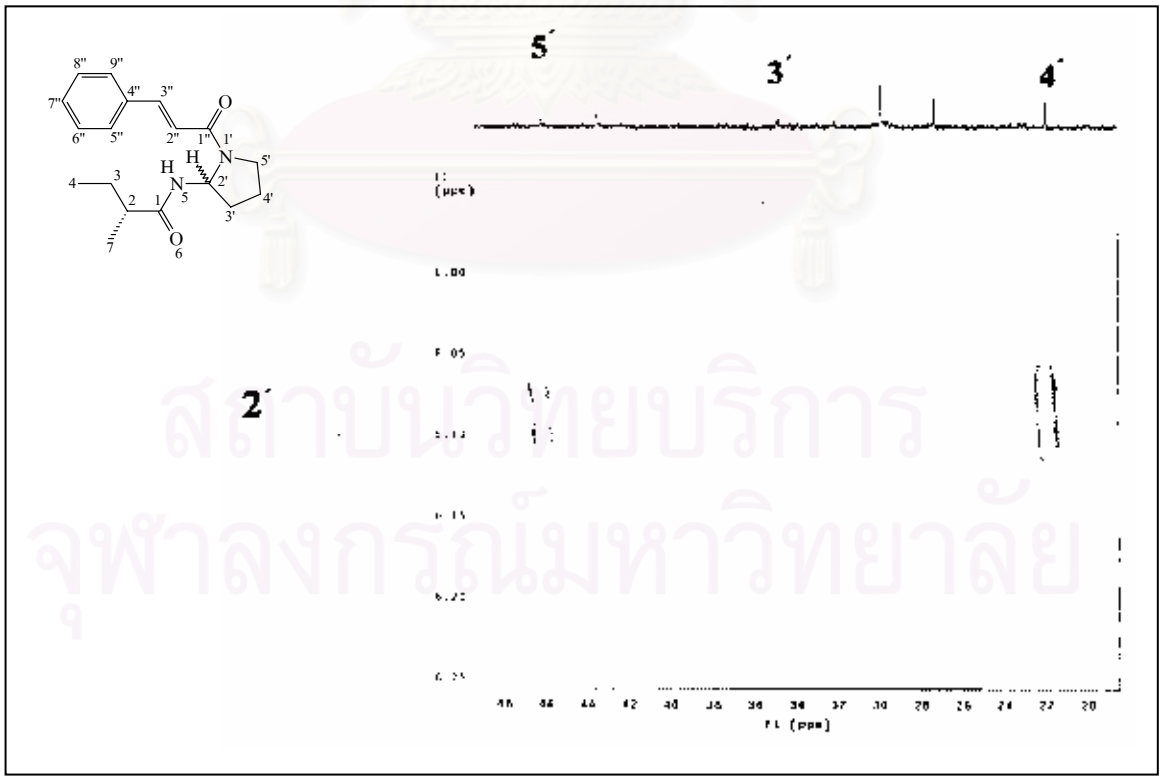

Figure 141. HMBC Spectrum of compound HAO6 ($CDCl_3$) [δ_H 6.0-6.2 ppm, δ_C 20-48 ppm]

สถาบันวิทยบริการ
จุฬาลงกรณ์มหาวิทยาลัย

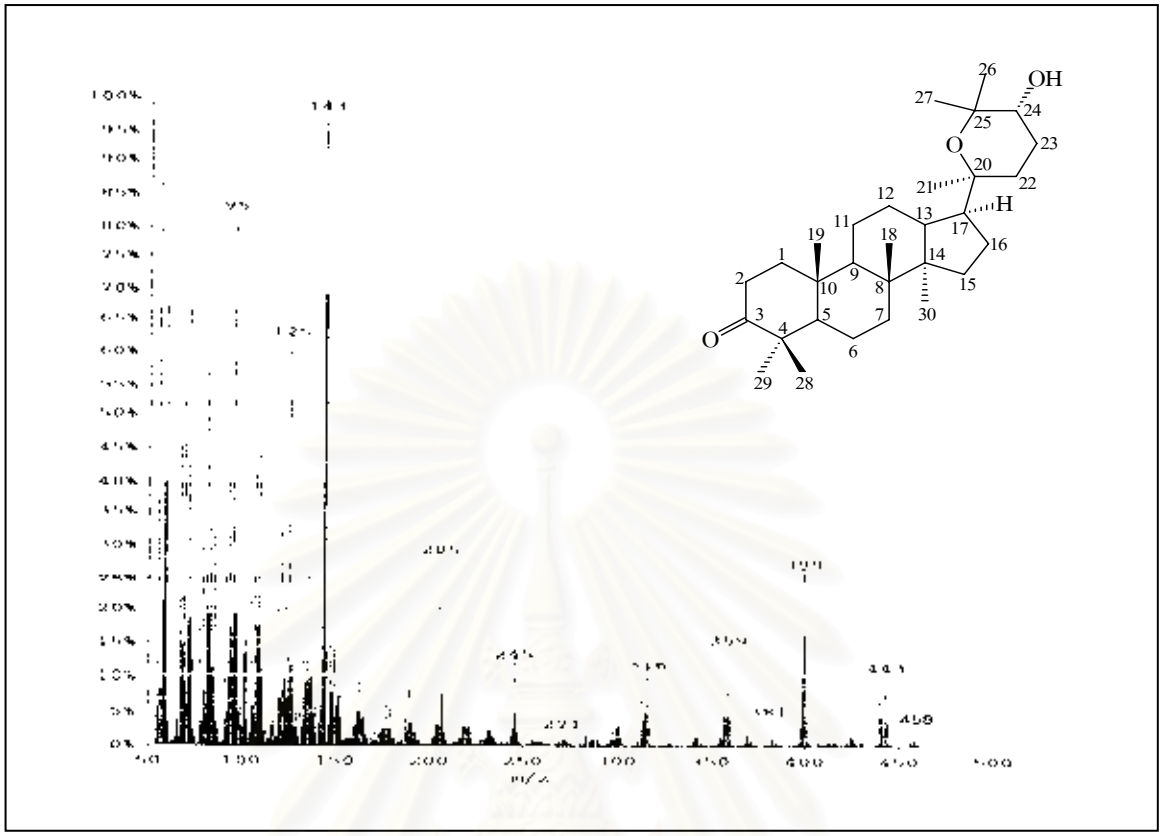

Figure 142. EI Mass spectrum of compound HAO7

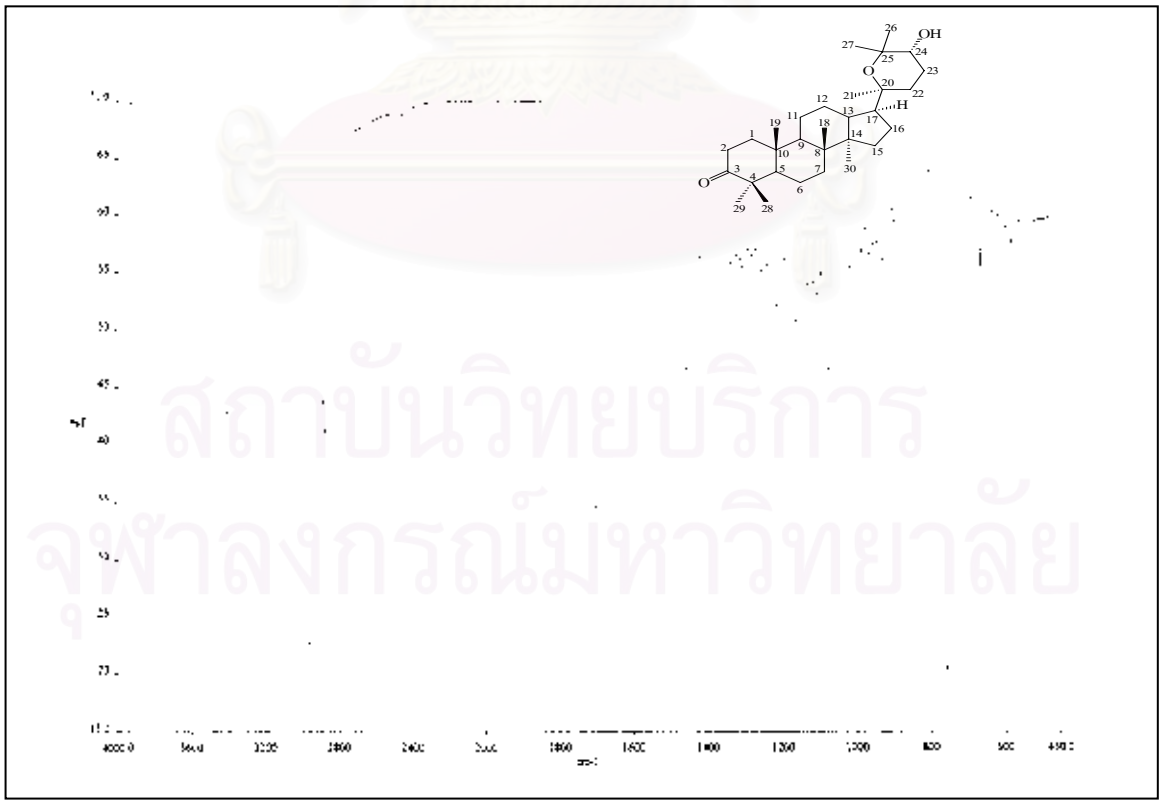

Figure 143. IR Spectrum of compound HAO7 (KBr disc)

สถาบันวิทยบริการ
จุฬาลงกรณ์มหาวิทยาลัย

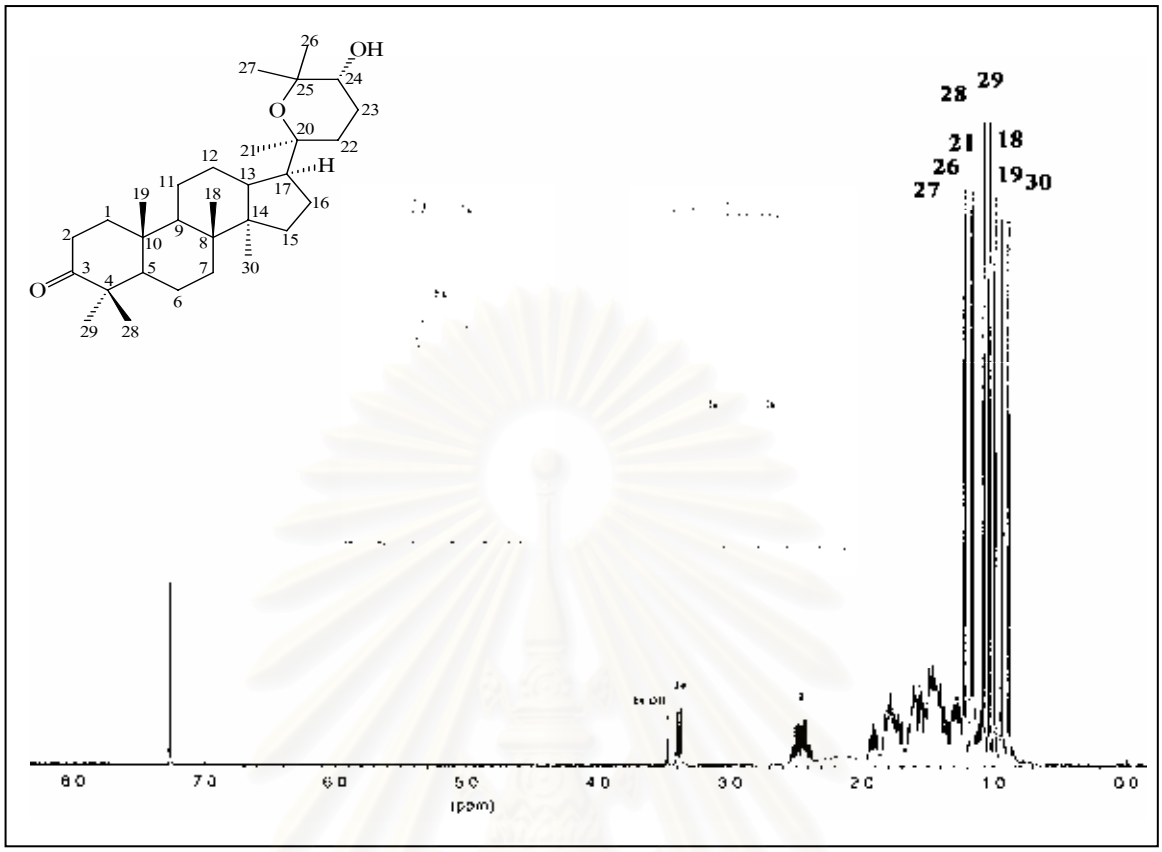

Figure 144. ^{1}H NMR (400 MHz) Spectrum of compound HAO7 ($CDCl_3$)

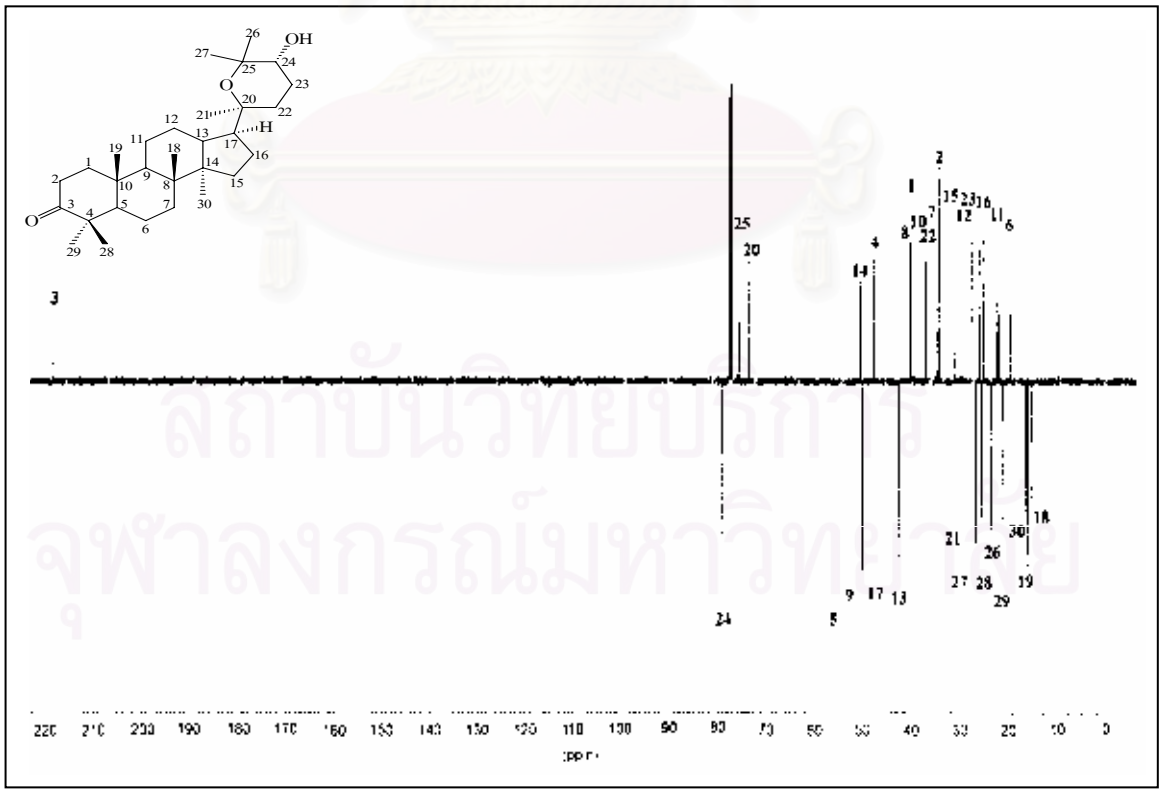

Figure 145. ^{13}C APT (100 MHz) Spectrum of compound HAO7 ($CDCl_3$)

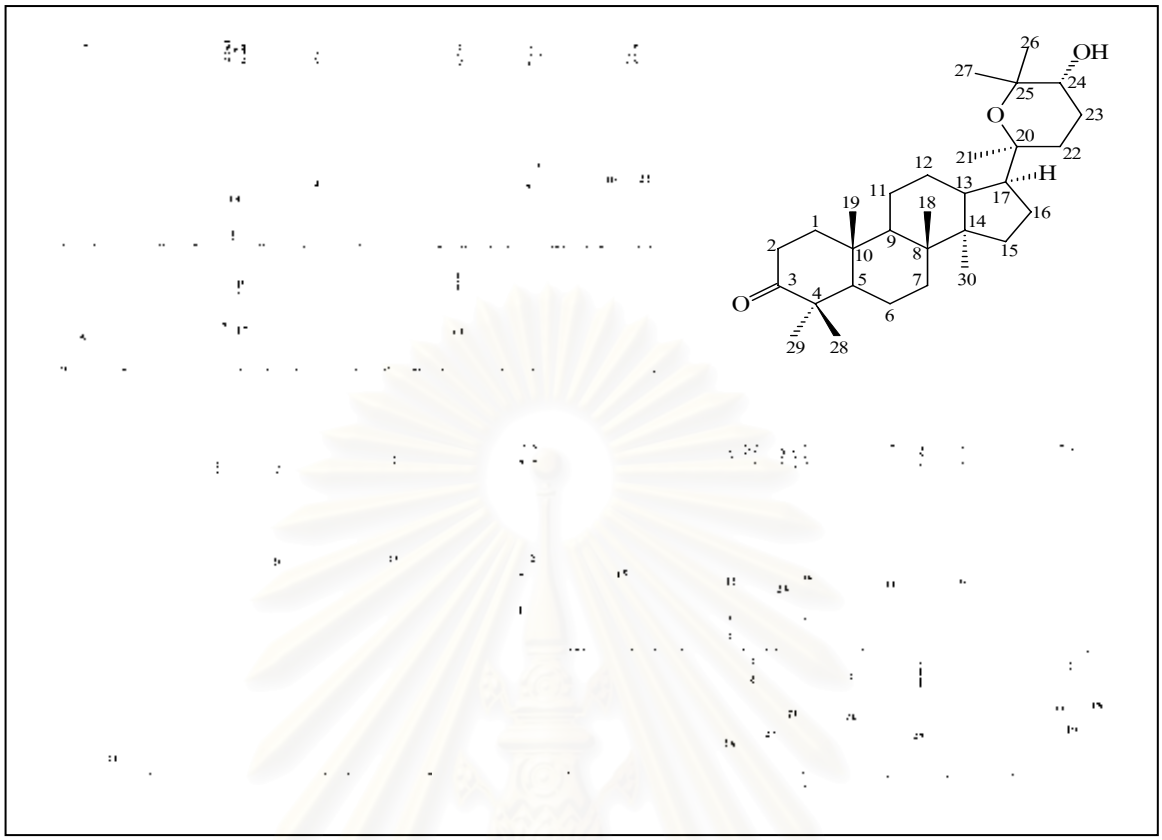

Figure 146. ^{13}C APT (100 MHz) Spectrum of compound HAO7 ($CDCl_3$) (expanded)

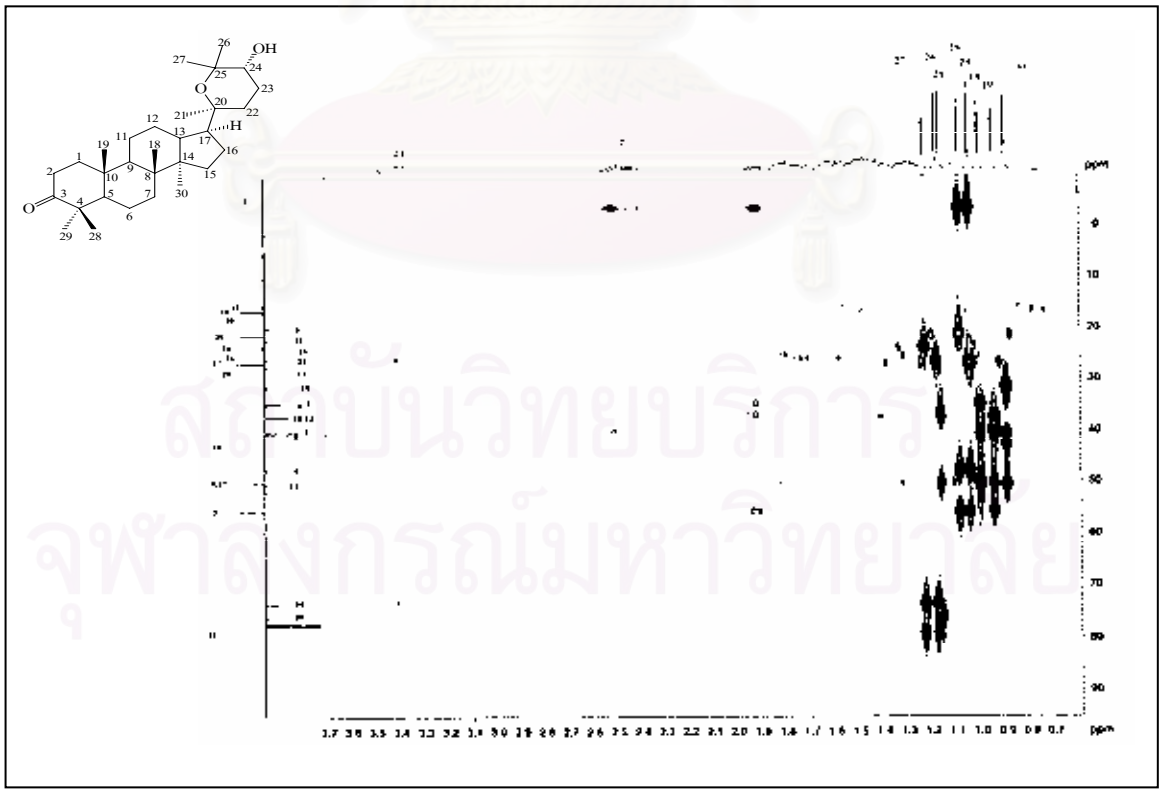

Figure 147. HMBC Spectrum of compound HAO7 ($CDCl_3$)

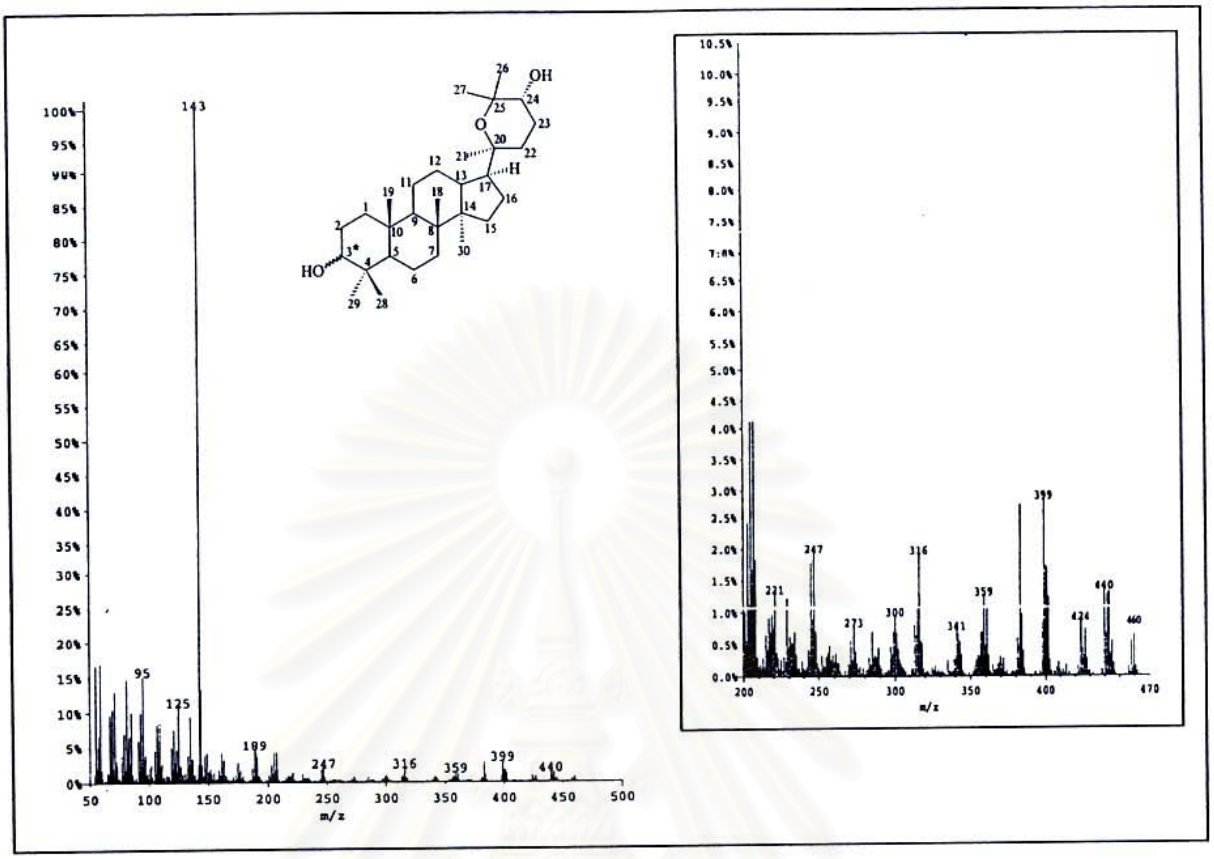

Figure 148. EI Mass spectrum of compound EAO1

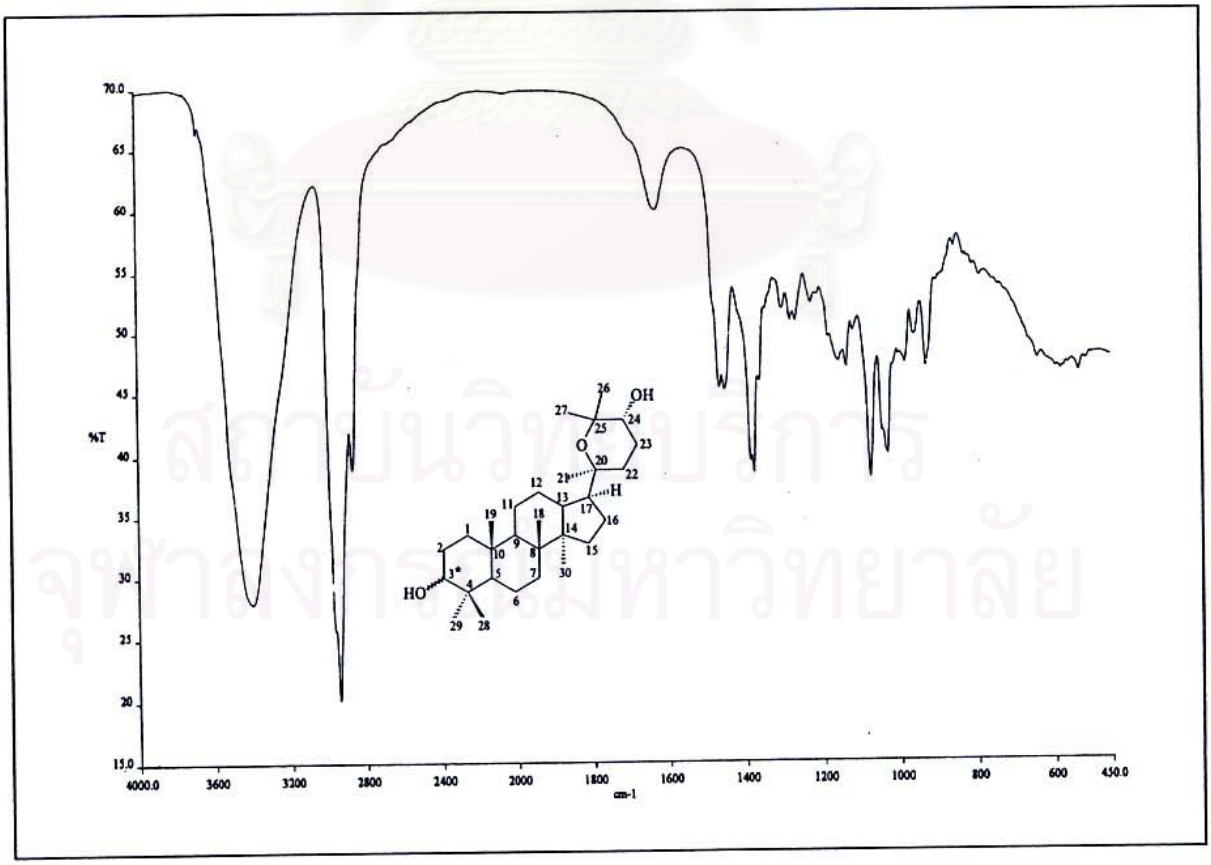

Figure 149. IR Spectrum of compound EAO1 (KBr disc)

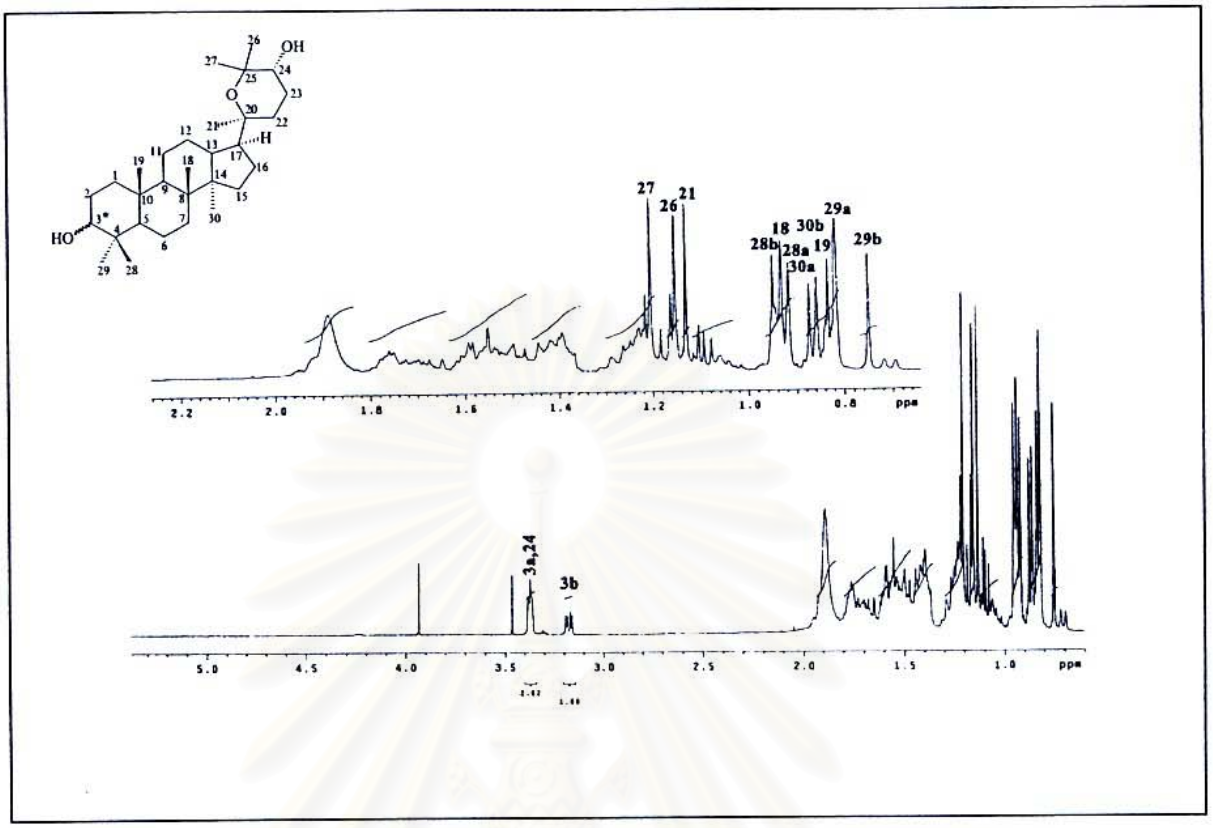

Figure 150. ^{1}H NMR (500 MHz) Spectrum of compound EAO1 ($CDCl_3$)

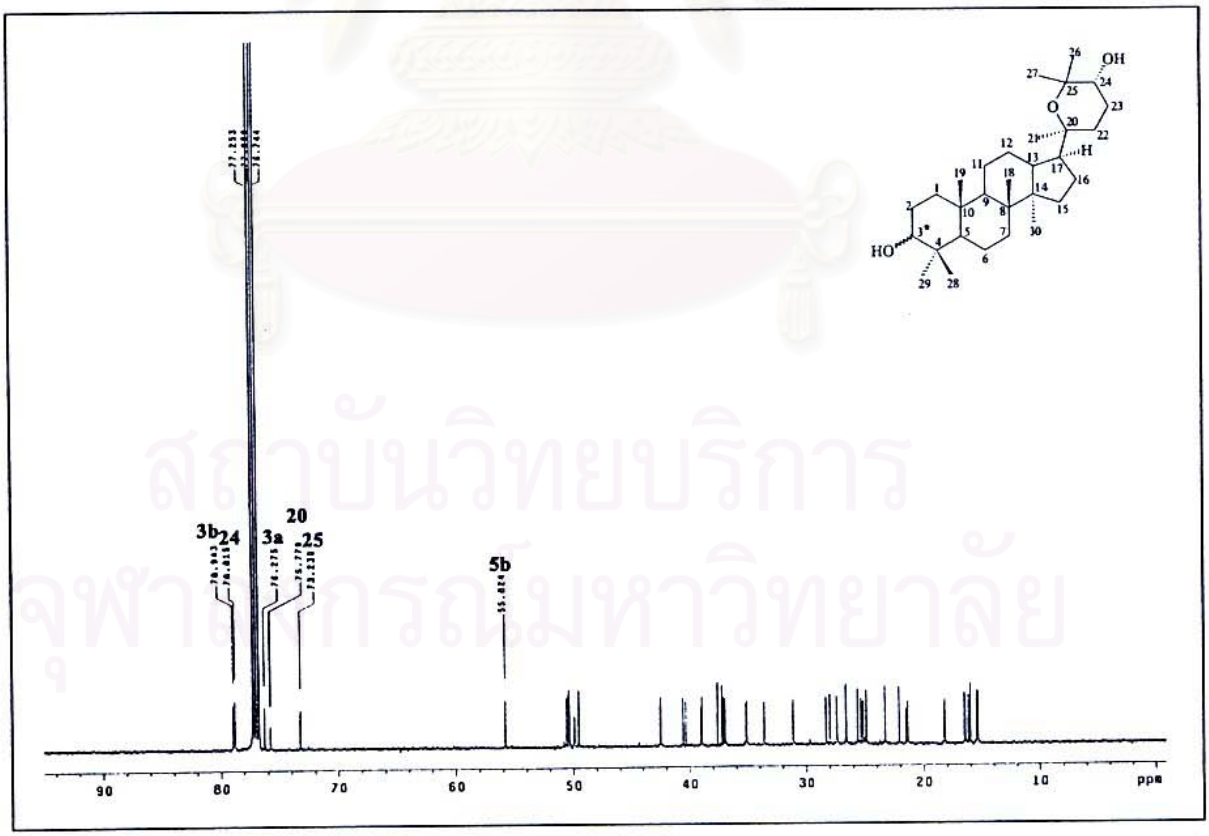

Figure 151. ^{13}C NMR (125 MHz) Spectrum of compound EAO1 ($CDCl_3$)

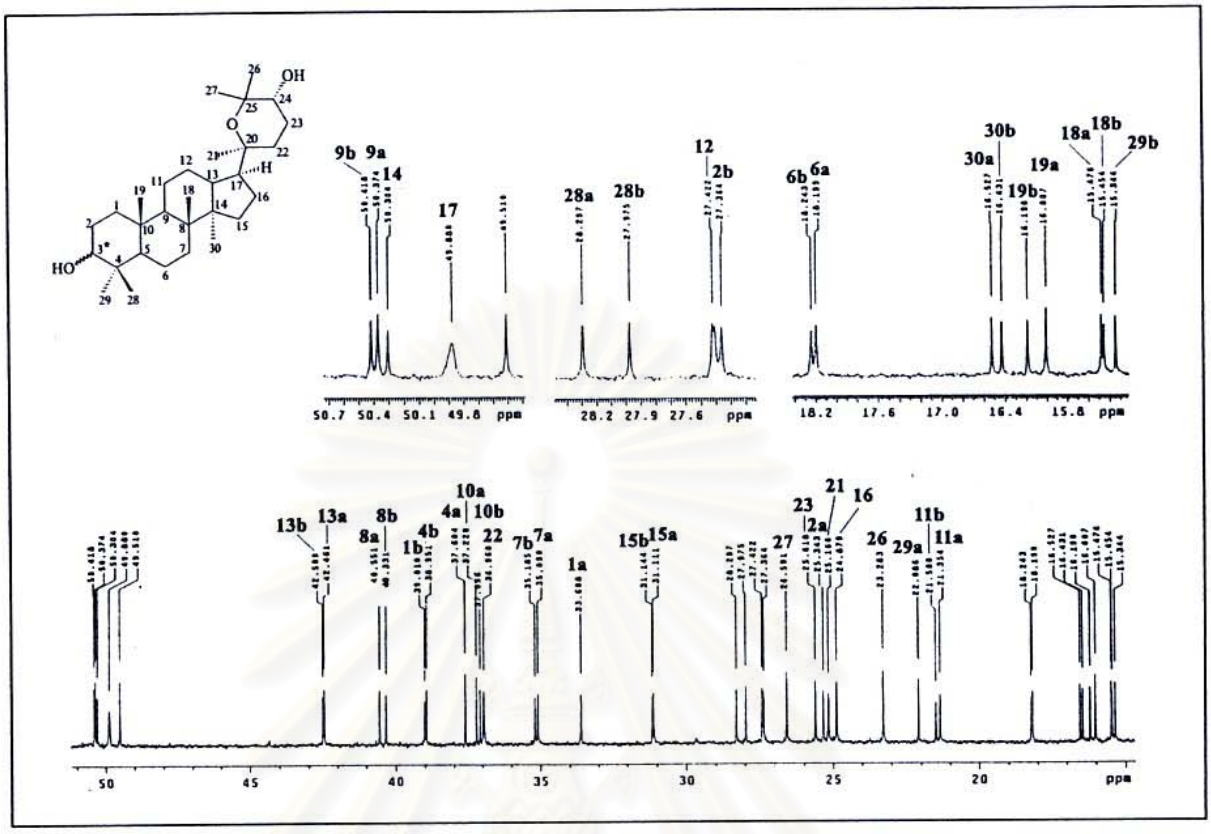

Figure 152. ^{13}C NMR (125 MHz) Spectrum of compound EAO1 ($CDCl_3$) (expanded)

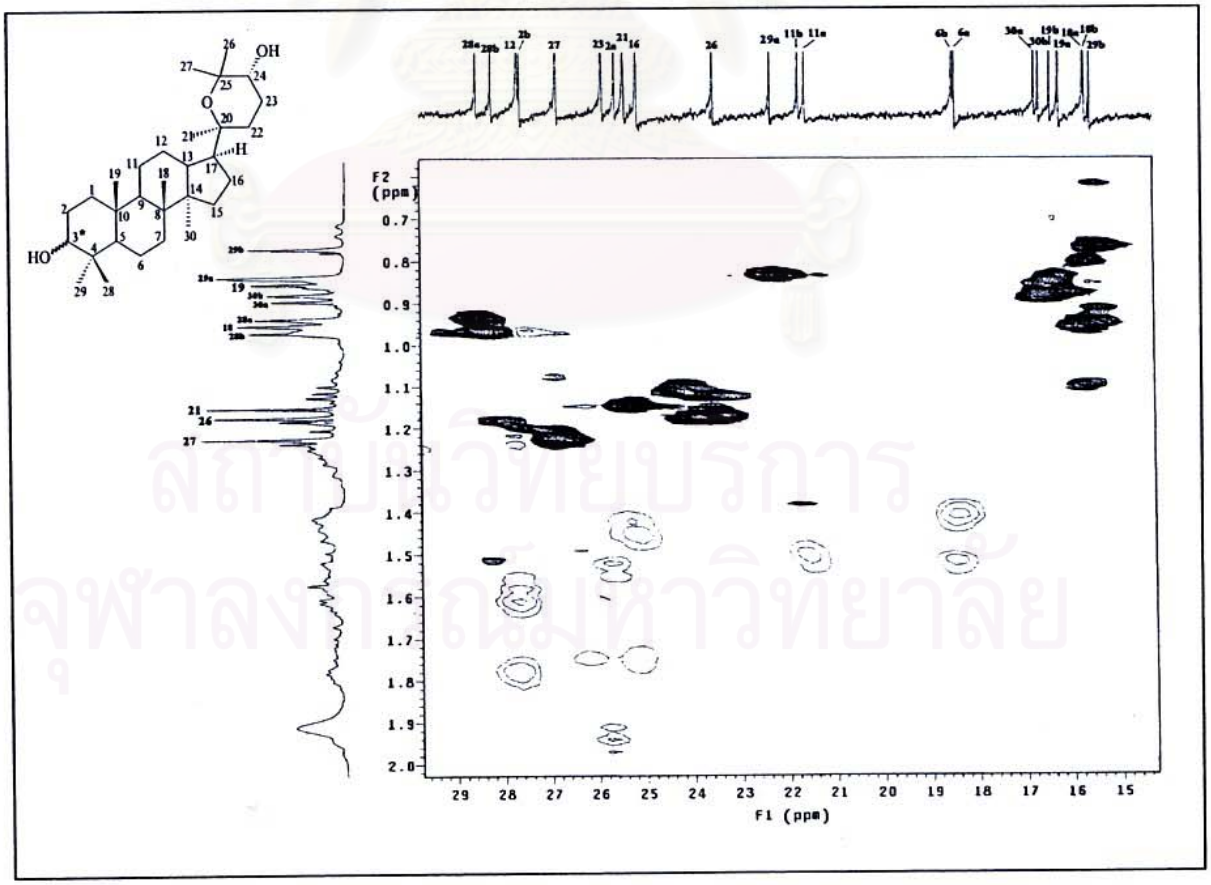

Figure 153. HSQC Spectrum of compound EAO1 ($CDCl_3$) [δ_H 0.7-2.0 ppm, δ_C 15-29 ppm]

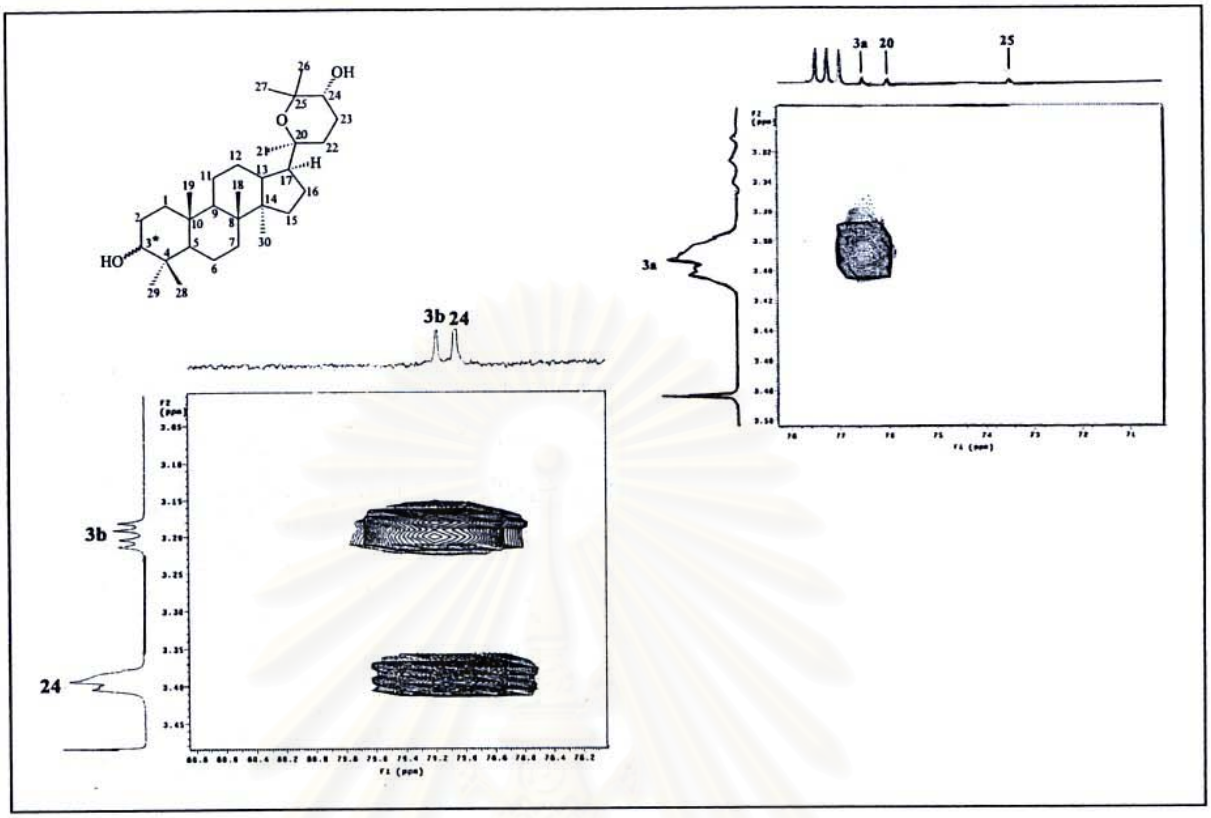

Figure 154. HSQC Spectrum of compound EAO1 ($CDCl_3$) [δ_H 3.2-3.4 ppm, δ_C 71-80 ppm]

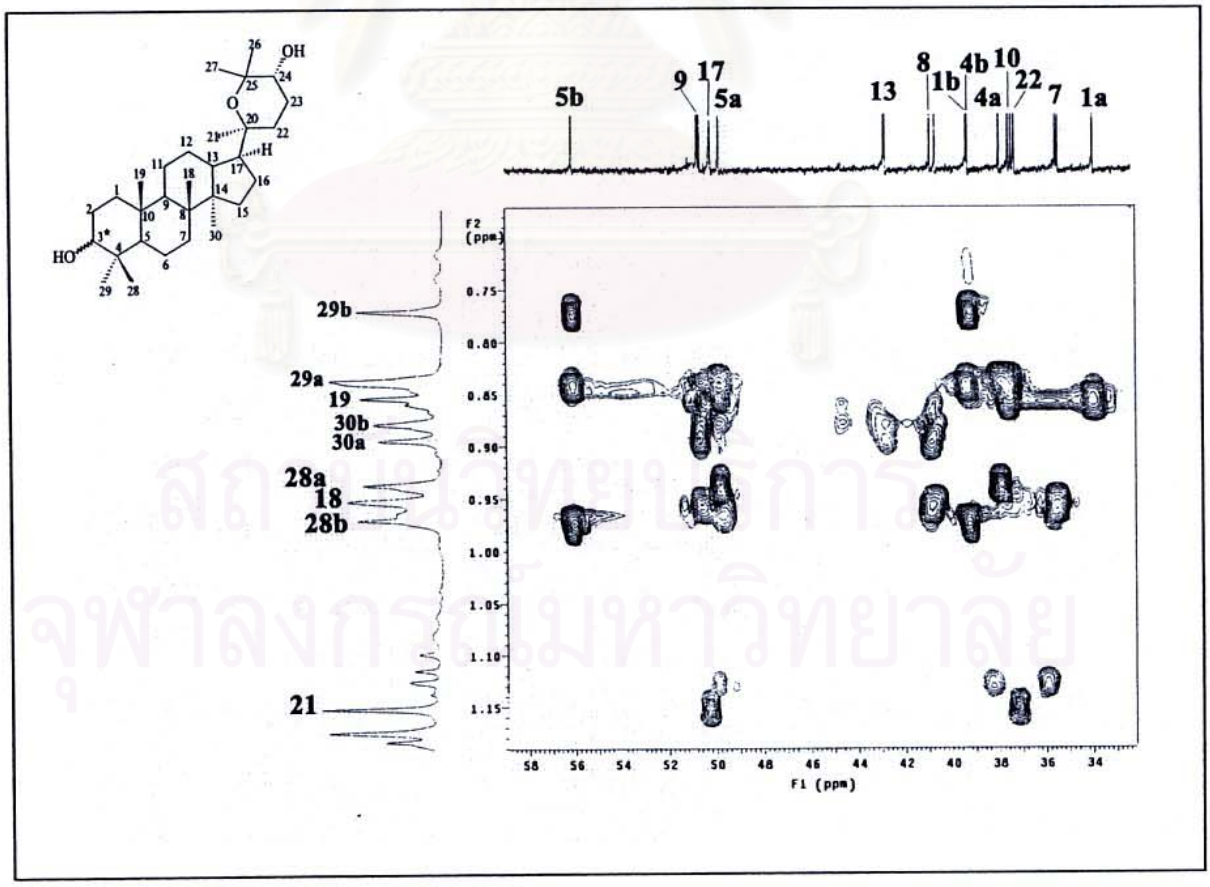

Figure 155. HMBC Spectrum of compound EAO1 ($CDCl_3$) [δ_H 0.7-1.2 ppm, δ_C 33-58 ppm]

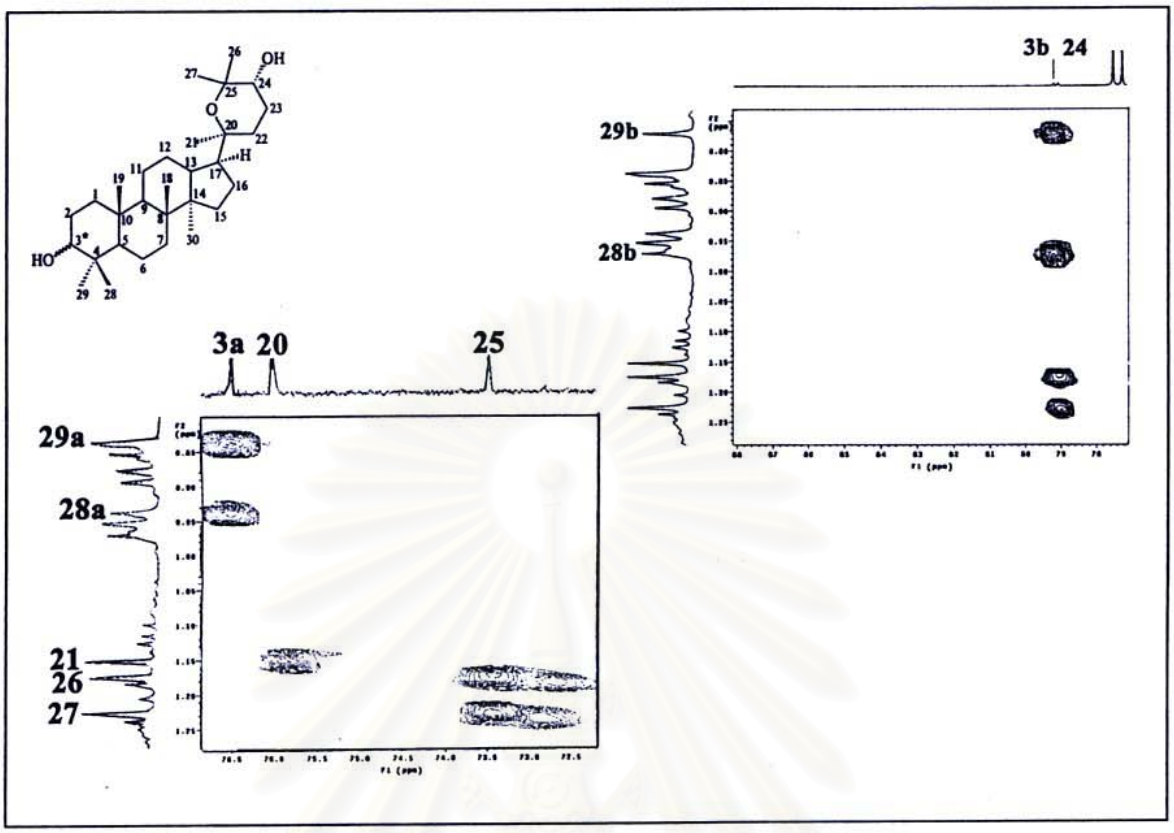

Figure 156. HMBC Spectrum of compound EAO1 ($CDCl_3$) [δ_H 0.7-1.3 ppm, δ_C 72-88 ppm]

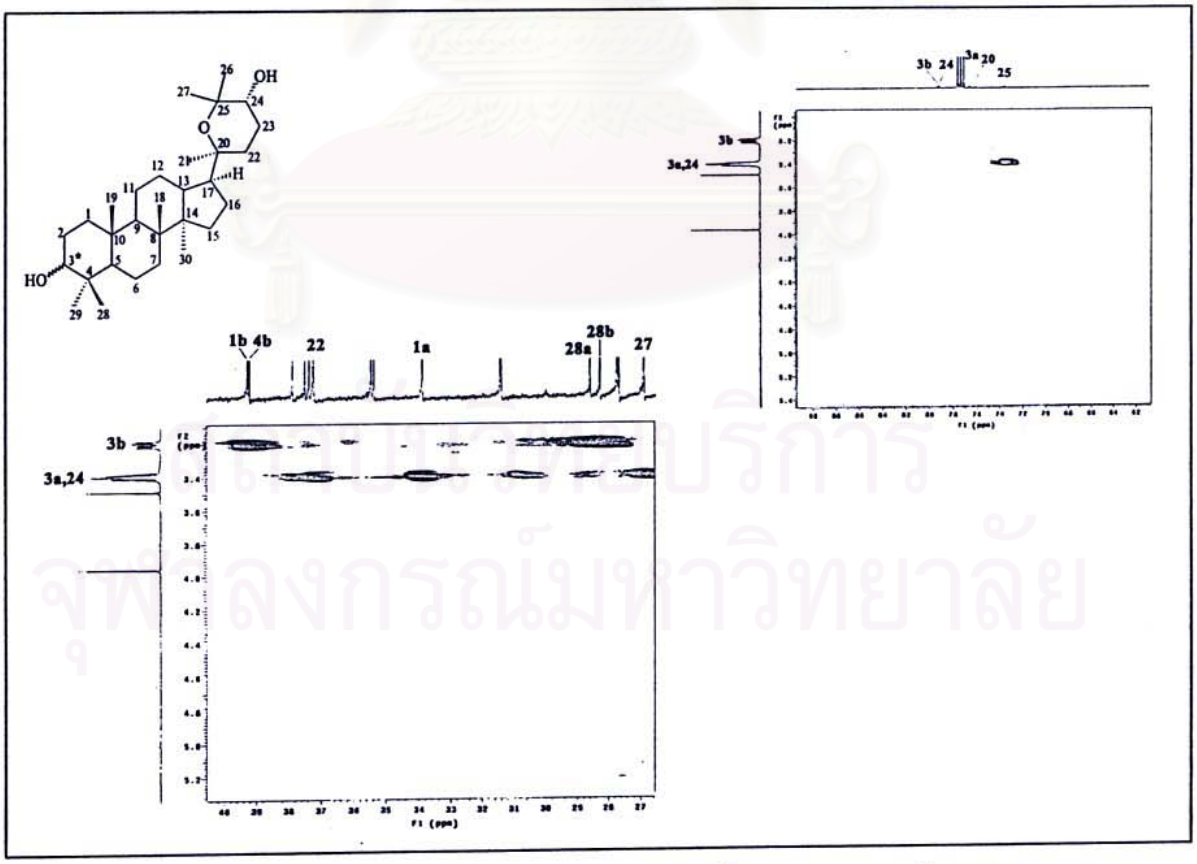

Figure 157. HMBC Spectrum of compound EAO1 ($CDCl_3$) [δ_H 3.1-3.6 ppm, δ_C 26-80 ppm]

VITA

Miss Nantiya Joycharat was born on August 25, 1979 in Bangkok, Thailand. She received her Bachelor's Degree of Science (Public Health) (1st class honor) from Mahidol University in 2000. She was granted a Royal Golden Jubilee Ph.D. Scholarship from the Thailand Research Fund (TRF) in 2003.

Publication

Joycharat , N., Greger, H., Hofer, O., Saifah, E. 2007. Flavaglines and triterpenoids from the leaves of *Aglaia forbesii*. Phytochemistry, available online 20 August 2007.

Poster presentation

Nantiya Joycharat, Harald Greger, Otmar Hofer, and Ekarin Saifah. 2007. Chemical Constituents of *Aglaia forbesii* Leaves. RGJ-Ph.D. Congress VIII, April 20-22, 2007, Chonburi, Thailand.

สถาบันวิทยบริการ
จุฬาลงกรณ์มหาวิทยาลัย